Enantioselective Synthesis of Bioactive Molecule and Development of Synthetic Methodologies Involving Formation of C-C, C-N Bonds

by

Kishor Dharmraj Mane

10CC17J26029

A thesis submitted to the
Academy of Scientific & Innovative Research
for the award of the degree of
DOCTOR OF PHILOSOPHY
in
SCIENCE

Under the supervision of

Dr. Gurunath Suryavanshi

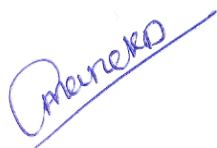and under the co-supervision of

Dr. Shafeek A. R. Mulla

CSIR- National Chemical Laboratory, Pune

Academy of Scientific and Innovative Research
AcSIR Headquarters, CSIR-HRDG Campus
Sector 19, Kamla Nehru Nagar,
Ghaziabad, U.P. – 201 002, India
April-2022

Certificate

This is to certify that the work incorporated in this Ph.D. thesis entitled, "*Enantioselective Synthesis of Bioactive Molecule and Development of Synthetic Methodologies Involving Formation of C-C, C-N Bonds*" submitted by *Mr. Kishor Dharmraj Mane* to the Academy of Scientific and Innovative Research (AcSIR), in partial fulfillment of the requirements for the award of the Degree of *Doctor of Philosophy in Science*, embodies original research work carried-out by the student. We, further certify that this work has not been submitted to any other University or Institution in part or full for the award of any degree or diploma. Research material(s) obtained from other source(s) and used in this research work has/have been duly acknowledged in the thesis. Image(s), illustration(s), figure(s), table(s) *etc.*, used in the thesis from other source(s), have also been duly cited and acknowledged.

Mr. Kishor Dharmraj Mane   Dr. Shafeek A. R. Mulla   Dr.Gurunath Suryavanshi

Research Student   Research Co-Supervisor   Research Supervisor

Date: 07/04/2022   Date: 07/04/2022   Date: 07/04/2022

STATEMENTS OF ACADEMIC INTEGRITY

I Mr. Kishor Dharmraj Mane, a Ph. D. student of the Academy of Scientific and Innovative Research (AcSIR) with Registration No. 10CC17J26029 hereby undertake that, the thesis entitled "Enantioselective Synthesis of Bioactive Molecule and Development of Synthetic Methodologies Involving Formation of C-C, C-N Bonds" has been prepared by me and that the document reports original work carried out by me and is free of any plagiarism in compliance with the UGC Regulations on *"Promotion of Academic Integrity and Prevention of Plagiarism in Higher Educational Institutions (2018)"* and the CSIR Guidelines for "*Ethics in Research and in Governance (2020)*".

Signature of the Student
Date   : 07/04/2022
Place : Pune

It is hereby certified that the work done by the student, under my/our supervision, is plagiarism-free in accordance with the UGC Regulations on *"Promotion of Academic Integrity and Prevention of Plagiarism in Higher Educational Institutions (2018)"* and the CSIR Guidelines for "*Ethics in Research and in Governance (2020)*".

Signature of the Co-Supervisor
Name : Dr. Shafeek A. R. Mulla
Date : 07/04/2022
Place : Pune

Signature of the Supervisor
Name : Dr. Gurunath Suryavanshi
Date : 07/04/2022
Place : Pune

"It is impossible to extend enough thanks to my family, especially my parents, who gave me the encouragement I needed throughout this process."

↑

personal language to thank friends & family

wikiHow

CONTENTS

Section II   **Visible Light Promoted, Photocatalyst Free C(sp^2)-H Bond Functionalization of Indolizines *via* EDA Complexes**

Chapter IV   **Synthesis of Congested Indolizine Amides From in situ Generated Azaoxyallyl Cations and Ti-superoxide Catalyzed Oxidative Amidation of Aldehydes**

Section I   **Metal-free Regioselective C-3 Alkylation of Indolizines *via* in situ Generated Azaoxyallyl Cations**

ABBREVIATIONS AND CHEMICAL FORMULAS

Ac	Acetyl
Ar	Aryl
Bn	Benzyl
Boc	N-tert-Butoxycarbonyl
Bz	Benzoyl
BBr$_3$	Boron tribromide
Br$_2$	Bromine
(Boc)$_2$O	Di-tert-butyl dicarbonate
n-Bu	n-Butyl
n-BuLi	n-Butyl lithium
t-Bu	*tert*-Butyl
CDC	Cross Dehydrogenative Coupling
CSA	Camphorsulfonic acid
CH$_3$CN	Acetonitrile
CH$_2$Cl$_2$	Dichloromethane
EtOH	Ethanol
DBU	1,8-Diazabicyclo[5.4.0]undec-7-ene
DDQ	2,3-Dichloro-5,6-dicyano-1,4-benzoquinone
DEAD	Diethyl azodicarboxylate
DIBAL-H	Diisobutyl aluminium hydride
DMP	Dess–Martin periodinane
DMF	Dimethyl formamide
DMS	Dimethyl sulfide
DMSO	Dimethyl sulphoxide
DMAP	N,N-dimethyl-4-aminopyridine
dr	Diastereomeric ratio

ee	Enantiomeric excess
Et	Ethyl
EtOAc	Ethyl acetate
g	Grams
h	Hours
HPLC	High performance liquid chromatography
HRMS	High resolution mass spectroscopy
I_2	Iodine
imid.	Imidazole
K_2CO_3	Potassium carbonate
IR	Infra-red
IBX	2-Iodoxybenzoic acid
LAH	Lithium aluminum hydride
LiHMDS	Lithium hexamethyldisilazide
M^+	Molecular ion
Me	Methyl
MOM	Methoxymethyl
*m*CPBA	meta-Chloroperoxybenzoic acid
min	Minutes
mg	Miligram
mL	Milliliter
mp	Melting point
MS	Mass spectrum
Ms	Mesyl
NBS	*N*-Bromosuccinimide
NaOH	Sodium Hydroxide
$NaHCO_3$	Sodium bicarbonate
NMR	Nuclear Magnetic Resonance
NMO	*N*-Methyl morpholine *N*-oxide

PCC	Pyridinium chlorochromate
Pd/C	Palladium on activated charcoal
PDC	Pyridinium dichromate
Ph	Phenyl
p-Ts	*p*-Tosyl
p-TSA	*p*-Toluene sulfonic acid
Py	Pyridine
PhI	Iodobenzene
PIDA	(Diacetoxyiodo)benzene
PIFA	bis(trifluoroacetoxy)iodobenzene
HTIB	Hydroxy(tosyloxy)iodobenzene
PPh_3	Triphenylphosphine
TBS	*tert*-Butyldimethylsilyl
TEMPO	(2,2,6,6-tetramethyl-1-piperidinyl)oxyl
THF	Tetrahydrofuran
TLC	Thin layer chromatography
TBAF	Tetrabutylammonium fluoride
TBDMSCl	*tert*-Butyldimethylsilyl chloride
TBDPSCl	*tert*-Butyldiphenylsilyl chloride
TFA	Trifluoroacetic acid
TfOH	Trifluoromethanesulfonic acid
EDA	Electron Donor Acceptor
TBACl	Tetrabutyl ammonium chloride
TBAB	Tetrabutyl ammonium bromide

GENERAL REMARKS

1. All reagents and starting materials from commercial suppliers were used as such without further purification.

2. Solvents were distilled and dried using standard protocols. Reactions were carried out in anhydrous solvents under argon, nitrogen atmosphere in oven-dried glassware.

3. Petroleum ether refers to the fraction collected in the boiling range 60-80 ^{0}C.

4. Organic layers after every extraction were dried over anhydrous sodium sulphate.

5. Air sensitive reagents and solutions were transferred *via* syringe or cannula and were introduced to the apparatus *via* rubber septa.

6. Column Chromatography was performed over silica gel (100-200 mesh and 230-400 mesh size).

7. All evaporations were carried out under reduced pressure on Heidolph rotary evaporator below 50 °C unless otherwise specified.

8. All reactions are monitored by thin layer chromatography (TLC) with 0.25 mm pre-coated E-Merck silica gel plates (60F-254). Visualization was accomplished with either UV light, Iodine adsorbed on silica gel or by immersion in an ethanolic solution of phosphomolybdic acid (PMA), p-anisaldehyde or KMnO4 followed by heating with a heat gun for ⁓15 sec.

9. ^{1}H and ^{13}C NMR spectra were recorded on Brucker FT AC-200 MHz, Brucker Advance 400 MHz, Brucker Advance 500 MHz and JEOL ECX 400 instruments using TMS as an internal standard. The following abbreviations were used: s=singlet, d=doublet, t=triplet, q=quartet, m multiplet, br. s.=broad singlet, dd=doublet of doublet, dt=doublet of triplet and ddd=doublet of doublet of doublet, app=apparent.

10. Chemical nomenclature (IUPAC) and structures were generated using Chem Draw Professional 20.0.0.41 software.

11. High-resolution mass spectra (HRMS) were recorded on a Thermo Scientific Q-Exactive, Accela 1250 pump and EI Mass spectra were recorded on Finnigan MAT-1020 spectrometer at 70 eV using a direct inlet system.

12. UV-vis absorption spectra were measured with a UV-Vis spectrum were recorded with a Shimadzu 1800 spectrophotometer.

13. All the melting points are uncorrected and were recorded using a scientific melting point apparatus (Buchi B-540) and the temperatures are in centigrade scale.

14. The compounds, scheme and reference numbers given in each chapter refers to that chapter only.

![AcSIR logo]	**Synopsis of the thesis to be submitted to the Academy of Scientific and Innovative Research for award of the degree of Doctor of philosophy in Chemical Sciences**
Name of the Candidate	Mr. Kishor Dharmraj Mane
Enrollment No. and Date	Ph. D in Chemical Sciences (10CC17J26029); January 2017
Title of the Thesis	Enantioselective Synthesis of Bioactive Molecule and Development of Synthetic Methodologies Involving Formation of C-C, C-N Bonds
Research Supervisor	Dr. Gurunath Suryavanshi

1. Introduction

Substituted piperidines are the most accessible structural motifs found among the biologically active N-heterocycles which occurred naturally as well as synthetically. It has become the most reputed and impressive core structure as it is present in 72 small drug molecules having piperidine as active site. Due to the impact of piperidines in pharmaceutical industry it has attracted the attention of chemists towards its synthesis.

1.1 Statement of Problem

Due to the increasing importance of tofacitinib in medicinal and pharmaceutical fields, several synthetic approaches have been well reported in the literature. Among the reported methods, asymmetric synthesis of tofacitinib is rarely explored. Substituted aryl carbonyls and quinoxaline-2(1H)-ones with ether cores are very important in the bioactive natural products. Indolizines are one of the vital fused *N*-heterocyclic compounds mainly isolated from different plants and fungal sources and further they come into spotlight due to their unique physical and pharmacological properties. Therefore, new methods are for synthesis of these core structure need to develop.

2. Objectives

1) Short Enantioselective Total Synthesis of (+)-Tofacitinib and Process for the production of key intermediate of (+)- Tofacitinib

2) Development of Metal-Free Regioselective Cross Dehydrogenative Coupling of Cyclic Ethers with Aryl Carbonyls and quinoxalin-2(1H)-ones.

3) Development of new synthetic methodologies for the C-H functionalization of indolizines.

4) Ti-superoxide catalysed oxidative amidation of aldehydes and synthesis of congested indolizine amides.

3. Methodology

The thesis is divided into four chapters. Chapter 1: Short Enantioselective Total Synthesis of (+)-Tofacitinib and Process for the production of key intermediate of (+)- Tofacitinib.

Chapter 2: Efforts to Access the Regioselective alkylation of aryl carbonyls and C-H functionalization of quinoxalin-2(1H)-ones. Chapter 3:   Development of new synthetic methodologies for the C-H functionalization of indolizines. Chapter 4:Ti-superoxide catalysed oxidative amidation of aldehydes and synthesis of congested indolizine amides.

Chapter 1: Short Enantioselective Total Synthesis of (+)-Tofacitinib and Process for the production of key intermediate of (+)- Tofacitinib.
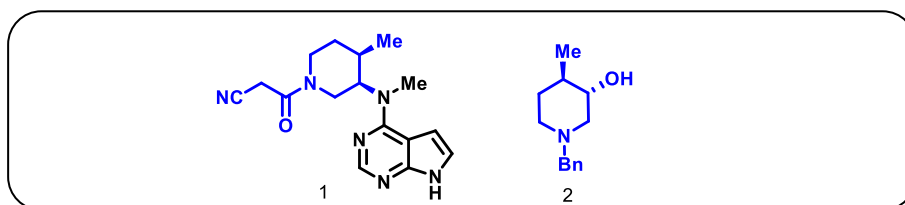
Section I: Short Enantioselective Total Synthesis of (+)-Tofacitinib
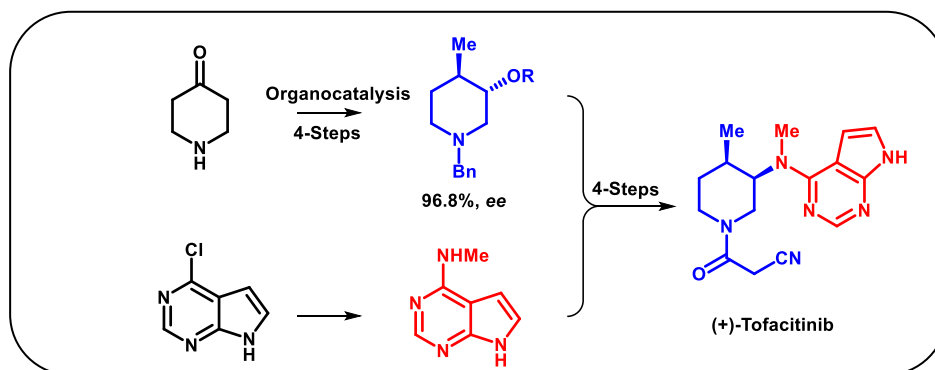
In recent studies, 3, 4-disubstituted piperidines have shown a promising candidate as JAK inhibitors. Whereas in 2012, tofacitinib (1) became the first JAK inhibitor drug approved by the Food and Drug Administration (FDA) for the treatment of rheumatoid arthritis, also in 2017 it was further approved for the treatment of active rheumatoid arthritis (RA), psoriatic arthritis, and ulcerative colitis.
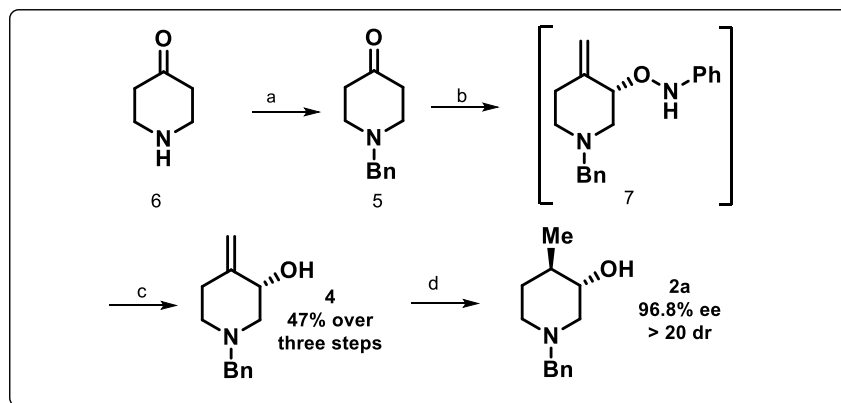
Due to the increasing importance of tofacitinib in medicinal and pharmaceutical fields, several synthetic approaches have been well reported in the literature. Among the reported methods, asymmetric synthesis of tofacitinib is rarely explored. We have planned the synthesis of tofacitinib (**1**) from stereoselective inversion of 1-benzyl-4-methylpiperidin-3-yl methanesulfonate**2b** via nucleophilic substitution reaction with N-methyl dezapurine amine **3**. Further, the key intermediate **2a** synthesized from the *N*-protected piperidone **5** by using proline catalysed one pot *α*-aminoxylation and Wittig reaction, followed by reduction of allylic alcohol **4**.
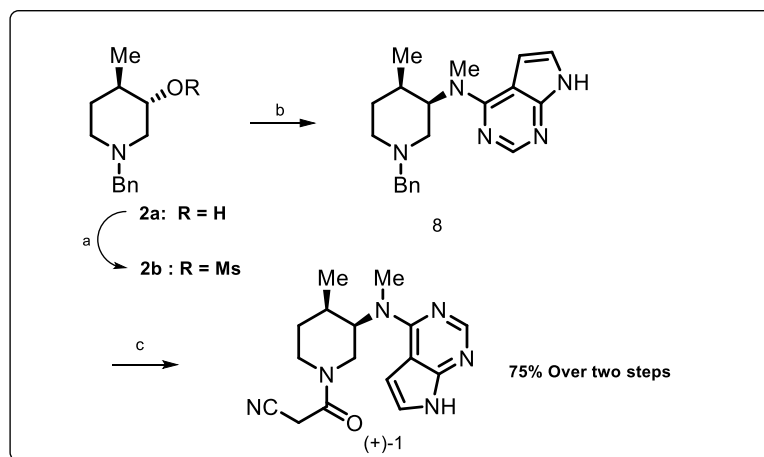
Finally, the S_N^2 nucleophilic addition of dezapurine amine with fragment **2b** producesIntermediate 8 and then within 2 step gives Tofacitinib (**1**)

Section II: Process for the Production of Key Intermediate of (+)- Tofacitinib *via* Overmann Rearrangement Reaction.
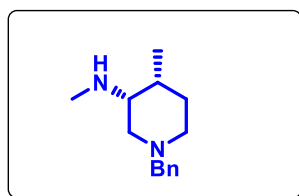
In the Literature very,few methods are available for the Synthesis of enantiomerically pure (+)-Tofacitinib. The present invention provides an efficient catalytic route for the key intermediate of (+)- Tofacitinib.It is the catalytic and enantioselective method for the synthesis of chiral pure (3R,4R)-1-benzyl-N,4-dimethylpiperidin-3-amine which is being developed for the first-time using Overmann rearrangement reaction. In recent studies, 3, 4-disubstituted piperidines have shown a promising candidate as JAK inhibitors.
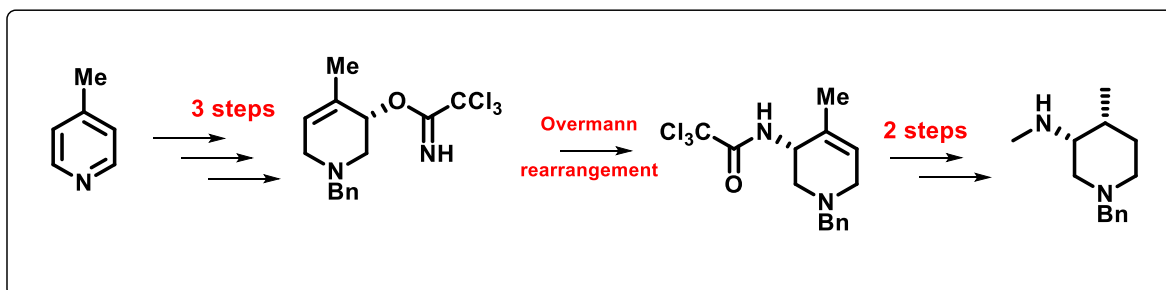
The existing method to synthesize 3, 4-disubstituted piperidines involves multistep reaction sequences thereby limiting the overall yield and the enantioselectivity as well as regioselectivity of the process particularly unsuitable for the atom economic synthesis. The literature methods in the synthesis of (+)-Tofacitinib employ either chiral starting materials or expensive reagents involving longer reaction sequences, often resulting in poor product selectivity. Present work describes a flexible and novel method that employs metal free Overmann rearrangement reaction for the enantioselective production of key intermediate of (+)- Tofacitinib in 8 Steps with excellent yield.

Chapter 2: Development of Metal-Free Regioselective Cross Dehydrogenative Coupling (CDC) of Cyclic Ethers with Aryl Carbonyls and Quinoxalin-2(1H)-ones.

Section I: Metal-Free Regioselective Cross Dehydrogenative Coupling of Cyclic Ethers and Aryl Carbonyls

Functionalized cyclic ethers are important scaffolds found in a variety of natural products and pharmaceutical ingredients. Generally, tetrahydrofuran (THF), 1,4-dioxane and tetrahydropyrans (THP) are the examples of cyclic ethers. These compounds show a broad spectrum of biological activity, including antibacterial, anti-inflammatory, anti-cancer, and anti-diabetic. They have also been employed in the synthesis of agricultural pesticide.
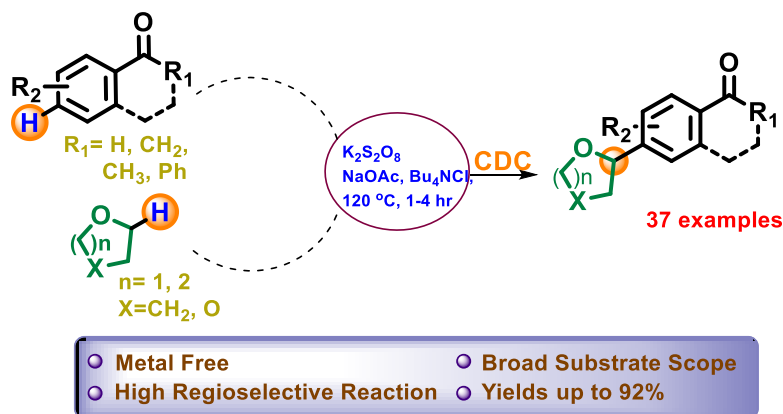
A highly regioselective, efficient and metal free oxidative cross dehydrogenative coupling (CDC) of aryl carbonyls with cyclic ethers has been developed. This method offers easy access to substituted α-arylated cyclic ethers with high functional group tolerance in good to excellent yields. Regioselectivity of this CDC reaction was confirmed by DFT calculation studies.In order to understand the reasons that the para product is formed exclusively, calculations have been done with density functional theory (DFT).In addition, this reaction tolerates various functional groups under oxidative conditions and can be applied to obtain a wide range of substituted aromatic carbonyls.

Section II: Visible Light Mediated, Metal and Oxidant Free Highly Efficient Cross Dehydrogenative Coupling (CDC) Reaction between Quinoxalin-2(1H)-ones and Ethers
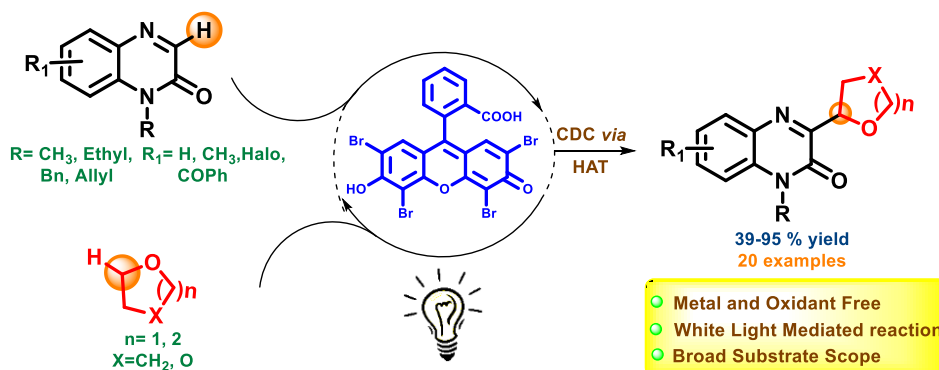
Carbon-carbon (C-C) bond formation has always been the most useful and fundamental reactions in the development of organic chemistry and is considered a backbone of nearly every organic molecule. Hence C-C bond formation reactions consistently contributed in the advancement of organic chemistry. The application of C-C bond formation is found in fine chemicals, agrochemicals, medicinal and pharmaceutical ingredients therefore makes this transformation one of the very crucial class of reaction in organic chemistry.

In this approach, we have developed an efficient white light mediated, eosin y catalyzed C-C bond formation reaction between ethers and quinoxalin-2(1H)-ones to give 3C-alkylated quinoxalin-2(1H)-ones. This approach has a wide substrate scope with high functional group tolerance. Also, it is a base and oxidant free approach under mild reaction conditions over previously reported methods. Further applications of the present methodology are underway in our laboratory.

Chapter 3:Development of New Synthetic Methods for the C-H Functionalization of Indolizines.

Section I: Acetic Acid Catalyzed Regioselective C(sp2)-H Bond Functionalization of Indolizines: Concomitant Involvement of Synthetic and Theoretical Studies

N-heterocyclic compounds are found ubiquitously in many natural products and the core structure of active pharmaceutical ingredients. Indolizines are one of the vital fused *N*-heterocyclic compounds mainly isolated from different plants and fungal sources and further they come into spotlight due to their unique physical and pharmacological properties. The natural and synthetic indolizine alkaloids are extensively used in SAR studies and this study reveals that the indolizine derivatives showed a broad-spectrum biological activity such as anticancer, antibiotics, antitubercular, antioxidant, antimicrobial, antimycobacterial, anticancer, anti-inflammatory and many more.

An atom economical and environment benign protocol has been developed for the regioselective C-C coupling of indolizines and quinone monoimine. The acetic acid catalyzed cross-coupling reaction proceeds under metal-free conditions; provide wide range of synthetically important indolizine derivatives. The present protocol showed good functional group tolerance and broad substrate scope in good to excellent yields. Quantum Mechanical Investigation using DensityFunctional Theory (DFT) has played a crucial role to understand acetic acid is the key player in determining the actual pathway as catalyst and its ultrafast nature. Different Pathways involving inter and intramolecular proton transfer, with or without

acetic acid were investigated. Calculated results revealed that a proton shuttle mechanism is involved for the least energetic most favorable acetic acid catalyzed pathway. Further, the regioselectivity has also been explained theoretically.

Section II: Visible Light Promoted, Photocatalyst Free C(sp^2)-H Bond Functionalization of Indolizines *via* EDA complexes
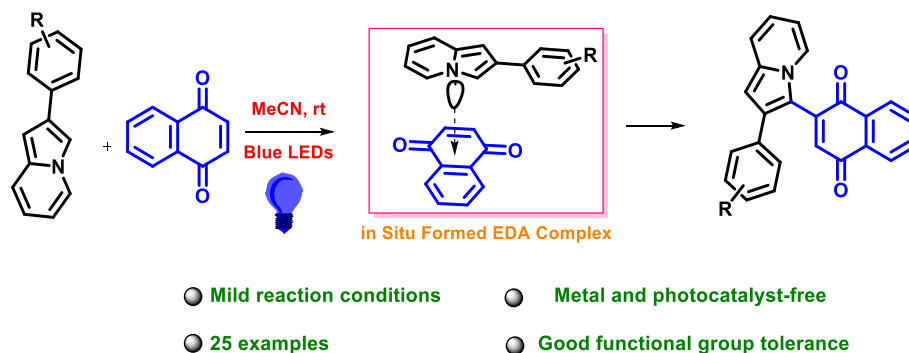
In the past decade, visible-light photocatalysis has become a hot area in synthetic organic chemistry for initiating various organic transformations under very mild reaction conditions and environmental friendliness. However, photoredox catalysis suffered from costly exogenous photosensitizers and complex organic dyes are usually required for the electron transfer (ET) processes. At present, with the increasing demand for the development of greener chemical processes, photodriven organic transformations in the absence of external photocatalysts have gained significant attention.

In this approach we have described a catalyst and additive free photodriven cross dehydrogenative coupling (CDC) reaction initiated by electron donor-acceptor (EDA) complexes between electron rich indolizines and electron poor quinones has been demonstrated. This green transformation reveals the advantages of operational simplicity, mild reaction conditions and good functional group tolerances.

Chapter 4: Synthesis of Congested Indolizine Amides from in situ Generated Azaoxyallyl Cations and Ti-superoxide Catalysed Oxidative Amidation of Aldehydes

Section I: Metal-free Regioselective C-3 Alkylation of Indolizines *via* in situ Generated Azaoxyallyl Cations
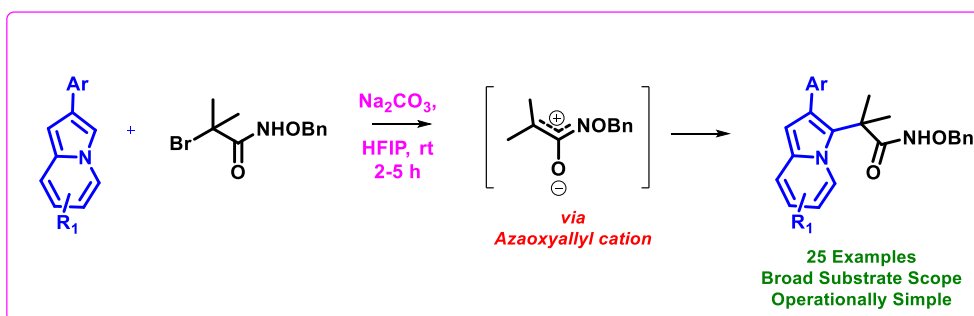
The amide bond constituting structural backbone of proteins and peptides, is abundantly found in natural products, pharmaceuticals, polymers and agrochemicals. In particular, primary amides ($RCONH_2$) play an important role in organic synthesis as building blocks exhibiting a wide range of industrial applications and pharmacological interests

In this approach we have synthesized hindered indolizine amides from in situ generated azaoxyallyl cation. We have synthesized broad range synthetically important C-3 functionalized indolizines with good to excellent yield by using simple reaction conditions.

Section II: Ti-Superoxide Catalyzed Oxidative Amidation of Aldehydes with Saccharin as Nitrogen Source: Synthesis of Primary Amides
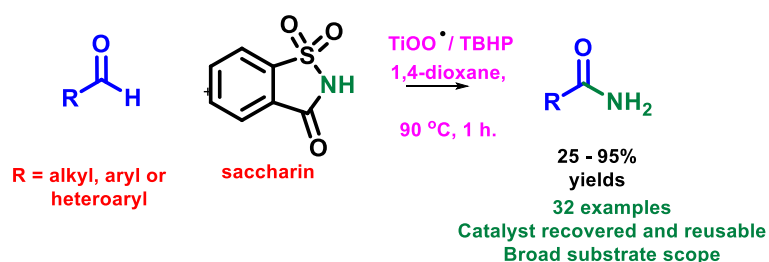
Traditionally, amide synthesis has been achieved by the reaction of an amine with an activated carboxylic acid derivative, that often employs coupling reagents. Subsequently, several alternate strategies emerged for amide formation that include: the Staudinger reaction, the Schmidt reaction, the Beckmann rearrangement, hydroamination of alkynes, dehydrogenative amidation of alcohols, hydroaminocarbonylation of alkenes, iodonium promoted nitroalkene amine coupling reaction and transamidation of primary amides. A new heterogeneous catalytic system (Ti-Superoxide/ saccharin/TBHP) has been developed that efficiently catalyzes oxidative amidation of aldehydes to produce various primary amides. The protocol employs saccharin as amine source and was found to tolerate a wide range of substrates with different functional groups. Moderate to excellent yields, catalyst reusability

and operational simplicity are the main highlights. A possible mechanism and the role of the catalyst in oxidative amidation have also been discussed

4. Summary

1) We have achieved the total synthesis of (+)-tofacitinib (1) in 8 steps commenced from 4-piperidinone in 22.4% overall yield with 96.8% *ee*. The key steps involved are *L*-proline catalyzed *α*-aminohydroxylation followed by Wittig olefination and hydrogenation reactions.

2) We have disclosed the metal free Overmann rearrangement reaction for the enantioselective production of key intermediate of (+)- Tofacitinib in 8 Steps with excellent yield

3) We have developed the first efficient and metal free CDC reaction of aromatic carbonyls with inactive cyclic ethers to give the desired *p*-alkylated aryl aldehydes and ketones in good to excellent yields with high regioselectivity.

4) We have described an efficient white light mediated, eosin y catalyzed C-C bond formation reaction between ethers and quinoxalin-2(1H)-ones to give C-3 alkylated quinoxalin-2(1H)-ones.

5) In conclusion we developed an operationally simple and environment friendly protocol for the regioselective C-H functionalization of indolizines by using catalytic amount of acetic acid.This theoretical result was also confirmed by synthetic experiments.

6) We have described the photodriven cross dehydrogenative coupling reaction between indolizines with quinones *via* EDA complexes for the synthesis of Broad range of synthetically important indolizine derivatives in good to excellent yields from a simple starting material.

7) We have described the simple, convenient and environment-friendly protocol for primary amide synthesis directly from aldehydes using Ti-superoxide as a mild and cheap catalyst and saccharin as amine source using TBHP as oxidant.

5. Future directions

1) We have targeted to complete the Metal-free Regioselective C-3 Alkylation of Indolizines *via* in situ generated azaoxyallyl Cations and communicated in due date.

6. Publications

1) **Kishor D. Mane**, Anagh Mukherjee, Kumar Vanka and Gurunath Suryavanshi, Metal-Free Regioselective Cross Dehydrogenative Coupling of Cyclic Ethers and Aryl Carbonyls. *J. Org. Chem.* **2019**, *84,* 2039-2047

2) **Kishor D. Mane**, Rohit B. Kamble and Gurunath Suryavanshi, A visible light mediated, metal and oxidant free highly efficient cross dehydrogenative coupling (CDC) reaction between quinoxalin-2(1H)-ones and ethers. *New J. Chem.*, **2019**, *43*, 7403-7408
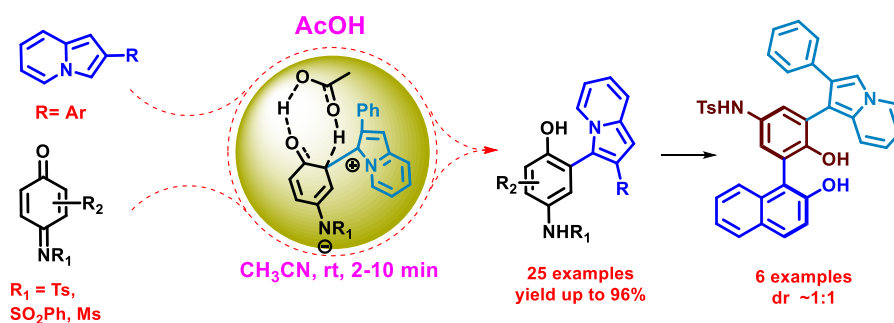
3) Rohit B. Kamble, **Kishor D. Mane**, Bapurao D. Rupanawar, Pranjal Korekar, A. Sudalai and Gurunath Suryavanshi, Ti-superoxide catalyzed oxidative amidation of aldehydes with saccharin as nitrogen source: synthesis of primary amides. *RSC Adv.*, **2020**, *10*, 724-728

4) **Kishor D. Mane**, Rohit B. Kamble and Gurunath Suryavanshi, Short enantioselective total synthesis of (+)-tofacitinib. *Tetrahedron Letters*, **2021**, *67*, 152838

5) **Kishor D. Mane,**Anirban Mukherjee, Gourab Kanti Das, and Gurunath Suryavanshi. Acetic Acid Catalyzed Regioselective C-(sp2)-H bond Functionalization of Indolizines: Concomitant Involvement of Synthetic and Theoretical Studies; *J. Org. Chem.* **2022**, *87* (8), 5097-5112.

6) **Kishor D. Mane,** Gurunath Suryavanshi, Visible Light Promoted, Photocatalyst Free C(sp^2)-H Bond Functionalization of Indolizines *via* EDAcomplexes (*Just Accepted*) Eur. J. Org. Chem. 2022, https://doi.org/10.1002/ejoc.202200261

7) **Kishor D. Mane,** Gurunath Suryavanshi, Metal-free Regioselective C-3 Alkylation of Indolizines *via* in situ generated azaoxyallyl Cations (*Manuscript under preparation*)

8) **Kishor D. Mane,** Satish G. More, Gurunath Suryavanshi. Lewis Acid Catalysed Ring Opening Reactions of Donor-Acceptor Cyclopropanes with Indolizines (work under progress)

7. References

1) D. R. Joshi, I. Kim, *Adv. Synth. Catal.* **2021**, *363*, 1.

2) Y. Wu, H. Ding, M. Zhao, Z.-H. Ni, J.-P. Cao, *Green Chem.* **2020**,*22*, 4906.

3) S. Lee, S. Kim, S. H. Yoon, A. Dagar, I. Kim, *J. Org. Chem.* **2021**, *86*, 12367.

4) J. Liu, Z. Zhua and F. Liu, *Org. Chem. Front.*, **2019**, 6, 241.

5) Cao, Z.-Y.; Ghosh, T.; Melchiorre, P. *Nat. Commun.* **2018**, 9, 3274.

6) Yang, L.; Pu, X.; Niu, D.; Fu, Z.; Zhang, X. *Org. Lett.***2019**, 21, 8553.

Chapter I

Short Enantioselective Total Synthesis of (+)-Tofacitinib and Process for Preparationof (*3R,4R*)-1-Benzyl-*N*-4-Dimethylpiperidin-3-Amine

1. "Short Enantioselective Total Synthesis of (+)-Tofacitinib." **Mane, K. D.**; Kamble, R. B.; Suryavanshi, G. *Tetrahedron Letters. https://doi.org/10.1016/j.tetlet.2021.152838*

2. "A Process for Preparation of (*3R,4R*)-1-Benzyl-*N*-4-Dimethylpiperidin-3-amine" **Mane, K. D.**; Kamble, R. B. Suryavanshi, G. (*Provisional patent filed*)

1.1.1 Introduction:

The heterocycles with the nitrogen atom are the frequent structures studied in natural product synthesis and medicinal chemistry.[1] Substituted piperidines are the unique class of pharmacophore having biological importance in pharmaceutical drug and natural product synthesis.[2] The 23 branded drugs out of 200 have the piperidine ring in common. Also it is most common FDA approved pharma materials.[3,4] Piperidines and their analogues display a huge biological activities including antimalarial, anticancer, antihypertensive, antibacterial, anti-inflammatory, antiviral, properties.[5] In recent studies, piperidine alkaloids showed a considerable amount of glycosides inhibitor activity. Glycosidases are intricated in numerous metabolic ways for therapeutics of diseases, including AIDS and diabetics.[6]
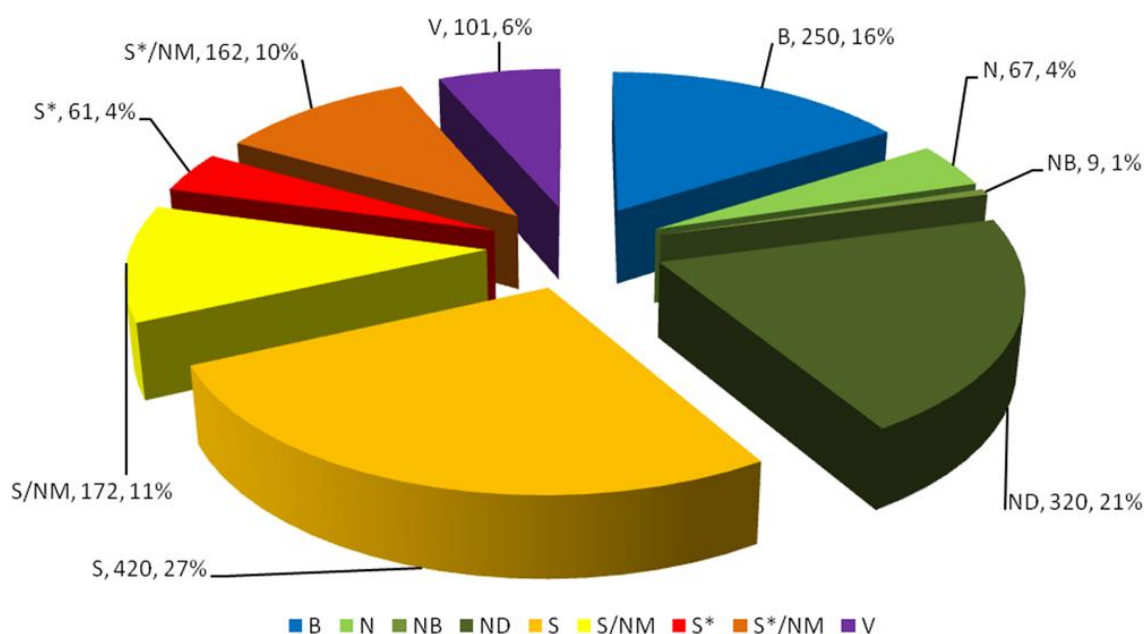
Fig 1: Distribution of Piperidines

Various compounds that accommodate the substituted piperidine nucleus are currently engaged in recent applications as a drug for the treatment of various diseases. Donepezil drug **1** is advised to patients to treat Alzheimer's disease. For schizophrenia patients Pipamperone **2** is a highly

advised drug.[8] Another class of substituted piperidine moieties has shown a broad range of biological activities in which paroxetine (**4**) is an antidepressant,[9a] fentanyl (**3**) is an active pain reliever,[9b] and levocabastine **5** [10] is an antihistamine drug as shown in **Figure 2**.
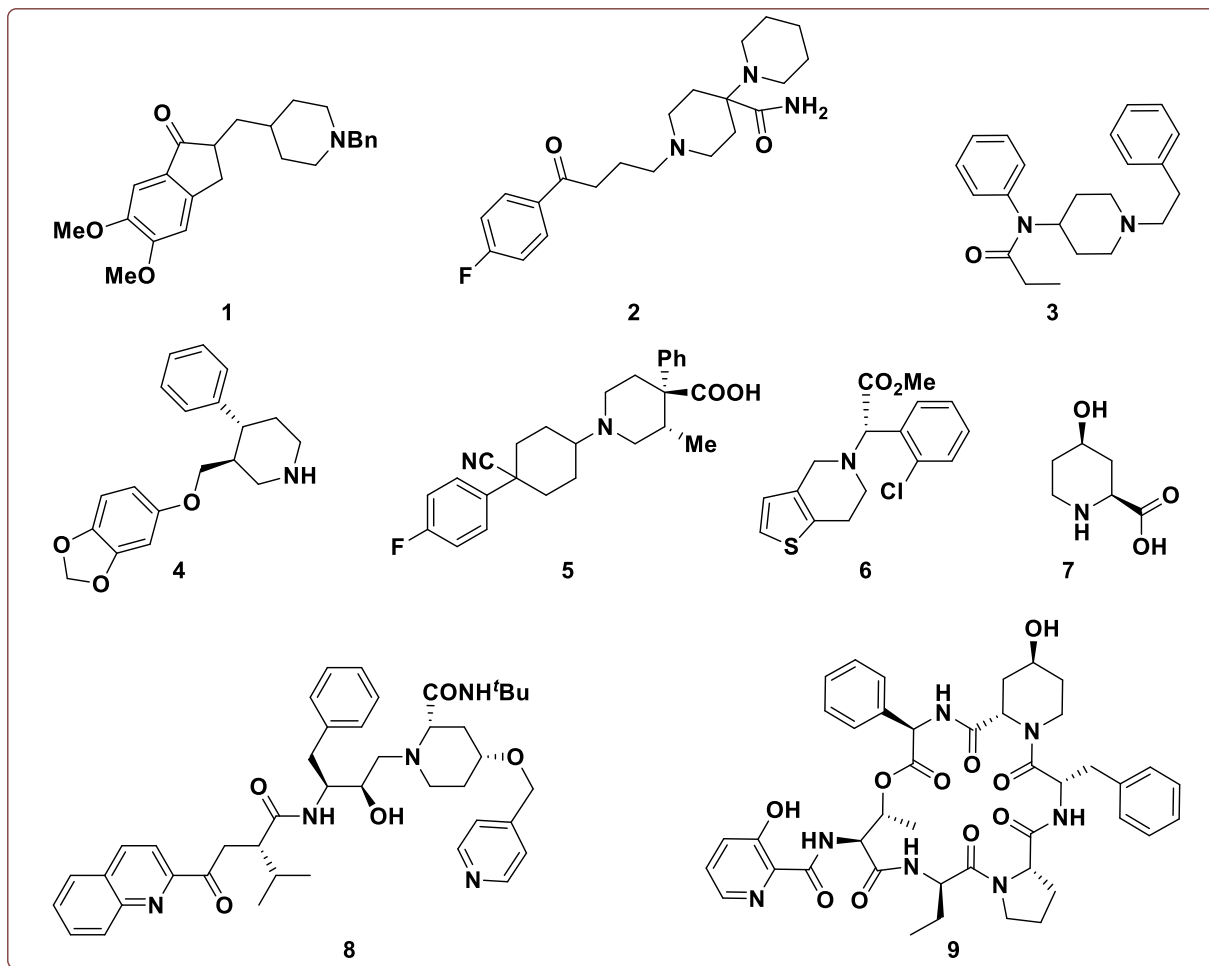
Figure 2: Biologically active piperidine molecules

Clopidogrel[11] **6** is a tetrahydrothienopyridines, as shown in **Figure 2,** is an antiplatelet agent that employs their movement after metabolic activation. In the literature, about 72 drugs that contain piperidine are found as the core structure. For the synthesis of piperidines and related structures, various reactions are known in the literature. Few general synthetic approaches for the synthesis of piperidine scaffold and their analogs for the last few decades are shown in **Figure 3**. A variety

of synthetic routes are known in the literature. Out of them few are ecofriendly such as minimum waste, scalability and few of them are some disadvantages such as harsh reaction conditions, low yield, and costly starting materials.[12]
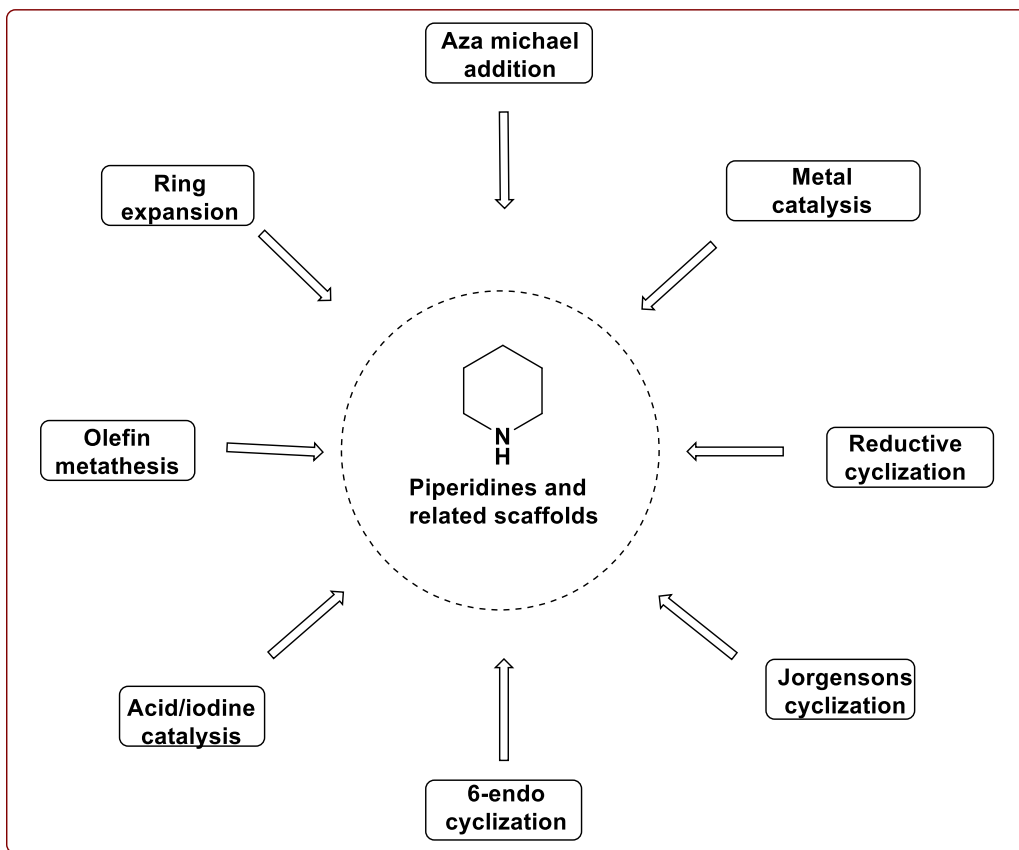
Figure 3. Biologically active piperidine synthesis

The traditional methods have been utilized for the preparation of piperidines and their active biological analogs such as ring expansion reaction, aldol, aza Michael addition, reductive amination, Mannich reaction, heterocyclic rearrangement, alkene, and alkyne metathesis, various metal-catalyzed and acid-catalyzed approaches for the cyclization, and various multicomponent reactions (MCR) are known in the literature.[13a-13f] Despite these conditions, some other approaches are available to synthesize of substituted piperidine moieties such as ring-opening of strained cyclopropanes, Diels-Alder cyclization reaction with imines, intramolecular Michael

addition reaction, and aza-Prins cyclization.[14] It is an ultimatum task for the researchers to find out a more efficient and straightforward way to synthesize piperidine analogs with a high magnitude of enantioselectivity.

Section I

Short Organocatalytic Enantioselective Total Synthesis of (+)-Tofacitinib

1.1.2 Introduction and Pharmacology
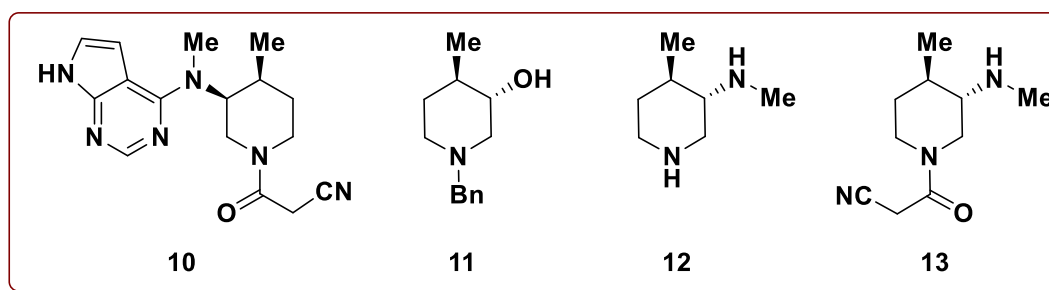
Figure 4. Structure of tofacitinib and key intermediates

Substituted piperidines are the most accessible structural motifs found among the biologically active *N*-heterocycles, which occurred naturally and synthetically.[15] It has become the most reputed and impressive core structure as it is present in 72 small drug molecules having piperidine as an active site.[16] Due to the impact of piperidines in the pharmaceutical industry, it has attracted the attention of chemists towards its synthesis.[17] The Janus protein tyrosine kinase, also known as jakinibs, is a medication that inhibits the movement of one or more of the Janus kinase family of enzymes (JAK1, JAK2, and JAK3), thereby interrupting the JAK-STAT signaling pathway.[18] Hence it has become an important task to develop JAK inhibitors that will prevent such uncontrolled inflammation.[19]

In recent studies, 3, 4-disubstituted piperidines have shown a promising candidate as JAK inhibitors.[20a] Whereas in 2012, tofacitinib (1) became the first JAK inhibitor drug approved by

the Food and Drug Administration (FDA) for the treatment of rheumatoid arthritis, also in 2017 it was further approved for the treatment of active rheumatoid arthritis (RA),[20b] psoriatic arthritis,[20c] and ulcerative colitis.[20d]

It is a promising immunosuppressant, developed by Pfizer and approved for treatment during organ transplant rejection.[21] Tofacitinib (CP-690,550) (**10**) with two chiral centers having the substituted piperidines and amino deazapurine core as shown in **Figure 4**. Also, it shows promising clinical activities against autoimmune related diseases such as psoriasis, inflammatory bowel disease, and Crohn's disease.[22]

1.1.3 Review of literature

Maricán's approach[24]

In 2013, Maricán *et al.* reported the preparation of key synthetic intermediate *tert*-butyl-(3*S*,4*R*)-3-hydroxy-4-methyl piperidine-1-carboxylate from (*S*)-5-hydroxypiperidin-2-one in 6 steps. Preliminary, the key steps of this route are selenoxide elimination, Grignard methyl cuprate addition, with an overall yield of 18 %.

Maricán *et al.* and coworkers describe the asymmetric total synthesis of (+)-**10** in nine steps beginning from the chiral 2-hydroxy-piperidone **14**. The alcohol group of 2-hydroxy-piperidone **14** was protected by using TBDPSCl in DMF solvent and imidazole as a base to give compound **15** in 96% yield. Then the *N*-H group of O-TBPS protected compound **15** was protected by using Boc anhydride to form the compound **16** in 85% yield. The compound **16** was then subjected to the synthesis of *α,β*-unsaturated piperidone by adding phenyl selenide chloride, then subsequently pyrolytic syn elimination with H_2O_2 (30%), achieving unsaturated piperidone amide **17** in 60% yield over the two steps. Then the compound **17** was subjected to the methylcuprate addition on *α,β*-unsaturated double bond, also known as Gillman reaction using

Grignard reagent to give compound **18** in 62% yield with >94% *de*. Then the reduction of the amide group in compound **18** to piperidine was accomplished under alane reduction to give the compound **19** in 78% yield. Then the TBPDS group was deprotected using tetrabutyl ammonium fluoride in THF, giving the compound **20** in 75% yield.
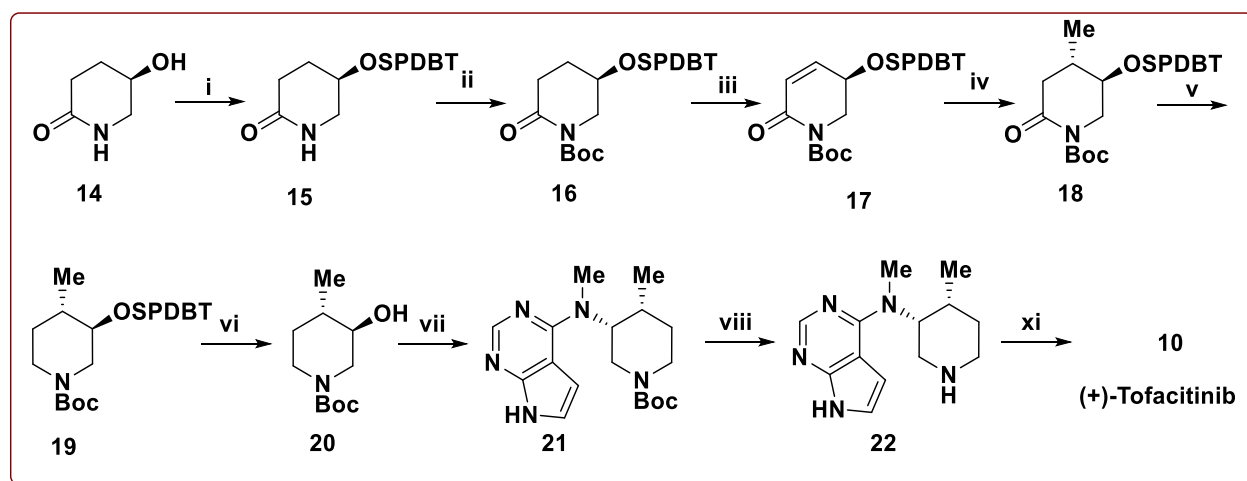
Scheme 1 :(i)TBDPSCl, imidazole, DMF, 96%; (ii) *n*BuLi, DABCO, Boc$_2$O, −78 °C, THF, 85%; (iii) (a) HMDS BuLi, PhSeCl, −78 °C, THF; (iii) H$_2$O$_2$, 60% (iv) MeMgBr, CuBr.S(CH$_3$)$_2$, (CH$_3$)$_3$SiCl, Et$_2$O, −78°C, 62%; (v) (a) AlH$_3$, THF, 78%; (vi). TBAF/THF, 75%; (vii) DIAD-Ph$_3$P, Dioxane, 100 °C, 2 h, 68% (viii) ZnBr$_2$, CH$_2$Cl$_2$, 95%; (ix) EDC/HOBt, CH$_2$Cl$_2$, Cyanoacetic acid.

Then the compound **20** was subjected to the Mitsunobu reaction with separately prepared *N*-Me azepine derivative, giving the 68 % yield of **21** employing DIAD-Ph$_3$P combination in 1,4-dioxane as solvent. Finally, the *N*-Boc group in compound **21** was deprotected using a catalytic amount of ZnBr$_2$ in DCM solvent, then the coupling of amine **22** with readily available cyanoacetic acid by using EDC/HOBt combination reaction to afford the **(+)-10** in 80% yield and 9.5% overall yield beginning from enantiopure hydroxypiperidin-2-one **(14)**.

Ripin's approach[25]

Initially, Ripin and co-workers from Pfizer have developed a synthetic route to prepare key intermediate **27** from 4-picoline, followed by late-stage resolution to achieve the enantiomeric purity in the overall five steps as shown in (**Scheme 2**). Synthesis begins with the carbamate group protection of 3-amino-4-methyl pyridine **23**, the carbamate protected pyridine **24** was reduced by Rhodium catalyzed hydrogenation to give (4-methyl-piperidin-3-yl)-carbamic acid methyl ester **25** with 5:1 (*cis/trans*) ratio.
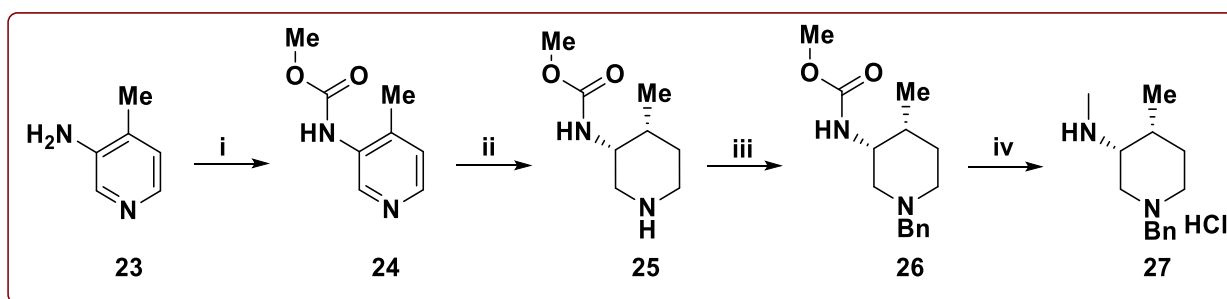
Scheme 2: (i) $(MeO_2C)_2O$, KO*t*Bu, THF, $0\,^{o}C$, 30 min, 89%; (ii) H_2 (100 psi), 5% Rh/Al_2O_3, EtOH, 100 ^{o}C, 24h, quantitative; (iii) (a) PhCHO, $NaBH(OAc)_3$, DCM, 20 ^{o}C, 30 min, 70%; (b) $LiAlH_4$, THF, 90%; (c) 36% HCl, EtOH, 38%

Then the amido piperidine compound **25** was then exposed to benzyl protection by using $NaBH(OAc)_3$ in DCM and benzaldehyde called reductive amination reaction to yield the benzyl protected methyl ((*3R,4R*)-1-benzyl-4-methyl piperidine-3-yl)carbamate **26**. Then the conversion of the *N*-carbamate functional group of compounds **26** to *N*-Me piperidine was accomplished by LAH reduction using anhydrous THF as a solvent to give cis-1-benzyl-N,4-dimethylpiperidin-3-amine in 90% yield. Then treatment of cis-1-benzyl-*N*,4-dimethylpiperidin-3-amine with HCl affords hydrochloride salt **27**.

Uang's approach[23d]

In 2017, Uang *et al.* accomplished the formal asymmetric synthesis of tofacitinib *via* a stereoselective Michael addition of the corresponding enolate of chiral 1,3-dioxolanone to

methyl crotonate. The enantioselectivity was introduced by using chiral auxiliary, *i.e.,* homochiral 1,3-dioxolanon synthesized from the derivative of camphor sulfonic acid and glycolic acid. [23d]

Uang's approach described the formal asymmetric synthesis of **(+)-10** from stereoselective Michael's addition of the corresponding enolate of chiral 1,3-dioxolanone to methyl crotonate (**Scheme 3**). The key step in this approach involvs Michael addition of
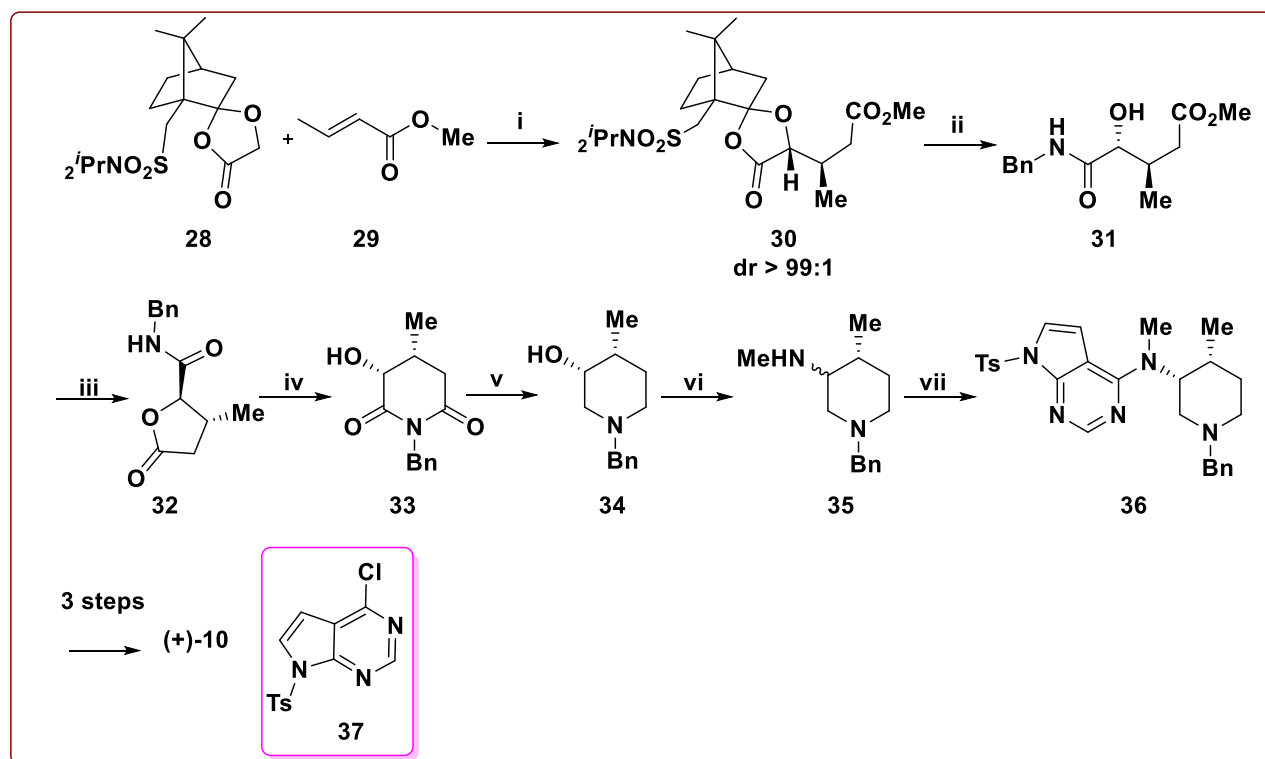
Scheme 3: (i) LDA, THF, −100 °C, 30 min,−100 to − 78 °C, 3 h; (ii) 3 equiv. BnNH₂, 80 °C, neat, 12 h,89%; (iii) TFA:H₂O (10:1), 60 °C, 9 h, 93%; (iv) LDA, THF, −78 °C, 30 min, then THF, −40 °C, 4.5 h, 81%; (v) LAH, THF, 0 °C to reflux, 12 h, 74%; (vi) (a) CrO₃, H₂SO₄, HOAc, acetone, H₂O, 0 °C to rt (< 18 °C), 5 h; (b) then MeNH₂(33% in EtOH), HOAc, NaBH(OAc)₃, DCM, rt, 16 h, (vii)**37**, K₂CO₃, H₂O, 120 °C, 16 h

enolate generated from the chiral auxiliary protected *α*-hydroxy acid **28** to *α,β*-unsaturated crotonate ester **29** to give the compound **30**. For the removal of chiral auxiliary from the compound **30** using benzylamine in neat reaction condition gives *α*-hydroxy amide intermediate

31in 89% yield. This was followed by the formation of lactone of compound **31,** achieved by using acid-catalyzed lactonization employing TFA–H$_2$O (10:1) to yield *γ*-lactone **32** in 93% yield. Then, *γ*-lactone **32** was treated for the ring expansion reaction using LDA as a base to yield imide **33** in 81% yield. The formed imide **33** was then transformed into 3,4-disubstituted piperidine **34**in 74% yield using LAH reduction. Then the disubstituted piperidine **34** was subjected to the reductive amination reaction sequentially as to Jone's oxidation come after reduction by using sodium triacetoxy borohydride to give the key precursor **35** which are useful for the total synthesis of (+)-tofacitinib**10**. In this approach, Uang and co-workers described the formal asymmetric total synthesis of **(+)-10** with 26 % overall yield in 8 steps.

1.1.4 Present Work

1.1.4.1 Objective

Several synthetic approaches have been well established in the literature[23a] due to the increasing importance of tofacitinib in the medicinal and pharmaceutical fields. Among the reported methods, asymmetric synthesis of tofacitinib is rarely explored.[23b-d] The methods mentioned above require late-stage resolution techniques for the synthesis of enantiopure piperidine moiety, which results in yield loss. Furthermore, the use of chiral auxiliary and harsh reaction conditions make the above approaches impractical. The enantiopure piperidine moiety as a core structure in tofacitinib and our efforts to synthesize these moieties, we have outlined a retrosynthetic approach for the tofacitinib **(10)**. The synthesis of tofacitinib **(10)** could be accomplished from stereoselective inversion of 1-benzyl-4-methyl piperidine-3-yl methanesulfonate **11b** *via* nucleophilic substitution reaction with *N*-methyl dezapurine amine **38.** Further, the key intermediate **11a** can be synthesized from the *N*-protected piperidone **40** by using proline

catalyzed one-pot α-aminoxylation and Wittig reaction, followed by reduction of allylic

alcohol **39** as shown in **Scheme 4**
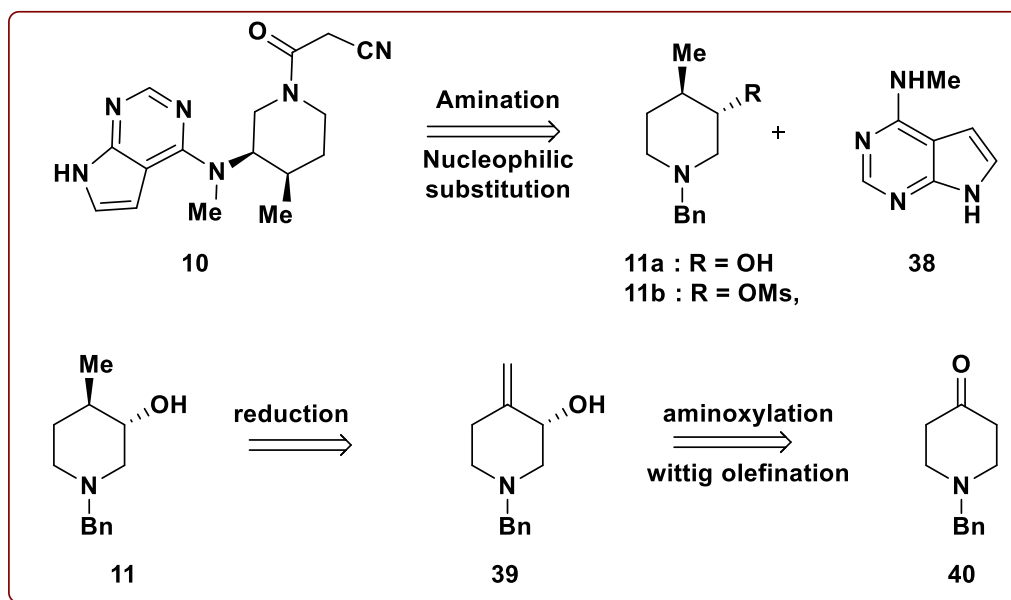
Scheme 4. Retrosynthetic analysis of tofacitinib (CP-690,550)

1.1.4.2 Results and Discussion

This method describes a straightforward and organocatalytic approach for synthesizing 3,4-

disubstituted piperidine, which plays a key intermediate in the enantioselective total synthesis

(+)-Tofacitinib. Our approach to synthesizing key intermediate **11a** commences from *N*-benzyl

protection of 4-piperidone **41** under basic conditions using K_2CO_3, BnBr in H_2O, and

chloroform, gives us the following: *N*-benzyl protected 4-piperidone **40** in 87% yield.[27] The

compound **40** was then subjected for the direct proline-catalyzed asymmetric α-aminoxylation

reaction using *L*-proline as organocatalyst and nitrosobenzene as aminoxylating source in DMF

under N_2 atmosphere for 62 hrs. In this step, we have optimized the various parameters for the

aminoxylation reaction and out of which best reaction condition is mentioned in this

transformation followed by one carbon Wittig reaction using methyl triphenylphosphonium iodide (CH_3PPh_3I) and *t*-BuOK as a base in THF for 12 hrs which gives intermediate **42** as shown in **Scheme 5**.
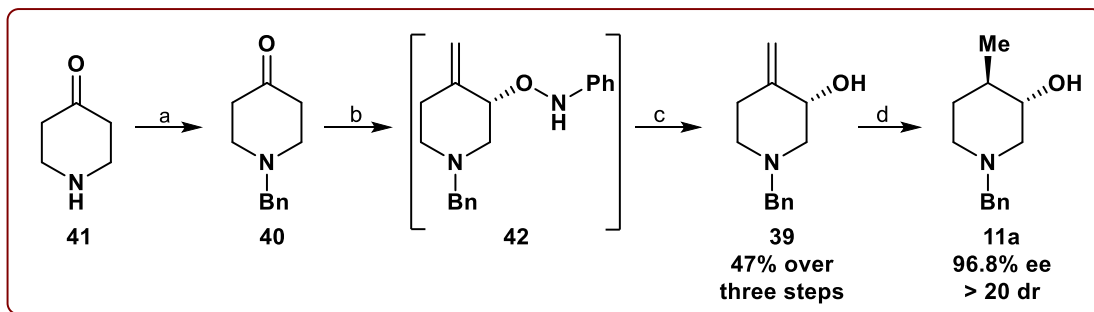
Scheme 5. Synthesis of enantiopure hydroxypiperidine *via* proline catalysed α-aminoxylation; reaction conditions: (a) BnBr, K_2CO_3, H_2O:$CHCl_3$ (1:1), 12 h, rt 87%; (b) (i) *L*-proline, PhNO, DMF, 0 °C, 62 h; (ii) CH_3PPh_3I, *t*-BuOK, LiCl (1.1 eq.), THF, 50 °C; (c) $CuSO_4.5H_2O$ (30 mol %), MeOH, 25 °C, 12 h; (d) 10% Pd/C, H_2 (1 atm), AcOEt, 5 h, rt, 93%

After consumption of starting material, the *O-N* bond cleavage of intermediate **42** was achieved in situ by addition of $CuSO_4.5H_2O$ in the reaction mixture. Further, the reaction kept for another 12h to give the corresponding chiral allylic alcohol **39** in 47% yield over three steps with 97% *ee*.[28] Furthermore, the formed allylic alcohol **39** was subjected for diastereoselective hydrogenation reaction using 1 atm pressure of hydrogen and 10 % Pd on carbon to form the compound **11a** in 93% yield with 96.8% *ee*.
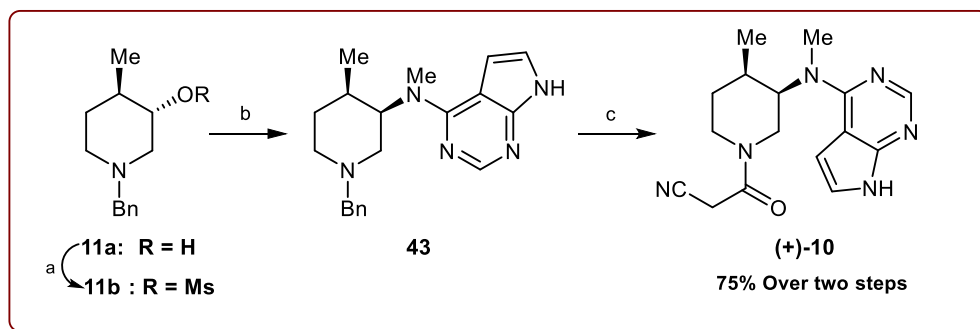
Scheme 6. Synthesis of (+)-Tofacitinib: (a) MsCl, TEA, DCM, 0 °C, 1 h, 97%; (b) **29**, K_2CO_3,

DMF, 60 °C, 12 h, 81%; (c) 20 wt % Pd(OH)$_2$, H$_2$ (1 atm), TFA, MeOH, 45 °C 12 h then, ClCOCH$_2$CN, DCM, TEA, 0 °C to rt, 2 h

The previous literature reports confirmed the formation of compound **11a**, and its optical rotation is in sound agreement with the reported value. Then the enantiopure piperidine alcohol **11a** was utilized for the synthesis of tofacitinib **10**.

Further, compound **11a** was utilized for mesylation reaction using MsCl and Et$_3$N, followed by base mediated S$_N$2 reaction with *N*-Methyl dezapurine **38** under the basic condition to give compound **43** in 81% yield as shown in **Scheme 6**. Then *N*-benzyl deprotection of compound **43** was carried out under hydrogenation condition using 20 *wt* % Pd(OH)$_2$ and 1 atm H$_2$ pressure followed by in situ *N*-acylation using 2-cyanoacetyl chloride to give (+)-tofacitinib **(10)** in 75 % yield over two steps. The formation of tofacitinib **(10)** was confirmed by ^{1}H, ^{13}C NMR, and its values are in good agreement with previous reports.[29]

CHLOROFORM-d

147.04 136.79 129.30 128.33 127.46 108.06 77.26 77.00 76.75 70.17 62.08 60.65 53.96 31.07

Chemical Shift (ppm)

Q5 #153 RT: 0.84 AV: 1 NL: 1.23E8
T: FTMS + p ESI Full ms [100.0000-1500.0000]

204.1385
R=79807
$C_{13}H_{18}ON = 204.1383$
0.9701 ppm

146.0812
R=94507
$C_9H_{10}N_2 = 146.0838$
-17.8812 ppm

314.1169
R=64207
$C_{16}H_{17}N_5Cl = 314.1167$
0.4839 ppm

260.2009
R=69707
$C_{13}H_{20}N_6 = 260.1744$
101.9656 ppm

358.9800
R=59606
$C_{16}H_6N_4Cl_3 = 358.9653$
41.0179 ppm

419.3157
R=54307

464.3735
R=51107

492.4049
R=46206

m/z

Figure 5. ^{1}H, ^{13}C NMR and mass spectrum of (*S*)-1-benzyl-4-methylenepiperidin-3-ol (**39**)

The formation of allylic alcohol **39** was confirmed by ^{1}H, ^{13}C NMR, and HRMS spectrum, as shown in **Figure 5**. In the ^{1}H (proton) NMR spectrum, the multiplets at 7.19-7.27 ppm correspond to five *N*-benzyl protected phenyl ring protons, and singlets at δ 3.54 are 2 protons of

N-benzyl CH$_2$ group on the nitrogen atom. δ 4.86 and 4.71 singlets are the 2 hydrogen on the allylic double bond. δ 3.82 sharp singlet corresponds to allylic OH group, and δ 2.45-2.58 multiplets are the aliphatic hydrogen atom piperidine ring. In the ^{13}C NMR spectrum, four phenyl ring carbons peaks shows at δ 147.04, 136.79, 129.30, and 128.33. The two peaks of the allylic double bond correspond to δ 127.46 and 108.06. The remaining 5 peaks at δ 70.17, 62.08, 60.65, 53.96, and 31.07 correspond to the aliphatic protons in the piperidine ring.

After concluding the structure of allylic alcohol **39** by ^{1}H and ^{13}C NMR spectrum we have also confirmed the compound **39** by mass spectrum, as shown in **Figure 5.** [M + H]$^{+}$ calculated for the molecular formula C$_{13}$H$_{17}$NO: 204.1383;and found at 204.1385.
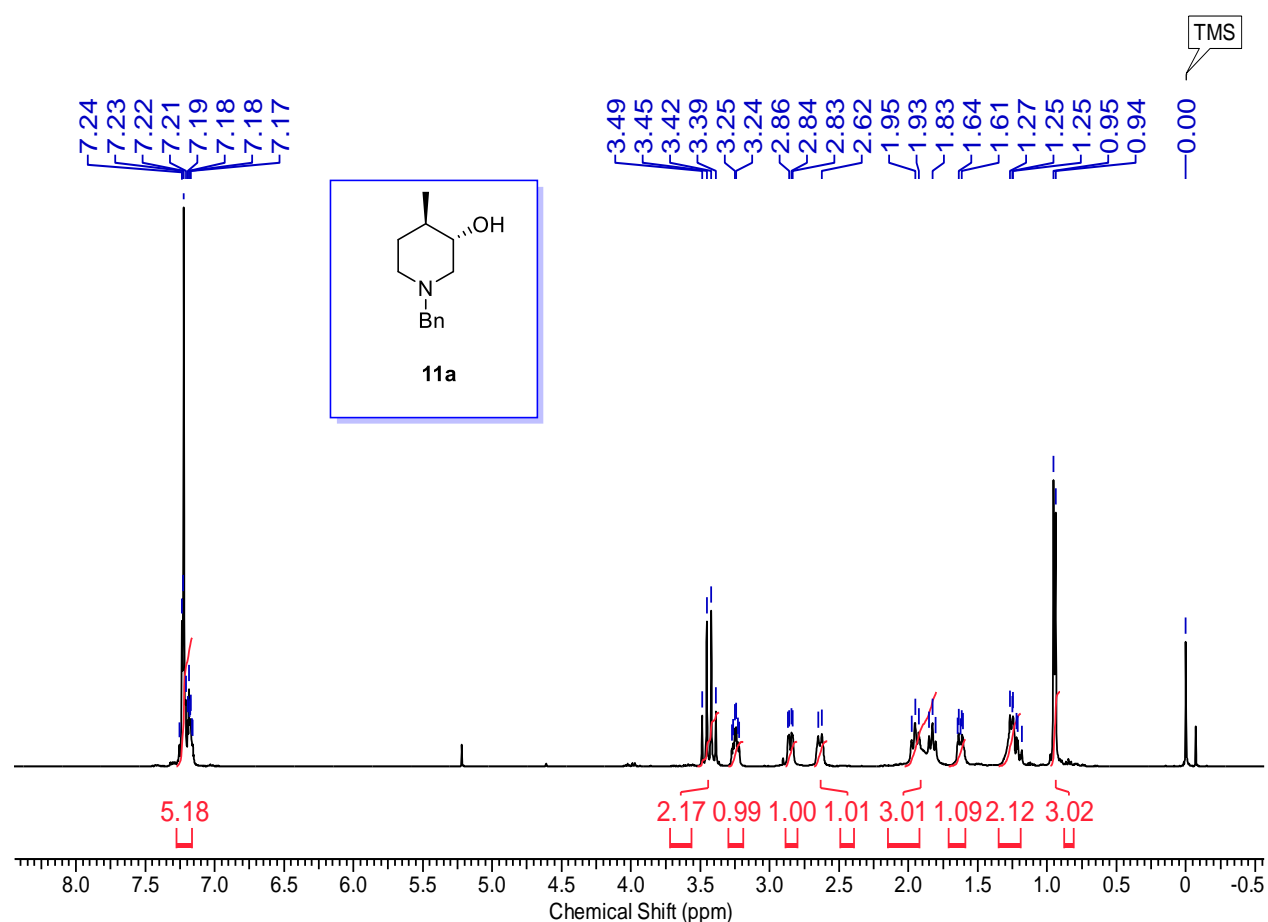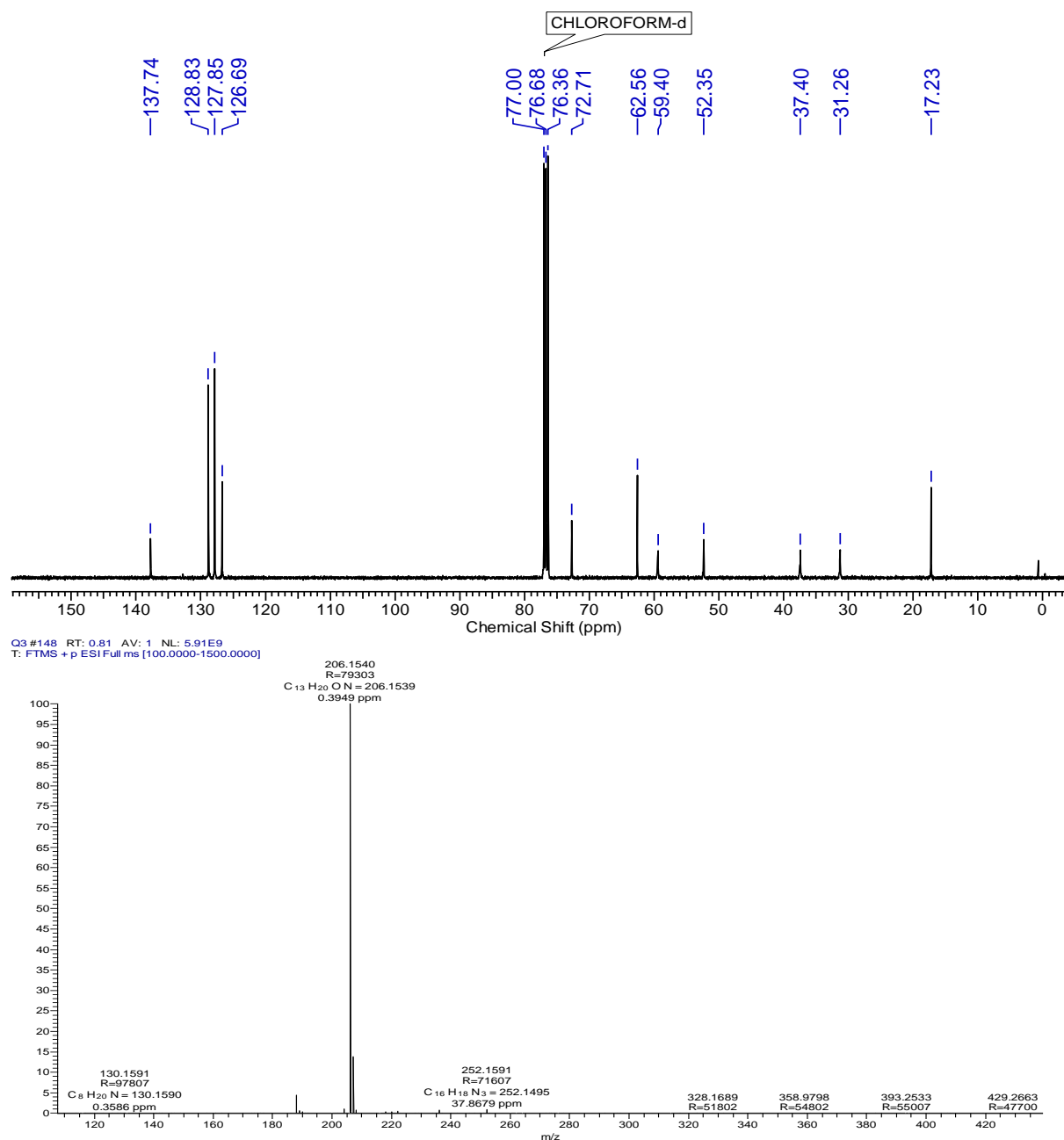
Figure 6. ^{1}H, ^{13}C and mass spectrum of(3*S*,4*R*)-1-benzyl-4-methylpiperidin-3-ol (**11a**)

The reduction of allylic alcohol **39** to the formation of our key intermediate **11a** was confirmed by ^{1}H, ^{13}C NMR, and mass spectroscopy, as shown in (**Figure 6**). In the ^{1}H spectrum of **11a**, the quartet at δ 0.94-1.25 (3H) corresponds to the methyl group on the piperidine ring. Multiplets at

δ 7.17 to 7.24 (5H) are the aromatic protons. In the ^{13}C NMR spectrum, peaks at δ 137.74, 128.83, 127.85, and 126.69 are the carbon present on the aromatic ring and the resonance of methyl carbon present on piperidine ring are at δ of 17.23 as shown in **Figure 6**.
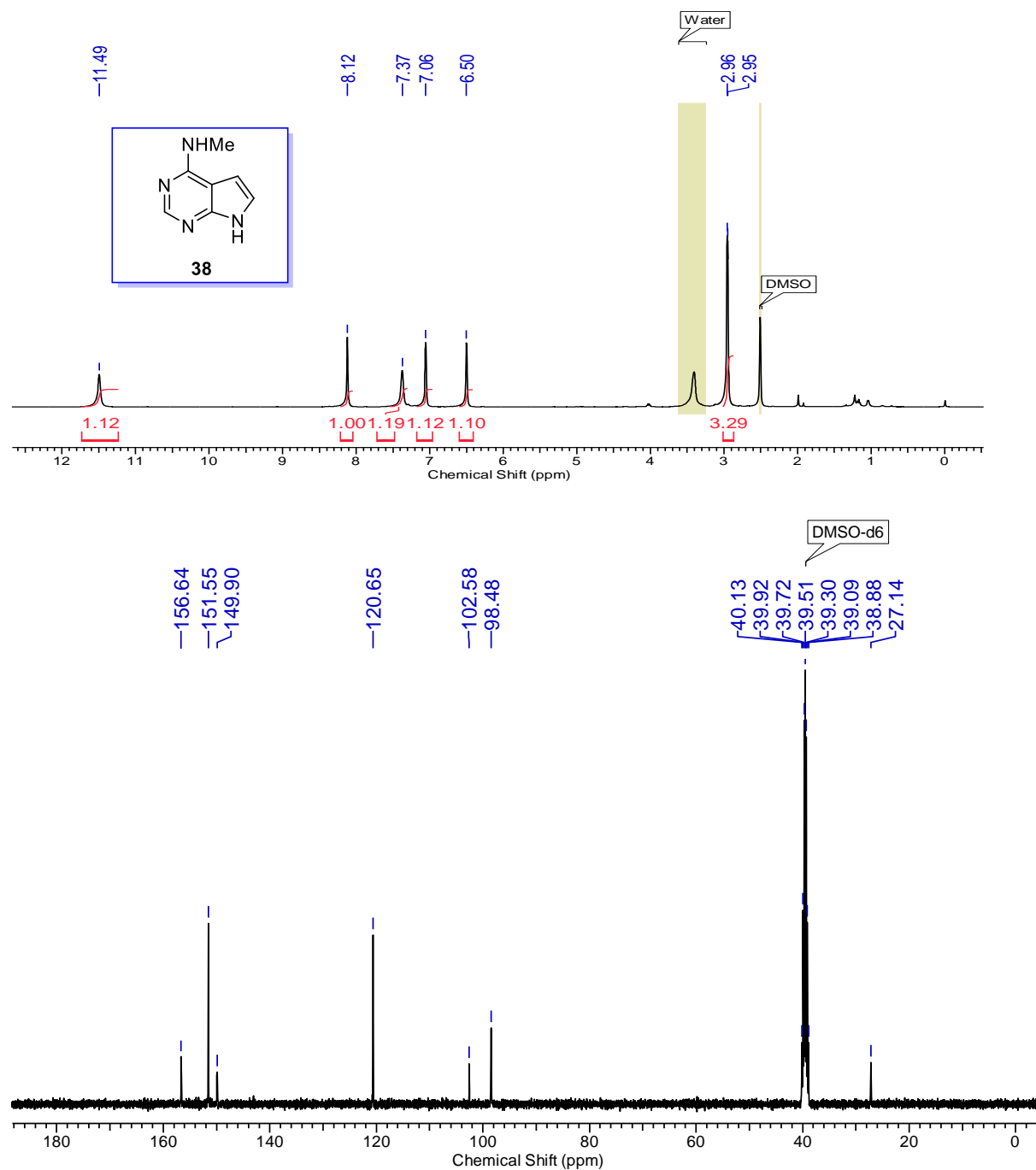
Figure 7. ^{1}H and ^{13}C NMR of *N*-methyl-7H-pyrrolo[2,3-d] pyrimidin-4-amine (**38**)

The introduction of the methyl group on deazapurine amine compound was confirmed by the ¹H and ¹³C NMR spectra, as shown in (**Figure 7**). In the proton NMR spectra of compound **38**, singlet peaks in the region of δ 3.29 (3H) correspond to the methyl group on the nitrogen atom of deazapurine amine. Peaks at δ 8.12, 7.06, and 6.50 are the aromatic protons, and peaks at 7.37 and 11.49 are the NH protons. In¹³C NMR spectra of compound **38** carbon peak resonate at δ 156.64, 151.55, 149.90, 120.65, 102.58, and 98.48 are corresponding to aromatic carbons as shown in (**Figure 7**).
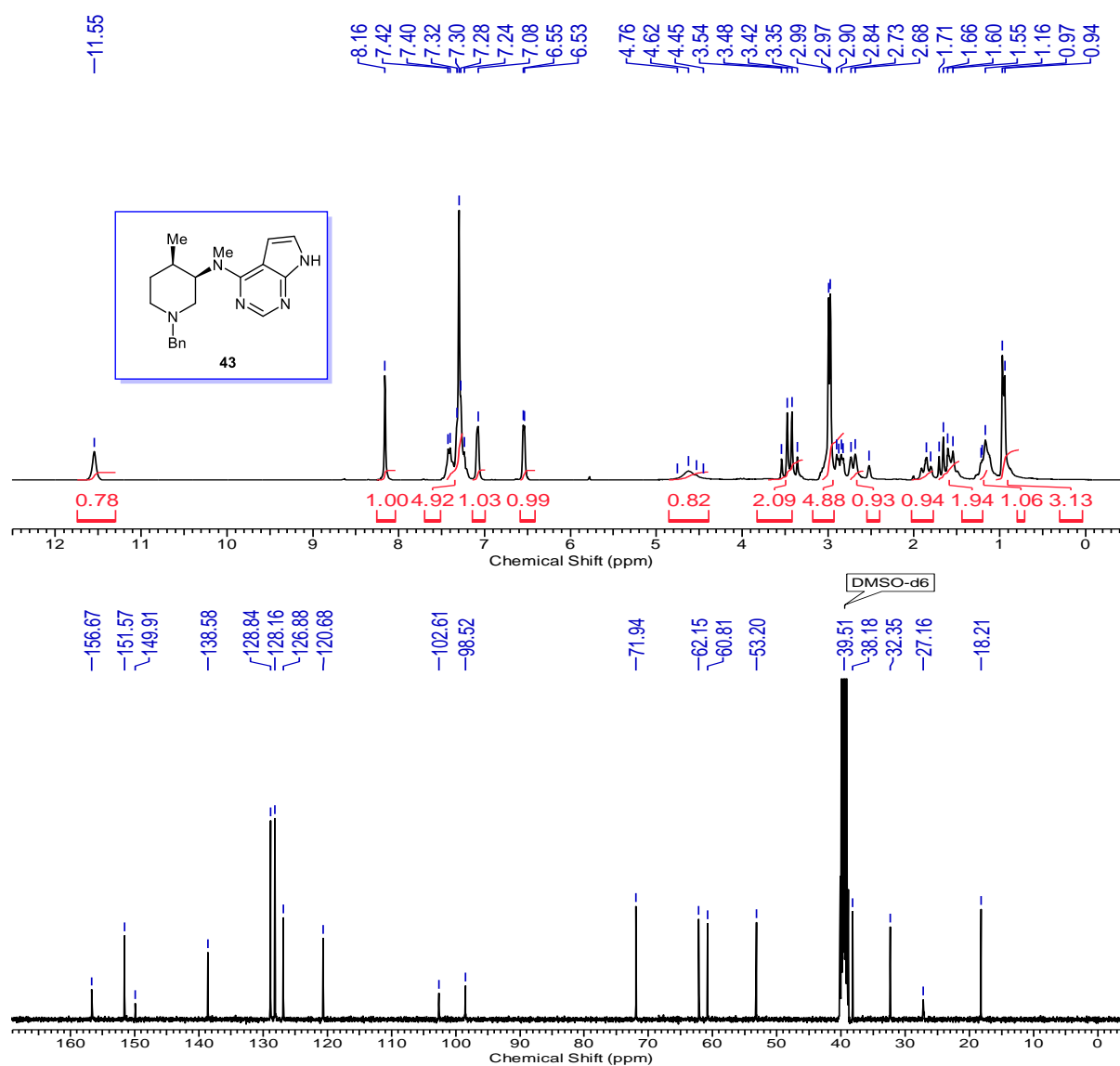
Figure 8.^{1}H and ^{13}C NMR of *N*-((*3R,4R*)-1-benzyl-4-methylpiperidin-3-yl)-*N*-methyl-7H-pyrrolo[2,3-d]pyrimidin-4-amine (**43**)

We have also confirmed the formation of **38** by using HRMS spectroscopy m/z [M +H]$^+$calculated for the molecular formula $C_7H_9N_4$: 149.0822; and found at 149.0821

In the proton NMR spectrum of compound **43**, as shown in **Figure 8**, quartet at δ 0.94 to 1.55 (3H) corresponds to the methyl group on piperidine ring. Protons resonate at δ 8.16 (singlet 1H), 7.24 to 7.28 (doublet 1H), and 6.56 to 6.55 (doublet 1H) are the aromatic protons present on compound **43** and remaining hydrogens in the range of δ 1.60 to 4.76 are the aliphatic hydrogens on piperidine ring. In ^{13}C NMR spectra of the intermediate compound, 34 carbon peaks at δ 18.21, 27.16, 32.35, 38.18, 53.20, 60.81, 62.15, and 71.94 are those aliphatic ring carbons that are present on the piperidine ring. The aromatic carbons resonate at δ 156.67, 151.57, 149.91, 138.58, 128.84, 128.16, 126.88, 120.68, 102.61 and 98.52 are the aromatic ring carbons.

161.99
161.81
157.30
152.11
150.87

121.17
116.62

102.61
102.12

70.18

DMSO-d6

53.17
45.58
42.83
42.19
39.51
34.36
31.38
25.30

14.13

Chemical Shift (ppm)
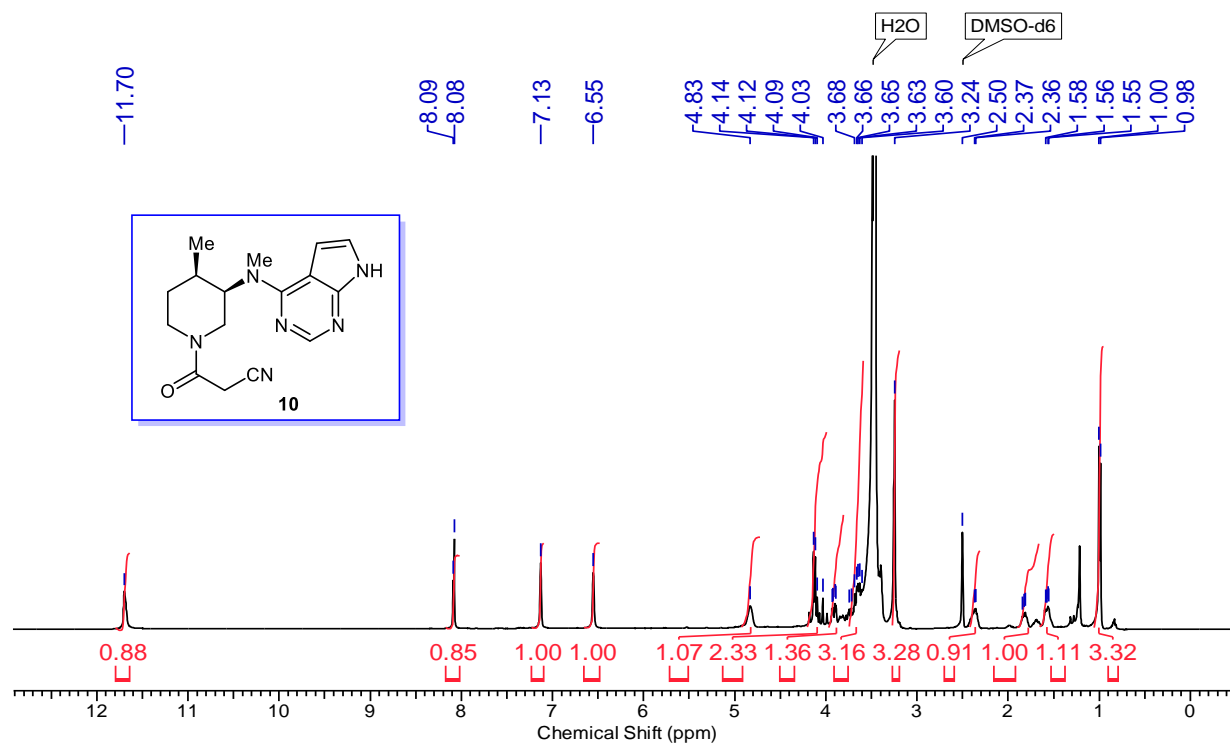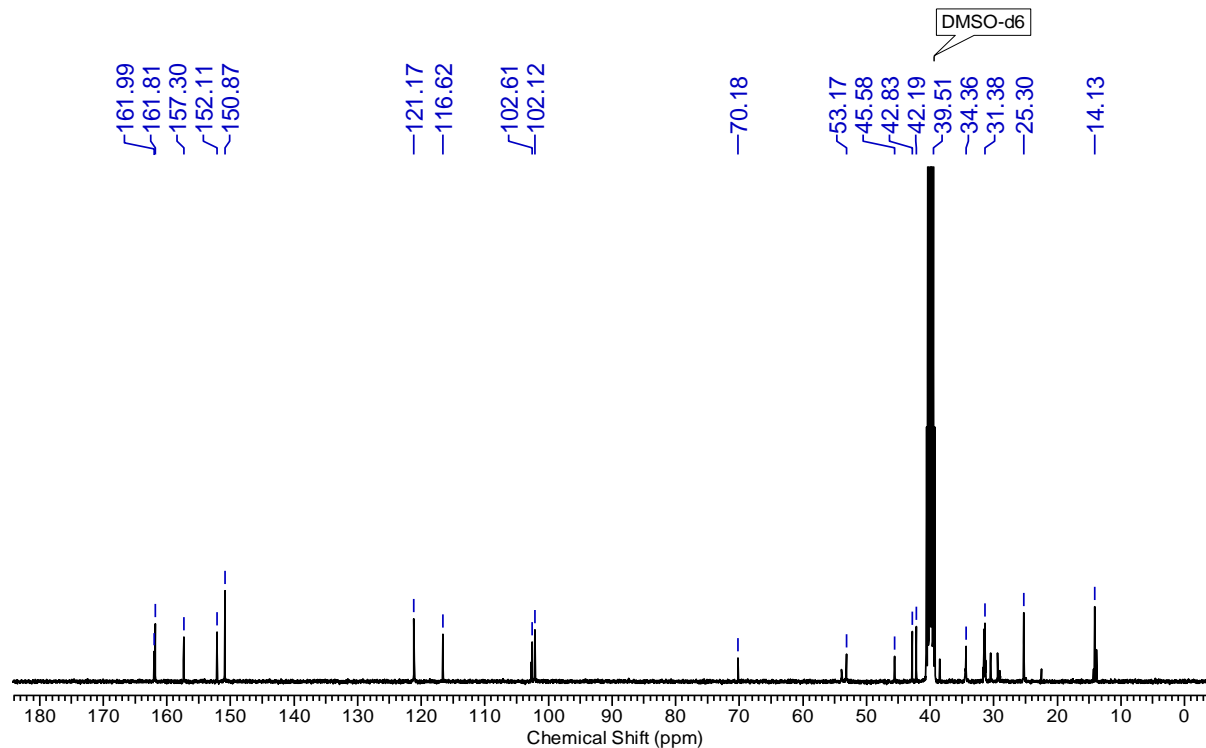
Q1 #202 RT: 1.10 AV: 1 NL: 1.89E9
T: FTMS + p E SI Full ms [100.0000-1500.0000]

313.1772
R=64007
C₁₆ H₂₁ O N₆ = 313.1771
0.0597 ppm

332.0692
R=62202

149.0818
R=85100
C₇ H₉ N₄ = 149.0822
-2.1782 ppm

242.2839
R=72007
C₁₅ H₂₀ N₃ = 242.1652
490.1113 ppm

335.1582
R=61507

375.2133
R=56707

426.2234
R=50607

489.1763
R=42500

546.4003
R=34000

587.3629
R=31400

647.3278
R=44307

699.2691
R=35502

Relative Abundance

m/z
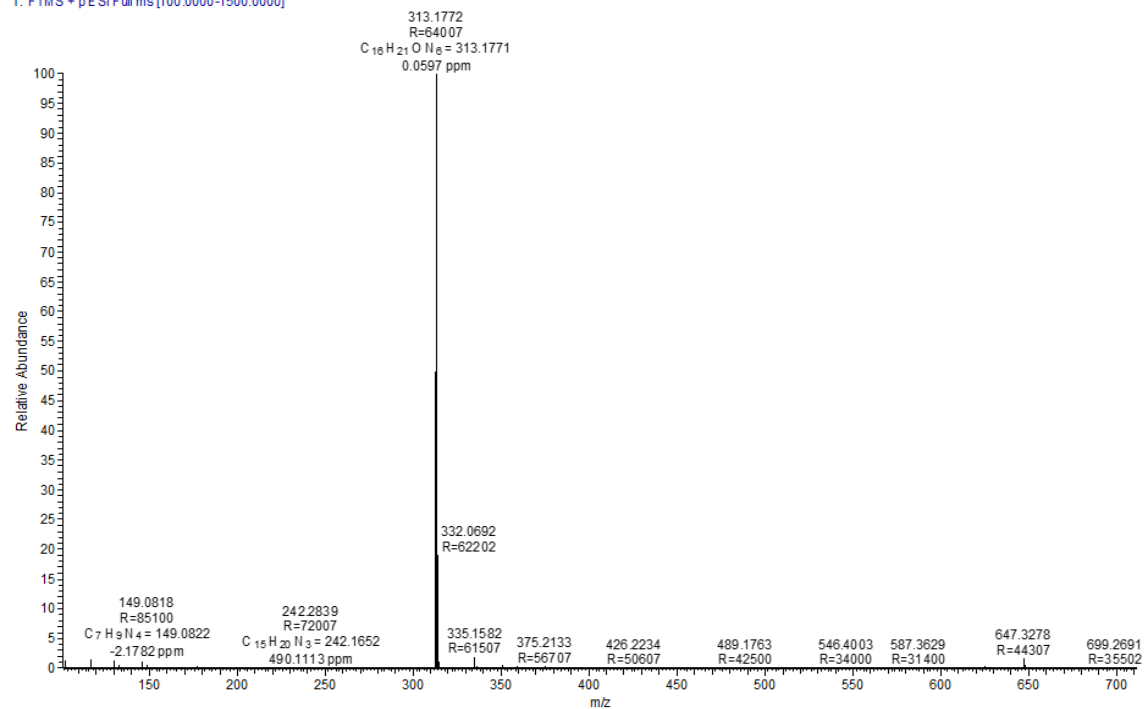
Figure 9. ^{1}H, ^{13}C and mass spectra of (+)-Tofacitinib **(10)**

After 8 steps, we have achieved the enantioselective total synthesis of tofacitinib**10** which was confirmed by the ^{1}H, ^{13}C NMR, and mass spectroscopy, as shown in (**Figure 9**). In[1]H NMR spectra of tofacitinib peaks resonate at δ 0.98 to 1.56 quartets (3H) for methyl group and peak at δ 11.70 corresponding to *N*-H proton. Protons resonate at δ 8.08 to 8.09 doublet (1H), 7.13 singlet (1H), and 6.55 singlet (1H) are the aromatic hydrogens on tofacitinib molecule. The Remaining peaks in the range of 1.58 to 4.83 are the aliphatic protons present on the piperidine ring of tofacitinib. The aromatic carbons displayed in the range of δ 161.99, 161.81, 152.11, 121.17, 116.62, 102.61, 102.12, and 150.87 in ^{13}C NMR spectra of Tofacitinib. Methyl carbon of aliphatic piperidine is ring present at δ 14.13 and aliphatic carbons are present in between the range of δ 25.30 to 70.18, respectively. For final analysis of Tofacitinib, we have also taken the mass and shown in **Figure 9**. m/z [M +H]$^{+}$ calculated for the molecular formula $C_{16}H_{21}ON_6$ is 313.1771 and found in 313.1772.

1.1.4.3 HPLC Data
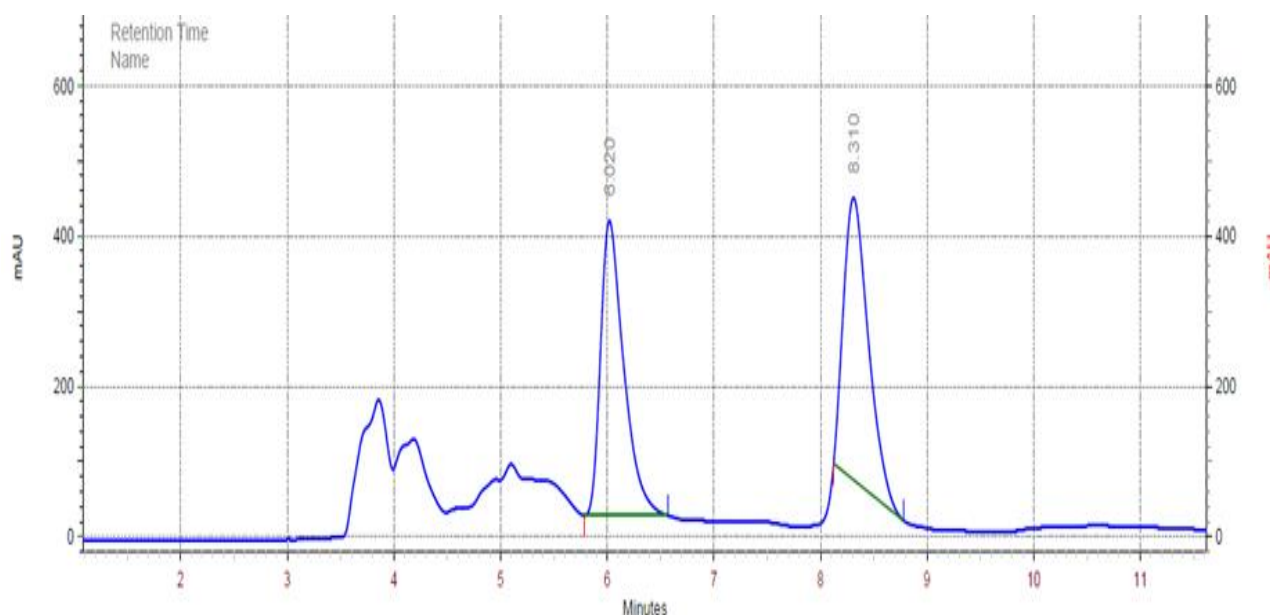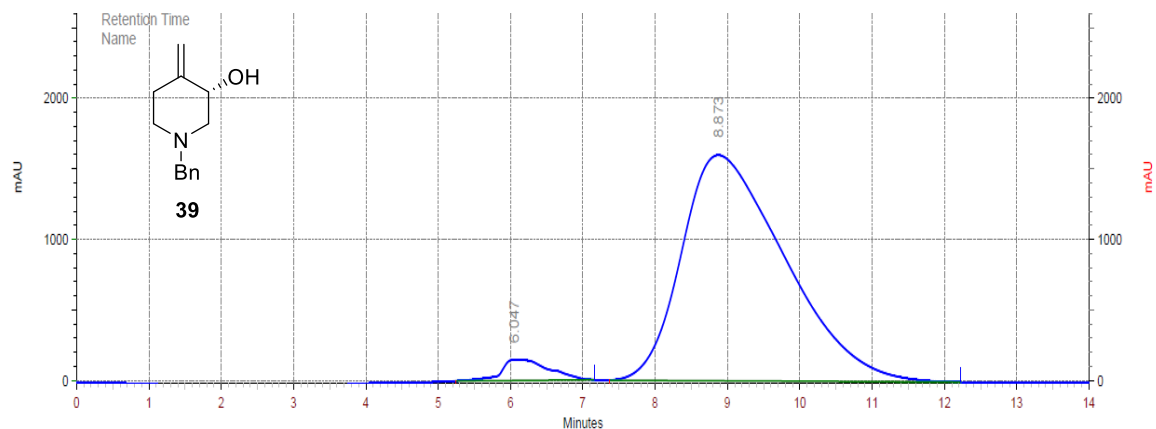
VWD: Signal A,

 254nm

Results

Retention Time	Area	Area %
6.047	41994648	1.51
8.873	2739107889	98.49
Total	2781102537	
		100.00

Column   : Chiracel ADH (4.6X250 nm)

Mobile Phase   : IPA:n-Hexane(10:90)

Wavelength   : 254 nm

Flow rate   : 1ml/min

(*S*)-1-benzyl-4-methylenepiperidin-3-ol (**39**)
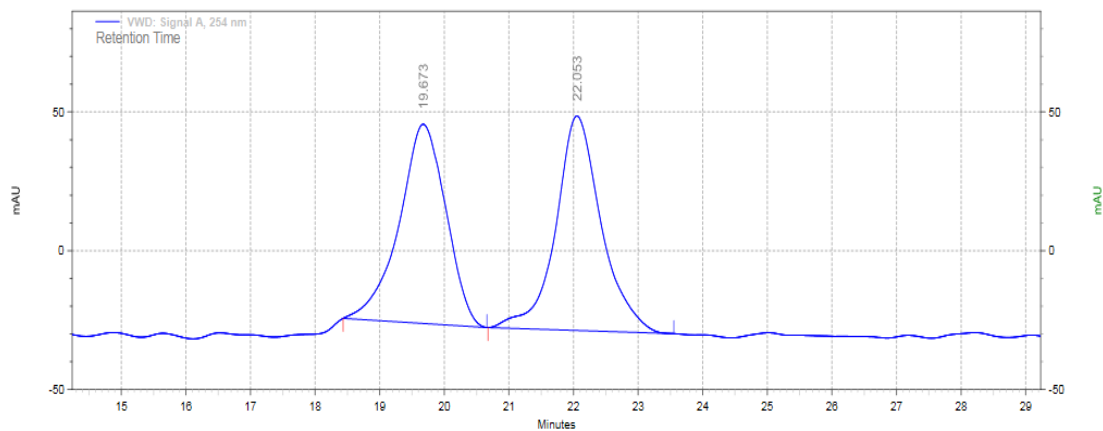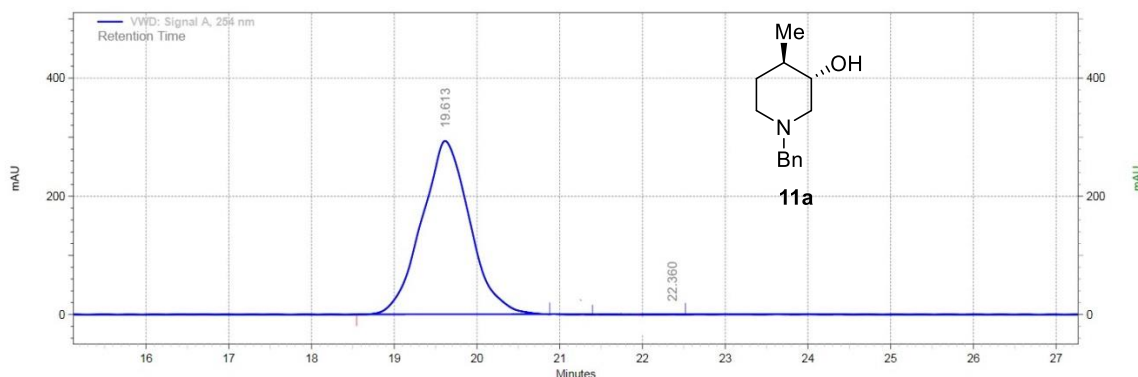
VWD: Signal A,

254nm

Results

Retention Time	Area	Area %
19.613	195059352.26	98.39
22.360	3171696.74	1.61
Total	198231049.00	100.00

Column   : Chiracel ADH (4.6X250 nm)

Mobile Phase   : IPA:n-Hexane (05:95)

Wavelength   : 254 nm

Flow rate   : 0.5 ml/min

(3*S*,4*R*)-1-benzyl-4-methylpiperidin-3-ol (**11a**)

1.1.5 Conclusion

In conclusion, the (+)-tofacitinib (**10**) synthesized in 8 steps commenced from 4-piperidinone in 22.4% overall yield with 96.8% *ee*. The key steps involved are *L*-proline catalyzed α-aminohydroxylation followed by Wittig olefination and hydrogenation reactions. An enantioselective total synthesis of Tofacitinib (CP-690,550), a Janus tyrosine kinase (JAK3) specific inhibitor, has been achieved from the readily available 4-piperidone. Proline catalyzed hydroxylation is the key step for the synthesizing of enantiopure 1-benzyl-4-methylpiperidin-3-ol. We have shown the simple organocatalyzed route for the enantioselective total synthesis of

(+)-Tofacitinib, and all the reagents are cheap and readily available are the key feature of our total synthesis.

1.1.6 Experimental Section

1-Benzylpiperidin-4-one (40)

K_2CO_3 (11.3 gm, 81.67 mmol) was added to a solution of 4-Piperidone monohydrate hydrochloride (5 gm, 32.67 mmol) in $CHCl_3$:H_2O (3:1, 50 mL) at 27 °C and stirred for 20 min. Followed by the addition of BnBr (7.2 gm, 43.0 mmol) at the same temperature and then stirred for 4hr. After completion of the reaction (monitored by TLC), another 20 mL of H_2O was added, and the organic layer was separated washed with brine. Further, the organic layer dried over anhydrous Na_2SO_4 and concentrated under vacuum to give pale yellow liquid in 87% yield.

(*S*)-1-Benzyl-4-methylenepiperidin-3-ol (39)

To a solution of nitrosobenzene (2.1 g, 19.83 mmol) and *L*-proline (0.304 g, 2.64 mmol) in DMF (90 mL) was added 1-benzylpiperidin-4-one **40**(5 g in 15 ml DMF) at 0 °C under N_2 over 24 h by using dropping funnel. Then the reaction mixture was stirred at the same temperature for 62 h. After consumption of starting material, freshly prepared aqueous ammonium chloride solution was added to the reaction and extracted with ethyl acetate (5*40 ml) and washed with brine; then, the organic layer evaporated under reduced pressure, and the crude product was then dissolved in anhydrous THF under N_2 atmosphere and used for subsequent sequential olefination reaction. To this reaction mixture dissolved in anhydrous THF, anhydrous LiCl (3.3 g, 79.35 mmol) was added, followed by phosphorous ylide in THF CH_2PPh_3 (Separately prepared in 100 ml of RB flask using tBuOK and CH_3PPh_3I in THF) using the cannula. Then this reaction mixture was stirred at 27 °C for 8 hrs. After stirring for 8 h, the reaction mixture was quenched with saturated NH_4Cl and extracted with ethyl acetate (120 mL). The combined organic layers

were washed with brine, dried over anhydrous Na$_2$SO$_4$, and concentrated under reduced pressure to give a crude(*S*)-*N*-phenylhydroxylamine intermediate **42**, which was used directly for the next step without further purification. To a well-stirred solution of crude intermediate **42**in MeOH (40 ml) was added CuSO$_4$.5H$_2$O (1.3 g, 30 mol %) at 25 °C. The reaction mixture was then allowed to stir for 12 h at this temperature. After the reaction (monitored by TLC), the solvent was evaporated under reduced pressure to afford the crude allylic alcohol. The crude product was then purified by column chromatography over silica gel using petroleum ether and ethyl acetate (8:2) as eluents to afford enantiopure alcohol **39** as light reddish oil. **Yield**: 47% (2.5 gm).

[α]^{25}$_D$: -5.8 (c 1, CHCl$_3$). **^{1}H NMR (500 MHz, *CDCl₃*)** δ 2.09 - 2.19 (m, 1H), 2.34 - 2.40 (m, 1H), 2.42 - 2.47 (m, 1H), 2.47 - 2.55 (m, 2H), 2.56 - 2.62 (m, 1H), 3.54 (s, 2H), 3.82 (br. s., 1H), 4.03 - 4.13 (m, 1H), 4.71 (s, 1H), 4.86 (s, 1H), 7.19 - 7.25 (m, 5H); **^{13}C NMR** (126 MHz,*CDCl₃*) δ 31.1, 54.0, 60.7, 62.1, 70.2, 108.1, 127.5, 128.3, 129.3, 136.8, 147.0 ; **HRMS** m/z [M + H]$^+$ calculated for C$_{13}$H$_{17}$NO: 204.1383; found: 204.1385.

(3*S*,4*R*)-1-Benzyl-4-methylpiperidin-3-ol (11a)

A mixture of **39** (500 mg, 2.46 mmol) and 10% Pd/C (15 mg) in AcOEt (25 mL) was stirred under an H$_2$ atmosphere (1 atm) for 5 h. After this time, the reaction was filtered through a Celite pad and washed with AcOEt (3 x 10 mL). The combined organic phase was concentrated under vacuum to afford the crude product, purified by column chromatography on silica gel using petroleum ether: ethyl acetate (7:3) as eluent to give hydroxy piperidine **11a** in pure form as a light yellow oil. **Yield:** 93% (469 mg), [α]^{25}$_D$ = +34.9 (c, 0.8 CHCl$_3$).

^{1}H NMR (400 MHz, CDCl$_3$)δ 0.95 (d, *J* = 6.0 Hz, 3H), 1.19 - 1.35 (m, 2H), 1.59 - 1.71 (m, 1H), 1.83 (t, *J* = 9.6 Hz, 1H), 1.89 - 2.03 (m, 2H), 2.64 (d, *J* =11.4 Hz, 1H), 2.85 (dd, *J* = 10.5, 3.2 Hz, 1H), 3.25 (td, *J* = 8.7, 4.1 Hz, 1H), 3.44 (q, *J* =13.1 Hz, 2H), 7.16 - 7.28 (m, 5H); **^{13}C NMR** (101

MHz, CDCl$_3$) δ 17.2, 31.3, 37.4, 52.4, 59.4, 62.6, 72.7, 126.7, 127.8, 128.8, 137.7; **HRMS** m/z [M + H]$^+$calculated for C$_{13}$H$_{20}$ON: 206.1539; found: 206.1540.

N-Methyl-7H-pyrrolo[2,3-d]pyrimidin-4-amine (38)

To a solution of 6-Chloro-7-dezapurine in EtOH were added a solution of Me-NH$_2$ in 33% EtOH in a 50 mL seal tube. Then this reaction mixture was stirred at 100 °C for 2 hrs. After completing the reaction (monitored by TLC), EtOH was evaporated in a vacuum, then 20 mL of THF was added to crude amine solution and extracted with 3*20 ml of ethyl acetate and washed with brine solution. Then the organics were evaporated under reduced pressure to afford amine **38** in quantitative yield as white amorphous solid.

^{1}H NMR (400 MHz, DMSO-d$_6$) δ 2.95 (d, *J* = 4.3 Hz, 3H), 6.49 (br. s., 1H), 7.05 (br. s., 1H), 7.37 (br. s., 1H), 8.11 (s, 1H), 11.49 (br. s., 1H). **^{13}C NMR** (101 MHz, DMSO-d$_6$) δ 27.1, 98.5, 102.6, 120.7, 149.9, 151.5, 156.6; **HRMS**m/z [M +H]$^+$calculated for C$_7$H$_9$N$_4$: 149.0822; found: 149.0821

1-Benzyl-4-methylpiperidin-3-yl methanesulfonate (11b)

Mesyl chloride (125 mg, 1.07 mmol) was added dropwise to an ice-cooled solution of hydroxy piperidine **11a** (200 mg, 0.97 mmol) and TEA (150 mg, 1.455 mmol) in DCM (4 mL) over 30 minutes. Stir the reaction mixture for another 2 hours. after completion of reaction monitored by TLC, add aqueous NaHCO$_3$ solution and extract with DCM (3*10 ml) and evaporated under reduced pressure to give the crude product mesylate as yellowish oil and was further used in next step without purification.

N-((3R,4R)-1-Benzyl-4-methylpiperidin-3-yl)-N-methyl-7H-pyrrolo[2,3-d]pyrimidin-4-amine (43)

In a sealed tube 1-benzyl-4-methylpiperidin-3-yl methanesulfonate **11b** (200 mg, 0.7 mmol) dissolved in 3 ml, DMF and then K_2CO_3 (290 mg, 2.1 mmol) was added at room temperature and stirred for 5 min followed by *N*-methyl-7H-pyrrolo[2,3-d]pyrimidin-4-amine **38** (105 mg, 0.7 mmol) was added, and the temperature was raised to 60 °C & reaction mixture stirred for overnight. After completion of the reaction, water was added to the reaction mixture, extracted with 3*20 ml of ethyl acetate, and washed with brine solution. Then the crude organics were evaporated under reduced pressure then purified by column chromatography over silica gel using petroleum ether and ethyl acetate (8:2) as eluents to afford corresponding amine **43** in 81 % yield. **Yield** (190 mg) as white solid; $[\alpha]_D^{25} = +26.5$ (*c* 1, MeOH).

¹H NMR (200 MHz, *DMSO-d_6*)δ 0.95 (d, *J* = 5.1 Hz, 3H), 1.14 - 1.23 (m, 1H), 1.47 - 1.71 (m, 2H), 1.77 - 2.03 (m, 1H), 2.71 (d, *J* = 10.3 Hz, 1H), 2.82 - 3.07 (m, 5H), 3.29 - 3.70 (m, 2H), 4.39 - 4.86 (m, 1H), 6.54 (d, *J* = 2.9 Hz, 1H), 7.08 (br. s., 1H), 7.26 - 7.44 (m, 5H), 8.16 (s, 1H), 11.55 (br. s., 1H); **¹³C NMR** (101 MHz, *DMSO-d_6*)δ 18.2, 27.2, 32.3, 38.2, 53.2, 60.8, 62.1, 71.9, 98.5, 102.6, 120.7, 126.9, 128.2, 128.8, 138.6, 149.9, 151.6, 156.7.

Tofacitinib (10)

To a solution of 20 wt % Pd(OH)$_2$ (50 mol %, 20 mg) in MeOH 10 ml was added TFA (0.2 ml) followed by addition of compound **43** at room temperature. The formed reaction mixture was stirred at 45 °C for 12 hrs under H$_2$ balloon pressure (1atm). After completion of the reaction (monitored by TLC), the reaction mixture was filtered on a celite pad and washed with aqueous NaHCO$_3$ (10 ml * 2) and EtOAc (10 ml * 2). Then the organic layer was evaporated under reduced pressure to give crude benzyl deprotected amine. Then this amine was directly used for the next sequential reaction. The amine was dissolved in DCM (10 ml) under N$_2$ atmosphere followed by sequential addition of TEA (0.4 ml) and cyanoacetyl chloride {17 mg (13.0 µl), 0.16

mmol} respectively. The reaction mixture was further stirred for 2 hours at room temperature. After completion of the reaction (monitored by TLC), the reaction mixture was washed with aqueous NaHCO$_3$ (10 ml * 2) and extracted with DCM (10 ml * 3). Then the organics were evaporated under reduced pressure to give crude product 1 as white semisolid. The crude product was purified on neutral alumina using 2:8 (EtOAc: Hexane) and offered tofacitinib (**10)** as an off-white solid. **Yield:** 75%, (32.9 mg); $[\alpha]^{25}_D$ = +9.6 (c 0.7, MeOH) {lit. value $[\alpha]^{25}_D$ = +10.4 (c 0.68, MeOH).[1]

^{1}H NMR (400 MHz, *DMSO-d$_6$*) δ 0.99 (d, *J* =7.3 Hz, 3H), 1.50 - 1.65 (m, 1H), 1.66 - 1.90 (m, 1H), 2.36 (d, *J* =5.5 Hz, 1H), 3.24 (br. s., 3H), 3.59 - 3.74 (m, 3H), 3.91 (dd, *J* =12.8, 3.7 Hz, 1H), 4.06 - 4.20 (m, 2H), 4.83 (br. s., 1H), 6.55 (br. s., 1H), 7.13 (br. s., 1H), 8.02 - 8.17 (m, 1H), 11.70 (br. s., 1H); **^{13}C NMR** (101 MHz, *DMSO-d$_6$*) δ 14.1, 25.3, 31.4, 34.4, 42.2, 42.8, 45.6, 53.2, 70.2, 102.1, 102.6, 116.6, 121.2, 150.9, 152.1, 157.3, 161.8, 162.0. **HRMS** m/z [M +H]$^+$ calculated for C$_{16}$H$_{21}$ON$_6$: 313.1771; found: 313.1772.

Section II

Process for the production of key intermediates of (+)-Tofacitinib *via* Overmann rearrangement reaction

1.2.1   Introduction

In the world's total population nearly 1% of people are affected by chronic autoimmune disorders steered by immune system dysregulation, such as rheumatoid arthritis. In the present situation, conventional antirheumatic drugs (DMARDs) are disease-modifying drugs indicated for the medicaments for autoimmune disorders and rheumatic arthritis, including inflammatory myositis, systemic sclerosis, systemic lupus erythematosus, spondyloarthritis, and inflammatory bowel disease.[30,31] Due to the active medicinal resistance and unfavorable effects of the DMARD, and MXTs, searching for new molecular structures with less risk is in progress. Janus kinase inhibitors, also called jakinibs or JAK inhibitors, are a type of medication that suppresses the activity of one or more enzymes of the Janus kinase enzyme families (TYK2, JAK1, JAK3, JAK2,) thereby inhibiting the signaling pathway in JAK-STAT.[32] Tofacitinib **10** (Fig. 1) is designed by Pfizer and approved by Food and Drug
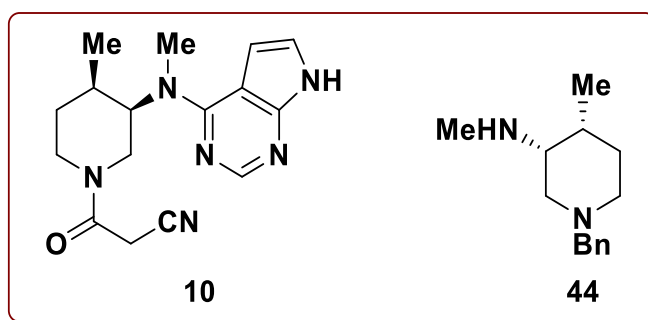
Figure 10: Structure of (+)-Tofacitinib (**10**) and *N*-benzyl-3-methylamino-4-methylpiperidine (**44**)

Administration (FDA) is a JAK 3 inhibitor and revolved as effective against plenty of disorders such as ulcerative colitis, rheumatoid arthritis (RA), and prevention of organ transplant rejection as well.[33]

1.2.2 Review of Literature

Due to the bioactivity of (+)-tofacitnib **10** against various disorders, a variety of synthetic approaches have been displayed in the literature reports.[10] Among the current approaches in the literature, stereoselective synthesis of key intermediate **44** for tofacitinib synthesis is rarely found.
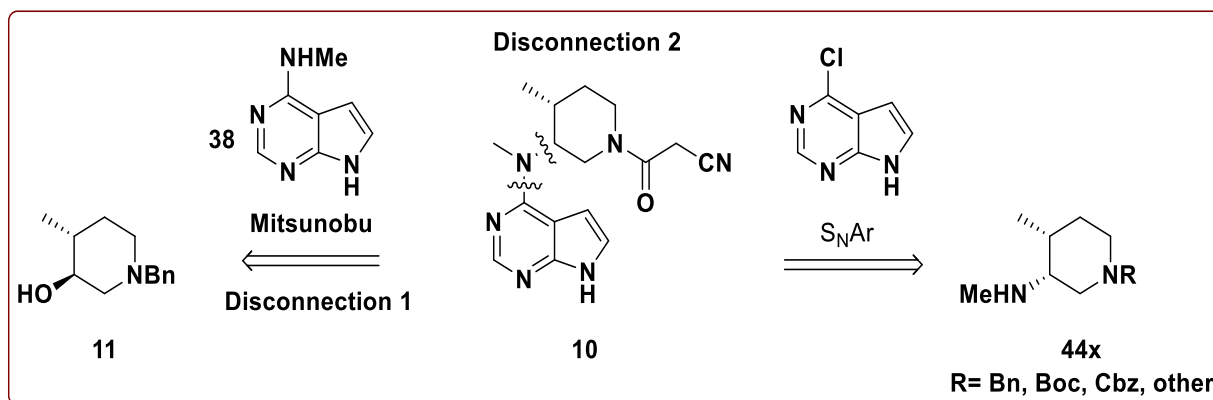
Figure 11: Common tofacitinib disconnections

The common retrosynthetic disconnections of tofacitinib can assume by two major fragments, in which the first fragment **11** was described in chapter one. We have shown the literature data and synthetic route for fragment **11** in the previous section. Now in this section, we have covered all the literature reports for the synthesis of common tofacitinib intermediate, as well as we have shown the few synthetic approaches *via* Overmann rearrangement reaction.

Ripin's first approach[34]

Ripin *et al.* developed the synthetic route for synthesizing a key intermediate **44** in 9 steps to get (±)-**10,** and the synthesis starts with the 4-picoline **45** (**Scheme 7**). For the synthesis of tetrahydropyridine **46**, the moiety 4-picoline is treated with benzyl chloride to get the quaternary ammonium salt of picoline. Then the formed salt intermediate is directly reduced by using sodium borohydride in ethanol to give the compound **46** in 73% yield. The formed olefin 46 is then treated with a hydroboration reaction using $BH_3.THF$ in combination with $BF_3.OEt_2$ followed by H_2O_2 mediated oxidation, and finally, the piperidine alcohol intermediate was isolated as tosylate salt **47** by using TsOH in acetone.
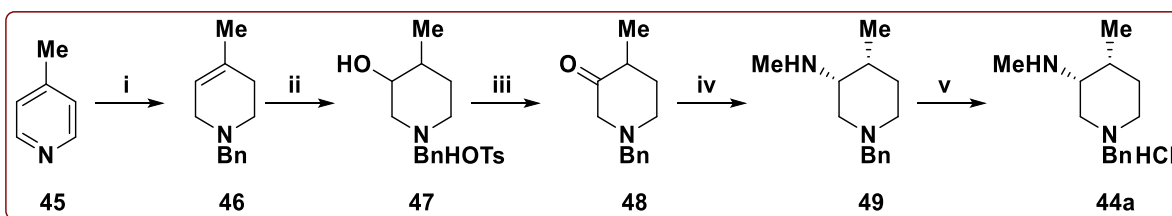
Scheme 7: (i) (a) acetone, BnCl, 16 h, 55 ^{o}C, 69% (b) EtOH, NaBH$_4$,10 h, 15 ^{o}C, 73%; (ii) (a) BF$_3$.OEt$_2$, BH$_3$.THF, 20 ^{o}C, THF, 14.5 h (b) 17.5% aq. H$_2$O$_2$, 68 h; 19-22 ^{o}C, (c) acetone, TsOH, -2 to 5 ^{o}C, 1.5 h, 88% over three steps; (iii) SO$_2$.Py, DMSO, TEA, 22 ^{o}C, 1 h, 93%; (iv) (a) 8 M MeNH$_2$ in EtOH, AcOH, Toluene: EtOH, 18-24 ^{o}C, 55 min; (b) NaBH$_4$, THF, AcOH, 2 ^{o}C, 13 h, 92%; (v) 32% HCl, Toluene: EtOH, 62%

The piperidine tosylate salt **47** is then oxidized using Parikh–Doering oxidation to yield ketone **48** in 93% yield. Further, the ketone **48** is treated for reductive amination with methylamine in ethanol followed by reduction of imine using NaBH$_4$ in acetic acid to give crude intermediate **49** in 92% yield, and it was then hydrolyzed with HCl to give diastereomerically pure HCl. salt of **44a.**

Ruggeri approach[35]

In 2007 Ruggeri and co-workers described the rhodium-catalyzed first enantioselective preparation of intermediate **44b** in only five steps. In this approach, Rh catalyzed hydrogenation

is the key step. The ferrocene substituted phosphine ligand with the Rh metal system is highly

selective for the *cis* conformation of compound **44b,** as shown in **Scheme 8**.
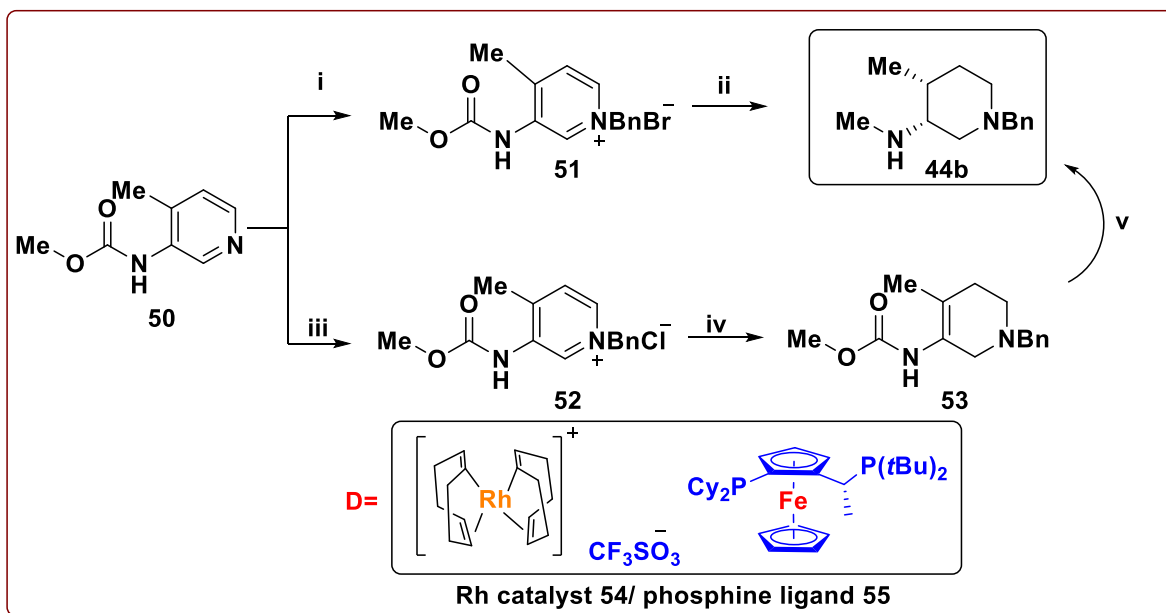
Scheme 8: (i) Toluene, BnBr, 110 ^{o}C, 20 h, 96%; (ii) D, H$_2$ (200 psi), THF:EtOH, 70°C, 48h, 68% *ee* and 84% *cis*; (iii) Toluene, BnCl, 80 ^{o}C, 16 h, 78% ; (iv) NaBH$_4$, EtOH, 16 h, rt, 72%; (v) D, H$_2$ (200 psi), THF:EtOH, 70°C, 48h, 66% *ee* and 90% *cis*.

Patil'sapproach[36]

Patil and co-workers from India have synthesized the common intermediate of tofacitinib from

the 3-amino-4-methyl pyridine **56**. The main advantage of this approach is that they have not

isolated any intermediates and completed their final molecule **49** in only 2 steps with an overall

yield 26 %, as shown in (**Scheme 9**). In first step of the synthesis, the amine group of picoline is

acylated using AcCl with a 95% yield of **57**. Then the *N*-acylated pyridine **57** was treated with

BnCl for the formation of to form quaternary pyridine salt **58** in toluene solvent at 110 °C then

the quaternary salt was subsequently reduced to compound **59** by using sodium borohydride in

ethanol with 91% yield. The formed enamide 59 was then treated with HCl for hydrolysis to

obtain the ketone **48** in a 95% yield**.** Further, the reductive amination of ketone was done using

titanium isopropoxide mediated to get **(±)-44c** in 96% yield, and the resolution of **(±)-44c** is achieved by using *L*-DTTA to give compound **60** in 37 % yield and 98.6 % *ee*.
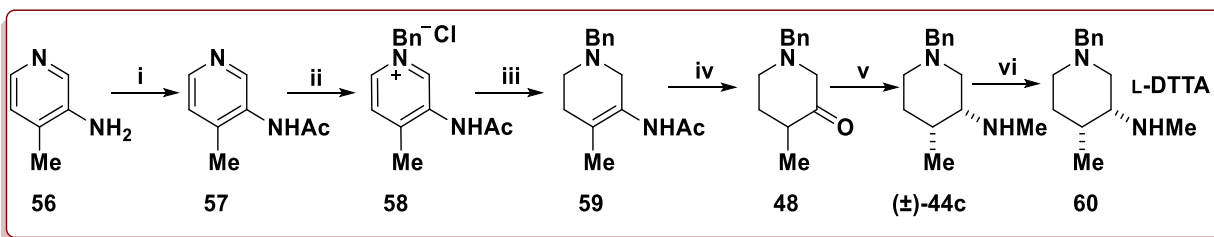
Scheme 9 : (i) AcCl, acetone, 8 h, rt, 95%; (ii) BnCl, Toluene, 5 h, 110 °C, 95%; (iii) NaBH$_4$, EtOH, 5 h, 50 °C, 91%; (iv) 35% HCl, 70 °C, 95 %; 4 h, (v) (a) Ti(OiPr)$_4$, 33% MeNH$_2$ in MeOH, 15 °C, 1 h; (b) MeOH, NaBH$_4$, rt, 3 h, 96%; (vi) di-*p*-toluolyl-*L*-tartaric acid, 1 h, MeOH/H$_2$O, 40%

Jiang's approach[37]

Jiang and coworkers have reported the enantioselective total synthesis of all the four stereoisomers having common piperidine intermediate from readily available Garner's aldehyde as shown in **Scheme 10,** and in this approach, they have applied the few steps in the previously reported methods. The compound **61** was reduced to tertiary alcohol using excess methyl magnesium chloride in THF to give **62** in 85% yield, followed by E$_2$ elimination of alcohol to obtain corresponding enantiopure compound **63** in 54% yield.
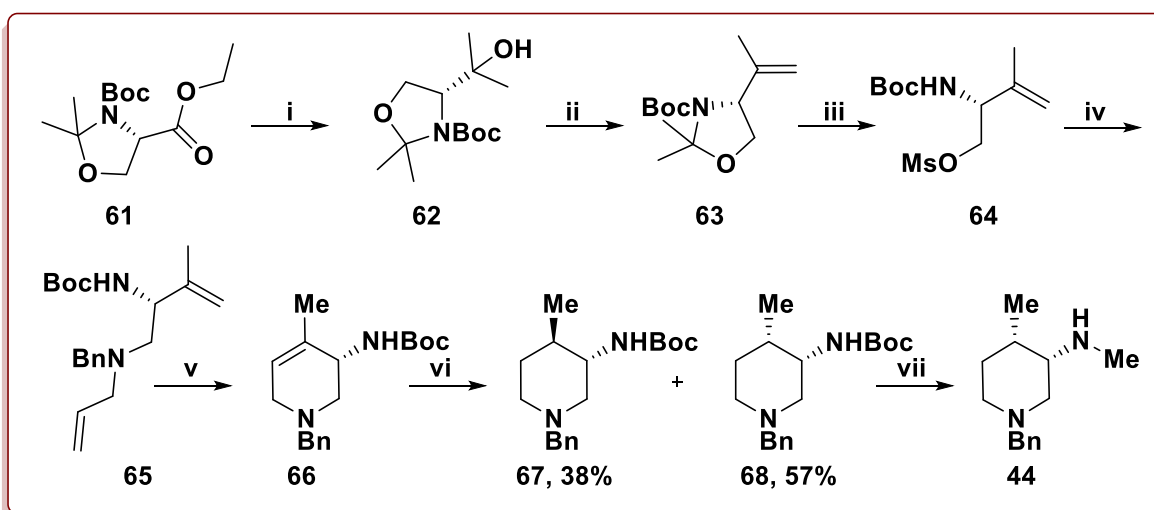
Scheme 10: i) MeMgCl (6 equiv.), THF, 0 °C, 85%; ii) (a) MsCl (5.0 equiv.), Et$_3$N (10 equiv.), DCM, 54%; (b) *p*-TSA, MeOH, 80%; iii) MsCl, Et$_3$N, DCM, 97%; iv) (a) allyamine, reflux; (b)

BnBr, K_2CO_3, ACN, 60%; v) Grubbs 2nd generation catalyst (5 mol%), DCM, reflux, 92%; vi) H_2, PtO_2 (10 mol %), MeOH, 95% (1.5:1.0 *trans:cis* ratio), vii) $LiAlH_4$, THF, reflux

The formed enantiopure alkene **63** was subjected to *p*-TSA-catalyzed ring-opening of oxazolidine followed by mesylation of alcohol using MsCl to give compound **64**. The mesylate **64** was subjected for S_N^2 reaction with allylamine, as a nucleophile, followed by in situ NH group is protection using benzyl bromide to give compound **65** in 60% yield. Then the prepared alkene moiety **65** was subjected for ring-closing metathesis using ^{2}nd generation Grubbs catalyst to achieve the piperidine moiety **66** in 92% yield. Then subsequently, H_2/PtO_2 mediated hydrogenation gives the mixture of compounds **67** and **68**, separated chromatographically. Then this mixture of two isomers is reduced to common intermediate **44** by using LAH in tetrahydrofuran solvent.

Hao's approach[38]

Hao and coworkers developed an alternative route for synthesizing Cbz protected compound **78** starting from the *L*-malic acid **69** as chiral auxiliary, as shown in **Scheme 11**. The synthesis of **78** was achieved in 16 steps, and the author claimed that this route has several advantages, such as mild reaction conditions, cheap starting materials, and the overall yield of compound **78** is 26 % with *ee* > 98 %. This approach synthesizes Cbz protected piperidine intermediate **78**, beginning with *L*-malic acid as a chiral pool starting material. In the first step, malic acid is converted into ester using thionyl chloride in methanol, then methylation at the alpha position, and $BH_3.DMS$ mediated acidification to give compound **70** in 85% yield. The key step in this method is the cyclization of compound **73** catalyzed by Raney Nickel to attain the piperidine **74** in 91% yield. After the Cbz protection using CbzCl in TEA, DCM condition, followed by deprotection of TBS group by using TBAF and then mesylation of accessible OH

using MsCl to give **75** in 99% yield. Then OMS group is removed by using S_N^2 substitution of

azide with inversion of configuration
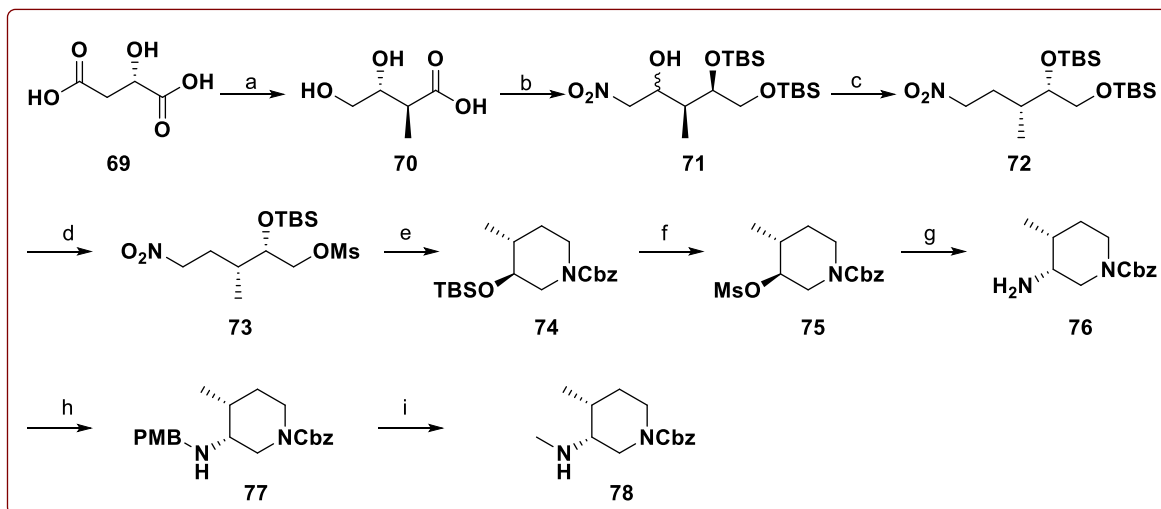
Scheme 11: (a) (i) SOCl$_2$, MeOH,98%; (ii) LHMDS, MeI, THF, 97%; (iii) CH$_3$SBH$_3$, NaBH$_4$, THF, 85% (b) (i) TBSCl, l m, DMF, 99%; (ii) DIBAL-H, DCM, 93%; (iii) MeNO$_2$, KO*t*-Bu, THF, *t*-BuOH, 94% (c) (i) MsCl, TEA, DCM (ii) NaBH$_4$, EtOH, 85% over 2 steps (d) (i) HF-Pyr, THF, 81% (ii) MsCl, TEA, DCM, 96% (e) (i) Ra-Ni, EtOH (ii) CbzCl, TEA, DCM, 91% over 2 steps (f) (i) 1 M TBAF in THF, 94% (ii) MsCl, TEA, DCM, 99% (g) (i) NaN$_3$, DMF, 80% (ii) PPh$_3$, 28% NH$_4$OH, 84% over 2 steps (h) *p*-anisaldehyde, NaBH(OAc)$_3$, DCM, 92% (i) (i) HCHO, NaBH(OAc)$_3$, DCM, 99% (ii) CAN, ACN:H$_2$O, 93%, 98% *ee*

followed by reduction of azide into amine by using PPh$_3$ in ammonium hydroxide to attain

piperidine amine **76** in 84% yield over 2 steps. In the final step, reductive amination was done to

protect the free amine group using *p*-anisaldehyde and NaBH(OAc)$_3$ as reducing agents. Further,

another reductive amination sequence was carried out using HCHO to form tertiary amine. The

PMB group is removed by using CAN to give Cbz protected piperidine intermediate **78** in 93%

yield with 98% *ee*, and the overall yield of the method is 26%

Stavber and Cluzeau, s approach[39]

Stavber and Cluzeau, in the year 2014 (from Lek Pharmaceuticals) have disclosed the various routes for the synthesis of intermediate **83** starting from the alkene **79.** The synthesis begins with bromonium ion formation of alkene **79** followed by the opening of this bromonium ion with sodium hydroxide to form the epoxide, and subsequently, the epoxide opening is done with

79　　　　　**80**　　　　　**81**　　　　**82**

1.9:1 (cis:trans ratio)

83
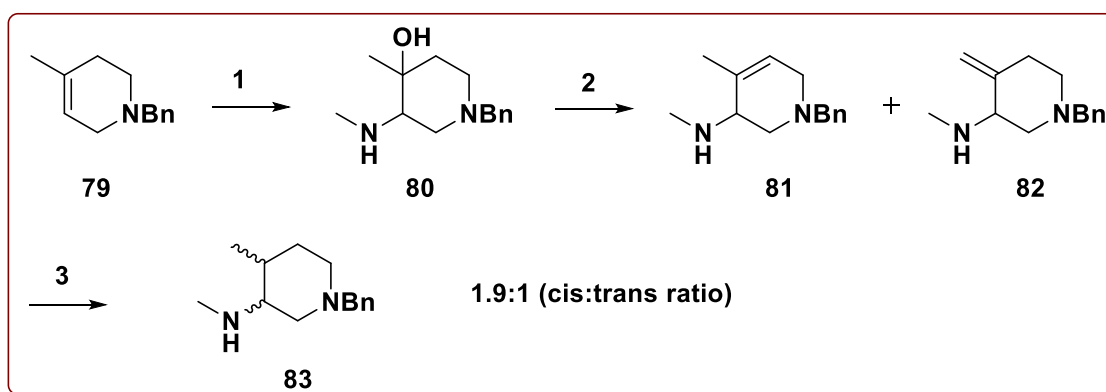
Scheme 12: (1) (a) NBS, TFA, *i*PrOH: H_2O, 50 ^{o}C, 20 h (b) NaOH, 30 ^{o}C, 12 h (c) 40% MeNH$_2$, 60 ^{o}C, overnight, 76% (2) H_2SO_4, 80 ^{o}C, 16 h, 79%, 1.9:1 endo: exo. (3) H_2 (20 atm), 5% Rh/C, AcOH, 40 ^{o}C, 81% (1.9:1, cis:trans)

methylamine to give compound **80** in 76% yield. Then acid-mediated hydrolysis of compound **80** gives the two isomers **81** and **82** Endo: Exo ratio 1.9:1. In this approach, the author has tested the reduction step with different conditions but using Rh/C catalyst gives the best cis/trans ratio of **83**.

Hao, s 2nd route 27[40]

In 2011, Hao *et al.* proposed another route for synthesizing Boc-protected piperidine intermediate **92** from easily and cheaply available starting materials, as shown in **Scheme13**. In the first step of this approach, the replacement of the Bn group by the Boc protection of nitrogen followed by reductive amination of ketone in the same reaction condition gives compound **86** in quantitative yield by using H_2 in Pd/C condition. This is the key step for this approach as chiral auxiliary is introduced in same step. The author screened the various metal catalyst for the

asymmetric reduction of **86**. Out of all screened reaction conditions, Cobalt catalyzed and (S)-Tol BINAP as the chiral catalyst in the system with the excess amount of $NaBH(OAc)_3$ is most suitable to achieve compound **87**. Then methyl group is introduced on amine by reductive amination reaction in the presence of formaldehyde and $NaBH(OAc)_3$ as a reducing agent to
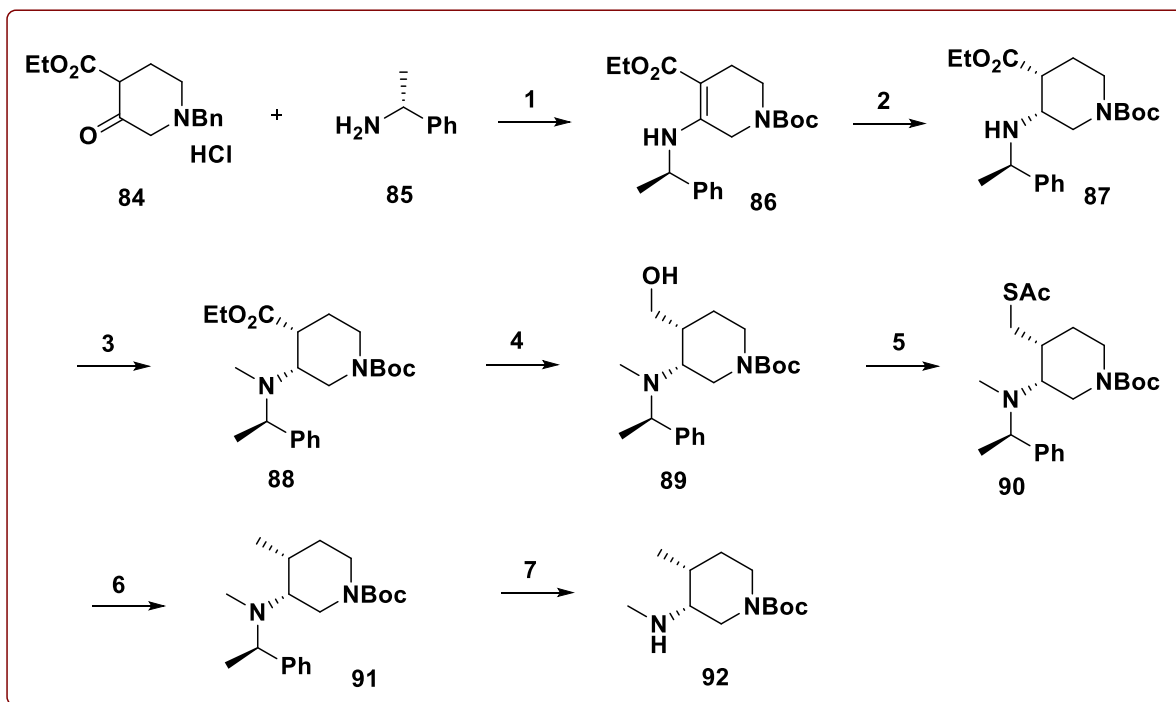
Scheme 13: (1) (a) H_2 (1 atm), 10% Pd/C, $(Boc)_2O$, TEA, 4 h, quantative (b) toluene, reflux, overnight, 91% (2) (a) $CoCl_2.6H_2O$ (1 mol%), (S)-TolBINAP, DCM: DMF, r.t, 1 h (b) $NaBH(OAc)_3$, r.t, overnight, 69% (de 71%). (3) (a) HCOH, DCM, r.t, 1.5 h (b) $NaBH(OAc)_3$, r.t, overnight, quant. (4) $LiALH_4$, THF, 30 min, 93% (5) CH_3COSH, PPh_3, DIAD, THF, reflux, overnight, 88% (6) H_2, Ra-Ni, EtOH, r.t, 4 h, 98% (7) $HCOONH_4$, 5% Pd/C, MeOH, reflux, 5 h, quant.

give compound **88** in quantitative yield. Then the ester group of intermediate **88** is converted to alcohol by using LAH and subsequently by applying Mitsonobou reaction on compound **89** in the presence of thioacetic acid, and DIAD gives compound **90** in 88% yield. Removal of thioacetate group is achieved by using hydrogenation catalyzed by Raney-Nickel. In the final

synthesis step the chiral auxiliary was removed using ammonium formate to give Boc protected

piperidine in quantitative yield with a 49% overall yield. The enantiomeric ratio of this method is

not described in this approach but stated that it was high in amount and not mentioned anywhere

in the paper.

Pfizer's approach[41,42]
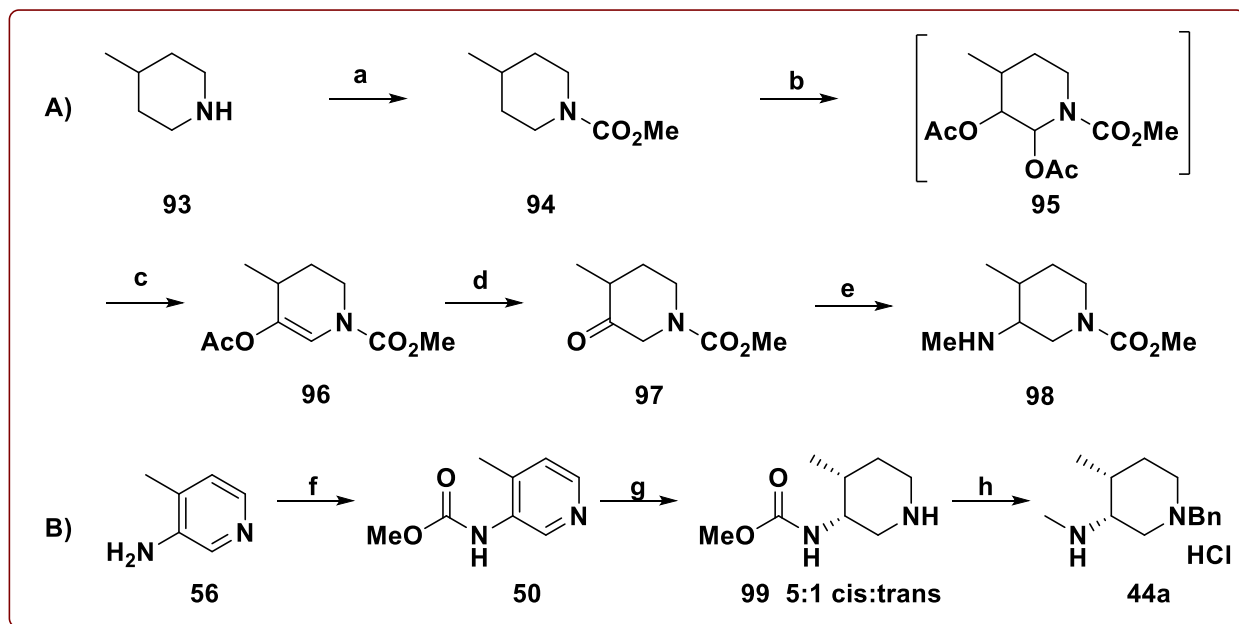
Scheme 14: (a) MeOCOCl, TEA, DCM, overnight, 20 °C, 59% (b) electrochemical oxidation, KOAc, AcOH (c) Ac$_2$O, 140 °C, 2 h, then r.t, overnight, 86% (d) 40% MeNH$_2$ in MeOH, MeOH, r.t, overnight, 27% (e) 2 M MeNH$_2$ in MeOH, NaBH$_4$, AcOH, EtOH, 19% (f) (MeO$_2$C)$_2$O, KOtBu, THF, 0 °C, 30 min. 89% (g) H$_2$ (100 psi), 5% Rh/Al$_2$O$_3$, EtOH, 100 °C, 24 h, quant. (h) (1) PhCHO, NaBH(OAc)$_3$, DCM, 20 °C, 30 min., 70% (ii) LAH, THF, 90% (iii) 36% HCl, EtOH, 38%

Alternative methods were developed by Pfizer for the synthesis of Bn and carboxylate-protected

piperidine, as shown in (**Scheme 14**). The first route starts with 3-amino 4-methyl picoline **56**

with carbamate protection of amine to give compound **50** in 89% yield. Then sequentially

hydrogenation of protected amine **50** by using Rh catalyst gives piperidine **99** in quantitative

yield with 5:1 cis/trans ratio. *N*-benzylation of piperidine amine is achieved by using reductive

amination reaction followed by acidification with HCl gives the Bn protected piperidine **100** in salt form with 38% yield. In this patent, the author does not describe the cis/trans ratio of the final compound. Also, in the same report, Pfizer reported a very similar method with a few minor changes in the approach, as shown in **Scheme 14**. In this approach, the synthesis begins with 4-methyl piperidine **93** with carboxylate protection in the initial step. Then the sequential electrochemical oxidation of compound **94** by sing potassium acetate in an acetic acid medium gives an intermediate **95**. The crude diacetate obtained from the previous step is transformed to ketone **96** using acetic anhydride mediated cleavage of diacetate. The methylamine moiety is inserted by using reductive amination reaction condition gives the carboxylate protected piperidine in 19% yield followed by preparation of salt by using HCl to give compound **44a** as salt.

1.2.3 Present Work

1.2.3.1 Objectives

After taking a literature survey for the synthesis of a key intermediate of (+)-tofacitinib, it can be seen that the previous methods employ costly starting material, complex metal catalysts, and expensive reagents are required, and also some reports have poor selectivities. To overcome the difficulties mentioned above and the selectivity issues in the synthesis of piperidine amine moiety, we describe the present section on metal-free Overmann rearrangement reaction to prepare key intermediate of (+)-tofacitinib from readily available starting materials in 8 steps.
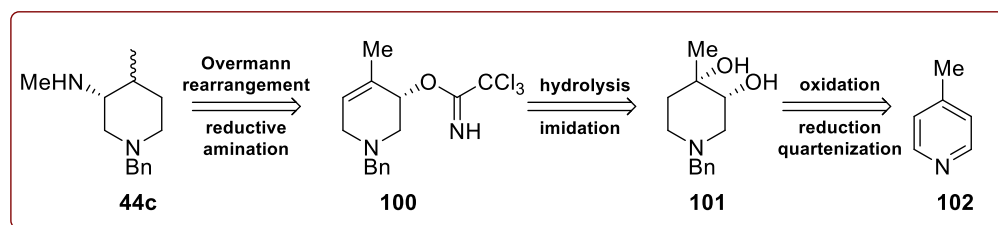
Fig. 10: Retrosynthetic analysis

The possible retrosynthetic analysis of key intermediate of tofacitinib is shown in **Figure 10**, and it can be synthesized from the commercially available starting material 4-picoline **102**. The piperidine amine **44c** can be obtained from allylic imidate moiety **100** *via* Overmann rearrangement and reduction strategy. The allylic imidate core can be obtained from chiral diol from imidation and hydrolysis sequence reactions. Piperidine diol **101** could be synthesized from 4-picoline moiety **102** *via* quaternization, reduction, and oxidation strategy.

1.2.3.2 Results and Discussion

The sequential pathway for synthesizing key molecule piperidine amine is shown in **Scheme 15**. The synthesis starts with the readily available and cheap starting material 4-picoline. Our synthetic approach begins with quaternization of 4-methyl pyridine by using benzyl bromide in
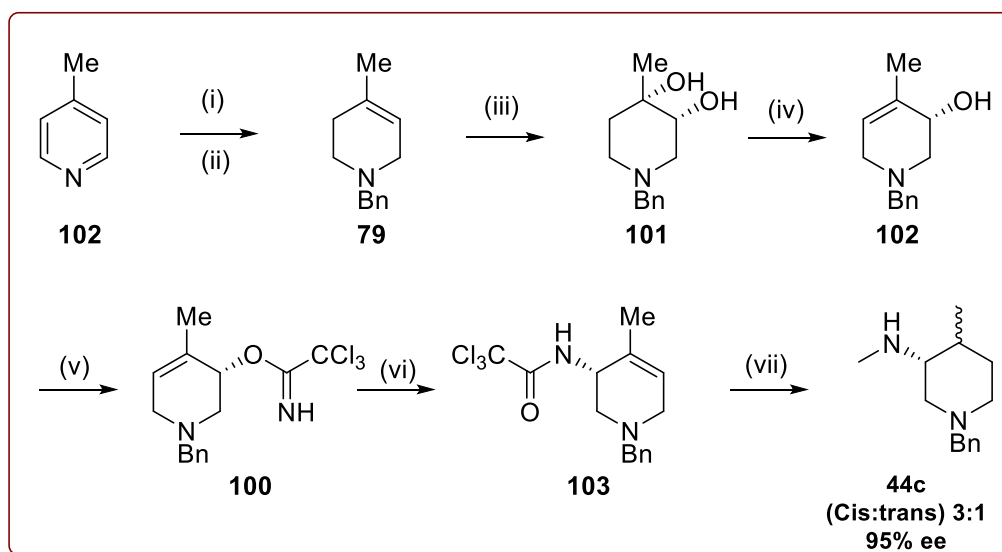
Scheme 15. Reaction Conditions: (i) BnBr, Acetone, 25 $^{\circ}$C ,3 h, 98% (ii) NaBH$_4$, MeOH, 0-25 $^{\circ}$C , 1 h, 97% (iii) K$_3$Fe(CN)$_6$, MeSO$_2$NH$_2$, K$_2$CO$_3$, K$_2$OSO$_4$.2H$_2$O, (DHQ)$_2$PHAL, t-BuOH:H$_2$O (1:1), 27 $^{\circ}$C, 5 h, 90% (iv) PTSA, toluene, reflux, 85% (v) CCl$_3$CN, DCM, DBU, 0 to 25 $^{\circ}$C, 24 h. (vi) Toluene, 110 $^{\circ}$C, 18 h, 81% (vii) a) NaOH, H$_2$O, Me$_2$CHOH, 75 $^{\circ}$C 1 h (b) CH$_2$O THF, then 10% Pd/C, H$_2$ (1 atm), AcOEt,12 h, 27 $^{\circ}$C 8

AV-400-20220121-150322-11816.001.001.1r.esp

AV-400-20220121-150322-11816.002.001.1r.esp
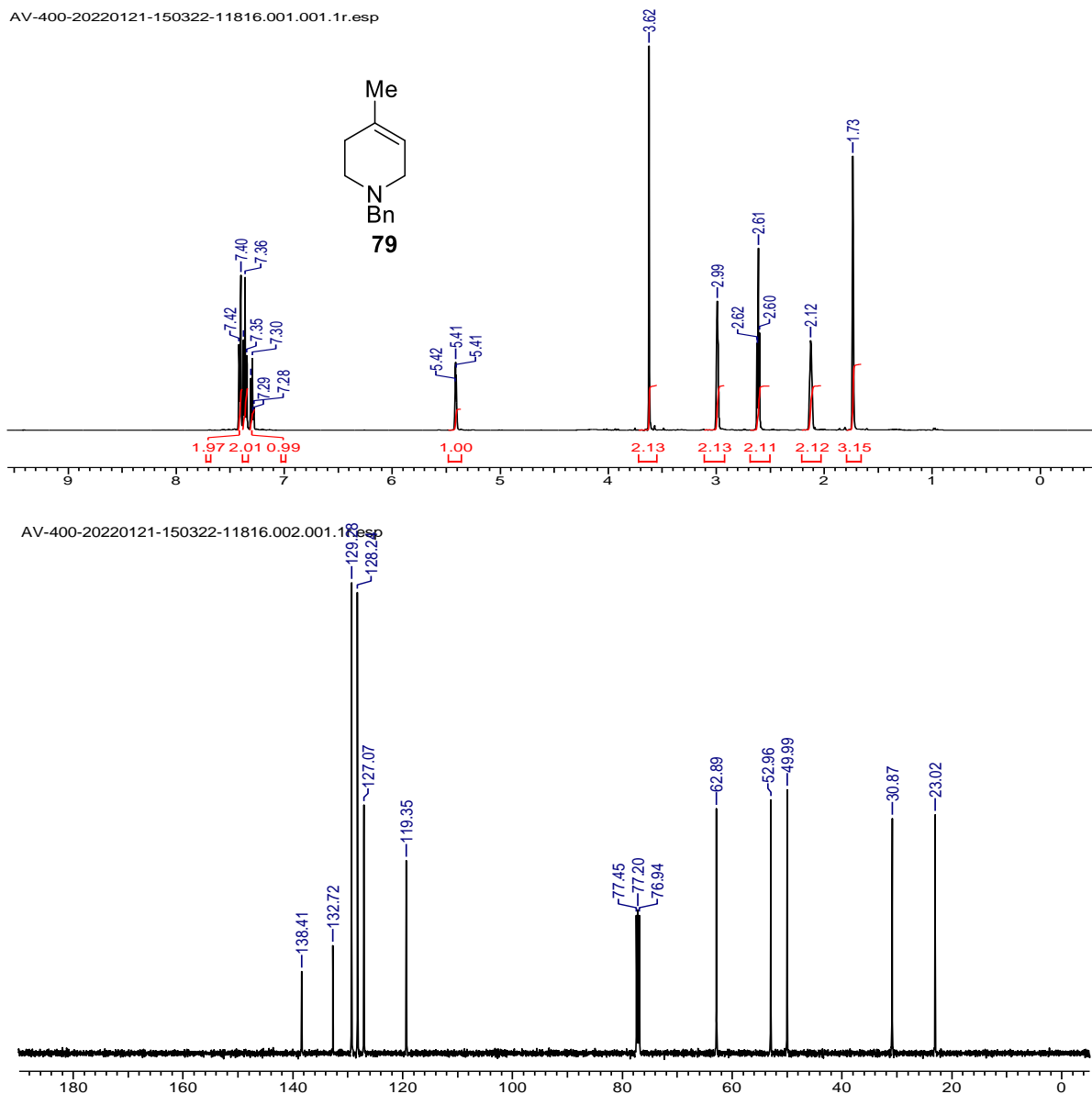
Fig. 11: ^{1}H and ^{13}C NMR of 1-benzyl-4-methyl-1,2,3,6-tetrahydropyridine (**79**)

acetone to give the quaternary salt of pyridine, then reduces this salt by using sodium borohydride in methanol to produce olefin **79** in 97% yield. Its ^{1}H and ^{13}C NMR analysis confirmed the formation of olefin **79 (fig.11)**. The characteristic peak of olefinic hydrogen showed at δ 5.41 (t, 1H) and hydrogens of benzyl protected ring showed in the range of δ 7.28-7.42. For protons of aliphatic ring displayed in the range of δ 1.73-3.62. Further ^{13}C NMR

spectrum of **6** having aliphatic carbons showed in the range of δ 23-62, and remaining aromatic/olefinic carbon showed in the range of δ 119-138.

Then the olefin is further subjected to the Sharpless asymmetric dihydroxylation reaction to form chiral diol **101** by using hydroquinidine 1,4-phthalazinediyl diether in tertiary butanol and water as solvent at room temperature to give diol **101** in 90% yield. Diol formation was confirmed by its ^{1}H and ^{13}C NMR analysis (**Fig. 12**). In the ^{1}H NMR spectrum, the aromatic hydrogens showed at δ 7.22-7.32, and the remaining aliphatic protons are shown in the range of δ 1.20-3.51. At the same time, its ^{13}C NMR spectrum shows aromatic carbons in the range of δ 127-137 and remaining aliphatic carbons in the range of 36-72.

Fig. 12: ^{1}H and ^{13}C NMR of (3R,4S)-1-benzyl-4-methylpiperidine-3,4-diol (**101**)
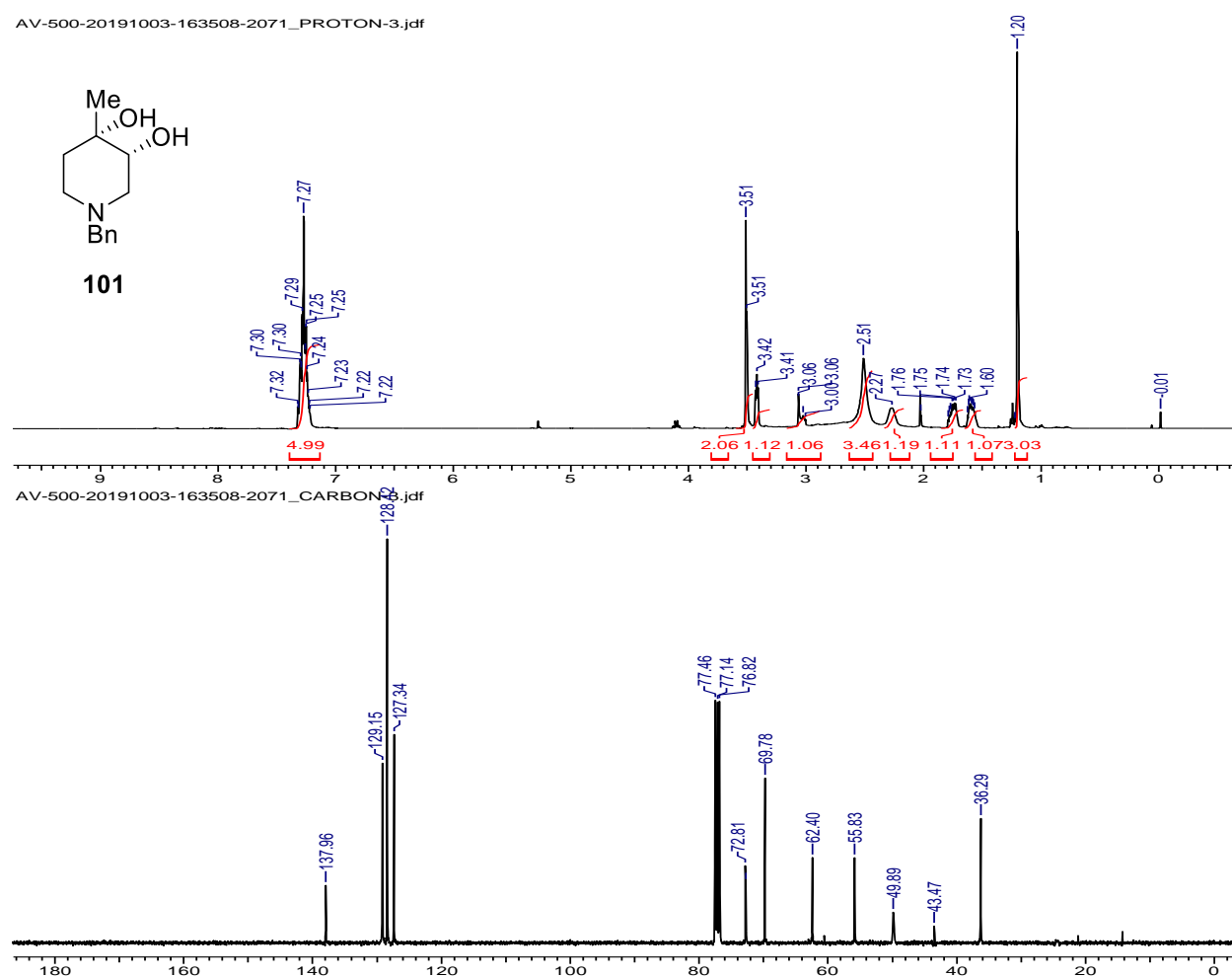
Then the chiral diol **101** was utilized for the next step, *i.e.*, hydrolysis reaction by using para toluene sulphonic acid in toluene to achieve allylic alcohol **102** in 85 % yield. Its ^{1}H and ^{13}C NMR analysis confirmed the formation of allylic alcohol moiety **102.** After allylic alcohol is in hand, we proceed further for formation imidate by using trichloroacetonitrile in DCM and DBU as a base to give allylic imidate moiety **100** in comparative yield. The formation of imidate moiety was confirmed by taking its ^{1}H and ^{13}C NMR analysis (**Fig. 13**). In the ^{1}H NMR spectrum of allylic imidate, aromatic hydrogens showed at δ 7.26-7.39, and remaining aliphatic protons showed in the range of δ 2.26-5.83. In the carbon NMR spectrum, the aromatic carbons showed in the range of δ 123-162 and remaining carbons at δ 26-91.

imidate tofa.003.001.1r.esp
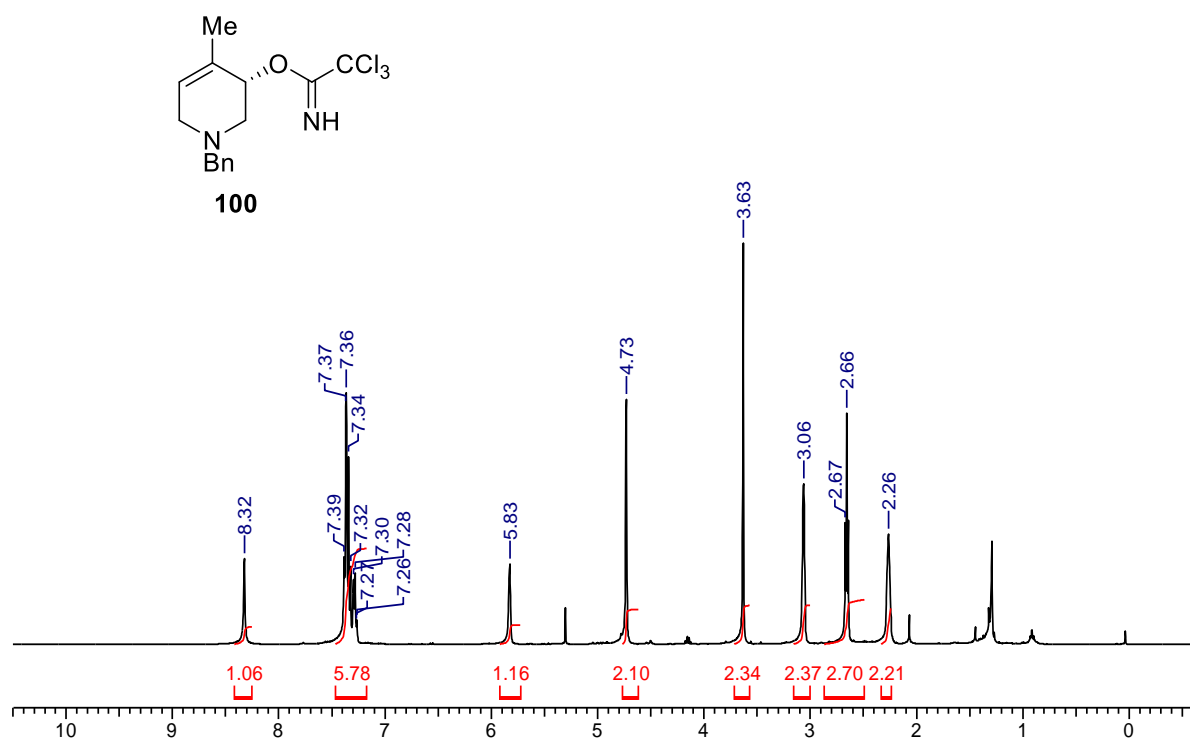
imidate tofa.004.001.1r.esp
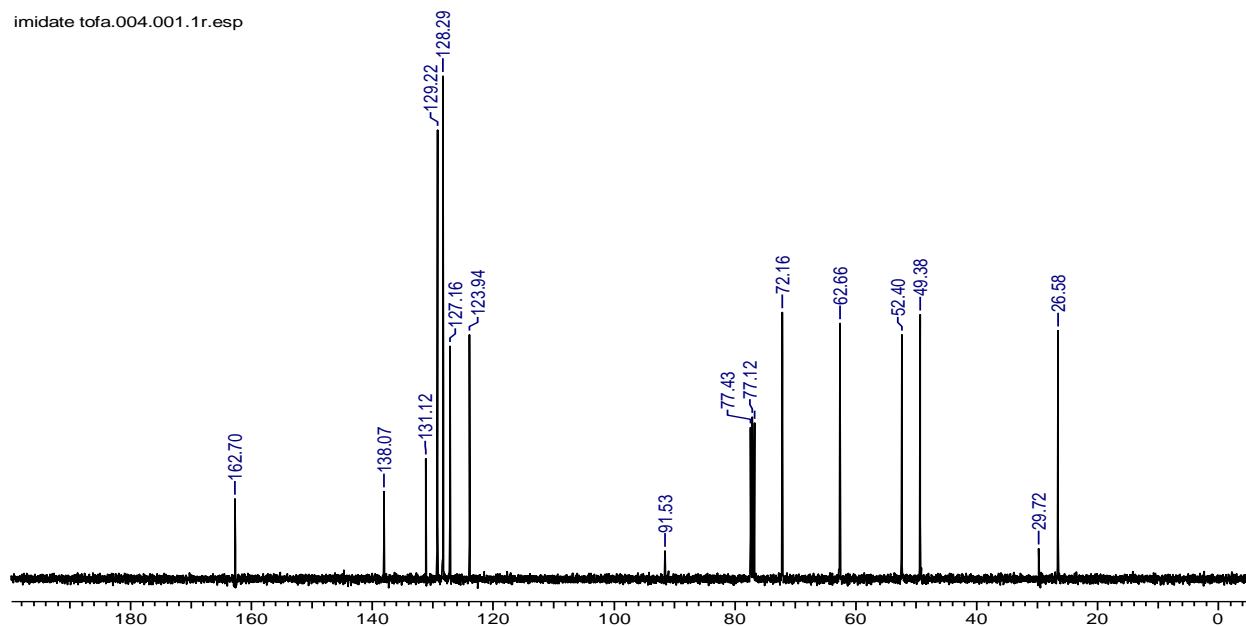
Fig. 13: ¹H and ¹³C NMR of (S)-1-benzyl-4-methyl-1,2,3,6-tetrahydropyridin-3-yl 2,2,2-trichloroacetimidate (**100**)

After allylic imidate in hand, we proceeded to this compound for our key reaction, *i.e.*, metal-free Overmann rearrangement reaction to achieve compound **103** by using toluene as solvent and refluxed for 18 hours to give compound **103** in 81% yield as shown in **Scheme 15**. The formation of allylic amide was further confirmed by its ¹H, ¹³C NMR, and HRMS analysis, as

AV-500-20190810-263553-11680_PROTON-3.jdf

AV-500-20190810-263553-11680_CARBON-3.jdf
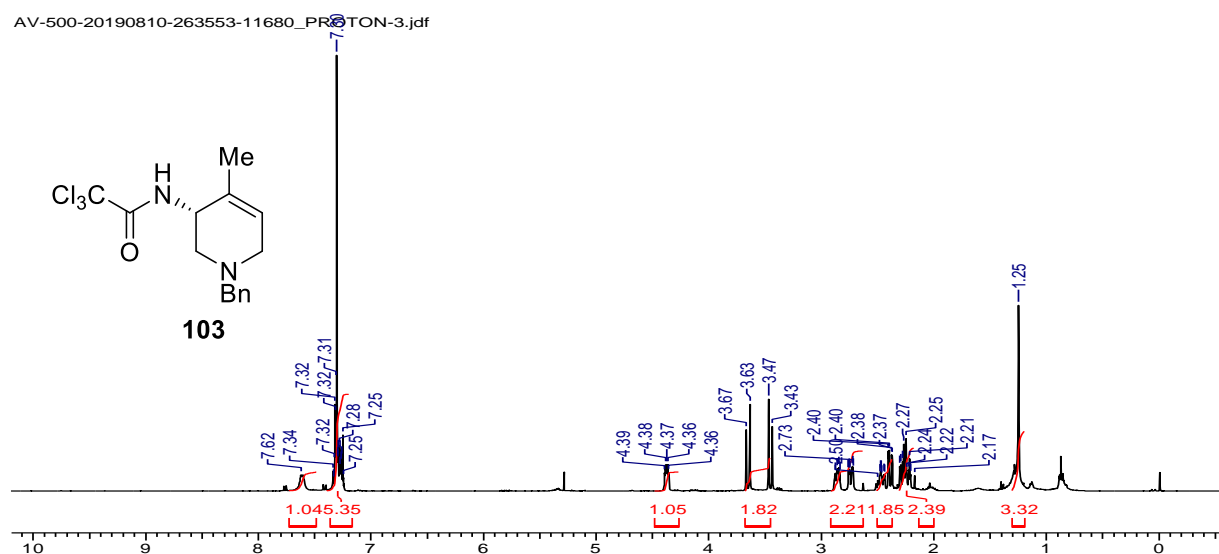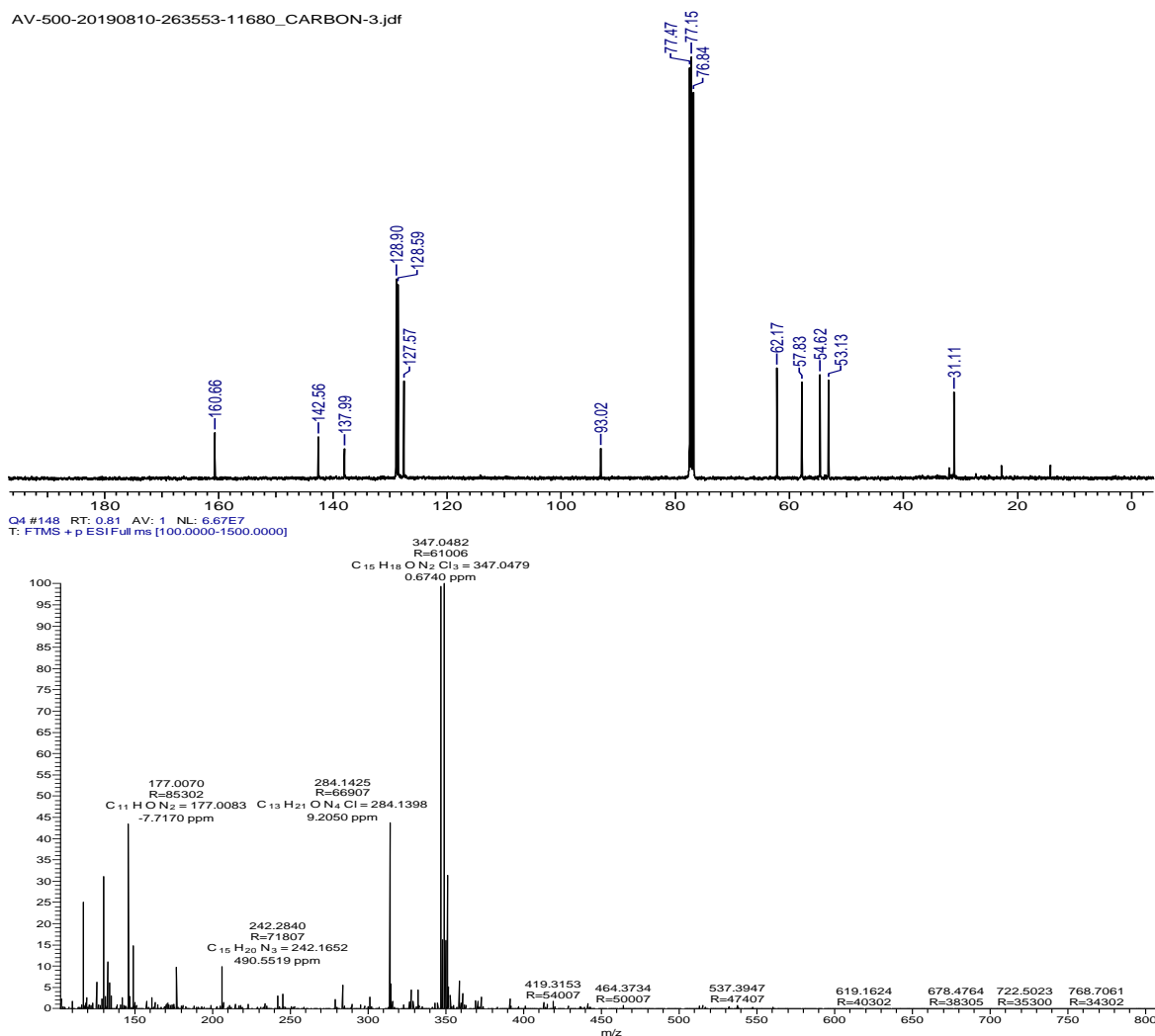
Fig. 14: ^{1}H, ^{13}C NMR and Mass spectra of (R)-N-(1-benzyl-4-methyl-1,2,3,6-tetrahydropyridin-3-yl)-2,2,2-trichloroacetamide **(103)**

shown in **Fig. 14**. In ^{1}H NMR, the aromatic protons of the phenyl ring are shown in the range of δ 7.25-7.32, and the remaining nonaromatic hydrogens showed at δ 1.25-4.39. In ^{13}C NMR, the characteristic amide functional group is shown at δ 160. Whereas the appearance of aromatic carbons in the range of δ 127-142 and nonaromatic carbons at δ 31-93. The formed allylic acetamide was further confirmed by taking its mass. Then the allylic trichloroacetamide moiety was subjected for the hydrolysis reaction by using aqueous sodium hydroxide in isopropanol solvent at room temperature to give allylic amine intermediate. Then, the crude amine (without

purifying) is treated for the subsequent reaction, *i.e.*, reductive amination reaction, giving the key intermediate of tofacitinib. Firstly the imine is formed when formaldehyde is added to the reaction followed by reduction using hydrogenation condition to give our key precursor of tofacitinib piperidine amine **44c** in 87% yield. The formation of **44c** was further confirmed by taking its ^{1}H and ^{13}C NMR analysis, as shown in **Fig.15**. In the ^{1}H NMR spectrum, the characteristic peak of methyl on piperidine ring and nitrogen atom is shown at δ 0.93-0.95 and 2.96-2.97. The benzyl-protected ring's protons showed δ 7.21-7.37 and aliphatic hydrogens of piperidine at δ 1.55-3.30. In the ^{13}C NMR spectrum, the aromatic carbons displayed at δ 126-138, and the remaining carbons of the piperidine ring showed at δ 18-71. The ^{1}H, ^{13}C NMR optical rotation and Mass data of obtained piperidine amine **11** is well-matched with the previous literature. Further use of this enantiopure piperidine amine **11** is undergoing in our laboratory.

AV-400-(11).002.001.1r.esp
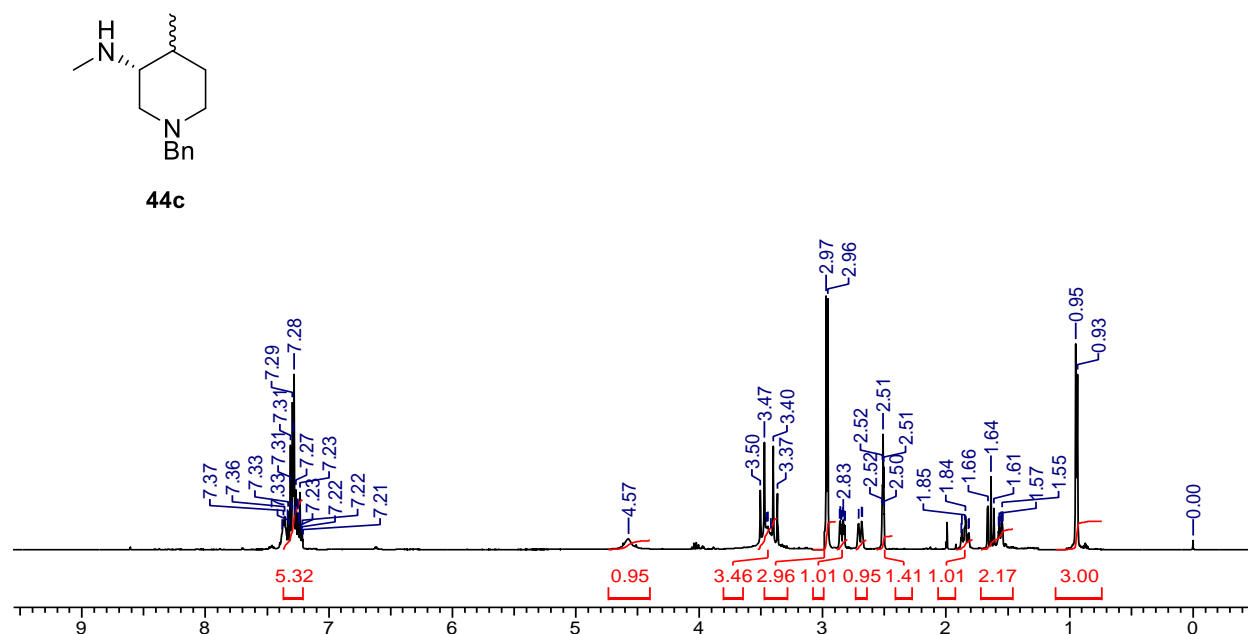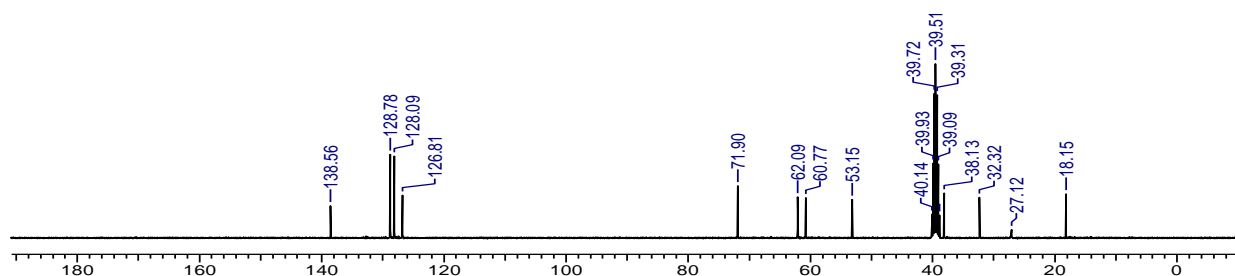
Fig. 15: ^{1}H and ^{13}C NMR of (3R)-1-benzyl-N,4-dimethylpiperidin-3-amine (**44c**)

1.2.4 Conclusion

In conclusion, we have developed the enantioselective synthesis of (3*R*)-1-benzyl-*N*,4-dimethylpiperidin-3-amine in 8 steps with nearly 98% *ee* and 32% overall yield. The compound **44c** is a crucial key intermediate of tofacitinib, and in this report, we have shown the straightforward and cheap route for their synthesis. The metal-free Overmann rearrangement is a key step for the present synthesis and other essential transformations employed in this route, such as Sharpless asymmetric dihydroxylation hydrolysis reaction. Further utilization of this key intermediate of tofacitinib is underway in our laboratory.

1.2.5 Experimental Section

1-Benzyl-4-methyl-1,2,3,6-tetrahydropyridine (79)

Add benzyl bromide (53.76 mmol) to a solution of 4-picoline (5 gm, 53.76 mmol) in acetone (50 mL) at 25 °C. Keep the mixture for 3 hours at 50-70 °C. Wash the formed precipitate with diethyl ether (3 x 15 mL). Dry the precipitate in vacuo to get 13.8 gm, 98% of quaternary pyridinium salt as white solid. Then this quaternary pyridinium salt was directly used for

subsequent reaction. Dissolve pyridinium salt (13.8 g, 52.47 mmol) in MeOH. Then the salt is reduced by slow addition of $NaBH_4$ (6 g, 157.41 mmol) over 1 hour at 0 °C. Leave the reaction mixture to stir for another 1 hour at room temperature. Then the reaction mixture is quenched by adding aqueous $NaHCO_3$ solution, extracted with ethyl acetate, and washed with brine. Dry the combined organic layers over Na_2SO_4 and concentrate the organic layer under reduced pressure to afford **79** light yellow oil.

Yield: 97% (9.5 g), fainy yellow oil. **^{1}H NMR** (500 MHz ,CDCl$_3$) δ 7.44 - 7.39 (m, 2 H), 7.36 (t, J = 7.5 Hz, 2 H), 7.32 - 7.28 (m, 1 H), 5.41 (td, J = 1.5, 3.1 Hz, 1 H), 3.62 (s, 2 H), 2.99 (br. s, 2 H), 2.69 - 2.50 (m, 2 H), 2.21 - 2.03 (m, 2 H), 1.73 (s, 3 H). **^{13}C NMR** (126 MHz,CDCl$_3$) δ 138.4, 132.7, 129.3, 128.2, 127.1, 119.3, 62.9, 53.0, 50.0, 30.9, 23.0.

(3R,4S)-1-Benzyl-4-methylpiperidine-3,4-diol (101)

Dissolve $K_3Fe(CN)_6$ (15.7 gm, 47.87 mmol), K_2CO_3 (6.6 gm, 47.87 mmol) and ligand (DHQ)$_2$PHAL (Hydroquinine 1,4-phthalazinediyl diether) (0.05 mmol) in tBuOH/H_2O (v/v = 1:1, 50 ml) at room temperature. Then add $K_2OsO_4.2H_2O$ (0.005 mmol) and then add $CH_3SO_2NH_2$ (1.6 gm, 15.95 mmol) to the reaction mixture at 0 °C. Stir the reaction mixture for 5 minutes. Add olefin **79** (3 gm, 15.95 mmol) to the mixture. Stir the reaction mixture vigorously at room temperature for 5 hours until TLC shows no olefin. Then quench the reaction by adding sodium sulfite to the mixture. Stir the reaction mixture for 30 min. Extract the aqueous phase with ethyl acetate (25 ml x 3). Wash the combined organic layers with brine solution. Dry the combined organic layers over anhydrous sodium sulfate. Evaporate the solvent under reduced pressure to obtain the crude product. Purify the crude product by flash column chromatography (pet. ether/EtOAc, 8:2) to afford the product **101** as white solid.

Yield: 90% (3.17 g), white solid. **^{1}H NMR** (400 MHz ,CDCl$_3$) δ 7.39 - 7.13 (m, 5 H), 3.60 - 3.45 (m, 2 H), 3.45 - 3.31 (m, 1 H), 3.16 - 2.88 (m, 1 H), 2.51 (br. s., 4 H), 2.27 (br. s., 1 H), 1.85 - 1.66 (m, 1 H), 1.60 (ddd, J = 3.9, 6.4, 13.5 Hz, 1 H), 1.22 - 1.12 (m, 3 H). **^{13}C NMR** (101 MHz ,CDCl$_3$) δ 138.0, 129.2, 128.4, 127.3, 72.8, 72.7, 69.8, 62.4, 55.8, 49.9, 43.5, 36.3. **HRMS** (ESI) m/z [M+H]$^+$ calcd for C$_{13}$H$_{20}$NO$_2$: 222.1741 found: 222.1738.

(S)-1-Benzyl-4-methyl-1,2,3,6-tetrahydropyridin-3-ol (102)

3 gm (*3R,4S*)-1-benzyl-4-methyl piperidine-3,4-diol **101** (13.57 mmol) in 30 mL toluene was stirred by adding 3.85 gm of para-toluenesulfonic acid monohydrate (20.36 mmol) at 100-110 °C for 8-12 hours. Then the reaction mixture was allowed to cool at room temperature and poured into cold water 50 mL contains 5 mL of aqueous ammonia. Extraction of the product with ethyl acetate (50 mL x 3) followed drying on sodium sulfate and concentration of organic layer under reduced pressure to afford the crude product. The crude product was purified using silica gel with ethyl acetate/pet. ether to obtain 2.06 gm of compound **102** in 85% yield as gummy semisolid.

Yield: 85% (2.06 g), gummy semisolid.**^{1}H NMR** (500 MHz ,CDCl$_3$) δ 7.35 - 7.25 (m, 5H), 4.96 (s, 1H), 4.81 (s, 1 H), 4.25 - 4.13 (m, 1H), 3.92 (br. s., 2H), 3.64 (s, 2 H), 2.77 - 2.65 (m, 1H), 2.65 - 2.50 (m, 3 H), 2.50 - 2.42 (m, 1H), 2.29 - 2.19 (m, 1H), 1.28 (br. s., 1H).**^{13}C NMR** (126 MHz ,CDCl$_3$) δ 147.1, 136.9, 129.8, 129.4, 128.7, 128.4, 128.3, 128.1, 127.5, 108.1, 70.2, 62.1, 60.7, 54.0, 31.1. **HRMS** (ESI) m/z [M+H]$^+$ calcd for C$_{13}$H$_{18}$NO: 204.1220 found: 204.1227.

(*S*)-1-Benzyl-4-methyl-1,2,3,6-tetrahydropyridin-3-yl 2,2,2-trichloroacetimidate (100)

2 gm of allylic alcohol 102 (9.85 mmol) was dissolved in 20 mL of dry DCM under a nitrogen atmosphere. Then 1.8 gm of DBU (1,8-Diazabicyclo[5.4.0]undec-7-ene) 11.82 mmol was added in the reaction vessel at 0 °C. After 5-minute, Trichloroacetonitrile (2.1 gm, 14.77 mmol) was

added, the reaction was allowed to stir at room temperature until the TLC showed no allylic alcohol. After complete conversion, water 20 mL was added to the reaction mixture and extracted with DCM. Crude product purified by using silica gel column chromatography with ethyl acetate /pet ether to obtain 3.30 gm, 97% of compound **100**.

(*R*)-*N*-(1-Benzyl-4-methyl-1,2,3,6-tetrahydropyridin-3-yl)-2,2,2-trichloroacetamide (103)

In an oven-dried 100 mL, round bottom flask, 2 gm of (*S*)-1-benzyl-4-methyl-1,2,3,6-tetrahydropyran-3-yl 2,2,2-trichloroacetimidate **100** (5.78 mmol) was dissolved in dry toluene, and then K_2CO_3 (1.6 gm, 11.56 mmol) was added at room temperature. Allow the reaction mixture to stir at 90-110 $^{\circ}$C for 12-18 hours until the complete conversion of **9**. After completion of reaction monitored by TLC, remove the solvent under reduced pressure, and water 10 mL was added in the reaction mixture. Extraction with ethyl acetate (50 mL x 3), drying on sodium sulfate, and concentration of organic layer under reduced pressure to afford the crude product. The crude product is purified using silica gel with ethyl acetate and pet ether to obtain 1.62 gm, compound **103** in 81% yield as faint yellow semisolid.

Yield: 81% (1.62 g), yellow semisolid. **^{1}H NMR** (400 MHz ,CDCl$_3$) δ 7.62 (br. s., 1 H), 7.39 - 7.20 (m, 6 H), 4.37 (td, *J* = 3.5, 7.6 Hz, 1 H), 3.65 (d, *J* = 13.3 Hz, 1 H), 3.47 (s, 1 H), 2.92 - 2.80 (m, 1 H), 2.74 (ddd, *J* = 1.6, 4.0, 11.3 Hz, 1 H), 2.51 - 2.37 (m, 2 H), 2.31 - 2.18 (m, 3 H), 1.25 (s, 3 H). **^{13}C NMR** (101 MHz ,CDCl$_3$) δ 160.7, 142.6, 138.0, 128.9, 128.6, 127.6, 93.0, 62.2, 57.8, 54.6, 53.1, 31.1. **HRMS** (ESI) m/z [M+H]$^{+}$ calcd for $C_{15}H_{18}OCl_3N_2$: 347.0479 found: 347.0482.

(*3R*)-1-Benzyl-N,4-dimethylpiperidin-3-amine (44c)

Dissolve (*R*)-N-(1-benzyl-4-methyl-1,2,3,6-tetrahydropyridin-3-yl)-2,2,2-trichloroacetamide (1 gm, 2.89 mmol) in Me$_2$CHOH (20 mL) and add 5.0 M aqueous sodium hydroxide solution (5.0 mL). Stir the reaction mixture for 1-2 hours at 25-75 $^{\circ}$C.; after completion of reaction monitored

by TLC, the solvent is concentrated in the vacuum. 10 mL water is added to the reaction mixture and extracted with CH_2CL_2 (3×15 mL). Dry the organic phase over sodium sulfate and concentrate under reduced pressure. Then the crude product is used for the next step without further purification. To a solution of crude amine obtained in the above step (430 mg, 2.10 mmol) dissolved in THF (10 mL) and then CH_2O (formaldehyde solution 37%) was added in the reaction vessel and stir the reaction for 1-2 hours at 25-50 $^{\circ}$C. After 1 hour, cool the reaction mixture to room temperature and then add ethyl acetate (5 mL), followed by adding 10% Pd/C (50 mg). Charge the mixture with H_2 (1 atm) and stir the reaction mixture at room temperature for 12 hours. After the completion of the reaction, it was filtered through a Celite pad and washed with EtOAc (3 x 15 mL). The combined organic phase was concentrated under vacuum to afford the crude product, purified by column chromatography on silica gel using CH_2Cl_2: MeOH as eluent to give (3*R*)-1-benzyl-N,4-dimethylpiperidin-3-amine **44c** in pure form as a light yellow oil (398 mg, 87% yield). 98.4 % *ee* and 32% overall yield.

Yield: 87% (398 mg), light yellow oil. **^{1}H NMR** (400 MHz , DMSO d$_6$) δ 7.37 - 7.21 (m, 6 H), 4.57 (br. s., 1 H), 3.52 - 3.37 (m, 4 H), 2.97 (d, *J* = 4.6 Hz, 3 H), 2.84 (ddd, *J* = 1.7, 4.4, 10.4 Hz, 1 H), 2.73 - 2.64 (m, 1 H), 2.51 (td, *J* = 1.8, 3.6 Hz, 1 H), 1.85 (dt, *J* = 2.5, 11.4 Hz, 1 H), 1.72 - 1.46 (m, 2 H), 0.94 (d, *J* = 5.9 Hz, 3 H).**^{13}C NMR** (101 MHz ,DMSO d$_6$) δ 138.6, 128.8, 128.1, 126.8, 71.9, 62.1, 60.8, 53.2, 38.1, 32.3, 27.1, 18.1. $[\alpha]^{25}_D$: -19.8 (c 1, MeOH).**HRMS** (ESI) m/z [M+H]$^+$ calcd for $C_{14}H_{23}N_2$: 219.1860 found: 219.1841.

1.2.6 References

1   Darout, E.; McClure, K. F.; Mascitti, V. Synthesis of spirofuranopyrimidine-piperidines. *Tetrahedron.***2012**, *68*, 4596–4599.

2   Mohite, A. R.; Sultane, P. R.; Bhat, R. G. BF$_3$·Et$_2$O and trifluoroacetic acid/triethyl amine-mediated synthesis of functionalized piperidines*.Tetrahedron Lett.***2012**, *53*, 30–35.

3   Vitaku, E.; Smith, D. T.; Njardarson, J. T. Analysis of the Structural Diversity, Substitution Patterns,

and Frequency of Nitrogen Heterocycles among U.S. FDA Approved Pharmaceuticals.*J. Med. Chem.***2014**, *57*, 10257–10274.

4   Taylor, R. D.; MacCoss, M.; Lawson, A. D. G. Rings in Drugs. *J. Med. Chem.***2014**, *57*, 5845–5859.

5   Sajadikhah, S. S.; Maghsoodlou, M. T.; Hazeri, N.; Habibi-Khorassani, S. M.; Willis, A. C. One-pot five-component synthesis of highly functionalized piperidines using oxalic acid dihydrate as a homogenous catalyst.*Chinese Chem.Lett.***2012**, *23*, 569–572.

6   Tite, T.; Lallemand, M.-C.; Poupon, E.; Kunesch, N.; Tillequin, F.; Gravier-Pelletier, C.; Merrer, Y. L.; Husson, H.-P. Synthesis of polyhydroxylated piperidines and evaluation as glycosidase inhibitors.*Bioorg. Med. Chem.* **2004**, *12*, 5091–5097.

7   Wilkinson, D. G.The pharmacology of donepezil: a new treatment for Alzheimer's disease.*Expert Opin. Pharmacother.***1999**, *1*, 121–135.

8   Schotte, A.; Janssen, P. F. M.; Gommeren, W.; Luyten, W. H. M. L.; Van Gompel, P.; Lesage, A. S.; De Loore, K.; Leysen, J. E.Risperidone compared with new and reference antipsychotic drugs: in vitro and in vivo receptor binding.*Psychopharmacology. (Berl)***1996**, *124*, 57–73.

9   (a)Li, F.; Wang, X.; Liu, Y. M.; Zhang, J.; Yang, J. J.Synthesis of 3,4,5-trisubstituted piperidine via S_N2' reaction.*Synth. Commun.* **2020,***50*, 56–62 (b) Mishra, S.; Ghosh, R.Efficient one-pot synthesis of functionalized piperidine scaffolds via $ZrOCl_2 \cdot 8H_2O$ catalyzed tandem reactions of aromatic aldehydes with amines and acetoacetic esters. *Tetrahedron Lett.* **2011**, *52*, 2857–2861.

10   Goel, P.; Alam, O.; Naim, M. J.; Nawaz, F.; Iqbal, M.; Alam, Md I. Recent advancement of piperidine moiety in treatment of cancer- A review. *Eur. J. Org. Chem.***2018**, *157*, 480-502.

11   Saeed, A.; Shahzad, D.; Faisal, M.; Larik, F. A.; El-Seedi, H. R.; Channar, P. A.Developments in the synthesis of the antiplatelet and antithrombotic drug (S)-clopidogrel**.** *Chirality.* **2017,***29*, 684 –707.

12   Bari, A.; Iqbal, A.; Khan, Z. A.; Shahzad, S. A.; Yar, M.Synthetic approaches toward piperidine related structures: A review. *Syn. Comm.***2020**, *17,* 2572–2589.

13   (a**)** Sales, M.; Charette, A. B. A Diels−Alder Approach to the Stereoselective Synthesis of 2,3,5,6-Tetra- and 2,3,4,5,6-Pentasubstituted Piperidines.*Org. Lett.***2005**, *7*, 5773–5776. (b) Dobbs, A. P.; Guesne, S. J. Rapid Access to *trans*-2,6-Disubstituted Piperidines: Expedient Total Syntheses of (-)-Solenopsin A and (+)-*epi*-Dihydropinidine.*Synlett.***2005**, *13*, 2101–2103. (c) Lebold, T. P.; Leduc, A. B.; Kerr, M. A. Zn(II)-Catalyzed Synthesis of Piperidines from Propargyl Amines and Cyclopropanes**.***Org. Lett.***2009**, *11*, 3770–3772. (d) Fustero, S.; Jimenez, D.; Moscardo, J.; Catalan, S.; Del Pozo, C.Enantioselective Organocatalytic Intramolecular Aza-Michael Reaction: a Concise Synthesis of (+)-Sedamine, (+)-Allosedamine, and (+)-Coniine**.***Org. Lett.***2007**, *9*, 5283–5286. (e) Brahmachari, G.; Das, S. Bismuth nitrate-catalyzed multicomponent reaction for efficient and one-pot synthesis of densely functionalized piperidine scaffolds at room temperature.*Tetrahedron Lett.* **2012**, *53*, 1479–1484. (f) Takasu, K.; Shindoh, N.; Tokuyama, H.; Ihara, M. Catalytic imino Diels–Alder reaction by triflic imide and its application to one-pot synthesis from three components.*Tetrahedron.***2006**, *62*, 11900–11906.

14   Khan, A. T.; Lal, M.; Khan, M. M. Synthesis of highly functionalized piperidines by one-pot multicomponent reaction using tetrabutylammonium tribromide (TBATB).*Tetrahedron Lett.* **2010,***51*, 4419–4424.

15   (a) Oefner, C.; Binggeli, A.; Breu, V.; Bur, D.; Clozel, J-P.; D'Arcy, A.; Dorn, A.; Fischli, W.; Grfininger, F.; Gtillert, R.; Hirth, G.; Marki, H.P.; Mathews, S.; Miiller, M.; Ridley, R. G.; Stadler, H.; Vieira, E.; Wilhelm, M.; Winkler F.K.; Wostl, W. Renin inhibition by substituted piperidines: A novel paradigm for the inhibition of monomeric aspartic proteinases.*Chemistry & Biology*.**1999,***6*, 127-131 (b) Fabio, R D.; Giovannini, R.; Bertani, B.; Borriello, M.; Bozzoli, A.; Donati, D.; Falchi, A.; Ghirlanda, D.; Leslie, C. P.; Pecunioso, A.; Rumboldt, G.; Spada, S. Synthesis and SAR of substituted tetrahydrocarbazole derivatives as new NPY-1 antagonists.*Bioorg. Med. Chem. Lett.* **2006**, *16,* 1749-1752.

16   (a) Vitaku, E.; Smith, D. T.; Njardarson, J. T.Analysis of the Structural Diversity, Substitution Patterns, and Frequency of Nitrogen Heterocycles among U.S. FDA Approved Pharmaceuticals.*J. Med. Chem.* **2014**, *57*, 10257-10274 (b) Taylor, R. D.; MacCoss, M.; Lawson, A. D. G. Rings in Drugs. *J. Med. Chem.***2014**, *57*, 5845–5859.

17   (a) Bailey, P. D.; Millwood, P. A.; Smith. P.D. Asymmetric routes to substituted piperidines**.***Chem. Commun.* **1998,** 633-640. (b) Jiang, J.; DeVita, R. J.; Doss, G. A.; Goulet, M. T.; Wyvratt. M. J.Asymmetric Synthesis of Chiral, Nonracemic Trifluoromethyl-Substituted Piperidines and Decahydroquinolines. *J. Am. Chem. Soc.***1999**, *121*, 593-594

18   Kaplan, M. H.; STAT signaling in inflammation, *JAKSTAT* 2, **2013**, 24198.

19   (a) Lightfoot, H. L.; Goldberg, F. W.; Sedelmeier, J. Evolution of Small Molecule Kinase Drugs.*ACS Med. Chem. Lett.* **2019**, *10*, 153-160. (b) Clark, J. D.; Flanagan, M. E.; Telliez, J-B. Discovery and Development of Janus Kinase (JAK) Inhibitors for Inflammatory Diseases. *J. Med. Chem.* **2014,***57*, 5023-5038. (c) Schwartz, D.M.; Kanno, Y.; Villarino, A.; Ward, M.; Gadina, M.; O'Shea, J. J. JAK inhibition as a therapeutic strategy for immune and inflammatory diseases. *Nat. Rev. Drug. Discov.* **2017,***16*, 843-862.

20   (a) Thorarensen, A.; Dowty, M. E.; Banker, M. E.; Juba, B.; Jussif, J.; Lin, T.; Vincent, F.; Czerwinski, R. M.; Casimiro-Garcia, A.; Unwalla, R.; Trujillo, J. I.; Liang, S.; Balbo, P.; Che, Y.; Gilbert, A. M.; Brown, M. F.; Hayward, M.; Montgomery, J.; Leung, L.; Yang, X.; Soucy, S.; Hegen, M.; Coe, J.; Langille, J.; Vajdos, F.; Chrencik, J.; Telliez, J. B. Design of a Janus Kinase 3 (JAK3) Specific Inhibitor   1-((2*S*,5*R*)-5-((7*H*-Pyrrolo[2,3-*d*]pyrimidin-4-yl)amino)-2-methylpiperidin-1-yl)prop-2-en-1-one (PF-06651600) Allowing for the Interrogation of JAK3 Signaling in Humans.*J. Med. Chem.* **2017**, *60*, 1971-1993. (b) Vijayakrishnan, L.; Venkataramana, R.; Gulati, P.Treating inflammation with the Janus Kinase inhibitor CP-690,550.*Trends Pharmacol. Sci.* **2011**, *32*, 25-34. (c) Seavey, M. M.; Dobrzanski, P. B. The many faces of Janus kinase.*Biochem. Pharmacol.* **2012**, *83*, 1136-1145. (d) Clark, J. D.; Flanagan, M. E.; Telliez, J.-B. Discovery and Development of Janus Kinase (JAK) Inhibitors for Inflammatory Diseases.*J. Med. Chem.* **2014**, *57*, 5023-5038.

21   Changelian, P. S.; Flanagan, M. E.; Ball, D. J.; Kent, C. R.; Magnuson, K. S.; Martin, W. H.; Rizzuti, B. J.;Sawyer, P. S.; Perry, B. D.; Brissette, W. H., McCurdy, S. P.; Kudlacz, E. M.; Conklyn, M. J.; Elliott, E. A.; Koslov, E. R.; Fisher, M. B.; Strelevitz, T. J.; Yoon, K.; Whipple, D. A.; Sun, J.; Munchhof, M. J.; Doty, J. L.; Casavant, J. M.; Blumenkopf, T. A.; Hines, M.; Brown, M. F. *et.al*. Prevention of Organ Allograft Rejection by a Specific Janus Kinase 3 Inhibitor. *Science,* **2003**, *302*, 875-878.

22   (a) Dhillon, S.Tofacitinib: A Review in Rheumatoid Arthritis.*Drugs*. **2017**, *77,* 1987-2001. (b) Berekmeri, A.; Mahmood, F.; Wittmann, M.; Helliwell, P.Tofacitinib for the treatment of psoriasis and psoriatic arthritis.*Expert Rev. Clin. Immunol.* **2018**, *14*, 719-730. (c) Fernandez-Clotet, A.; Castro-Poceiro, J.; Panes, J. Tofacitinib for the treatment of ulcerative colitis. *Expert Rev. Clin. Immunol.* **2018**, *14*, 881. (d) Zand, M. S.Tofacitinab in Renal Transplantation.*Transplant. Rev. (Copenhagen, Den.)*, **2013**, *27*, 85-89. (e) De Vries, L. C. S.; Wildenberg, M. E.; De Jonge, W. J.; D′Haens, G. R. The Future of Janus Kinase Inhibitors in Inflammatory Bowel Disease.*J. Crohn's Colitis*. **2017**, *11*, 885-893.

23   (a) Carvalho, L.C.R.; Lourenço, A.; Ferreira, L. M.; Branco, P.S. Tofacitinib synthesis–an asymmetric challenge*Eur. J. Org. Chem.* **2019**, 615-624. (b) Hao, B.-Y.; Liu, J.-Q.; Zhang, W.-H.; Chen, X.-Z. **A** Novel Asymmetric Synthesis of *cis*-(3*R*,4*R*)-*N*-(*tert*-Butoxycarbonyl)-4-methyl-3-(methylamino)piperidine.*Synthesis,* **2011**, *8*, 1208-1212. (c). Liao, H.C.; Uang, B.J.Formal asymmetric synthesis of (+)-tofacitinib.*Tetrahedron: Asymmetry*, **2017**, *28*, 105-109.

24   A. Maricán, M. J. Simirgiotis, L. S. Santos. Asymmetric total synthesis of Tofacitinib.*Tetrahedron Lett.***2013**, *54*,5096-5098.

25   Cai, W.;Colony, J. L.; Frost, H.; Hudspeth, J. P.; Kendall, P. M.; Krishnan, A. M.; Makowski, T.; Mazur, D. J.; Phillips, J.; Brown Ripin, D. H. An Improved and Efficient Process for the Preparation of Tofacitinib Citrate.*Org. Process Res. Dev.* **2005,** *9*, 51.

26   (a) Kamble, R. B.; Gadre, S. H.; Suryavanshi, G. M.A formal asymmetric synthesis of (2*S*,4*R*)-4-hydroxypipecolic acid via Co(III)(salen)-catalyzed two stereocentered HKR of racemic azido epoxide. *Tetrahedron Lett.* **2015**, *56,* 1263-1265. (b) Kamble, R. B.; Suryavanshi, G. M.Synthesis of key intermediate for (+)-tofacitinib through Co^III(salen)-catalyzed two stereocentered hydrolytic kinetic resolution of (±)-methyl-3-(oxiran-2-yl)butanoate.*Synth. Commun*.**2018,***48*, 1045-1051.

27   Moustafa, M. M. A. R.; Pagenkopf, B. L. Ytterbium Triflate Catalyzed Synthesis of Alkoxy-Substituted Donor−Acceptor Cyclobutanes and Their Formal [4 + 2] Cycloaddition with Imines: Stereoselective Synthesis of Piperidines. *Org. Lett.* **2010***, 12*,3168-3171.

28   (a) Devalankar, D. A.; Chouthaiwale, P. V.; Sudalai, A.Organocatalytic sequential α-aminoxylation and *cis*-Wittig olefination of aldehydes: synthesis of enantiopure γ-butenolides.*Tetrahedron:Asymmetry,***2012**, *23*, 240-244 (b) Hayashi, Y.; Yamaguchi, J.; Sumiya, T.; Hibino, K.; Shoji, M.Direct Proline-Catalyzed Asymmetric α-Aminoxylation of Aldehydes and Ketones. *J. Org. Chem*.**2004,** 69, 5966-5973

29   Jiang, J-k.; Ghoreschi, K.; Deflorian, F.; Chen, Z.; Perreira, M.; Pesu, M.; Smith, J.; Liu, E.; Leister, W.; Costanzic, S.; O'Shea, J. J.; Thomas, C. J. *J. Med. Chem.* **2008**, *51*, 8012-8018.

30   (a) Maryanoff, B. E.; Zhang, H.-C.; Cohen, J. H.; Turchi, I. J.; Maryanoff, C. A.;Cyclizations of N-acyliminium ions. *Chem. Rev.* **2004**, *104*, 1431-1628. (b) Royer, J.; Bonin, M.; Micouin, L.Chiral heterocycles by iminium ion cyclization. *Chem. Rev.* **2004**, *104*, 2311-2352.

31   (a) Goel, P.; Alam, O.; Naim, M. J.; Nawaz, F.; Iqbal, M.; Alam, M.I.; Recent advancement of piperidine moiety in treatment of cancer-A review. *Eur. J. of Med. Chem.* **2018**, *157*, 480-502. (b) Vikatu, E.; Smith, D.T.; Njardason, J. T.; Analysis of the structural diversity, substitution patterns, and frequency of nitrogen heterocycles among US FDA approved pharmaceuticals: miniperspective. *J. med. Chem.* **2014**, *57*, 10257.

32   Kulagowski, J. J.; Blair, W.; Bull, R. J.; Chang, C.; Deshmukh, G.; Dyke, H. J.; Eigenbrot, C.;Ghilardi, N.; Gibbons, P.; Harrison, T. K.;Identification of imidazo-pyrrolopyridines as novel and potent JAK1 inhibitors. *J. Med. Chem.* **2012,** *55*, 5901.

33   (a) Vijayakrishnan, L.; Venkataramana, R.; Gulati, P.Treating inflammation with the Janus kinase inhibitor CP-690,550. *Trends Pharmacol. Sci.* **2011**, *32*, 25-34. (b) Seavey, M. M.; Dobrzanski, P. B.The many faces of Janus kinase. *Biochem. Pharmacol.* **2012**, *83*, 1136-1145. (c) Clark, J. D.; Flanagan, M. E.; Telliez, J.-B. Discovery and development of Janus Kinase (JAK) inhibitors for inflammatory diseases: Miniperspective. *J. Med. Chem.* **2014**, *57*, 5023-5038. (d) Haan, G.; Kreis, S.; Margue, C.; Behrmann, I. Jaks and cytokine receptors-an intimate relationship. *Biochem. Pharmacol.* **2006**, *72*, 1538-1546. (e) Ghoreschi, K.; Laurence, A. O.; Shea, J. J.Janus kinases in immune cell signaling. *Immunol. Rev.* **2009**, *228*, 273-287. (f) Shuai, K.; Liu, B.Regulation of JAK–STAT signalling in the immune system. *Nat. Rev. Immunol.* **2003**, *3*, 900-911. (g) O'Shea, J. J.; Plenge, R.JAK and STAT signaling molecules in immunoregulation and immune-mediated disease. *Immunity* **2012**, *36*, 542-550. (h) Clark, J. D.; Flanagan, M. E.; Telliez, J.-B.Discovery and development of Janus Kinase (JAK) inhibitors for inflammatory diseases: Miniperspective. *J. Med. Chem.* **2014**, *57*, 5023-5038. (i) Changelian, P. S.; Flanagan, M. E.; Ball, D. J.; Kent, C. R.; Magnuson, K. S.; Martin, W. H.; Rizzuti, B. J.;Sawyer, P. S.; Perry, B. D.; Brissette, W. H.Prevention of organ allograft rejection by a specific Janus kinase 3 inhibitor. *Science* **2003**, *302*, 875-878.

34   Brown Ripin, D. H.; Abele, S.; Cai, W.; Blumenkopf, T.; Casavant, J. M.; Doty, J. L.; Flanagan,M.; Koecher, C.; Laue, K. W.; McCarthy, K.Development of a Scaleable Route for the Production of cis-N-Benzyl-3-methylamino-4-methylpiperidine. *Org. Process Res. Dev.* **2003**, *7*, 115-120.

35   Ruggeri, S. G.; Hawkins, J.; Makowski, T.; Rutherford, J.;Pyrrolo[2,3-D]pyrimidinederivatives ; their intermediates and synthesis.**F. Urban, WO/2007/ 012953, 2007**

36   Patil, Y. S.; Bonde, N. L.; Kekan, A. S.; Sathe, D. G.; Das, A.;An improved and efficient process for the preparation of tofacitinib citrate. *Org. Process Res. Dev.* **2014,** *18*, 1714-1720.

37   Jiang, J.; Ghoreschi, K.; Deflorian, F.; Chen, Z.; Perreira, M.; Pesu, M.; Smith, J.; Nguyen, D.; Liu, E. H.; Leister, W.; Costanzi, S.; Shea, J. J. O.; Thomas, C. J.Examining the Chirality, Conformation and

Selective Kinase Inhibition of 3-((3 R, 4 R)-4-methyl-3-(methyl (7H-pyrrolo [2, 3-d] pyrimidin-4-yl) amino) piperidin-1-yl)-3-oxopropanenitrile (CP-690,550). *J. Med. Chem.* **2008**, *51*, 8012-8018.

38 Hao, B.-Y.; Liu, J.-Q.; Zhang, W.-H.; Chen, X.-Z.Chiral Pool Synthesis of N-Cbz-cis-(3R, 4R)-3-methylamino-4-methylpiperidine from L-Malic acid. *Bull. Korean Chem. Soc.* 2013,34, 1371–1377.

39 Stavber, G.; Cluzeau, J. New synthetic route for the preparation of 3-amino-piperidine compounds.**WO/2014/016338, 2014.**

40 Hao, B.-Y.; Liu, J.-Q.; Zhang, W.-H.; Chen, X.-Z.A Novel Asymmetric Synthesis of cis-(3R, 4R)-N-(tert-Butoxycarbonyl)-4-methyl-3-(methylamino) piperidine. *Synthesis,* 2011,8, 1208-1212.

41 Cai, W.; Colony, J. L.; Frost, H.; Hudspeth, J. P.; Kendall, P. M.; Krishnan, A. M.; Makowski, T.; Mazur, D. J.; Phillips, J.; B. Ripin, D. H.; Ruggeri, S. G.; Stearns, J. F.; White,, T. D.Investigation of practical routes for the kilogram-scale production of cis-3-methylamino-4-methylpiperidines. *Org. Process Res. Dev.***2005**, *9*, 51–56.

42 Ripin, D. H. B. 3-amino-piperidine derivatives and process for their preparation. **WO/2004/046112,2004**

Chapter II

Development of Metal-Free Regioselective Cross Dehydrogenative Coupling (CDC) of Cyclic Ethers with Aryl Carbonyls and Quinoxalin-2(1H)-ones

1.   "Metal-Free Regioselective Cross Dehydrogenative Coupling of Cyclic Ethers and Aryl Carbonyls." **Mane, K. D.;** Mukherjee, A.; Vanka, K.; Suryavanshi, G. *J. Org. Chem.* **2019**, *84*, 4, 2039-2047.

2.   "Visible Light Mediated, Metal and Oxidant Free Highly Efficient Cross Dehydrogenative Coupling (CDC) Reaction between Quinoxalin-2(1H)-ones and Ethers." **Mane**, **K. D.;** Kamble, R. B.; Suryavanshi, G. *New J. Chem.*, **2019**, *43*, 7403-7408.

2.1.1 Introduction

The C-C bond formation *via* C-H bond activation of sp^3, sp^2 hybridized carbons as cross-coupling participants have received renewed attention over the last few decades.[6a-b] However, sp^3 C-H bond activation is a challenging task due to their inertness, gained from high bond energy and high Pka value. Hence, CDC reactions have attracted the attention of organic chemists to prepare C-C bonds under metal and metal-free conditions in academic and industrial research.[6c-f]
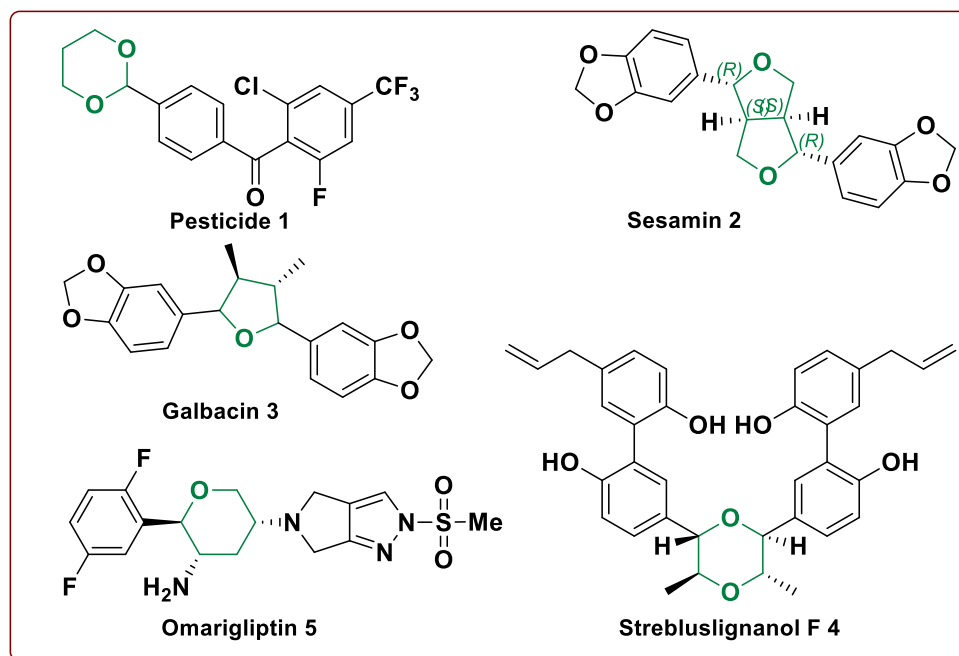
Figure 1. Biologically active cyclic ethers

From the last decades, CDC reactions have grabbed the attention of organic chemists for the formation of new C-C bonds. The coupling between $C(sp^2)$-H bonds has been extensively carried out using the CDC approach due to the easy accessibility of the starting material and makes this transformation an important tool for the formation of C-C bonds. In most of the C-C bond formation reactions, pre-functionalization of starting material is needed. The important aspect of the CDC reaction is that the pre-functionalization of starting material is averted.

Section I

Metal-Free Regioselective Cross Dehydrogenative Coupling of Cyclic Ethers and Aryl Carbonyls

Functional functionalized cyclic ethers are necessary scaffolds found in various natural products and pharmaceutical ingredients.[1] Generally, tetrahydrofuran (THF), 1,4-dioxane, and tetrahydropyrans (THP) are examples of cyclic ethers. These compounds show a broad spectrum of biological activity, including antibacterial,[2a] anti-inflammatory,[2b] anti-cancer,[2c-e] and anti-diabetic.[2f-g] They have also been employed in synthesizing agricultural pesticide **1**(Figure 1).[3] Lignins are the class of natural compounds that exclusively contain substituted THF as a core unit.[5] Examples of lignins includes Sesamin **2** and Galbacin **3** (Figure 1): these exhibit anti-cancer,[4a] anti-oxidant,[4b] anti-inflammatory,[4c] and anti-obesity [4d] activities. Strebluslignanol F **4**, a natural product that contains 1, 4-dioxane is a core unit and shows potent anti-hepatitis B virus activity.[5a] On the other hand, omaragliptin **5** is an oral anti-diabetic drug with substituted THP as the core moiety.[5b]

2.1.2 Review of Literature

After a careful survey of the literature, we realized that both metal and metal-free approaches had been used for the oxidative cross dehydrogenative coupling of cyclic ethers with arenes and heteroarenes. Some of these important methods include the use of transition metals such as Cu (I) catalyzed cross-coupling between substituted 1,1'-diarylethenes and cyclic ethers, [7] Cu (II) catalyzed addition of α-oxyalkyl radical to isoquinolinium salts [8] and Fe (II) catalyzed α-arylation of cyclic and acyclic ethers with azoles.[9]

Doyle's Approach (2016)[10]

In 2016 Doyle and co-workers had achieved α-arylation of cyclic ethers through Ni (II) catalyzed photo-redox coupling between an aryl halide and cyclic ethers, as shown in **Scheme 1**. In this approach, the author reported the nickel catalyzed oxidative addition of aryl chlorides followed by reductive elimination to form the aryl ethers in the catalytic amount of photocatalyst.
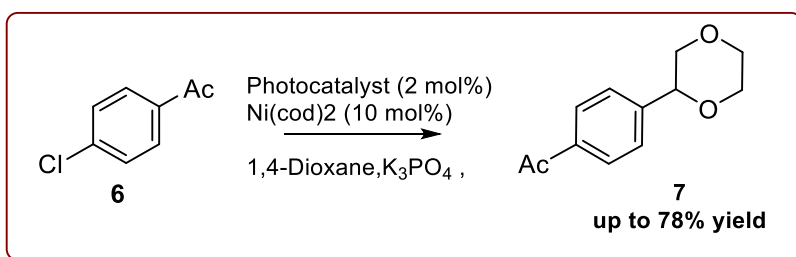
Scheme 1: Arylation of ethers by Ni catalyst

Shirakawa's Approach (2017)[15]

Various electron-deficient heterocyclic arenes were subjected for *α*-arylation of cyclic and acyclic ethers under oxidative metal-free conditions using a variety of oxidants such as DTBP, TBHP, BPO, and $K_2S_2O_8$. These heterocycles contain substituted pyridines,[11] thiophenes,[12] indoles,[13] quinines,[14] azoles,[15] and chromanes.[16] Although these methods efficiently yields the CDC product, but they are limited to activated heterocyclic systems. Recently, Shirakawa et al. reported base promoted oxidative dehydrogenative coupling between a substituted benzene derivative and cyclic ethers and amides in the presence of DTBP oxidant and NatBuO base (**Scheme 2**).[17]
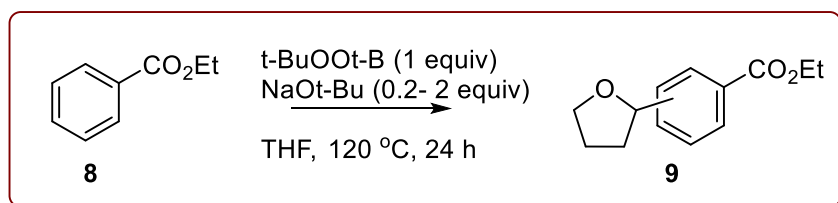
Scheme 2. Alkylation of ethers on aryl carbonyls

Despite some advantages, the reaction suffers from limitations such as, poor yields and regioselectivity when electron withdrawing substituents were present on the aryl rings.

Lei's Approach (2014)[23]

In 2014 the Lei and a co-worker reported the synthesis of allylic ethers from various substituted styrenes with ether derivatives. The CuI was the ideal catalyst for this transformation, and DTBP as an oxidant in an inert condition of N_2 reaction proceeded well to give the allylic ethers in good to excellent yields (**Scheme 3**).
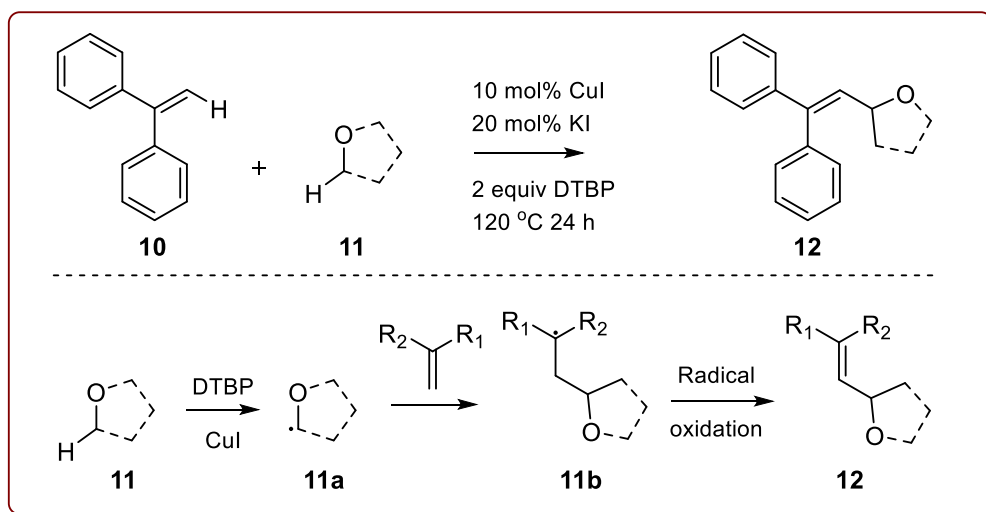
Scheme 3. Oxidative alkenylation of cyclic ethers

2.1.3 Present Work

2.1.3.1 Objective

 Inspired by the metal-free approach,[18] our motive has been to develop a synthetic method for the α-functionalization of cyclic ethers with better yields and regioselectivity (**Scheme 4**). Thus, we have described the metal-free CDC reaction *via* Csp^3-Csp^2 coupling between various cyclic ethers and aromatic carbonyls to generate a wide range of α-arylated cyclic ethers. The key

features of this reaction are short reaction time, good to excellent yields, and high
regioselectivity.
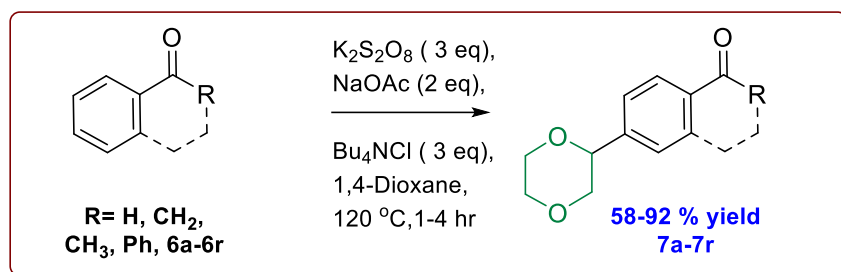
Scheme 4. CDC coupling of aryl carbonyls with ethers

2.1.4 Result and Discussion

We have started our investigation by taking acetophenone as a model substrate and 1,4-dioxane
as a coupling partner and solvent. The results are summarised in **Table 1**. Initially, when
acetophenone **6a** (1 equiv) and 1,4-dioxane (30 equiv., also acts as the solvent) are reacted at 120
°C in the presence of oxidant $K_2S_2O_8$ (3 equiv), tetra butyl ammonium bromide (A) (2 equiv) as
an additive and NaOAc (2 equiv), to our delight we got the expected product **7a** in 51% yield
within 4 h of reaction time (Table1, entry 1). Increase in reaction time from 4 h to 12 h, the yield
of **7a** reduces to 45% due to the decomposition of the obtained product (Table1, entry 2). With
increased equivalence of tetra butyl ammonium bromide (A) from 2 to 3 and refluxing at 120 °C,
we obtained a 57% yield of the desired product (Table1, entry 3). When tetrabutyl ammonium
chloride (B) was used instead of tetra butyl ammonium bromide (A) as an additive, and the
mixture refluxed for 4 h, we got the expected product in 81% yield, which was a significant
improvement (Table1, entry 4) in comparison to the first 3 entries (Table1, entry 1 to 3). We also
observed that the reaction did not proceed in the absence of additive as well as base (Table1,
entries 5 & 6) and resulted in the recovery of the starting material. By increasing the additive

tetra butyl ammonium chloride (B) from 3 to 4 equiv, we observed an increase in yields only by

4% (Table1, entry 7).

Table 1. Optimization of Reaction Conditions[a]

Entry	Oxidant (3 equiv.)	Addtive (equiv.)	Base (equiv.)	Time (h)	Yield (%)[a]
1	$K_2S_2O_8$	A (2)	NaOAc (2)	4	51
2	$K_2S_2O_8$	A (2)	NaOAc (2)	12	45
3	$K_2S_2O_8$	A (3)	NaOAc (2)	4	57
4[b]	$K_2S_2O_8$	B (3)	NaOAc (2)	4	81
5	$K_2S_2O_8$	B (3)	-	4	N.R.
6	$K_2S_2O_8$	-	NaOAc (2)	12	N.R.
7	$K_2S_2O_8$	B (4)	NaOAc (2)	4	85
8	$K_2S_2O_8$	B (3)	NaOAc (4)	4	79
9	$Na_2S_2O_8$	B (3)	NaOAc (2)	12	31
10	$(NH_4)_2S_2O_8$	B (3)	NaOAc (2)	12	N.R.
11[c]	$K_2S_2O_8$	B (3)	NaOAc (2)	12	N.R.
12[d]	$K_2S_2O_8$	C (3)	NaOAc (2)	4	67
13	$K_2S_2O_8$	B (3)	K_2CO_3 (2)	4	N.R.
14	$K_2S_2O_8$	B (3)	NaOEt (2)	4	70
15	$K_2S_2O_8$	B (3)	Cs_2CO_3 (2)	4	N.R.
16	$K_2S_2O_8$	B (3)	NaOtBu (2)	4	N.R.
17	$K_2S_2O_8$	-	Bu4NOH	4	N.R.

18	$K_2S_2O_8$	D (2)	NaOAc (2)	12	55
19	$K_2S_2O_8$	D (2)	-	12	N.R.
20	Oxone	B (3)	NaOAc (2)	4	17
21	TBHP	B (3)	NaOAc (2)	4	N.R.
22	DTBP	B (3)	NaOAc (2)	4	Trace
23	BPO	B (3)	NaOAc (2)	4	N.R.

[a] Reaction condition: 6a (0.83 mmol), $K_2S_2O_8$ (2.5 mmol), TBACl (2.5 mmol 50% aq. solution), Na**O**Ac (1.66 mmol), 1,4-Dioxane (3 ml) and Temp. 120 °C. [b] TBACl in 50% aq. solution. [c] Temp. 80 °C. [d] $Bu_4NF.3H_2O$. N.R. = No Reaction.

Keeping the tetra butyl ammonium chloride (B) (3 equiv), $K_2S_2O_8$ (3 equiv) constant and increasing the stoichiometry of NaOAc (2 to 4 equiv) lead to 79 % yield for the CDC product (Table 1, entry 8). The oxidant $Na_2S_2O_8$ offers only 31% yield of the desired product (Table 1, entry 9). No conversion was observed using $(NH_4)_2S_2O_8$ (Table 1, entry 10). However, no significant improvement was observed with use of the different combinations of additives and bases. Instead, most of the attempts were not fruitful (Table 1, entries 11-23). However, changing the bases didn't lead to an enhancement in the yields. We examined the effect of atmospheric oxygen by conducting the reaction under an inert atmosphere, which did not affect the yield. In addition to this, the impact of the solvent was also studied. Therefore, we achieved the best regioselectivity and the highest yield of the isolated product using $K_2S_2O_8$ (3 equiv.), tetra butyl ammonium chloride (B) (3 equiv.), and NaOAc (2 equiv.) for the reaction at 120 °C for 4 h (Table1, entry 4).).

With these optimized reaction conditions in hand (**Table 1**, entry 4), we studied the substrate scope of this unique transformation, and limitations of the CDC reaction were studied by

Table 2. CDC Reaction between Aromatic Ketones and Cyclic Ethers
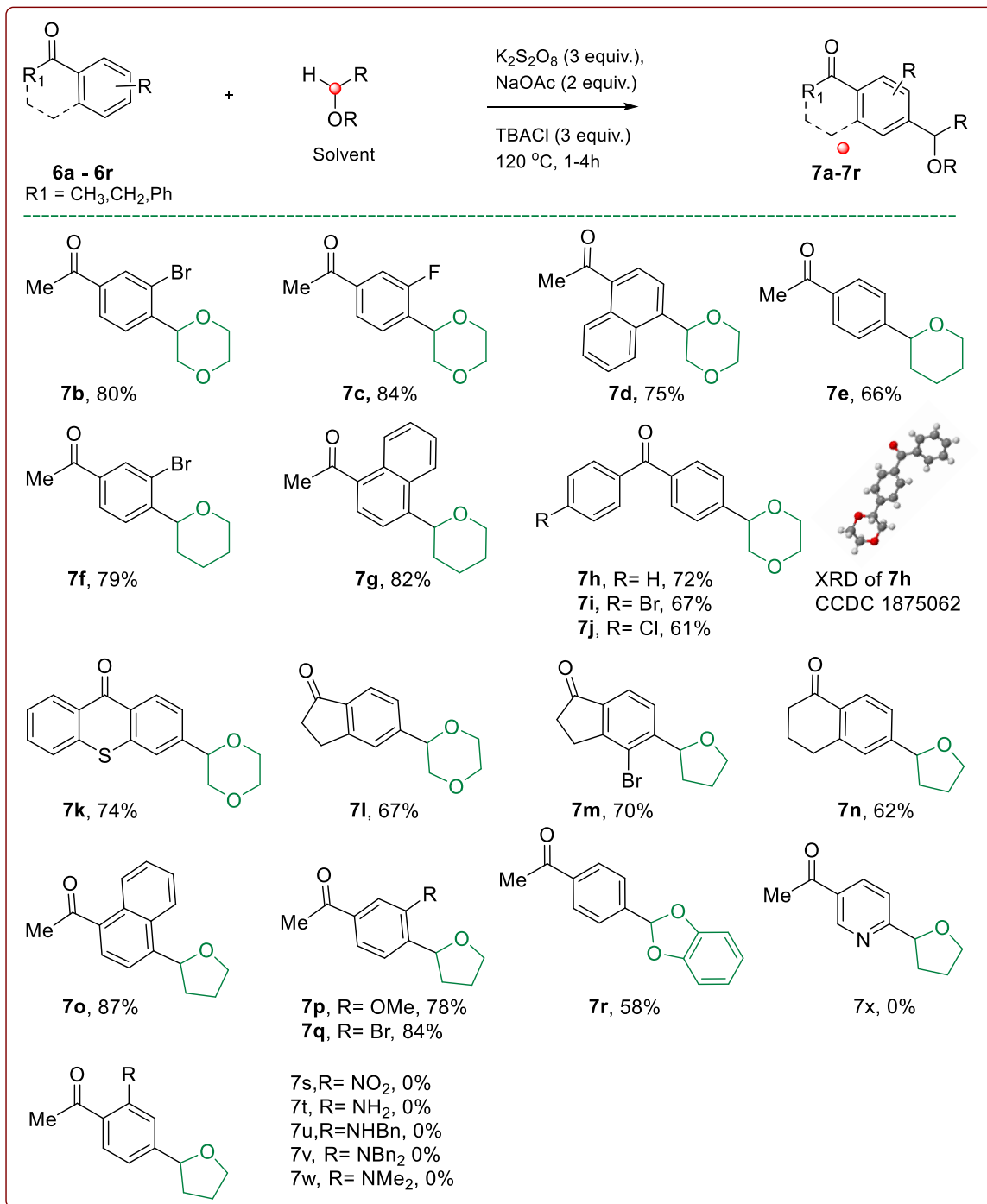
6a - 6r
R1 = CH₃,CH₂,Ph

K₂S₂O₈ (3 equiv.), NaOAc (2 equiv.)

TBACl (3 equiv.)
120 °C, 1-4h

7a-7r

7b, 80%

7c, 84%

7d, 75%

7e, 66%

7f, 79%

7g, 82%

7h, R= H, 72%
7i, R= Br, 67%
7j, R= Cl, 61%

XRD of **7h**
CCDC 1875062

7k, 74%

7l, 67%

7m, 70%

7n, 62%

7o, 87%

7p, R= OMe, 78%
7q, R= Br, 84%

7r, 58%

7x, 0%

7s,R= NO₂, 0%
7t, R= NH₂, 0%
7u,R=NHBn, 0%
7v, R= NBn₂ 0%
7w, R= NMe₂, 0%

Reaction condition: 6a (0.83 mmol), K₂S₂O₈ (2.5 mmol), TBACl (2.5 mmol 50% aq. solution), NaOAc (1.66 mmol), 1,4-Dioxane (3 ml) and Temp. 120 °C.

evaluating a variety of aryl carbonyls to investigate the generality of this reaction. As shown in **Table 2**, the CDC reaction proceeds without any difficulty for a wide range of substrates bearing various substituents at different positions on the aryl ketones, providing the coupling products in moderate to good yields. When the electron-withdrawing and electron-donating groups were present at the meta position to the acetyl group and the reaction was done under optimised conditions, the desired products were obtained in excellent yields (**7b**, **7c, 7f**). The unsubstituted acetophenone was subjected to the standard reaction conditions with THP as coupling ether, and gave the desired product **7e** in 66% yield. 1-Acetonaphthone also gave the expected α-arylated products of different cyclic ethers with excellent yields (**7d**, **7g**, **7o**). On the other hand, substituted cyclic ketones such as indanone and tetralone resulted in moderate yields of the products (**7l-7n**). It is noteworthy that thioxanthone successively delivered CDC product **7k** under oxidation condition without any diverse effect on sulfur. When acetophenone was subjected to standardized reaction conditions using 1,3-benzodioxole as a solvent, it offered a corresponding product **7r** in 58 % yield. Also, acyclic ethers were subjected as a coupling partner, leading to the formation of undesired polymerization. Unfortunately, this approach failed to give expected CDC products when the reaction was carried out on N-substituted aryl carbonyls and heterocyclic aryl ketones (**7s-7x**). The formation of **7a-7r** was confirmed by measuring their corresponding ^{1}H, ^{13}C and HRMS spectral data.

Example 1:

The structure of 1-(4-(1,4-dioxan-2-yl)phenyl)ethan-1-one **7a** was confirmed from its ^{1}H and ^{13}C NMR spectrum. In ^{1}H NMR spectrum, which showed singlet for methyl group hydrogen at δ 2.59 (s, 3 H), multiples for aromatic hydrogens at δ 7.99 - 7.87 (m, J = 8.4 Hz, 2H) and 7.54 - 7.39 (m, J = 8.0 Hz, 2H). The hydrogens present in the ether moiety are showed in the range of

4.68 (dd, J = 2.3, 9.9 Hz, 1H), 3.98 - 3.94 (m, 1H), 3.92 (dd, J = 2.3, 11.1 Hz, 1H), 3.89 - 3.86 (m, 1H), 3.83 - 3.79 (m, 1H), 3.74 (dd, J = 3.1, 11.4 Hz, 1H) and 3.41 (t, J = 10.9 Hz. In ^{13}C NMR spectrum of compound **7a** the characteristic peak of carbonyl group was showed in at δ 197 (**Figure 2**).
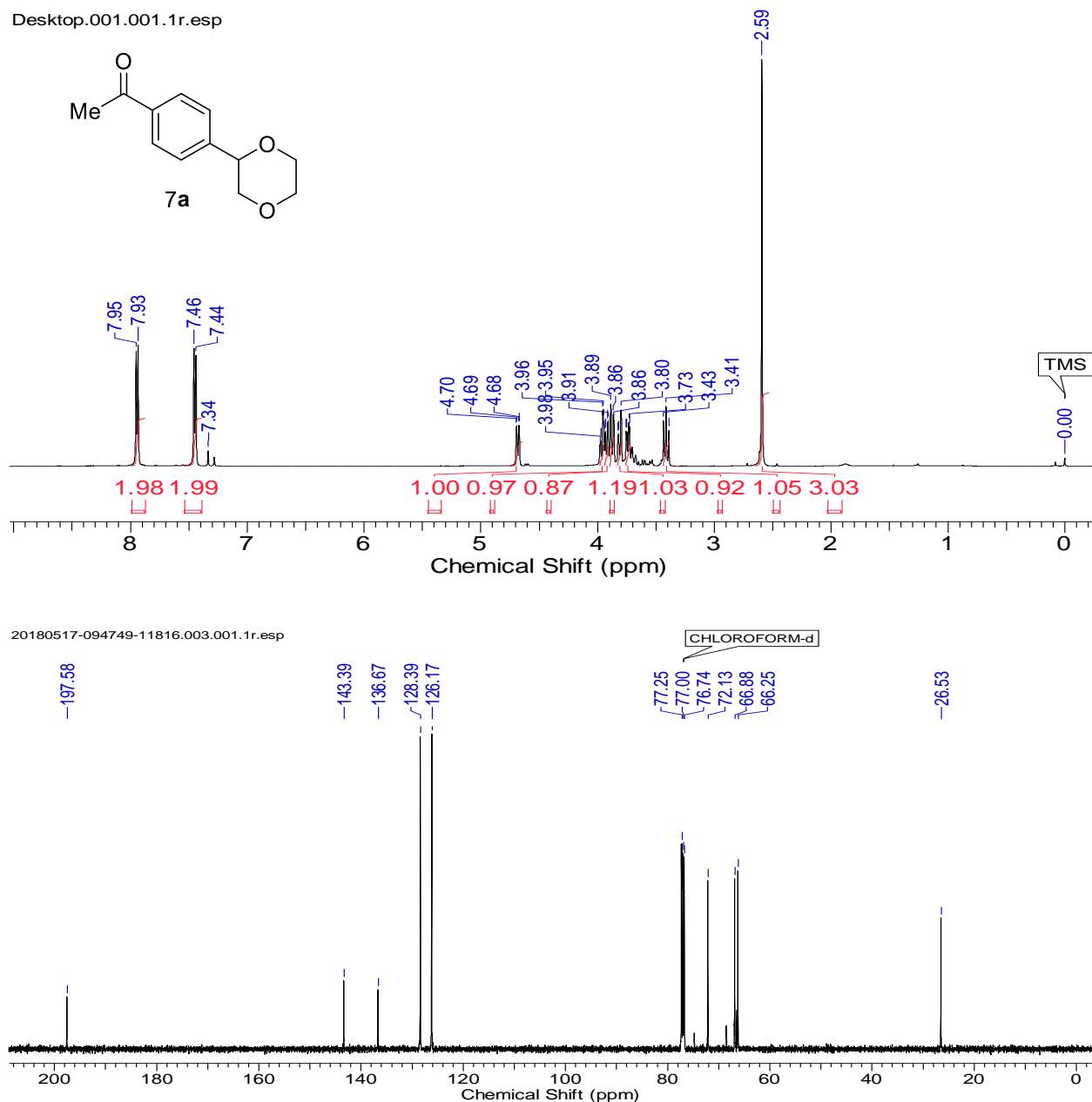
Figure 2. ^{1}H and ^{13}C NMR of 1-(4-(1,4-dioxan-2-yl)phenyl)ethan-1-one (**7a**)

Table 3. CDC Reaction between Aromatic Aldehydes and Cyclic Ethers[a]
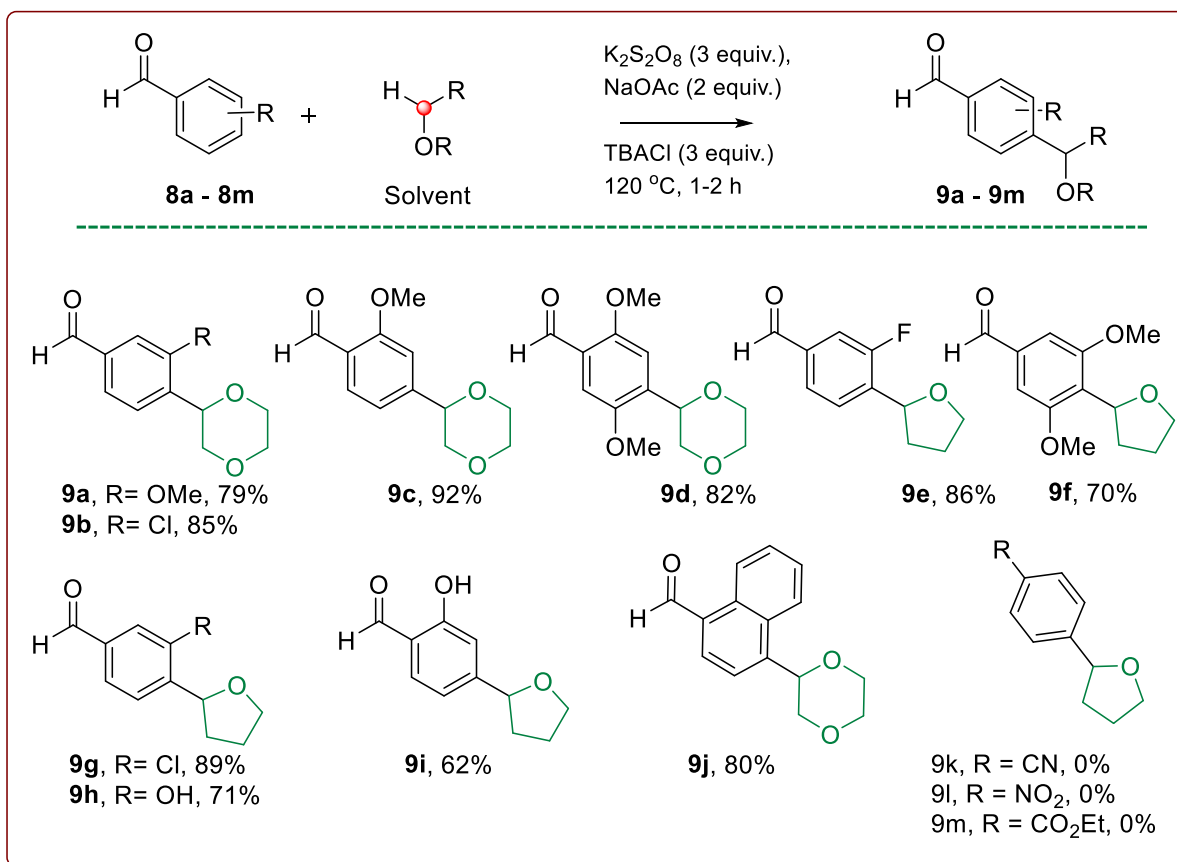
[a]Reaction condition: 8a (0.73 mmol), $K_2S_2O_8$ (2.20 mmol), TBACl (2.20 mmol 50% aq. solution), NaOAc (1.47 mmol), 1,4-Dioxane (3 ml) at 120 °C.

Next, we examined the efficiency of substituted aldehydes as coupling partners under the optimized experimental conditions. Notably, it was observed that the rate of the CDC reaction between benzaldehydes and cyclic ethers was faster than for the aryl ketones (**Table 3**). Various substrates having electron-withdrawing substituents, such as Cl, Br, and F groups on the aromatic ring of the aldehydes were efficiently reacted to produce the substituted para-alkylated benzalehydes with excellent yields (**Table 3**, entries **9b**, **9e,** and **9g**). Surprisingly, hydroxyl-substituted benzaldehydes also offer good yields of alkylated aryl carbonyls under oxidative conditions (**9h** and **9i**). Benzaldehydes with different electron-donating substituents also led to

the corresponding product with good to excellent yields (**9c**, **9d** & **9f**). A reaction performed with 2,5-dimethoxy benzaldehyde on a 6 mmol scale provided **9d** in 79% yield. Cyano, nitro, and carboxylate substituted aryl derivatives were unable to give the desired product with our optimized reaction conditions (**9k-m**).

Example 2:
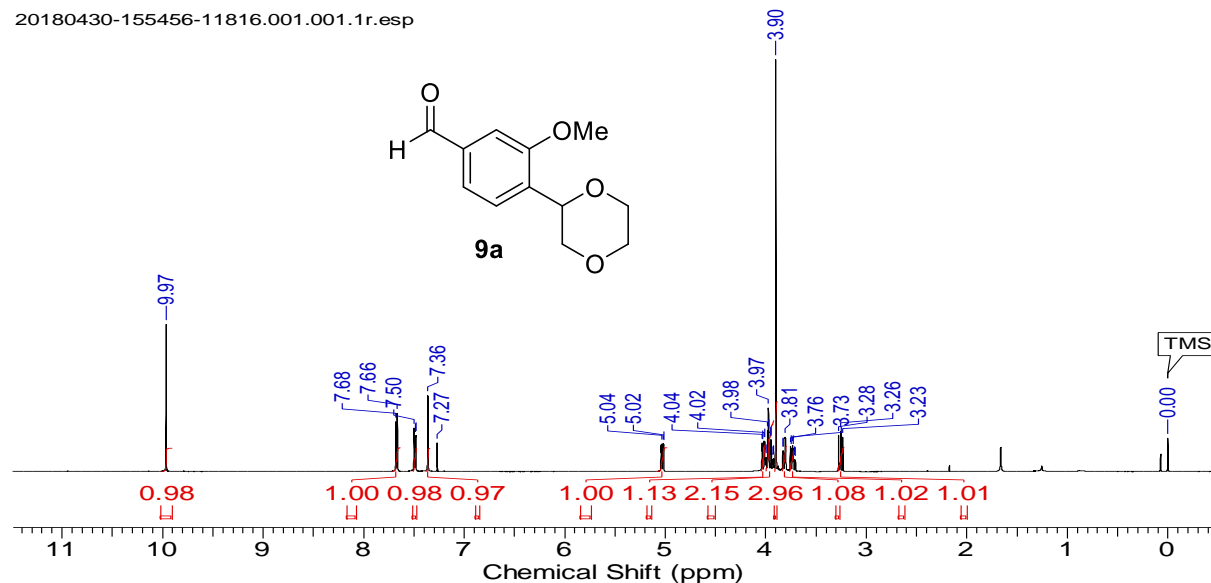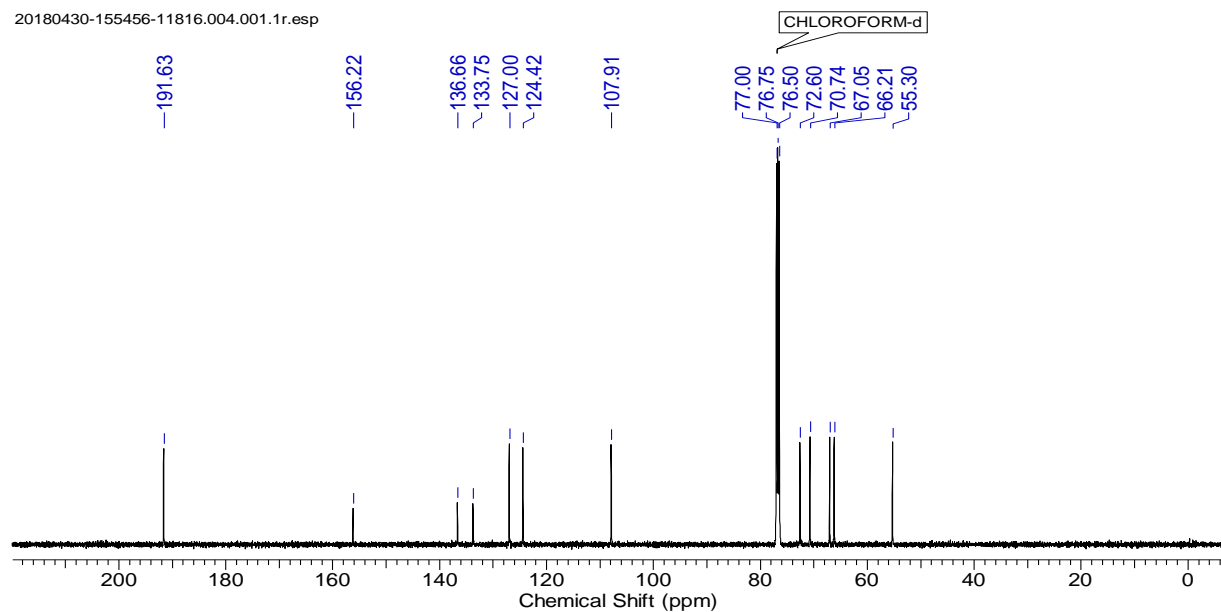
Fig. 3: ^{1}H and ^{13}C NMR of 4-(1,4-dioxan-2-yl)-3-methoxybenzaldehyde (**9a**)

The formed para alkylated aldehydes 4-(1,4-dioxan-2-yl)-3-methoxybenzaldehyde **9a** is further confirmed by the ^{1}H, ^{13}C, and HRMS analysis (**Fig.3**). In the ^{1}H NMR spectrum of compound **9a,** the characteristic peak of aldehyde hydrogen showed at δ 9.97 (s, 1H) and aromatic hydrogens appeared in the region of 7.67 (d, *J* = 7.6 Hz, 1H), 7.46 - 7.52 (m, 1H) and 7.33 - 7.39 (m, 1H). Methyl peak of methoxy group showed in the region of δ 3.90 (s, 3H) and remaining hydrogens present on ether moiety appear in the region of 5.03 (dd, *J* = 9.7, 2.5 Hz, 1H), 4.02 (dd, *J* = 11.4, 2.7 Hz, 1H) and 3.92 - 4.00 (m, 2H). Further, the formed product is clarified by using 13C NMR analysis, and the characteristic peak aldehyde carbonyl is shown in the region of δ 191.63, and HRMS analysis of 9a is matched with the formed product.
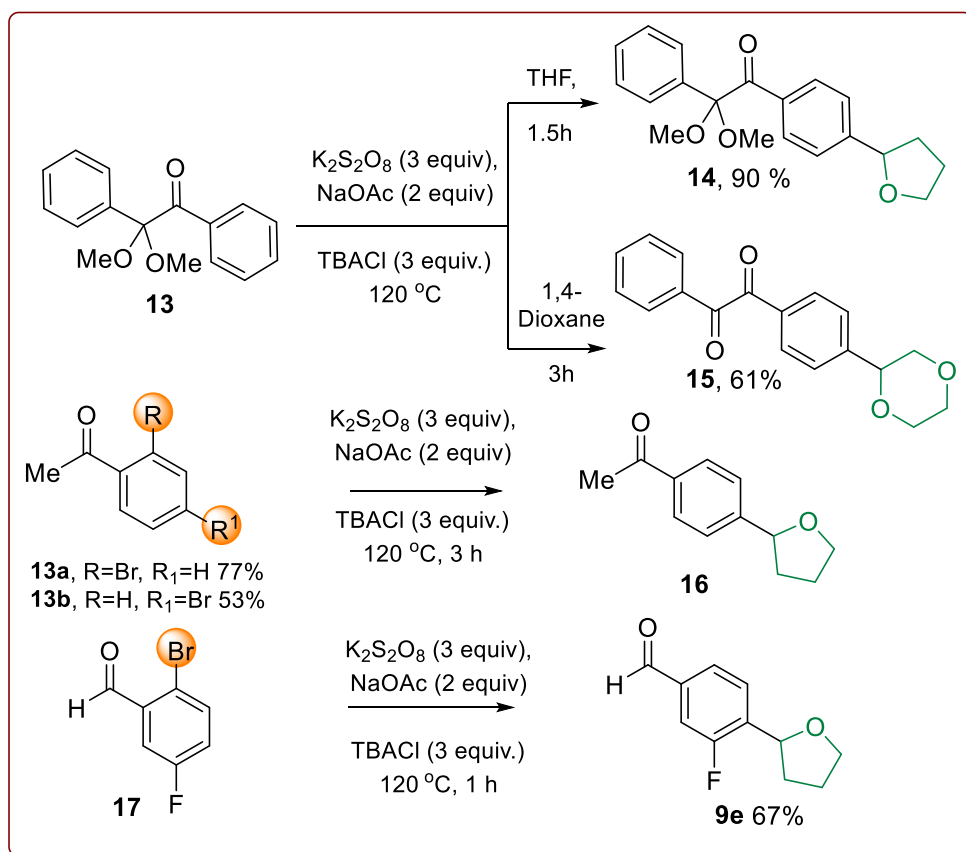
Scheme 5. Some unexpected results of CDC reaction

When benzil, α, α'-dimethyl acetal was subjected to the reaction under standard reaction conditions, it gave unexpected products. In THF, the acetal group remained unaffected, whereas, in 1,4-dioxane, it got deprotected to ketone (**Scheme 5**). It has observed the uncommon phenomenon in the presence of bromine on ortho or para position to the aryl carbonyls, and it delivers unexpected debrominated products, i.e., **16** and **9e,** as shown in **Scheme 5**.
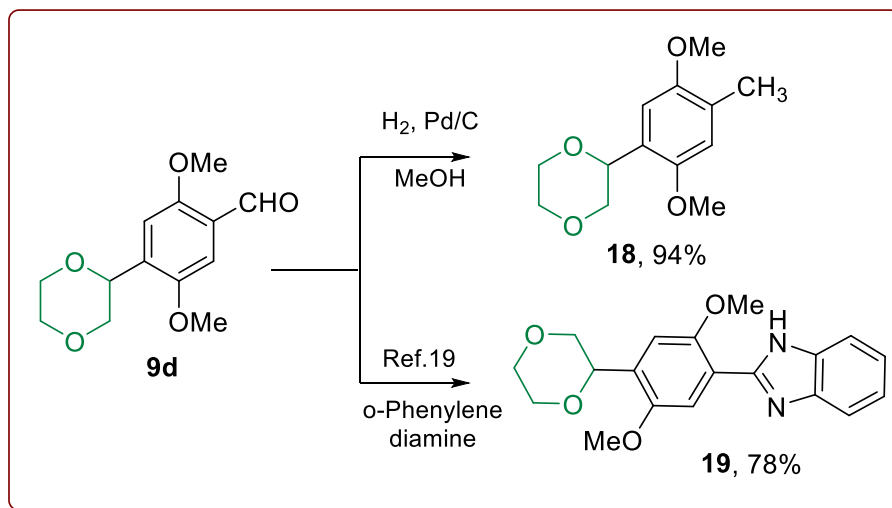
Scheme 6: Synthetic transformations of the products

Example 3:

Formed product of synthetic transformation 2-(4-(1,4-dioxan-2-yl)-2,5-dimethoxyphenyl)-1H-benzo[d]imidazole (**17**) was confirmed by ^{1}H, ^{13}C NMR and Mass analysis.

To show the utility of the reaction, the para-alkylated aryl carbonyl derivatives were further functionalized under various reaction conditions, as shown in **Scheme 6**. The compound **9d** was subjected to the hydrogenation reaction using Pd/C; the aldehyde group of **9d** got reduced to methyl to give the toluene derivative **18** in quantitative yield. Subsequently, the same compound **9d** was converted into its 1,2-benzimidazole derivative **19** under the known protocol.[19]

AV-500-20180611-140744-11816.001.001.1r.esp

AV-500-20180611-140744-11816.003.001.1r.esp
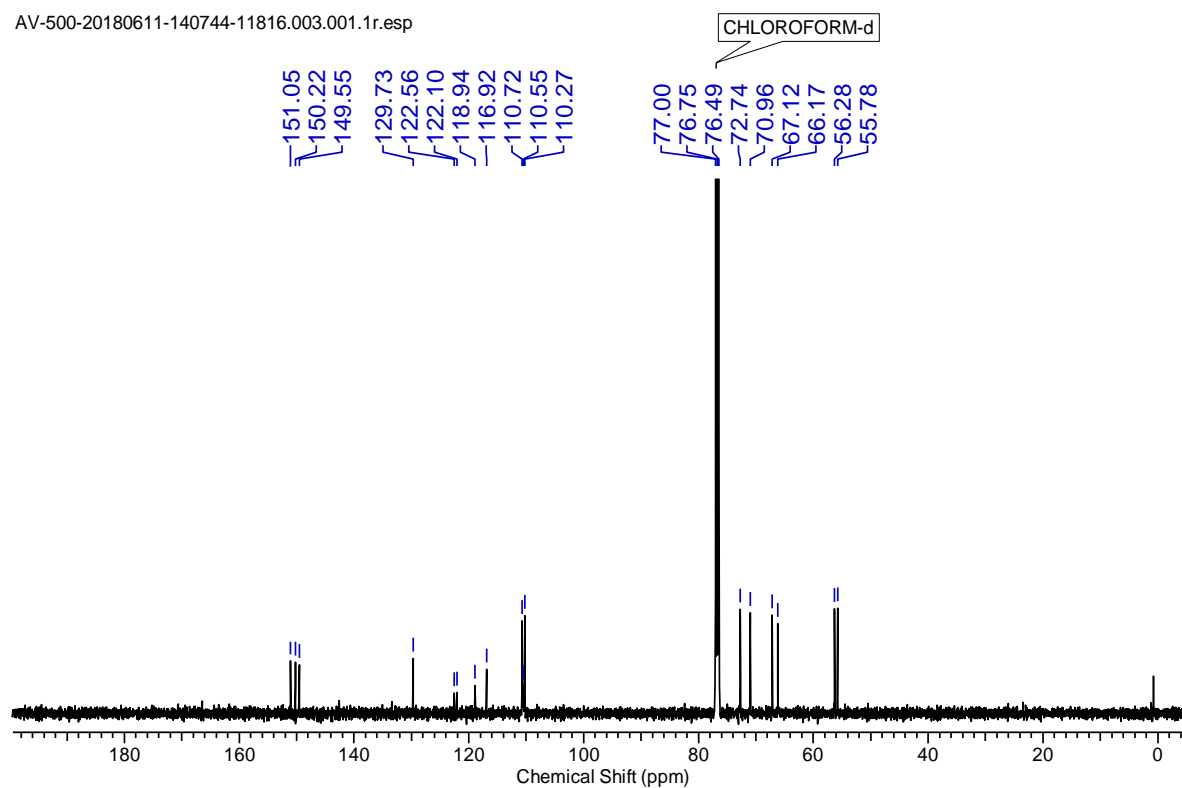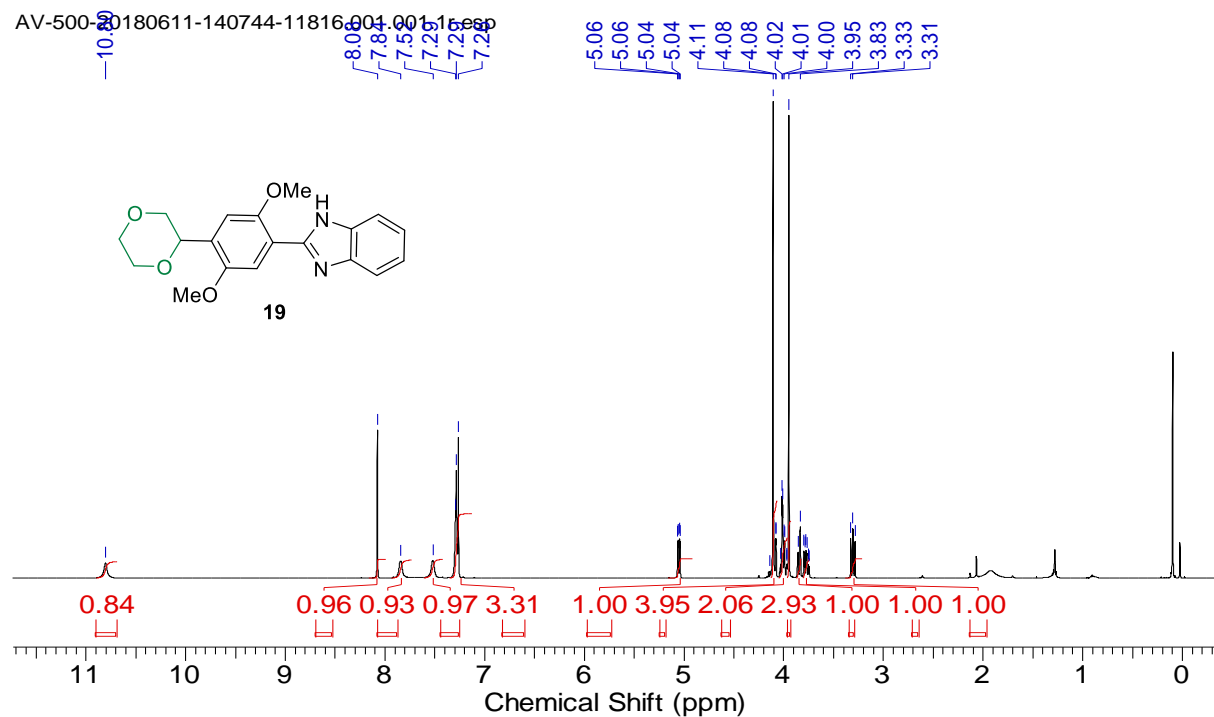
Fig. 4: ^{1}H and ^{13}C NMR of 2-(4-(1,4-dioxan-2-yl)-2,5-dimethoxyphenyl)-1H-benzo[d]imidazole (17)

To understand the mechanism of this CDC reaction, we carried out control experiments (**Scheme 7**), where two equivalents of TEMPO (2,2,6,6-tetramethyl piperidine-*N*-0xide) were added into the reaction system under optimized reaction conditions. It was observed that the THF radical coupled with TEMPO to from a TEMPO-THF adduct **20**, instead of the expected product **7a**. It indicates that the reaction might be proceeding via the radical pathway. In the second control experiment, when the reaction was performed with p-substituted aryl ketone, we did not obtain the expected ortho alkylated product **20**. It indicates that the
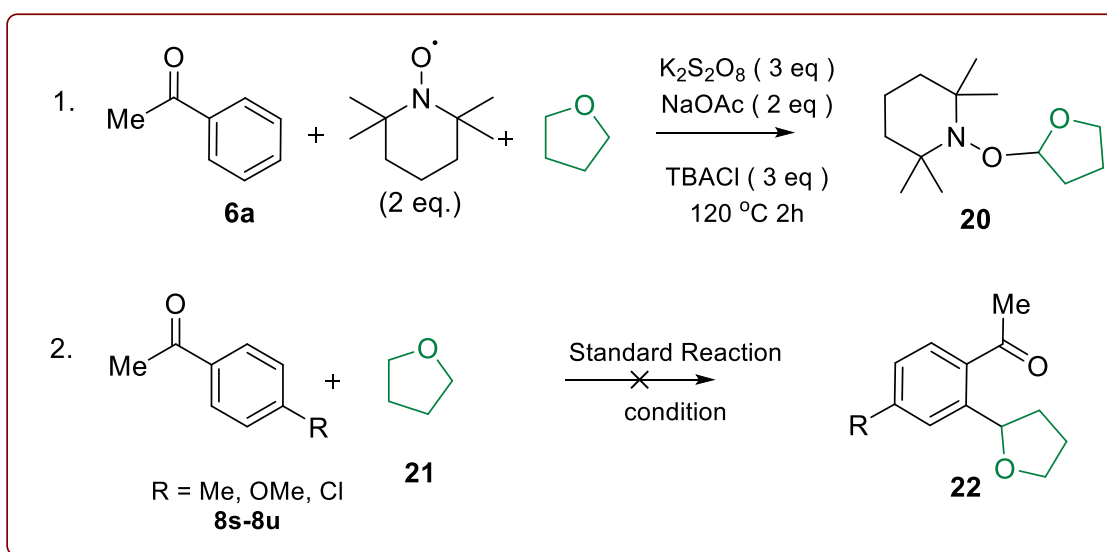
Scheme 7. Control experiments

reaction regioselectively goes only to the *para* position. Based on the above control experiments and the reported literature,[21, 22] the possible catalytic cycle was then initially proposed in **Scheme 8**, as the α-oxyalkyl radical **23** was generated via hydrogen atom abstraction from 1,4-dioxane by persulfate.[21a-c] Then, this α-oxyalkyl radical **23** reacted with acetophenone **6a** to generate the aryl radical species **24**. It was followed by single-electron oxidation to form the aryl cation species

25.[22] The aryl cationic species further underwent aromatization to form the desired product **7a**. In order to understand the reasons that the *para* product is formed exclusively, calculations have been done with density functional theory (DFT). We propose that two molecules of acetophenone can form a chelate with the bare Na$^+$, with the counter anion present in its vicinity in the *ortho* or *para* positions of the acetophenone.
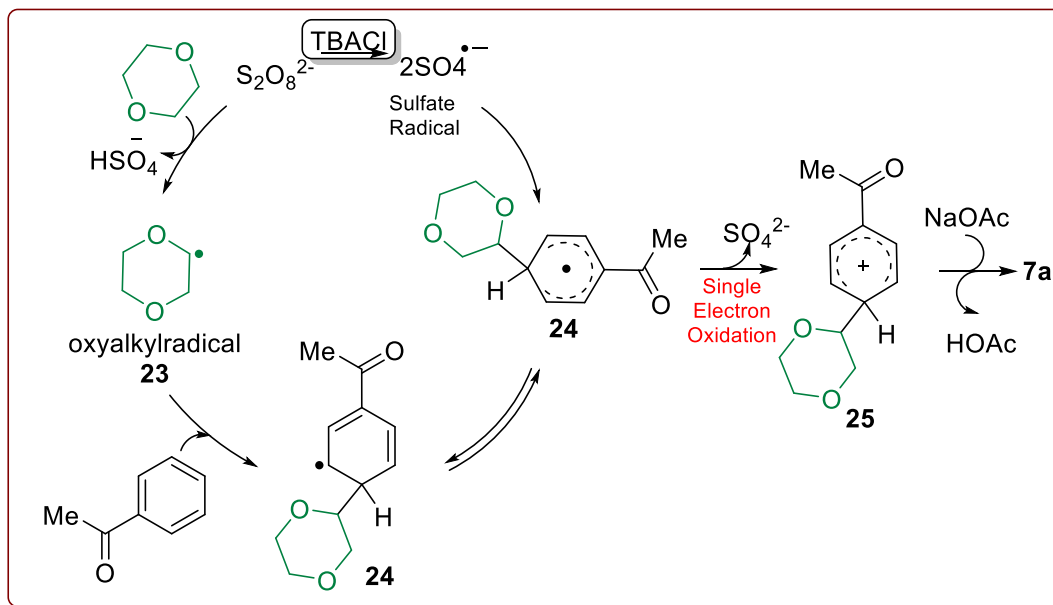
Scheme 8: Expected reaction mechanism of dehydrogenative coupling

2.1.5. Conclusion

In conclusion, we have developed the first efficient and metal free CDC reaction of aromatic carbonyls with inactive cyclic ethers to give the desired *p*-alkylated aryl aldehydes and ketones in good to excellent yields with high regioselectivity. In addition, this reaction tolerates various functional groups under oxidative conditions and can be applied to obtain a wide range of substituted aromatic carbonyls. The utility of the products of CDC were shown by converting them to benzimidazole heterocycles.

2.1.6. Experimental Section

Experimental Procedure for the Synthesis of 1-(4-(1,4-dioxan-2-yl) phenyl) ethan-1-one (7a):

To a 25 mL round-bottom flask acetophenone **6a** (0.833 mmol, 100 mg), $K_2S_2O_8$ (2.5 mmol, 676 mg), tetrabutylammonium chloride (TBACl, 2.5 mmol, 1.4 ml) and NaOAc (1.66 mmol, 136 mg) was taken in 1,4-dioxane (3 ml). The round-bottom flask was equipped with a condenser, and the resulting reaction mixture was refluxed to 120 °C for 4 h, and TLC monitored the progress of the reaction. The reaction mixture was dried under vacuum on completion of the reaction. Then the crude reaction mixture was diluted with ethyl acetate (10 mL) and washed with brine. Eluted with EtOAc (25 mL * 2). The organics were evaporated, and the crude residue was preadsorbed on silica gel and purified by column chromatography (100-200 mesh silica Using 80/20 petroleum ether/ethyl acetate as the eluent to afford the corresponding compound **7a** in 81% yield.

Experimental Procedure for the Synthesis of 4-(1,4-dioxan-2-yl)-3-methoxybenzaldehyde (9a):

To a 25 mL round-bottom flask 3-methoxybenzaldehyde **8a** (0.73 mmol), $K_2S_2O_8$ (2.20 mmol, 594 mg), tetrabutylammonium chloride (TBACl, 2.20 mmol, 1.2 ml) and NaOAc (1.47 mmol, 121 mg) was taken in 1,4-dioxane (3 ml). The round-bottom flask was equipped with a condenser, and the resulting reaction mixture was refluxed to 120 °C for 1.5 h, and TLC monitored the progress of the reaction. It was dried the reaction mixture under vacuum on completion of the reaction. Then the crude reaction mixture was diluted with ethyl acetate (10 mL) and washed with brine. Eluted with EtOAc (20 mL * 2). The organics were evaporated, and the crude residue was preadsorbed on silica gel and purified by column chromatography (100-

200 mesh silica Using 85/15 petroleum ether/ethyl acetate as the eluent to afford the corresponding compound **9a** in 79% yield.

Experimental Procedure for synthesis of 2-(2,5-dimethoxy-4-methylphenyl)-1,4-dioxane (18): Degassed methanol (4.0 ml) was added to the mixture of Pd/C (10 wt %) and **9d** (0.3 mmol,76 mg). After stirring under 1 atm hydrogen pressure for 12 h at room temperature, the reaction mixture was filtered and evaporated under reduced pressure. The crude product was then purified by flash column chromatography (eluent: 90/10 pet. ether/ethyl acetate) to give 16 (67 mg) hydrogenated product as a clear oil.

Experimental Procedure for synthesis of 2-(4-(1,4-dioxan-2-yl)-2,5-dimethoxyphenyl)-1H-benzo[d]imidazole (19):

To a 25 mL round-bottom flask 4-(1,4-dioxan-2-yl)-2,5-dimethoxybenzaldehyde (0.396 mmol,100 mg), *o*-phenylenediamine (0.396 mmol,42 mg), 30% H_2O_2 in water (94 mg, 0.82 ml) and HCl 37% in water (50.5 mg, 0.15 mL) was taken in acetonitrile (3 ml). After stirring for 1 h at rt, the reaction mixture was evaporated under reduced pressure. Then the crude reaction mixture was diluted with ethyl acetate (10 mL) and washed with brine. Eluted with EtOAc (15 mL * 2). The organics were evaporated, and the crude residue was preadsorbed on silica gel and purified by column chromatography (100-200 mesh silica Using 70/30 petroleum ether/ethyl acetate as the eluent to afford the corresponding compound **17** in 78% yield as a white solid.

1-(4-(1,4-Dioxan-2-yl)phenyl)ethan-1-one (7a): white solid. Yield: 81% (139 mg); M.P.: 91-93 °C. ^{1}H NMR (500 MHz , CDCl$_3$): δ 7.99 - 7.87 (m, *J* = 8.4 Hz, 2H), 7.54 - 7.39 (m, *J* = 8.0 Hz, 2H), 4.68 (dd, *J* = 2.3, 9.9 Hz, 1H), 3.98 - 3.94 (m, 1H), 3.92 (dd, *J* = 2.3, 11.1 Hz, 1H), 3.89 - 3.86 (m, 1H), 3.83 - 3.79 (m, 1H), 3.74 (dd, *J* = 3.1, 11.4 Hz, 1H), 3.41 (t, *J* = 10.9 Hz, 1H), 2.59

(s, 3H)). $^{13}C\{^{1}H\}$ NMR (126 MHz, CDCl$_3$): δ 197.6, 143.4, 136.7, 128.4, 126.2, 77.3, 72.1, 66.9, 66.2, 26.5; HRMS (ESI) m/z calculated for C$_{12}$H$_{15}$O$_3$ [(M+H)$^+$] 207.1016, found 207.1019.

1-(3-Bromo-4-(1,4-dioxan-2-yl)phenyl)ethan-1-one (7b): white solid. Yield: 80% (114 mg); M.P.: 87-89 ^{o}C. ^{1}H NMR (500 MHz , CDCl$_3$): δ 8.02 (d, J = 1.5 Hz, 1H), 7.83 (dd, J = 1.5, 8.0 Hz, 1H), 7.60 (d, J = 8.0 Hz, 1H), 4.92 (dd, J = 2.5, 9.7 Hz, 1H), 4.01 (dd, J = 2.5, 11.6 Hz, 1H), 3.91 (s, 1H), 3.90 - 3.88 (m, 1H), 3.77 - 3.74 (m, 1H), 3.69 - 3.63 (m, 1H), 3.15 (dd, J = 9.7, 11.6 Hz, 1H), 2.51 (s, 3H)). $^{13}C\{^{1}H\}$ NMR (126 MHz, CDCl$_3$): δ 196.3, 142.6, 137.8, 132.4, 128.2, 127.4, 122.0, 77.0, 70.5, 67.1, 66.3, 26.6; HRMS (ESI) m/z calculated for C$_{12}$H$_{14}$O$_3$Br [(M+H)$^+$] 285.0121, found 285.0127.

1-(4-(1,4-Dioxan-2-yl)-3-fluorophenyl)ethan-1-one (7c): white solid. Yield: 84% (136 mg); M.P.: 116-118 ^{o}C. ^{1}H NMR (500 MHz, CDCl$_3$): δ 7.72 - 7.78 (m, 1H), 7.57 - 7.66 (m, 2H), 4.97 (dd, J = 9.9, 2.3 Hz, 1H), 3.91 - 4.00 (m, 3H), 3.80 - 3.84 (m, 1H), 3.70 - 3.77 (m, 1H), 3.36 (dd, J = 11.4, 9.9 Hz, 1H), 2.59 (s, 3H). $^{13}C\{^{1}H\}$ NMR (126 MHz, CDCl$_3$): δ 196.4 , 160.4-158.4 (d, J_{F-C} = 247.96 Hz), 138.4-138.3 (d, J_{F-C} = 6.68 Hz), 130.8-130.7 (d, J_{F-C} = 14.31 Hz), 128.04-128.01 (d, J_{F-C} = 3.81 Hz), 124.4, 114.8-114.6 (d, J_{F-C} = 22.89 Hz), 71.9 , 70.9, 67.2 , 66.3, 26.6 ; HRMS (ESI) m/z calculated for C$_{12}$H$_{14}$O$_3$F [(M+H)$^+$] 225.0921, found 225.0928.

1-(4-(1,4-Dioxan-2-yl)naphthalen-1-yl)ethan-1-one (7d): gummy liquid. Yield: 75% (113 mg). ^{1}H NMR (200 MHz , CDCl$_3$): δ 8.87 - 8.64 (m, 1H), 8.15 - 8.05 (m, 1H), 7.93 (d, J = 7.6 Hz, 1H), 7.75 (d, J = 7.6 Hz, 1H), 7.66 - 7.51 (m, 2H), 5.43 (dd, J = 2.4, 9.7 Hz, 1H), 4.18 - 4.04 (m, 3H), 3.95 - 3.76 (m, 2H), 3.50 (dd, J = 10.0, 11.9 Hz, 1H), 2.75 (s, 3H). $^{13}C\{^{1}H\}$ NMR (126 MHz, CDCl$_3$): δ 201.7, 138.7, 135.5, 130.4, 129.9, 127.7, 127.3, 126.6, 126.5, 122.5, 122.1, 74.7, 71.9, 67.2, 66.4, 29.8; HRMS (ESI) m/z calculated for C$_{16}$H$_{17}$O$_3$ [(M+H)$^+$] 257.1172, found 257.1171.

1-(4-(Tetrahydro-2H-pyran-2-yl)phenyl)ethan-1one (7e)): whitish semisolid. Yield: 66% (112 mg). ^{1}H NMR (200 MHz, CDCl$_3$): δ 7.97 - 7.86 (m, J = 8.3 Hz, 2H), 7.49 - 7.38 (m, J = 8.2 Hz, 2H), 4.39 (d, J = 10.6 Hz, 1H), 4.17 (dd, J = 2.9, 10.9 Hz, 1H), 3.71 - 3.56 (m, 1H), 2.60 (s, 3H), 1.86 (d, J = 12.3 Hz, 1H), 1.75 - 1.47 (m, 5H). ^{13}C{^{1}H} NMR (101 MHz, CDCl$_3$): δ 197.9, 148.7, 136.1, 128.4, 125.8, 79.5, 68.9, 34.1, 26.6, 25.7, 23.9; HRMS (ESI) m/z calculated for C$_{13}$H$_{17}$O$_2$ [(M+H)$^+$] 205.1223, found 205.1222.

1-(3-Bromo-4-(tetrahydro-2H-pyran-2-yl)phenyl)ethan-1-one (7f): Clear oil. Yield: 79% (113 mg). ^{1}H NMR (500 MHz , CDCl$_3$): δ 8.08 (s, 1H), 7.88 (d, J = 8.0 Hz, 1H), 7.64 (d, J = 8.0 Hz, 1H), 4.65 (d, J = 10.7 Hz, 1H), 4.16 (d, J = 11.1 Hz, 1H), 3.65 (t, J = 10.7 Hz, 1H), 2.57 (s, 3H), 2.03 (d, J = 13.4 Hz, 1H), 1.93 (br. s., 1H), 1.74 - 1.65 (m, 2H), 1.60 (d, J = 8.4 Hz, 1H), 1.31 - 1.24 (m, 1H).^{13}C{^{1}H} NMR (126 MHz, CDCl$_3$): δ 196.4, 147.7, 137.1, 132.3, 127.5, 127.4, 121.5, 78.9, 69.0, 32.6, 26.5, 25.7, 23.7; HRMS (ESI) m/z calculated for C$_{13}$H$_{16}$O$_2$Br [(M+H)$^+$] 283.0328, found 283.0333.

1-(4-(Tetrahydro-2H-pyran-2-yl)naphthalen-1-yl)ethan-1-one (7g): Gummy oil. Yield: 82% (123 mg). ^{1}H NMR (400 MHz , CDCl$_3$): δ 8.78 (d, J = 7.9 Hz, 1H), 8.07 (d, J = 7.9 Hz, 1H), 7.93 (d, J = 7.9 Hz, 1H), 7.71 (d, J = 7.3 Hz, 1H), 7.62 - 7.51 (m, 2H), 5.09 (d, J = 11.0 Hz, 1H), 4.31 - 4.22 (m, 1H), 3.85 - 3.73 (m, 1H), 2.74 (s, 3H), 2.11 - 1.99 (m, 2H), 1.86 - 1.78 (m, 2H), 1.72 - 1.64 (m, 2H). ^{13}C{^{1}H} NMR (101 MHz, CDCl$_3$): δ 201.6, 143.8, 134.5, 130.2, 130.0, 128.0, 126.9, 126.3, 125.9, 122.9, 121.0, 76.6, 69.0, 33.2, 29.7, 25.6, 23.8; HRMS (ESI) m/z calculated for C$_{17}$H$_{19}$O$_2$ [(M+H)$^+$] 255.1380, found 255.1378

(4-(1,4-Dioxan-2-yl)phenyl)(Phenyl)methanone(7h)*:* White solid. Yield: 72% (106 mg); M.P.: 70-72 ^{o}C. ^{1}H NMR (200 MHz, CDCl$_3$): δ 7.84 - 7.77 (m, 4H), 7.65 - 7.55 (m, 1H), 7.54 - 7.44 (m, 4H), 4.73 (dd, J = 2.7, 10.2 Hz, 1H), 4.01 - 3.93 (m, 2H), 3.92 - 3.85 (m, 1H), 3.85 - 3.69 (m,

2H), 3.48 (dd, J = 10.2, 11.5 Hz, 1H)). $^{13}C\{^1H\}$ NMR (101 MHz, CDCl$_3$): δ 195.6, 142.5, 137.3, 137.0, 132.0, 129.9, 129.7, 128.0, 126.3, 125.6, 125.1, 77.1, 72.0, 66.7, 66.0; HRMS (ESI) m/z calculated for C$_{17}$H$_{17}$O$_3$ [(M+H)$^+$] 269.1172, found 269.1174.

(4-(1,4-Dioxan-2-yl)phenyl)(4-bromophenyl)methanone (7i): White solid. Yield: 67% (89 mg); M.P.: 88-90 ^{o}C. ^1H NMR (200 MHz , CDCl$_3$): δ 7.81 - 7.74 (m, J = 8.3 Hz, 2H), 7.71 - 7.60 (m, 4H), 7.54 - 7.43 (m, J = 8.1 Hz, 2H), 4.73 (dd, J = 2.6, 10.0 Hz, 1H), 4.01 - 3.92 (m, 2H), 3.89 (d, J = 2.7 Hz, 1H), 3.84 - 3.69 (m, 2H), 3.46 (dd, J = 10.2, 11.6 Hz, 1H). $^{13}C\{^1H\}$ NMR (50 MHz, CDCl$_3$): δ 194.5, 142.4, 136.1, 135.6, 131.0, 130.8, 129.4, 127.6, 126.9, 126.6, 125.5, 76.7, 71.6, 66.3, 65.7; HRMS (ESI) m/z calculated for C$_{17}$H$_{16}$O$_3$Br [(M+H)$^+$] 347.0277, found 347.0285.

(4-(1,4-Dioxan-2-yl)phenyl)(4-chlorophenyl)methanone (7j): White solid. Yield: 61% (85 mg); M.P.: 90-92 ^{o}C. ^1H NMR (500 MHz, CDCl$_3$): δ 7.75 (d, J = 8.4 Hz, 2H), 7.77 (d, J = 8.0 Hz, 2H), 7.48 (dd, J = 9.9, 8.4 Hz, 4H), 4.73 (dd, J = 10.3, 2.7 Hz, 1H), 3.97 - 4.00 (m, 1H), 3.90 - 3.95 (m, 2H), 3.82 - 3.86 (m, 1H), 3.76 (td, J = 11.3, 3.2 Hz, 1H), 3.47 (dd, J = 11.4, 10.3 Hz, 1H). $^{13}C\{^1H\}$ NMR (101 MHz, CDCl$_3$): δ 194.7, 142.7, 138.6, 136.5, 135.5, 131.1, 129.8, 128.3, 125.8, 77.1, 71.9, 66.7, 66.0; HRMS (ESI) m/z calculated for C$_{17}$H$_{16}$O$_3$Cl [(M+H)$^+$] 303.0782, found 303.0789.

3-(1,4-Dioxan-2-yl)-9H-thioxanthen-9-one (7k): White solid. Yield: 74% (104 mg); M.P.: 163-165 ^{o}C. ^1H NMR (400 MHz, CDCl$_3$): δ 8.54 - 8.66 (m, 2H), 7.56 - 7.66 (m, 3H), 7.46 - 7.53 (m, 1H), 7.42 (dd, J = 8.2, 1.8 Hz, 1H), 4.76 (dd, J = 10.1, 2.7 Hz, 1H), 3.91 - 4.05 (m, 3H), 3.85 (dd, J = 11.4, 2.7 Hz, 1H), 3.76 (td, J = 11.3, 3.4 Hz, 1H), 3.46 (dd, J = 11.9, 10.1 Hz, 1H). $^{13}C\{^1H\}$ NMR (101 MHz, CDCl$_3$): δ179.7, 142.9, 137.6, 137.2, 132.3, 130.0, 129.8, 129.2,

128.8, 126.4, 126.0, 124.1, 123.2, 72.1, 67.0, 66.3; HRMS (ESI) m/z calculated for $C_{17}H_{15}O_3S$ [(M+H)$^+$] 299.0736, found 299.0733.

5-(1,4-Dioxan-2-yl)-2,3-dihydro-1H-inden-1-one (7l): White solid. Yield: 67% (110 mg); M.P.: 128-130 ^{o}C. ^{1}H NMR (400 MHz, CDCl$_3$): δ 7.50 - 7.70 (m, 2H), 7.39 (d, J = 6.7 Hz, 1H), 5.68 (d, J = 9.2 Hz, 1H), 3.92 - 4.08 (m, 3H), 3.82 (d, J = 11.0 Hz, 1H), 3.72 (td, J = 11.0, 3.7 Hz, 1H), 3.22 (t, J = 10.4 Hz, 1H), 3.05 - 3.17 (m, 2H), 2.58 - 2.83 (m, 2H). ^{13}C{^{1}H} NMR (101 MHz, CDCl$_3$): δ 207.0, 155.7, 138.5, 134.6, 132.6, 125.9, 124.6, 73.2, 71.7, 67.0, 66.3, 36.6, 25.6; HRMS (ESI) m/z calculated for $C_{13}H_{15}O_3$ [(M+H)$^+$] 219.1016, found 219.1018.

4-Bromo-5-(tetrahydrofuran-2-yl)-2,3-dihydro-1H-inden-1-one (7m): off white solid. Yield: 70% (93 mg); M.P.: 116-118 ^{o}C. ^{1}H NMR (200 MHz, CDCl$_3$): δ 7.62 (d, J = 8.2 Hz, 1H), 7.39 (d, J = 8.1 Hz, 1H), 5.64 (t, J = 6.9 Hz, 1H), 4.06 (q, J = 7.1 Hz, 1H), 3.79 - 3.97 (m, 1H), 2.92 - 3.06 (m, 2H), 2.43 - 2.69 (m, 3H), 1.72 - 2.06 (m, 2H), 1.34 - 1.55 (m, 1H). ^{13}C{^{1}H} NMR (126 MHz, CDCl$_3$): δ 206.5, 155.1, 144.2, 137.1, 134.5, 125.2, 120.1, 76.4, 69.1, 36.4, 34.0, 26.9, 25.8; HRMS (ESI) m/z calculated for $C_{13}H_{14}O_2Br$ [(M+H)$^+$] 281.0172, found 281.0170.

6-(Tetrahydrofuran-2-yl)-3,4-dihydronaphthalen-1(2H)-one (7n): Clear oil. Yield: 62% (91 mg). ^{1}H NMR (400 MHz, CDCl$_3$): δ 7.93 (d, J = 8.5 Hz, 1H), 7.13 - 7.24 (m, 2H), 4.85 (d, J = 6.7 Hz, 1H), 4.04 (d, J = 7.9 Hz, 1H), 3.89 (d, J = 7.3 Hz, 1H), 2.85 - 2.97 (m, 2H), 2.52 - 2.64 (m, 2H), 2.21 - 2.36 (m, 1H), 2.01 - 2.13 (m, 2H), 1.91 - 2.00 (m, 2H), 1.65 - 1.79 (m, 1H). ^{13}C{^{1}H} NMR (101 MHz, CDCl$_3$): δ 197.9, 149.1, 144.4, 131.3, 127.0, 125.2, 123.6, 79.9, 68.6, 38.8, 34.3, 29.5, 29.4, 25.7, 23.0; HRMS (ESI) m/z calculated for $C_{14}H_{17}O_2$ [(M+H)$^+$] 217.1223, found 217.1222.

1-(4-(Tetrahydrofuran-2-yl)naphthalen-1-yl)ethan-1-one (7o): White solid. Yield: 87% (123 mg); M.P.: 65-67 ^{o}C. ^{1}H NMR (400 MHz, CDCl$_3$): δ 8.80 (d, J = 8.5 Hz, 1H), 7.94 (d, J = 7.3

Hz, 1H), 7.98 (d, *J* = 7.9 Hz, 1H), 7.70 (d, *J* = 7.3 Hz, 1H), 7.52 - 7.65 (m, 2H), 5.61 - 5.76 (m, 1H), 4.20 - 4.37 (m, 1H), 4.06 (q, *J* = 7.7 Hz, 1H), 2.75 (s, 3H), 2.54 - 2.70 (m, 1H), 1.96 - 2.13 (m, 2H), 1.87 (dt, *J* = 12.5, 6.6 Hz, 1H). $^{13}C\{^1H\}$ NMR (101 MHz, CDCl$_3$): δ 201.8, 144.9, 134.7, 130.6, 130.4, 128.5, 127.4, 126.8, 126.3, 123.4, 120.2, 77.7, 68.9, 34.0, 30.0, 25.9; HRMS (ESI) m/z calculated for C$_{16}$H$_{17}$O$_2$ [(M+H)$^+$] 241.1223, found 241.1226.

1-(3-Methoxy-4-(tetrahydrofuran-2-yl)phenyl)ethan-1-one (7p): Clear oil. Yield: 78% (114 mg). ^{1}H NMR (400 MHz , CDCl$_3$): δ 7.48 - 7.43 (m, 2H), 7.38 (s, 1H), 5.09 (t, *J* = 7.0 Hz, 1H), 4.10 - 4.00 (m, 1H), 3.90 - 3.85 (m, 1H), 3.84 - 3.80 (m, 3H), 2.52 (s, 3H), 2.36 (dd, *J* = 6.7, 12.8 Hz, 1H), 1.88 (qd, *J* = 6.9, 14.2 Hz, 2H), 1.62 - 1.55 (m, 1H). $^{13}C\{^1H\}$ NMR (101 MHz, CDCl$_3$): δ 197.8, 156.2, 138.4, 137.0, 125.3, 121.6, 108.6, 75.8, 68.6, 55.4, 33.0, 26.5, 25.8; HRMS (ESI) m/z calculated for C$_{13}$H$_{17}$O$_3$ [(M+H)$^+$] 221.1172, found 221.1177.

1-(3-Bromo-4-(tetrahydrofuran-2-yl)phenyl)ethan-1-one (7q): Clear oil. Yield: 84% (113 mg). ^{1}H NMR (400 MHz, CDCl$_3$): δ 8.08 (d, *J* = 1.5 Hz, 1H), 7.86 (dd, *J* = 8.0, 1.5 Hz, 1H), 7.59 (d, *J* = 8.0 Hz, 1H), 5.15 (t, *J* = 7.1 Hz, 1H), 4.17 (td, *J* = 7.6, 6.1 Hz, 1H), 3.97 (q, *J* = 7.2 Hz, 1H), 2.51 - 2.64 (m, 4H), 1.98 (td, *J* = 14.0, 7.1 Hz, 2H), 1.65 (dd, *J* = 12.6, 7.6 Hz, 1H). $^{13}C\{^1H\}$ NMR (126 MHz, CDCl$_3$): δ 196.4, 148.5, 137.2, 132.4, 127.3, 126.6, 121.5, 79.7, 69.2, 33.2, 26.5, 25.7; HRMS (ESI) m/z calculated for C$_{12}$H$_{14}$O$_2$Br [(M+H)$^+$] 269.0172, found 269.0178.

1-(4-(Benzo[d][1,3]dioxol-2-yl)phenyl)ethan-1-one (7r): white solid. Yield: 58% (116 mg); M.P.: 70-72 ^{o}C. ^{1}H NMR (500 MHz, CDCl$_3$): δ 8.04 (s, 1H), 8.02 (s, 1H), 7.70 (s, 1H), 7.68 (s, 1H), 7.01 (s, 1H), 6.89 (s, 4H), 2.63 (s, 3H). $^{13}C\{^1H\}$ NMR (126 MHz, CDCl$_3$): δ 197.5, 147.2, 140.9, 138.4, 128.6, 126.6, 121.9, 108.8, 108.7, 26.7; HRMS (ESI) m/z calculated for C$_{15}$H$_{13}$O$_3$ [(M+H)$^+$] 241.0859, found 241.0864.

4-(1,4-Dioxan-2-yl)-3-methoxybenzaldehyde (9a): Clear oil. Yield: 79% (128 mg). ^{1}H NMR (500 MHz, CDCl$_3$): δ 9.97 (s, 1H), 7.67 (d, J = 7.6 Hz, 1H), 7.46 - 7.52 (m, 1H), 7.33 - 7.39 (m, 1H), 5.03 (dd, J = 9.7, 2.5 Hz, 1H), 4.02 (dd, J = 11.4, 2.7 Hz, 1H), 3.92 - 4.00 (m, 2H), 3.90 (s, 3H), 3.79 - 3.84 (m, 1H), 3.69 - 3.76 (m, 1H), 3.26 (dd, J = 11.3, 9.7 Hz, 1H). ^{13}C{^{1}H} NMR (126 MHz, CDCl$_3$): δ 191.6, 156.2, 136.7, 133.8, 127.0, 124.4, 107.9, 72.6, 70.7, 67.1, 66.2, 55.3; HRMS (ESI) m/z calculated for C$_{12}$H$_{15}$O$_4$ [(M+H)$^+$] 223.0965, found 223.0964.

3-Chloro-4-(1,4-dioxan-2-yl)benzaldehyde (9b): Pale yellow solid. Yield: 85% (137 mg); M.P.: 72-74 °C. ^{1}H NMR (400 MHz, CDCl$_3$): 9.96 (s, 1H), 8.04 - 7.75 (m, 3H), 5.18 - 5.00 (m, 1H), 4.08 (d, J = 11.6 Hz, 1H), 4.04 - 3.93 (m, 2H), 3.84 (d, J = 12.2 Hz, 1H), 3.75 (dd, J = 4.0, 10.1 Hz, 1H), 3.36 - 3.17 (m, 1H). ^{13}C{^{1}H} NMR (101 MHz, CDCl$_3$): δ 190.1, 142.1, 136.5, 132.4, 129.6, 128.1, 127.9, 74.5, 70.1, 66.8, 66.0; HRMS (ESI) m/z calculated for C$_{11}$H$_{12}$O$_3$Cl [(M+H)$^+$] 227.0469, found 227.0467.

4-(1,4-Dioxan-2-yl)-2-methoxybenzaldehyde (9c): Clear oil. Yield: 92% (150 mg). ^{1}H NMR (500 MHz , CDCl$_3$): δ 10.43 (s, 1H), 7.79 (d, J = 8.0 Hz, 1H), 7.04 (s, 1H), 6.95 (d, J = 8.0 Hz, 1H), 4.66 (dd, J = 2.7, 10.3 Hz, 1H), 3.98 - 3.93 (m, 4H), 3.91 (t, J = 3.4 Hz, 1H), 3.89 - 3.87 (m, 1H), 3.83 - 3.79 (m, 1H), 3.76 - 3.72 (m, 1H), 3.41 (dd, J = 10.3, 11.4 Hz, 1H). ^{13}C{^{1}H} NMR (126 MHz, CDCl$_3$): δ 189.1, 161.7, 146.5, 128.3, 124.0, 117.9, 108.8, 77.1, 71.8, 66.6, 66.0, 55.4; HRMS (ESI) m/z calculated for C$_{12}$H$_{15}$O$_4$ [(M+H)$^+$] 223.0965, found 223.0963.

4-(1,4-Dioxan-2-yl)-2,5-dimethoxybenzaldehyde (9d): Yellow solid. Yield: 82% (124 mg); M.P.: 118-120 °C. ^{1}H NMR (500 MHz, CDCl$_3$): δ 10.43 (s, 1H), 7.27 (s, 1H), 7.19 (s, 1H), 4.98 (dd, J = 9.5, 2.3 Hz, 1H), 4.04 (dd, J = 11.3, 2.5 Hz, 1H), 3.96 - 3.99 (m, 1H), 3.92 - 3.96 (m, 4H), 3.82 (s, 3H), 3.79 - 3.81 (m, 1H), 3.69 - 3.76 (m, 1H), 3.22 (dd, J = 11.1, 9.9 Hz, 1H). ^{13}C{^{1}H} NMR (126 MHz, CDCl$_3$): δ 189.2, 156.9, 149.9, 135.5, 123.8, 110.8, 108.1, 73.1, 70.9,

67.3, 66.4, 56.2, 55.7; HRMS (ESI) m/z calculated for $C_{13}H_{17}O_5$ [(M+H)$^+$] 253.1071, found 253.1069.

3-Fluoro-4-(tetrahydrofuran-2-yl) benzaldehyde (9e): Clear oil. Yield: 86% (135 mg) & 67% (105 mg). ^{1}H NMR (200 MHz, CDCl$_3$): 9.96 (s, 1H), 7.72 - 7.61 (m, 2H), 7.52 (d, *J* = 9.9 Hz, 1H), 5.16 (t, *J* = 7.1 Hz, 1H), 4.12 (q, *J* = 6.8 Hz, 1H), 4.03 - 3.87 (m, 1H), 2.59 - 2.39 (m, 1H), 2.09 - 1.93 (m, 2H), 1.75 (dd, *J* = 7.6, 12.1 Hz, 1H). ^{13}C{^{1}H} NMR (50 MHz, CDCl$_3$): δ 190.7 , 162.3-157.3 (d, J = 248.82 Hz), 138.4-138.1 (d, J = 14.27 Hz), 137.0-136.9 (d, J = 6.22 Hz,), 127.4-127.3 (d, J = 4.39 Hz), 126.3-126.2 (d, J = 2.93 Hz,), 115.0-114.6 (d, J = 22.32 Hz), 74.9-74.8 (d, J = 1.83 Hz), 68.8 , 33.4 , 25.9; HRMS (ESI) m/z calculated for $C_{11}H_{12}O_2F$ [(M+H)$^+$] 195.0816, found 195.0815.

3,5-Dimethoxy-4-(tetrahydrofuran-2-yl)benzaldehyde (9f): Clear oil. Yield: 70% (99 mg). ^{1}HNMR (500 MHz , CDCl$_3$): 10.43 (s, 1H), 7.27 (s, 1H), 7.19 (s, 1H), 4.98 (dd, *J* = 2.3, 9.5 Hz, 1H), 4.04 (dd, *J* = 2.5, 11.3 Hz, 1H), 3.99 - 3.97 (m, 1H), 3.96 - 3.91 (m, 4H), 3.82 (s, 3H), 3.81 - 3.79 (m, 1H), 3.75 - 3.70 (m, 1H), 3.22 (dd, *J* = 9.9, 11.1 Hz, 1H). ^{13}C{^{1}H} NMR (101 MHz, CDCl$_3$): δ 191.4, 158.8, 136.2, 124.5, 104.9, 71.8, 68.7, 55.6, 29.9, 27.4; HRMS (ESI) m/z calculated for $C_{13}H_{17}O_4$ [(M+H)$^+$] 237.1121, found 237.1119.

3-Chloro-4-(tetrahydrofuran-2-yl)benzaldehyde (9g): Clear oil. Yield: 89% (134 mg). ^{1}H NMR (400 MHz, CDCl$_3$): δ 9.86 (s, 1H), 7.75 (d, *J* = 1.5 Hz, 1H), 7.60 - 7.70 (m, 2H), 5.14 (t, *J* = 7.1 Hz, 1H), 4.03 - 4.17 (m, 1H), 3.90 (q, *J* = 7.3 Hz, 1H), 2.50 (dd, *J* = 12.5, 6.4 Hz, 1H), 1.83 - 2.02 (m, 2H), 1.51 - 1.65 (m, 1H). ^{13}C{^{1}H} NMR (101 MHz, CDCl$_3$): δ 190.3, 148.2, 135.9, 132.0, 129.6, 127.9, 126.6, 77.4, 68.8, 32.7, 25; HRMS (ESI) m/z calculated for $C_{11}H_{12}O_2Cl$ [(M+H)$^+$] 211.0520, found 211.0519

3-Hydroxy-4-(tetrahydrofuran-2-yl)benzaldehyde (9h): Yellow oil. Yield: 71% (111 mg). ^{1}H NMR (200 MHz, CDCl$_3$): δ 9.98 (s, 1H), 9.80 (s, 1H), 7.20 - 7.46 (m, 2H), 7.10 (dd, J = 7.5, 1.8 Hz, 1H), 5.89 (dd, J = 9.6, 6.2 Hz, 1H), 4.09 - 4.35 (m, 1H), 3.77 - 4.04 (m, 1H), 2.49 - 2.70 (m, 1H), 1.96 - 2.23 (m, 2H), 1.63 - 1.84 (m, 1H). ^{13}C{^{1}H} NMR (50 MHz, CDCl$_3$): δ 193.3, 157.2, 134.0, 128.5, 127.8, 124.7, 123.5, 80.2, 68.6, 32.9, 25.6; HRMS (ESI) m/z calculated for C$_{11}$H$_{11}$O$_3$ [(M-H)$^+$] 191.0703, found 191.0702

2-Hydroxy-4-(tetrahydrofuran-2-yl)benzaldehyde (9i): Clear oil. Yield: 62% (98 mg). ^{1}H NMR (200 MHz, CDCl$_3$): δ 11.07 (s, 1H), 9.86 (s, 1H), 7.52 (d, J = 8.5 Hz, 1H), 6.89 - 7.07 (m, 2H), 4.92 (t, J = 7.1 Hz, 1H), 3.90 - 4.16 (m, 2H), 2.37 (dd, J = 11.9, 6.3 Hz, 1H), 1.93 - 2.07 (m, 2H), 1.70 - 1.87 (m, 1H). ^{13}C{^{1}H} NMR (50 MHz, CDCl$_3$): δ 195.3, 161.1, 153.7, 133.1, 119.0, 116.4, 113.5, 79.3, 68.4, 33.9, 25.2; HRMS (ESI) m/z calculated for C$_{11}$H$_{12}$O$_3$ [(M+H)$^+$] 193.0859, found : 193.0858.

4-(1,4-Dioxan-2-yl)-1-naphthaldehyde (9j): Clear oil. Yield: 80% (131 mg). ^{1}H NMR (200 MHz, CDCl$_3$): δ 10.29 (s, 1H), 9.17 - 9.35 (m, 1H), 8.01 - 8.10 (m, 1H), 7.93 (d, J = 7.5 Hz, 1H), 7.82 (d, J = 7.5 Hz, 1H), 7.50 - 7.68 (m, 2H), 5.37 (dd, J = 9.9, 2.3 Hz, 1H), 3.98 - 4.11 (m, 3H), 3.73 - 3.84 (m, 2H), 3.41 (dd, J = 11.9, 9.9 Hz, 1H). ^{13}C{^{1}H} NMR (50 MHz, CDCl$_3$): δ 192.7, 141.0, 135.7, 130.4, 130.0, 129.7, 128.0, 126.6, 125.1, 122.3, 122.2, 74.4, 71.5, 66.8, 66.0; HRMS (ESI) m/z calculated for C$_{15}$H$_{14}$O$_3$Na [(M+Na)$^+$] 265.0835, found 265.0832.

2,2-Dimethoxy-2-phenyl-1-(4-(tetrahydrofuran-2-yl)phenyl)ethan-1-one   (14):   White semisolid. Yield: 90% (114 mg). ^{1}H NMR (400 MHz, CDCl$_3$): δ 8.04 (d, J = 7.9 Hz, 2H), 7.61 (d, J = 7.3 Hz, 2H), 7.20 - 7.46 (m, 5H), 4.74 - 4.98 (m, 1H), 4.00 - 4.12 (m, 1H), 3.81 - 3.98 (m, 1H), 3.21 (s, 6H), 2.21 - 2.40 (m, 1H), 1.90 - 2.07 (m, 2H), 1.72 (dt, J = 12.4, 7.9 Hz, 1H). ^{13}C{^{1}H} NMR (50 MHz, CDCl$_3$): δ 194.6, 148.8, 136.9, 133.0, 130.2, 128.8, 128.4, 126.9,

125.2, 103.5, 80.1, 68.8, 50.0, 34.4, 25.9; HRMS (ESI) m/z calculated for $C_{20}H_{22}O_4Na$ [(M+Na)$^+$] 349.1410, found 349.1406.

1-(4-(1,4-Dioxan-2-yl)phenyl)-2-phenylethane-1,2-dione (15): Yellow oil. Yield: 61% (70 mg). ^{1}H NMR (500 MHz, CDCl$_3$): δ 7.97 (d, *J* = 7.6 Hz, 4H), 7.61 - 7.73 (m, 1H), 7.43 - 7.58 (m, 4H), 4.61 - 4.81 (m, 1H), 3.86 - 4.00 (m, 3H), 3.82 (d, *J* = 10.7 Hz, 1H), 3.73 (td, *J* = 11.3, 2.9 Hz, 1H), 3.40 (t, *J* = 10.9 Hz, 1H). ^{13}C{^{1}H} NMR (50 MHz, CDCl$_3$): δ 194.4, 194.0, 145.5, 134.9, 132.9, 132.5, 130.0, 129.9, 129.0, 126.6, 77.2, 72.1, 66.9, 66.3; HRMS (ESI) m/z calculated for $C_{18}H_{16}O_4Na$ [(M+Na)$^+$] 319.0941, found 319.0936.

1-(4-(Tetrahydrofuran-2-yl)phenyl)ethan-1-one(16): Clear oil   Yield 77% (121 mg) & 53% (83 mg). ^{1}H NMR (400 MHz , CDCl$_3$): 7.93 (d, *J* = 8.5 Hz, 2H), 7.42 (d, *J* = 8.5 Hz, 2H), 4.95 (t, *J* = 7.3 Hz, 1H), 4.14 - 4.07 (m, 1H), 3.97 (q, *J* = 7.3 Hz, 1H), 2.60 (s, 3H), 2.37 (dd, *J* = 6.4, 12.5 Hz, 1H), 2.02 (td, *J* = 7.0, 14.0 Hz, 2H), 1.81 - 1.74 (m, 1H). ^{13}C{^{1}H} NMR (101 MHz, CDCl$_3$): δ 197.8, 149.2, 136.1, 128.4, 125.6, 80.1, 68.9, 34.7, 26.6, 25.9. HRMS (ESI) m/z calculated for $C_{12}H_{14}O_2$ [(M+H)$^+$] 191.1067, found 191.1062.

2-(2,5-Dimethoxy-4-methylphenyl)-1,4-dioxane (18): clear oil yield: 94% (71 mg). ^{1}H NMR (400 MHz, CDCl$_3$): 6.89 (s, 1H), 6.59 (s, 1H), 4.95 - 4.82 (m, 1H), 3.92 - 3.83 (m, 3H), 3.75 (s, 3H), 3.72 - 3.62 (m, 5H), 3.22 (t, *J* = 10.4 Hz, 1H), 2.14 (s, 3H). ^{13}C{^{1}H} NMR (101 MHz, CDCl$_3$): δ 151.6, 149.2, 126.1, 124.1, 113.2, 108.8, 72.5, 71.2, 67.1, 66.1, 55.7, 55.6, 15.9; HRMS (ESI) m/z calculated for $C_{13}H_{18}O_4Na$ [(M+Na)$^+$] 261.1097, found 261.1093.

2-(4-(1,4-Dioxan-2-yl)-2,5-dimethoxyphenyl)-1H-benzo[d]imidazole (19): White solid. Yield: 78% (159 mg). ^{1}H NMR (500 MHz, CDCl$_3$): δ 10.80 (br. s., 1H), 8.08 (s, 1H), 7.84 (br. s., 1H), 7.52 (br. s., 1H), 7.13 - 7.35 (m, 3H), 5.05 (dd, *J* = 9.7, 2.5 Hz, 1H), 4.07 - 4.13 (m, 4H), 3.96 - 4.05 (m, 2H), 3.95 (s, 3H), 3.82 - 3.87 (m, 1H), 3.74 - 3.81 (m, 1H), 3.31 (dd, *J* = 11.1, 10.3 Hz,

1H). $^{13}C\{^1H\}$ NMR (126 MHz, CDCl$_3$): δ 151.1, 150.2, 149.6, 129.7, 122.6, 122.1, 118.9, 116.9, 110.7, 110.5, 110.3, 72.7, 71.0, 67.1, 66.2, 56.3, 55.8; HRMS (ESI) m/z calculated for C$_{19}$H$_{21}$O$_4$N$_2$ [(M+H)$^+$] 341.1496, found 341.1502.

X-ray crystal data of compounds 7h
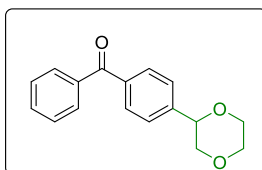
checkCIF/PLATON report

Structure factors have been supplied for datablock(s) mo_kdm_123_0m_pl
THIS REPORT IS FOR GUIDANCE ONLY. IF USED AS PART OF A REVIEW PROCEDURE
FOR PUBLICATION, IT SHOULD NOT REPLACE THE EXPERTISE OF AN EXPERIENCED
CRYSTALLOGRAPHIC REFEREE.

No syntax errors found.   CIF dictionary   Interpreting this report

Datablock: mo_kdm_123_0m_pl

```
Bond precision:    C-C = 0.0012 A          Wavelength=0.71073

Cell:    a=11.8124(4)      b=10.5930(4)      c=11.7212(4)
         alpha =90         beta=115.715(1)   gamma=90

Temperature: 100 K

                  Calculated              Reported
Volume            1321.41(8)              1321.41(8)
Space group       P 21/c                  P 21/c
Hall group        -P 2ybc                 -P 2ybc
Moiety formula    C17 H16 O3              C17 H16 O3
Sum formula       C17 H16 O3              C17 H16 O3
Mr                268.30                  268.30
Dx,g cm-3         1.349                   1.349
Z                 4                       4
Mu (mm-1)         0.092                   0.092
F000              568.0                   568.0
F000'             568.29
h,k,lmax          17,16,17                17,16,17
Nref              4802                    4653
Tmin,Tmax         0.986,0.992             0.981,0.992
Tmin'             0.981
```

```
Correction method= # Reported T Limits: Tmin=0.981 Tmax=0.992
AbsCorr = MULTI-SCAN

Data completeness=    0.969          Theta(max)= 32.592

R(reflections)=       0.0384( 4321)  wR2(reflections)= 0.1076( 4653)

S = 1.063             Npar= 181
```

The following ALERTS were generated. Each ALERT has the format
test-name_ALERT_alert-type_alert-level.
                   Click on the hyperlinks for more details of the test.

The thermal ellipsoid was drawn at the 50% probability level
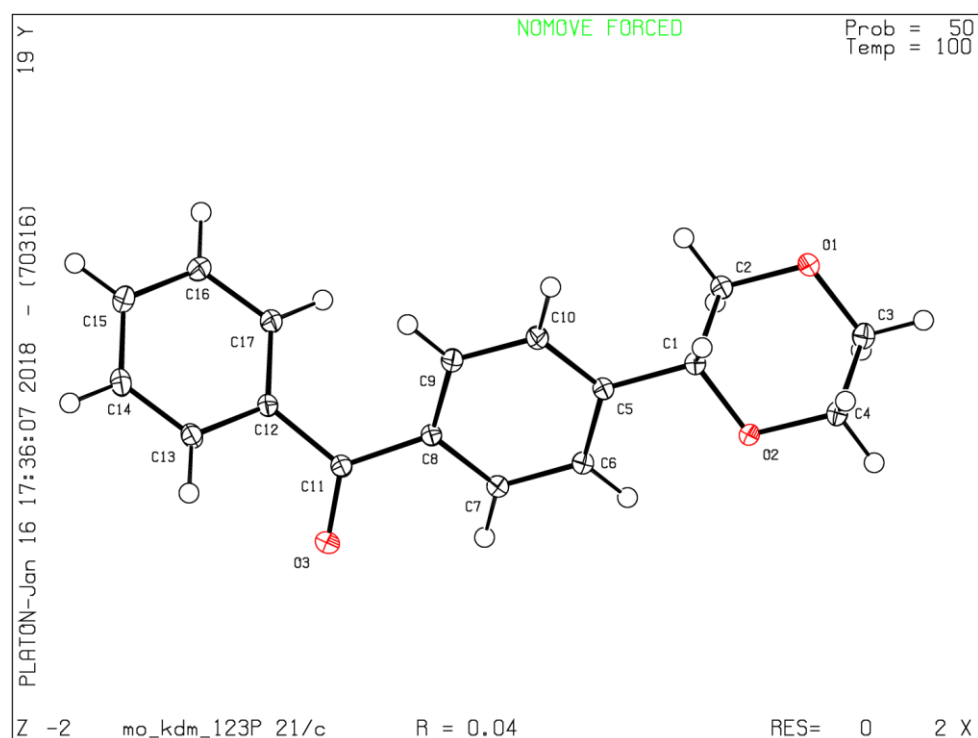
Section II

Visible Light Mediated, Metal and Oxidant Free Highly Efficient Cross Dehydrogenative Coupling (CDC) Reaction between Quinoxalin-2(1H)-ones and Ethers

2.2.1 Introduction

Carbon-carbon (C-C) bond formation has always been the most valuable and fundamental reaction in the development of organic chemistry and is considered a backbone of nearly every organic molecule. Hence C-C bond formation reactions consistently contributed in the advancement of organic chemistry. The application of C-C bond formation is found in fine chemicals, agrochemicals, medicinal and pharmaceutical ingredients; therefore, these transformations are one of the crucial class of reactions in organic chemistry.[24] Among the group of the methods developed over years,[25] metal-catalyzed and metal-free cross-dehydrogenative coupling (CDC) reactions have been reported as a straightforward and strong approach for the
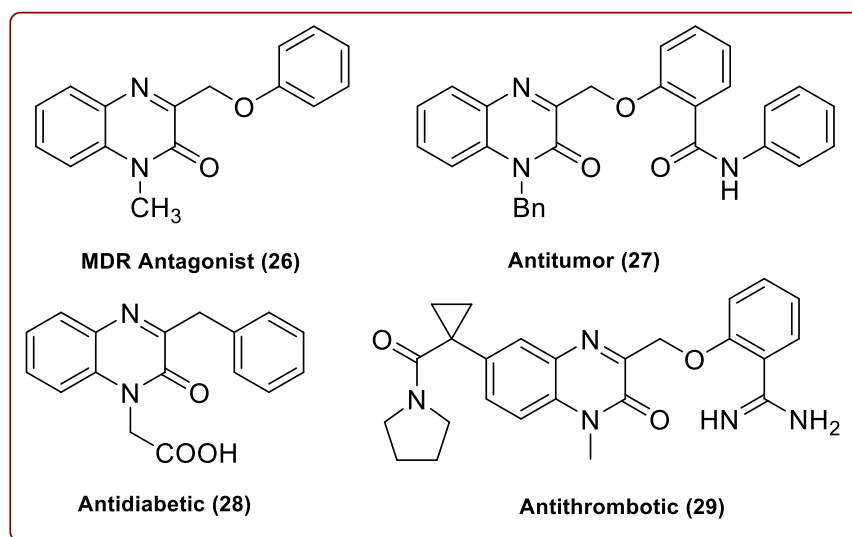
Figure 6. Biologically active ether molecules

preparation of C-C bonds.[26] Recently, photocatalyzed CDC reactions are emerging as a powerful tool to the transition metals as it has overcome with an effective way out for coupling of two C-H bonds with different chemical properties. Moreover, photocatalytic C-H functionalization has earned more attention due to its high atom economy and follows green chemistry principle. The major advantage in performing CDC reaction as compared to traditional metal catalyzed methods shows that the elimination of most important step i.e. prefunctionalization of starting materials. Furthermore, cyclic ethers follow green chemistry principle and ethers are important synthons in organic chemistry which serve as most versatile CDC reaction partner which we generally observe in various natural as well as synthetic molecules.[27a]

2.2.2 Review of Literature

The metal and metal-free CDC reactions on various electron-deficient heterocyclic, cyclic, and acyclic ethers have been studied comprehensively. These heterocycles contain substituted pyridines, thiophenes, indoles, quinines, isoquinines, azoles, and chromanes.[28] In addition to this, some attempts were made for C-N bond formation using photocatalytic CDC reaction.[29]

Furthermore, Wu and co-workers have developed photocatalyzed hydrogen atom transfer (HAT) reaction for C-H activation of ethers and subsequent 1, 4-addition to various SOMO-philes as shown in Scheme1.[31a] These CDC reactions are highly step and atom economy which provides unconventional approaches towards connecting molecular fragments that are often complementary to conventional methods. The development of this area by photocatalysis and first-row transition metal catalysis, and also with the help of peroxides and radical initiators has become successful. Initially, CDC reactions were carried out using metal catalysts, whereas recently, metal-free approaches were extensively applied for these transformations as these are much greener and more eco-friendly.

Adimurthys Work (2017)[30a]
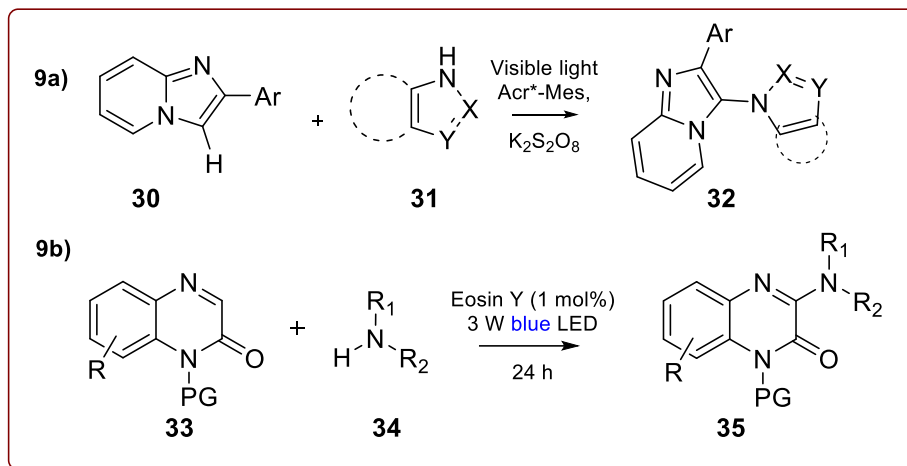
Scheme 9: C-H amination of imidazo heterocycles

Recently, Adimurthy *et al.* studied C-H amination of imidazo [1,2-a] pyridines (**Scheme 9a**) under photocatalytic conditions using benzotriazoles, benzoimidazoles, triazoles, pyrazoles, imidazoles, and indazoles as amine source[30a] with $K_2S_2O_8$ as external oxidant, whereas Wei *et al.* efficiently carried out CDC amination reaction of quinoxalin-2(1H)-ones using blue LED and eosin Y as a photocatalyst (**Scheme 9b**).[30b]

Wu's Work (2018)[31a]
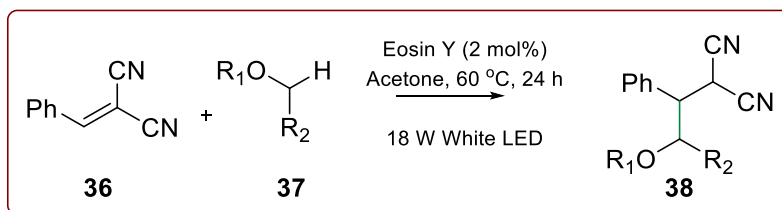
Scheme 10. Hydrogen atom transfer reactions

Furthermore, Wu and co-workers have developed a photocatalyzed hydrogen atom transfer (HAT) reaction for C-H activation of ethers and subsequent 1, 4-addition to various SOMO-

philes as shown in **Scheme 10**. Recently, Wei *et al.* has reported the photocatalytic CDC reaction between substituted quinoxalin-2(1H)-ones and ethers. Even though this approach needs the TBHP as oxidant and DABCO as a base in stoichiometric amount.[31b]

Correa's Approach (2014)[8c]
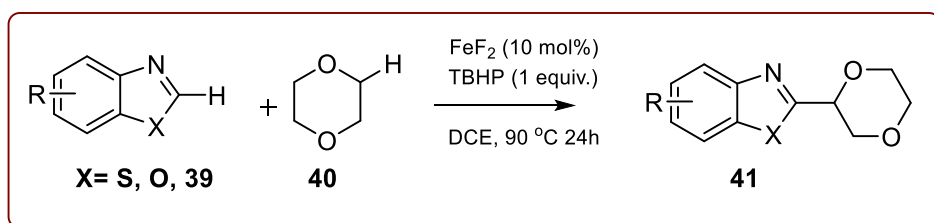
Scheme 11. Coupling between ethers and azoles

Correa and co-workers reported Fe-catalysed cross-coupling between cyclic ethers and azoles.[30] THF coupled with benzothiazole in the presence of the stoichiometric amount of TBHP in the presence of 10 mol-% of FeF_2 in DCE at 90 °C for 24 h to afford the corresponding product in good to excellent yields (**Scheme 11**). The iron salt and oxidant were critical for the transformation. Differently substituted azoles were coupled with THF, dioxane and 1,3-dioxolane to afford the products in good yields. Acyclic ether such as 1,2-dimethoxyethane also underwent the reaction to give both methylene and methyl-substituted products with high regioselectivities.

2.2.3 Present Work

2.2.3.1 Objectives

The 3-alkyl substituted quinoxalin-2(1H)-ones and their derivatives show broad range of biological activities as pharmaceuticals and agrochemicals.[32] Some important activities include MDR antagonists **26**,[33] antitumor **27**,[34] anti-viral, anti-microbial[35] and anti-diabetic activity **28**[36] (**Fig 6**). These molecules are widely used in the organic synthesis and synthesis of advanced

materials. The high importance of these moieties attracts more attention of chemist towards new and easy routes for alkylation/arylation of quinoxalin-2(1H)-ones.[37] Numerous reports were accessible in the literature for 3C activation of quinoxalin-2(1H)-ones *via* C-H bond activation under metal-free conditions.[38] Keeping in mind the importance of CDC reaction and our previous efforts towards developing metal free approaches [39] herein, we report a metal free photocatalytic CDC reaction for 3C alkylation of quinoxalin-2(1H)-ones with ethers (**Scheme 12**).
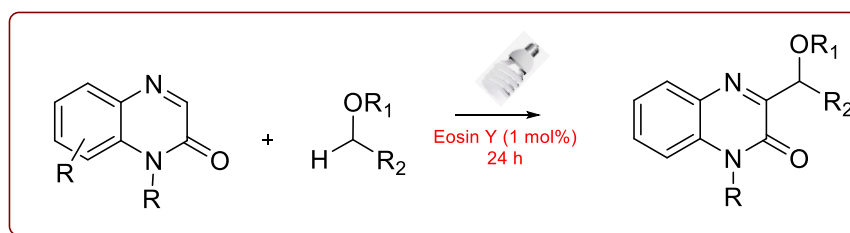
Scheme 12. CDC reaction for 3C alkylation of quinoxalin-2(1H)-ones with ethers

2.2.4 Results and Discussion

To investigate our assumption on CDC reaction, our initial attempts commences with coupling between 1-methylquinoxalin-2(1H)-one **42** and THF, using photocatalyst rose bengal (1 mol %) at 25 °C for 24 hrs. To our delight the desired C-alkylated product was formed in 27 % yield (**Table 4,** Entry 1). With this result, to enhance yield of product we vary the time and concentration of rose Bengal. Unfortunately yields were not promising and increased only up to 43 % (Entry 2-4). Hence, after careful analysis we speculated to use eosin Y as photocatalyst as an alternative to rose bengal. When eosin Y (1 mol %) was used as catalyst surprisingly, the yield of desired product increased to 68% in comparison with rose bengal (Entry 5). Further addition of TBHP as additive didn't enhance the yield (Entry 6) whereas increasing the concentration of eosin Y to 2 mol% for 18 h desired product was obtained in 88 % yield (Entry 7). Moreover, elaboration of reaction time from 18 to 24 h keeping concentration of eosin y in 1

mol%, yield of product boosted dramatically to 95% (Entry 8). With these results it can be concluded that time of the reaction plays an important role in the formation of product (Entry 9 and 10).

Table 4: Optimization Table for CDC reaction[a]
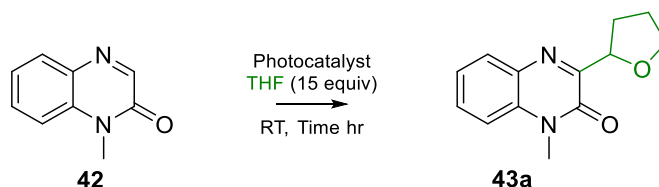
Entry	Photocatalyst	Time (h)	(Yield %)[a]
1	Rose Bengal (1 mol%)	24	27
2	Rose Bengal (1 mol%)	36	35
3	Rose Bengal (2 mol%)	24	42
4	Rose Bengal (2 mol%)	48	43
5	Eosin Y (1 mol%)	18	68
6	Eosin Y (1 mol%)	18	69
7	Eosin Y (2 mol%)	18	88
8	**Eosin Y (1 mol%)**	**24**	**95**
9	Eosin Y (2 mol%)	24	94
10	Eosin Y (2 mol%)	36	96
11	Eosin Y (1 mol%)	24	61
12	-	36	Nr
13	Eosin B (1 mol%)	24	30

Reaction conditions: [a]Isolated Yields; [b] Oxidant TBHP used 2 equiva.; nr = No Reaction; c Water:THF used in 1:0.3

It is noteworthy that, the reaction works well in the presence of water to offer 3C-alkylated product in 61% yield (Entry 11). However, no reaction was observed in absence of photocatalyst (Entry 12). The reaction was attempted with eosin B as photocatalyst offer only 30% yield of the

desired product (Entry 13). From the above observation it was concluded that, entry 8 is the suitable condition for the CDC reaction between 1-methylquinoxalin-2(1H)-one and ethers.

Table 5: Substrate Scope for CDC Reaction

43a, R= Me, 95 %
43b, R= Bn,   90 %
43c, R= allyl, 92%

43d, R= Me, 49 %
43e, R= Bn,   42%
43f, R= allyl, 52%

43g, R= Me, 51%
43h, R= Bn,   39%

43i, 89 %

43j, X=CH₂, 55%
43k, X= O, 59%

43l, 41 %

43m, 84 %

43n, R= Br, 89 %
43o, R= Cl, 86 %

43p, 81%

43q, 83%

43r, 0%
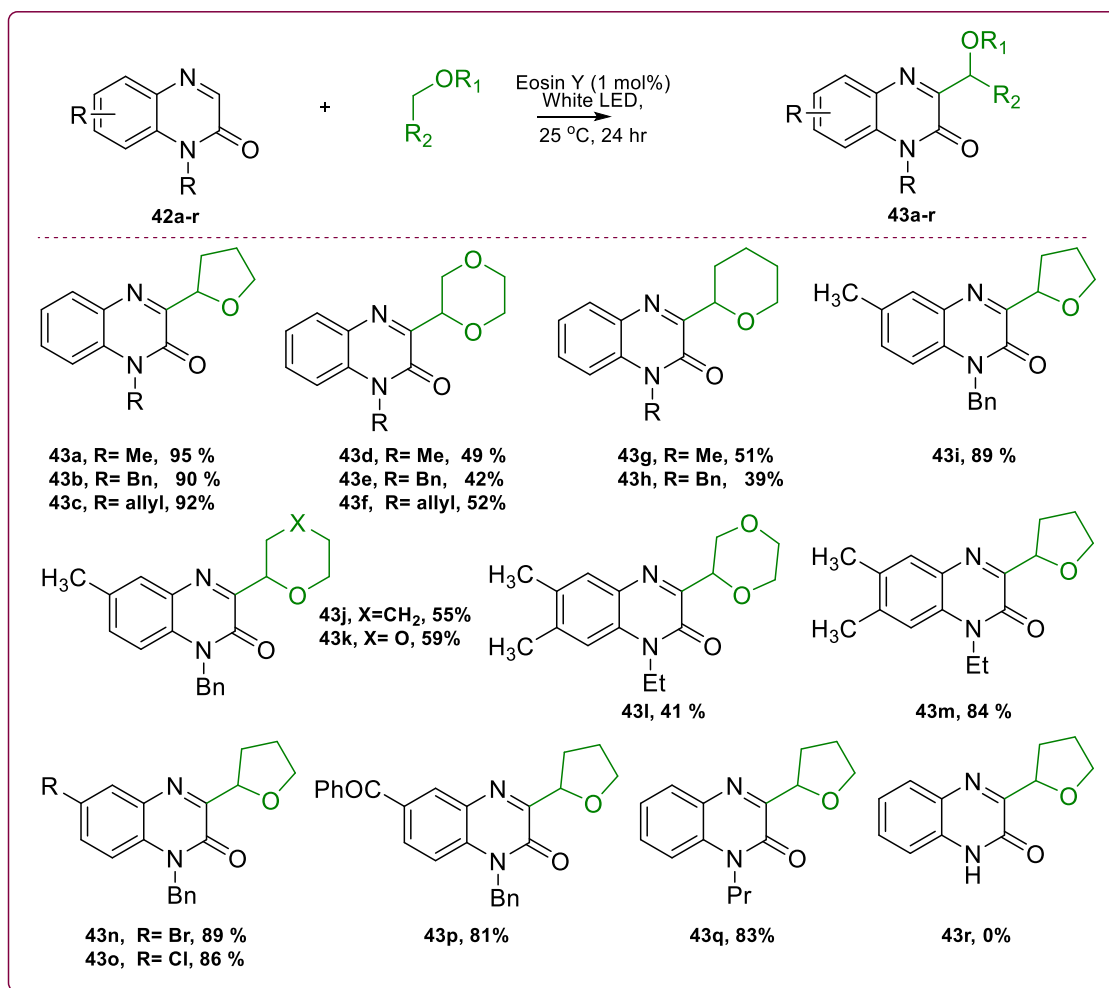
[a]Reaction conditions: Substituted 2-Quinazolinones (42a,1 mmol), Eosin Y (0.01 mmol), in THF (15 mmol) at 25 °C under air for 24 h. [b]The isolated yields were calculated based on quinoxalin-2(1H)-ones

With the optimized reaction conditions in hand, we next examined the substrate scope for this CDC reaction on the various substituted quinoxalin-2(1H)-one derivative (**Table 5**). To our delight, the reaction serves as a really appreciable protocol to the syntheses of various 3C substituted quinoxalin-2(1H)-one, affording moderate to excellent yields bearing both electron-

donating and electron-withdrawing substituent. While amide group of quinoxalin-2(1H)-one alkylated with groups such as methyl, benzyl and allyl groups subjected for photocatalytic CDC reaction condition, high yields of desired product was observed without any diverse effect (**43a-43h, Table 5**). We were glad to find that various cyclic ethers such as THF, THP and 1,4-dioxanes were compatible with the reaction conditions and yields of the corresponding 3C alkylated quinoxalin-2(1H)-one products in satisfactory yields. It is noteworthy that, quinoxalin-2(1H)-one bearing electron donating groups such as methyl and dimethyl provided the highest yields (**43i-43m**) whereas quinoxalin-2(1H)-one with electron withdrawing group such as -Br, -Cl gave slightly less yields of desired (**43n-43o**). Also, the 6-benzoyl substituted quinoxalin-2(1H)-one subjected under optimized reaction condition to form the desired product in 81% yields (**43p**). Also, *N*-propylated quinoxalin-2(1H)-one derivative subjected under optimized reaction conditions yields 3C alkylated product in 83% yield (**43q, Table 5**). The formation of **43a**-**43r** was confirmed and predicted by their corresponding ^{1}H, ^{13}C, and Mass data.

Example 1:
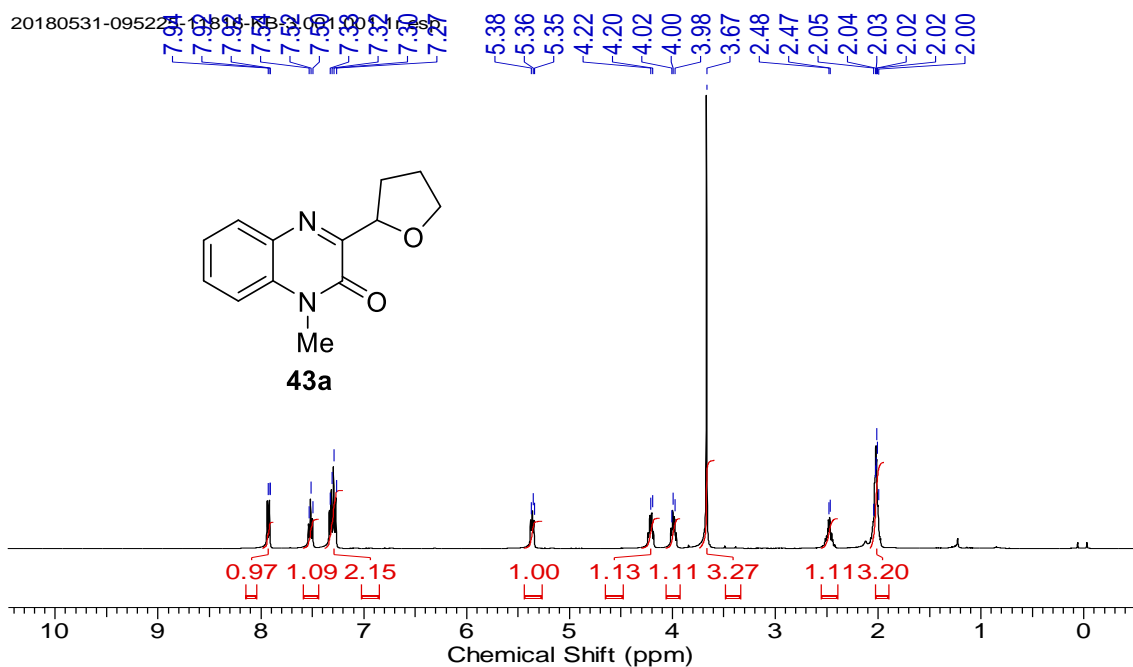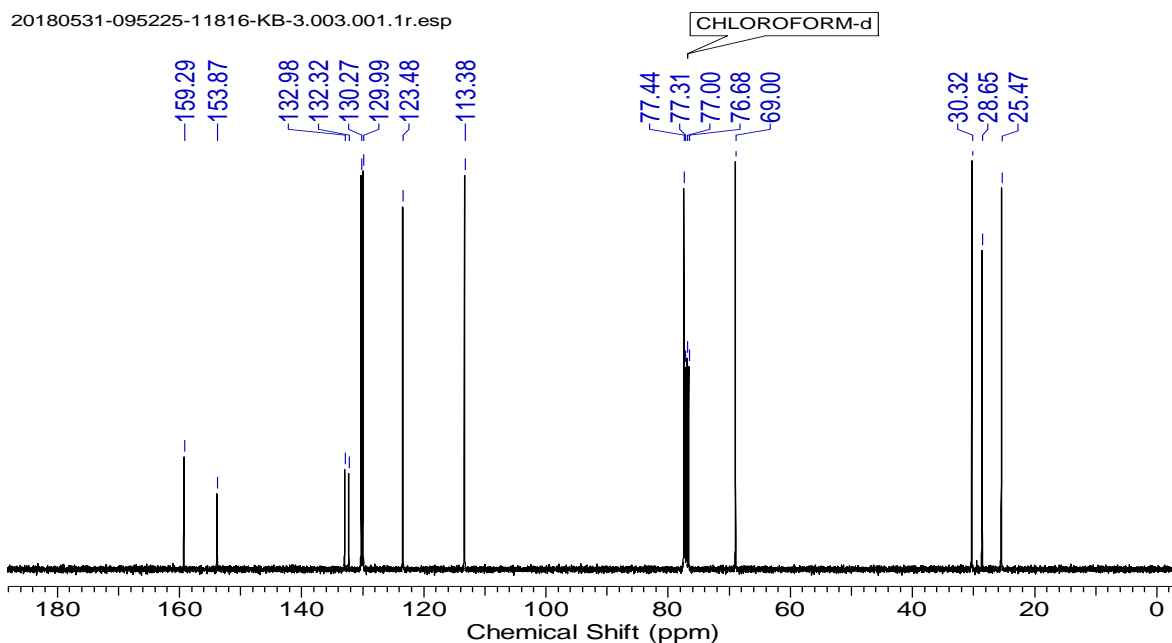
Figure 7. ^{1}H and ^{13}C NMR of 1-methyl-3-(tetrahydrofuran-2-yl)quinoxalin-2(1H)-one (**43a**)

The confirmation of the product, i.e., 1-methyl-3-(tetrahydrofuran-2-yl) quinoxalin-2(1H)-one (**43a**) was done by checking its ^{1}H and ^{13}C NMR spectrum. The peak showed in ^{1}H NMR at δ 2.00 (s, 3H) for three methyl protons attached to nitrogen of amide group in compound **43a** and 4 aromatic protons in the range of δ 7.88 -7.98 (m, 1H), 7.44 -7.59 (m, 1H) and 7.20 -7.37 (m, 2H). In its ^{13}C NMR spectrum, aromatic carbons showed in the range of δ 113-159, and remaining carbons of ether moiety are in the range of δ 25-77 (**43a**) (**Figure 7**).

Alkylated (3C) 2-quinazolinone derivatives were further functionalised as shown in **Scheme 13** to show the synthetic utility of the developed protocol. 1-Allyl-3-(1,4-dioxan-2-yl) quinoxalin-2(1H)-one subjected to hydrogenation using Pd/C as the catalyst to give compound **44** in 94% yield. Next, 1-allyl-3-(1,4-dioxan-2-yl) quinoxalin-2(1H)-one subjected for oxidative 1,3-dipolar addition[40] with 4-methoxybenzaldehyde oxime using PIDA as oxidant under nitrogen atmosphere to afford compound **45** in 75% yield (**Scheme 13**).
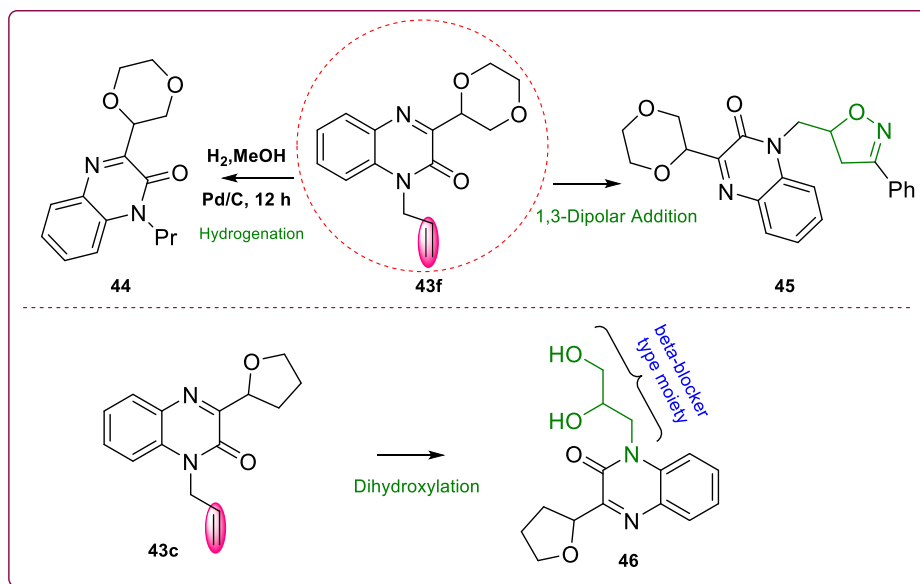
Scheme 13: Synthetic transformations of the products

Besides, 1-allyl-3-(tetrahydrofuran-2-yl) quinoxalin-2(1H)-one **43c** could also be converted into the dihydroxylated product **46** in 89% yield, which appears as a β-blocker type core structure (**Scheme 13**).

Example 2:

AV-200-20180913 155620334 190 12 00 001 1r.esp

161.4
156.8
154.6
154.0
132.8
131.
130.7
128.4
124.2
121.3
114.6
114.

78.17
77.70
77.07
76.43
74.47
67.56
66.36
55.42
46.08
39.17
29.72
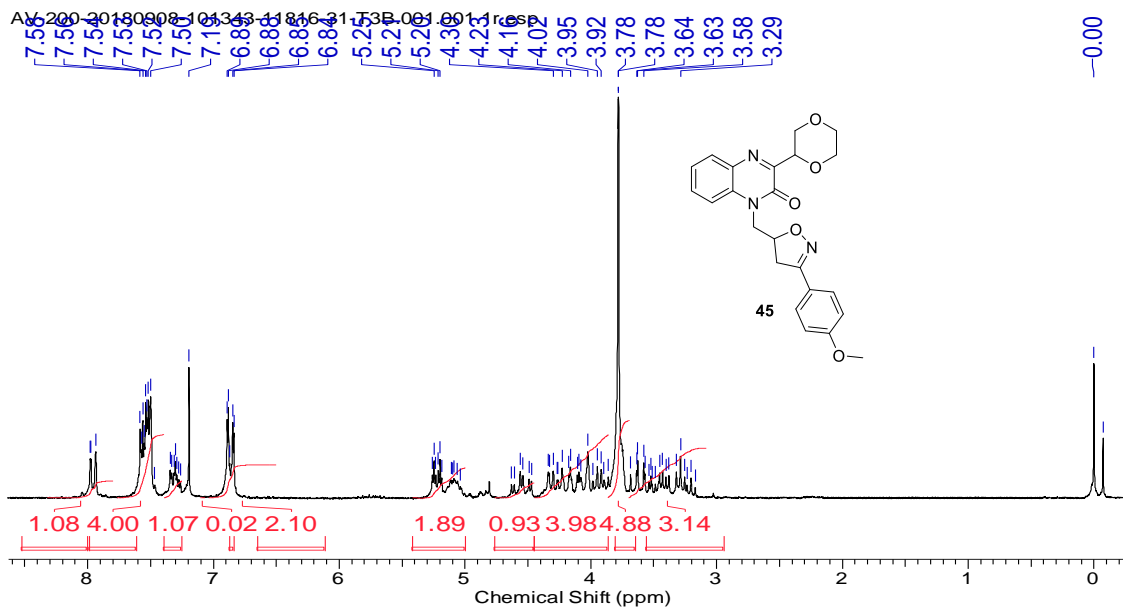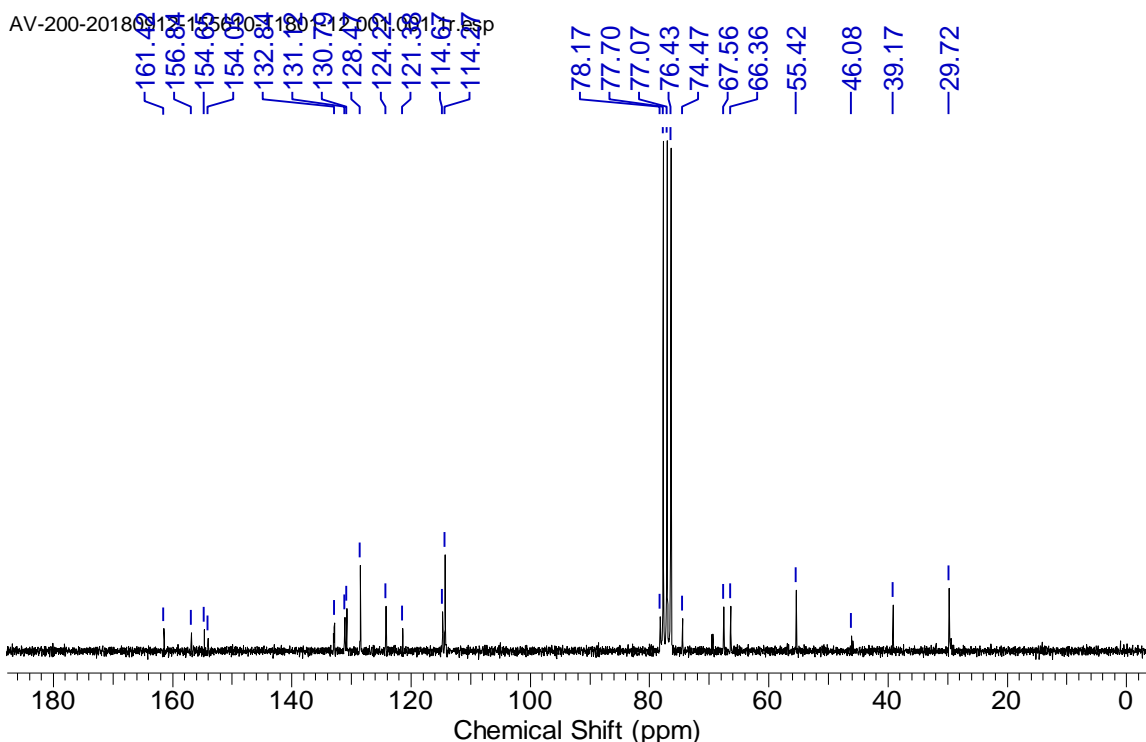
Figure 8. ¹H and ¹³C NMR of 3-(1,4-dioxan-2-yl)-1-((3-(4-methoxyphenyl)-4,5-dihydroisoxazol-5-yl) methyl) quinoxalin-2(1H)-one (**45**)

The comp. **45** (3-(1,4-dioxan-2-yl)-1-((3-(4-methoxyphenyl)-4,5-dihydroisoxazol-5-yl) methyl) quinoxalin-2(1H)-one) was confirmed by ¹H,¹³C NMR and HRMS analysis (**Figure 8**.). In the proton NMR spectrum, the signals for aromatic hydrogens appeared at δ 7.80-8.32 (m, 1H), 7.39-7.77 (m, 4H), 7.25-7.39 (m, 1H) and 6.50-7.04 (m, 2H). The remaining aliphatic hydrogens showed in the range of δ 3.70-5.42 and ¹³C NMR spectrum appearance of aromatic carbons in the range of δ 114-161 ppm and δ 29-78 (**Figure 8**).

Example 3:

The formation of *β-blocker* type moiety 1-(2,3-dihydroxypropyl)-3-(tetrahydrofuran-2-yl) quinoxalin-2(1H)-one (**46**) was confirmed by ¹H,¹³C NMR and HRMS analysis (**Figure 9**.). In the proton NMR spectrum, the signals for aromatic hydrogens appeared in the range of δ 7.24-7.89, and the remaining aliphatic hydrogens showed in the range of δ 1.18-5.31 ppm. The

aromatic carbons displayed in the range of δ 113.51-158.06 and nonaromatic carbons in the range of δ 24.95-68.89 in the[13]C NMR spectrum.
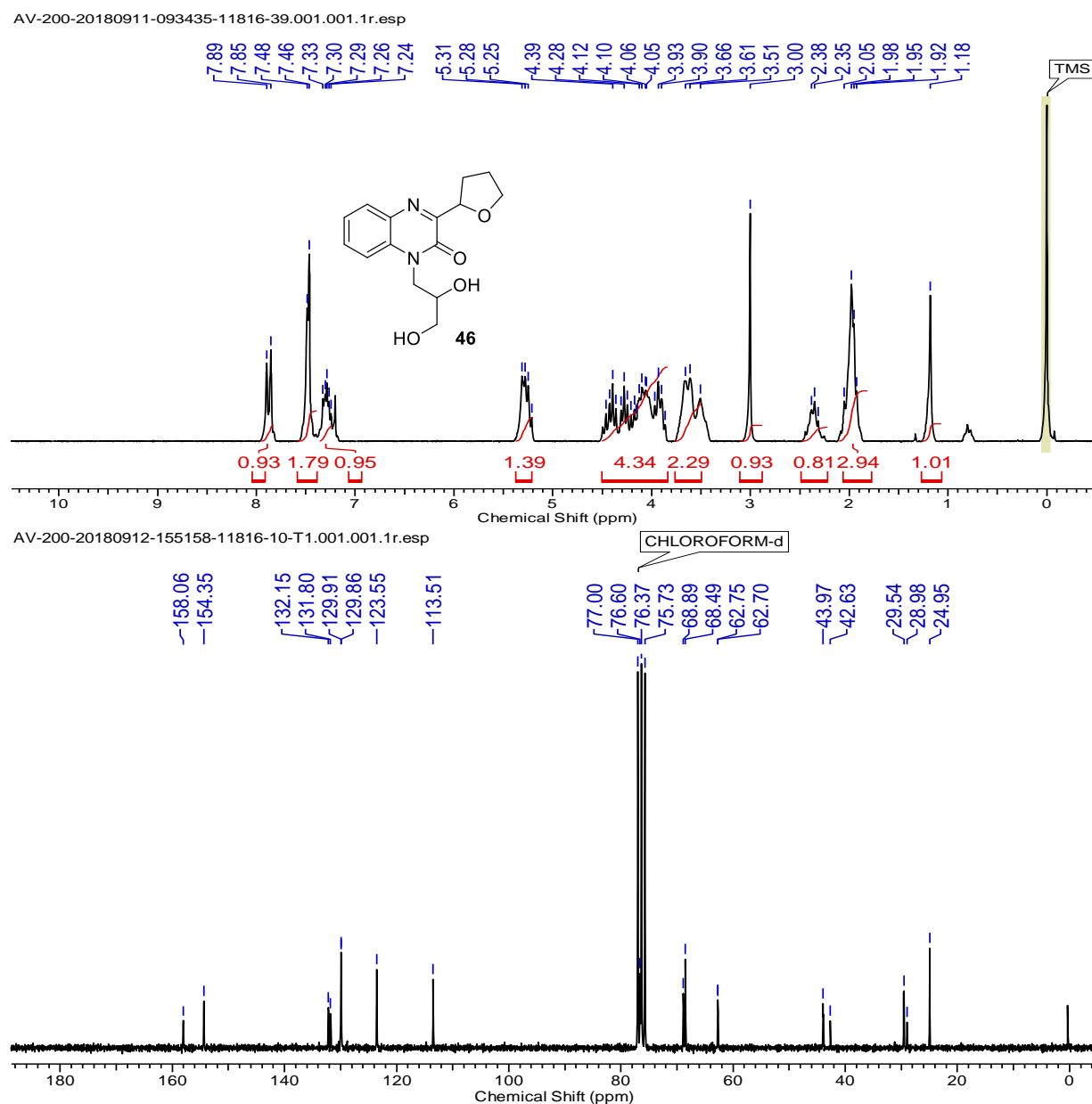
Figure 9. ^{1}H and ^{13}C NMR of 1-(2,3-dihydroxypropyl)-3-(tetrahydrofuran-2-yl) quinoxalin-2(1H)-one (**46**)

In order to gain insight into the reaction mechanism, the control experiment was performed between 1-methylquinoxalin-2(1H)-on **43** and THF by addition of 2 equivalents TEMPO as

radical scavenger (**Scheme 14**). We observed the formation TEMPO-THF adduct **20** with trace amount of desired product. The formation of TEMPO-THF adduct **20** were confirmed by LCMS.
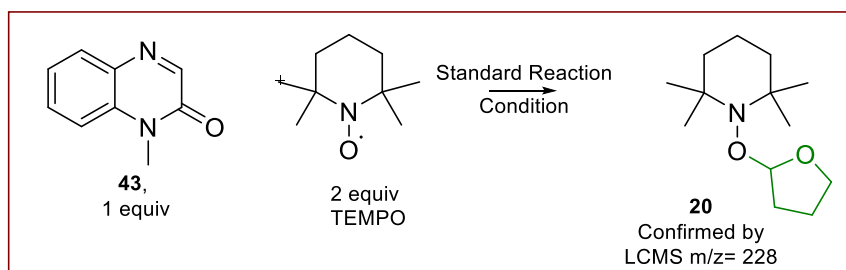
Scheme 14. Control experiments for oxidative rearrangement reaction

From above experiment it can conclude that reaction works by formation of radical. On the basis of control experiment and known literature, we are proposing a plausible reaction pathway for the eosin y catalyzed CDC reaction (**Scheme 15**).
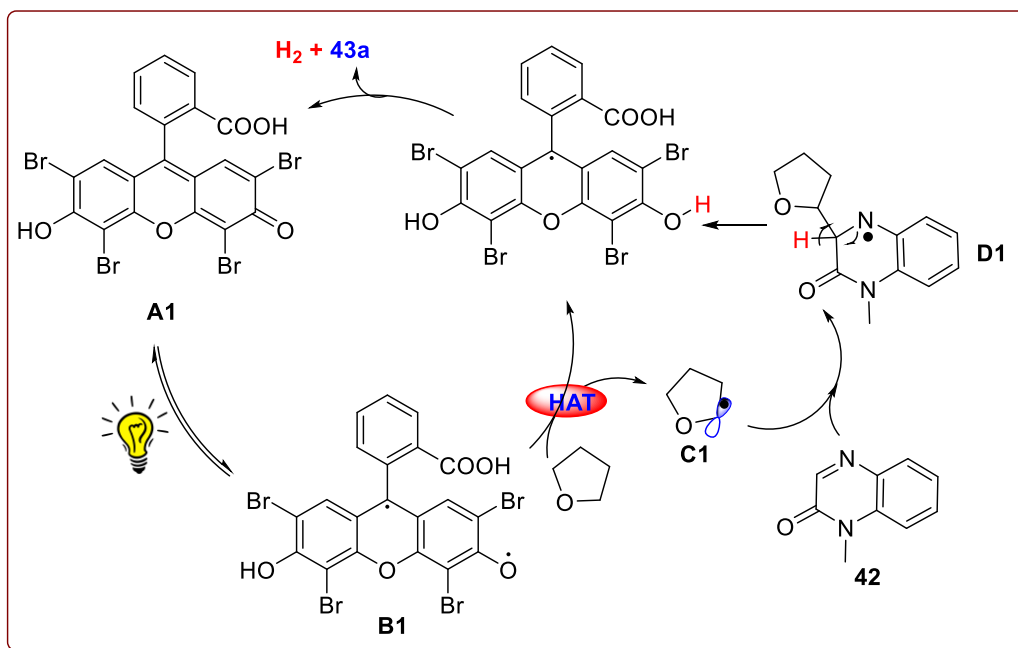
Scheme 15: Plausible reaction mechanism

The anionic eosin y species A1 activated in presence of white light which promotes HAT process[8] for the formation of carbon centered radical C1. The formed radical C1 adds on 1-

methylquinoxalin-2(1H)-on **42** to generate *N*-centered radical D1. Then the species D1 undergoes dehydrogenative aromatization reaction to give the desired product 43a and eosin y which will further used for the next catalytic cycle.

2.2.5 Conclusion

In conclusion, we have developed an efficient white light-mediated eosin y catalyzed C-C bond formation reaction between ethers and quinoxalin-2(1H) to give 3C-alkylated quinoxalin-2(1H)-ones. This approach has a broad substrate scope with high functional group tolerance. Also, it is a base and oxidant-free approach under mild reaction conditions over previously reported methods. Further applications of the present methodology are underway in our laboratory.

2.2.6 Experimental Section

General Procedure for the Cross Dehydrogenative Coupling of quinoxalin-2(H)-one with Ethers
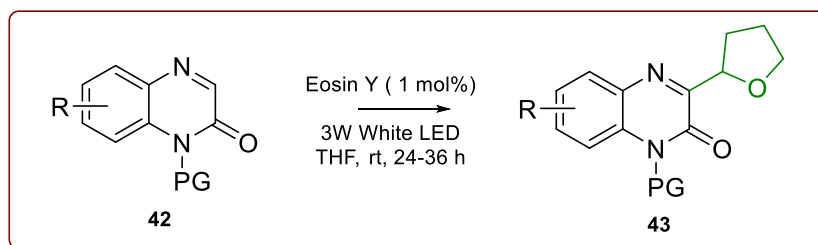
To a solution of quinoxalin-2(H)-one **42** (0.2 mmol), Eosin Y (1 mol %), ether (3 mL) was added, and the reaction mixture was kept open to the air and stirred under the irradiation of 3 W White LEDs at room temperature (27 $^{\circ}$C) for 24h. After completion of the reaction (monitored by TLC), the reaction mixture was dried under a vacuum. Then the crude reaction mixture was diluted with ethyl acetate (10 mL) and washed with brine. Eluted with EtOAc (10 mL * 2) and dried over anhydrous Na_2SO_4. The organics were evaporated, and the crude residue was purified

by flash column chromatography using a mixture of petroleum ether and ethyl acetate (70:30) as eluent to give the desired product **43**.

General procedure for the synthesis of 3-(1,4-dioxan-2-yl)-1-propylquinoxalin-2(1H)-one (44):
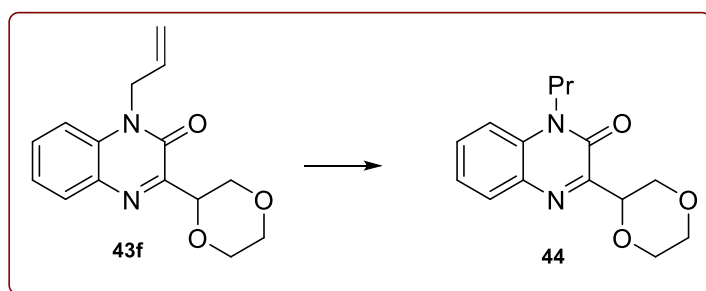
The solution of allyl moiety (**43f**) formed in the present work is reduced using the hydrogenation condition. Formed product (**43f**) (1 mmol) dissolved in methanol 5 mL, then in this solution was added Pd/C (10% on carbon 20 mg) and the mixture was stirred under H_2 atmosphere at room temperature for about 12 h. After completion of the reaction mixture, it was filtered over celite pad using methanol as eluent and organic solvent evaporated under reduced pressure to give the crude product of reduced allyl group (monitored by TLC). The crude organics were purified by using silica gel column chromatography. (100−200 mesh) using an appropriate concentration of ethyl acetate and petroleum ether (EtOAc/PE = 2:98) as an eluent to give the **44** in good yield.

 Experimental procedure for the Synthesis of 3-(1,4-dioxan-2-yl)-1-((3-(4-methoxyphenyl)-4,5-dihydroisoxazol-5-yl)methyl)quinoxalin-2(1H)-one (45):

The solution of oxime (1.5 mmol) in MeOH (2 mL) was added slowly at room temperature to a stirred solution of DIB (1.1 equiv) and olefin (1.1 equiv.) in Methanol 2 mL containing TFA. A white precipitate formed slowly and then slowly dissolved as the reaction progressed. Upon completion of the reaction (as monitored by TLC), the reaction mixture was added to water and extracted with ethyl acetate (5 mL × 3). A combined organic layer was washed with anhydrous

Na$_2$SO$_4$ and dried over reduced pressure. The crude product was purified by column chromatography on silica gel (100−200 mesh, EtOAc/PE = 10:90 to 30:70 as step gradient) to afford compound **8** as a white solid.

Experimental procedure for the synthesis of 1-(2,3-dihydroxypropyl)-3-(tetrahydrofuran-2-yl) quinoxalin-2(1H)-one (46):

In a 100 mL oven-dried round bottom A flask NMO (1.5 equiv.) and OsO$_4$ (10 mol%) were added. In the 100 mL round bottom flask B, prepare the solution of olefin (1 equiv.) in acetone (10 mL) and water (5 mL) at room temperature. Mix the olefin solution in round bottom flask A and above reaction mixture was stirred for 5 h and after completion of the reaction (monitored by TLC), quenched with a saturated solution of aqueous sodium thiosulphate. The above bilayer solution of the reaction mixture was stirred for another 1 h at room temperature. Then above reaction mixture was extracted with EtOAc. The obtained organic layers were concentrated under reduced pressure. The crude residue was purified by silica gel column chromatography to afford the desired product **46** in excellent yield.

1-Methyl-3-(tetrahydrofuran-2-yl)quinoxalin-2(1H)-one (43a):

Yield: 95 % (95 mg); White Solid; ^{1}HNMR (400 MHz, CDCl$_3$): δ 7.88 - 7.98 (m, 1H), 7.44 - 7.59 (m, 1H), 7.20 - 7.37 (m, 2H), 5.36 (dd, *J* = 7.32, 6.10 Hz, 1H), 4.21 (d, *J* = 6.71 Hz, 1H), 3.92 - 4.06 (m, 1H), 3.67 (s, 3H), 2.48 (d, *J* = 5.49 Hz, 1H), 1.95 - 2.08 (m, 3H).^{13}C NMR(101 MHz, CDCl$_3$): δ 159.3, 153.9, 133.0, 132.3, 130.3, 130.0, 123.5, 113.4, 77.4, 69.0, 30.3, 28.7, 25.5;

1-Benzyl-3-(tetrahydrofuran-2-yl)quinoxalin-2(1H)-one (43b):

Yield: 90 % (70 mg); White Solid; ^{1}H NMR (200 MHz, CDCl$_3$): δ 8.10 (dd, *J* = 8.02, 1.58 Hz, 1H), 7.85 (dd, *J* = 7.96, 1.64 Hz, 1H), 7.48 - 7.72 (m, 4H), 7.30 - 7.48 (m, 3H), 5.50 - 5.72 (m,

2H), 5.43 (dd, *J* = 7.45, 6.06 Hz, 1H), 4.13 - 4.33 (m, 1H), 3.92 - 4.11 (m, 1H), 2.34 - 2.57 (m, 1H), 1.94 - 2.23 (m, 3H). ^{13}C NMR (50 MHz, CDCl$_3$): δ 154.7, 149.7, 139.8, 138.2, 136.3, 129.3, 128.9, 128.3, 127.9, 126.5, 126.4, 76.8, 69.0, 67.9, 30.6, 25.6; HRMS (ESI) calculated [M+H]$^+$ for C$_{19}$H$_{19}$O$_2$N$_2$: 307.1441, found: 307.1442

1-Allyl-3-(tetrahydrofuran-2-yl)quinoxalin-2(1H)-one (43c):

Yield: 92 % (88 mg); yellow gummy oil; ^{1}H NMR (500 MHz, CDCl$_3$): δ 7.85 (d, *J* = 8.01 Hz, 1H), 7.33 - 7.48 (m, 1H), 7.13 - 7.30 (m, 2H), 5.73 - 5.95 (m, 1H), 5.26 - 5.35 (m, 1H), 5.15 (d, *J* = 10.30 Hz, 1H), 5.06 (d, *J* = 17.55 Hz, 1H), 4.80 (br. s., 2H), 4.13 (q, *J* = 6.61 Hz, 1H), 3.82 - 3.98 (m, 1H), 2.26 - 2.48 (m,1H), 1.83 - 2.05 (m, 3H). ^{13}C NMR (126 MHz, CDCl$_3$): δ 159.2, 153.3, 132.3, 132.1, 130.3, 130.2, 129.8, 123.3, 117.8, 113.8, 77.2, 68.9, 44.0, 30.2, 25.4.

3-(1,4-Dioxan-2-yl)-1-methylquinoxalin-2(1H)-one (43d):

Yield: 49 % (52 mg); Yellow Solid ; ^{1}H NMR (400 MHz, CDCl$_3$): δ 7.94 (d, *J* = 7.93 Hz, 1H), 7.50 (t, *J* = 7.93 Hz, 1H), 7.21 - 7.32 (m, 2H), 5.21 (dd, *J* = 9.46, 2.14 Hz, 1H), 4.19 (dd, *J* = 10.99, 1.83 Hz, 1H), 4.03 (d, *J* = 11.60 Hz, 1H), 3.86 - 3.95 (m, 1H), 3.75 (d, *J* = 6.10 Hz, 2H), 3.62 (s, 3H), 3.53 - 3.60 (m, 1H). ^{13}C NMR (101 MHz, CDCl$_3$): δ 155.0, 153.5, 133.0, 132.4, 130.7, 130.5, 123.7, 113.5, 74.5, 69.3, 67.4, 66.2, 28.9; HRMS (ESI) calculated [M+Na]$^+$ for C$_{13}$H$_{14}$O$_3$N$_2$Na: 269.0897, found: 269.0898

1-Benzyl-3-(1,4-dioxan-2-yl)quinoxalin-2(1H)-one (43e):

Yield: 42 % (35 mg); White Solid; ^{1}H NMR (500 MHz, CDCl$_3$): δ 8.07 (d, *J* = 8.01 Hz, 1H), 7.76 (d, J = 8.01 Hz, 1H), 7.57 (t, *J* = 7.63 Hz, 1H), 7.46 - 7.51 (m, 1H), 7.43 (d, *J* = 7.25 Hz, 2H), 7.29 - 7.35 (m, 2H), 7.23 - 7.28 (m, 1H), 5.38 - 5.61 (m, 2H), 5.19 (dd, *J* = 9.54, 2.29 Hz, 1H), 4.00 - 4.10 (m, 2H), 3.91 (td, *J* = 11.44, 3.05 Hz, 1H), 3.71 - 3.82 (m, 2H), 3.64 (t, *J* = 10.68 Hz, 1H). ^{13}C NMR (126 MHz, CDCl$_3$): δ 154.1, 144.8, 139.7, 138.3, 135.8, 129.8, 128.9,

128.3, 127.9, 127.9, 126.5, 126.5, 73.8, 69.2, 68.0, 67.2, 66.0; HRMS (ESI) calculated [M+H]$^+$

for $C_{19}H_{19}O_3N_2$: 323.1390, found: 323.1391

1-Allyl-3-(1,4-dioxan-2-yl)quinoxalin-2(1H)-one (43f):

Yield: 52 % (53 mg); Yellow Solid; ^{1}H NMR (500 MHz, CDCl$_3$): δ 7.95 (dd, *J* = 8.20, 1.34 Hz,

1H), 7.39 - 7.55 (m, 1H), 7.10 - 7.33 (m, 2H), 5.74 - 5.95 (m, 1H), 5.15 - 5.27 (m, 2H), 5.08 (d, *J*

= 17.17 Hz, 1H), 4.74 - 4.88 (m, 2H), 4.19 (dd, *J* = 11.44, 2.67 Hz, 1H), 4.03 (d, *J* = 11.44 Hz,

1H), 3.86 - 3.94 (m, 1H), 3.70 - 3.80 (m, 2H), 3.60 (dd, *J* = 11.06, 9.54 Hz, 1H).^{13}C NMR (126

MHz, CDCl$_3$): δ 155.1, 153.2, 132.7, 132.2, 130.7, 130.7, 130.3, 123.7, 118.2, 114.1, 74.4, 69.3,

67.4, 66.2, 44.4;

1-Methyl-3-(tetrahydro-2H-pyran-2-yl)quinoxalin-2(1H)-one (43g):

Yield: 51 % (54 mg); Yellow Solid; ^{1}H NMR (500 MHz, CDCl$_3$): δ 8.05 (d, *J* = 8.0 Hz, 1H),

7.55 (t, *J* = 7.6 Hz, 1H), 7.25 - 7.41 (m, 2H), 5.00 (d, *J* = 10.7 Hz, 1H), 4.29 (d, *J* = 10.7 Hz, 1H),

3.62 - 3.80 (m, 4H), 2.15 (d, J = 12.6 Hz, 1H), 1.98 (d, *J* = 10.3 Hz, 1H), 1.72 - 1.90 (m, 2H),

1.52 - 1.68 (m, 2H). ^{13}C NMR (126 MHz, CDCl$_3$): δ 158.5, 153.3, 132.7, 132.4, 130.3, 129.9,

123.4, 113.2, 76.1, 69.1, 29.9, 28.6, 25.3, 23.3; HRMS (ESI) calculated [M+H]$^+$ for $C_{14}H_{17}O_2N_2$:

245.1285 found: 245.1279

1-Benzyl-3-(tetrahydro-2H-pyran-2-yl)quinoxalin-2(1H)-one (43h):

Yield: 39 % (32 mg); White Solid; ^{1}H NMR (200 MHz, CDCl$_3$): δ 8.06 (dd, *J* = 7.89, 1.58 Hz,

1H), 7.37 - 7.47 (m, 1H), 7.22 - 7.36 (m, 7H), 5.32 - 5.68 (m, 2H), 4.87 - 5.20 (m, 1H), 4.32 (dd,

J = 10.55, 3.09 Hz, 1H), 3.60 - 3.89 (m, 1H), 2.20 (d, *J* = 10.74 Hz, 1H), 1.53 - 2.08 (m, 6H).^{13}C

NMR (50 MHz, CDCl$_3$): δ 158.3, 153.1, 134.5, 132.3, 131.7, 130.0, 129.6, 128.2, 127.0, 126.1,

123.1, 113.6, 68.8, 45.1, 29.6, 24.9, 23.0;

1-Methyl-3-(tetrahydrofuran-2-yl)quinoxalin-2(1H)-one (43i):

Yield: 89 % (79 mg); Colorless Oil; ^{1}H NMR (200 MHz, CDCl$_3$): δ 7.54 - 7.91 (m, 1H), 7.06 - 7.33 (m, 7H), 5.30 - 5.52 (m, 2H), 3.86 - 4.07 (m, 1H), 2.39 - 2.56 (m, 1H), 2.26 - 2.38 (m, 3H), 2.12 - 2.25 (m, 1H), 1.89 - 2.11 (m, 3H).

1-Benzyl-7-methyl-3-(tetrahydro-2H-pyran-2-yl)quinoxalin-2(1H)-one (43j):

Yield: 55 % (51 mg); Colorless Oil; ^{1}H NMR (200 MHz, CDCl$_3$): δ 7.73 - 7.91 (m, 1H), 6.93 - 7.28 (m, 7H), 5.17 - 5.57 (m, 2H), 4.89 - 5.07 (m, 1H), 4.14 - 4.31 (m, 1H), 3.54 - 3.76 (m, 1H), 2.30 (s, 3H), 2.01 - 2.16 (m, 1H), 1.39 - 1.99 (m, 5H). ^{13}C NMR (50 MHz, CDCl$_3$): δ 157.5, 153.6, 141.0, 135.2, 133.5, 131.4, 131.1, 130.4, 130.3, 128.8, 127.6, 126.9, 126.7, 125.0, 114.2, 114.0, 69.4, 45.7, 30.2, 25.6, 23.6, 22.0, 20.5; HRMS (ESI) calculated [M+H]$^+$ for C$_{21}$H$_{23}$O$_2$N$_2$: 335.1754, found: 335.1741

1-Benzyl-3-(1,4-dioxan-2-yl)-7-methylquinoxalin-2(1H)-one (43k):

Yield: 59 % (55 mg); Colorless Oil; ^{1}H NMR (400 MHz, CDCl$_3$): δ 7.77 (s, 1H), 7.17 - 7.26 (m, 4H), 7.13 (t, *J* = 6.49 Hz, 2H), 7.04 - 7.10 (m, 1H), 5.41 - 5.51 (m, 1H), 5.23 - 5.40 (m, 2H), 4.23 (dd, *J* = 11.44, 2.29 Hz, 1H), 4.01 - 4.10 (m, 1H), 3.86 - 3.98 (m, 1H), 3.72 - 3.84 (m, 2H), 3.63 (dd, *J* = 11.06, 9.54 Hz, 1H), 2.32 (s, 3H). ^{13}C NMR (101 MHz, CDCl$_3$): δ 154.7, 153.4, 141.4, 134.6, 133.5, 132.4, 131.7, 130.2, 130.1, 129.8, 128.6, 127.4, 126.4, 125.0 , 114.0, 113.8, 74.2, 69.1, 67.2, 67.1, 66.0, 45.4, 45.4 , 29.3, 20.2; HRMS (ESI) calculated [M+H]$^+$ for C$_{20}$H$_{21}$O$_3$N$_2$: 337.1547, found: 337.1534

3-(1,4-Dioxan-2-yl)-1-ethyl-6,7-dimethylquinoxalin-2(1H)-one (43l):

Yield: 41 % (40 mg); White solid; ^{1}H NMR (400 MHz, CDCl$_3$): δ 7.89 (s, 1H), 7.55 (s, 1H), 5.21(dd, *J* = 9.77, 2.44 Hz, 1H), 4.42 - 4.68 (m, 2H), 4.07 - 4.19 (m, 2H), 3.99 (td, *J* = 11.29, 3.05 Hz, 1H), 3.79 - 3.92 (m, 2H), 3.69 (t, *J* = 10.68 Hz, 1H), 2.41 (d, *J* = 6.10 Hz, 6H), 1.46 (t, *J* = 7.02 Hz, 3H). ^{13}C NMR (101 MHz, CDCl$_3$): δ 154.1, 143.4, 139.9, 138.4, 136.8, 136.0, 128.2,

125.8, 73.8, 69.3, 67.2, 65.9, 62.0, 29.3, 19.9, 19.6, 14.1; HRMS (ESI) calculated [M+H]$^+$ for C$_{16}$H$_{21}$O$_3$N$_2$: 289.1547, found: 289.1543

1-Ethyl-6,7-dimethyl-3-(tetrahydrofuran-2-yl)quinoxalin-2(1H)-one (43m):

Yield: 84 % (79 mg); Semi Solid; ^{1}H NMR (200 MHz, CDCl$_3$): δ 7.73 (s, 1H), 7.48 (s, 1H), 5.19 - 5.42 (m, 1H), 4.34 - 4.60 (m, 2H), 4.08 - 4.25 (m, 1H), 3.86 - 4.02 (m, 1H), 2.34 (d, J = 2.40 Hz, 7H), 1.95 - 2.11 (m, 3H), 1.39 (t, J = 7.07 Hz, 3H).^{13}C NMR (101 MHz, CDCl$_3$): δ 155.0, 148.5, 139.5, 138.7, 136.9, 136.0, 128.4, 126.1, 77.2, 69.1, 62.1, 30.7, 25.9, 20.2, 19.9, 14.5; HRMS (ESI) calculated [M+H]$^+$ for C$_{16}$H$_{21}$O$_2$N$_2$: 273.1598, found: 273.1598

1-Benzyl-6-bromo-3-(tetrahydrofuran-2-yl)quinoxalin-2(1H)-one (43n):

Yield: 89 % (76 mg); White Solid; ^{1}H NMR (200 MHz, CDCl$_3$): δ 7.88 (q, J = 2.06 Hz, 2H), 7.21 - 7.50 (m, 6H), 5.38 - 5.53 (m, 3H), 4.14 (q, J = 7.33 Hz, 1H), 3.96 (td, J = 7.67, 5.75 Hz, 1H), 2.20 - 2.31 (m, 2H), 1.89 - 2.16 (m, 2H).^{13}C NMR (101 MHz, CDCl$_3$): δ 155.6, 150.8, 141.1 , 135.6, 134.7, 132.6, 128.6, 128.3, 128.0, 127.9, 124.5, 122.6, 76.2, 68.9, 68.4, 29.6, 25.3; HRMS (ESI) calculated [M+H]$^+$ for C$_{19}$H$_{18}$O$_2$N$_2$Br: 385.0546, found: 385.0543

1-Benzyl-7-chloro-3-(tetrahydrofuran-2-yl) quinoxalin-2(1H)-one (43o):

Yield: 86 % (76 mg); Reddish viscous Oil; ^{1}H NMR (200 MHz, CDCl$_3$): δ 7.75 - 8.12 (m, 1H), 7.17 - 7.40 (m, 7H), 5.32 - 5.65 (m, 3H), 4.17 - 4.34 (m, 1H), 3.97 - 4.16 (m, 1H), 2.40 - 2.67 (m, 1H), 1.95 - 2.26 (m, 3H). ^{13}C NMR (50 MHz, CDCl$_3$): δ 160.5, 153.2, 134.1, 132.6, 130.9, 130.5, 129.5, 129.2, 128.4, 127.2, 126.1, 123.5, 114.9, 113.6, 76.8, 68.6, 62.7, 45.2, 29.9, 25.0; HRMS (ESI) calculated [M+H]$^+$ for C$_{19}$H$_{18}$O$_2$N$_2$Cl: 341.1051, found: 341.1040

6-Benzoyl-1-benzyl-3-(tetrahydrofuran-2-yl) quinoxalin-2(1H)-one (43p):

Yield: 81% (68 mg); Gummy Oil; ^{1}H NMR (200 MHz, CDCl$_3$): δ 7.95 - 8.19 (m, 1H), 7.70 - 7.83 (m, 2H), 7.59 - 7.68 (m, 2H), 7.36 - 7.57 (m, 3H), 7.26 - 7.34 (m, 3H), 7.14 - 7.26 (m, 2H),

5.31 - 5.69 (m, 3H), 4.19 - 4.42 (m, 1H), 3.93 - 4.16 (m, 1H), 2.41 - 2.80 (m, 1H), 1.97 - 2.21 (m, 3H).^{13}C NMR (101 MHz, CDCl$_3$): δ 194.8, 161.9, 153.7, 137.8, 136.4, 134.6, 134.5, 132.9, 132.4, 132.2, 131.7, 130.9, 130.2, 129.6, 129.5, 128.8, 128.1, 127.7, 127.6, 126.7, 126.5, 124.7, 116.3, 77.3, 69.0, 45.3, 30.4, 25.4; HRMS (ESI) calculated [M+H]$^+$ for C$_{26}$H$_{23}$O$_3$N$_2$: 411.1703, found: 411.1715

1-Propyl-3-(tetrahydrofuran-2-yl) quinoxalin-2(1H)-one(43q):

Yield: 83 % (79 mg); Gummy Oil; ^{1}H NMR (400 MHz, CDCl$_3$): δ 7.97 (d, *J* = 7.9 Hz, 1H), 7.54 (t, *J* = 7.6 Hz, 1H), 7.23 - 7.39 (m, 2H), 5.29 - 5.53 (m, 1H), 4.15 - 4.38 (m, 3H), 3.94 - 4.10 (m, 1H), 2.42 - 2.64 (m, 1H), 2.05 (br. s., 3H), 1.74 - 1.88 (m, 2H), 1.05 (t, *J* = 7.6 Hz, 3H). ^{13}C NMR (101 MHz, CDCl$_3$): δ 159.5, 153.8, 132.8, 132.3, 130.7, 130.0, 123.4, 113.6, 77.6, 69.2, 43.6, 30.5, 25.6, 20.6, 11.4; HRMS (ESI) calculated [M+H]$^+$ for C$_{15}$H$_{19}$O$_2$N$_2$: 259.1441, found: 259.1435

3-(1,4-Dioxan-2-yl)-1-propylquinoxalin-2(1H)-one (44):

Yield: 94 % (57 mg); Off white solid; ^{1}H NMR (500 MHz, CDCl$_3$): δ 8.04 (d, *J* = 7.6 Hz, 1H), 7.57 (t, *J* = 7.4 Hz, 1H), 7.26 - 7.41 (m, 2H), 5.23 - 5.44 (m, 1H), 4.17 - 4.31 (m, 3H), 4.12 (d, *J* = 11.4 Hz, 1H), 3.95 - 4.04 (m, 1H), 3.84 (d, *J* = 5.0 Hz, 2H), 3.67 (t, J = 10.3 Hz, 1H), 1.73 - 1.88 (m, 2H), 1.05 (t, J = 7.2 Hz, 3H).^{13}C NMR (126 MHz, CDCl$_3$): δ 154.8, 153.1, 132.5, 132.0, 130.6, 130.4, 123.3, 113.3, 74.2, 69.1, 67.2, 66.0, 43.4, 20.3, 11.0; HRMS (ESI) calculated [M+H]$^+$ for C$_{15}$H$_{18}$N$_2$O$_3$: 274.1308 Found: 274.1309

3-(1,4-Dioxan-2-yl)-1-((3-(4-methoxyphenyl)-4,5-dihydroisoxazol-5-yl)methyl)quinoxalin-2(1H)-one (45):

Yield: 75 % (65 mg); White solid; ^{1}H NMR(200 MHz, CDCl$_3$): δ 7.80 - 8.32 (m, 1H), 7.39 - 7.77 (m, 4H), 7.25 - 7.39 (m, 1H), 6.50 - 7.04 (m, 2H), 5.00 - 5.42 (m, 2H), 4.55 (td, *J* = 13.8,

4.3 Hz, 1H), 3.86 - 4.45 (m, 4H), 3.70 - 3.86 (m, 5H), 3.12 - 3.70 (m, 3H); ^{13}C NMR (50 MHz, CDCl$_3$): δ 161.4, 156.8, 154.6, 154.1, 132.8, 131.1, 130.8, 128.5, 124.2, 121.4, 114.7, 114.3, 78.2, 74.5, 67.6, 66.4, 55.4, 46.1, 39.2, 29.7; HRMS (ESI) calculated [M+H]$^+$ for C$_{23}$H$_{24}$O$_5$N$_3$: 422.1710, found: 422.1698

1-(2,3-Dihydroxypropyl)-3-(tetrahydrofuran-2-yl)quinoxalin-2(1H)-one (46):

Yield: 89 % (60 mg); colourless gummy oil; ^{1}H NMR (200 MHz, CDCl$_3$): δ 7.87 (d, *J* = 7.83 Hz, 1H), 7.47 (d, *J* = 3.79 Hz, 2H), 7.23 - 7.36 (m, 1H), 5.21 - 5.37 (m, 1H), 4.35 - 4.50 (m, 1H), 3.86 - 4.32 (m, 4H), 3.63 (d, *J* = 9.35 Hz, 2H), 3.51 (br. s., 1H), 3.00 (s, 1H), 2.22 - 2.49 (m, 1H), 1.81 - 2.11 (m, 3H), 1.18 (s, 1H).^{13}C NMR (50 MHz, CDCl$_3$): δ 158.1, 154.3, 132.2, 131.8, 129.9, 129.9, 123.6, 113.5, 76.6, 68.9, 68.5, 62.7, 62.7, 44.0, 42.6, 29.6, 29.5, 29.0, 25.0; HRMS (ESI) calculated [M+H]$^+$ for C$_{15}$H$_{19}$O$_4$N$_2$: 291.1339, found: 291.1345.

2.2.7. References

1   (a) Lorente, A.; Lamariano-Merketegi, J.; Albericio, F.; Álvareza, M. Tetrahydrofuran-Containing Macrolides: A Fascinating Gift from the Deep-Sea *Chem. Rev*. **2013**, 113, 4567−4610. (b) Ward, R. S. Lignans, neolignans and related compounds. *Nat. Prod. Rep*. **1999**, 16, 75–96. (c) Li, G.; Ju, H. K.; Chang, H. W.; Jahng, Y.; Lee, S.-H.; Son, J.-K. Melanin Biosynthesis Inhibitors from the Bark of Machilus thunbergii. *Biol. Pharm. Bull*. **2003**, 26, 1039-1041. (d) Zhai, H.; Inoue, T.; Moriyama, M.; EsumiI, T.; Mitsumoto, Y.; Fukuyama, Y. Neuroprotective Effects of 2,5-Diaryl-3,4-dimethyltetrahydrofuran Neolignans. *Biol. Pharm. Bull*. **2005**, 28, 289-293. (e) Teponno, R. B.; Kusari, S.; Spiteller, M. Recent advances in research on lignans and Neolignans. *Nat. Prod. Rep*. **2016**, 33, 1044–1092. (f) Lee, W. S.; Baek, Y.; Kim, J-R.; Cho, K-H.; Sok, D-E.; Jeong, T-S. Antioxidant activities of a new lignan and a neolignan from Saururus chinensis. *Bioorg. Med. Chem. Lett*. **2004**, 14, 5623-5628. (g) Saleem, M.; Kim, H. J.; Ali, M. S.; Lee, Y. S. An update on bioactive plant lignans. *Nat. Prod. Rep*. **2005**, 22, 696-716. (h) Pan, J.-Y.; Chen, S.-L.; Yang, M.-H.; Wu, J.; Sinkkonen, J.; Zou, K. An update on lignans: natural products and synthesis. *Nat. Prod*. *Rep.* **2009**, 26, 1251-1296, and references therein.

2   (a) (a) Surivet, J-P.; Zumbrunn, C.; Bruyere, T.; Bur, D.; Kohl, C.; Locher, H. H.; Seiler, P.; Ertel, E. A.; Hess, P.; Enderlin-Paput, M.; Enderlin-Paput, S.; Gauvin, J-C.; Mirre, A.; Hubschwerlen, C.; Ritz, D.; Rueedi, G. Synthesis and Characterization of Tetrahydropyran-Based Bacterial Topoisomerase

Inhibitors with Antibacterial Activity against Gram-Negative Bacteria. *J. Med. Chem.* **2017**, 60, 3776−3794. (b) Saluja, B.; Thakkar, J. N.; Li, H.; Desai, U. R.; Sakagami, M. Novel low molecular weight lignins as potential anti-emphysema agents: In vitro triple inhibitory activity against elastase, oxidation and inflammation. *Pulmonary Phar-macology & Therapeutics.* **2013**, 26, 296-304. (c) Lee, M-A.; Kim, W. K.; Park, H. J.; Kang, S. S.; Lee, S. K. Anti-proliferative activity of hydnocarpin, a natural lignan, is associated with the suppression of Wnt/b-catenin signaling pathway in colon cancer cells. *Bioorg. Med. Chem. Lett*. **2013**, 23, 5511–5514. (d) Katz, J. D.; Jewell, J. P.; Guerin, D. J.; Lim, J.; Dinsmore, C. J.; Deshmukh, S. V.; Pan, B-S.; Marshall, C. G.; Lu, W.; Altman, M. D.; Dahlberg, W. K.; Davis, L.; Falcone, D.; Gabarda, A. E.; Hang, G.; Hatch, H.; Holmes, R.; Kunii, K.; Lumb, K. J.; Lutterbach, B.; Mathvink, R.; Nazef, N.; Patel, S. B.; Qu, X.; Reilly, J. F.; Rickert, K. W.; Rosenstein, C.; Soisson, S. M.; Spencer, K. B.; Szewczak, A. A.; Walker, D.; Wang, W.; Young, J.; Zeng, Q. Discovery of a 5H-Benzo[4,5]cyclohepta[1,2-b]pyridin-5-one (MK-2461) Inhibitor of c-Met Kinase for the Treatment of Cancer. *J. Med. Chem*. **2011**, 54, 4092–4108. (e) Gonza´lez, A. G.; Silva, M. H.; Padro´n, J. I.; Leo´n, F.; Reyes, E.; lvarez-Mon, M. AÄ.; Pivel, J. P.; Quintana, J.; Este´vez, F.; Bermejo, J. Synthesis and Antiproliferative Activity of a New Compound Containing an α-Methylene-γ-Lactone Group. *J. Med. Chem.* **2002**, 45, 2358-2361. (f) Li, S.; Xu, H.; Cui, S.; Wu, F.; Zhang, Y.; Su, M.; Gong, Y.; Qiu, S.; Jiao, Q.; Qin, C.; Shan, J.; Zhang, M.; Wang, J.; Yin, Q.; Xu, M.; Liu, X.; Wang, R.,; Zhu, L.; Li, J.; Xu, Y.; Jiang, H.; Zhao, Z.; Li, J.; Li, H. Discovery and Rational Design of Natural-Product-Derived 2-Phenyl- 3,4-dihydro-2H-benzo[f]chromen-3-amine Analogs as Novel and Potent Dipeptidyl Peptidase 4 (DPP-4) Inhibitors for the Treatment of Type 2 Diabetes *J. Med. Chem*. **2016**, 59, 6772−6790. (g) Goodwin, N. C.; Ding, Z-M.; Harrison, B. A.; Strobel, E. D.; Harris, A. L.; Smith, M.; Thompson, A. Y.; Xiong, W.; Mseeh, F.; Bruce, D. J.; Diaz, D.; Gopinathan, S.; Li, L.; O'Neill, E.; Thiel, M.; Wilson, A. G. E.; Carson, K. G.; Powell, D.; Rawlins, D. B. Discovery of LX2761, a Sodium-Dependent Glucose Cotransporter 1 (SGLT1) Inhibitor Restricted to the Intestinal Lumen, for the Treatment of Diabetes. *J. Med. Chem.* **2017**, 60, 710−721.

3   Miyazaki, H.; Uneme, H.; Katagiri, Y.; Yasser, S. A-K. S.; Salunke, G. B. Preparation of benzaldehyde oxime ether and phenyl alkyl ketone oxime ether compounds as pesticides. Patent No. **JP 2014080385**

4   (a) Liu, Z.; Saarinen, N. M.; Thompson, L. U. Sesamin Is One of the Major Precursors of Mammalian Lignans in Sesame Seed (Sesamum indicum) as Observed In Vitro and in Rats. *J. Nutr.* **2006**, 136, 906-912. (b) Kiso, Y. Antioxidative roles of sesamin, a functional lignan in sesame seed, and its effect on lipidand alcohol-metabolism in the liver: A DNA microarray study. *Biofactors*, **2004**, 21, 191-196. (c) Kong, P.; Chen, G.; Jiang, A.; Wang, Y.; Song, C.; Zhuang, J.; Xi, C.; Wang, G.; Ji, Y.; Yan, J. Sesamin inhibits IL-1β-stimulated inflammatory response in human osteoarthritis chondrocytes by activating Nrf2 signaling pathway. *Oncotarget*. **2016**, 7, 83720-83726. (d) Nguyen, P. H.; Le, T. V. T.; Kang, H. W.; Chae, J.; Kim, S. K.; Kwon, K-i.; Seo, D. B.; Lee, S. J.; Oh, W. K. AMP-activated protein kinase (AMPK) activators from Myristica fragrans (nutmeg) and their anti-obesity effect. *Bioorg. Med. Chem. Lett*. **2010**, 20, 4128-4131.

5   (a) Li, J.; Meng, A-P.; Guan, X-L.; Li, J.; Wu, Q.; Deng, S-P.; Su, X-J.; Yang, R-Y. Anti-hepatitis B virus lignans from the root of Streblus asper. *Bioorg. Med. Chem. Lett*. **2013**, 23, 2238–2244. (b) Burness, C. B. *Drugs*. **2015**, 75, 1947-1952.

6   (a) Zhang, S.; Guo, L.; Wang, H.; Duan, X. Bu4NI-catalyzed decarboxylative acyloxylation of an sp3 C–H bond adjacent to a heteroatom with α-oxocarboxylic acids. *Org. Biomol. Chem*. **2013**, 11, 4308–4311. (b) Doan, S. H.; Nguyen, V. H. H.; Nguyen, T. H.; Pham, P. H.; Nguyen, N. N.; Phan, A. N. Q.; Tu, T. N.; Phan, N. T. S. Cross-dehydrogenative coupling of coumarins with Csp3–H bonds using an iron-organic framework as a productive heterogeneous catalyst. *RSC Adv*. **2018**, 8, 10736–10745. (c) Majji, G.; Rout, S. K.; Rajamanickam, S.; Guin, S.; Patel, B. K. Synthesis of esters via sp3 C–H functionalisation. *Org. Biomol. Chem.* **2016**, 14, 8178-8211. (d) Evano, G.; Blanchard, N. and Toumi, M. Copper-Mediated Coupling Reactions and Their Applications in Natural Products and Designed Biomolecules Synthesis. *Chem. Rev*. **2008**, 108, 3054. (e) Wang, H.; Guo, L.; Duan, X. Silver-catalyzed oxidative coupling/cyclization of acrylamides with 1,3-dicarbonyl compounds. *Chem. Commun.* **2013**, 49, 10370-10372. (f) Lakshman, M. K.; Vurama, P. K. Cross-dehydrogenative coupling and oxidative-amination reactions of ethers and alcohols with aromatics and heteroaromatics. *Chem. Sci.* **2017,** 8, 5845–5888.

7   Liu, D.; Liu, C.; Lia, H.; Lei, A. Copper-catalysed oxidative C–H/C–H coupling between olefins and simple ethers. *Chem. Commun.* **2014**, 50, 3623-3626.

8   Sun, Q.; Zhang, Y-Y.; Sun, J.; Han, Y.; Jia, X.; Yan, C-G. Construction of C (sp2)-X (X = Br, Cl) Bonds through a Copper-Catalyzed Atom-Transfer Radical Process: Application for the 1,4-Difunctionalization of Isoquinolinium Salts. *Org. Lett.* **2018**, 20, 987-990.

9   Correa, A.; Fiser, B.; Go´mez-Bengoa, E. Iron-catalyzed direct a-arylation of ethers with azoles. *Chem. Commun*. **2015**, 51, 13365-13368.

10   Shields, B. J.; Doyle, A. G. Direct C(sp3)-H Cross Coupling Enabled by Catalytic Generation of Chlorine Radicals *J. Am. Chem. Soc.* **2016**,138, 12719-12722.

11   Li, X.; Wanga, H-Y.; Shi, Z-J. Transition-metal-free cross-dehydrogenative alkylation of pyridines under neutral conditions. *New J. Chem*. **2013**, 37, 1704-1706.

12   Kianmehr, E.; Fardpour, M.; Khan, K. M. Direct Regioselective Alkylation of Non-Basic Heterocycles with Alcohols and Cyclic Ethers through a Dehydrogenative Cross- Coupling Reaction under Metal-Free Conditions. *Eur. J. Org. Chem*. **2017**, 2661-2668.

13   Jin, L.; Feng, J.; Lu, G.; Cai, C. Di-tert-butyl Peroxide (DTBP)-Mediated Oxidative Cross- Coupling of Isochroman and Indole Derivatives. *Adv. Synth. Catal*. **2015**, 357, 2105-2110.

14   (a) Devariab, S.; Shah, B. A. Visible light-promoted C–H functionalization of ethers and electron-deficient arenes. *Chem. Commun*. **2016**, 52, 1490-1493. (b) Okugawa, N.; Moriyama, K.; Togo, H. Introduction of Ether Groups onto Electron-Deficient Nitrogen-Containing Heteroaromatics Using Radical Chemistry under Transition-Metal-Free Conditions. Eur. *J. Org. Chem*. **2015**, 4973–4981. (c) Zhou, L.; Okugawa, N.; Togo, H. Hydroxymethylation of Quinolines with $Na_2S_2O_8$ by a Radical

Pathway. *Eur. J. Org. Chem*. **2017,** 6239–6245.

15 (a) Liu, S.; Liu, A.; Zhang, Y.; Wang, W. Direct Ca-heteroarylation of structurally diverse ethers via a mild N-hydroxysuccinimide mediated cross-dehydrogenative coupling reaction. *Chem. Sci.* **2017**, 8, 4044-4050. (b) Xie, Z.; Cai, Y.; Hu, H.; Lin, C.; Chen, Z.; Wang, L.; and Pan, Y. Cu-Catalyzed Cross-Dehydrogenative Coupling Reactions of (Benzo)thiazoles with Cyclic Ethers. *Org. Lett*. **2013**, 15, 4600-4603.

16 Jafarpour, F.; Darvishmolla, M. Peroxy mediated Csp^2-Csp^3 dehydrogenative coupling: regioselective functionalization of coumarins and coumarin-3-carboxylic acids. *Org. Biomol. Chem.* **2018**, 16, 3396–3401.

17 Ueno, R.; Shirakawa, E. Base-promoted dehydrogenative coupling of benzene derivatives with amides or ethers. *Org. Biomol. Chem.* **2014**, 12, 7469–7473

18 (a) Chavan, S. S.; Rupanawar, B. D.; Kamble, R. B.; Shelke, A. M.; Suryavanshi, G. Metal-free annulation of β-acylamino ketones: facile access to spirooxazolines and oxazolines via oxidative C–O bond formation. *Org. Chem. Front*. **2018**, 5, 544-548. (b) Rupanawar, B. D.; Chavan, S. S.; Shelke, A. M.; Suryavanshi, G. Triflic acid-catalyzed metal-free synthesis of (E)-2-cyanoacrylamides and 3-substituted azetidine-2,4-diones. *New J. Chem.* **2018**, 42, 6433-6440.

19 Bahrami, K.; Khodaei, M. M.; Kavianinia, I. A Simple and Efficient One-Pot Synthesis of 2-Substituted Benzimidazoles. *Synthesis*. **2007,** 4, 547–550.

20 Corey, E. J.; Helal, C. J. Reduction of Carbonyl Compounds with Chiral Oxazaborolidine Catalysts: A New Paradigm for Enantioselective Catalysis and a Powerful New Synthetic Method. *Angew. Chem. Int. Ed*. **1998**, 37, 1986 -2012.

21 (a) Ji, P.-Y.; Liu, Y.-F.; Xu, J.-W.; Luo, W.-P.; Liu, Q.; Guo, C.-C. Transition-Metal-Free Oxidative Decarboxylative Cross Coupling of α,β-Unsaturated Carboxylic Acids with Cyclic Ethers under Air Conditions: Mild Synthesis of α-Oxyalkyl Ketones. *J. Org. Chem*. **2017,** 82, 2965−2971. (b) Handa, S.; Fennewald, J.C.; Lipshutz, B. H. Aerobic Oxidation in Nanomicelles of Aryl Alkynes, in Water at Room Temperature. *Angew. Chem. Int. Ed*. **2014,** 53, 3432-3435. (c) Ledwith, A.; Russel, P. J,; Sutcliffe, L. H. J. Chem. Soc. D, *Chem. Commun*. **1971**, 964.

22 (a) Shi, Z.; Glorius, F. Synthesis of fluorenones via quaternary ammonium salt-promoted intramolecular dehydrogenative arylation of aldehydes. *Chem. Sci.,* **2013**, 4, 829–833. (b) Shirakawa, E.; Itoh, K.; Higashino, T.; and Hayashi, T. tert-Butoxide-Mediated Arylation of Benzene with Aryl Halides in the Presence of a Catalytic 1,10-Phenanthroline Derivative. *J. Am. Chem. Soc*. **2010**, 132, 15537-15539; (c) Devariab, S.; Shah, B. A. Visible light-promoted C–H functionalization of ethers and electron-deficient arenes. Chem. *Commun.,* **2016,** 52, 1490-1493. (d) House, D. A. Kinetics and Mechanism of Oxidations by Peroxydisulfate. *Chem. Rev*. **1962**, 62, 185. (e) Avetta, P.; Pensato, A.; Minella, M.; Malan-drino, M.; Maurino, V.; Minero, C.; Hanna, K.; Vione, D. Activation of Persulfate by Irradiated Magnetite: Implications for the Degradation of Phenol under Heterogeneous Photo-Fenton-Like Conditions. *Environ. Sci. Technol*. **2015**, 49, 1043. (f) Dai, C.; Meschini, F.; Narayanam,

J. M. R.; and Stephenson, C. R. J. Friedel-Crafts Amidoalkylation via Thermolysis and Oxidative Photocatalysis. *J. Org. Chem.* **2012**, 77, 4425, and refrences therein

23   Liu, D.; Liu, C.; Li, H.; Lei, A. Copper-catalysed oxidative C-H/C–H coupling between olefins and simple ethers. *Chem. Commun*. **2014**, 50, 3623-3626.

24   (a) Brahmachari, G. Design for carbon-carbon bond forming reactions under ambient conditions**.** *RSC Adv*., **2016**, *6*, 64676-64725 (b) Resch, V.; Schrittwieser, J. H.; Siirola, E.; Kroutil, W. Novel carbon–carbon bond formations for biocatalysis. *Current Opinion in Biotechnology*, **2011**, *22*, 793-799 (c) Hart, D. J. Free-radical carbon-carbon bond formation in organic synthesis. *Science*, **1984**, *223*, 883-887 (d) Yamaguchi, J.; Yamaguchi, A. D.; Itami, K. C-H Bond Functionalization: Emerging Synthetic Tools for Natural Products and Pharmaceuticals. *Angew. Chem. Int. Ed.* **2012**, *51*, 8960-9009

25   Jun, C-H. Transition metal-catalyzed carbon–carbon bond activation. Chem. Soc. Rev. **2004**, *33*, 610-618

26   (a) Lakshman, M. K.; Vurama, P. K. Cross-dehydrogenative coupling and oxidative-amination reactions of ethers and alcohols with aromatics and heteroaromatics. *Chem. Sci.,* 2017, *8*, 5845- 5888. (b) Varun, B. V.; Dhineshkumar, J.; Bettadapur, K. R.; Siddaraju, Y.; Alagiri, K.; Prabhu, K. R. Recent advancements in dehydrogenative cross coupling reactions for CC bond formation. *Tetrahedron Lett.,* **2017**, *58*, 803-824 (c) Li, Z.; Bohle, D. S.; Li, C-J. Cu-catalyzed cross-dehydrogenative coupling: A versatile strategy for C–C bond formations via the oxidative activation of sp3 C–H bonds. *PNAS*, **2006,** *24*, 8928-8933 (d) Li, C-J. Cross-dehydrogenative coupling (CDC): exploring C− C bond formations beyond functional group transformations. *Acc. Chem. Res.,* **2009**, *42*, 335-344 (e) Yeung, C. S.; Dong, V. M. Catalytic dehydrogenative cross-coupling: forming carbon-carbon bonds by oxidizing two carbon− hydrogen bonds. *Chem. Rev*. **2011**, 1*11*, 1215-1292 (f) Girard, S. A.; Knauber, T.; Li, C-J. The Cross-Dehydrogenative Coupling of C-H Bonds: A Versatile Strategy for C-C Bond Formations. *Angew. Chem. Int. Ed.,* **2014**, *53*, 74-100 (g) Zhang, C.; Tanga, C.; Jiao, N. Recent advances in copper-catalyzed dehydrogenative functionalization via a single electron transfer (SET) process. *Chem. Soc. Rev*., **2012**, *41*, 3464-3484 (h) Ravelli, D.; Protti, S.; Fagnoni, M. Carbon–carbon bond forming reactions via photogenerated intermediates. *Chem. Rev*. **2016**, *116*, 9850-9913 (i) Hari, D. P.; KÖnig, B. Eosin Y catalyzed visible light oxidative C–C and C–P bond formation. *Org. Lett.,* **2011**, *13*, 3852-3855 (j) Wei, G.; Basheer, C.; Tan, C.-H.; Jiang, Z. Visible light photocatalysis in chemoselective functionalization of C (sp3) H bonds enabled by organic dyes. *Tetrahedron Lett.* **2016**, *57,* 3801-3809.

27   (a) Martín, T.; Padrón, J. I.; Martín, V. S. Strategies for the Synthesis of Cyclic Ethers of Marine Natural Products. *Synlett*, **2014**, *25,* 12-32 (b) Rutkowski, J.; Brzezinski, B. Structures and properties of naturally occurring polyether antibiotics**.** *Biomed. Res. Int.* **2013**, 162513 (c) Kadota, I.; Yamamoto, Y. Synthetic strategies of marine polycyclic ethers via intramolecular allylations: linear and convergent approaches. *Acc. Chem. Res.* **2005**, *38,* 423-432 (d) Li, N.; Shi, Z.; Tang, Y.; Chen, J.; Li, X. Recent progress on the total synthesis of acetogenins from Annonaceae. *Beilstein J. Org. Chem.* **2008**, *4*, 1-62 (e) Nakata, T. Total synthesis of marine polycyclic ethers. *Chem. Rev.* **2005**, *105*, 4314-4347.

28   (a) Li, X.; Wanga, H-Y.; Shi, Z-J. Transition-metal-free cross-dehydrogenative alkylation of pyridines under neutral conditions. *New J. Chem.* **2013**, *37*, 1704-1706 (b) Kianmehr, E.; Fardpour, M.; Khan, K. M. Direct Regioselective Alkylation of Non-Basic Heterocycles with Alcohols and Cyclic Ethers through a Dehydrogenative Cross-Coupling Reaction under Metal-Free Conditions. *Eur. J. Org. Chem.* **2017**, *18*, 2661-2668 (c) Jin, L.; Feng, J.; Lu, G.; Cai, C. Di-tert-butyl Peroxide (DTBP)-Mediated Oxidative Cross-Coupling of Isochroman and Indole Derivatives. *Adv. Synth. Catal.* **2015**, *357*, 2105-2110 (d) Devariab, S.; Shah, B. A. Visible light-promoted C–H functionalization of ethers and electron-deficient arenes. *Chem. Commun.* **2016,** *52*, 1490-1493 (e) Okugawa, N.; Moriyama, K.; Togo, H. Introduction of Ether Groups onto Electron-Deficient Nitrogen-Containing Heteroaromatics Using Radical Chemistry under Transition-Metal-Free Conditions. *Eur. J. Org. Chem.* **2015,** *22*, 4973-4981 (f) Zhou, L.; Okugawa, N.; Togo, H. Hydroxymethylation of Quinolines with $Na_2S_2O_8$ by a Radical Pathway. *Eur. J. Org. Chem.* **2017**, *41*, 6239-6243 (g) Liu, S.; Liu, A.; Zhang, Y.; Wang, W. Direct Cα-heteroarylation of structurally diverse ethers *via* a mild *N*-hydroxysuccinimide mediated cross-dehydrogenative coupling reaction. *Chem. Sci.* **2017**, *8*, 4044-4050 (h) Xie, Z.; Cai, Y.; Hu, H.; Lin, C.; Chen, Z.; Wang, L.; Pan, Y. Cu-catalyzed cross-dehydrogenative coupling reactions of (benzo) thiazoles with cyclic ethers. *Org. Lett.* **2013,** *15*, 4600-4603 (i) Jafarpour, F.; Darvishmolla, M. Peroxy mediated Csp2–Csp3 dehydrogenative coupling: regioselective functionalization of coumarins and coumarin-3-carboxylic acids. *Org. Biomol. Chem.* **2018**, *16*, 3396-3401.

29   (a) Zhao, Y.; Huang, B.; Yang, C.; Li, B.; Gou, B.; Xia,;W. Photocatalytic cross-dehydrogenative amination reactions between phenols and diarylamines. *ACS Catal.* **2017**, *7,* 2446-2451 (b) Zhaoa, Y.; Xia, W. Recent advances in radical-based C–N bond formation via photo-/electrochemistry. *Chem. Soc. Rev*., **2018**, *47,* 2591-2608 (c) Zhao, Y.; Huang, B.; Yang, C.; Xia, W. Visible-light-promoted direct amination of phenols via oxidative cross-dehydrogenative coupling reaction. *Org. Lett.* **2016**, *18*, 3326-3329.

30   (a) Samanta, S.; Ravi, C.; Rao, S. N.; Joshi, A.; Adimurthy, S. Visible-light-promoted selective C–H amination of heteroarenes with heteroaromatic amines under metal-free conditions. *Org. Biomol. Chem.,* **2017**, *15*, 9590-9594 (b) Wei, W.; Wang, L.; Bao, P.; Shao, Y.; Yue, H.; Yang, D.; Yang, X.; Zhao X.; Wang, H. Metal-Free C(sp[2])–H/N–H Cross-Dehydrogenative Coupling of Quinoxalinones with Aliphatic Amines under Visible-Light Photoredox Catalysis. *Org. Lett.* **2018**, *20*, 7125-7130.

31   (a) Fan, X-Z.; Rong, J.-W.; Wu, H-L.; Zhou, Q.; Deng, H-P.; Tan, J. D.; Xue, C.-W.; Wu, L-Z.; Tao, H-R.; Wu, J. Eosin Y as a Direct Hydrogen-Atom Transfer Photocatalyst for the Functionalization of C− H Bonds. *Angew. Chem. Int. Ed.* **2018**, *57*, 8514-8518 (b) Wei, W.; Wang, L.; Yue, H.; Bao, P.; Liu, W.; Hu, C.; Yang D.; Wang, H. Metal-Free Visible-Light-Induced C–H/C–H Cross-Dehydrogenative-Coupling of Quinoxalin-2(H)-ones with Simple Ethers**.** *ACS Sustainable Chem. Eng*. **2018**, *6*, 17252−17257 (c) Correa, A.; Fiser, B.; Bengoa, E. G. Iron-catalyzed direct α-arylation of ethers with azoles. *Chem. Commun*. **2015**, *51*, 13365–13368.

32   (a) Ajani, O. O. Present status of quinoxaline motifs: Excellent pathfinders in therapeutic medicine.

Eur. J. Med. Chem. **2014**, *85*, 688-715 (b) Wang, D.; Gao, F. Quinazoline derivatives: synthesis and bioactivities. *Chemistry Central Journal,* **2013**, *7*, 95; references therein

33　　Lawrence, D. S.; Copper, J. E.; Smith, C. D. Structure− activity studies of substituted quinoxalinones as multiple-drug-resistance antagonists. *J. Med. Chem*. **2001**, *44*, 594-601.

34　　Liu, Z.; Yu, S.; Chen, D.; Shen, G.; Wang, Y.; Hou, L.; Lin, D.; Zhang, J.; Ye, F. Design, synthesis, and biological evaluation of 3-vinyl-quinoxalin-2 (1H)-one derivatives as novel antitumor inhibitors of FGFR1. *Drug Design, Development and Therapy*, **2016**, *10,* 1489-1500.

35　　(a) Harmenberg, J.; Akesson-Johansson, A.; Graslund, A.; Malmfors, T.; Bergman, J.; Wahren, B.; Akerfeldt, S.; Lundblad, L.; Cox, S. The mechanism of action of the anti-herpes virus compound 2, 3-dimethyl-6 (2-dimethylaminoethyl)-6H-indolo-(2, 3-b) quinoxaline. *Antiviral Res.* **1991**, 1*5*, 193–204 (b) Desai, N. C.; Dodiya, A.; Shihory, N. Synthesis and antimicrobial activity of novel quinazolinone–thiazolidine–quinoline compounds. *J. of Saudi Chem. Soci*. **2013**, *17*, 259-267.

36　　Qin, X.; Hao, X.; Han, H.; Zhu, S.; Yang, Y.; Wu, B.; Hussain, S.; Parveen, S.; Jing, C.; Ma, B.; Zhu, C. Design and synthesis of potent and multifunctional aldose reductase inhibitors based on quinoxalinones. *J. Med. Chem.* **2015**, *58*, 1254-1267.

37　　(a) Ramesh, B.; Reddy, R.; Kumar, G. R.; Reddy, B.V.S. Mn (OAc)3. 2H$_2$O promoted addition of arylboronic acids to quinoxalin-2-ones. *Tetrahedron Lett*. **2018**, *59*, 628-631 (b) Yin, K.; Zhang, R. Transition-Metal-Free Direct C–H Arylation of Quinoxalin-2 (1 H)-ones with Diaryliodonium Salts at Room Temperature. *Org. Lett.* **2017**, *19*, 1530-1533 (c) Yang, L.; Gao, P.; Duan, X.-H.; Gu, Y.-R.; Guo, L.-N. Direct C–H cyanoalkylation of quinoxalin-2 (1 H)-ones via radical C–C bond cleavage. *Org. Lett.* **2018**, 20, 1034-1037.

38　　(a) Jung, H. I.; Lee, J. H.; Kim, D. Y. Photocatalyst-free Photoredox Arylation of Quinoxalin-2(1*H*)-Ones with Aryldiazo Sulfones. *Bull. Korean Chem. Soc.* **2018**, *39*, 1003-1006 (b) Akula, P. S.; Hong, B-C.; Lee, G-H. Visible-light-induced C(sp^3)–H activation for a C–C bond forming reaction of 3,4-dihydroquinoxalin-2(1H)-one with nucleophiles using oxygen with a photoredox catalyst or under catalyst-free conditions. *RSC Adv*., **2018**, *8,* 19580-19584 (c) Yuan, J.; Liu, S.; Qu, L. Transition Metal-Free Direct C-3 Arylation of Quinoxalin-2 (1H)-ones with Arylamines under Mild Conditions. *Adv. Synth. Catal.* **2017**, *359*, 4197-4207 (d) Paul, S.; Ha, J. H.; Park, G. E.; Lee, Y. R. Transition Metal-Free Iodosobenzene-Promoted Direct Oxidative 3-Arylation of Quinoxalin-2 (H)-ones with Arylhydrazines. *Adv. Synth. Catal.* **2017**, *359*, 1515-1521.

39　　(a) Chavan, S. S.; Rupanawar, B. D.; Kamble, R. B.; Shelke, A. M.; Suryavanshi, G. Metal-free annulation of β-acylamino ketones: facile access to spirooxazolines and oxazolines via oxidative C–O bond formation. *Org. Chem. Front*., **2018**, *5,* 544-548 (b) Rupanawar, B. D.; Chavan, S. S.; Shelke, A. M.; Suryavanshi, G. Triflic acid-catalyzed metal-free synthesis of (E)-2-cyanoacrylamides and 3-substituted azetidine-2, 4-diones. *New J. Chem*., **2018**, *42*, 6433-6440 (c) Bansode, A. H.; Suryavanshi, G. Metal-free hypervalent iodine/TEMPO mediated oxidation of amines and mechanistic insight into the reaction pathways. *RSC Adv*., **2018**, *8,* 32055-32062 (d) Mane, K. D.; Mukherjee, A.; Vanka, K.;

Suryavanshi, G. Metal-Free Regioselective Cross Dehydrogenative Coupling of Cyclic Ethers and Aryl Carbonyls. *J. Org. Chem.* **2019,** *84*, 2039−2047 (e) S. G. More, G. Suryavanshi, Org. Biomol. Chem., 2019, 17, 3239-3248

40   Mendelsohn, B. A.; Lee, S.; Kim, S.; Teyssier, F.; Aulakh, V. S.; Ciufolini, M. A. Oxidation of oximes to nitrile oxides with hypervalent iodine reagents. *Org. Lett.* **2009**, *11*, 1539-1542.

41   (*TURBOMOLE* V7.0, 2015; University of Karlsruhe and Forschungszentrum Karlsruhe GmbH, 1989–2007; TURBOMOLE GmbH, since 2007; (http://www.turbomole.com.)

42   Perdew, J. P.; Burke, K.; Ernzerhof, M. Generalized Gradient Approximation Made Simple. *Phys. Rev. Lett*. **1996**, 77, 3865.

43   Ansgar, S.; Christian, H.; Reinhart, A. Fully optimized contracted Gaussian basis sets of triple zeta valence quality for atoms Li to Kr. *J. Chem. Phys*. **1994**, 100, 5829−5835.

44   Eichkorn, K.; Treutler, O.; Öhm, H.; Haser, M.; Ahlrichs, R. Auxiliary basis sets to approximate Coulomb potentials.¨*Chem. Phys. Lett.* **1995**, 240, 283−289.

45   Sierka, M.; Hogekamp, A.; Ahlrichs, R. Fast evaluation of the Coulomb potential for electron densities using multipole accelerated resolution of identity approximation. *J Chem. Phys.*. **2003**, 118, 9136-9148.

46   Klamt, A.; Schuurmann, G. COSMO: a new approach to dielectric screening in solvents with explicit expressions for the screening energy and its gradient. *J. Chem. Soc., Perkin Trans.* 2 **1993**, 799−805.

Chapter III

Development of New Synthetic Methods for the C-H Functionalization of Indolizines

1. "Acetic Acid Catalyzed Regioselective $C(sp^2)$-H Bond Functionalization of Indolizines: Concomitant Involvement of Synthetic and Theoretical Studies." **Mane**, **K. D.;** Mukherjee, A.; Das, G.K.; Suryavanshi, G. *J. Org. Chem.* **2022**, 87 (8), 5097-5112.

2. "Visible Light Promoted, Photocatalyst Free $C(sp^2)$-H Bond Functionalization of Indolizines *via* EDA complexes." **Mane**, **K. D.;** Rupanawar, B. D.; Suryavanshi, G. *E. J. Org. Chem.***2022,** (*Just Accepted*) https://doi.org/10.1002/ejoc.202200261

3.1.1 Introduction

N-heterocyclic compounds are found ubiquitously in many natural products and the core structure of active pharmaceutical ingredients. Indolizines are one of the vital fused *N*-heterocyclic compounds mainly isolated from different plants and fungal sources[1] and further they come into spotlight due to their unique physical and pharmacological properties. The natural and synthetic indolizine alkaloids are extensively used in SAR studies and this study reveals that the indolizine derivatives showed a broad spectrum biological activity such as anticancer, antibiotics, antitubercular, antioxidant, antimicrobial, antimycobacterial, anticancer, anti-inflammatory and many more (fig.1).[2,3] The fluorescent indolizine derivatives effectively used in Alzheimer disease (a neurodegenerative disorder) to detect accumulated amyloid-*β* (Aβ) peptides monomers, dimers, and plaques in the brain of 5XFAD Alzheimer transgenic mouse model.[4] The fluorescent indolizines core derivative have been used for preparing drug-biotin conjugates to find out mode of action of antiangiogenic drug.[5]

Additionally, the fluorescent properties of substituted indolizine make them valuable candidate in dye-sensitized solar cells as organic sensitizer,[6] FRET fluorescence sensors to detect Hg^{2+} and Cu^{2+} in living cell,[7] pH fluorescent probe for imaging of living cells,[8] and fluorescent blue-emitting indolizines for organic light-emitting device.[9] The fluorescent indolizine β-cyclodextrin compounds used as a molecular chemo sensor to detect volatile organic compounds and biological markers.[10]

Section I

Acetic Acid Catalyzed Regioselective C(sp^2)-H Bond Functionalization of

Indolizines: Concomitant Involvement of Synthetic and Theoretical Studies
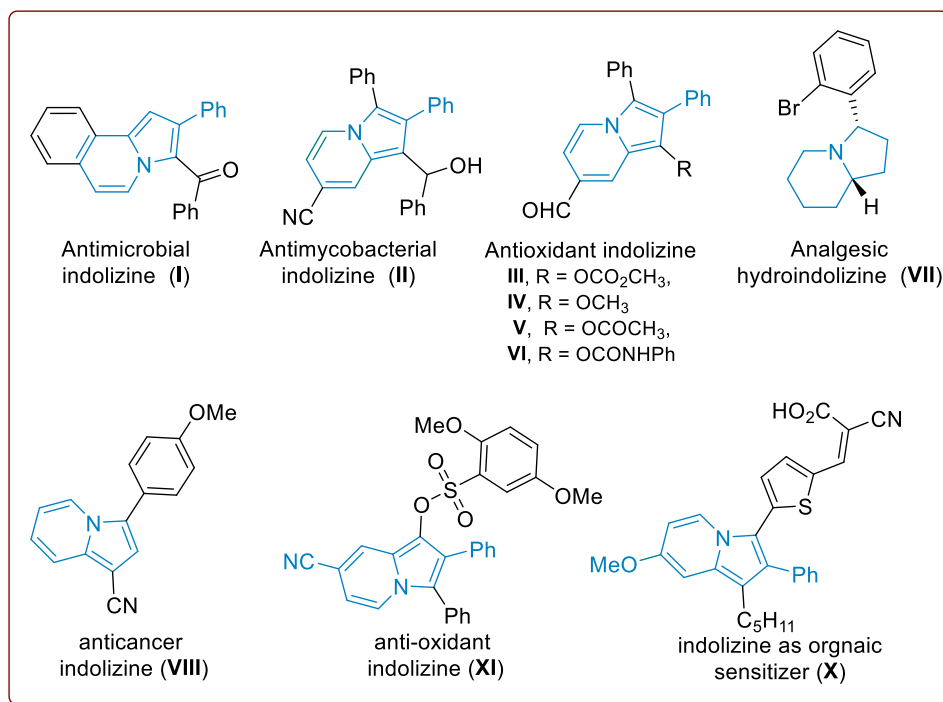
Figure 1. Fluorescent and biologically active indolizines

The unique physical and pharmacological properties of indolizines derivative were able to draw attention among research groups. Consequently, diverse strategies have been reported for the synthesis[11] and functionalization of indolizines, [12] among these transformations, C-C coupling reactions plays an important role in the development of new set of indolizines.[13] Quinone monoimines shows excellent electrophilic properties and effectively used with various nucleophiles such as Thiols,[14a] thiocyanation,[14b] and cyanoacrylate.[14c] Quinone monoimines also used as dienophiles in Diels Alder reactions with dines,[15a, b] [3+3] cyclization reaction of 2-

indolylmethanols,[15c] imino exchange reaction to synthesize *N*-acyl diarylamines and phenothiazines.[15d]

3.1.2 Review of Literature

Gevorgyan's Approach (2004)[13e]

In 2004, Gevorgyan and co-workers developed C−H functionalization of heteroaryls such as indolizines with heteroaryl bromides by using palladium catalyst and it provided a wide range of biheteroaryl structural motif in excellent yields (**Scheme 1**).
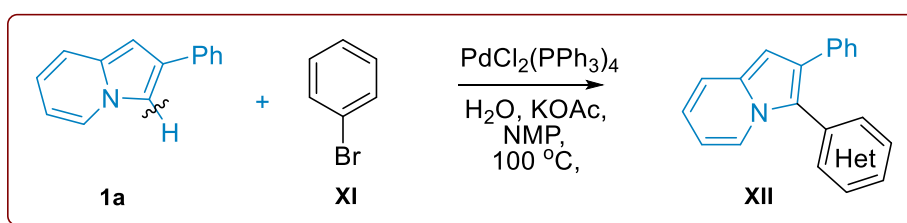
Scheme 1: C-C coupling of indolizines with heteroaryl bromides

Kim's Approach (2015)[17]

In 2015 Ikon Kim and co-workers developed the indium triflate catalysed aza-Friedel-Crafts type three component coupling for the C-H functionalization of indolizines by using the combination of aldehydes and morpholine to generate alkylated indolizine in good to excellent yields (**Scheme 2**). This report showed the three-component coupling of morpholine, aldehyde and indolizine to generate the aminoalkyl group at C-3 position of indolizine.
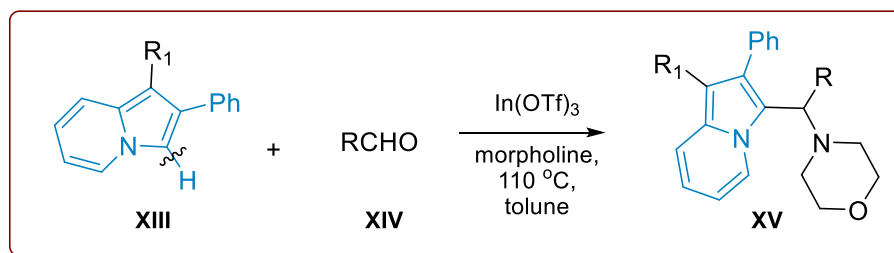
Scheme 2. Previous report on C-H functionalization of indolizines

3.1.3 Present Work

3.1.3.1 Objective

To the best of our knowledge, there are limited reports present so far for the metal-free C-H functionalization of indolizines. In continuation of our research interest in the development of simple and efficient methodologies,[17] herein we have developed an acetic acid catalyzed, metal-free regioselective C-C coupling of indolizine and quinone monoimine derivatives to get the corresponding C-3 functionalized indolizines.
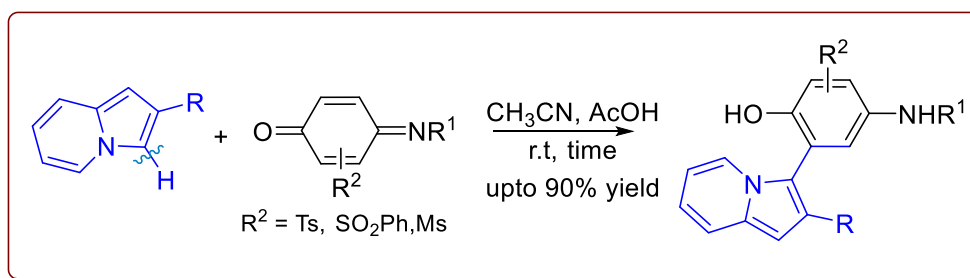
Scheme 3. C-C coupling of indolizine with quinone monoimine

As the reaction involves only two starting materials and solvent while investigating the reaction pathway, theoretically our initial assumption was a simple nucleophilic attack of indolizine to the electrophilic monoimine may take place followed by the intramolecular four or five membered proton abstractions. Based on prior research[18] upon calculating the energetics against our initial hypothesis using DFT, it was observed that the activation barriers for different transition states did not fit with the reaction condition. Hence this hypothesis won't stand. At this point the complexity arises and we started connecting the missing dots and it came out of the discussion that the monoimine we were using, is the crude mixture for which we did not do the column. For the synthesis of the quinone monoimine, (Diacetoxyiodo)benzene (PIDA) was used and as a biproduct we got acetic acid in the system which can also easily be recognizable by its smell.

Since we were using the crude monoimine with acetic acid for the reported reaction, the presence of acetic acid might cause the reaction to happen very fast, our next assumption. Based on this hypothesis, we again performed DFT quantum mechanical studies which showed the energetics to fit finely with the reaction condition which have a global activation barrier of only 17.67 kcal mol^{-1}. With these computational results in our hand, we now started looking into the synthetic evidences and support. We have removed acetic acid impurity present in starting material. The purified quinone monoimine subjected for optimized reaction condition but the yield of product reduced drastically. This is the first and direct support of our hypothesis and theory. Yield was substantially increased when one drop of acetic acid added externally in the reaction mixture. Hence, we have shown a delicate control over synthesis and computation: a computation driven synthesis and a synthesis driven computation. We now were interested to find the origin of regioselectivity, which upon investigation showed transition state for the nucleophilic attack from C-3 position is 5.68 kcal mol-1 more stabilized than C-1 position of indolizine. Three different gauche conformations have been studied to identify the most stable transition state for the nucleophilic attack.

3.1.4 Result and Discussion

As an initial investigation, indolizine (**1a**) and quinone monoimine (**2a**) were used as a model substrate for the optimization of reaction conditions (Table 1). First, the desired product C-3 functionalized indolizine **3a** was observed in a trace amount of isolated yield in the presence of HCl or without any additive at rt in 12 hours (Table 1, entries 1&2). Further, we found that the reaction works well in acetonitrile with a catalytic amount of acetic acid as an additive (Table 1, entry 3). With CH$_3$CN as a solvent, we investigated different concentrations of acetic acid and reaction times at room temperature, which resulted in comparative yields of the expected product

(see Table 1, entries 3-6). Excellent yields were obtained even when reactions were conducted for a short period of time, beginning with 1 hour, 20 minutes, 10 minutes, and 2 minutes (Table 1, entries 7-10). Further, different solvents were screened to promote the reaction yields (Table 1, entries 11-13). Entries 11-13 demonstrate that the reaction works well in all the solvents but not

Table 1. Optimization of the Reaction Condition for C-C Coupling[a]
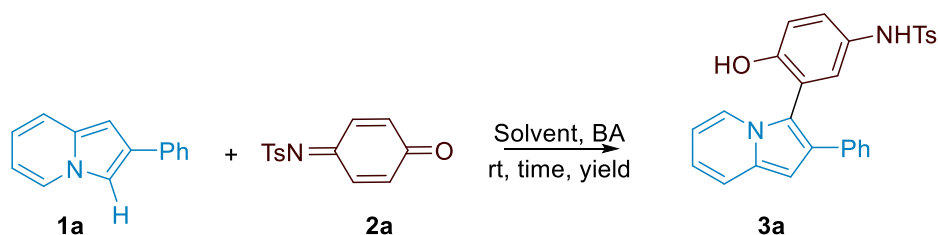
entry	Addtive (equiv.)	Solvent	Time (h)	Yield (%)[a]
1	-	CH$_3$CN	12h	trace
2	HCl	CH$_3$CN	12h	trace
3	AcOH (10 mol%)	CH$_3$CN	12h	88
4	AcOH (20 mol%)	CH$_3$CN	12h	87
5	AcOH (50 mol%)	CH$_3$CN	12h	74
6	AcOH(100 mol%)	CH$_3$CN	12h	69
7	AcOH (20 mol%)	CH$_3$CN	1h	88
8	AcOH (20 mol%)	CH$_3$CN	20 min	89
9	AcOH (20 mol%)	CH$_3$CN	10 min	92
10	**AcOH (20 mol%)**	**CH$_3$CN**	**2 min**	**92**
11	AcOH (20 mol%)	DCE	10 min	71
12	AcOH (20 mol%)	THF	10 min	78
13	AcOH (20 mol%)	DCM	10 min	81
14	AcOH (20 mol%)	CH$_3$CN	10 min	55[b]

[a] Reaction condition: **1a** (1 equiv.), **2a** (1 equiv.), AcOH (20 mol%), CH$_3$CN, rt, 2 min. [b] reaction carried out at 0 °C

Table 2. Scope for Substituted Indolizines
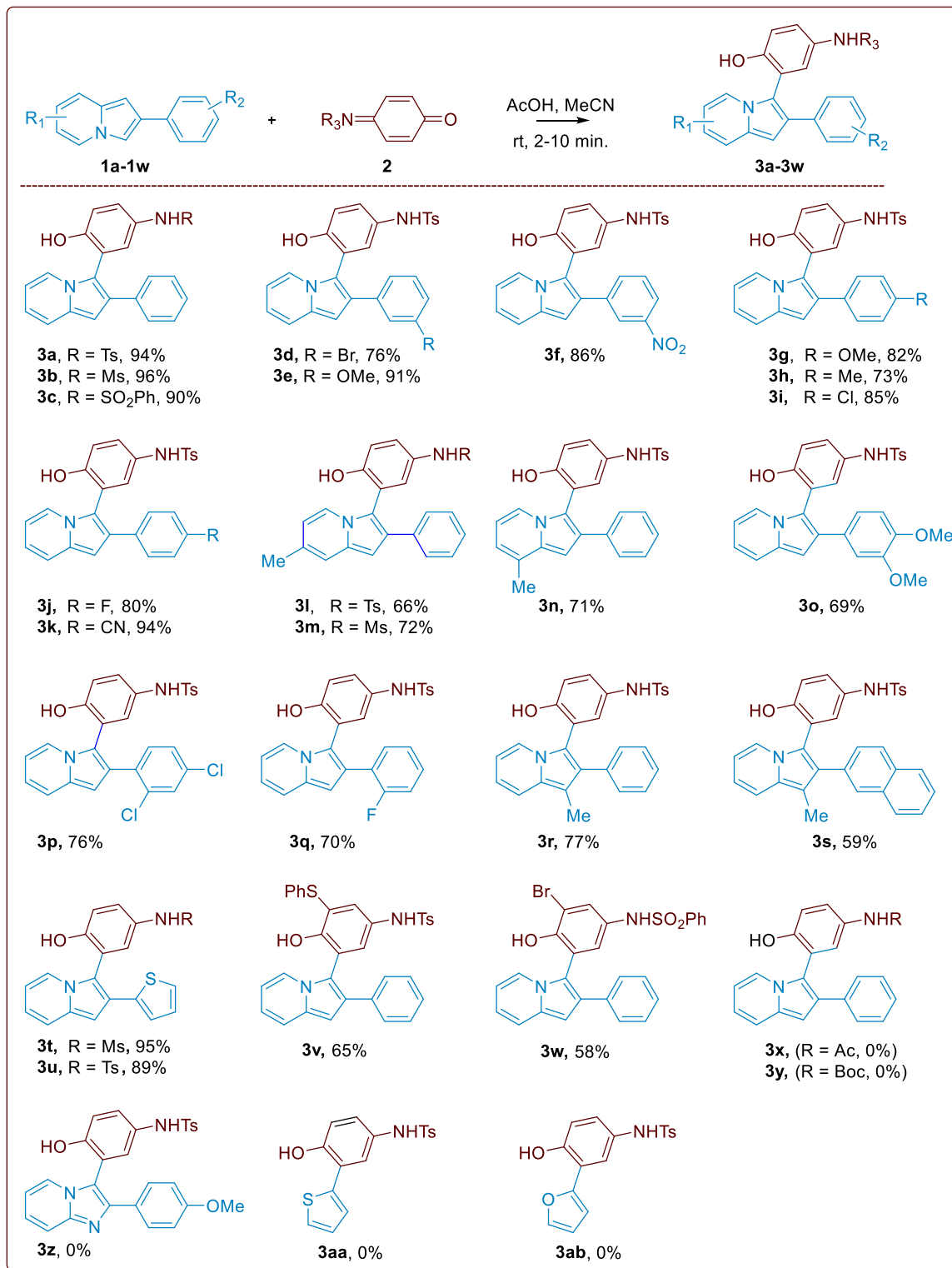
Reaction condition: **1a** (1 equiv.), **2a** (1 equiv.), AcOH (20 mol%), CH$_3$CN, rt, 2-10 min

better than acetonitrile. With lowering reaction temperature, the rate of reaction slows down (Table 1, entry 14). Thus, we choose entry 10 as the most optimal reaction condition to form **3a**. With optimized reaction condition in hand (Table 1, entry 10), we investigated the scope of the reported reaction by screening wide range of indolizines and quinone monoimine derivatives (Table 2). In the reaction of *N*-sulfonyl prepared quinone monoimines with substituted indolizines containing electron withdrawing, electron donating, halo and hetero substituents, coupled products (**3a-3w**) are obtained in good to excellent yields, as shown in Table 2. Using standard reaction conditions, *N*-tosyl, mesyl and sulfonyl protected quinone monoimines gave 90-96% yields for the expected products (**3a-3c**) upon reaction with indolizine. With ortho, meta, and para substituted electron donating groups on the phenyl rings of indolizines, we obtained the desired products (**3e, 3g, 3h, 3o**) in good yields (up to 91 %). Halogen substitutions at ortho, meta, and para positions on indolizines were also examined under optimized reaction conditions that gave the corresponding products (**3d**, **3i**, **3j**, **3p**, **3q**) with good to excellent yields.

In addition, electron withdrawing substitution on indolizine offered desired products (**3f, 3k**) in 86 and 94% yields respectively. With substituents present at the C-1, C-6, and C-7 positions of indolizines, the reaction gave the coupled products (**3l-3n, 3r-3s**) with 59-77% yields. Furthermore, indolizines with heterocyclic rings are also capable of forming coupled products (**3t** and **3u**) with comparable yields. The substituted quinone monoimines also gave moderate yields of the coupled products **3v** and **3w**. Unfortunately, *N*-acyl protected quinone monoimine, and various electron-rich heterocycles failed to give the expected products (**3x-3ab**).

Example 1:

The structure of compound 3a *N*-(4-hydroxy-3-(2-phenylindolizin-3-yl) phenyl)-4-methylbenzene -sulfonamide was confirmed from its ^{1}H and ^{13}C NMR spectrum. In proton NMR

spectrum, the peak showed at δ 2.36 singlet for methyl group of *N*-protected tosyl group and δ5.21 singlet corresponding to hydrogen of amide group. The peaks at δ 6.40 to 7.58 are the aromatic hydrogens. In carbon NMR spectrum of product **3a** the methyl carbon was showed at δ21.24 and aromatic carbons showed in the region of 98.72 to 152.67 (**Figure 2**).
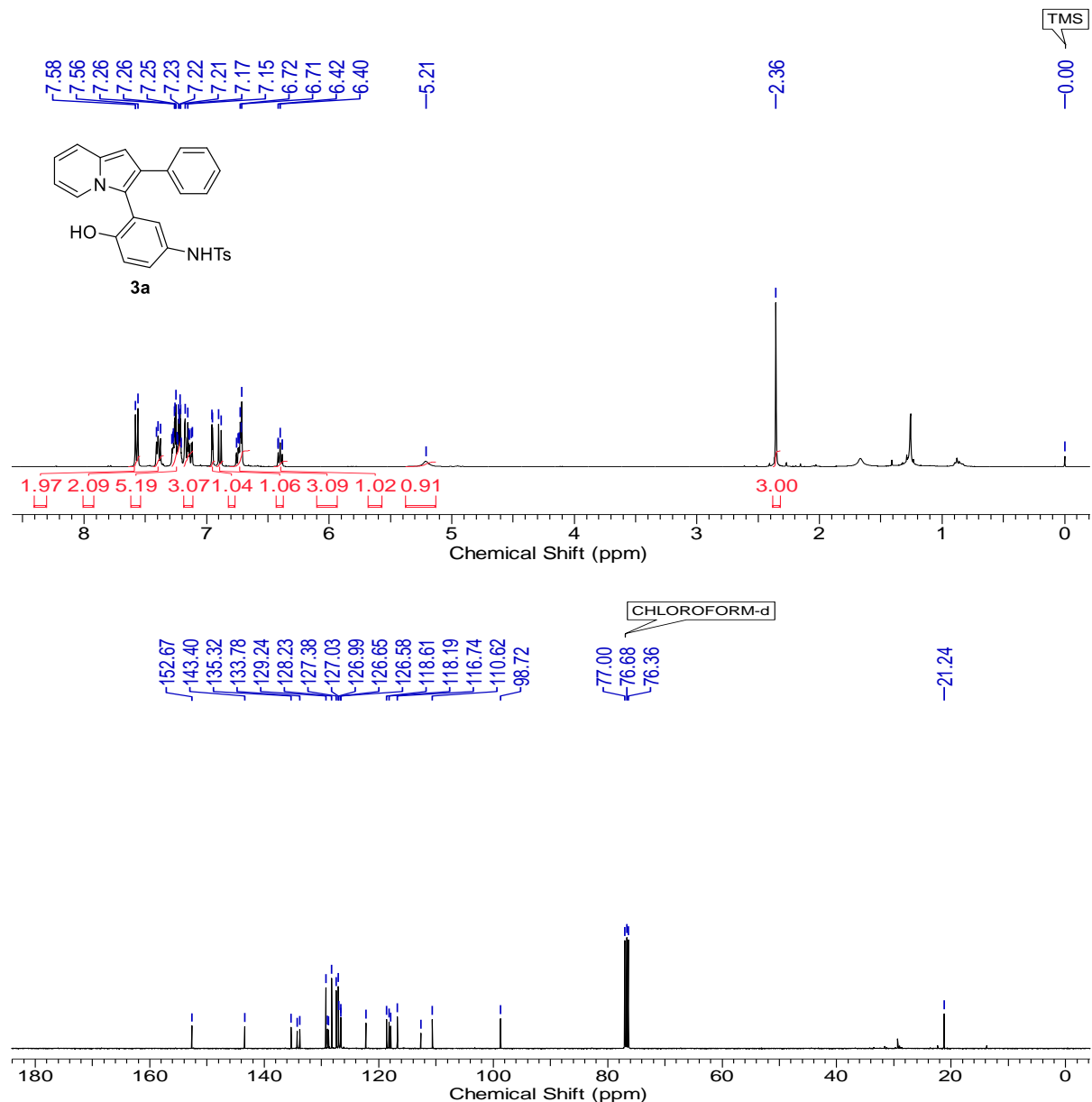
Figure 2. ^{1}H and ^{13}C NMR of *N*-(4-hydroxy-3-(2-phenylindolizin-3-yl)phenyl)-4-methylbenzenesulfonamide(3a)

Table 3. Synthesis of Indolizine Functionalized BINOLs

6a, 69%
dr (1:1)

6b, 60%
dr (1:1)

6c, 57%
dr (1:1)

6g, 57%
dr (1:1)

6d, 65%
dr (1:1)

6e, 74%
dr (1:1)

6f, 55%
dr (1:1)

6h, 55%
dr (1:1)
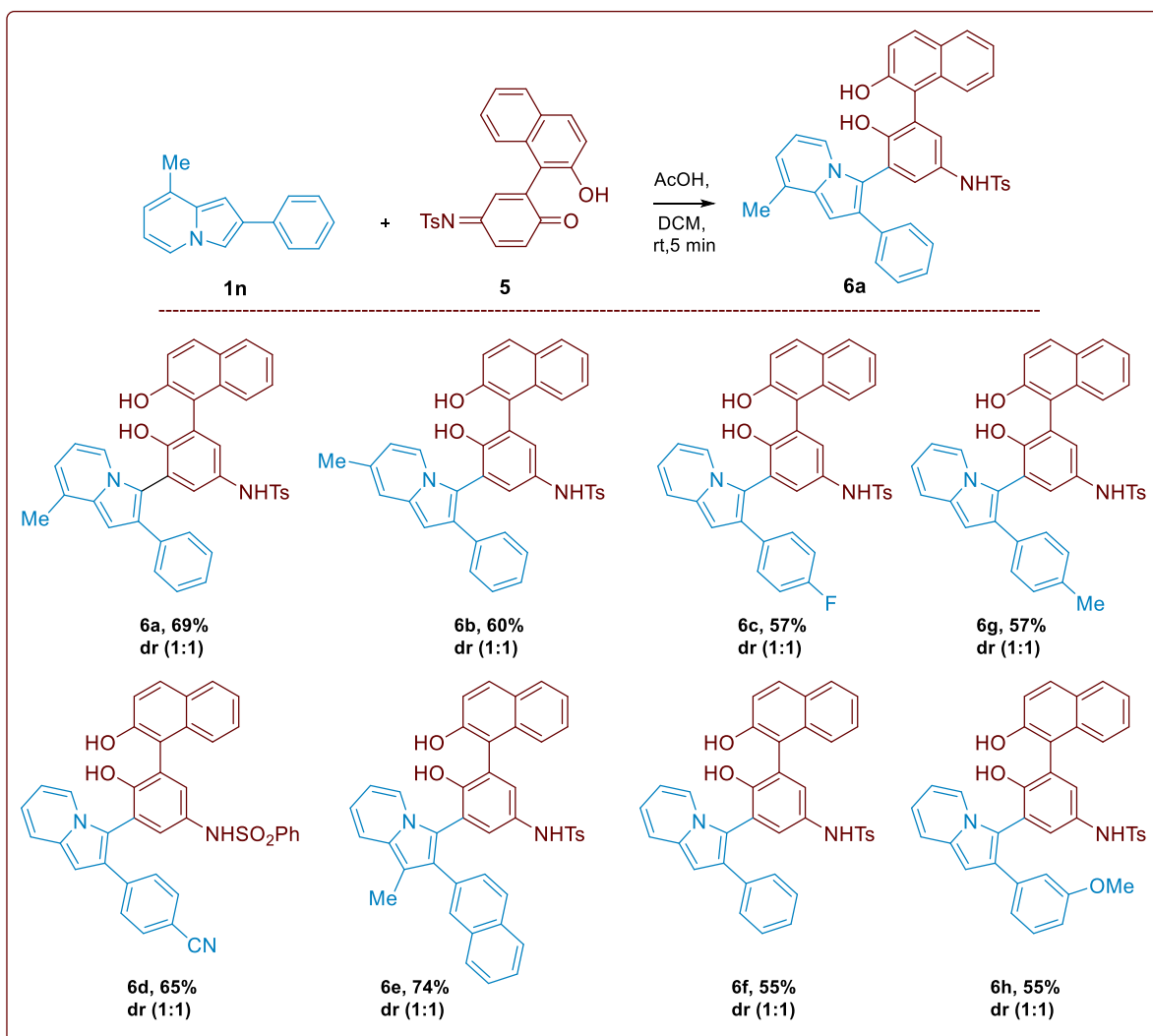
[a]Reaction condition: **1n** (1 equiv., 0.197 mmol), **5** (1 equiv., 0.197 mmol), AcOH (20 mol%), DCM, rt, 5 min.

Additionally, we investigated the effect of other quinone monoimines reaction with different indolizines and the results are summarized in Table 3 & Scheme 4. For the quinone monoimine derivative (**5**), the standard reaction conditions were applied to produce a wide range of synthetically important molecules of axially chiral BINOLs with substituted indolizine cores.
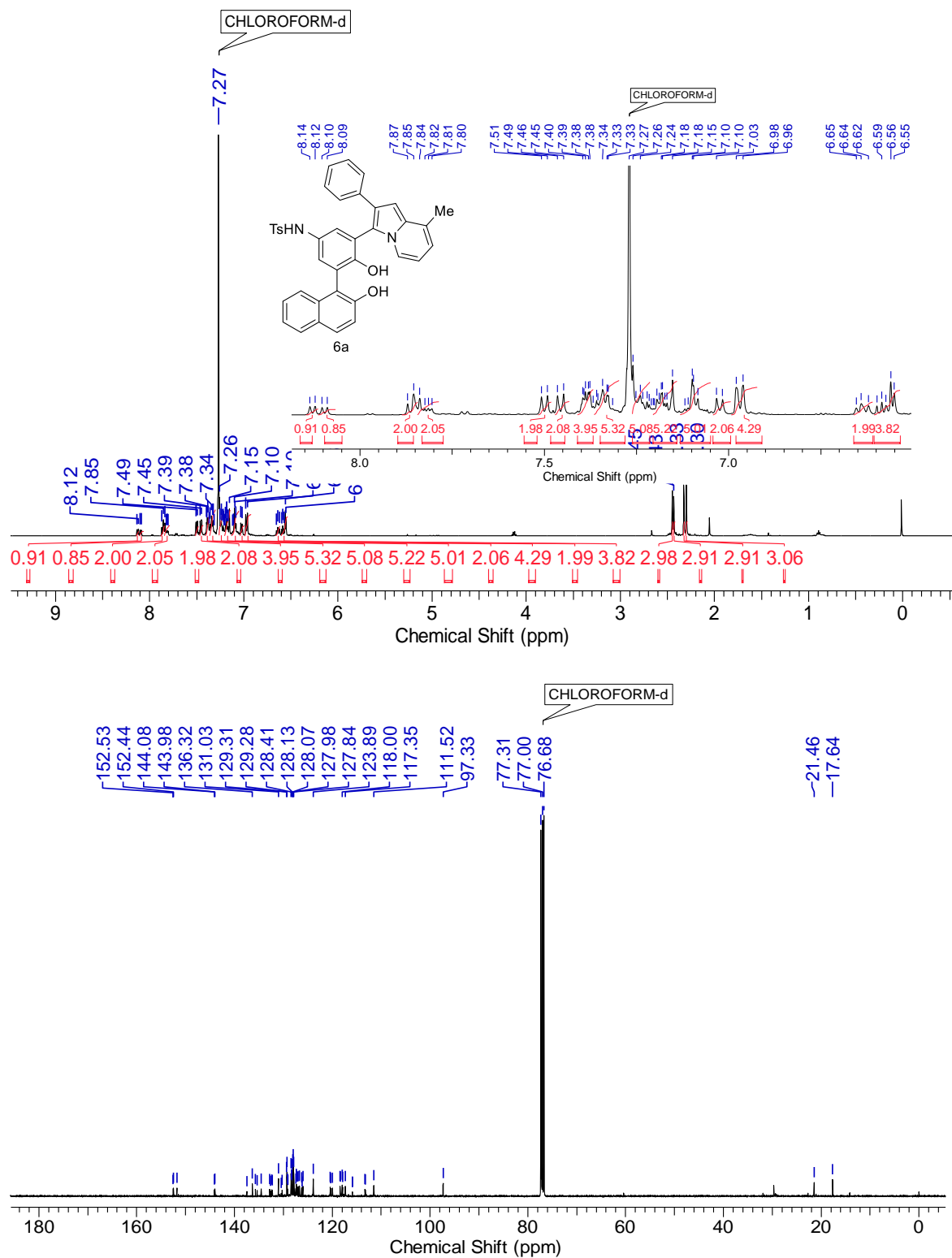
Figure 3: ^{1}H and ^{13}C NMR of *N*-(4-hydroxy-3-(2-hydroxynaphthalen-1-yl)-5-(8-methyl-2-phenylindolizin-3-yl)phenyl)-4-methylbenzenesulfonamide (6a)

The formed binol functionalized indolizine **6a** was further confirmed by it's the ^{1}H, ^{13}C and HRMS analysis (**Fig.3**). As shown in Table 3, several indolizines with electron donating, electron withdrawing, and halo group reacted well with quinone monoimine **5** under standard reaction conditions and provided corresponding products (**6a-6f**) in 57-74% yields. For the axially chiral BINOL products, four possible stereoisomers are possible. Since we have used racemic starting material, a pair of diastereomers have formed, each of which exists as a racemic mixture.
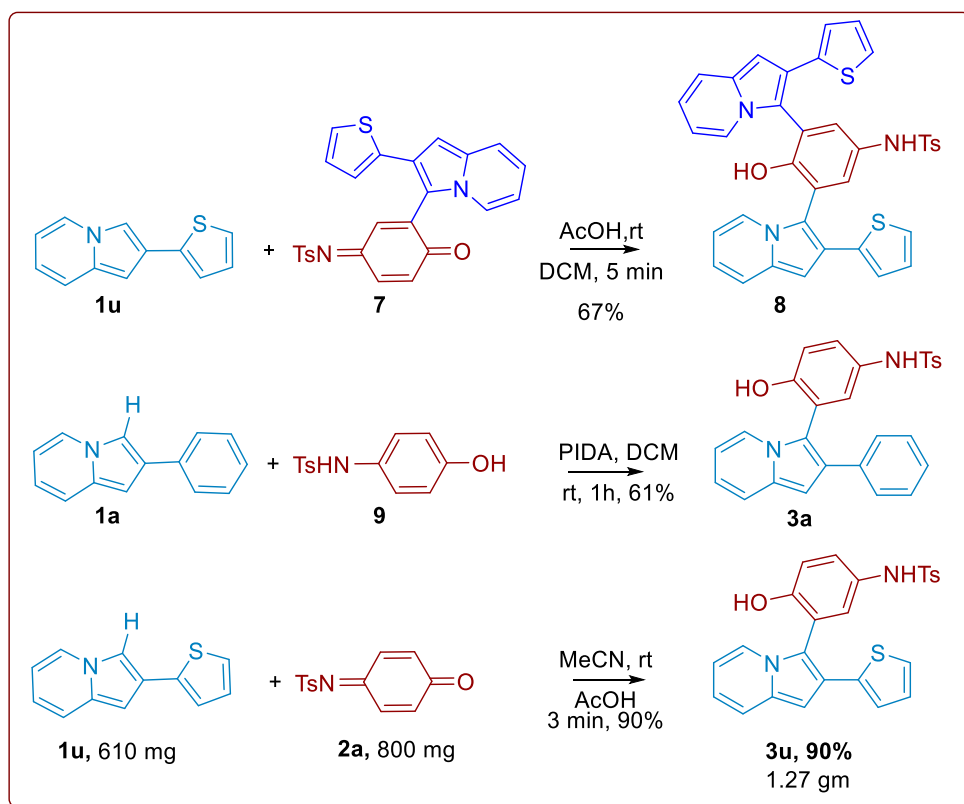
Scheme 4. Synthetic utility and scale-up experiment

Example 2:

In the ^{1}H NMR spectrum of indolizine binol **6a** the characteristic peaks of two methyl group are showed at δ 2.30-2.33 (s, 1H) and δ 2.43-2.45 respectively in near about 1:1 diastereomeric ratio.

Aromatic hydrogens appeared in the region of δ 6.55 to 8.12. The indolizine binol moiety was further confirmed by using ^{13}C NMR and Mass analysis. We also synthesized symmetric indolizine **8** and one pot synthesis **3a** from *N*-tosyl-*p*-aminophenol **9** as shown in Scheme 4. The compound **3u** is oxidized to give quinonone monoimine derivative **7**, followed by an addition of heterocyclic indolizine **1u**, which yields symmetric indolizine **8** in 67% yield. Additionally, we successfully synthesized product **3a** directly from *N*-tosyl-*p*-aminophenol **9** in one-pot reaction by using PIDA with 61% yield. In a scale-up reaction of **1u** with quinone monoimine **2a**, 1.27 grams of compound **3u** were obtained with 90% yield.

Example 3:

Formed product of symmetric indolizine moiety (**8**) was further confirmed by ^{1}H, ^{13}C NMR and HRMS analysis. In proton NMR spectrum the characteristic peak of methyl group is showed at δ
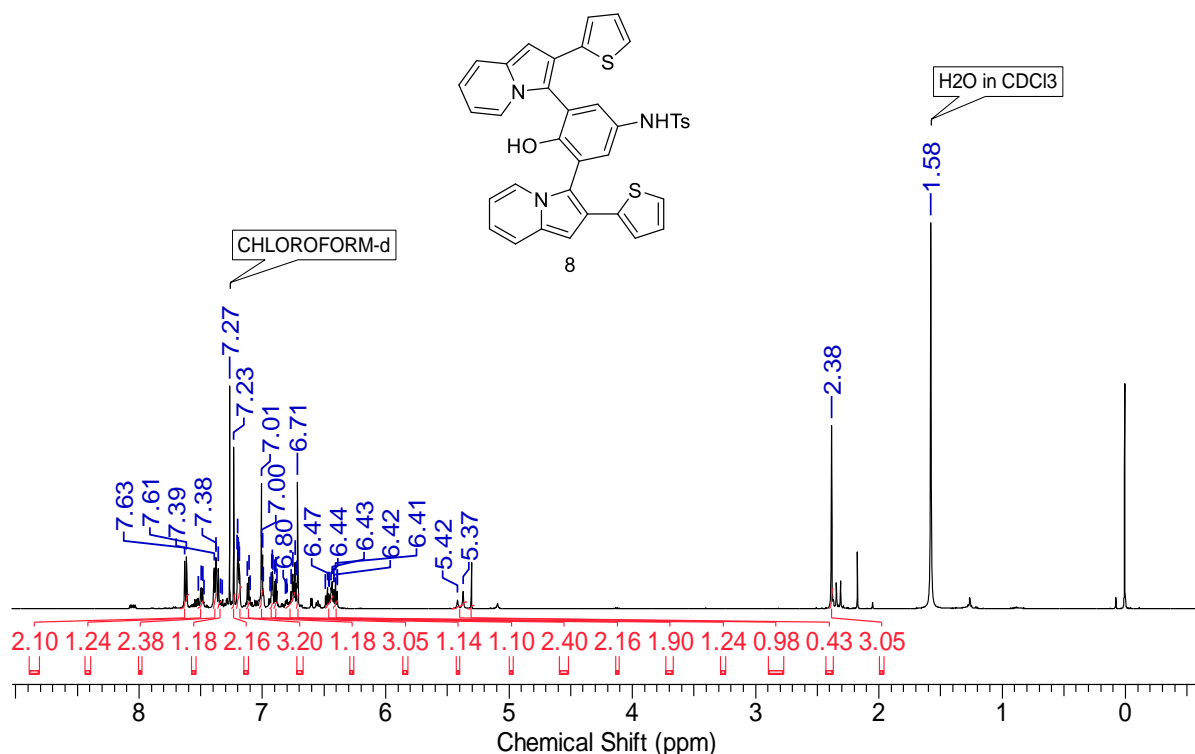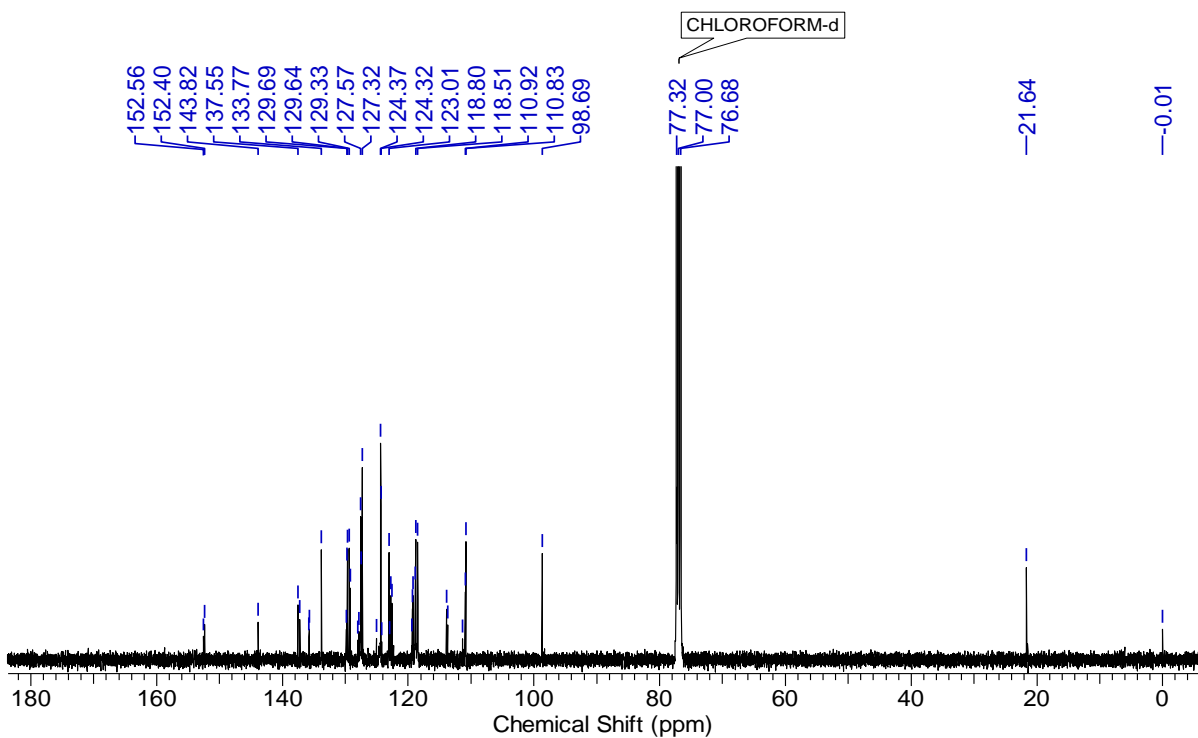
Fig. 4: ^{1}H and ^{13}C NMR of *N*-(4-hydroxy-3,5-bis(2-(thiophen-2-yl)indolizin-3-yl)phenyl)-4-methylbenzenesulfonamide(8)

2.38 and δ 5.42, 5.37 are N-H and O-H hydrogens respectively. Aromatic hydrogens displayed in the range of 6.41 to 7.63 ppm. Also the carbon and mass spectra is matched with our desired product.

3.1.5. DFT Studies
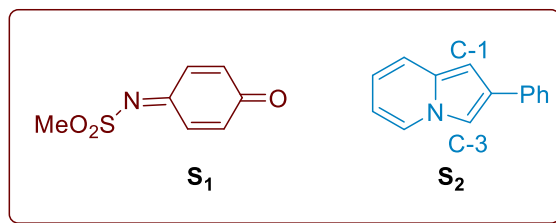
Figure 5. Structure of the model starting materials

Design of Reaction Pathways: We selected model structure of monoimine S_1 and indolizine S_2 in **Figure 5** have been used to investigate the probable mechanistic pathways for the reaction. Overviews of the investigated pathways are shown in **Scheme 5**.
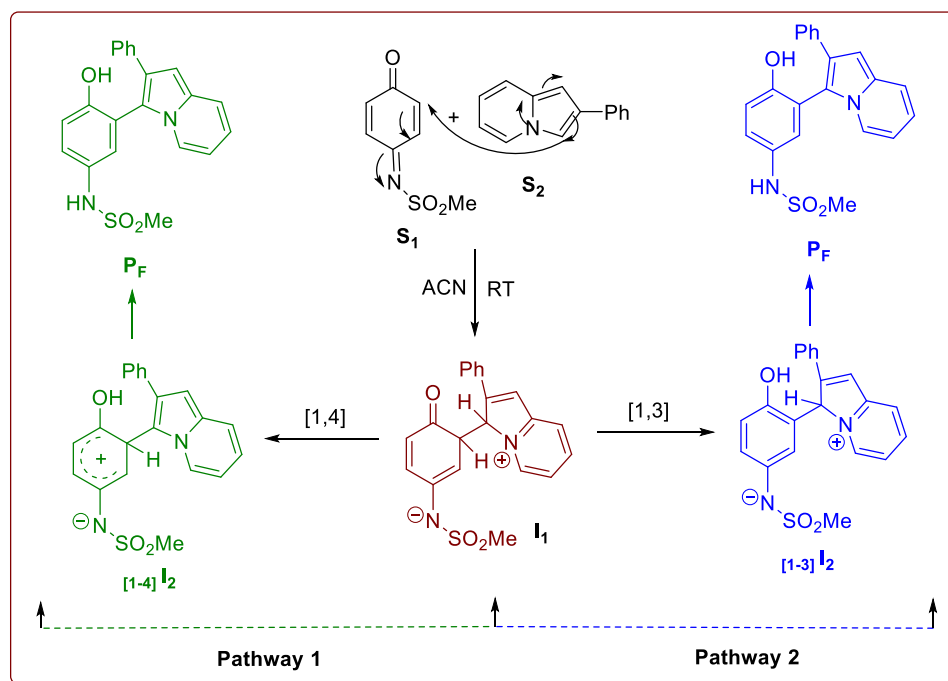
Scheme 5. Initial hypothesis for the probable reaction pathways

In pathway 1 the reaction goes *via* a [1, 4] proton transfer. Whereas, a [1, 3] proton abstraction mechanism is seen in pathway 2. Pathway 3 shows an acetic acid catalyzed proton shuttle mechanism for the formation of the product (**Scheme 5**). Summary of the free energy of activation and activation energy related to the individual step and overall reaction for different pathways using substrate S_1 and S_2 are shown respectively in Table SI1, SI2. Potential Energy Surface (PES) of the studied pathways are shown respectively in figure 6, 7, 8 and 9. Stationary points for the minima have been designated using the letters **'S'**, **'I'** and **'P'**. **'TS'** is used for the saddle point. Subscript on the right- and left-hand side respectively indicates the species number

and the pathway it belongs. '**F**' in subscript represents 'final', '**Ac**' represents 'acetic acid catalyzed pathway' and '**PT**' represents proton transfer.
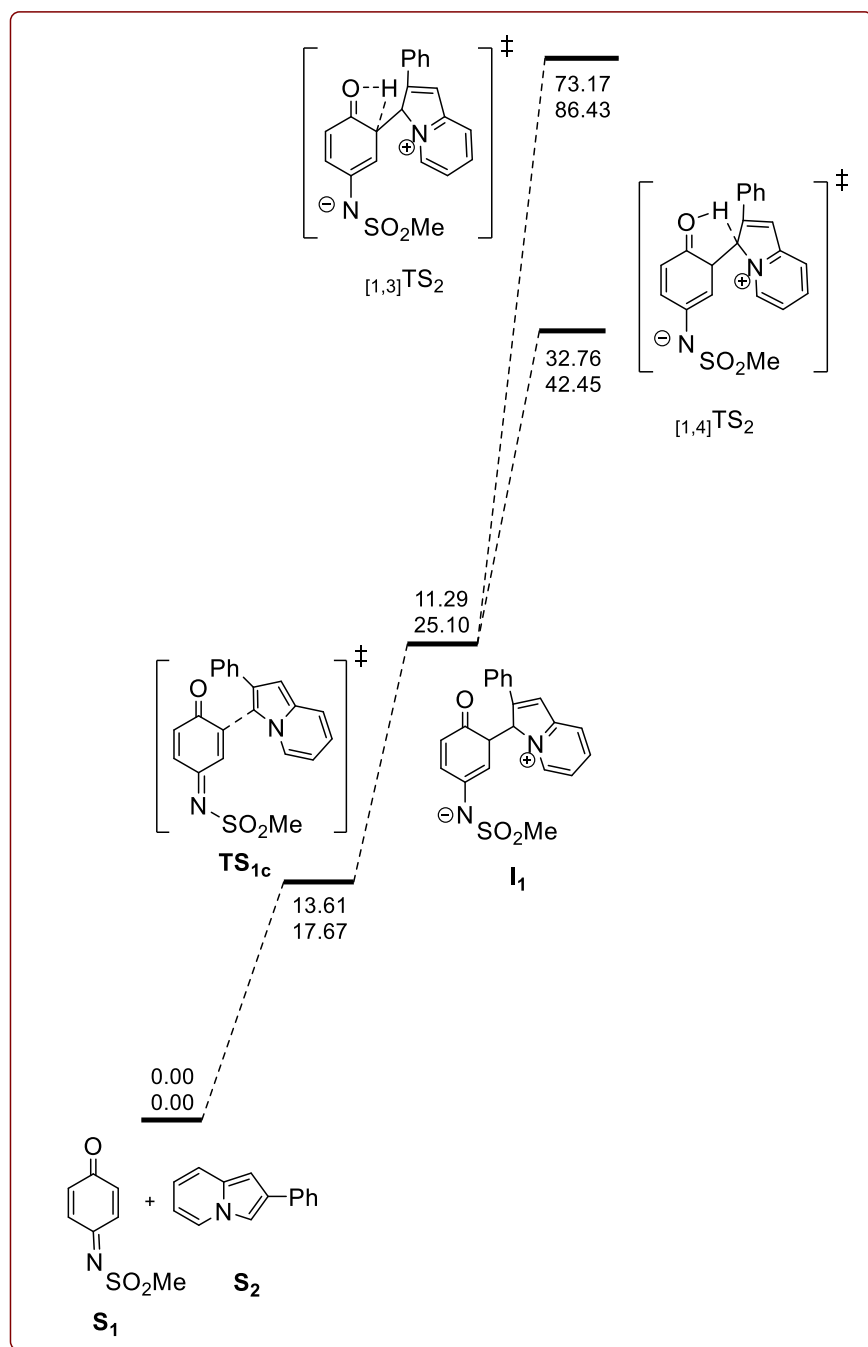
Figure 6. PES for Pathway 1 and Pathway 2

Analysis of the Pathways

Conformational Analysis for the nucleophilic attack: Initially the indolizine S_2 from its C-3 position does the nucleophilic attack to the electrophilic monoimine S_1 through TS_1 to produce the intermediate I_1. We found three different gauche conformations can be possible for TS_1 which are indicated as TS_{1a}, TS_{1b} and TS_{1c} in **figure 7**. DFT quantum mechanical calculations revealed that the activation barrier for TS_{1a}, TS_{1b} and TS_{1c} are 24.09, 20.54 and 17.67 kcal mol^{-1} respectively. Hence, TS_{1c} is the most stable conformer for the nucleophilic attack.
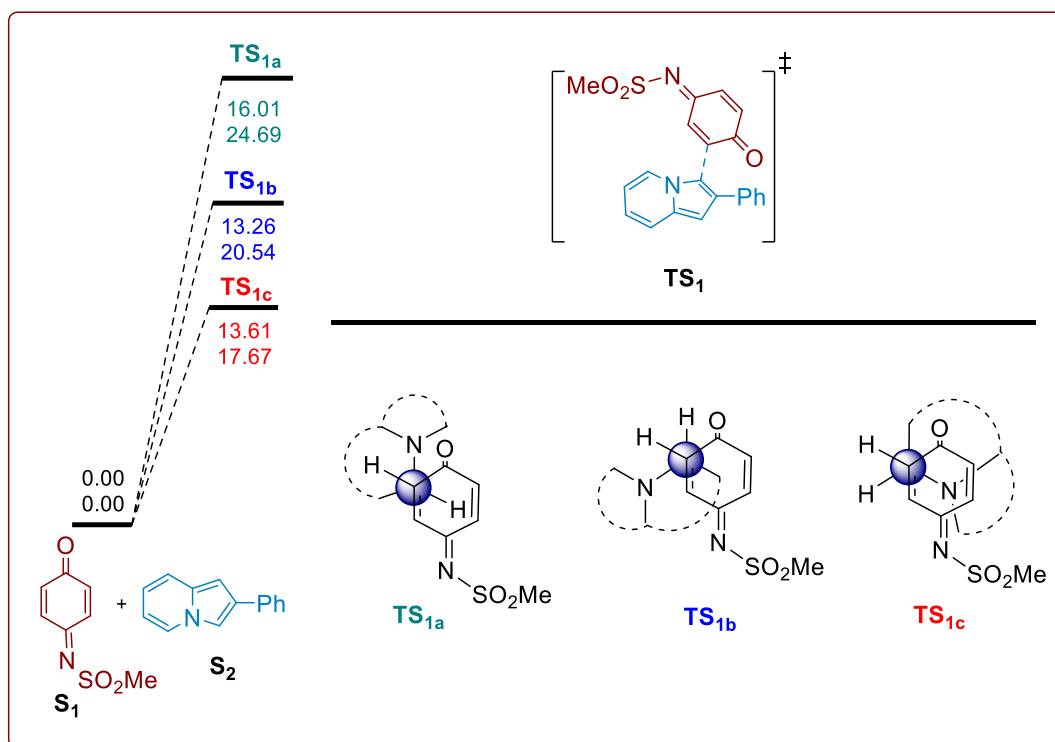
Figure 7. Conformation analysis for the nucleophilic attack

Pathway 1 and 2. We suspect that two different ways of proton transfer could be possible after the nucleophilic attack. In pathway 1 an intramolecular [1, 4] proton transfer is observed which has an activation barrier of 17.35 kcal mol^{-1} but has a global energy barrier of 42.45 kcal mol^{-1}. A [1, 3] intramolecular proton transfer is associated with pathway 2. The TS for [1, 3] proton abstraction has an energy barrier of 61.33 kcal mol^{-1}. Both the pathways involve the intermediate

I_1, which is also destabilized by an amount of 7.43 kcal mol^{-1}. Therefore, the observed energetics did not fit with the current reaction condition. Hence, our initial hypothesis for the intramolecular proton abstraction pathways did not stand any more.
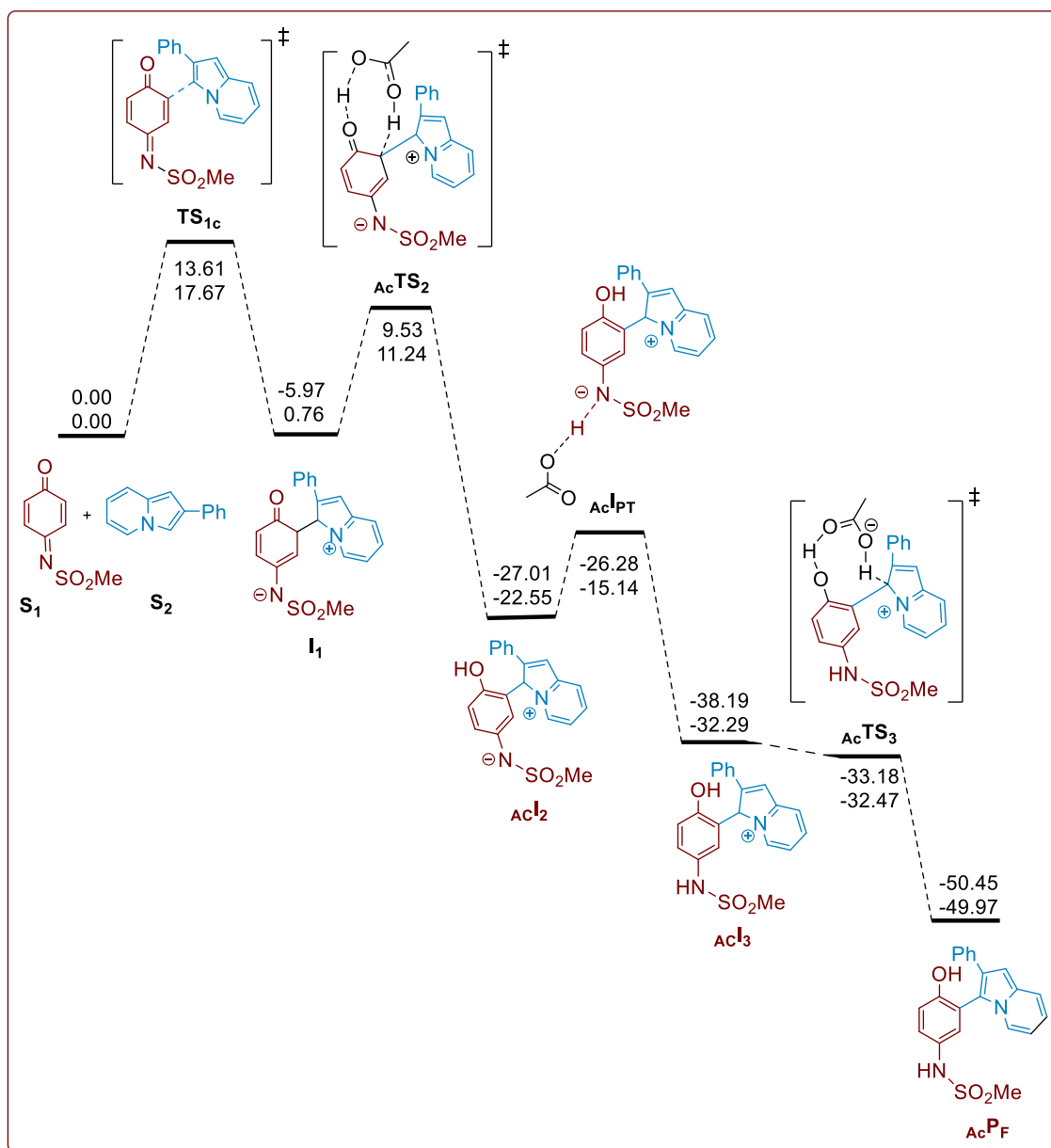
Figure 8. PES along with structures and thermodynamic parameters for pathway 3

Pathway 3. At this point we again started understanding the system and found acetic acid has an important role to make the reaction catalytic and very fast which led us to pathway 3(**Figure 8**).

After the initial nucleophilic attack, intermediate I_1 is formed through TS_{1c} associated with activation barrier of 17.67 kcal mol^{-1}. Here in this pathway 3, I_1 is getting far more stabilized than pathway 1 and 2 due to the acetic acid support in the system through, hydrogen bonding. An eight membered proton shuttle mechanism was observed in the very next step by which an intermolecular proton abstraction from acetic acid to I_1 and from I_1 to acetic acid is occurring simultaneously through $_{Ac}TS_2$ to form $_{Ac}I_2$ and therefore we are getting acetic acid back (**Scheme 6**). This step has an activation barrier of 10.48 kcal mol^{-1}. The intermediate $_{Ac}I_2$ forms $_{Ac}I_3$ and acetate anion through $_{Ac}I_{PT}$ by crossing a barrier of 7.41 kcal mol^{-1}. Lastly the aromatization occurs through a proton transfer from $_{Ac}I_3$ to acetate anion *via* $_{Ac}TS_3$ which has an activation barrier of -0.18 kcal mol^{-1} and hence we obtain the final desired product $_{Ac}P_F$ with recovery the acetic acid which is further used to perform the next catalytic cycle. Hence, this pathway 3 is a
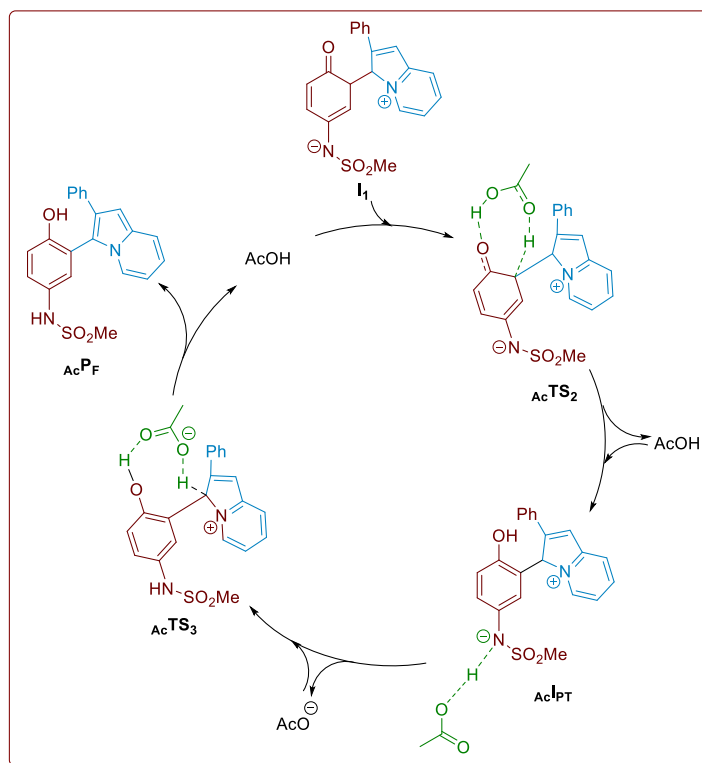
Scheme 6. Catalytic cycle for the acetic acid catalyzed pathway

direct support for the crucial role of acetic acid catalytically to make the reaction very fast and

the energetics for the pathway 3 now exactly fits with our current reaction condition.
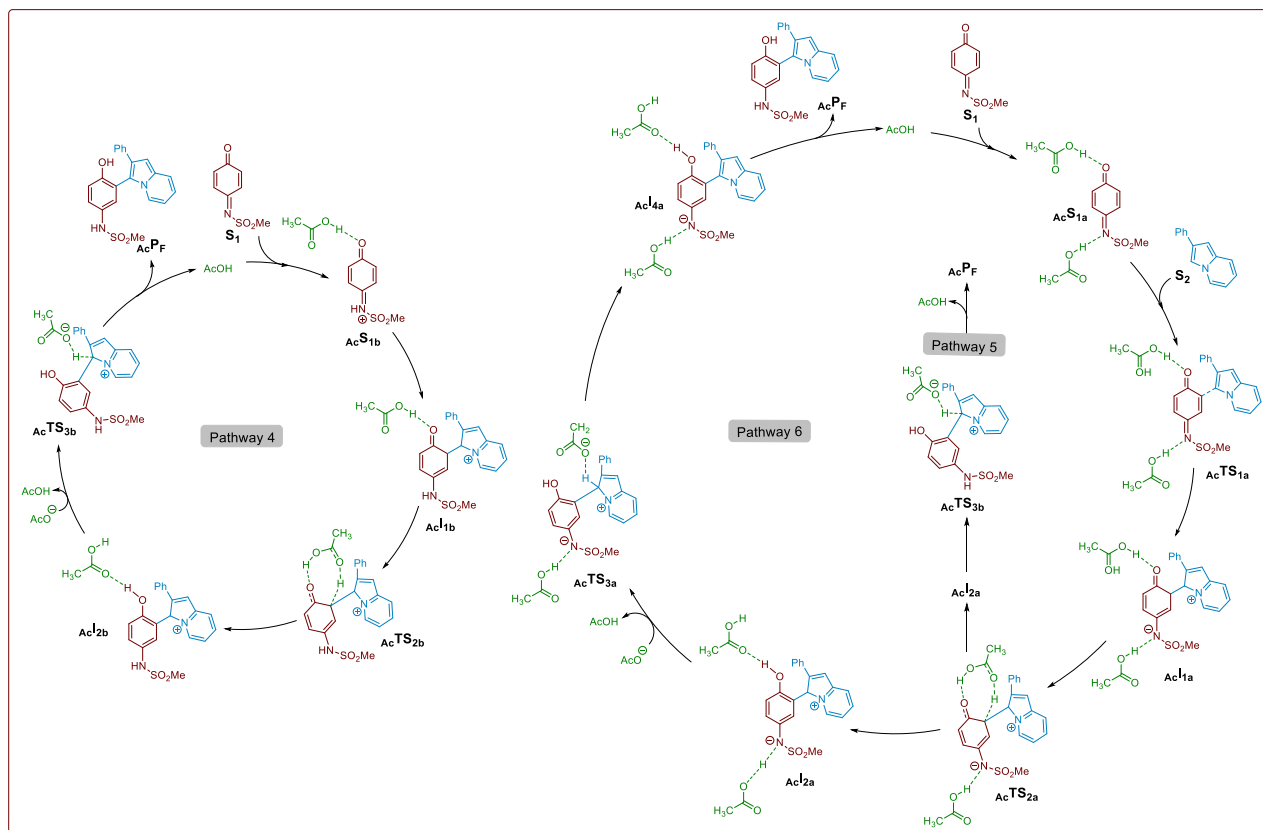
Scheme 7. Outline of the pathway 4, 5 and 6

But, as shown in Scheme 6 and in pathway 3, the acetic acid participates after the initial

nucleophilic attack and also, there are various negatively charged intermediates and TS in the

mechanistic route. At this point few questions may arise, viz. why acetic acid is not taking part in

the initial nucleophilic attack step by activating the reactant and also why the negatively charged

intermediates and TS are not getting stabilized by the acetic acid in the catalytic cycle.

Considering these facts, our further investigation led us to three different pathways (pathway 4, 5

and 6) as shown in Scheme 7 and Figure 9. Based on our conformational analysis as shown in

Figure 3, we chose the most stable conformer TS_{1c} to probe the effect of activation by acetic acid.

Pathway 4. In pathway 4 the quinone monoimine gets protonated ($_{Ac}S_{1b}$) for activation at the very first step. This protonation leads to a barrier less TS for the nucleophilic attack by indolizine S_2 to form the intermediate $_{Ac}I_{1b}$. Now the proton abstraction takes place by a proton shuttle mechanism through $_{Ac}TS_{2b}$ with an activation barrier of 13.57 kcal mol^{-1}. The intermediate $_{Ac}I_{2b}$ is further stabilized when one acetate molecule got inserted by replacing one molecule of acetic acid, forming the intermediate $_{Ac}I_{3b.}$ Next protonation occurs to give rise to the hydrogen bonded aromatized intermediate $_{Ac}I_{4b}$ through $_{Ac}TS_{3b}$ having -0.18 kcal mol^{-1} activation energy barrier. Lastly, $_{Ac}P_F$ is formed.

Pathway 5. In pathway 5 the quinone monoimine S_1 initially gets activated by the acetic acid through hydrogen bonding ($_{Ac}S_{1a}$) which facilitates the nucleophilic attack by the indolizine S_2 through $_{Ac}TS_{1a}$ with an energy barrier of 8.48 kcal mol^{-1} forming the intermediate $_{Ac}I_{1a}$ that undergo a proton shuttle mechanism through $_{Ac}TS_{2a}$ which has an activation barrier of 17.85 kcal mol^{-1} end up with intermediate $_{Ac}I_{2a}$. Now at this point the nitrogen on the quinone monoimine moiety gets protonated by the acetic acid and forms the intermediate $_{Ac}I_{3b}$. The further proton abstraction to give the aromatized hydrogen bonded intermediate $_{Ac}I_{4b}$ occurs through $_{Ac}TS_{3b}$ with an activation barrier of -0.18 kcal mol^{-1}. Finally, $_{Ac}P_F$ is formed.

Pathway 6. Pathway 6 also follows the common step up to intermediate $_{Ac}I_{2a}$. Then instead of protonating the nitrogen (pathway 5), one acetic acid molecule goes out and one acetate molecule gets inserted to provide intermediate $_{Ac}I_{3a}$ that undergo proton abstraction through $_{Ac}TS_{3a}$ by crossing an activation barrier of only 0.18 kcal mol^{-1}. Further, the hydrogen bonded negatively charged aromatized intermediate $_{Ac}I_{4a}$ gets protonated to provide final product $_{Ac}P_F$

with initializing another catalytic cycle. Comparing all the possible mechanistic pathways it can be concluded from the energy profile that pathway 6 has the least energetic or most favorable geometries of intermediates and transition states. Therefore pathway 6 is the most plausible investigated path for the reported reaction which has a global free energy barrier of 19.73 kcal mol^{-1}.
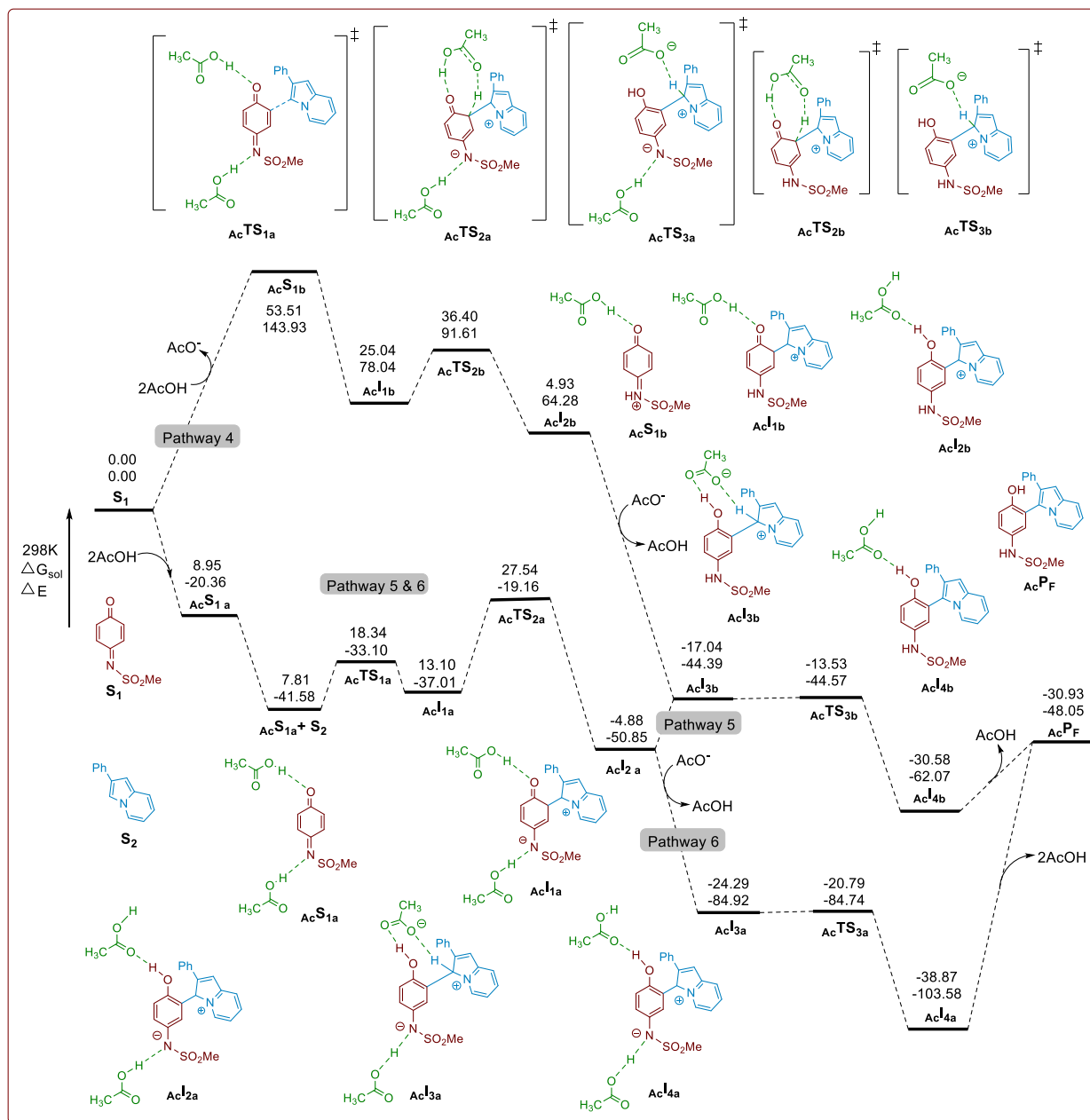
Figure 9. PES along with structures and thermodynamic parameters for pathway 4, 5 and 6

Regioselectivity: The indolizine S_2 has two reactive sites for the nucleophilic attack. In our current reaction condition, we have shown a selective control for the functionalization of C-3 hydrogen over C-1 (Figure 5). In order to understand such regioselectivity we again performed DFT quantum mechanical calculations for determining the transition state involving C-1 site of indolizine and compared the energetics between C-1 and C-3. It can clearly be seen from the
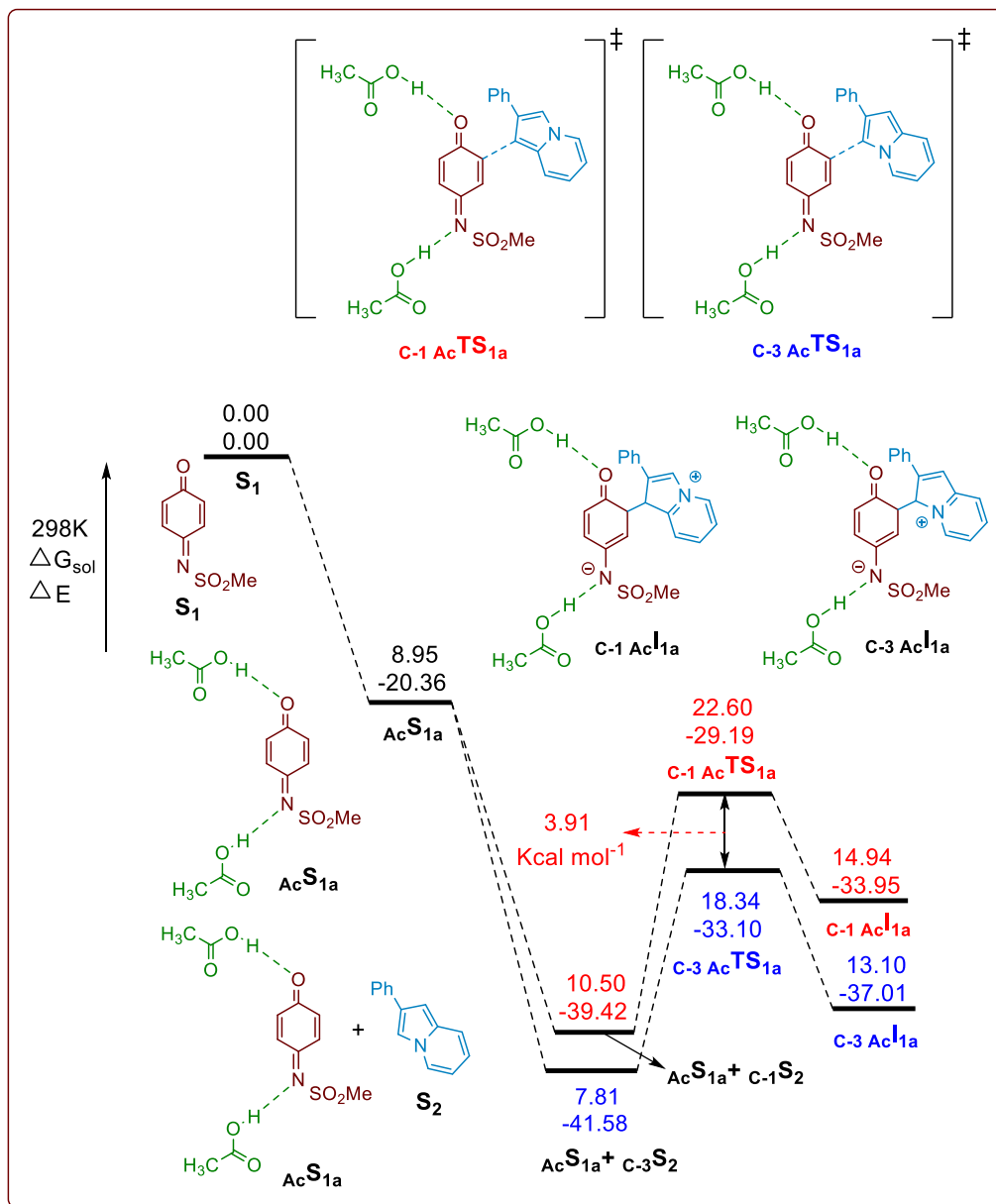
Figure 10. PES for regioselectivity

energy profile in Figure 10 that after activating by acetic acid the quinone monoimine ($_{Ac}S_{1a}$) when comes into contact with the indolizine S_2, the drop of energy leading to the respective transition states is much more in case of C-3 than C-1 which is due to the additional pi-stacking interaction between the molecules. Further, the transition state involving C-3 site is more stabilized by an amount 3.91 kcal mol^{-1}. Finally, the thermodynamic stability of the intermediate ($_{C-3Ac}I_{1a}$) *via* C-3 TS is much higher than the intermediate ($_{C-1Ac}I_{1a}$) *via* C-1 TS. Hence the C-3 site is the chosen one for the reported reaction.

3.1.6. Conclusion

In conclusion we developed an operationally simple and environment friendly protocol for the regioselective C-H functionalization of indolizines by using catalytic amount of acetic acid. We have shown the application of present methodology by synthesizing functionally important binol substituted derivatives of indolizines. The energetics from DFT quantum mechanical investigations showed that our preliminary hypothesis of intramolecular proton abstractions did not fit with the current reaction condition; instead, it gave rise to some complex path which revealed the role of acetic acid toward unfolding the inherent mechanism for this ultrafast catalytic reaction. This theoretical result was also confirmed by synthetic experiments. Additionally, the choice of regioselectivity was also addressed.

3.1.7. Experimental Section

Typical procedure for the synthesis of quinone monoimines

N-tosyl-p-aminophenol (2.64 g) was added in DCM 50 mL followed by addition of PhI(OAc)$_2$ (1 equiv., 3.23 g) and stirred for 1h at room temperature. Add 25 mL water to the mixture and extract with EtOAc (25 mL x 3). The combined organic layers were washed with brine dried

over sodium sulphate. The solvent evaporated under reduced pressure. The crude residue is purified by using flash column chromatography (100-200 mesh silica using 85/15 petroleum ether/ethyl acetate as the eluent to afford the corresponding compound as orange solid. All quinone monoimines (2a-2c, 5 and 7) are synthesized by using above method.

General procedure for the synthesis of 3a

To a 25 mL oven dried round-bottom flask indolizine **1a** (0.191 mmol, 37 mg), quinone monoimine **2a** (0.191 mmol, 50 mg) and AcOH (0.038 mmol, 0.2 mL) was taken in CH_3CN (1 ml). Then the resulting reaction mixture was stirred to 25 °C for 2 min. Upon completion of the reaction, the reaction mixture was dried under vacuum. Then the crude reaction mixture was diluted with ethyl acetate (5 mL) and washed with brine and eluted with EtOAc (5 mL x 2). The organic layer was evaporated and the crude residue was preadsorbed on silica gel and purified by column chromatography (100-200 mesh silica Using 80/20 to 80/30 petroleum ether/ethyl acetate as the eluent to afford the corresponding compound **3a** in 94 % yield as faint yellow semisolid (81 mg).

***N*-(4-Hydroxy-3-(2-phenylindolizin-3-yl)phenyl)-4-methylbenzenesulfonamide (3a).** White semisolid, 94% yield (81 mg). ^{1}H NMR (400 MHz, CDCl$_3$) δ 7.57 (d, *J* = 8.4 Hz, 2H), 7.35 - 7.44 (m, 2H), 7.20 - 7.29 (m, 5H), 7.11 - 7.19 (m, 3H), 6.95 (d, *J* = 2.6 Hz, 1H), 6.89 (d, *J* = 8.8 Hz, 1H), 6.65 - 6.81 (m, 3H), 6.34 - 6.45 (m, 1H), 5.21 (br. s., 1H), 2.36 (s, 3H). ^{13}C{^{1}H} NMR (101 MHz, CDCl$_3$) δ 152.7, 143.4, 135.3, 134.3, 133.8, 129.2, 128.9, 128.8, 128.2, 127.4, 127.0, 127.0, 126.6, 126.6, 122.2, 118.6, 118.2, 117.9, 116.7, 112.7, 110.6, 98.7, 21.2. HRMS (ESI) m/z calculated for $C_{27}H_{23}O_3N_2S$ [(M+H)$^+$] 455.1424 found 455.1417.

***N*-(4-Hydroxy-3-(2-phenylindolizin-3-yl)phenyl)methanesulfonamide (3b).** White solid, 96% yield (94 mg). ^{1}H NMR (500 MHz, CDCl$_3$) δ 7.65 (d, *J* = 7.2 Hz, 1H), 7.45 (d, *J* = 9.2 Hz, 1H),

7.34 (d, J = 7.6 Hz, 2H), 7.24 - 7.29 (m, 4H), 7.17 - 7.23 (m, 1H), 7.11 (d, J = 2.3 Hz, 1H), 7.04 (d, J = 8.8 Hz, 1H), 6.70 - 6.87 (m, 2H), 6.52 (t, J = 6.7 Hz, 1H), 6.38 (br. s., 1H), 2.84 (s, 3H). ^{13}C{^{1}H} NMR (126 MHz, CDCl$_3$) δ 153.0, 134.6, 133.9, 129.3, 129.0, 128.3, 127.9, 127.1, 126.6, 125.9, 122.6, 118.8, 118.6, 118.3, 117.1, 113.3, 111.0, 99.2, 38.7. HRMS (ESI) m/z calculated for C$_{21}$H$_{18}$O$_3$N$_2$NaS [(M+Na)$^+$] 401.0930 found 401.0911.

N-(4-Hydroxy-3-(2-phenylindolizin-3-yl)phenyl)benzene-sulfonamide (3c). White amorphous solid, 90% yield (101 mg). ^{1}H NMR (500 MHz, CDCl$_3$) δ 7.70 (d, J = 8.0 Hz, 2H), 7.47 - 7.58 (m, 1H), 7.33 - 7.45 (m, 4H), 7.18 - 7.31 (m, 5H), 7.14 (dd, J = 8.8, 2.7 Hz, 1H), 6.95 (d, J = 2.3 Hz, 1H), 6.89 (d, J = 8.8 Hz, 1H), 6.67 - 6.78 (m, 2H), 6.40 (t, J = 6.7 Hz, 1H). ^{13}C{^{1}H} NMR (126 MHz, CDCl$_3$) δ 152.8, 138.3, 134.3, 133.9, 132.6, 128.8, 128.8, 128.7, 128.3, 127.5, 127.1, 127.1, 126.8, 126.7, 122.3, 118.7, 118.3, 118.0, 116.9, 112.6, 110.8, 98.8. HRMS (ESI) m/z calculated for C$_{26}$H$_{21}$O$_3$N$_2$S [(M+H)$^+$] 441.1267 found 441.1260.

N-(3-(2-(3-Bromophenyl)indolizin-3-yl)-4-hydroxyphenyl)4-methylbenzenesulfonamide (3d). White amorphous solid, 76% yield (74 mg). ^{1}H NMR (500 MHz, CDCl$_3$) δ 7.58 (m, J = 8.4 Hz, 2H), 7.51 (t, J = 1.5 Hz, 1H), 7.40 - 7.47 (m, 2H), 7.36 (d, J = 8.0 Hz, 1H), 7.20 (m, J = 8.0 Hz, 2H), 7.13 - 7.17 (m, 2H), 7.06 - 7.11 (m, 1H), 6.93 - 6.99 (m, 2H), 6.79 (dd, J = 8.6, 7.1 Hz, 1H), 6.72 (s, 1H), 6.44 - 6.50 (m, 1H), 6.41 (s, 1H), 5.11 (s, 1H), 2.38 (s, 3H). ^{13}C{^{1}H} NMR (126 MHz, CDCl$_3$) δ 153.1, 147.3, 143.8, 136.9, 135.8, 134.2, 130.7, 130.0, 129.8, 129.6, 129.3, 127.6, 127.5, 127.3, 126.1, 122.7, 122.6, 119.1, 118.8, 117.8, 117.2, 113.2, 111.3, 99.1, 21.6. HRMS (ESI) m/z calculated for C$_{27}$H$_{22}$O$_3$N$_2$BrS [(M+H)$^+$] 533.0529 found 533.0527.

N-(4-Hydroxy-3-(2-(3-methoxyphenyl)indolizin-3-yl)phenyl)-4-methylbenzenesulfonamide (3e). White solid, 91% yield (98 mg). ^{1}H NMR (500 MHz, CDCl$_3$) δ 7.52 - 7.62 (m, 2H), 7.38 - 7.45 (m, 2H), 7.10 - 7.19 (m, 4H), 6.96 (d, J = 2.7 Hz, 1H), 6.87 - 6.92 (m, 2H), 6.81 - 6.85 (m,

1H), 6.71 - 6.78 (m, 3H), 6.65 - 6.68 (m, 1H), 6.36 - 6.45 (m, 1H), 5.22 (br. s., 1H), 3.62 (s, 3H), 2.36 (s, 3H). ^{13}C{^{1}H} NMR (126 MHz, CDCl$_3$) δ 159.6, 153.1, 143.8, 135.9, 135.7, 134.1, 129.6, 129.5, 129.3, 128.9, 127.4, 127.3, 127.1, 125.7, 122.5, 120.2, 119.0, 118.6, 118.3, 117.0, 115.9, 113.0, 112.7, 111.0, 99.1, 55.0, 21.5. HRMS (ESI) m/z calculated for C$_{28}$H$_{25}$O$_4$N$_2$S [(M+H)$^+$] 485.1530 found 485.1524.

N-(4-Hydroxy-3-(2-(3-nitrophenyl)indolizin-3-yl)phenyl)-4-methylbenzenesulfonamide (3f). Yellow solid, 86% yield (89 mg). ^{1}H NMR (400 MHz, CDCl$_3$) δ 8.20 (t, *J* = 2.0 Hz, 1H), 8.05 (ddd, *J* = 8.3, 2.3, 1.0 Hz, 1H), 7.54 - 7.61 (m, 3H), 7.43 - 7.50 (m, 2H), 7.37 (t, *J* = 8.0 Hz, 1H), 7.20 (d, *J* = 8.0 Hz, 2H), 7.10 (dd, *J* = 8.8, 2.8 Hz, 1H), 7.03 (d, *J* = 2.5 Hz, 1H), 6.94 (d, *J* = 8.8 Hz, 1H), 6.78 - 6.85 (m, 2H), 6.59 (s, 1H), 6.50 (td, *J* = 6.9, 1.0 Hz, 1H), 2.38 (s, 3H). ^{13}C{^{1}H} NMR (101 MHz, CDCl$_3$) δ 152.6, 148.2, 143.6, 136.4, 135.4, 134.0, 133.0, 129.3, 129.0, 127.2, 127.0, 126.9, 126.2, 122.4, 122.0, 121.1, 118.9, 118.8, 117.2, 116.9, 113.5, 111.3, 98.7, 21.2. HRMS (ESI) m/z calculated for C$_{27}$H$_{22}$O$_5$N$_3$S [(M+H)$^+$] 500.1275 found 500.1268.

N-(4-Hydroxy-3-(2-(4-methoxyphenyl)indolizin-3-yl)phenyl)-4-methylbenzenesulfonamide (3g). White solid, 82% yield (88 mg). ^{1}H NMR (500 MHz, CDCl$_3$) δ 7.5 - 7.6 (m, 2 H), 7.3 - 7.5 (m, 2 H), 7.2 - 7.2 (m, 4 H), 7.1 (dd, *J* = 8.4, 2.7 Hz, 1 H), 7.0 (d, *J* = 2.7 Hz, 1 H), 6.9 (d, *J* = 8.8 Hz, 1 H), 6.8 - 6.8 (m, 2 H), 6.7 - 6.8 (m, 1 H), 6.7 (s, 1 H), 6.3 - 6.5 (m, 2 H), 5.1 (s, 1 H), 3.8 (s, 3 H), 2.4 (s, 3 H). ^{13}C{^{1}H} NMR (101 MHz, CDCl$_3$) δ 158.7, 153.0, 143.7, 135.7, 134.1, 129.6, 129.2, 128.8, 127.4, 127.3, 126.9, 125.7, 122.5, 118.8, 118.4, 118.4, 117.1, 115.9, 114.1, 112.5, 110.7, 98.7, 55.2, 21.5. HRMS (ESI) m/z calculated for C$_{28}$H$_{25}$O$_4$N$_2$S [(M+H)$^+$] 485.1530 found 485.1509.

N-(4-Hydroxy-3-(2-(p-tolyl)indolizin-3-yl)phenyl)-4-methylbenzenesulfonamide (3h). White semisolid, 73% yield (82 mg). ^{1}H NMR (500 MHz, CDCl$_3$) δ 7.60 (m, *J* = 7.6 Hz, 2H), 7.35 -

7.48 (m, 2H), 7.15 - 7.24 (m, 5H), 7.04 - 7.10 (m, 2H), 6.98 (br. s., 1H), 6.92 (d, *J* = 8.4 Hz, 1H), 6.68 - 6.80 (m, 2H), 6.50 (s, 1H), 6.42 (t, *J* = 6.7 Hz, 1H), 5.17 (br. s., 1H), 2.39 (s, 3H), 2.34 (s, 3H). ^{13}C{^{1}H} NMR (126 MHz, CDCl$_3$) δ 153.0, 143.7, 136.7, 135.8, 134.2, 131.6, 129.6, 129.4, 129.2, 129.1, 127.6, 127.4, 127.1, 126.4, 122.5, 118.9, 118.5, 118.4, 117.1, 112.6, 110.9, 99.0, 21.6, 21.2. HRMS (ESI) m/z calculated for C$_{28}$H$_{25}$O$_3$N$_2$S [(M+H)$^+$] 469.1580 found 469.1577.

N-(3-(2-(4-Chlorophenyl)indolizin-3-yl)-4-hydroxyphenyl)-4-methylbenzenesulfonamide

(3i). White semisolid, 85% yield (90 mg). ^{1}H NMR (500 MHz, CDCl$_3$) δ 7.57 (d, *J* = 8.0 Hz, 2H), 7.38 - 7.46 (m, 2H), 7.26 (s, 1H), 7.21 (s, 1H), 7.18 (s, 4H), 7.14 (dd, *J* = 8.8, 2.7 Hz, 1H), 6.89 - 7.01 (m, 2H), 6.73 - 6.81 (m, 1H), 6.69 (s, 1H), 6.54 (s, 1H), 6.37 - 6.49 (m, 1H), 5.15 (s, 1H), 2.39 (s, 3H). ^{13}C{^{1}H} NMR (126 MHz, CDCl$_3$) δ 153.0, 143.9, 135.7, 134.2, 133.2, 132.7, 129.6, 129.4, 128.9, 128.7, 127.9, 127.4, 127.2, 126.9, 122.6, 119.0, 118.8, 118.0, 117.1, 113.0, 111.2, 98.9, 21.6. HRMS (ESI) m/z calculated for C$_{27}$H$_{22}$O$_3$N$_2$SCl [(M+H)$^+$] 489.1034 found 489.1025.

N-(3-(2-(4-Fluorophenyl)indolizin-3-yl)-4-hydroxyphenyl)4-methylbenzenesulfonamide

(3j). White solid, 80% yield (87 mg). ^{1}H NMR (500 MHz, CDCl$_3$) δ 7.58 (d, *J* = 8.0 Hz, 2H), 7.38 - 7.46 (m, 2H), 7.18 - 7.25 (m, 4H), 7.14 (dd, *J* = 8.8, 2.7 Hz, 1H), 6.98 (d, *J* = 2.7 Hz, 1H), 6.89 - 6.96 (m, 3H), 6.77 (dd, *J* = 9.0, 6.7 Hz, 1H), 6.68 (s, 1H), 6.39 - 6.52 (m, 2H), 2.39 (s, 3H). ^{13}C{^{1}H} NMR (101 MHz, CDCl$_3$) δ 163.1, 160.7, 152.9, 148.2, 147.3, 145.5, 143.8, 143.6, 135.7, 134.1, 131.3, 130.7, 129.7, 129.6, 129.5, 129.3, 129.3, 129.2, 128.8, 128.2, 127.4, 127.3, 127.2, 126.9, 126.4, 125.7, 122.6, 118.9, 118.7, 118.0, 117.1, 115.9, 115.6, 115.4, 112.9, 111.1, 98.9, 21.5. ^{19}F NMR (376 MHz, CDCl$_3$) δ -115.41 (s, 1F). HRMS (ESI) m/z calculated for C$_{27}$H$_{22}$O$_3$N$_2$FS [(M+H)$^+$] 473.1330 found 473.1321.

***N*-(3-(2-(4-Cyanophenyl)indolizin-3-yl)-4-hydroxyphenyl)4-methylbenzenesulfonamide**

(3k). White solid, 94% yield (103 mg). ^{1}H NMR (500 MHz, DMSO-d$_6$) δ 9.75 (d, *J* = 9.5 Hz, 2H), 7.66 (d, *J* = 8.4 Hz, 2H), 7.49 - 7.56 (m, 1H), 7.46 (m, *J* = 8.0 Hz, 2H), 7.36 - 7.43 (m, 2H), 7.25 - 7.34 (m, 3H), 7.13 (dd, *J* = 8.8, 2.7 Hz, 1H), 6.96 (d, *J* = 8.8 Hz, 1H), 6.83 - 6.87 (m, 1H), 6.79 (dd, *J* = 8.8, 6.9 Hz, 1H), 6.64 (d, *J* = 2.7 Hz, 1H), 6.51 - 6.59 (m, 1H), 2.34 (s, 3H). ^{13}C{^{1}H} NMR (126 MHz, DMSO-d$_6$) δ 153.9, 142.9, 140.6, 136.4, 132.2, 129.4, 127.9, 126.6, 126.4, 125.6, 125.0, 123.9, 123.1, 119.1, 118.9, 118.4, 118.0, 117.5, 116.8, 115.5, 110.9, 108.2, 98.6, 21.0. HRMS (ESI) m/z calculated for C$_{28}$H$_{22}$O$_3$N$_3$S [(M+H)$^+$] 480.1376 found 480.1371

***N*-(4-Hydroxy-3-(7-methyl-2-phenylindolizin-3-yl)phenyl)-4-methylbenzenesulfonamide**

(3l). White solid, 66% yield (74 mg). ^{1}H NMR (500 MHz, CDCl$_3$) δ 7.60 (d, *J* = 8.0 Hz, 2H), 7.36 (d, *J* = 6.9 Hz, 1H), 7.24 - 7.31 (m, 5H), 7.18 - 7.23 (m, 3H), 7.16 (dd, *J* = 8.8, 2.7 Hz, 1H), 6.98 (d, *J* = 2.7 Hz, 1H), 6.93 (d, *J* = 8.8 Hz, 1H), 6.61 (s, 1H), 6.54 (s, 1H), 6.28 (dd, *J* = 7.2, 1.5 Hz, 1H), 5.20 (br. s., 1H), 2.40 (s, 3H), 2.32 (s, 3H). ^{13}C{^{1}H} NMR (126 MHz, CDCl$_3$) δ 152.8, 143.5, 135.5, 134.5, 134.3, 129.3, 128.9, 128.8, 128.6, 128.3, 127.4, 127.2, 127.1, 126.7, 126.6, 121.8, 118.2, 116.7, 113.5, 111.7, 97.3, 21.3, 20.7. HRMS (ESI) m/z calculated for C$_{28}$H$_{25}$O$_3$N$_2$S [(M+H)$^+$] 469.1580 found 469.1566.

***N*-(4-Hydroxy-3-(7-methyl-2-phenylindolizin-3-yl)phenyl)methanesulfonamide (3m).** White semisolid, 72% yield (67 mg). ^{1}H NMR (500 MHz, CD$_3$CN) δ 7.55 (d, *J* = 7.1 Hz, 1H), 7.47 (s, 1H), 7.39 (d, *J* = 2.7 Hz, 1H), 7.31 - 7.34 (m, 2H), 7.26 (d, *J* = 7.6 Hz, 2H), 7.21 - 7.23 (m, 2H), 7.15 - 7.18 (m, 1H), 7.03 (d, *J* = 8.7 Hz, 1H), 6.92 (d, *J* = 2.7 Hz, 1H), 6.60 (s, 1H), 6.38 (d, *J* = 5.5 Hz, 1H), 2.67 (s, 3H), 2.28 (s, 4H). ^{13}C{^{1}H} NMR (101 MHz, CD$_3$CN) δ 155.1, 137.1, 134.4, 131.0, 130.1, 129.4, 129.3, 129.2, 129.1, 128.7, 127.6, 127.2, 126.4, 124.2, 120.1, 118.0, 117.6,

114.0, 98.4, 38.8, 21.0. HRMS (ESI) m/z calculated for $C_{22}H_{21}O_3N_2S$ [(M+H)$^+$] 393.1267 found 393.1259.

***N*-(4-Hydroxy-3-(8-methyl-2-phenylindolizin-3-yl)phenyl)-4-methylbenzenesulfonamide**

(3n). White semisolid, 71% yield (80 mg). ^{1}H NMR (400 MHz, CD$_3$CN) δ 7.54 - 7.59 (m, 1H), 7.45 - 7.50 (m, 2H), 7.28 - 7.32 (m, 2H), 7.19 - 7.26 (m, 6H), 7.11 (dd, *J* = 8.7, 2.7 Hz, 1H), 6.91 (d, *J* = 8.6 Hz, 1H), 6.75 (s, 1H), 6.71 (d, *J* = 2.6 Hz, 1H), 6.58 (d, *J* = 6.6 Hz, 1H), 6.43 (t, *J* = 6.8 Hz, 1H), 2.44 (s, 3H), 2.32 (s, 3H). ^{13}C{^{1}H} NMR (101 MHz, CD$_3$CN) δ 155.2, 144.9, 137.1, 136.9, 134.9, 130.8, 130.6, 129.4, 129.0, 128.9, 128.9, 128.2, 127.3, 127.0, 122.0, 120.1, 117.9, 117.8, 117.5, 116.9, 111.7, 98.5, 21.6, 18.2. HRMS (ESI) m/z calculated for $C_{28}H_{25}O_3N_2S$ [(M+H)$^+$] 469.1580 found 469.1566.

***N*-(3-(2-(3,4-Dimethoxyphenyl)indolizin-3-yl)-4-hydroxyphenyl)-4-methylbenzenesulfon -**

amide (3o). White solid, 69% yield (69 mg). ^{1}H NMR (500 MHz, CDCl$_3$) δ 7.61 (m, *J* = 8.4 Hz, 2H), 7.39 - 7.46 (m, 2H), 7.22 (m, *J* = 8.0 Hz, 2H), 7.16 (dd, *J* = 8.8, 2.7 Hz, 1H), 7.01 - 7.08 (m, 1H), 6.92 - 6.98 (m, 2H), 6.76 - 6.84 (m, 3H), 6.73 (s, 1H), 6.53 (s, 1H), 6.36 - 6.47 (m, 1H), 5.23 (br. s., 1H), 3.89 (s, 3H), 3.59 (s, 3H), 2.40 (s, 3H). ^{13}C{^{1}H} NMR (126 MHz, CDCl$_3$) δ 153.0, 148.7, 148.0, 143.8, 135.7, 134.1, 129.6, 129.3, 129.2, 128.8, 127.3, 127.2, 127.0, 126.6, 122.4, 119.9, 118.7, 118.5, 116.9, 115.9, 112.5, 111.3, 110.8, 98.5, 55.7, 55.4, 21.5. HRMS (ESI) m/z calculated for $C_{29}H_{27}O_5N_2S$ [(M+H)$^+$] 515.1635 found 515.1619.

***N*-(3-(2-(2,4-Dichlorophenyl)indolizin-3-yl)-4-hydroxyphenyl)-4-methylbenzenesulfonamide**

(3p). White solid, 76% yield (75 mg). ^{1}H NMR (500 MHz, CDCl$_3$) δ 7.49 - 7.58 (m, 3H), 7.46 (d, *J* = 8.8 Hz, 1H), 7.42 (d, *J* = 1.9 Hz, 1H), 7.24 (d, *J* = 8.0 Hz, 2H), 7.09 (dd, *J* = 8.4, 2.3 Hz, 1H), 7.04 (d, *J* = 8.4 Hz, 1H), 6.97 - 7.01 (m, 2H), 6.79 - 6.85 (m, 2H), 6.75 (s, 1H), 6.45 - 6.56 (m, 1H), 5.23 (br. s., 1H), 2.43 (s, 3H). ^{13}C{^{1}H} NMR (126 MHz, CDCl$_3$) δ 152.4, 143.5, 135.5,

133.8, 133.3, 133.2, 132.6, 132.4, 129.3, 128.8, 127.0, 126.8, 126.6, 126.0, 125.7, 122.5, 118.9, 118.3, 117.3, 116.7, 115.0, 111.0, 101.2, 21.3. HRMS (ESI) m/z calculated for $C_{27}H_{21}O_3N_2Cl_2S$ [(M+H)$^+$] 523.0644 found 523.0630.

N-(3-(2-(2-Fluorophenyl)indolizin-3-yl)-4-hydroxyphenyl)4-methylbenzenesulfonamide

(3q). White solid, 70% yield (77 mg). ^{1}H NMR (500 MHz, CDCl$_3$) δ 7.54 (d, *J* = 8.4 Hz, 2H), 7.38 - 7.49 (m, 2H), 7.15 - 7.24 (m, 3H), 7.11 (td, *J* = 7.6, 1.5 Hz, 1H), 7.02 - 7.08 (m, 2H), 6.96 - 7.00 (m, 1H), 6.93 (d, *J* = 2.7 Hz, 1H), 6.87 (d, *J* = 8.8 Hz, 1H), 6.73 - 6.81 (m, 2H), 6.54 (br. s., 1H), 6.39 - 6.49 (m, 1H), 5.19 (br. s., 1H), 2.38 (s, 3H). ^{13}C{^{1}H} NMR (126 MHz, CDCl$_3$) δ 160.8, 158.8, 153.0, 143.7, 135.8, 133.8, 131.0, 131.03, 131.0, 129.7, 129.5, 129.1, 128.8, 128.7, 127.4, 127.3, 126.9, 125.8, 124.0, 123.2, 122.6, 122.5, 119.1, 118.4, 118.1, 116.9, 116.0, 115.9, 115.8, 114.5, 111.1, 101.1, 21.6. ^{19}F NMR (376 MHz, CDCl$_3$) δ -115.13 (s, 1F). HRMS (ESI) m/z calculated for $C_{27}H_{22}O_3N_2FS$ [(M+H)$^+$] 473.1330 found 473.1314.

N-(4-Hydroxy-3-(1-methyl-2-phenylindolizin-3-yl)phenyl)-4-methylbenzenesulfonamide

(3r). White semisolid, 77% yield (87 mg). ^{1}H NMR (400 MHz, CDCl$_3$) δ 7.54 (d, *J* = 8.3 Hz, 2H), 7.42 (d, *J* =7.1 Hz, 1H), 7.36 - 7.39 (m, 1H), 7.23 - 7.28 (m, 3H), 7.13 - 7.21 (m, 4H), 6.94 - 7.02 (m, 2H), 6.78 (d, *J* = 8.5 Hz, 1H), 6.70 (dd, *J* = 8.8, 7.3 Hz, 1H), 6.33 - 6.41 (m, 1H), 2.38 (s, 3H), 2.37 (s, 3H). ^{13}C{^{1}H} NMR (101 MHz, CDCl$_3$) δ 152.8, 148.1, 147.2, 145.5, 143.6, 135.7, 134.2, 131.6, 129.7, 129.5, 128.9, 128.3, 127.3, 126.7, 126.4, 122.3, 118.1, 117.4, 116.9, 116.8, 113.5, 110.7, 106.9, 21.6, 9.4. HRMS (ESI) m/z calculated for $C_{28}H_{25}O_3N_2S$ [(M+H)$^+$] 469.1580 found 469.1576

N-(4-Hydroxy-3-(1-methyl-2-(naphthalen-2-yl)indolizin-3-yl)phenyl)-4-methylbenzenesulfo-namide (3s). White solid, 59% yield (58 mg). ^{1}H NMR (500 MHz, CDCl$_3$) δ 7.79 - 7.86 (m, 1H), 7.68 - 7.77 (m, 3H), 7.42 - 7.55 (m, 6H), 7.18 - 7.30 (m, 2H), 7.03 - 7.11 (m, 3H), 6.97 (dd,

J = 8.8, 2.7 Hz, 1H), 6.70 - 6.81 (m, 2H), 6.42 (t, *J* = 6.7 Hz, 2H), 2.43 (s, 3H), 2.34 (s, 3H). ^{13}C{^{1}H} NMR (126 MHz, CDCl$_3$) δ 152.6, 143.4, 135.6, 133.1, 131.9, 131.6, 129.2, 128.7, 128.6, 128.3, 127.7, 127.6, 127.6, 127.4, 127.3, 127.0, 126.3, 125.8, 125.6, 122.1, 118.0, 117.3, 116.8, 116.6, 113.3, 110.6, 107.0, 21.3, 9.2. HRMS (ESI) m/z calculated for C$_{32}$H$_{26}$O$_3$N$_2$NaS [(M+Na)$^+$] 541.1556 found 541.1538.

N-(4-Hydroxy-3-(2-(thiophen-2-yl)indolizin-3-yl)phenyl)methanesulfonamide   (3t).   White solid, 95% yield (91 mg). ^{1}H NMR (500 MHz, CDCl$_3$) δ 7.55 (d, *J* = 6.9 Hz, 1H), 7.38 (d, *J* = 8.8 Hz, 1H), 7.33 (dd, *J* = 8.8, 2.7 Hz, 1H), 7.19 (d, *J* = 2.7 Hz, 1H), 7.11 - 7.15 (m, 1H), 7.07 (d, *J* = 8.4 Hz, 1H), 6.96 - 7.00 (m, 1H), 6.92 (dd, *J* = 5.0, 3.8 Hz, 1H), 6.67 - 6.84 (m, 2H), 6.55 (br. s., 1H), 6.43 - 6.51 (m, 1H), 5.33 (br. s., 1H), 2.93 (s, 3H). ^{13}C{^{1}H} NMR (126 MHz, CDCl$_3$) δ 153.7, 137.0, 134.1, 129.5, 127.4, 126.7, 124.6, 124.2, 123.2, 122.8, 118.9, 118.8, 118.1, 117.5, 112.7, 111.3, 98.5, 39.0. HRMS (ESI) m/z calculated for C$_{19}$H$_{16}$O$_3$N$_2$NaS$_2$ [(M+H)$^+$] 407.0495 found 407.0479.

N-(4-Hydroxy-3-(2-(thiophen-2-yl)indolizin-3-yl)phenyl)-4-methylbenzenesulfonamide (3u). White solid, 89% yield (102 mg). ^{1}H NMR (500 MHz, CDCl$_3$) δ 7.59 (m, *J* = 8.0 Hz, 2H), 7.31 - 7.38 (m, 2H), 7.22 (dd, J = 8.8, 2.7 Hz, 1H), 7.17 (m, *J* = 8.4 Hz, 2H), 7.13 (dd, *J* = 5.0, 1.1 Hz, 1H), 6.97 (d, *J* = 8.8 Hz, 1H), 6.89 - 6.94 (m, 2H), 6.87 (dd, *J* = 3.6, 1.0 Hz, 1H), 6.70 - 6.77 (m, 2H), 6.62 (s, 1H), 6.35 - 6.48 (m, 1H), 5.21 (s, 1H), 2.35 (s, 3H). ^{13}C{^{1}H} NMR (126 MHz, CDCl$_3$) δ 153.4, 143.5, 136.7, 135.4, 133.8, 129.3, 129.2, 127.5, 127.4, 127.2, 124.2, 123.7, 122.8, 122.3, 118.6, 118.5, 117.3, 116.9, 112.0, 110.8, 98.1, 21.3. HRMS (ESI) m/z calculated for C$_{25}$H$_{21}$O$_3$N$_2$S$_2$ [(M+H)$^+$] 461.0988 found 461.0971.

N-(4-Hydroxy-3-(2-phenylindolizin-3-yl)-5-(phenylthio)phenyl)-4-methylbenzene

sulfonamide (3v). White semisolid, 65% yield (92 mg). ^{1}H NMR (500 MHz, CDCl$_3$) δ 7.54 (d, *J*

= 7.6 Hz, 2H), 7.39 - 7.46 (m, 2H), 7.23 - 7.35 (m, 10H), 7.12 - 7.20 (m, 3H), 7.06 - 7.12 (m, 2H), 6.98 - 7.04 (m, 1H), 6.81 - 6.88 (m, 1H), 6.70 - 6.80 (m, 1H), 6.44 (t, J = 6.5 Hz, 1H), 2.39 (s, 3H). $^{13}C\{^1H\}$ NMR (126 MHz, CDCl$_3$) δ 153.2, 143.5, 135.5, 135.2, 134.3, 130.7, 129.3, 129.2, 129.0, 128.3, 128.2, 128.1, 127.9, 127.7, 127.2, 127.1, 126.6, 126.2, 125.2, 122.6, 121.6, 120.1, 119.1, 118.7, 117.7, 114.7, 110.4, 98.9, 21.3. HRMS (ESI) m/z calculated for C$_{33}$H$_{27}$O$_3$N$_2$S$_2$ [(M+H)$^+$] 563.1458 found 563.1446.

N-(3-Bromo-4-hydroxy-5-(2-phenylindolizin-3-yl)phenyl)-benzenesulfonamide (3w). White semisolid, 58% yield (76 mg). ^1H NMR (500 MHz, CDCl$_3$) δ 7.69 - 7.77 (m, 2H), 7.48 - 7.55 (m, 2H), 7.36 - 7.44 (m, 4H), 7.33 (d, J = 7.6 Hz, 1H), 7.10 - 7.17 (m, 2H), 7.03 - 7.08 (m, 1H), 6.89 - 6.99 (m, 2H), 6.71 - 6.79 (m, 2H), 6.68 (s, 1H), 6.43 (t, J = 6.7 Hz, 1H). $^{13}C\{^1H\}$ NMR (126 MHz, CDCl$_3$) δ 153.1, 138.6, 136.9, 134.1, 132.9, 130.6, 130.0, 129.8, 129.1, 129.0, 128.4, 127.5, 127.3, 126.1, 123.3, 122.6, 119.1, 118.8, 117.9, 117.2, 113.2, 111.3, 99.1. HRMS (ESI) m/z calculated for C$_{26}$H$_{20}$O$_3$N$_2$BrS [(M+H)$^+$] 519.0373 found 519.0358.

Experimental procedure for the synthesis of 6

To a 25 mL oven dried round-bottom flask quinone monoimine **5** (0.197 mmol, 80 mg) indolizine **1n** (0.197 mmol, 45 mg), and AcOH (0.039 mmol) was taken in DCM (3 ml). Then the resulting reaction mixture was stirred at room temperature for 5 min. Upon completion of the reaction (monitored by TLC), the reaction mixture was dried under vacuum. Then the crude reaction mixture was diluted with ethyl acetate (5 mL) and washed with brine and eluted with EtOAc (5 mL x 3). The organic layer was evaporated and the crude residue was preadsorbed on silica gel and purified by column chromatography (100-200 mesh silica Using 80/20 to 80/50 petroleum ether/ethyl acetate as the eluent to afford the corresponding product **6a** in 69% yield (91 mg).

***N*-(4-Hydroxy-3-(2-hydroxynaphthalen-1-yl)-5-(8-methyl-2-phenylindolizin-3-yl)phenyl)-4-methylbenzenesulfonamide (6a).** White gummy semisolid, 69% yield (91 mg). ^{1}H NMR (500 MHz, CDCl$_3$) δ 8.13 (d, J = 6.9 Hz, 1H), 8.10 (d, J = 6.9 Hz, 1H), 7.84 - 7.89 (m, 2H), 7.79 - 7.84 (m, 2H), 7.50 (d, J = 8.0 Hz, 2H), 7.46 (m, J = 8.4 Hz, 2H), 7.37 - 7.41 (m, 4H), 7.30 - 7.36 (m, 5H), 7.21 - 7.26 (m, 5H), 7.14 - 7.21 (m, 5H), 7.05 - 7.13 (m, 5H), 7.02 (m, J = 8.0 Hz, 2H), 6.97 (d, J = 9.2 Hz, 4H), 6.61 - 6.66 (m, 2H), 6.53 - 6.61 (m, 4H), 2.45 (s, 3H), 2.43 (s, 3H), 2.33 (s, 3H), 2.30 (s, 3H). ^{13}C{^{1}H} NMR (101 MHz, CDCl$_3$) δ 152.5, 152.4, 151.8, 151.8, 144.1, 144.0, 137.5, 136.3, 135.7, 135.4, 134.6, 134.5, 132.8, 132.6, 132.3, 132.2, 131.0, 130.4, 130.2, 129.3, 129.3, 129.1, 129.1, 129.1, 128.4, 128.4, 128.3, 128.3, 128.1, 128.1, 128.0, 127.8, 127.5, 127.4, 127.4, 127.4, 127.3, 127.2, 127.1, 126.8, 126.7, 126.3, 126.2, 126.0, 123.9, 123.9, 120.4, 120.3, 119.9, 119.9, 118.4, 118.4, 118.0, 117.9, 117.3, 117.3, 115.9, 115.8, 113.3, 113.2, 111.5, 111.5, 97.3, 97.3, 21.5, 21.5, 17.6, 17.6. HRMS (ESI) m/z calculated for C$_{38}$H$_{31}$O$_4$N$_2$S [(M+H)$^+$] 611.1999 found 611.1984.

***N*-(4-Hydroxy-3-(2-hydroxynaphthalen-1-yl)-5-(7-methyl-2-phenylindolizin-1-yl)phenyl)-4-methylbenzenesulfonamide (6b).** White gummy semisolid, 60% yield (45 mg). ^{1}H NMR (500 MHz, CDCl$_3$) δ 8.22 (s, 1H), 8.14 (dd, J = 14.8, 7.2 Hz, 1H), 7.82 - 7.87 (m, 2H), 7.77 - 7.81 (m, 2H), 7.74 (dd, J = 9.0, 5.3 Hz, 1H), 7.60 - 7.67 (m, 1H), 7.55 (dd, J = 8.1, 4.1 Hz, 1H), 7.47 (d, J = 8.5 Hz, 1H), 7.43 (d, J = 8.2 Hz, 1H), 7.33 - 7.39 (m, 7H), 7.27 - 7.32 (m, 7H), 7.19 - 7.26 (m, 4H), 7.13 - 7.18 (m, 5H), 7.08 - 7.12 (m, 1H), 7.03 - 7.07 (m, 1H), 6.99 (d, J = 7.9 Hz, 3H), 6.86 - 6.96 (m, 3H), 6.62 - 6.66 (m, 1H), 6.58 (d, J = 11.9 Hz, 1H), 6.43 - 6.50 (m, 2H), 6.38 - 6.42 (m, 1H), 6.26 (d, J = 2.7 Hz, 1H), 2.43 (s, 3H), 2.31 (s, 3H), 2.27 - 2.30 (m, 6H). ^{13}C{^{1}H} NMR (126 MHz, CDCl$_3$) δ 151.8, 151.5, 147.8, 142.4, 141.6, 139.7, 136.2, 134.5, 132.8, 132.2, 131.5, 131.0, 130.8, 130.7, 129.7, 129.4, 129.2, 129.1, 129.0, 128.7, 128.6, 128.3, 128.1, 128.0,

127.9, 127.8, 127.6, 127.4, 127.3, 127.3, 127.1, 127.0, 126.7, 126.6, 126.3, 126.1, 125.8, 125.0, 124.2, 124.1, 123.9, 123.9, 123.8, 123.5, 122.0, 121.9, 121.5, 120.1, 118.0, 117.9, 117.7, 117.4, 117.3, 117.1, 116.6, 116.5, 115.7, 114.1, 106.3, 97.2, 29.7, 29.3, 21.4, 21.0. HRMS (ESI) m/z calculated for $C_{38}H_{31}O_4N_2S$ [(M+H)$^+$] 611.1999 found 611.1990.

N-(3-(2-(4-Fluorophenyl)indolizin-1-yl)-4-hydroxy-5-(2-hydroxynaphthalen-1-yl)phenyl)-4-methylbenzenesulfonamide (6c). Off white solid, 57% yield (52 mg). ^{1}H NMR (500 MHz, CDCl$_3$) δ 8.21 (d, *J* = 6.9 Hz, 1H), 8.17 (d, *J* = 6.9 Hz, 1H), 7.85 - 7.88 (m, 2H), 7.78 - 7.84 (m, 2H), 7.64 (d, *J* = 8.0 Hz, 1H), 7.50 (d, *J* = 8.4 Hz, 2H), 7.46 (m, *J* = 8.0 Hz, 2H), 7.33 - 7.42 (m, 7H), 7.30 - 7.33 (m, 2H), 7.18 - 7.25 (m, 4H), 7.13 - 7.16 (m, 2H), 7.08 - 7.11 (m, 1H), 7.05 (m, *J* = 8.0 Hz, 2H), 6.96 - 7.03 (m, 6H), 6.85 - 6.92 (m, 2H), 6.80 - 6.85 (m, 2H), 6.75 - 6.79 (m, 2H), 6.57 - 6.67 (m, 2H), 6.52 (d, *J* = 4.2 Hz, 2H), 6.40 - 6.49 (m, 1H), 2.35 (s, 3H), 2.32 (s, 3H). ^{13}C{^{1}H} NMR (126 MHz, CDCl$_3$) δ 162.9, 162.7, 160.9, 160.7, 152.4, 152.4, 151.5, 151.2, 147.7, 147.6, 144.0, 143.8, 142.5, 141.0, 139.1, 138.6, 138.2, 136.0, 135.2, 134.9, 132.5, 132.3, 132.2, 130.8, 130.5, 130.3, 129.8, 129.7, 129.5, 129.4, 129.1, 128.8, 128.1, 128.0, 127.7, 127.5, 127.3, 127.1, 126.9, 126.1, 125.9, 125.6, 125.3, 123.7, 123.6, 123.5, 123.3, 122.1, 122.0, 121.6, 120.7, 120.5, 120.3, 120.0, 119.0, 118.7, 117.8, 117.7, 117.4, 117.2, 117.1, 116.4, 116.2, 116.2, 115.6, 115.4, 114.8, 114.8, 114.6, 114.4, 113.1, 112.9, 111.2, 110.8, 106.7, 102.8, 98.4, 21.3, 21.2. ^{19}F NMR (376 MHz, CDCl$_3$) δ -113.77 (s, 1F), -114.58 (s, 1F), -115.56 (s, 1F). HRMS (ESI) m/z calculated for $C_{37}H_{28}O_4N_2FS$ [(M+H)$^+$] 615.1748 found 615.1734.

N-(3-(2-(4-Cyanophenyl)indolizin-1-yl)-4-hydroxy-5-(2-hydroxynaphthalen-1-yl)phenyl) -benzenesulfonamide (6d). Off white gummy semisolid, 65% yield (40 mg). ^{1}H NMR (500 MHz, CDCl$_3$) δ 8.13 (dd, *J* = 6.5, 4.6 Hz, 1H), 7.81 - 7.85 (m, 2H), 7.77 - 7.80 (m, 2H), 7.65 - 7.75 (m, 3H), 7.56 - 7.63 (m, 4H), 7.44 - 7.50 (m, 6H), 7.36 - 7.41 (m, 6H), 7.29 - 7.34 (m, 4H),

7.22 - 7.26 (m, 6H), 7.12 - 7.20 (m, 4H), 7.08 - 7.11 (m, 1H), 7.02 - 7.07 (m, 1H), 6.97 (d, *J* = 9.5 Hz, 2H), 6.87 - 6.92 (m, 1H), 6.81 - 6.87 (m, 2H), 6.74 - 6.81 (m, 1H), 6.66 - 6.73 (m, 1H), 6.54 - 6.65 (m, 3H), 6.34 - 6.47 (m, 1H). $^{13}C\{^1H\}$ NMR (101 MHz, CDCl$_3$) δ 152.5, 152.4, 151.2, 151.0, 147.7, 138.9, 138.9, 138.8, 138.8, 134.5, 134.3, 133.1, 132.5, 132.3, 131.9, 131.8, 131.6, 131.6, 131.2, 131.0, 130.7, 130.7, 128.7, 128.7, 128.6, 128.6, 128.4, 128.3, 128.1, 128.0, 127.7, 127.4, 127.4, 126.9, 126.9, 126.9, 126.8, 125.7, 125.3, 125.3, 125.2, 123.6, 123.6, 123.5, 123.5, 123.3, 121.9, 121.9, 120.6, 120.5, 119.4, 118.9, 118.4, 118.3, 117.6, 117.6, 117.4, 117.2, 117.2, 115.4, 115.4, 113.2, 113.2, 111.8, 109.7, 109.7, 98.4. HRMS (ESI) m/z calculated for C$_{37}$H$_{26}$O$_4$N$_3$S [(M+H)$^+$] 608.1639 found 608.1629.

N-(4-Hydroxy-3-(2-hydroxynaphthalen-1-yl)-5-(1-methyl-2-(naphthalen-2-yl)indolizin-3-yl)phenyl)-4-methylbenzenesulfonamide (6e). Gummy semisolid, 74% yield (57 mg). ^{1}H NMR (400 MHz, CDCl$_3$) δ 8.12 (d, *J* = 6.9 Hz, 2H), 7.78 - 7.88 (m, 4H), 7.44 (d, *J* = 8.3 Hz, 3H), 7.49 (d, *J* = 8.1 Hz, 2H), 7.30 - 7.40 (m, 11H), 7.20 - 7.25 (m, 5H), 7.14 - 7.20 (m, 5H), 7.04 - 7.14 (m, 7H), 6.93 - 7.04 (m, 7H), 6.57 - 6.66 (m, 3H), 6.50 - 6.57 (m, 3H), 2.44 (s, 3H), 2.42 (s, 3H), 2.31 (s, 3H), 2.29 (s, 3H). $^{13}C\{^1H\}$ NMR (126 MHz, CDCl$_3$) δ 152.8, 151.5, 151.4, 151.2, 147.5, 143.5, 139.0, 138.6, 137.2, 136.0, 136.0, 135.2, 135.0, 133.1, 132.8, 132.6, 132.5, 132.4, 132.1, 131.9, 131.3, 131.2, 130.7, 130.4, 130.0, 129.6, 128.9, 128.9, 128.7, 128.5, 128.1, 128.0, 127.9, 127.8, 127.7, 127.5, 127.4, 127.2, 127.2, 127.1, 127.0, 126.9, 126.0, 125.9, 125.6, 125.5, 125.4, 123.8, 123.7, 123.6, 123.5, 121.9, 121.8, 121.7, 121.2, 119.9, 119.8, 119.3, 117.7, 117.6, 117.6, 117.4, 117.4, 117.1, 116.9, 116.8, 116.5, 116.4, 115.5, 113.9, 113.1, 113.0, 112.6, 110.9, 106.4, 106.3, 94.1, 21.3, 21.0, 9.6, 9.1. HRMS (ESI) m/z calculated for C$_{42}$H$_{33}$O$_4$N$_2$S [(M+H)$^+$] 661.2156 found 661.2154.

N-(4-Hydroxy-3-(2-hydroxynaphthalen-1-yl)-5-(2-phenylindolizin-3-yl)phenyl)-4-

methylbenzene sulfonamide (6f). Off white semisolid, 55% yield (49 mg). ^{1}H NMR (500 MHz,

CDCl$_3$) δ 8.26 (d, *J* = 7.1 Hz, 1H), 8.23 (d, *J* = 6.9 Hz, 1H), 8.05 (t, *J* = 1.8 Hz, 1H), 8.02 (t, *J* =

1.8 Hz, 1H), 7.93 (dd, *J* = 8.1, 1.5 Hz, 1H), 7.90 (dd, *J* = 8.2, 1.6 Hz, 1H), 7.80 - 7.85 (m, 4H),

7.74 - 7.79 (m, 2H), 7.72 (d, *J* = 8.0 Hz, 2H), 7.45 (dd, *J* = 8.2, 5.7 Hz, 5H), 7.40 - 7.42 (m, 2H),

7.36 - 7.39 (m, 2H), 7.33 - 7.36 (m, 4H), 7.28 - 7.32 (m, 2H), 7.24 - 7.26 (m, 4H), 7.18 - 7.23 (m,

2H), 7.07 - 7.15 (m, 1H), 7.03 - 7.05 (m, 1H), 7.02 (s, 1H), 6.90 - 6.97 (m, 4H), 6.88 (s, 1H),

6.82 - 6.86 (m, 1H), 6.64 - 6.69 (m, 2H), 6.63 (s, 2H), 5.22 (br. s., 1H), 2.25 (s, 6H). [13]C{[1]H}

NMR (126 MHz, CDCl$_3$) δ 152.5, 151.7, 151.6, 148.0, 147.4, 144.4, 137.4, 136.0, 135.9, 135.2,

135.1, 133.9, 133.9, 132.8, 132.7, 131.9, 131.0, 130.2, 129.3, 129.1, 128.9, 128.9, 128.6, 128.3,

128.3, 127.7, 127.4, 127.3, 126.3, 126.1, 125.2, 124.9, 124.8, 124.7, 124.6, 124.2, 123.9, 123.8,

122.7, 122.6, 122.4, 122.1, 121.2, 120.8, 120.7, 119.9, 119.1, 118.7, 118.0, 118.0, 117.8, 117.7,

117.6, 117.5, 116.4, 116.1, 115.6, 115.5, 114.0, 113.5, 113.5, 112.0, 98.4, 98.3, 21.3, 21.3.

Experimental procedure for the synthesis of 8

To a 25 mL oven dried round-bottom flask quinone monoimine **7** (0.108 mmol, 50 mg)

indolizine **1u** (0.108 mmol, 22 mg), and AcOH (0.021 mmol) was taken in DCM (3 ml). Then

the resulting reaction mixture was stirred to room temperature for 5 min. Upon completion of the

reaction (monitored by TLC), the reaction mixture was dried under vacuum and purified by

column chromatography (100-200 mesh silica Using 80/10 to 80/20 petroleum ether/ethyl

acetate as the eluent to afford the corresponding product **8** in 67% yield (48 mg).

N-(4-Hydroxy-3,5-bis(2-(thiophen-2-yl)indolizin-3-yl)phenyl)-4-methylbenzenesulfonamide

(8). White semisolid, 67% yield (48 mg). ^{1}H NMR (500 MHz, CDCl$_3$) δ 7.62 (d, *J* = 8.4 Hz,

2H), 7.48 - 7.52 (m, 1H), 7.37 - 7.40 (m, 2H), 7.32 - 7.36 (m, 1H), 7.23 (s, 2H), 7.20 (dt, *J* = 4.4,

2.4 Hz, 3H), 7.10 - 7.13 (m, 1H), 6.99 - 7.03 (m, 3H), 6.92 - 6.94 (m, 1H), 6.88 - 6.91 (m, 1H), 6.74 - 6.81 (m, 2H), 6.70 - 6.73 (m, 2H), 6.43 - 6.49 (m, 2H), 6.39 - 6.42 (m, 1H), 5.37 (s, 1H), 2.38 (s, 3H). ^{13}C{^{1}H} NMR (101 MHz, CDCl$_3$) δ 152.6, 152.4, 143.8, 137.5, 137.2, 135.8, 135.7, 133.8, 129.9, 129.7, 129.7, 129.6, 129.3, 129.2, 127.8, 127.6, 127.5, 127.3, 125.0, 124.4, 124.3, 124.2, 123.0, 122.9, 122.8, 122.7, 122.6, 119.4, 119.3, 119.2, 118.9, 118.8, 118.5, 118.4, 113.9, 113.7, 111.4, 110.9, 110.8, 98.7, 98.7, 21.6. HRMS (ESI) m/z calculated for C$_{37}$H$_{28}$O$_3$N$_3$S$_3$ [(M+H)$^+$] 658.1287 found 658.1271.

Experimental procedure for the synthesis of 3a from *N*-tosyl-*p*-aminophenol

To a 50 mL round-bottom flask N-tosyl-p-aminophenol **9** (0.380 mmol, 100 mg) indolizine **1a** (0.380 mmol, 74 mg), and PIDA (0.418 mmol, 135 mg) was taken in DCM (10 ml). Then the resulting reaction mixture was stirred at room temperature for 1h. Upon completion of the reaction (monitored by TLC), the reaction mixture was dried under vacuum. Then the crude reaction mixture was diluted with ethyl acetate (10 mL) and washed with brine eluted with EtOAc (10 mL x 3). The organic layer was evaporated and the crude residue was preadsorbed on silica gel and purified by column chromatography (100-200 mesh silica Using 80/30 petroleum ether/ethyl acetate as the eluent to afford the corresponding product **3a** in 61% yield (105 mg).

Scale-up experiment

Reaction with **1u** (3.065 mmol, 610 mg), **2a** (3.065 mmol, 800 mg) and AcOH (0.6 mL) in MeCN stirred at rt for 10 min and reaction mixture dried under vacuum. Then the crude reaction mixture was diluted with ethyl acetate (30 mL) and washed with brine eluted with EtOAc (25 mL x 3). Then the crude residue was purified by column chromatography (100-200 mesh silica Using 80/30 petroleum ether/ethyl acetate as the eluent to produce **3u** in 90% yield (1.27 gm).

Section II

Visible Light Promoted, Photocatalyst Free C(sp²)-H Bond Functionalization of Indolizines *via* EDA Complexes

3.2.1 Introduction

In the past decade, visible-light photocatalysis has become a hot area in synthetic organic chemistry for initiating various organic transformations under environmentally friendly and very mild reaction conditions. However, photoredox catalysis suffered from costly exogenous photosensitizers and complex organic dyes used in electron transfer (ET) processes.[18] In recent, with the increasing demand for greener chemical processes, photo-driven organic transformations without external photocatalysts have gained significant attention due to their excellent synthetic value and high atom economy. The development of new organic transformations triggered by the photoexcitation of electron donor-acceptor (EDA) complexes is a field in its golden age.[19]
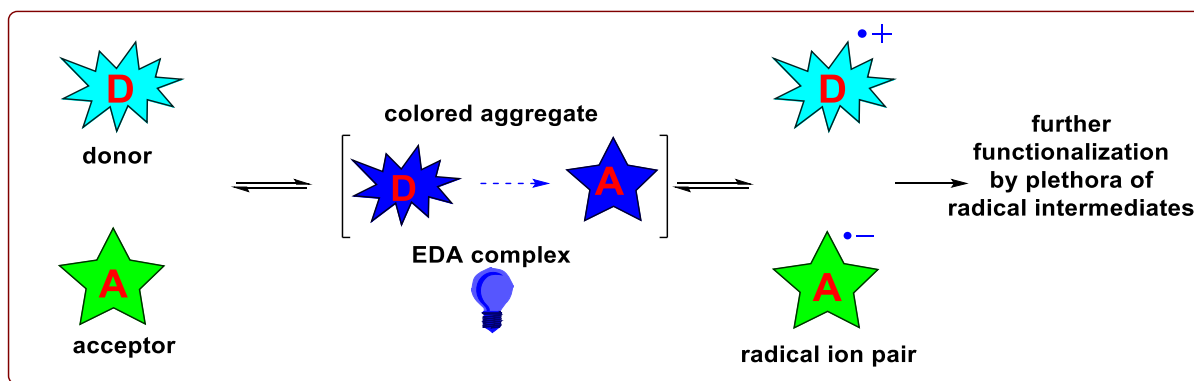
Figure 11: EDA complex driven photoionization

In recent years, the construction of important organic products by photoactivation using electron donor-acceptor (EDA) complexes turn up as an efficient and straightforward pathway.[20] Generally, typical EDA complexes are a novel class of molecular cluster having the combination

of electron rich donor molecule and electron poor acceptor substrate which generally are called the charge-transfer (CT) complexes.[21] While the electron acceptor molecule (A) and donor (D) may be colorless on their own whereas, after charge transfer, interlinkage between D and A results in a bathochromic shift to produce a visible light which absorbing colored aggregate upon excitation under visible light, gives reactive intermediates (charged radical ions) without the assistance of external photocatalyst *via* single electron transfer (SET) mechanism. (**Figure 11**).[22]
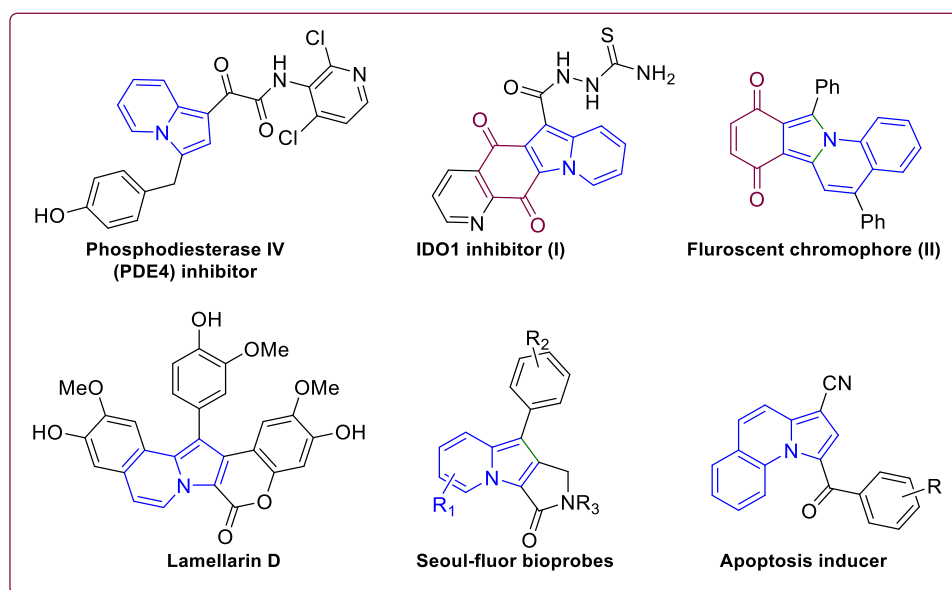
Figure 12: Some bioactive indolizine and quinones[25]

Indolizine and quinones are two privileged structures widely common in numerous bioactive natural products, pharmaceuticals, agrochemicals, approved commercial drugs, and functional organic materials.[23] The reduced form of indolizine derivative is a well-known core nucleus in many alkaloids[24] in natural product chemistry. Indolizines are a biostere for indole, widely present in many biologically active molecules. They can apply in important fluorescent sensors and fluorescent materials in materials chemistry (**Figure 12**),[25] thus justifying current efforts towards C-H functionalization of indolizines to synthesize this core.

3.2.2 Review of Literature

In the past few years, chemists have spent a great deal of time for synthesizing C-H functionalized indolizines.[26] Direct C-H functionalization of indolizines at C-3 position has provided an ideal and dynamic method to grant the useful indolizine derivatives. Transition metals are commonly employed in catalyzing borylation,[27] arylation,[28] acyloxylation[29], and propargylation[30] reactions. Even though these few metal free approaches are available in the literature for C-H functionalization of indolizines such as electrochemical sulfonylation,[31] alkylation,[32] and C-H dithiocarbamation[33] reactions. More recently, visible light-induced operations on indolizines have arisen as a new functionalization strategy.[34] Nevertheless, examples of visible light-mediated $C(sp^2)$-H bond activation reactions by using indolizine as a donor are still unknown in the literature.

Lenardao,s Work (2020)[35]
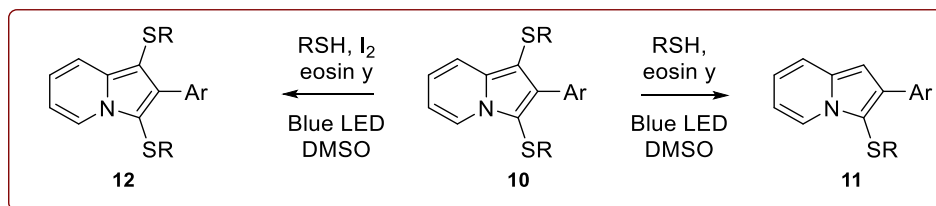
Scheme 8: C-H thiolation of indolizines

Recently in 2020, Lenardao and a co-worker reported the visible light-mediated mono and dithiolation of indolizines by using eosin y as a photocatalyst (**Scheme 8**). The advantages of this method is that controlled thiolation and dithiolation under very mild reaction conditions.

Cao's Work (2018)[36]

Also, Cao *et.al;* developed the cross dehydrogenative coupling (CDC) between oxoaldehyde and indolizine (**Scheme 9**) catalyzed by visible light under mild reaction conditions. This CDC

methodology is utilized for the synthesis of indolizine dicaronyls in good to excellent yield and
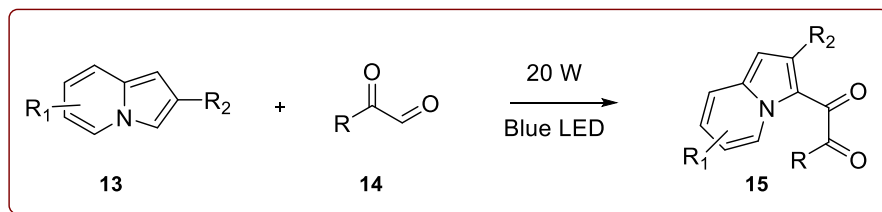
Scheme 9. CDC coupling of indolizine with oxoaldehyde

further useful application in the synthetic organic chemistry. Also avoiding of costly metal, photocatalyst and oxidants makes this approach very useful.

Hosoya's Approach (2021)[40]
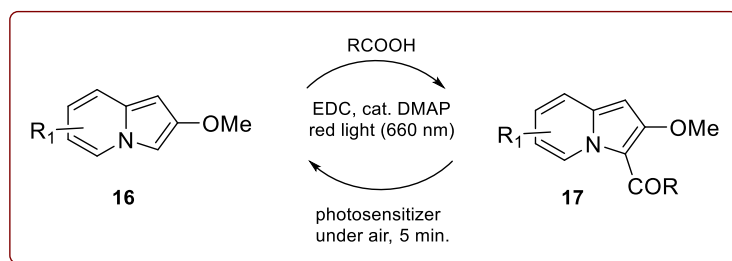
Scheme 10. Direct C-3 acylation of indolizines

Furthermore, Hosoya and co-workers have developed the direct 3-acylation of indolizines from carboxylic acids in good to excellent yields (**Scheme 10**). Previousely the condensation reagents are required for the peptide synthesis but in this method Hosoya group reported for the acylation reaction. Also the acyl group is released by using red light irridation and it is confirmed by neutral buffered solution. This method is further utilized for the water soluble photoreactive precursor with conjugated with photosensitizers and it was effectively release the carboxylic acid under red light.

3.2.3 Present Work

3.2.3.1 Objectives

Our continues research towards the C-H functionalization of indolizines by using various bronsted acid as well as metal free, visible light mediated reactions we have first time showed the indolizine as a donar moiety in present work (**Scheme 10**). Inspired by the previous literature reports and our continuous efforts towards visible-light-induced C-H functionalization of heteroarenes,[37] herein we have described the photo-driven cross dehydrogenative coupling reaction between indolizines with quinones *via* EDA complexes as shown in (**Scheme 11**).
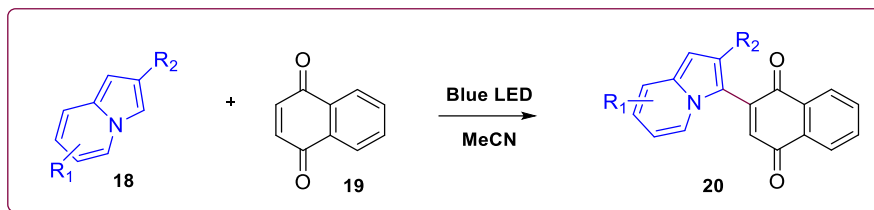
Scheme 11. CDC reaction between quinone and indolizines

3.2.4 Results and Discussion

To supplementary prospect, the formation of electron donor-acceptor complexes from **1** and **2**, we investigated the UV-vis absorption spectroscopic properties of 0.05 M solutions **1** and **2** and the mixture of **1** and **2** in acetonitrile, respectively (**Figure 13A**). A blue color appeared when yellow colored **1** was mixed with colorless **2**, a new band appeared, which could be attributed to the generation of charge-transfer (CT) band (**Figure 13B**). Sunden and co-workers reported that the visible light promoted annulation reaction between N,N-substituted dialkyl anilines, and alkenes to synthesize substituted tetrahydroquinolines *via* EDA complexes.[38]
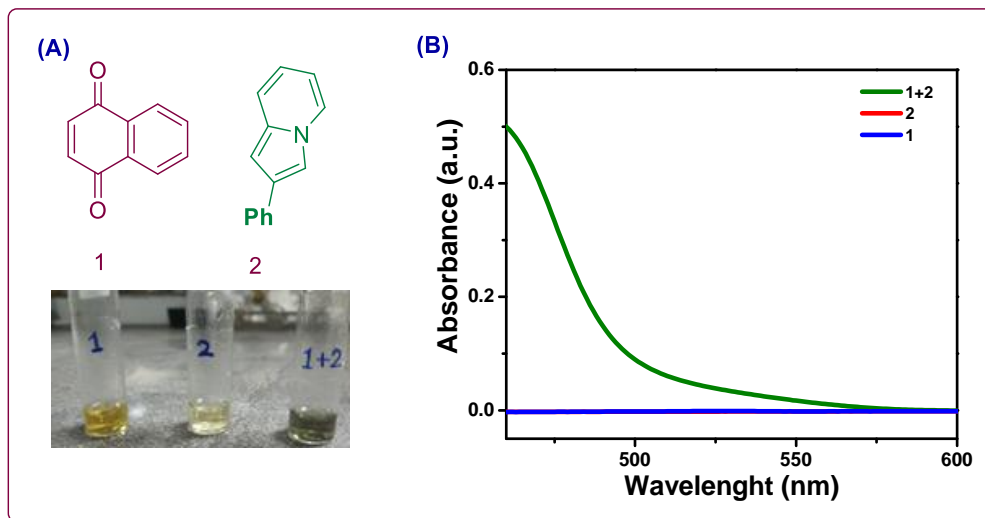
Figure 13. (A) Photos of 1, 2, and 1 + 2 in CH$_3$CN (0.05 M) (B) the charge transfer band of (1 + 2) EDA complex

Accordingly, we began our investigation by taking naphthoquinone **19**, and indolizine **18a** as a model substrate in DCM under irradiation with Blue led the desired product **20a** was formed in 35% yield (Table 4, entry 1). To our delight, the desired product **20a** was isolated in 61% yield along with difunctionalized byproduct **20a'** in 6% yield, when MeCN is used as a solvent instead of DCM (Table 4, entry 2). An examination of other routine solvents, such as dichloroethane (DCE), 1,4-dioxane, tetrahydrofuran (THF), and dimethyl sulfoxide (DMSO), and the experimental results showed that DCE displayed a higher efficiency compared with other solvents (Table 4, entries 3-6). When the reaction was carried out with 2 equiv. of naphthoquinone, the desired product **20a** was isolated in 64% yield and slightly increment of **20a'** (13% yield) in 8 hours of reaction time (Table 4, entry 7). The yield of **20a** and **20a'** was dramatically reduced to 21% and 0%, respectively, when the reaction time was increased to 16 hours (Table 4, entry 8). Surprisingly when reaction duration was reduced from 8 to 4 h, then the product **20a** was observed in 67% yield (Table 4, entry 9).

Table 4. Reaction Optimization
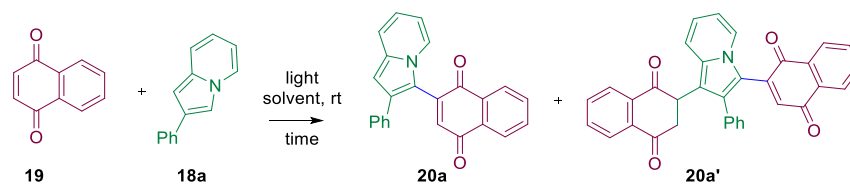
entry	solvent	light source	Time (hrs)	Yield of 20a (%)	Yield of 20a' (%)
1	DCM	Blue LED	8	35	0
2	MeCN	Blue LED	8	61	6
3	DCE	Blue LED	8	27	0
4	1,4-Dioxane	Blue LED	8	trace	0
5	THF	Blue LED	8	0	0
6	DMSO	Blue LED	8	trace	0
7[b]	MeCN	Blue LED	8	64	13
8[c]	MeCN	Blue LED	16	21	0
9	**MeCN**	**Blue LED**	**4**	**67**	**8**
10[d]	MeCN	-	6	trace	0
11	MeCN	dark	6	trace	0
12	MeCN	White LED	4	51	0
13[e]	MeCN	Blue LED	4	42	0

[a]Reaction condition:1a (0.14 mmol), 2a (0.14 mmol) in 2 mL of solvent irradiated with homemade setup of light in room temperature (Blue LED 12 W); [b,c] Reaction was carried out by using 0.28 mmol of 1a; [d] in the absence of light; [e]Under N_2 atmosphere

From entries 8 and 9, it can conclude that reaction time plays a crucial role in the formation of desired product; as the reaction is stirred for a longer time, the decomposition of products may occur. The absence of light suppressed the formation of product **20a**, confirming the requirement

Table 5: Substrate Scope for CDC Reaction
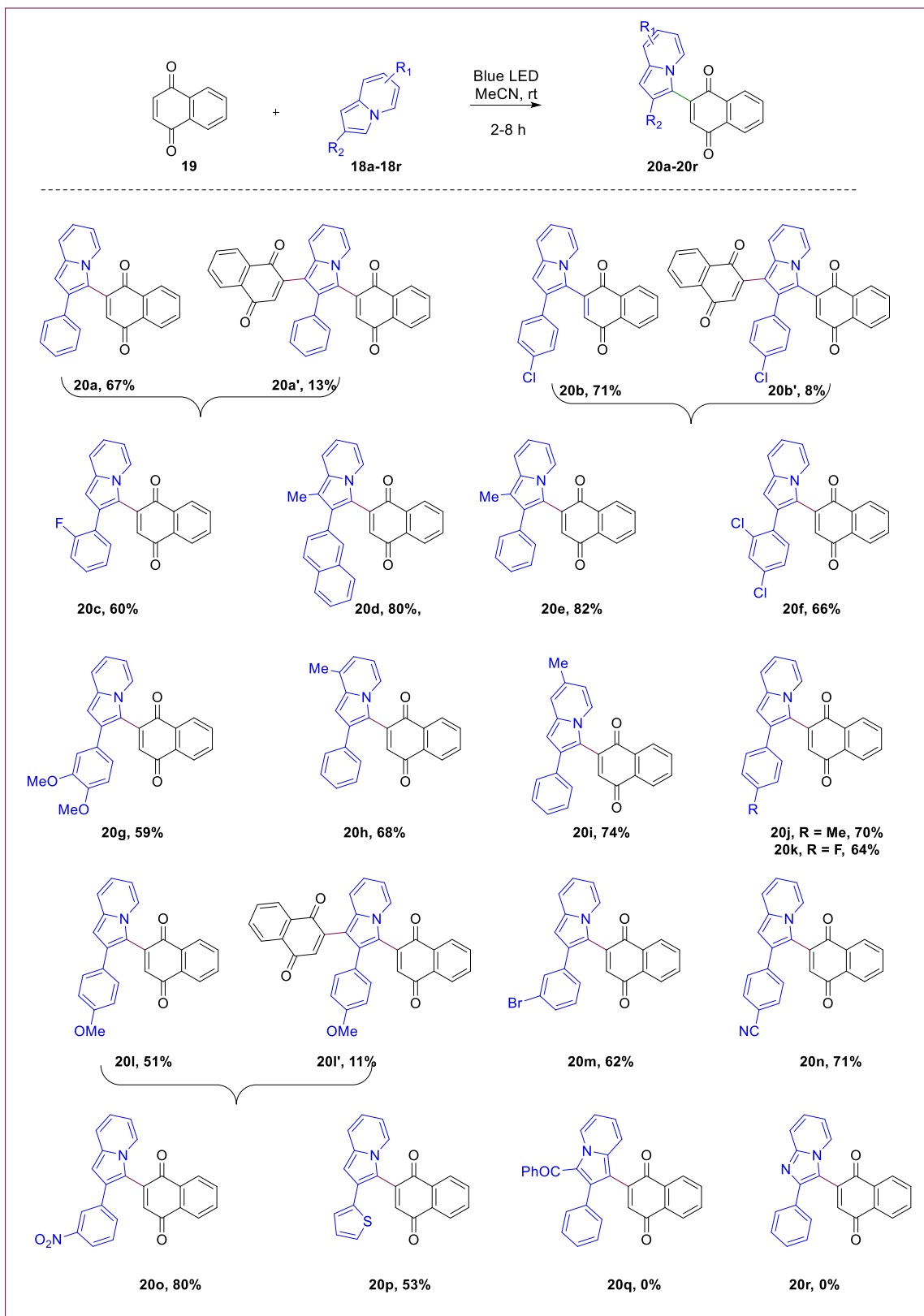
for an excitation source (Table 4, entry 10). When the reaction was carried out in the dark, then the trace amount conversion of the product was observed (Table 4, entry 11). Whereas, no such improvement in the yield of the expected product was observed on using White LED instead of Blue LED (Table 4, entry 12). When the same reaction was performed under an inert atmosphere, a decrease in the yield of **20a** was observed (Table 4, entry 13). Several indolizines with different substitution patterns, such as electron-withdrawing, electron releasing, halo groups (Cl, Br, and F), were compatible with our cross dehydrogenative coupling (CDC) protocol. The reaction between naphthoquinone and a wide variety of **18a-18r** has been evaluated. Para position of phenyl ring on indolizine substituted with -H, Cl, and OMe groups produce the expected CDC products (**20a,20b** & **20l**) in good yields with the minimal amount of side product (**20a'**, **20b'**, & **20l'**) (**Table 5**). Methyl group present on C1, C6, and C7 position of indolizine gave the desired products in compatible yields (**20d, 20e, 20h** & **20i**). Halo substituted indolizines such as F, Cl, and Br are suitable donors and gave the expected products with 60-66% yields (**20c, 20f, 20k** & **20m**). Electron releasing group such as OMe, Me produces the coupled products (**20g** & **20j**) with 59% and 70%, respectively. Electron withdrawing groups present on indolizine ring gave excellent yields of CDC products (**20n** & **20o**). Heterocyclic indolizine also forms EDA complex and produces the desired product (**20p**) in 53% yield. Imidazopyridine and C-3 substituted indolizine is not suitable donors for the present transformation (**20r** & **20q**). The reason behind the not formation of desired product may be the not formation of stable EDA complex or further radical transformation. The formation of **20a-20q** was further confirmed and predicted by their corresponding ^{1}H, ^{13}C and Mass data.

Example 1:

The confirmation of compound 2-(2-phenylindolizin-3-yl)naphthalene-1,4-dione (**20a**) was done by its ^{1}H and ^{13}C NMR spectrum. The peak showed in ^{1}H NMR at δ 6.70 (s, 1H) and δ 6.96 (s, 1H) for two protons attached to quinone and five membered ring of indolizine respectively.
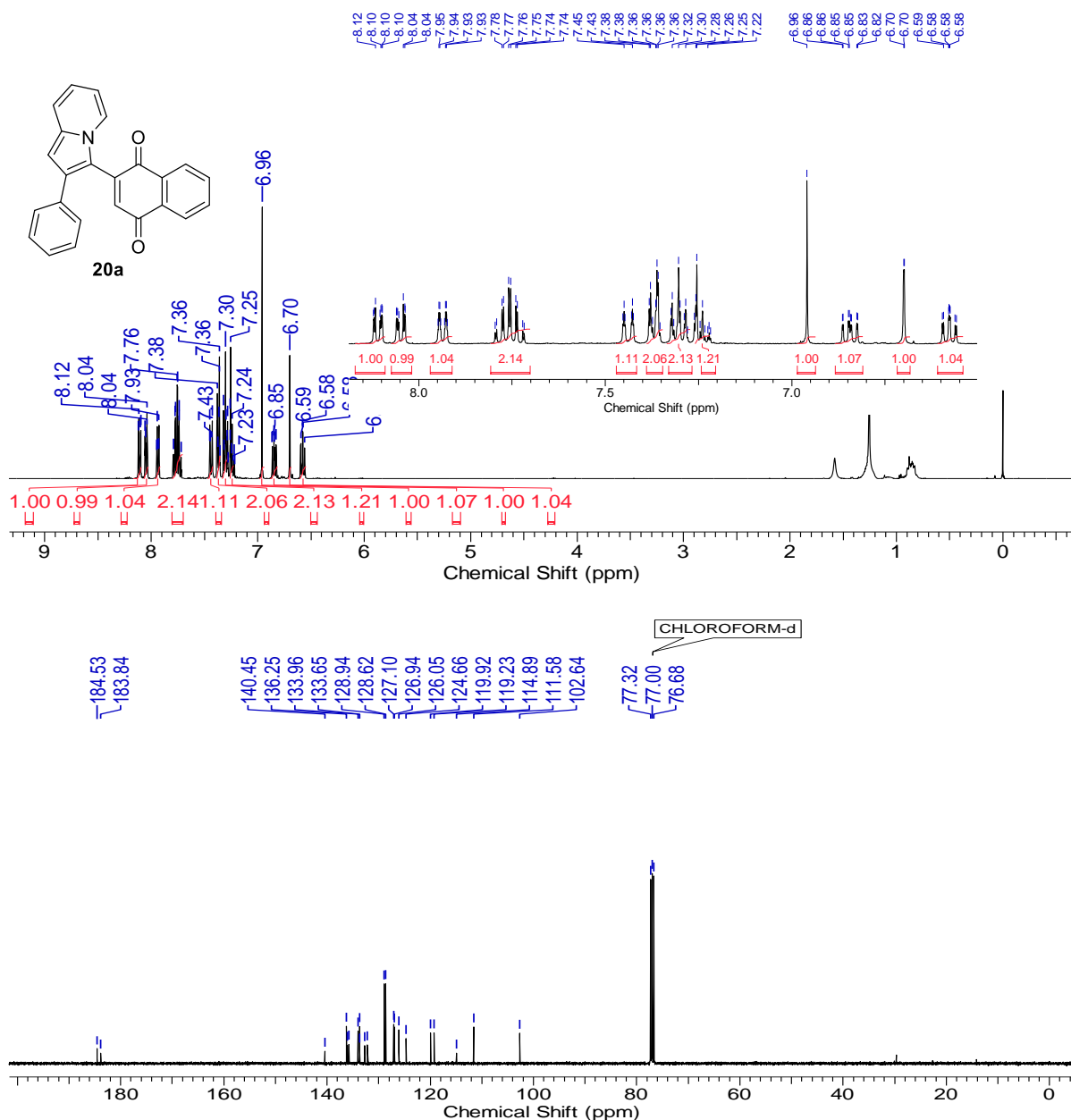
Figure 14. ^{1}H and ^{13}C NMR of 2-(2-phenylindolizin-3-yl)naphthalene-1,4-dione (**20a**)

The aromatic protons in the range of δ 6.58-8.12 ppm. In its ^{13}C NMR spectrum the characteristic Peak of two carbonyls showed as δ 183 and 184 respectively and remaining aromatic carbons are displayed in the range of δ 102-140 (**Figure 14**).

After examining the substrate scope for indolizines, we next focused on investigating the scope of substituted quinones (**Table 6**). Naphthoquinones substituted with groups like Cl, NO2, and bromo can form the stable EDA complex and give the CDC products with good yields (**22a, 22c & 22d**). Electron donating groups present on the quinone moiety are not suitable for forming EDA complex (**22b, & 22e**). Also, the heterocyclic naphthoquinone and substituted benzoquinone could not produce the desired products (**22f, 22g & 22h**). It was reasoned that the electron deficient conjugated π-system might be essential for forming the EDA complex and the following electron transfer process.

Table 6: Reaction Scope for Quinones[a]
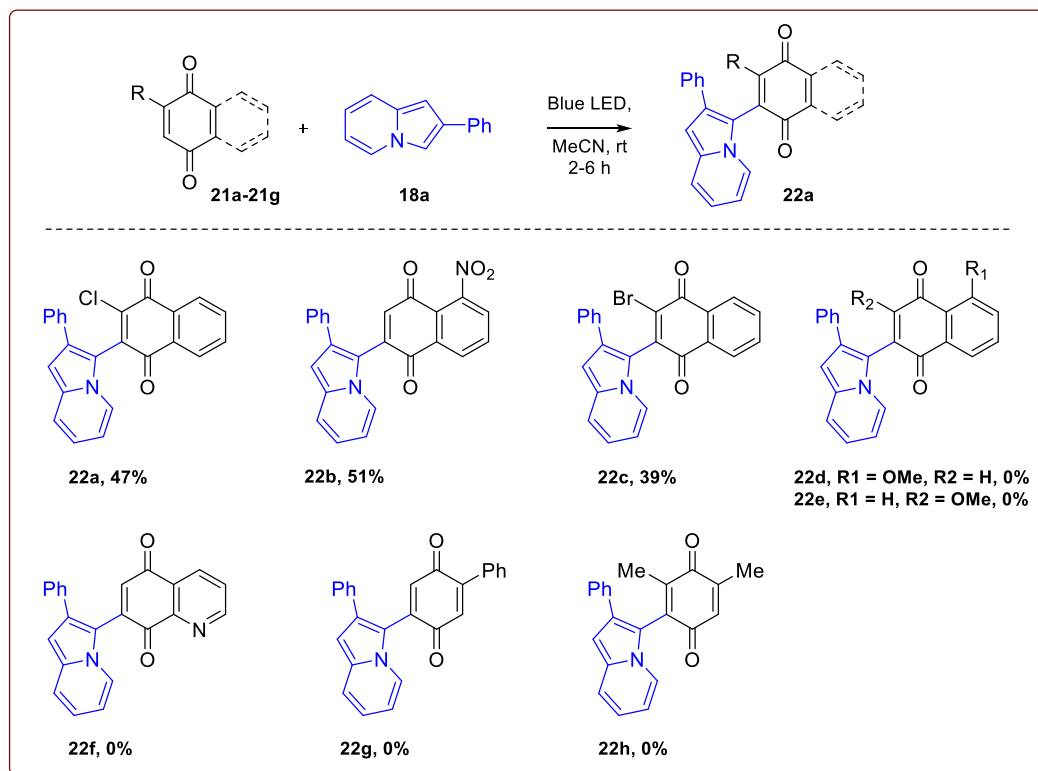
22a, 47%

22b, 51%

22c, 39%

22d, R1 = OMe, R2 = H, 0%
22e, R1 = H, R2 = OMe, 0%

22f, 0%

22g, 0%

22h, 0%

Concerning the mechanistic aspects, when the 2,2,6,6-tetramethylpiperidine-1-oxyl (TEMPO) was added in the standard reaction condition, only a trace amount of the product was obtained (**Scheme 12a**). Based on previous reports[39] and experimental observations, a possible reaction mechanism is depicted in **Scheme 12b**. The interaction between indolizine **1** and naphthoquinone **2** can produce an EDA complex, followed by visible light (Blue LED) initiated single electron transfer (SET) to give a radical ion pair **A**. Upon irradiation with visible light,
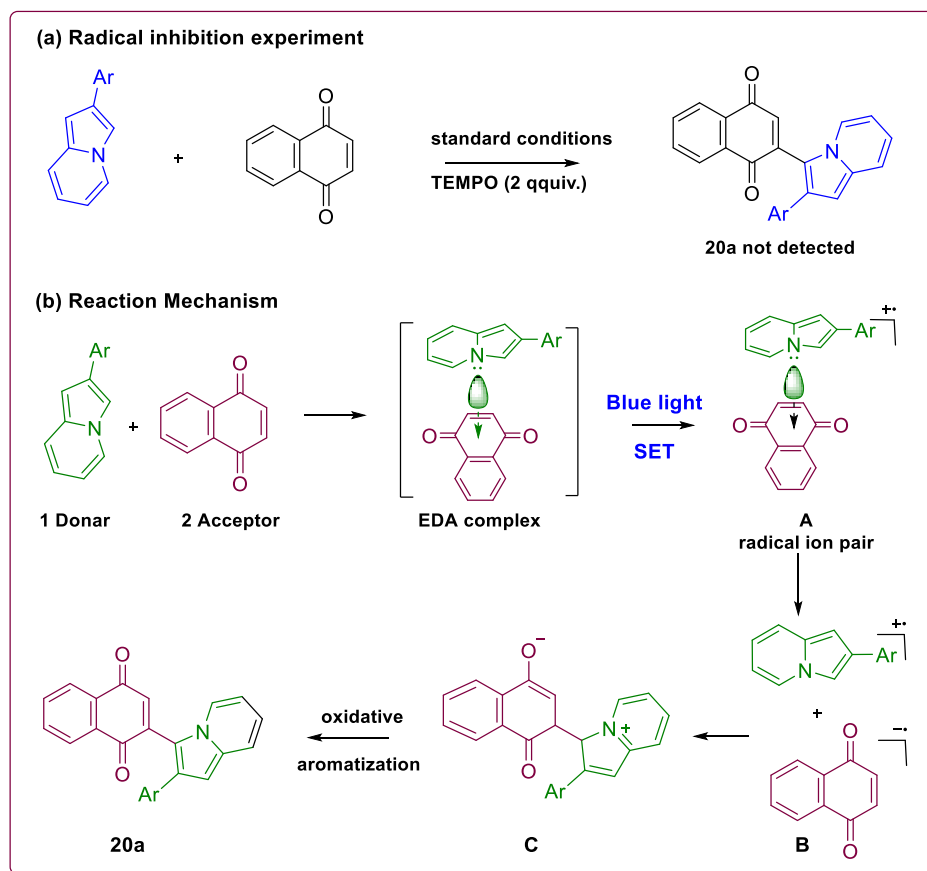
Scheme 12: Control experiment and possible reaction mechanism

generating the aryl radical ion pairs (**B**) simultaneously, followed by the oxidative addition of radical ion pairs, furnishes the expected coupled product **20a**.

3.2.5 Conclusion

In conclusion, we have developed a visible light promoted operationally simple under mild reaction conditions to construct functionally important derivatives of indolizine. Interestingly, this photo-driven CDC transformation can go ahead without adding any photocatalyst or additive. In place of catalyst, the formation of EDA complex between indolizine and quinone drives this photochemical reaction. Further attempts are ongoing in our laboratory to employ the freshly developed predecessors in other transformations, which will report in due course.

3.2.6 Experimental Section

General Experimental Procedure for synthesis of 20a

A solution of indolizine **1a** (0.31 mmol, 50 mg), quinone **2a** (0.31 mmol, 61 mg), and CH_3CN (3 mL) was added into a 25 mL oven-dried quartz tube. Then the mixture was stirred under Blue LED (12 W) at room temperature for 4 h monitored by TLC. The crude reaction mixture was diluted with ethyl acetate (5 mL) and water 5 mL, washed with brine and eluted with EtOAc (5 mL x 2). The collected organic layer was evaporated, and the crude residue was purified by using silica gel column chromatography (100-200 mesh silica) and isolated by using 98/05 to 90/10 petroleum ether/ethyl acetate to give the product **20a**.

2-(2-Phenylindolizin-3-yl)naphthalene-1,4-dione(20a).

Blue colored solid, yield: 67% (74 mg). ^{1}H NMR (400 MHz,CDCl$_3$)δ8.09 - 8.17 (m, 1H), 8.02 - 8.07 (m, 1H), 7.94 (dq, J = 7.2, 0.9 Hz, 1H), 7.76 (quind, J = 7.4, 7.4, 7.4, 7.4, 1.6 Hz, 2H), 7.44 (dt, J = 9.0, 1.1 Hz, 1H), 7.35 - 7.39 (m, 2H), 7.27 - 7.33 (m, 2H), 7.22 - 7.26 (m, 1H), 6.96 (s, 1H), 6.84 (ddd, J = 8.9, 6.6, 0.9 Hz, 1H), 6.68 - 6.72 (m, 1H), 6.54 - 6.61 (m, 1H).[13]C{[1]H}

NMR(101 MHz, CDCl$_3$) δ 184.5, 183.8, 140.4, 136.3, 136.0, 135.7, 134.0, 133.7, 133.7, 132.7, 132.2, 128.9, 128.6, 127.1, 126.9, 126.1, 124.7, 119.9, 119.2, 114.9, 111.6, 102.6. HRMS (ESI) m/z calculated for C$_{24}$H$_{16}$O$_2$N [(M+H)$^+$] 350.1176, found 350.1173

2,2'-(2-Phenylindolizine-1,3-diyl)bis(naphthalene-1,4-dione) (20a').

Blue colored solid, yield: 13% (20 mg).^{1}H NMR (400 MHz, CDCl$_3$) δ 8.06 - 8.13 (m, 3H), 7.98 - 8.04 (m, 1H), 7.90 (dt, *J* = 7.0, 1.0 Hz, 1H), 7.76 - 7.81 (m, 2H), 7.68 - 7.75 (m, 2H), 7.50 (dt, *J* = 9.1, 1.1 Hz, 1H), 7.16 - 7.26 (m, 5H), 7.04 (ddd, *J* = 9.1, 6.7, 1.0 Hz, 1H), 6.84 (s, 1H), 6.81 (s, 1H), 6.73 (td, *J* = 6.9, 1.3 Hz, 1H).^{13}C{^{1}H} NMR (101 MHz, CDCl$_3$) δ 184.7, 184.4, 184.4, 183.5, 143.7, 139.8, 138.6, 136.1, 135.2, 134.2, 133.9, 133.9, 133.6, 133.5, 133.0, 132.7, 132.5, 132.2, 132.0, 130.0, 128.7, 127.4, 127.2, 126.9, 126.3, 125.9, 125.2, 122.2, 118.8, 117.8, 112.6, 108.0.HRMS (ESI) m/z calculated for C$_{34}$H$_{20}$O$_4$N [(M+H)$^+$] 506.1387, found 506.1387.

2-(2-(4-Chlorophenyl)indolizin-3-yl)naphthalene-1,4-dione (20b).

Blue colored solid, yield: 71% (86 mg).^{1}H NMR (400 MHz, CDCl$_3$) δ 8.10 - 8.15 (m, 1 H), 8.02 - 8.09 (m, 1 H), 7.90 - 7.98 (m, 1 H), 7.78 (quind, *J*=7.2, 7.2, 7.2, 7.2, 1.6 Hz, 2H), 7.44 (dt, *J* = 8.9, 1.1 Hz, 1H), 7.27 - 7.33 (m, 4H), 6.97 (s, 1H), 6.86 (ddd, *J* = 8.9, 6.6, 1.0 Hz, 1H), 6.65 - 6.69 (m, 1H), 6.55 - 6.63 (m, 1H).^{13}C{^{1}H} NMR (101 MHz, CDCl$_3$) δ 184.5, 183.7, 140.2, 136.4, 136.1, 134.3, 134.1, 133.8, 133.0, 132.6, 132.4, 132.2, 130.1, 128.9, 128.0, 127.2, 126.1, 124.6, 120.1, 119.3, 111.8, 102.5.HRMS (ESI) m/z calculated for C$_{24}$H$_{15}$O$_2$NCl [(M+H)$^+$] 384.0786, found 384.0771.

2,2'-(2-(4-Chlorophenyl)indolizine-1,3-diyl)bis(naphthalene-1,4-dione) (20b').

Off white solid, yield: 8% (13 mg).^{1}H NMR (400 MHz, CDCl$_3$) δ 8.09 - 8.13 (m, 3H), 7.99 - 8.04 (m, 1H), 7.91 (dt, *J* = 7.0, 1.0 Hz, 1H), 7.78 - 7.83 (m, 2H), 7.70 - 7.77 (m, 2H), 7.51 (dt, *J* = 9.0, 1.1 Hz, 1H), 7.20 - 7.24 (m, 2H), 7.13 - 7.17 (m, 2H), 7.05 (ddd, *J* = 9.1, 6.7, 1.0 Hz, 1H),

6.88 (s, 1H), 6.86 (s, 1H), 6.74 (td, *J* = 6.8, 1.3 Hz, 1H).^{13}C{^{1}H} NMR(101 MHz, CDCl$_3$) δ 184.7, 184.3, 183.3, 143.4, 139.6, 138.7, 136.2, 135.1, 134.3, 134.0, 133.8, 133.6, 133.5, 132.6, 132.6, 132.3, 132.2, 132.0, 131.6, 131.1, 129.0, 127.2, 127.0, 126.3, 126.0, 125.1, 122.3, 118.7, 117.6, 112.8, 107.9.HRMS (ESI) m/z calculated for C$_{34}$H$_{19}$O$_4$NCl [(M+H)$^+$] 540.0997, found 540.0996.

2-(2-(2-Fluorophenyl)indolizin-3-yl)naphthalene-1,4-dione (20c).

Blue colored solid, yield: 60% (69 mg). ^{1}H NMR (500 MHz, CDCl$_3$) δ 8.10 (d, *J*=7.2 Hz, 2H), 7.93 (d, *J*=6.9 Hz, 1H), 7.71-7.81 (m, 2H), 7.46 (d, *J*=8.8 Hz, 1H), 7.40 (td, *J*=7.4, 1.5 Hz, 1H), 7.23 - 7.27 (m, 1H), 7.11 - 7.17 (m, 1H), 6.96 - 7.07 (m, 1H), 6.81 - 6.90 (m, 2H), 6.71 (s, 1H), 6.60 (t, *J*=6.3 Hz, 1 H). ^{13}C{^{1}H} NMR (126 MHz, CDCl$_3$) δ 184.8, 183.5, 160.2, 158.2, 140.5, 138.7, 135.8, 135.4, 134.0, 133.7, 132.6, 132.1, 131.6, 129.0, 129.0, 127.1, 126.7, 126.4, 126.1, 124.8, 124.4, 123.4, 123.3, 119.8, 119.3, 116.1, 116.0, 115.9, 111.7, 103.3. ^{19}F NMR (376 MHz, CDCl$_3$) δ -114.9 (s, 1F). HRMS (ESI) m/z calculated for C$_{24}$H$_{15}$O$_2$NF [(M+H)$^+$] 368.1081, found 368.1068.

2-(1-Methyl-2-(naphthalen-2-yl)indolizin-3-yl)naphthalene-1,4-dione (20d).

Blue colored solid, yield: 80% (100 mg).^{1}H NMR (400 MHz, CD$_3$CN) δ 8.02 (dt, *J* = 7.2, 1.0 Hz, 1H), 7.93 - 7.98 (m, 1H), 7.87 - 7.91 (m, 1H), 7.84 - 7.87 (m, 1H), 7.79 - 7.82 (m, 2H), 7.69 - 7.78 (m, 2H), 7.41 - 7.51 (m, 4H), 7.26 - 7.36 (m, 1H), 6.85 - 6.91 (m, 1H), 6.70 (s, 1H), 6.53 - 6.61 (m, 1H), 2.32 (s, 3H). ^{13}C{^{1}H} NMR (126 MHz, CD$_3$CN) δ 184.3, 183.8, 140.0, 136.0, 134.0, 133.7, 133.4, 132.9, 132.7, 132.1, 132.1, 128.9, 128.6, 127.8, 127.6, 127.2, 126.5, 126.3, 126.0, 125.5, 125.3, 125.1, 123.8, 119.0, 115.6, 111.2, 109.6, 108.9, 8.5. HRMS (ESI) m/z calculated for C$_{29}$H$_{20}$O$_2$N [(M+H)$^+$] 414.1489, found 414.1489.

2-(1-Methyl-2-phenylindolizin-3-yl)naphthalene-1,4-dione (20e).

Blue colored solid, yield: 82% (94 mg).^{1}H NMR (400 MHz, CDCl$_3$) δ 8.04 - 8.09 (m, 1H), 7.96 - 8.01 (m, 1H), 7.93 (dt, J = 7.1, 1.0 Hz, 1H), 7.66 - 7.76 (m, 2H), 7.41 (dt, J = 8.9, 1.2 Hz, 1H), 7.30 - 7.36 (m, 2H), 7.23 - 7.29 (m, 3H), 6.81 - 6.85 (m, 1H), 6.79 (s, 1H), 6.47 - 6.65 (m, 1H), 2.30 (s, 3H).^{13}C{^{1}H} NMR (101 MHz, CDCl$_3$) δ 184.4, 184.0, 140.1, 135.0, 134.9, 134.4, 133.8, 133.4, 133.0, 132.8, 132.2, 130.1, 128.4, 126.9, 126.9, 125.9, 124.9, 119.0, 117.7, 115.5, 111.4, 110.2, 9.2.HRMS (ESI) m/z calculated for C$_{25}$H$_{18}$O$_2$N [(M+H)$^+$] 364.1332, found 364.1332.

2-(2-(2,4-Dichlorophenyl)indolizin-3-yl)naphthalene-1,4-dione (20f).

Blue colored solid, yield: 66% (86 mg).^{1}H NMR (500 MHz, CDCl$_3$) δ 8.08 - 8.14 (m, 2H), 7.95 (d, J = 6.9 Hz, 1H), 7.76 - 7.81 (m, 2H), 7.47 (d, J = 9.2 Hz, 1H), 7.43 (d, J = 1.9 Hz, 1H), 7.29 (d, J = 1.5 Hz, 1H), 7.23 - 7.27 (m, 1H), 6.86 - 6.95 (m, 1H), 6.76 (s, 1H), 6.60 - 6.67 (m, 2H). ^{13}C{^{1}H} NMR (126 MHz, CDCl$_3$) δ 184.3, 183.2, 139.7, 135.3, 135.1, 133.8, 133.6, 133.5, 132.6, 132.2, 131.7, 129.5, 129.0, 126.9, 126.8, 125.9, 124.8, 121.4, 119.9, 119.0, 116.1, 111.5, 109.7, 103.4. HRMS (ESI) m/z calculated for C$_{24}$H$_{14}$O$_2$NCl$_2$ [(M+H)$^+$] 418.0396, found 418.0392.

2-(2-(3,4-Dimethoxyphenyl)indolizin-3-yl)naphthalene-1,4-dione (20g).

Blue colored solid, yield: 59% (76 mg).^{1}H NMR (500 MHz, CDCl$_3$) δ 8.14 (dd, J = 7.2, 1.1 Hz, 1H), 8.06 (dd, J = 7.6, 1.1 Hz, 1H), 8.00 (d, J = 7.2 Hz, 1H), 7.74 - 7.83 (m, 2H), 7.46 (d, J = 9.2 Hz, 1H), 7.07 (s, 1H), 6.93 (dq, J = 4.2, 2.0 Hz, 2H), 6.87 (dd, J = 8.6, 6.7 Hz, 1H), 6.81 - 6.85 (m, 1H), 6.71 (s, 1H), 6.58 - 6.64 (m, 1H), 3.89 (s, 3H), 3.74 (s, 3H). ^{13}C{^{1}H} NMR (101 MHz, CDCl$_3$) δ 184.2, 183.6, 148.6, 147.8, 140.4, 135.8, 135.3, 133.6, 133.4, 133.3, 132.4, 131.8, 128.2, 126.8, 125.7, 124.2, 120.9, 119.7, 118.8, 114.4, 111.8, 111.2, 111.1, 102.1, 55.5, 55.4. HRMS (ESI) m/z calculated for C$_{26}$H$_{20}$O$_4$N [(M+H)$^+$] 410.1387, found 410.1381.

2-(8-Methyl-2-phenylindolizin-3-yl)naphthalene-1,4-dione (20h).

Blue colored solid, yield: 68% (77 mg).^{1}H NMR (400 MHz, CD$_3$CN) δ 8.04 - 8.09 (m, 1H), 7.97 - 8.01 (m, 1H), 7.91 (d, J = 0.8 Hz, 1H), 7.83 (ddd, J = 7.6, 5.3, 1.7 Hz, 2H), 7.41 - 7.50 (m, 2H), 7.28 - 7.33 (m, 2H), 7.26 (d, J = 7.3 Hz, 1H), 6.94 (s, 1H), 6.77 (d, J = 0.8 Hz, 1H), 6.70 (s, 1H), 6.50 - 6.61 (m, 1H), 2.46 (s, 3H). ^{13}C{^{1}H} NMR (101 MHz, CD$_3$CN) δ 185.8, 185.1, 141.9, 138.9, 137.3, 137.1, 135.4, 135.2, 134.1, 133.5, 133.3, 130.1, 129.9, 129.4, 128.0, 127.9, 126.9, 124.1, 120.1, 116.3, 112.7, 101.5, 18.4. HRMS (ESI) m/z calculated for C$_{25}$H$_{18}$O$_2$N [(M+H)$^+$] 364.1332, found 364.1321.

2-(7-Methyl-2-phenylindolizin-3-yl)naphthalene-1,4-dione (20i).

Blue colored solid, yield: 74% (68 mg).^{1}H NMR (500 MHz, CDCl$_3$) δ 8.13 (d, J = 7.2 Hz, 1H), 8.02 - 8.08 (m, 1H), 7.92 (d, J = 7.2 Hz, 1H), 7.71 - 7.85 (m, 2H), 7.36 - 7.43 (m, 2H), 7.33 (t, J = 7.4 Hz, 2H), 7.23 - 7.28 (m, 1H), 6.96 (s, 1H), 6.60 (s, 1H), 6.46 (dd, J = 7.2, 1.5 Hz, 1H), 2.35 (s, 3H). ^{13}C{^{1}H} NMR (101 MHz, CDCl$_3$) δ 184.6, 184.1, 140.4, 136.7, 136.0, 135.1, 134.2, 133.9, 133.6, 132.9, 132.3, 130.8, 128.9, 128.6, 127.1, 126.9, 126.0, 124.4, 117.5, 114.4, 114.4, 101.7, 21.0. HRMS (ESI) m/z calculated for C$_{25}$H$_{18}$O$_2$N [(M+H)$^+$] 364.1332, found 364.1320.

2-(2-(*p*-Tolyl)indolizin-3-yl)naphthalene-1,4-dione (20j).

Blue colored solid, yield: 70% (63 mg).^{1}H NMR (500 MHz, CD$_3$CN) δ 8.06 (dd, J=7.2, 1.5 Hz, 1H), 7.97 - 8.03 (m, 2H), 7.75 - 7.91 (m, 2H), 7.46 (d, J=8.8 Hz, 1H), 7.31 (m, J=8.0 Hz, 2H), 7.12 (m, J=8.0 Hz, 2H), 6.91 (s, 1H), 6.86 (dd, J=9.0, 6.7 Hz, 1H), 6.70 (s, 1H), 6.51 - 6.64 (m, 1H), 2.30 (s, 3H). ^{13}C{^{1}H} NMR (126 MHz, CD$_3$CN) δ 185.6, 184.9, 141.6, 138.6, 137.7, 136.4, 135.2, 135.0, 133.9, 133.8, 133.6, 133.3, 130.3, 129.8, 127.7, 126.7, 126.0, 120.8, 119.8, 115.6, 112.3, 102.6, 21.2. HRMS (ESI) m/z calculated for C$_{25}$H$_{18}$O$_2$N [(M+H)$^+$] 364.1332, found 364.1333.

2-(2-(4-Fluorophenyl)indolizin-3-yl)naphthalene-1,4-dione (20k).

Blue colored solid, yield: 64% (59 mg).^{1}H NMR (400 MHz, CDCl$_3$) δ 8.10 - 8.16 (m, 1H), 8.04 - 8.09 (m, 1H), 7.95 (dd, J = 7.2, 0.8 Hz, 1H), 7.78 (quind, J = 7.3, 7.3, 7.3, 7.3, 1.6 Hz, 2H), 7.41 - 7.49 (m, 1H), 7.31 - 7.39 (m, 2H), 6.94 - 7.05 (m, 3H), 6.84 - 6.91 (m, 1H), 6.65 - 6.69 (m, 1H), 6.60 (td, J = 6.9, 1.3 Hz, 1H). ^{13}C{^{1}H} NMR (101 MHz, CDCl$_3$) δ 184.2, 183.5, 139.9, 135.9, 135.7, 133.8, 133.4, 132.3, 131.8, 131.5, 130.1, 130.0, 126.8, 125.8, 124.3, 122.5, 120.4, 119.8, 118.9, 115.4, 115.2, 114.5, 111.4, 102.3. HRMS (ESI) m/z calculated for C$_{24}$H$_{15}$O$_2$NF [(M+H)$^+$] 368.1081, found 368.1080.

2-(2-(4-Methoxyphenyl)indolizin-3-yl)naphthalene-1,4-dione (20l).

Blue colored solid, yield: 51% (49 mg).^{1}H NMR (400 MHz, CDCl$_3$) δ 8.09 - 8.16 (m, 1H), 8.03 - 8.08 (m, 1H), 7.96 (dd, J = 7.1, 0.8 Hz, 1H), 7.77 (quind, J = 7.3, 7.3, 7.3, 7.3, 1.6 Hz, 2H), 7.45 (d, J = 8.9 Hz, 1H), 7.21 (t, J = 7.9 Hz, 1H), 7.00 (s, 1H), 6.91 - 6.97 (m, 2H), 6.86 (ddd, J = 8.9, 6.6, 0.8 Hz, 1H), 6.77 - 6.83 (m, 1H), 6.71 (s, 1H), 6.53 - 6.64 (m, 1H), 3.73 (s, 3H). ^{13}C{^{1}H} NMR (101 MHz, CDCl$_3$) δ 184.6, 183.9, 159.7, 140.5, 137.2, 136.1, 136.0, 134.0, 133.7, 133.6, 132.8, 132.2, 129.6, 127.1, 126.1, 124.6, 121.5, 120.0, 119.3, 115.0, 114.5, 112.5, 111.7, 102.6, 55.2. HRMS (ESI) m/z calculated for C$_{25}$H$_{18}$O$_3$N [(M+H)$^+$] 380.1281, found 380.1264.

2,2'-(2-(4-Methoxyphenyl)indolizine-1,3-diyl)bis (naphthalene-1,4-dione) (20l').

Blue colored solid, yield: 11% (14 mg).^{1}H NMR (500 MHz, CDCl$_3$) δ 8.06 - 8.17 (m, 3H), 8.04 (dd, J = 7.4, 1.3 Hz, 1H), 7.88 (d, J = 6.9 Hz, 1H), 7.68 - 7.82 (m, 4H), 7.48 (d, J = 9.2 Hz, 1H), 7.09 - 7.15 (m, 2H), 6.97 - 7.05 (m, 1H), 6.85 (s, 1H), 6.75 - 6.82 (m, 3H), 6.64 - 6.74 (m, 1H), 3.75 (s, 3H). ^{13}C{^{1}H} NMR (101 MHz, CDCl$_3$) δ 184.8, 184.5, 184.4, 183.6, 158.8, 143.8, 139.9, 138.6, 136.2, 135.2, 134.2, 133.9, 133.7, 133.5, 132.7, 132.7, 132.5, 132.2, 132.0, 131.1,

127.2, 127.0, 126.3, 125.9, 125.2, 122.1, 118.7, 117.7, 114.3, 112.5, 108.0, 55.1. HRMS (ESI) m/z calculated for $C_{35}H_{22}O_5N$ [(M+H)$^+$] 536.1492, found 536.1490.

2-(2-(3-Bromophenyl)indolizin-3-yl)naphthalene-1,4-dione (20m).

Blue colored solid, yield: 62% (67 mg). ^{1}H NMR (500 MHz, CDCl$_3$) δ 8.15 (dd, J = 7.4, 1.3 Hz, 1H), 8.09 (dd, J = 7.4, 1.3 Hz, 1H), 7.97 (d, J = 7.2 Hz, 1H), 7.75 - 7.86 (m, 2H), 7.60 (t, J = 1.7 Hz, 1H), 7.47 (d, J = 8.8 Hz, 1H), 7.40 (d, J = 8.0 Hz, 1H), 7.27 - 7.31 (m, 1H), 7.12 - 7.21 (m, 1H), 7.00 (s, 1H), 6.89 (dd, J = 8.6, 6.7 Hz, 1H), 6.72 (s, 1H), 6.59 - 6.67 (m, 1H). ^{13}C{^{1}H} NMR (126 MHz, CDCl$_3$) δ 184.2, 183.5, 139.9, 137.7, 136.1, 135.8, 133.8, 133.5, 132.4, 131.9, 131.7, 131.5, 129.8, 129.7, 127.3, 126.9, 125.9, 124.3, 122.5, 119.9, 119.1, 114.6, 111.7, 102.3. HRMS (ESI) m/z calculated for $C_{24}H_{15}O_2NBr$ [(M+H)$^+$] 428.0281, found 428.0277.

4-(3-(1,4-Dioxo-1,4-dihydronaphthalen-2-yl)indolizin-2-yl)benzonitrile (20n).

Blue colored solid, yield: 71% (66 mg). ^{1}H NMR (500 MHz, CD$_3$CN) δ 8.05 - 8.13 (m, 2H), 7.98 - 8.03 (m, 1H), 7.80 - 7.89 (m, 2H), 7.64 (m, J = 8.4 Hz, 2H), 7.60 (m, J = 8.4 Hz, 2H), 7.52 (d, J = 8.8 Hz, 1H), 7.03 (s, 1H), 6.91 (dd, J = 8.6, 6.7 Hz, 1H), 6.82 (s, 1H), 6.60 - 6.71 (m, 1H). ^{13}C{^{1}H} NMR (126 MHz, CD$_3$CN) δ 185.6, 184.7, 141.8, 140.9, 139.2, 136.5, 135.4, 135.1, 133.8, 133.5, 131.4, 130.5, 127.8, 126.8, 125.9, 121.2, 120.2, 119.9, 117.7, 115.9, 113.0, 111.0, 102.6. HRMS (ESI) m/z calculated for $C_{25}H_{15}O_2N_2$ [(M+H)$^+$] 375.1128, found 375.1125.

2-(2-(3-Nitrophenyl)indolizin-3-yl)naphthalene-1,4-dione (20o).

Blue colored solid, yield: 80% (79 mg). ^{1}H NMR (400 MHz, CDCl$_3$) δ 8.29 (t, J = 1.9 Hz, 1H), 8.08 - 8.15 (m, 2H), 8.02 - 8.06 (m, 1H), 7.99 (dd, J = 7.2, 0.8 Hz, 1H), 7.74 - 7.83 (m, 2H), 7.66 (dt, J = 7.7, 1.4 Hz, 1H), 7.43 - 7.51 (m, 2H), 7.01 (s, 1H), 6.86 - 6.94 (m, 1H), 6.77 (s, 1H), 6.61 - 6.69 (m, 1H). ^{13}C{^{1}H} NMR (101 MHz, CDCl$_3$) δ 184.3, 183.6, 148.5, 139.7, 137.7, 136.6, 136.1, 134.7, 134.3, 133.9, 132.4, 132.0, 130.8, 129.5, 127.1, 126.2, 124.5, 123.5, 121.7, 120.4,

119.5, 114.8, 112.3, 102.6. HRMS (ESI) m/z calculated for $C_{24}H_{15}O_4N_2$ [(M+H)$^+$] 395.1026, found 395.1023.

2-Chloro-3-(2-phenylindolizin-3-yl)naphthalene-1,4-dione (22a).

Blue colored solid, yield: 47% (46 mg). ^{1}H NMR (500 MHz, CDCl$_3$) δ 8.12 (d, J = 7.2 Hz, 1H), 8.06 (d, J = 7.2 Hz, 1H), 8.01 (d, J = 7.6 Hz, 1H), 7.95 (d, J = 6.9 Hz, 1H), 7.73 - 7.82 (m, 2H), 7.44 - 7.59 (m, 2H), 7.37 - 7.42 (m, 2H), 7.28 - 7.32 (m, 3H), 7.23 (d, J = 5.3 Hz, 1H), 6.88 - 6.94 (m, 1H), 6.82 (s, 1H), 6.71 (s, 1H), 6.66 (t, J = 6.5 Hz, 1H). ^{13}C{^{1}H} NMR (101 MHz, CDCl$_3$) δ 184.2, 183.5, 140.1, 135.9, 135.4, 134.0, 133.6, 133.3, 132.4, 131.8, 128.6, 128.3, 127.8, 127.2, 126.8, 126.6, 125.7, 124.3, 119.6, 118.9, 114.6, 111.3, 111.0, 102.3, 101.3. HRMS (ESI) m/z calculated for $C_{24}H_{15}O_2NCl$ [(M+H)$^+$] 384.0786, found 384.0775.

5-Nitro-2-(2-phenylindolizin-3-yl)naphthalene-1,4-dione (22b).

Blue colored solid, yield: 51% (36 mg). ^{1}H NMR (500 MHz, CDCl$_3$) δ 8.17 (d, *J* = 7.2 Hz, 1H), 8.06 (d, *J* = 7.6 Hz, 1H), 8.01 (d, *J* = 6.9 Hz, 1H), 7.79 - 7.86 (m, 2H), 7.57 - 7.70 (m, 3H), 7.49 - 7.54 (m, 3H), 7.05 (s, 1H), 6.92 (t, *J* = 7.8 Hz, 1H), 6.67 (t, *J* = 6.5 Hz, 1H). ^{13}C{^{1}H} NMR (126 MHz, CDCl$_3$) δ 184.6, 183.8, 141.1, 140.0, 136.8, 136.4, 134.6, 134.2, 132.7, 132.3, 131.7, 130.3, 129.6, 127.4, 126.5, 124.6, 120.7, 119.8, 119.2, 115.0, 112.6, 110.7, 102.8. HRMS (ESI) m/z calculated for $C_{24}H_{15}O_2NCl$ [(M+H)$^+$] 384.0786, found

3.2.7. References

1   (a) Tewari, D.; Kumar, P.; Sharma, P. Pharmacognostical Evaluation of Elaeocarpus sphaericus (Rudraksha) Leaves. *Int. J. Pharmacognosy and Phytochemical Res.* **2013**, *5*, 147-150. (b) Colegate, S. M.; Dorling, P. R. in Handbook of Plant and Fungal Toxicants, ed. J. P. F. D'Mello, CRC Press, Boca Raton, **1997**, ch.1, pp. 1–18.

2   (a) Mehta, L. K.; Parrick, J. The Synthesis of Three Indolizine Derivatives of Interest as Non-Isomerizable Analogues of Tamoxifen. *J. Heterocyclic chem.* **1995**, *32*, 391-394. (b) Sharma, V.; Kumar, V. Indolizine: A Biologically Active Moiety. *Med. Chem. Res.* **2014**, *23*, 3593-3606. (c) Hazra, A.; Mondal, S.; Maity, A.; Naskar, S.; Saha, P.; Paira, R.; Sahu, K. B.; Paira, P.; Ghosh, S.; Sinha, C.; Samanta, A.; Banerjee, S.;

Mondal, N. B. Amberlite-IRA-402(OH): Ion Exchange Resin Mediated Synthesis of Indolizines, Pyrrolo [1,2-a] Quinolines and Isoquinolines: Antibacterial and Antifungal Evaluation of the Products. *Eur. J. Med. Chem.* **2011**, *46*, 2132-2140. (d) Gundersen, L. L.; Negussie, A. H.; Rise, F.; Ostby, O. B. Antimycobacterial Activity of 1-Substituted Indolizines. *Arch. Pharm. Med. Chem.* **2003**, *336*, 191-195. (e) Nasir, A. I.; Gundersen, L-L.; Rise, F.; Antonsen, O.; Kristensen, T.; Langhelle, B.; Bast, A.; Custers, I.; Haenen, G. R.; Wikstrom, H. Inhibition of Lipid Peroxidation Mediated by Indolizines. *Bioorg. Med. Chem. Lett.* **1998**, *8*, 1829-1832.

3   (a) Gundersen, L-L.; Charnock, C.; Negussie, A-H.; Rise, F.; Teklu, S. Synthesis of indolizine derivatives with selective antibacterial activity against Mycobacterium tuberculosis. *Eur. J. Pharm. Sci.* **2007**, *30*, 26-35. (b) Narajji, C.; Karvekar, M.D.; Das, A. K. Synthesis and antioxidant activity of 3,3'-diselanediylbis (N, N-disubstituted indolizine-1-carboxamide) and derivatives. S. *Afr. J. Chem.* **2008**, *61*, 53-55. (c) Sandeep, C.; Venugopala, K.N.; Gleiser, R.M.; Chetram, A.; Padmashali, B.; Kulkarni, R. S. Greener synthesis of indolizine analogue using water as a base and solvent: Study for larvicidal activity against Anopheles arabiensis. *Chem. Biol. Drug. Des.* **2016**, 899-904. (d) Huang, W.; Zuo, T.; Luo, X.; Jin, H.; Liu, Z.; Yang, Z. Indolizine derivatives as HIV-1 VIF-Elongin C interaction inhibitors. *Chem. Biol. Drug Des.* **2013**, *81*, 730-41.

4   (a) Kim, D.; Lee, J. H.; Kim, H. Y.; Shin, J.; Kim, K.; Lee, S.; Park, J.; Kim, J.; Kim, Y. Fluorescent indolizine derivative YI-13 detects amyloid-β monomers, dimers, and plaques in the brain of 5XFAD Alzheimer transgenic mouse model. *Plos one* **2020**, *15*, e0243041.

5   Arvin-Berod, M.; Desroches-Castan, A.; Bonte, S.; Brugière, S.; Coute, Y.; Guyon, L.; Feige, J.-J.; Baussanne, I.; Demeunynck, M. Indolizine-based scaffolds as efficient and versatile tools: Application to the synthesis of biotin-tagged antiangiogenic drugs. *ACS omega* **2017**, *2*, 9221-9230.

6   (a) Huckaba, A. J.; Giordano, F.; McNamara, L. E.; Dreux, K. M.; Hammer, N. I.; Tschumper, G. S.; Zakeeruddin, S. M.; Grätzel, M.; Nazeeruddin, M. K.; Delcamp, J. H. Indolizine-Based Donors as Organic Sensitizer Components for Dye-Sensitized Solar Cells. *Adv. Energy Mater.* **2014**, *5*, 1401629. (b) Huckaba, A. J.; Yella, A.; Brogdon, P.; Murphy, J. S.; Nazeeruddin, M. K.; Grätzel, M.; Delcamp, J. H. A Low Recombination Rate Indolizine Sensitizer for Dye-Sensitized Solar Cells. *Chem. Commun.* **2016**, *52*, 8424-8427.

7   Ji, R.; Liu, A.; Shen, S.; Cao, X.; Li, F.; Ge, Y. An indolizine-rhodamine-based FRET fluorescence sensor for highly sensitive and selective detection of Hg^{2+} in living cells. *RSC advances* **2017**, *7*, 40829-40833. (b) Zheng, X.; Ji, R.; Cao, X.; Ge, Y. FRET-based radiometric fluorescent probe for Cu^{2+} with a new indolizine fluorophore. *Analytica chimica acta* **2017**, *978*, 48-54.

8   Ge, Y.; Liu, A.; Dong, J.; Duan, G.; Cao, X.; Li, F. A simple pH fluorescent probe based on new fluorophore indolizine for imaging of living cells. *Sensors and Actuators B* **2017**, *247*, 46-52.

9   Song, Y. R.; Lim, C. W.; Kim, T. W.; Synthesis and photophysical properties of 1,2-diphenylindolizine derivatives: fluorescent blue-emitting materials for organic light-emitting device. *Luminescence* **2016**, *31*, 364-371.

10   (a) Becuwe, M.; Landy, D.; Delattre, F.; Cazier, F.; Fourmentin, S. Fluorescent Indolizine-*β*-Cyclodextrin Derivatives for the Detection of Volatile Organic Compounds. *Sensors* **2008**, *8*, 3689-3705. (b) Surpateanu, G. G.; Becuwe, M.; Lungu, N. C.; Dron, P. I.; Fourmentin, S.; Landy, D.; Surpateanu, G. Photochemical behaviour upon the inclusion for some volatile organic compounds in new fluorescent indolizine β-cyclodextrin sensors. *J. Photochem. and Photobiology A: Chemistry*, **2007**, *185*, 312-320.

11   (a) Sadowski, B.; Klajn, J.; Gryko, D. T. Recent advances in the synthesis of indolizines and their π-expanded analogues. *Org. biomol. Chem.***2016**, *14*, 7804-7828. (b) Lee, J. H.; Kim, I. Cycloaromatization Approach to Polysubstituted Indolizines from 2-Acetylpyrroles: Decoration of the Pyridine Unit. *J. Org. Chem.* **2013**, *78*, 1283-1288. (c) Joshi, D. R.; Kim, I. Correction to "Michael-Aldol Double Elimination Cascade to Make Pyridines: Use of Chromone for the Synthesis of Indolizines. *J. Org. Chem.* **2021**, *86*, 10235-10248

12   (a) Lins, C. L.; Block, J. H.; Doerge, R. F. Nitro-para-and meta-substituted 2-phenylindolizines as potential antimicrobial agents. *J. of pharma. sci.* **1982**, *71*, 556-561. (b) Wu, Y.; Ding, H.; Zhao, M.; Ni, Z.-H.; Cao, J.-P. Electrochemical and direct C-H methylthiolation of electron-rich aromatics. *Green Chem.* **2020**, *22*, 4906-4911. (c) Yu, Y.; Yue, Z.; Ding, L. G.; Zhou, Y.; Cao, H. Mn (OAc)$_3$ -Mediated Regioselective C-H Phosphonylation of Indolizines with H-Phosphonates. *Chem. Select* **2019**, *4*, 1117-1120. (d) Penteado, F.; Gomes, C. S.; Monzon, L. I.; Perin, G.; Silveira, C. C.; Lenardão, E. J. Photocatalytic Synthesis of 3-Sulfanyl- and 1,3-Bis(sulfanyl)indolizines Mediated by Visible Light. *Eur. J. Org. Chem.* **2020**, 2110-2115. (e) Xia, J-B.; Wang, X-Q.; You, S-L. Synthesis of Biindolizines through Highly Regioselective Palladium-Catalyzed C-H Functionalization. *J. Org. Chem.* **2009**, *74*, 1, 456-458. (f) Xia, J-B.; You, S-L. Synthesis of 3-Haloindolizines by Copper(II) Halide Mediated Direct Functionalization of Indolizines. *Org. Lett.* **2009**, *11*, 5, 1187-1190. (g) Seregin, I. V.; Ryabova, V.; Gevorgyan, V. Direct Palladium-Catalyzed Alkynylation of N-Fused Heterocycles. *J. Am. Chem. Soc.* **2007**, 129, 25, 7742-7743. (h) Yang, Y.; Cheng, K.; Zhang, Y. Highly Regioselective Palladium-Catalyzed Oxidative Coupling of Indolizines and Vinylarenes via C-H Bond Cleavage. *Org. Lett.* **2009**, *11*, 24, 5606-5609. (i) Jung, Y.; Kim, I. C3 functionalization of indolizines via In(III)-catalyzed three-component reaction. *Org. Biomol. Chem.*, **2015**, *13*, 10986-10994

13   (a) Teng, L.; Liu, X.; Guo, P.; Yu, Y.; Cao, H. Visible-Light-Induced Regioselective Dicarbonylation of Indolizines with Oxoaldehydes via Direct C−H Functionalization. *Org. Lett.* **2020**, *22*, 3841-3845. (b) Masumura, M. Addition reactions of indolizine derivatives with diethyl azodicarboxylate. *Heterocycles* **1979**, *12*, 787-790. (c) Joshi, D. R.; Seo, Y.; Heo, Y.; Park, S-h.; Lee, Y.; Namkung, W.; Kim, I. Domino [4 + 2] Annulation Access to Quinone–Indolizine Hybrids: Anticancer *N*-Fused Polycycles**.** *J. Org. Chem.* **2020**, *85*, 10994-11005. (d) Lee, S.; Kim, S.; Yoon, S. H.; Dagar, A.; Kim, I. Diastereoselective Synthesis of Densely Functionalized 3a,8a-Dihydro-8*H*-furo[3,2-*a*]pyrrolizines through One-Pot Three-Component Assembly**.** *J. Org. Chem.* **2021**, *86*, 12367-12377. (e) Park, C-H.; Ryabova, V.; Seregin, I. V.; Sromek, A. W.; Gevorgyan, V. Palladium-Catalyzed Arylation and Heteroarylation of Indolizines. *Org. Lett*. **2004**, 6, 1159-1162.

14   (a) Chen, F.-M.; Huang, F.-D.; Yao, X.-Y.; Li, T.; Liu, F.S. Direct C–H heteroarylation by an acenaphthyl based α-diimine palladium complex: improvement of the reaction efficiency for bi(hetero)aryls under aerobic

conditions. *Org. Chem. Front.* **2017**, *4*, 2336-2342. (b) Correia, J. T. M.; List, B.; Coelho, f. Catalytic Asymmetric Conjugate Addition of Indolizines to α,β-Unsaturated Ketones. *Angew.Chem. Int.Ed.* **2017**, *56*,7967-7970. (c) Zhang, Y-Z.; Sheng, F-T.; Zhu, Z.; Li, Z-M.; Zhang, S.; Tan, W.; Shi, F. Organocatalytic C3-functionalization of indolizines: synthesis of biologically important indolizine derivatives. *Org. Biomol. Chem.*, **2020**, 18, 5688-5696.

15   (a) Bansode, A. H.; Suryavanshi, G. Visible-Light-Induced Controlled Oxidation of N-Substituted 1,2,3,4-Tetrahydroisoquinolines for the Synthesis of 3,4-Dihydroisoquinolin-1(2*H*)-ones and Isoquinolin-1(2*H*)-ones. *Adv. Synth. Catal.* **2021**, *363*,1390-1400. (b) Bhoite, S. P.; Bansode, A. H.; Suryavanshi, G. Radical Rearrangement of Aryl/Alkylidene Malononitriles via Aza Michael Addition/Decynoformylation/Addition Sequence: An Access to α-Aminonitriles and α-Aminoamides. *J. Org. Chem.* **2020**, *85*, 14858-14865. (c) More, S. G.; Kamble, R. B.; Suryavanshi, G. Oxidative Radical-Mediated Addition of Ethers to Quinone Imine Ketals: An Access to Hemiaminals. *J. Org. Chem.* **2021**, *86*, 2107-2116.

16   Mukherjee, A.; Ansari, AJ.; Reddy, S. R.; Das, G. K.; Singh, R. Mechanistic Investigations for the Formation of Active Hexafluoroisopropyl Benzoates Involving Aza-Oxyallyl Cation and Anthranils. *Asian J. Org. Chem.* **2020**, 9. 2136-2143.

17   Jung, y.; Kim, I. C3 functionalization of indolizines via In(III)-catalyzed three-component reaction. Org. Biomol. Chem., 2015, 13, 10986–10994.

18   (a) Romero, N. A.; Nicewicz, D. A. Organic Photoredox Catalysis. *Chem. Rev.* **2016**, *116*, 10075-10166 (b) Prier, C. K.; Rankic, D. A.; MacMillan, D. W. C. Visible Light Photoredox Catalysis with Transition Metal Complexes: Applications in Organic Synthesis. *Chem. Rev.* **2013**, *113*, 5322-5363 (c) Xi, Y.; Yi, H.; Lei, A. Synthetic Applications of Photoredox Catalysis with Visible Light. *Org. Biomol. Chem.* **2013**, *11*, 2387-2403. (d) Narayanam, J. M. R.; Stephenson, C. R. J. Visible Light Photoredox Catalysis: Applications in Organic Synthesis. *Chem. Soc. Rev.* **2011**, *40*, 102-113. (e) Reckenthaler, M.; Griesbeck, A. G. Photoredox Catalysis for Organic Syntheses. *Adv. Synth. Catal*. **2013**, *355*, 2727-2744.

19   (a) Crisenza, G. E. M.; Mazzarella, D.; Melchiorre, P. Synthetic Methods Driven by the Photoactivity of Electron Donor-Acceptor Complexes. *J. Am. Chem. Soc.* **2020**, *142*, 5461-5476 (b) Yuan, Y.-Q.; Majumder, S.; Yang, M.-H.; Guo, S.-R. Recent advances in catalyst-free photochemical reactions *via* electron-donor-acceptor (EDA) complex process. *Tetrahedron Letters* **2020**, *61*, (8),151506.

20   (a) Lima, C. G. S.; Lima, T. de M.; Duarte, M.; Jurberg, I. D.; Paixao, M. W. Organic Synthesis Enabled by Light-Irradiation of EDA Complexes: Theoretical Background and Synthetic Applications. *ACS Catal.* **2016**, *6*, 1389-1407.

21   Rosokha, S. V.; Kochi, J. K. Fresh Look at Electron-Transfer Mechanisms via the Donor/Acceptor Bindings in the Critical Encouter Complex. *Acc. Chem. Res.* **2008**, *41*, 641-653.

22   (a) Mulliken, R. S. Molecular Compounds and their Spectra. II. *J. Am. Chem. Soc.* **1952**, *74*, 811-824. (b) Cao, Z.-Y.; Ghosh, T.; Melchiorre, P. Enantioselective radical conjugate additions driven by a photoactive intramolecular iminium ion-based EDA complex. *Nat. Commun.* **2018**, *9*, 3274-3283. (c) Liu, J.; Zhua, Z.; Liu, F. Cyanofluorination of vinyl ethers enabled by electron donor-acceptor complexes, *Org. Chem. Front.*,

2019, *6*, 241-244.

23   (a) Singh, G. S.; Mmatli, E. E. Recent progress in synthesis and bioactivity studies of indolizines. *Eur. J. Med. Chem.* **2011**, *46*, 5237-5257 (b) Chai, W.; Breitenbucher, J. G.; Kwok, A.; Li, X.; Wong, V.; Carruthers, N. I.; Lovenberg, T. W.; Mazur, C.; Wilson, S. J.; Axe, F. U.; Jones, T. K. Non-imidazole heterocyclic histamine H₃ receptor antagonists. *Bioorg. Med. Chem. Lett.*, **2003**, *13*, 1767-1770 (c) Dawood, K. M.; Abbas, A. A.; Inhibitory activities of indolizine derivatives: a patent review. https://doi.org/10.1080/13543776.2020.1798402

24   (a) Michael, J. P. Indolizidine and quinolizidine alkaloids. *Nat. Prod. Rep.*, **2008**, *25*, 139-165. (b) Movassaghi, M.; Ondrus, A. E.; Chen, B. Efficient and Stereoselective Dimerization of Pyrroloindolizine Derivatives Inspired by a Hypothesis for the Biosynthesis of Complex Myrmicarin Alkaloids. *J. Org. Chem.* **2007**, *72*, 10065-10074.

25   (a) Chen, S.; Xia, Z.; Nagai, M.; Lu, R.; Kostik, E.; Przewloka, T.; Song, M.; Chimmanamada, D.; James, D.; Zhang, S. Novel Indolizine Compounds as Potent Inhibitors of Phosphodiesterase IV (PDE4): Structure-Activity Relationship. *Med. Chem. Commun.* **2011**, *2*, 176-180 (b) Yang, H.; Wang, H.-W.; Zhu, T.-W.; Yu, L.-M.; Chen, J.-W.; Wang, L.-X.; Shi, L.; Li, D.; Gu, L.-Q.; Huang, Z.-S.; An, L.-K. Syntheses and Antibacterial Activity of Soluble 9-Bromo Substituted Indolizinoquinoline-5,12-dione Derivatives. *Eur. J. Med. Chem.* **2017**, *127*, 166-173. (c) Yang, R.; Chen, Y.; Pan, L.; Yang, Y.; Zheng, Q.; Hu, Y.; Wang, Y.; Zhang, L.; Sun, Y.; Li, Z.; Meng, X. Design, Synthesis and Structure-Activity Relationship Study of Novel Naphthoindolizine and Indolizinoquinoline-5,12-dione Derivatives as IDO1 Inhibitors. *Bioorg. Med. Chem.* **2018**, *26,* 4886-4897. (d) Zheng, L.; Gao, T.; Ge, Z.; Maa, Z.; Xu, J.; Ding, W.; Shena, L. Design, Synthesis and Structure-Activity Relationship Studies of Glycosylated Derivatives of Marine Natural Product Lamellarin D. *Eur. J. Med. Chem.* **2021**, *214*, 1132262 (e) Sharma, V.; Kumar, V. Indolizine: a biologically active moiety. *Med. Chem. Res.* **2014**, *23,*3593-3606. (f) Kim, E.; Lee, Y.; Lee, S.; Park, S. B. Discovery, Understanding, and Bioapplication of Organic Fluorophore: A Case Study with an Indolizine-Based Novel Fluorophore, Seoul-Fluor. *Acc. Chem. Res.* **2015**, *48*, 538-547. (g) Park, S.; Kwon, D. I.; Lee, J.; Kim, I. When Indolizine Meets Quinoline: Diversity-Oriented Synthesis of New Polyheterocycles and Their Optical Properties. *ACS Comb. Sci.* **2015**, *17*, 459-469.

26   (a) Sadowski, B.; Klajn, J.; Gryko, D. T. Recent advances in the synthesis of indolizines and their π-expanded analogues. *Org. Biomol. Chem.* **2016**, *14*, 7804-7828. (b) Shen, Y. M.; Grampp, G.; Leesakul, N.; Hu, H. W.; Xu, J.-H. Synthesis and Emitting Properties of the Blue-Light Fluorophores Indolizino[3,4,5-ab]isoindole Derivatives. *Eur. J. Org. Chem.* **2007**, *22*, 3718-3726. (c) Sung, J.; Lee, Y.; Cha, J. H.; Park, S. B.; Kim, E. Development of fluorescent mitochondria probe based on 1,2- dihydropyrrolo[3,4-b] indolizine-3-one. *Dyes Pigm.* **2017**, *145*, 461-468. (d) Yang, D-T.; Radtke, J.; Mellerup, S. K.; Yuan, K.; Wang, X.; Wagner, M.; Wang, S. One-Pot Synthesis of Brightly Fluorescent Mes2B-Functionalized Indolizine Derivatives via Cycloaddition Reactions. *Org. Lett.* **2015**, *17*, 2486-2489.

27   Bertallo, C. R. d. S.; Arroio, T. R.; Toledo, M. F. Z. J.; Sadler, S. A.; Vessecchi, R.; Steel, P. G.; Clososki, G. C. C-H Activation/ Metalation Approaches for the Synthesis of Indolizine Derivatives. *Eur. J. Org. Chem.*

2019, *2019*, 5205-5213.

28   (a) Wang, C.; Jia, H.; Li, Z.; Zhang, H.; Zhao, B. Palladium-Catalyzed C-3 Desulfitative Arylation of Indolizines with Sodium Arylsulfinates and Arylsulfonyl Hydrazides. *RSC Adv*. **2016**, *6,* 21814-21821. (b) Park, C.-H.; Ryabova, V.; Seregin, I. V.; Sromek, A. W.; Gevorgyan, V. Palladium Catalyzed Arylation and Heteroarylation of Indolizines. *Org. Lett.* **2004**, *6,* 1159-1162.

29   Sun, J.; Wang, F.; Shen, Y.; Zhi, H.; Wu, H.; Liu, Y. Palladium-catalyzed direct and regioselective C-H acyloxylation of indolizines. *Org. Biomol. Chem*., **2015**, *13*, 10236-10243

30   Yang, L.; Pu, X.; Niu, D.; Fu, Z.; Zhang, X. Copper-Catalyzed Asymmetric Propargylation of Indolizines. *Org. Lett.* **2019**, *21*, 8553- 8557

31   Kim, W.; Kim, H. Y.; Oh, K. Oxidation Potential-Guided Electrochemical Radical-Radical Cross-Coupling Approaches to 3-Sulfonylated Imidazopyridines and Indolizines. *J. Org. Chem.* **2021**, *86*, 22, 15973-15991**.**

32   Zhanga, Y-Z.; Sheng, F-T.; Zhu, Z.; Li, Z-M.; Zhang, S.; Tan, W.; Shi, F. Organocatalytic C3-Functionalization of Indolizines: Synthesis of Biologically Important Indolizine Derivatives. *Org. Biomol. Chem.*, **2020***,18*, 5688-5696.

33   Liu, X.; Song, D.; Zhang, Z.; Lin, J.; Zhuang, C.; Zhan, H.; Cao, H. Regioselective C-H dithiocarbamation of indolizines with tetraalkylthiuram disulfide under metal-free conditions. *Org. Biomol. Chem.*, **2021***,19*, 5284-5288

34   (a) Zhang, Y.; Yu, Y.; Liang, B.; Pei, Y-y.; Liu, X.; Yao, H.; Cao, H. Synthesis of Pyrrolo[2,1,5-cd] indolizine Rings *via* Visible-Light Induced Intermolecular [3+2] Cycloaddition of Indolizines and Alkynes. *J. Org. Chem.* **2020**, *85*, 10719-10727 (b) Liang, Y.; Teng, L.; Wang, Y.; He, Q.; Cao, H. A Visible-Light Induced Intermolecular [3 + 2] Alkenylation-Cyclization Strategy: Metal-Free Construction of Pyrrolo[2,1,5-cd] indolizine Rings. *Green Chem.* **2019**, *21*, 4025-4029.

35   Penteado, F.; Gomes, C. S.; Monzon, L. I.; Perin, G.; Silveira, C. C.; Lenardão, E. J. Photocatalytic Synthesis of 3-Sulfanyl- and 1,3- Bis(sulfanyl)indolizines Mediated by Visible Light. *Eur. J. Org. Chem.* **2020**, 2110-2115.

36   Teng, L.; Liu, X.; Guo, P.; Yu, Y.; Cao, H. Visible-Light-Induced Regioselective Dicarbonylation of Indolizines with Oxoaldehydes via Direct C-H Functionalization. *Org. Lett.* **2020**, *22*, 10, 3841-3845.

37   Mane, K. D.; Kamble, R. B.; Suryavanshi, G. A visible light mediated, metal and oxidant free highly efficient cross dehydrogenative coupling (CDC) reaction between quinoxalin-2(1H)-ones and ethers. *New J. Chem.*, **2019***,43*, 7403-7408.

38   Runemark, A.; Zacharias, S. C.; Sunden, H. Visible-Light-Driven Stereoselective Annulation of Alkyl Anilines and Dibenzoylethylenes via Electron Donor-Acceptor Complexes. *J. Org. Chem.* **2021**, *86*, 1901-1910.

39   (a) C. Hu, F-Q. Shen, G. Feng, J. Jin. Visible-Light-Induced α-Amino C-H Bond Arylation Enabled by Electron Donor-Acceptor Complexes. *Org. Lett.* **2021**, *23*, 10, 3913-3918. (b) V. Quint, N. Chouchène, M. Askri, J. Lalevée, A-C. Gaumonta, S. Lakhdar. Visible-light-mediated α-phosphorylation of N-aryl tertiary amines through the formation of electron donor-acceptor complexes: synthetic and mechanistic studies. *Org.*

Chem. Front., **2019**, *6,* 41-44. (c) J. Kaur, A. Shahin, J. P. Barham. Photocatalyst-Free, Visible-Light-Mediated C (sp3)-H Arylation of Amides via a Solvent-Caged EDA Complex. *Org. Lett.* **2021,** *23*, 6, 2002-2006. (d) L. Zheng, Y-E. Qian, Y-Z. Hu, J-A, Xiao, Z-P, Ye, K. Chen, H-Y, Xiang, X-Q. Chen, H. Yang. O-Perhalopyridin-4-yl Hydroxylamines: Amidyl-Radical Generation Scaffolds in Photoinduced Direct Amination of Heterocycles. *Org. Lett.* **2021**, *23*, 5, 1643-1647.

40   Watanabe, K.; Terao, N.; Niwa, T.; Hosoya,T. Direct 3-Acylation of Indolizines by Carboxylic Acids for the PracticalSynthesis of Red Light-Releasable Caged Carboxylic Acids. *J. Org. Chem.* **2021**, 86, 11822-11834.

Chapter IV

Synthesis of Congested Indolizine Amides from In-situ Generated Azaoxyallyl Cations and Ti-superoxide Catalysed Oxidative Amidation of Aldehydes

1. **Mane, K. D.;** More, S. G.; Suryavanshi, G. "Metal-free Regioselective C-3 Alkylation of Indolizines with in Azaoxyallyl Cations Generated Situ from α-bromoamides" (*Manuscript under preparation)*

2. Kamble, R. B.; **Mane, K. D.;** Rupanawar, B. D.; Korekar, P.; Suryavanshi, G. "Ti-Superoxide Catalyzed Oxidative Amidation of Aldehydes with Saccharin as Nitrogen Source: Synthesis of Primary Amides" *RSC Adv*., **2020**, *10*, 724-728

Section I

Metal-free Regioselective C-3 Alkylation of Indolizines with Azaoxyallyl Cations Generated In-situ from α-Bromoamides

4.1.1 Introduction

Functionalized Indolizine heterocycle plays a crucial role in both pharmaceuticals and materials chemistry.[1] It shows various biological activities such as antimicrobial, anticancer, antiproliferative, anti-inflammatory, and antitubercular activity.[2] In the past decade, numerous studies on indolizine skeletons exhibit their suitability for employment in organic electroluminescent (organic EL) diode and dye-sensitized solar cells (DSSC).[3]
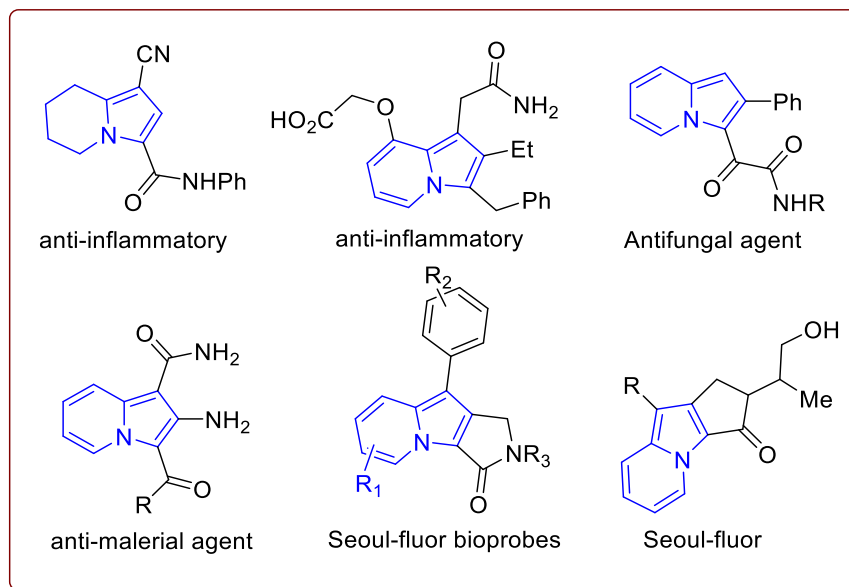
Figure 1: Some important indolizine derivatives

Indolizines substituted amides are essential scaffolds that show various biological activities such as anti-inflammatory, antifungal, and antimalarial agents, as shown in Figure 1.[2,4] Therefore considering the practical application of indolizine derivatives in medicinal and material chemistry, developing efficient and straightforward methods for synthesizing their analog is

highly desirable. Indolizine is generally synthesized from pyridines and pyrroles by applying a plethora of synthetic methods.[5] The π-excessive nature of the indolizine ring can easily undergo an electrophilic substitution reaction at C-3 or C-1 position.[6]

4.1.2 Review of Literature

Various reports are available for the selective C-3 substitution of indolizines rings in literature, such as arylation, heteroarylation,[7] decarbonylations[8] thiolations[9], etc. Nevertheless, selective alkylation of indolizine at the C-3 position is rarely explored.[10] Azaoxyallyl cation, an impermanently formed reactive species, has attracted considerable attention in constructing of important nitrogen-containing heterocycles.[11] Recently the azaoxyallyl cation as a 1,3-dipoles has been widely applied in [4+3], [3+3], and [3+2] cycloaddition reactions. Those are with cyclopentadienes, furan, dienes, azides, and carbonyl compounds to produce important heterocycles.[12] Remarkably, the direct nucleophilic addition at α-position of azaoxyallyl cation intermediate generated from α-broamides is rarely reported.

Amination on Azaoxyallyl Cations [13]
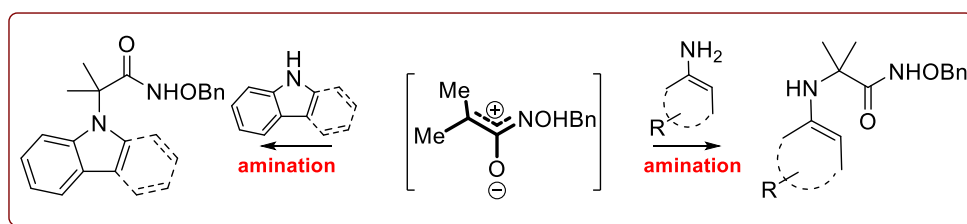
Scheme 1: Amination of azaoxyallyl cations

To date, only limited examples of direct nucleophilic substitution at α-position of bromoamides *via* azaoxyallyl cation intermediate has been reported for the synthesis of *α*-substituted carbonyl compounds (Scheme 1). In 2020 Singh and co-workers reported the metal-free amination of congested alkyl bromides at ambient temperature. When *α*-broamides in the presence of sodium

carbonate as a base and HFIP is solvent generates reactive species azaoxyallyl cation. This in situ generated azaoxyallyl cation is then functionalized using amine nucleophiles.

Cycloaddition Reaction on Azaoxyallyl Cation (2017)[12]
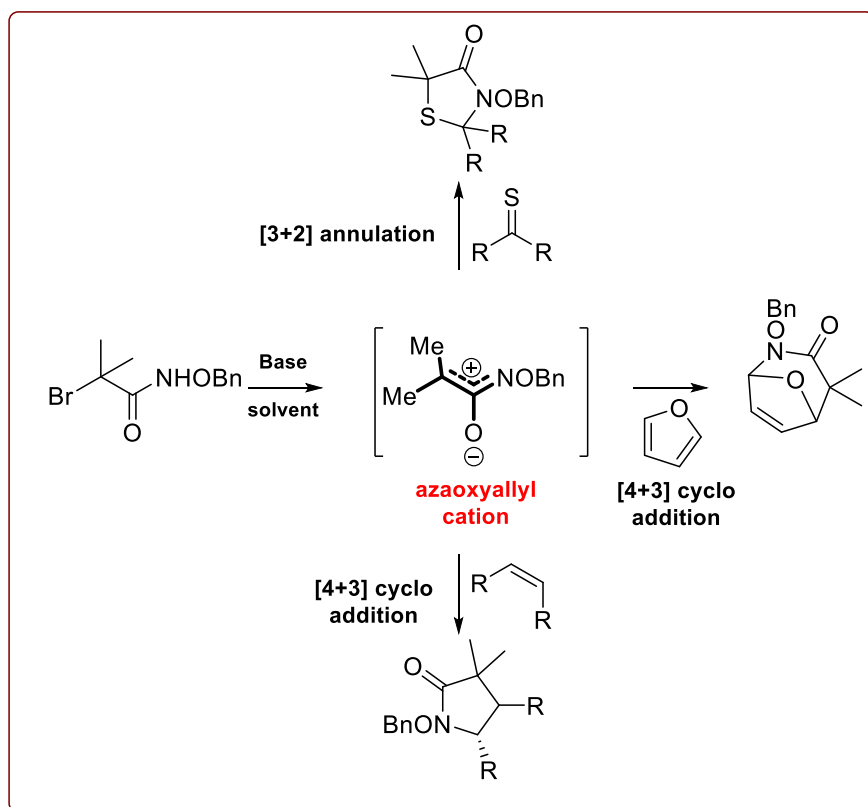
Scheme 2. Cycloaddition reactions on azaoxyallyl cations

Azaoxyallyl cation generated from alkyl bromides is highly reactive species and it can further functionalized by using various dienes, thioketones, furans and anthranils. Jeffrey and co-workers in 2011 reported the [4+3] cycloaddition reaction of cyclopentadiene and furan with reactive azaoxyallyl cation for the synthesis of heterocyclic ring system. Further, reactive species were utilized by Saha and the group in 2019 for the synthesis of thiazolidin-4-ones by using thiocarbonyls *via* the [3+2] annulation strategy. Also, various dienes and anthranils are beneficial species for the synthesis of important heterocyclic compounds by using azaoxyallyl cation

4.1.3 Present Work

4.1.3.1 Objective

Very recently Kim and co-workers reported the nucleophilic alkoxylation of in situ generated azaoxyallyl cation to synthesize hindered dialkyl ether derivatives.[14] Encouraged by these excellent results and our continuous efforts towards C-H activation of heteroarenes,[15] herein we have described the metal-free C-3 alkylation of indolizines by using α-bromohydroxamates in basic condition.
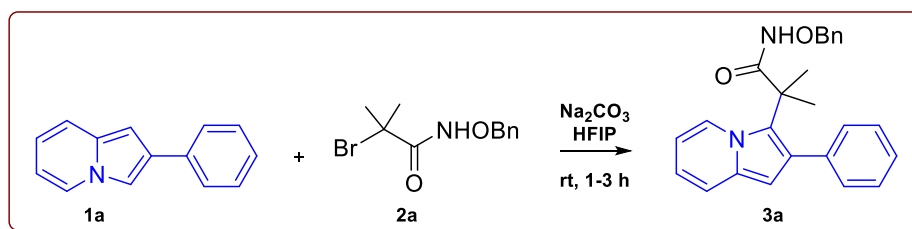
Scheme 3. C-3 alkylation of indolizine

4.1.4 Result and Discussion

We started our investigation by taking indolizine **1a** and α-bromohydroxamates **2a** as a model substrate, and the results are summarised in Table 1.

Initially, the reaction was carried out using indolizine **1a** (1 equiv.) and α-bromohydroxamates **2a** as the aza-oxyallyl cation precursor (1.1 equiv.) by using sodium carbonate (2 equiv.) as the base in DCM for 12 hours but failed to give the expected product **3a** (Table 1, entry 1). Then we have checked the utility of other routine solvents such as MeCN, DCE, 1,4-dioxane, THF, and DMSO, and the results show that none of the above solvents are effective for the formation of desired product **3a** (Table 1, entries 2-6). It is noteworthy that the expected product **3a** was obtained in 91% yield when the reaction was carried out by using HFIP as the solvent within 3 hours of reaction time (Table 1, entry 7). However, no significant improvement in the yields of

the product was observed with the use of different combinations of bases (Table 1, entries 8-11).

Further usage of 1:1 mixture of HFIP and DCE gave the corresponding product **3a** only in trace

amount (Table 1, entry 12).

Table 1. Optimization of Reaction Conditions[a]
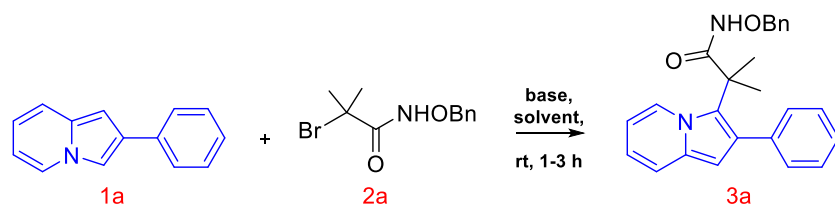
Sr. no	solvent	Base (equiv.)	Time (h)	Yield of 3a
1	DCM	Na_2CO_3	12	0
2	MeCN	Na_2CO_3	12	0
3	DCE	Na_2CO_3	12	0
4	1,4-Dioxane	Na_2CO_3	12	0
5	THF	Na_2CO_3	12	0
6	DMSO	Na_2CO_3	12	0
7	**HFIP**	**Na_2CO_3**	**3**	**91**
8	HFIP	K_2CO_3	3	71
9	HFIP	Cs_2CO_3	3	67
10	HFIP	NaOH	3	55
11	HFIP	DBU	3	76
12	HFIP/DCE (1:1)	Na_2CO_3	3	Trace

[a] Reaction condition: 1a (1 equiv., xx mmol), 2a (1.1 equiv., xx mmol),
Na_2CO_3 (2.5 equiv., xx mmol) and HFIP (1 ml) at room temperature

Therefore we achieved the best regioselectivity and excellent yield of **3a** using 1 equiv.

indolizine, 1.1 equiv. α-bromohydroxamates, and 2.5 equiv. sodium carbonate as a base and

HFIP as solvent at room temperature (Table 1, entry 7). With the optimized reaction in hand (Table 1, entry 7), we attempted the α-substitution of various indolizines with α-bromoamides, as shown in Table 2.

Table 2. Substrate Scope for Indolizines
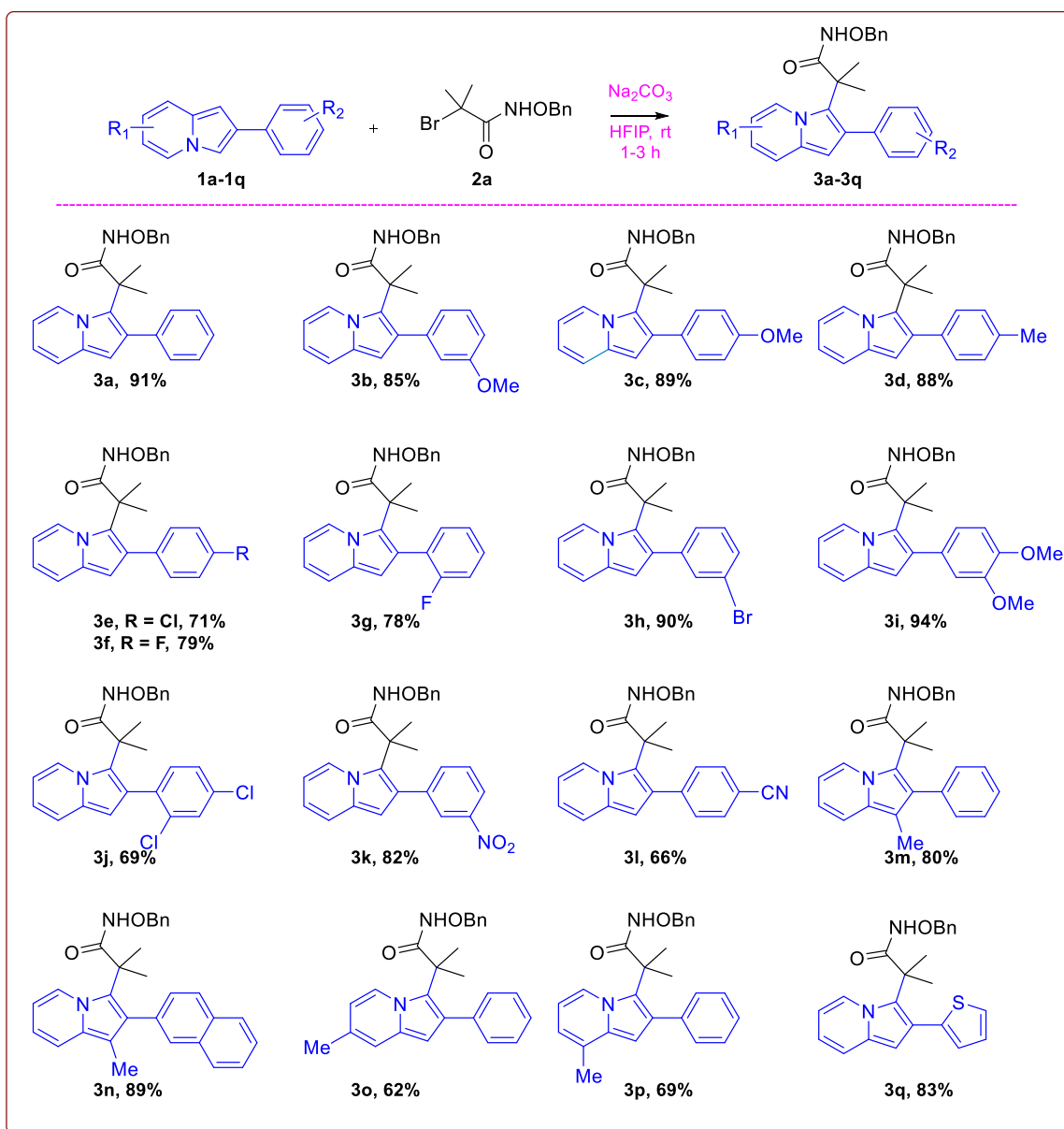
Reaction condition: 1a (1 equiv.,), 2a (1.1 equiv.,), Na$_2$CO$_3$ (2.5 equiv.,) and HFIP (1 ml) at room temperature for 1 to 3 h.

Indolizines substituted with a broad range of functional groups on reaction with in situ generated azaoxyallyl cation from alkyl bromides produce good to excellent yields of the corresponding products (Table 2). Substituted indolizines having electron-donating group, halogens on phenyl ring produce the desired products in 69-94% yields (Table 2, entries **3a-3j**). Electron-withdrawing group substituted indolizines ring also gives the excellent yields of the desired C-3 functionalized indolizineamides in excellent yields (entries, **3k** and **3l**). Also, indolizines substituted with C1, C3, and C7 positions can yield the expected products in good yields (entries, **3m-3p**). Heterocyclic indolizine produces the desired product **3q** in 83% yield.
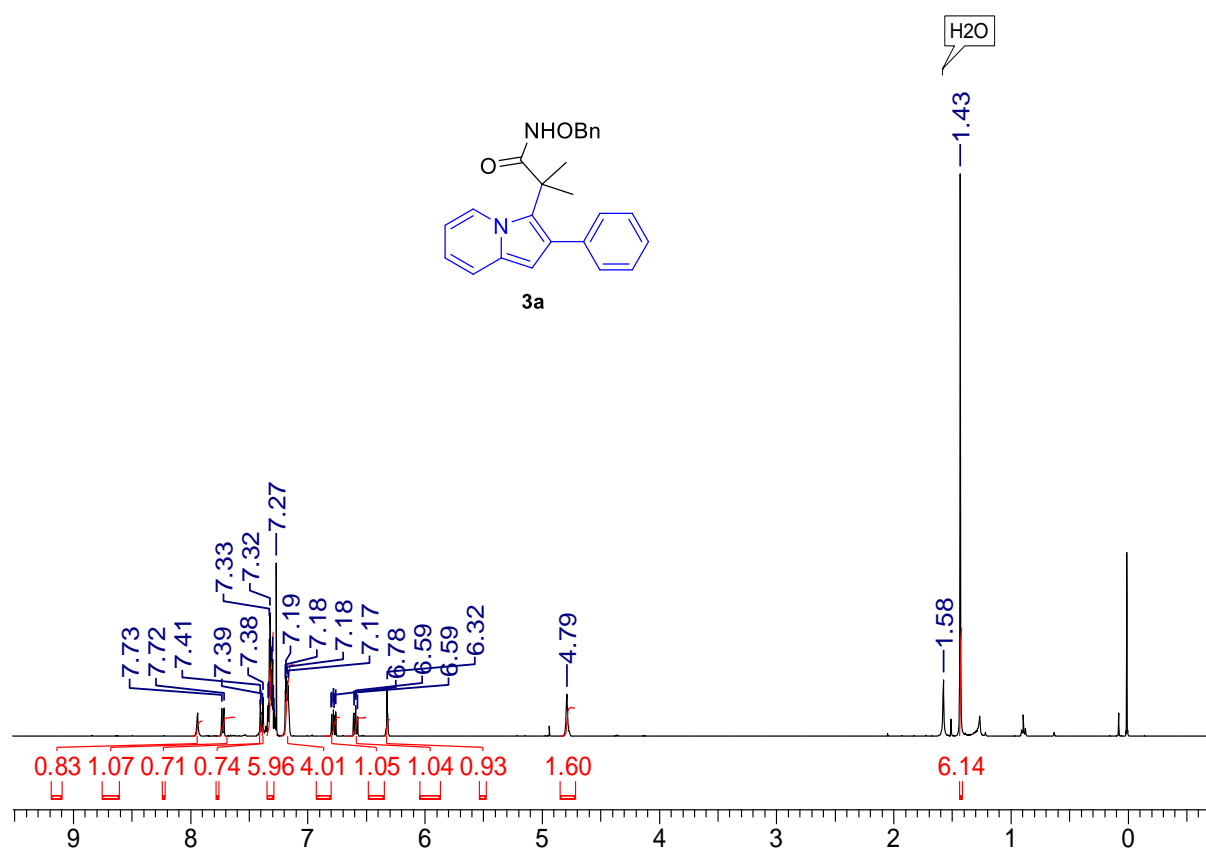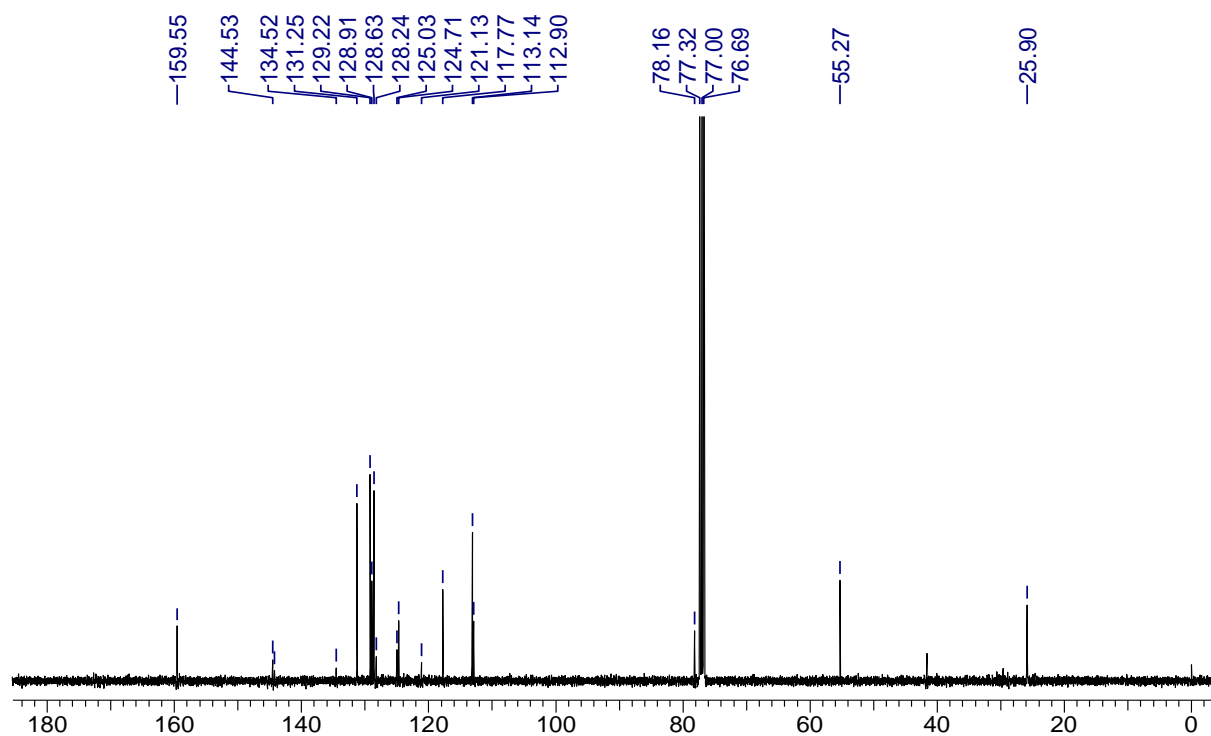
Figure 2. ^{1}H and ^{13}C NMR of *N*-(benzyloxy)-2-methyl-2-(2-phenylindolizin-3-yl)propanamide **(3a)**

Example 1:

The structure of *N*-(benzyloxy)-2-methyl-2-(2-phenylindolizin-3-yl) propanamide **3a** was confirmed from its ^{1}H and ^{13}C NMR spectrum. In ^{1}H NMR spectrum δ 1.43 (s, 6 H), for two methyl group hydrogens. Benzylic hydrogens of the CH$_2$ group are shown in the region δ 4.79 (s, 2 H), and aromatic hydrogens showed in the range of *δ* 6.32-7.73. In ^{13}C NMR spectrum of the compound, **3a** showed the amide peak of the carbonyl group at *δ* 159.5 (**Figure 2**).

Next, we examined the reactivity of other functional groups substituted alkyl bromides reaction with indolizine, and the results are summarized in Table 3. The broad range of alkyl bromides with electron-releasing and electron-withdrawing groups reacted with indolizine produces excellent yields of the expected products (**5a-5g**). Alkyl bromide substituted with halogens such as I, Cl, and Br gives excellent yields of the desired C-3 substituted indolizines (Table 3, entries **5a, 5b,** and **5d**). Electron withdrawal on alkyl bromide is also suitable for forming desired

products in good yields (Table 3, entries **5c** and **5e**). Other alkyl group substituted alkyl bromides are not suitable for forming azaoxyallyl cation and resulted in 0% yields of expected products (entries, **5h**, and **5i**).

Example 2:

The structure of **5g** was confirmed by using ^{1}H and ^{13}C NMR analysis (Fig. 3). In the ^{1}H NMR spectrum, the characteristic peak of 6 hydrogens of two methyl groups is shown at δ 1.43 (s, 6H),

Table 3. CDC Reaction between Aromatic Aldehydes and Cyclic Ethers[a]
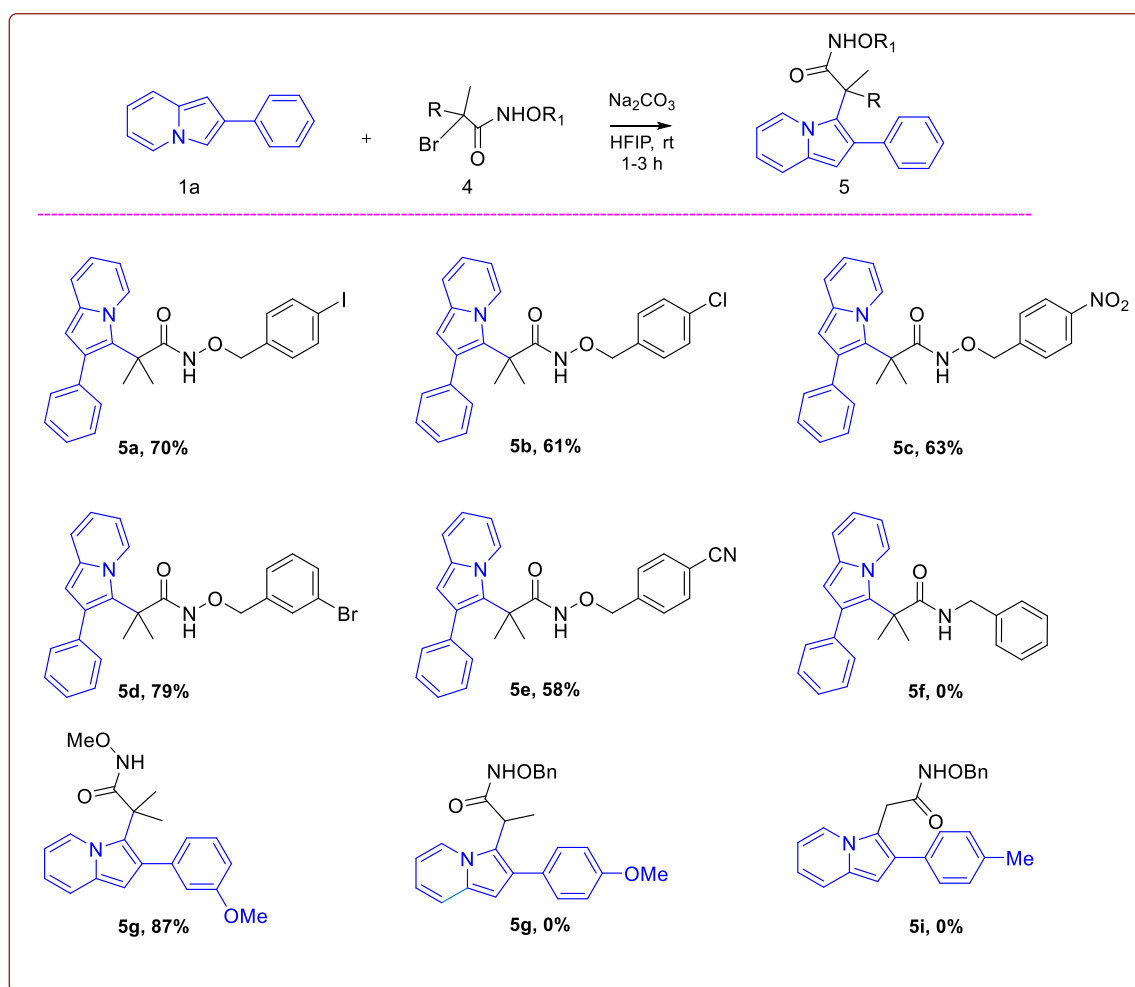
[a]Reaction condition: 1a (1 equiv.,), 4 (1.1 equiv.,), Na$_2$CO$_3$ (2.5 equiv.,) and HFIP (1 mL) at room temperature for 1 to 3 h.

and two methoxy groups present in the structure are shown at δ 2.05 and 3.66, respectively. Aromatic hydrogen's demonstrated in the range of δ 6.55-7.64. In ^{13}C, the NMR spectrum shows the aliphatic carbons in the range of δ 8.7-64.1 and aromatic carbons δ 108.6-174.5. After successful scope for substituted indolizine and alkyl bromide, we have proposed the possible reaction mechanism for the present transformation (Scheme 4). When alkyl bromide is reacted with the base in hexafluoroisopropanol, it will generate an azaoxyallyl cation intermediate. The formed azaoxyallyl cation then reacts with nucleophilic indolizine moiety to generate the cationic species **3**, which on further aromatization gives the desired product **3a**.
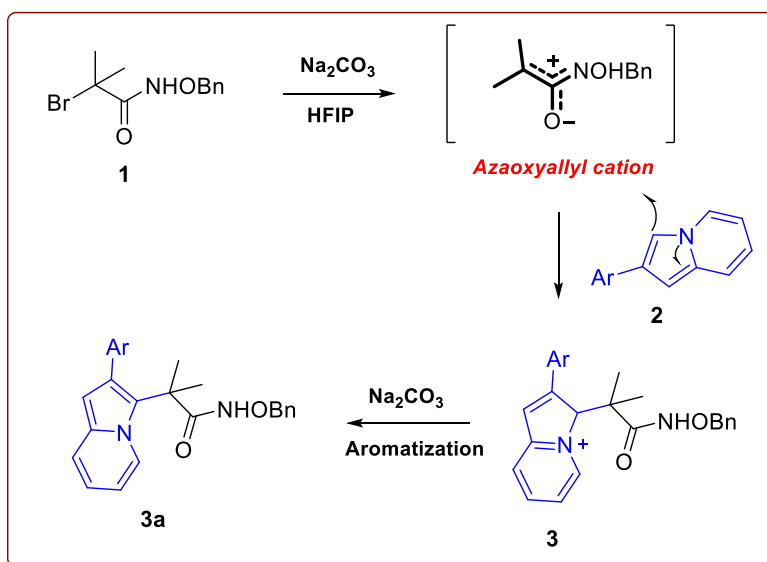
Scheme 4: Reaction mechanism

4.1.5. Conclusion

In conclusion, we have developed the regioselective $C(sp^2)$-H bond functionalization of indolizines from in-situ generated azaoxyallyl cations from alkyl bromides. The key features of the present protocol are metal-free, good to excellent yields, and easy operations. The current method is applicable for synthesizing functionally important derivatives of congested indolizine

amides. Further trapping of in situ generated azaoxyallyl cation is under progress in our laboratory.
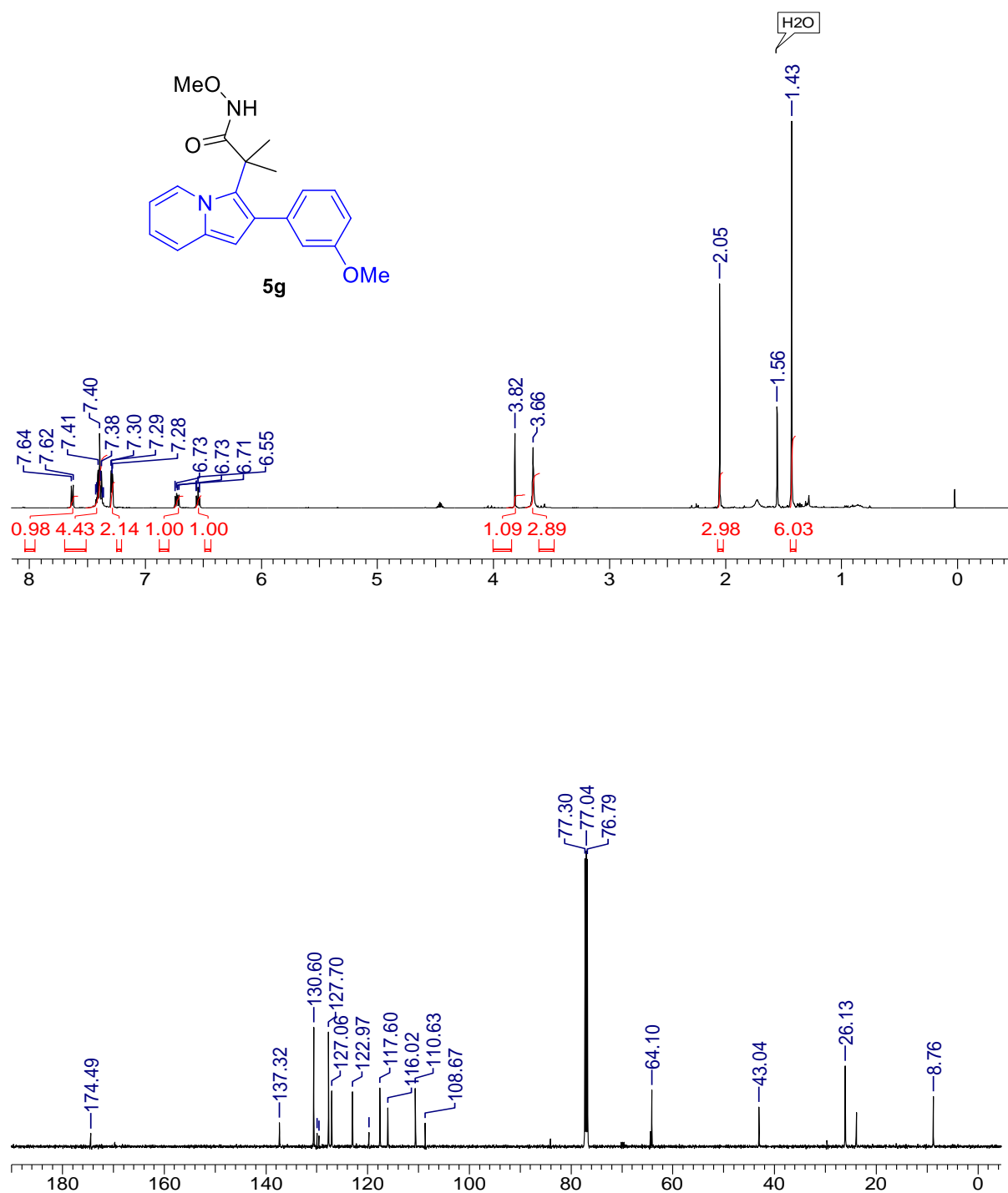
Fig. 3: ^{1}H and ^{13}C NMR of N-methoxy-2-methyl-2-(1-methyl-2-phenylindolizin-3-yl)propanamide

4.1.6. Experimental Section

Experimental Procedure for the Synthesis of *N*-(benzyloxy)-2-methyl-2-(2-phenylindolizin-3-yl)propanamide (3a): Indolizine **1a** (1 equiv.) was added in HFIP 1 mL, followed by the addition of *α*-bromohydroxamates 2a (1.1 equiv.) and anhydrous sodium carbonate (2.5 equiv.). Then the reaction mixture is stirred at room temperature for 3 hours. After completion of the reaction (monitored by TLC), the crude residue is purified by using flash column chromatography (100-200 mesh silica using 80/20 petroleum ether/ethyl acetate as the eluent to afford the corresponding product 3a as a white colored sticky liquid in 91% yield.

N-(benzyloxy)-2-methyl-2-(2-phenylindolizin-3-yl)propanamide (3a).

White colored gummy liquid, yield: 91% (74 mg).^{1}H NMR (400 MHz, CDCl$_3$) δ 7.72 (d, *J* = 7.3 Hz, 1H), 7.41 (t, *J* = 1.2 Hz, 1H), 7.38 (t, *J* = 1.2 Hz, 1H), 7.35 - 7.29 (m, 6H), 7.18 (dt, *J* = 1.6, 4.7 Hz, 4H), 6.78 (ddd, *J* = 0.9, 6.5, 8.9 Hz, 1H), 6.68 - 6.50 (m, 1H), 6.32 (s, 1H), 4.79 (s, 2H), 1.43 (s, 6H). ^{13}C NMR (101 MHz, CDCl$_3$) δ 159.5, 144.5, 144.3, 134.5, 131.2, 129.2, 128.9, 128.6, 128.2, 125.0, 124.7, 121.1, 117.8, 113.1, 112.9, 78.2, 55.3, 25.9.

N-(benzyloxy)-2-(2-(3-methoxyphenyl)indolizin-3-yl)-2-methylpropanamide (3b).

faint yellow gummy liquid; ^{1}H NMR (400 MHz , CDCl$_3$) δ 7.92 (s, 1H), 7.63 (d, *J* = 7.1 Hz, 1 H), 7.35 - 7.25 (m, 2H), 7.21 - 7.17 (m, 2H), 7.16 - 7.10 (m, 1H), 7.07 (d, *J* = 6.3 Hz, 2H), 6.79 (ddd, *J* = 0.9, 2.6, 8.3 Hz, 1H), 6.74 - 6.71 (m, 1H), 6.70 - 6.65 (m, 2H), 6.54 - 6.38 (m, 1H), 6.24 (s, 1H), 4.68 (br. s., 2H), 3.72 (s, 3H), 1.37 (s, 6H). ^{13}C NMR (101 MHz , CDCl$_3$) δ 173.9, 158.6, 139.6, 134.6, 132.3, 129.3, 128.7, 128.6, 128.5, 128.2, 123.4, 123.0, 120.1, 119.1, 117.5, 116.2, 112.1, 111.0, 102.6, 78.2, 55.2, 43.1, 26.0.

N-(benzyloxy)-2-(2-(4-methoxyphenyl)indolizin-3-yl)-2-methylpropanamide (3c).

^{1}H NMR (500 MHz , CDCl$_3$) δ 8.02 (s, 1 H), 7.44 - 7.37 (m, 5 H), 7.18 (d, *J* = 6.9 Hz, 2 H), 7.15 - 7.06 (m, *J* = 8.4 Hz, 2 H), 6.93 - 6.85 (m, 2 H), 6.78 (dd, *J* = 6.5, 8.8 Hz, 1 H), 6.67 - 6.48 (m, 1 H), 6.32 (s, 1 H), 4.80 (s, 2 H), 3.99 - 3.80 (m, 3 H), 1.45 (s, 6 H). ^{13}C NMR (126 MHz, CDCl$_3$) δ 174.0, 158.7, 134.7, 131.1, 129.4, 128.8, 128.7, 128.6, 128.6, 123.5, 119.1, 117.5, 112.8, 111.0, 103.0, 78.2, 55.3, 30.5, 26.2, 23.9

N-(benzyloxy)-2-(2-(4-fluorophenyl)indolizin-3-yl)-2-methylpropanamide (3f)

^{1}H NMR (500 MHz , CDCl$_3$) δ 7.96 (br. s., 1 H), 7.71 (d, *J* = 7.2 Hz, 1 H), 7.42 - 7.35 (m, 2 H), 7.33 - 7.29 (m, 2 H), 7.17 (d, *J* = 6.9 Hz, 2 H), 7.14 - 7.09 (m, 2 H), 7.03 - 6.95 (m, 2 H), 6.84 - 6.72 (m, 1 H), 6.64 - 6.49 (m, 1 H), 6.29 (s, 1 H), 4.79 (s, 2 H), 1.42 (s, 6 H). ^{13}C NMR (126 MHz , CDCl$_3$) δ 173.8, 163.0, 161.1, 134.7, 134.2, 132.4, 131.6, 131.5, 129.4, 129.0, 128.8, 128.6, 123.5, 120.4, 119.1, 117.7, 114.4, 114.2, 111.2, 102.9, 78.2, 43.2, 26.2. ^{19}F NMR (376 MHz, CDCl$_3$) δ -115.58.

N-(benzyloxy)-2-(2-(3,4-dimethoxyphenyl)indolizin-3-yl)-2-methylpropanamide (3i)

^{1}H NMR (500 MHz , CDCl$_3$) δ 8.00 (s, 1 H), 7.74 (d, *J* = 7.2 Hz, 1 H), 7.41 (d, *J* = 9.2 Hz, 1 H), 7.35 - 7.26 (m, 3 H), 7.18 (d, *J* = 6.9 Hz, 2 H), 6.85 - 6.76 (m, 3 H), 6.73 (dd, *J* = 1.9, 8.0 Hz, 1 H), 6.65 - 6.54 (m, 1 H), 6.35 (s, 1 H), 4.80 (s, 2 H), 3.95 (s, 3 H), 3.85 (s, 3 H), 1.48 (s, 6 H). ^{13}C NMR (126 MHz , CDCl$_3$) δ 174.1, 148.2, 147.9, 134.8, 132.3, 130.8, 129.7, 129.4, 128.8, 128.5, 123.4, 122.6, 120.4, 119.1, 117.6, 113.7, 111.1, 110.2, 102.9, 78.2, 55.9, 55.9, 43.2, 26.1

Experimental Procedure for the Synthesis (5a):

Indolizine **1a** (1 equiv.) was added in HFIP 1 mL, followed by the addition of α-bromohydroxamates 4 (1.1 equiv.) and anhydrous sodium carbonate (2.5 equiv.). Then the reaction mixture is stirred at room temperature for 2 hours. After completion of the reaction (monitored by TLC), the crude residue is purified using flash column chromatography (100-200

mesh silica using 80/30 petroleum ether/ethyl acetate as the eluent to afford the corresponding product **5a** as a white colored gummy liquid in 70% yield**.**

N-methoxy-2-methyl-2-(1-methyl-2-phenylindolizin-3-yl)propanamide (5g)

^{1}H NMR (500 MHz , CDCl$_3$) δ 7.63 (d, *J* = 7.2 Hz, 1 H), 7.51 – 7.33 (m, 5 H), 7.31 – 7.26 (m, 2 H), 6.73 (dd, *J* = 6.5, 8.8 Hz, 1 H), 6.57 – 6.52 (m, 1 H), 3.82 (s, 1 H), 3.66 (s, 3 H), 2.05 (s, 3 H), 1.43 (s, 6 H). ^{13}C NMR (126 MHz, CDCl$_3$) δ 174.5, 137.3, 130.6, 130.0, 129.6, 127.7, 127.1, 123.0, 119.8, 117.6, 116.0, 110.6, 108.7, 64.1, 43.0, 26.1, 8.8.

Section II

Ti-Superoxide Catalyzed Oxidative Amidation of Aldehydes with Saccharin as Nitrogen Source: Synthesis of Primary Amides

4.2.1 Introduction

The amide bond constituting the structural backbone of proteins and peptides is abundantly found in natural products, pharmaceuticals, polymers, and agrochemicals.[16] In particular, primary amides ($RCONH_2$) play an important role in organic synthesis as building blocks exhibiting a wide range of industrial applications and pharmacological interests[17] (Fig. 4). Traditionally, amide synthesis has been achieved by the reaction of an amine with an activated carboxylic acid derivative that often employs coupling reagents.[18]
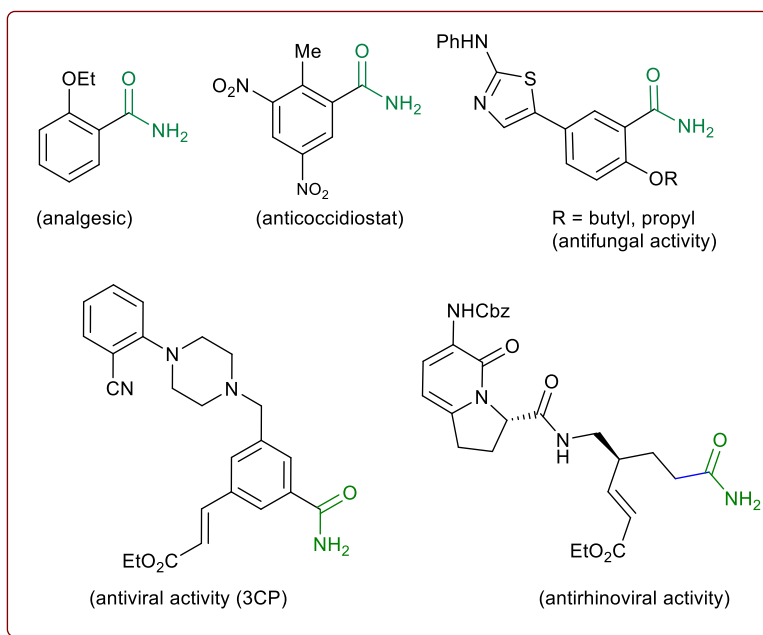
Figure 4. Some biologically important primary amides

Subsequently, several alternate strategies[19] emerged for amide formation that includes: (i) the Staudinger reaction; (ii) the Schmidt reaction; (iii) the Beckmann rearrangement; (iv)

hydroamination of alkynes; (v) dehydrogenative amidation of alcohols; (vi) hydroaminocarbonylation of alkenes; (vii) iodonium promoted nitroalkene amine coupling reaction; (viii) transamidation of primary amides; etc.

4.2.2 Review of Literature

In this context, oxidative amidation of aldehydes with amine salts are synthetically preferred and has been achieved with a variety of reagent systems[20] (e.g., I$_2$, NBS, MnO$_2$, 3,3',5,5'-tetra-*tert*-butyldiphenoquinone and TBHP as oxidant, *N*-heterocyclic carbene, transition metals such as Pd, Rh, Ru, Ni, Cu/Ag, Fe. Au, Pt, and lanthanides). It may also be noted that several researchers have developed catalyst-free methods using TBHP and H$_2$O$_2$ as oxidants.[21] Quite recently, visible light was utilized to trigger a photoredox catalytic oxidative amidation of aldehydes.[22] This reaction, however, relied on phenazinium salt, rose Bengal, or anthraquinone-based organophotocatalyst and air as the oxidant. Also, oxidative amidation of methylarenes catalyzed by Mn or Fe in combination with NH$_3$ or urea as amine source and oxidants has been reported [23] for amide synthesis (**Scheme 5**).
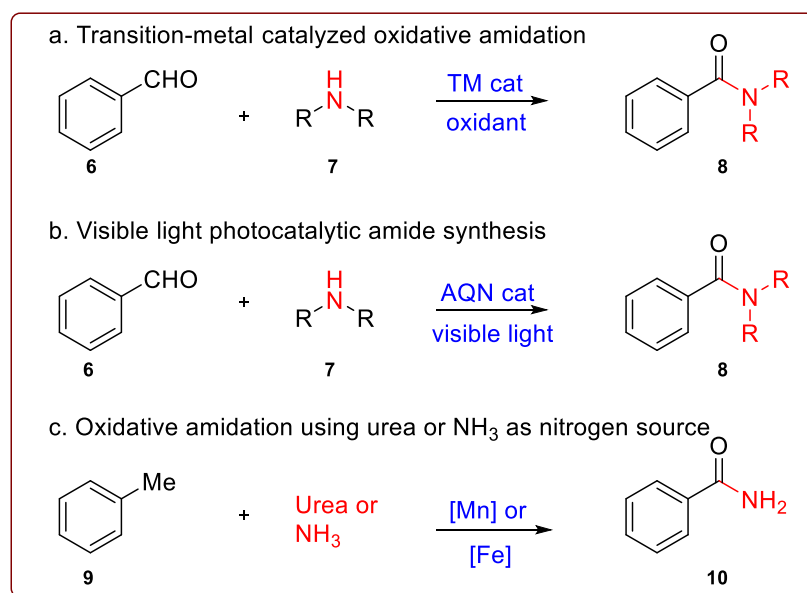
Scheme 5: Traditional amidation methods

Yuan's Work (2016)[5d]

Recently, Yuan and co-workers showed that heteropolyanion-based ionic liquids catalyzed oxidative amidation of aldehydes by using various primary and secondary amines in good yields (**Scheme 6**).
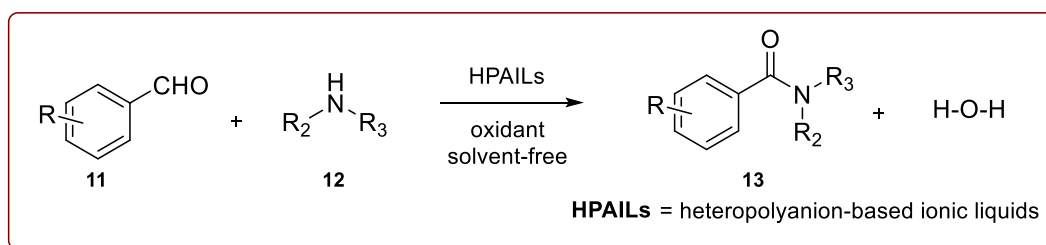
Scheme 6. HPAIL catalyzed amidation of aldehyde

The key feature of this methodology is that it is solvent-free, and various amines are tolerated in this approach. Furthermore, the catalyst used for this transformation is easily reusable, but the HPAIL is more costly than our heterogeneous catalysis method. Generally, various primary and secondary amines are required as amine sources in this work.

Maji's Work (2017)[5k]
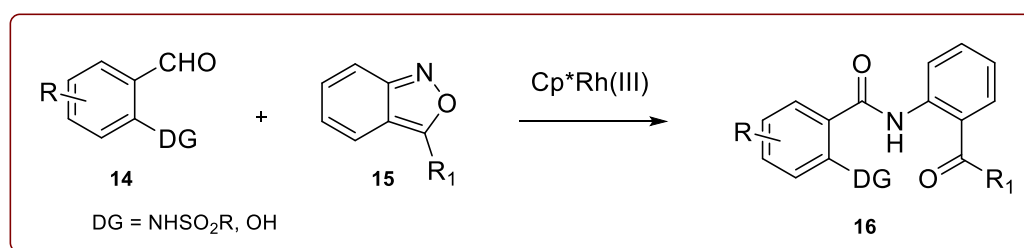
Scheme 7. Cp*Rh(III) catalysed direct amidation of aldehyde

In 2017 Maji and a co-worker developed the chelation-assisted Rh catalyzed oxidative amidation of aldehyde by using anthranil as the amine source (**Scheme 7**). In this work, the scope of aldehyde is limited, and generally, the aldehyde requires directing groups. The key advantages of

this protocol are catalytic amount of metal is required, and it is oxidant free. The incorporation of costly metals and limited substrate scope are a few limitations of this work. Also, the yield of a few substrates is significantly less as the reaction requires complex reagents.

4.2.3 Present Work

4.2.3.1 Objectives

The existing methods utilize homogeneous, rare, and costly transition metals as a catalyst. Also, these homogeneous reaction mixtures did not allow the recyclability of used metals. To the best of our knowledge, metal-catalyzed direct oxidative amidation of aldehydes under heterogeneous conditions has not been explored. In this strategy, we wish to report Ti-superoxide catalyzed oxidative amidation of aldehydes and catalyst reused for more than three catalytic cycles (**scheme 8**).
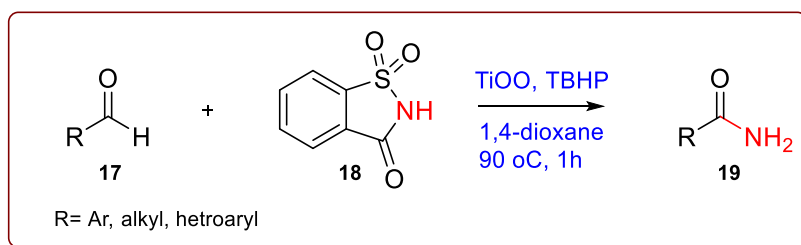
Scheme 8. Oxidative amidation of aldehyde

Saccharin (**2**) is an artificial sweetener used in the production of various foods and pharmaceutical products. It is also used in the preparation of disubstituted amines from halides via nucleophilic substitution followed by Gabriel synthesis.[24] Some time ago, we have reported an elegant synthesis and catalytic applications of exceptionally stable titanium superoxide for C-O, C-N, and C-Br bond-forming reactions.[25]

It was interesting to explore the cross dehydrogenative coupling between benzaldehyde and saccharin under Ti-superoxide catalysis in the presence of TBHP as an oxidant to produce N-

benzoylsaccharin (**8**). Surprisingly, the reaction underwent oxidative amidation to produce benzamide (56%). Thus, to develop a general condition for amide synthesis, we proposed that saccharin (**2**) could serve as a nitrogen source. In this paper, we wish to report, for the first time, that titanium superoxide efficiently catalyzes oxidative amidation of aldehydes under indeed heterogeneous conditions to produce primary amides (**3**) in excellent yields employing saccharin (**2**), an amine source, and TBHP as oxidant (**Scheme 8**).

4.2.4 Results and Discussion

Table 4 shows the optimization studies of oxidative amidation of anisaldehyde with saccharin as amine source over Ti-superoxide using TBHP as oxidant.

Table 4: Optimization of oxidative amidation of anisaldehyde with saccharin as amine source over Ti-superoxide [a]
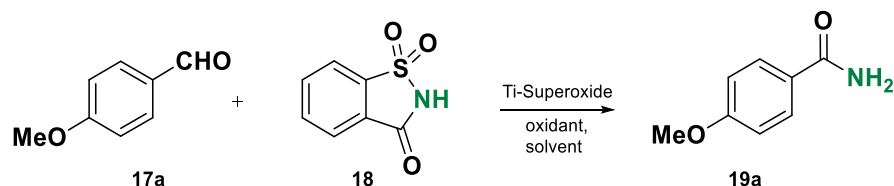
Entry	Catalyst [b] (wt%)	Oxidant (equiv.)	Solvent	T (°C)	Time (h)	Yield (%) [c]
1	10	TBHP (1)	DCE	25	12	N R
2	10	TBHP (2)	DCE	90	12	19
3	10	TBHP (3)	DCE	90	12	22
4	10	TBHP (3)	1,4-dioxane	90	12	41 (22) [d]
5	20	TBHP (3)	1,4-dioxane	90	12	65
6	20	TBHP (3)	1,4-dioxane	90	8	71
7	20	TBHP (3)	1,4-dioxane	90	4	83
8	**20**	**TBHP (3)**	**1,4-dioxane**	**90**	**1**	**95**
9	20	TBHP (2)	1,4-dioxane	90	1	51
10	20	DTBP (3) or	1,4-dioxane	90	1	N R

		K$_2$S$_2$O$_8$ (3)				
11	20	30% H$_2$O$_2$ (3)	1,4-dioxane	90	1	11

Reaction conditions[a]: Anisaldehyde (1 mmol), saccharin (1.2 mmol), solvent (4 mL); [b]titanium superoxide; [c] isolated yield; d: 5-6 in hexane was m TBHP used; [d]temperature was 110 ⁰C

Anisaldehyde **17a** and saccharin **18** was chosen as model substrates for the optimization of reaction conditions. When they were combined in equimolar amounts in 1,2-dichloroethane with Ti-superoxide (10 wt %) as a catalyst at RT, no reaction took place (Table 4, entry 1). However, with an increase in TBHP concentration (2-3 equiv.) and temperature at 90 ^{o}C, amide **19a** was obtained in low yields (entries 2-3, 19-22%). With the change of solvent to 1,4-dioxane, a considerable improvement in yield of **19a** was achieved (41%). Further, an increase in temperature to 110 ^{o}C had a deleterious effect on yield (22%) (entry 4). When the catalyst concentration was increased to 20 wt%, yield of **19a** was increased to 65% (entry 5). Interestingly, a substantial improvement in yield was observed from 65 to 83% as the reaction time was decreased from 12 h to 4 h. Finally, a dramatic improvement in yield (95%) was realized by reducing time to 1 h. Further, reduction in TBHP concentration to 2 equiv. resulted in a lowered yield of amide **19a** (51%) (entry 9). Unfortunately, other solvents such as CH$_3$CN, DMSO, DMF, and THF were found to be unsuitable for the reaction. Also, several oxidants such as DTBP, K$_2$S$_2$O$_8$, H$_2$O$_2$, and other Ti catalysts (titanium silicalite-1 and TiO$_2$) were found to be less favored for oxidative amidation. It may be noted that the reaction failed to proceed with other amine sources such as ammonia or its salts (Cl$^-$, OAc$^-$ or NO$_3^-$) as well.

To determine the scope and limitations of this reaction, a wide range of aldehydes were reacted under the optimized reaction conditions (Table 4). In general, good to excellent yields of primary

amides were obtained in most cases. For instance, aromatic aldehydes, bearing electron-donating and electron-withdrawing groups in different ring positions, gave the desired products (**19a-w**) in good to excellent yields (27-95 %), indicating that the reaction is not sensitive to electronic

Table 5: Substrate scope for the oxidative amidation of aldehydes[a]

17a-17aaf
R = alkyl, aryl or ,heteroaryl

19

19 (a-z & aa-af)
Yield : 25-95%b

19a, R = H, 93%
19b, R = Me, 95%
19c, R = OMe, 91%
19d, R = t-Bu, 88%
19e, R = Cl, 79%
19f, R = I, 75%
19g, R = OH, 36%
19h, R = NH$_2$, 38%

19i, 78%

19j, R = NO$_2$, 71%
19k, R = F, 74%
19l, R = CF$_3$, 71%
19m, R = OMe, 84%

19n, R = Me, 91%
19o, R = I, 79%
19p, R = Br, 73%
19q, R = OH, 48%
19r, R = NH$_2$, 27%
19s, R = OEt, 79%

19t, R = NO$_2$, 72%
19u, R = Me, 95%

19v, R = F, R$_1$ = H; 85%
19w, R = H, R$_1$ = F; 81%

19x, R = H, 71%
19y, R = Br, 74%
19z, R = OH, 55%

19aa, R, R$_1$= OMe, 86%
19ab, R, R$_1$= Cl, 74%

19ac, n = 4, 42%
19ad, n = 6, 39%

19ae, 61%

19af, 25%
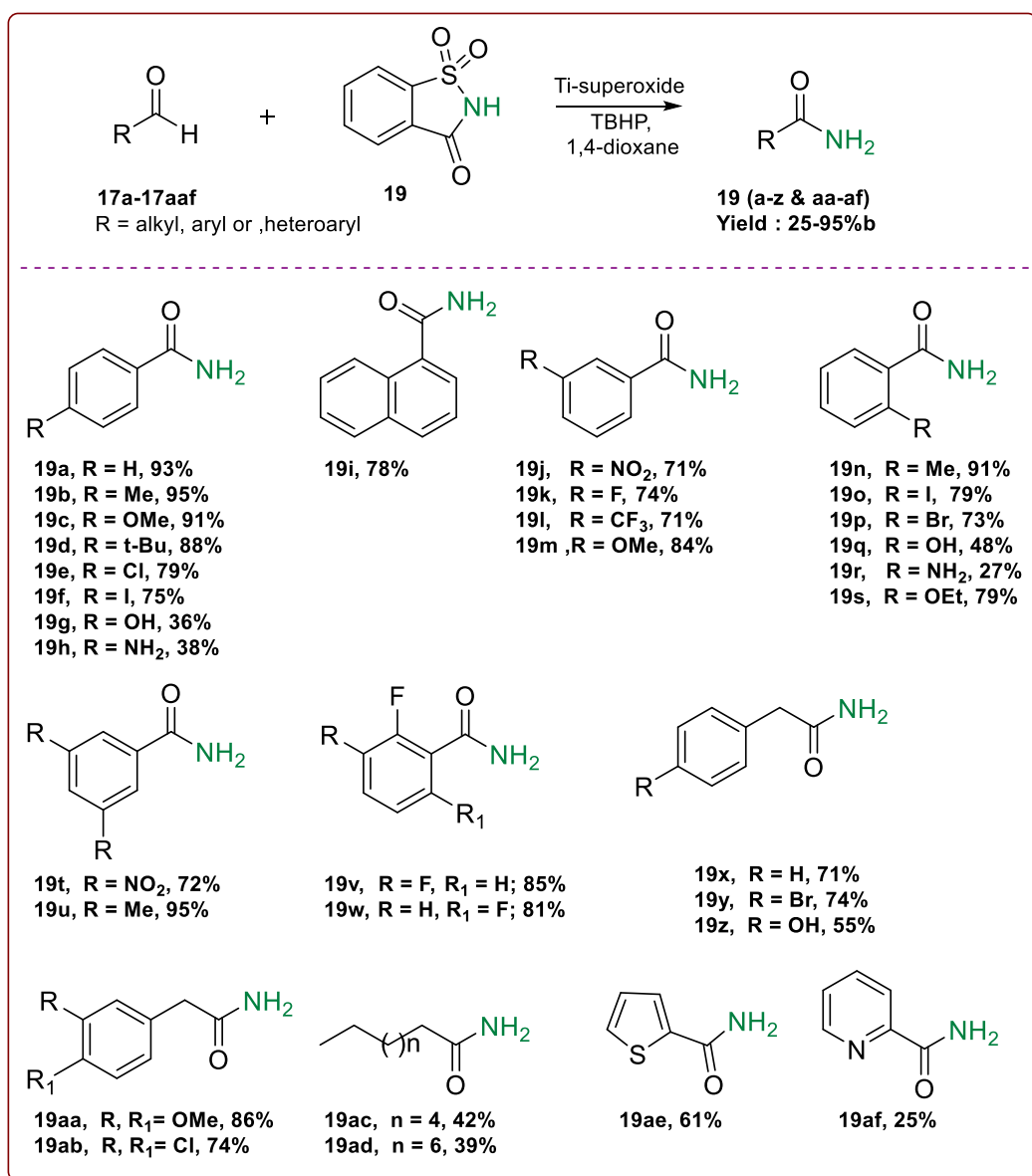
Reaction conditions: a: Aldehyde (1 mmol), saccharin (1.2 mmol),5-6 M TBHP in hexane (3 mmol), Ti-Superoxide (20 wt%), 1,4-dioxane (4 mL), 90 ^{o}C, 1 h: b : Isolated yield.

effects (Table 5). Thus, various functional groups with potential synthetic applications are well-suited for this reaction, although substrates with sensitive NH_2 and OH groups yielded a diminished yield (27-36%). Interestingly, phenyl acetaldehydes possessing a variety of substituents with different electronic effects (Br, OH, OMe and Cl) gave the desired primary amides (**19x-z** & **19aa-3ab**) in high yields (36-86%). Aliphatic (C_8- and C_{10}-), heteroaryl (2-thienyl and 2-pyridyl), and naphthyl aldehydes were tolerated as well, thus providing the desired amides (**19ae, 19af** & **19i**) in good yields (25-78%). Nevertheless, it should be noted that unsaturated aldehydes such as cinnamaldehyde and acrolein are less favored substrates under the oxidative amidation condition. The formation of **19a**-**19af** was confirmed and analyzed by ^{1}H, ^{13}C, and Mass data.

Example 1:

The confirmation of benzamide **(19a)** was done by its ^{1}H and ^{13}C NMR spectrum. In the ^{1}H NMR spectrum, the aromatic peaks displayed at δ 7.42-7.94, and N-H hydrogen showed at δ 8.07 (s, 1H). In the ^{13}C NMR spectrum of benzamide, the characteristic amide carbon showed at δ 168.62 and remaining saturated carbons in the range of δ 128-134(**3a**) (**Figure 5**).

In order to get an insight into the mechanism of this reaction, we have conducted the following two experiments (Scheme 8). When *N*-benzoyl saccharin **20** was subjected to the optimized reaction conditions, benzamide (**19a**) was indeed isolated in a 39% yield, confirming the involvement of **20** as the key intermediate.
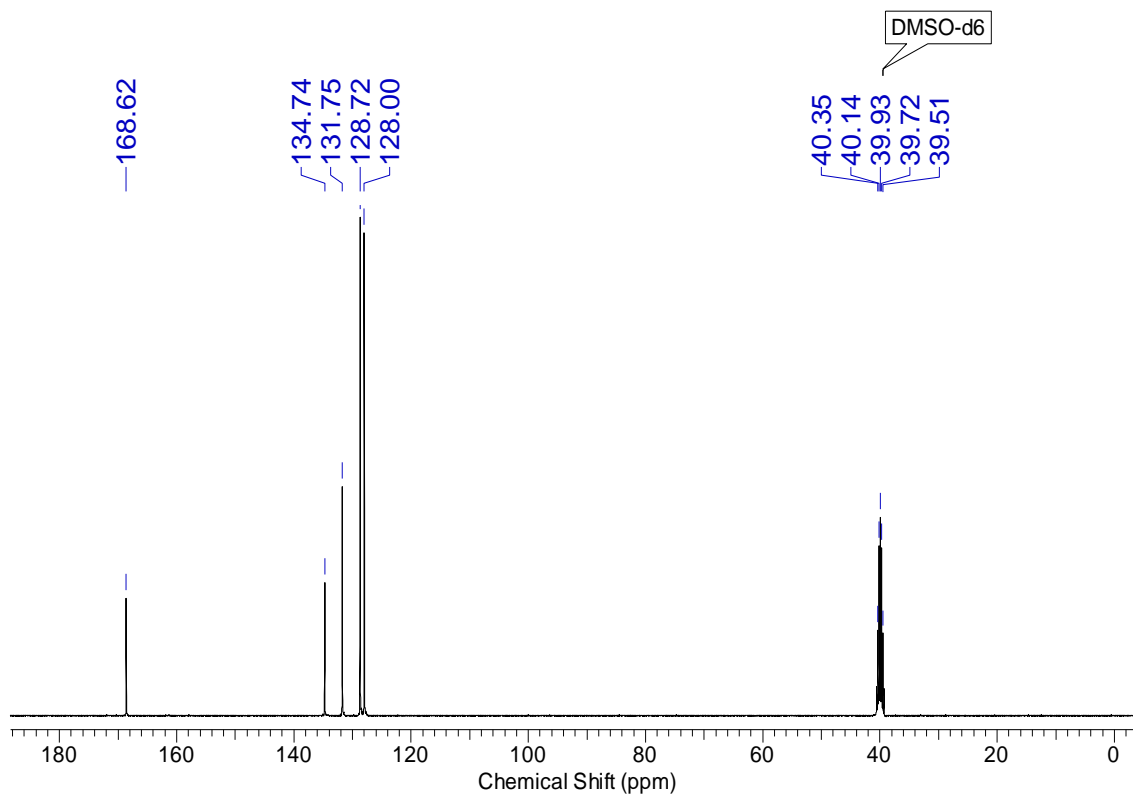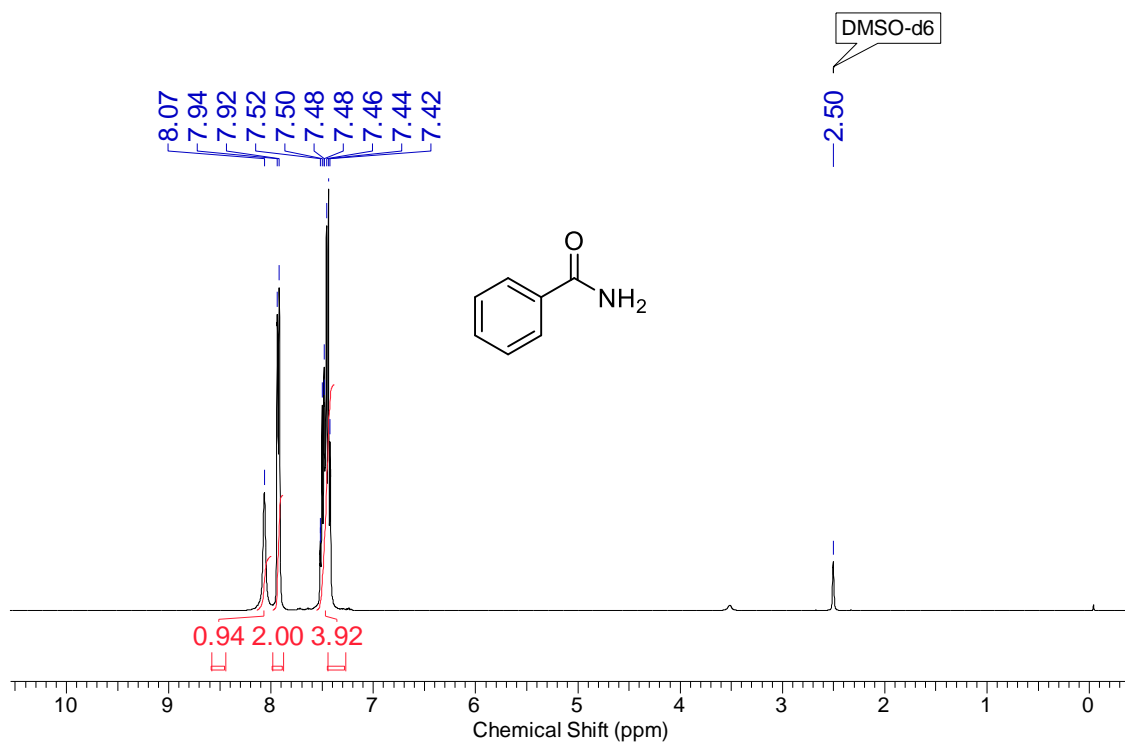
Figure 5. ^{1}H and ^{13}C NMR of benzamide (**19a**)
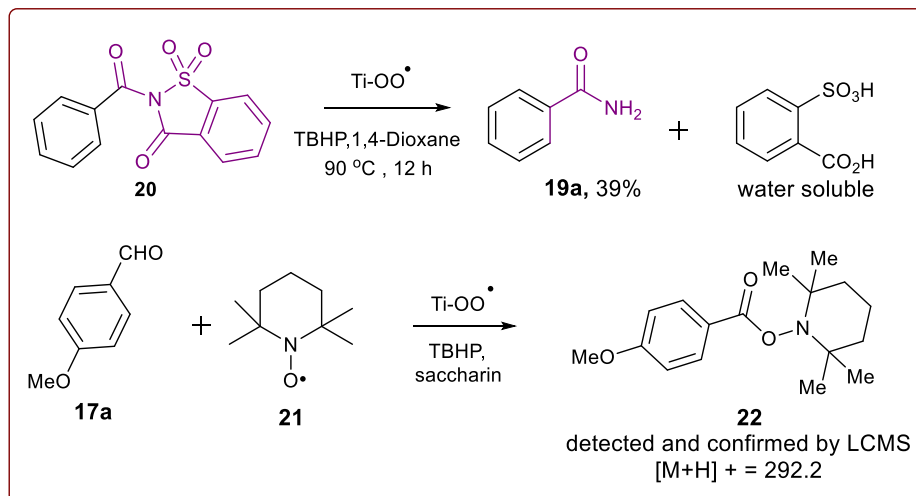
Scheme 8: Mechanistic studies to establish the involvement of radical pathway

Also, when oxidative amidation of anisaldehyde was carried out in the presence of radical scavenger TEMPO (1.1 equiv.), the corresponding TEMPO adduct **22** was detected and confirmed by LCMS, thus establishing the formation of benzoyl radical that underwent radical coupling in the reaction. Based on the above experiments and literature precedence,[26] a
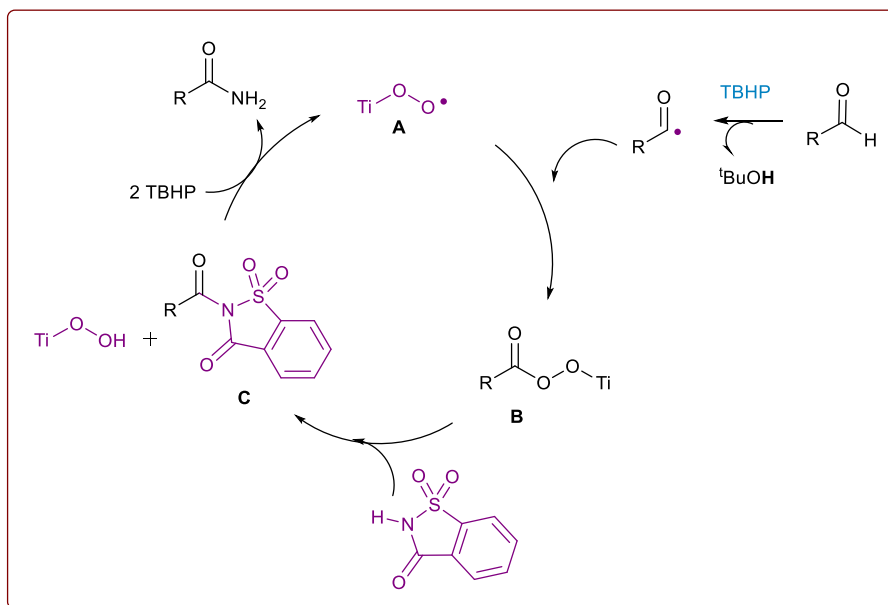
Scheme 9: Catalytic cycle for the oxidative amination of aldehydes

plausible catalytic cycle is proposed in Scheme 9. Initially, the combination of an acyl radical, generated from aldehyde on oxidation with TBHP, in the presence of Ti catalyst A produces Ti peroxo species B. Subsequently, B undergoes displacement with saccharin to produce *N*-acylsaccharin C along with TiOOH. Finally, 2 equiv. of TBHP is utilized: (i) to regenerate Ti catalyst A; (ii) to form amides from intermediate C *via* oxidative hydrolysis.
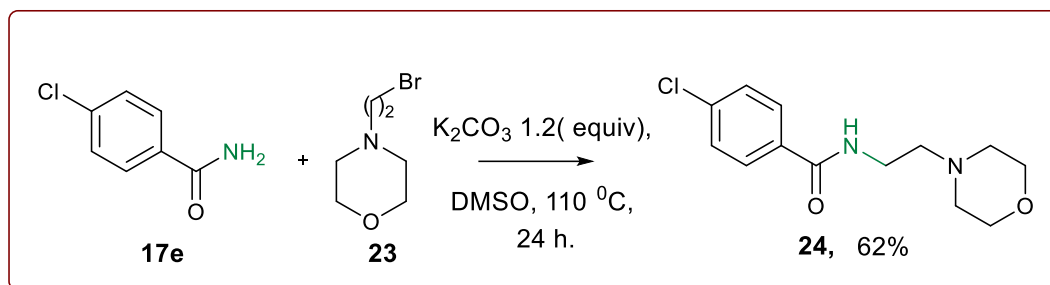
Scheme 10: Synthesis of moclobemide on 5 g scale
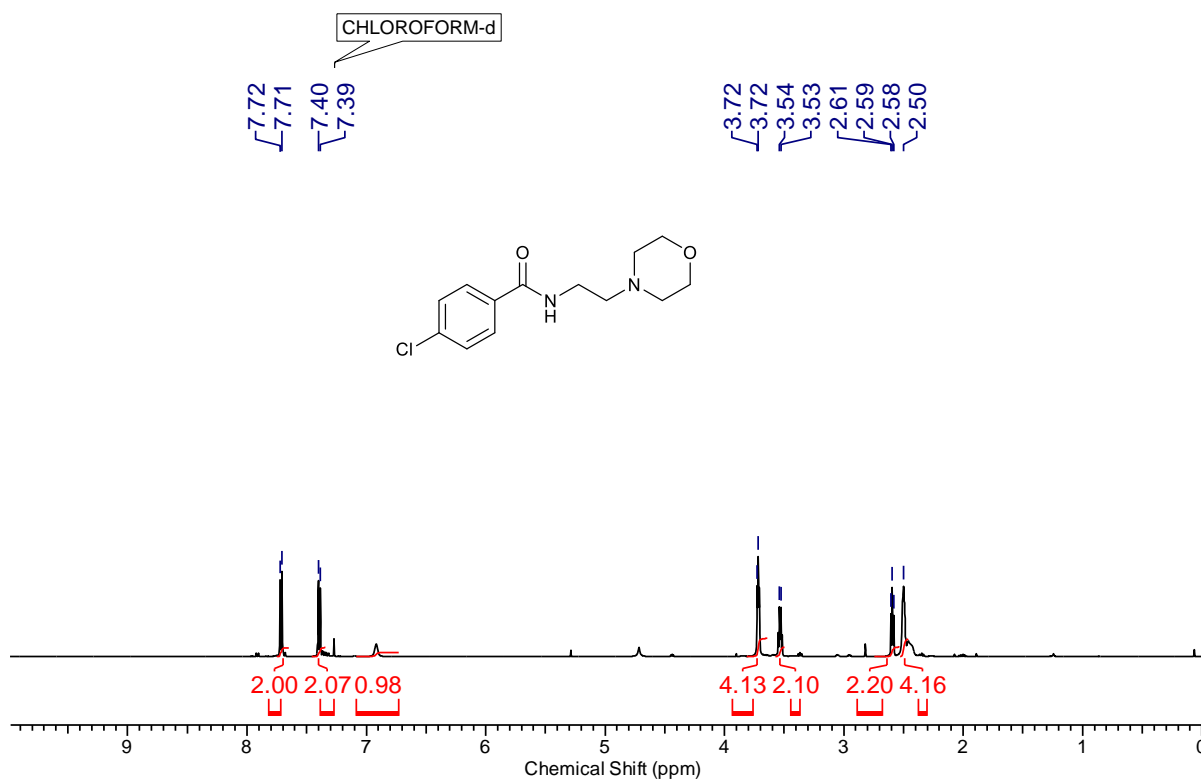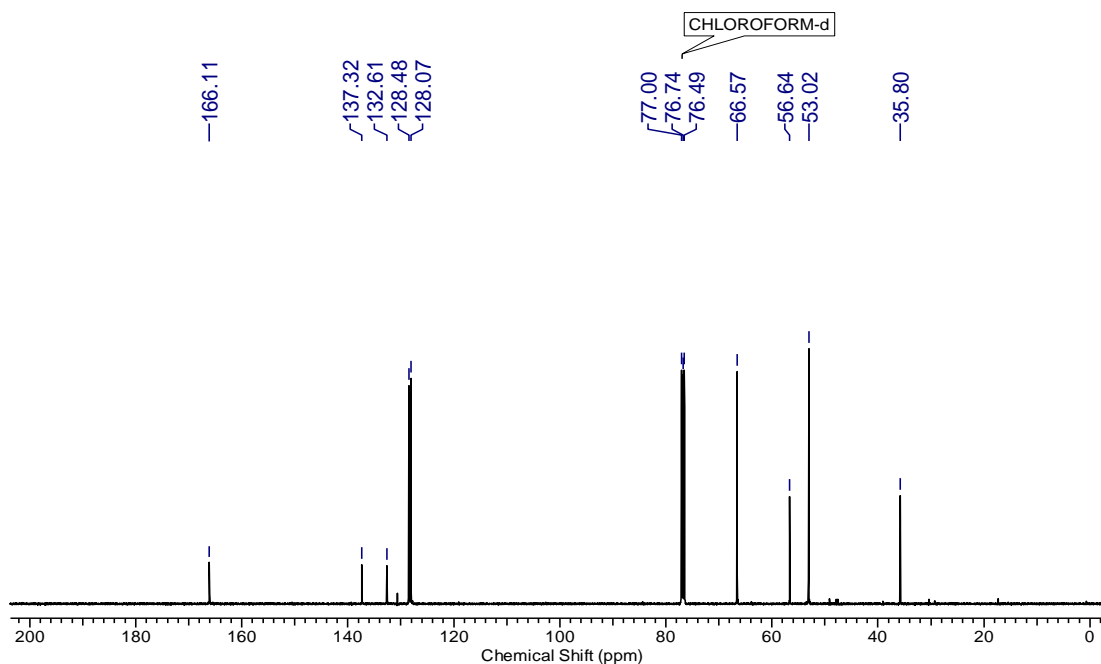
Figure 6. ^{1}H and ^{13}C NMR of Moclobemide (7)

This methodology is amply demonstrated in the synthesis of drugs, namely ethenzamide **19s** and moclobemide **24**. Scheme 10 shows the single-step synthesis of moclobemide, a reversible inhibitor of monoamine oxidase A *via N*-alkylation of **17e** with **23**.

Figure 7: Reusability studies of Ti catalyst[a]
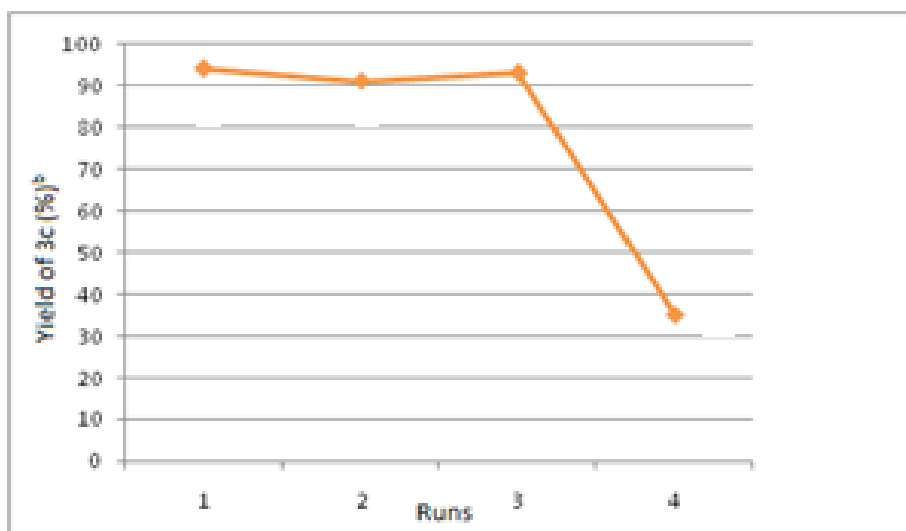
[a]Reaction conditions: Anisaldehyde (2 mmol), saccharin (2.4 mmol), TBHP (6 mmol), 1,4-dioxane, 90 $^{\circ}$C, 1 h; b: isolated yield.

Example 2:

Moclobemide formation was confirmed by measuring its ^{1}H,^{13}C NMR, and HRMS analysis (**Figure 6**). Aliphatic hydrogens showed in the range of δ 2.50 to 3.72 and aromatic four hydrogens in the range of δ 7.39-7.72. In carbon NMR, aliphatic carbons are displayed in the range of δ 35-66 and aromatic carbons in the range of δ 128-166. Fig. 7 shows the results of reusability studies. Ti-superoxide catalyst was readily recovered quantitatively by simple filtration and reused again at least for 3 cycles without the loss of catalytic activity (runs 1-3). The catalyst was performed ia a truly heterogeneous manner as no leaching of Ti was observed in the aqueous part.

4.2.5 Conclusion

In conclusion, we have described a simple, convenient, and environment-friendly protocol for primary amide synthesis directly from aldehydes using Ti-superoxide as a mild and cheap catalyst and saccharin as an amine source using TBHP oxidant. The presented strategy has several advantages that include: (i) Ti catalyst is recyclable; (ii) good functional group compatibility; (iii) wide range of substrate scope; (iv) mild reaction conditions; (v) no additives and can be easily scaled up; (vi) saccharin as cheaply available amine source. We envisage that this new catalytic method would be an alternative to other methods for primary amide synthesis.

4.2.6 Experimental Section

4.2.6.1 Preparation of the titanium superoxide catalyst:

Titanium tetraisopropoxide (Ti(OiPr)$_4$ (2.51 g, 0.0875 mmol) in anhydrous methanol (30 mL) was added to the stirred solution of 50% aq. H$_2$O$_2$ (3 g, 0.0875 mmol) for 30 min under a

nitrogen atmosphere with continuous stirring at room temp for 2 h. The yellow color solid formed was filtered on a sintered funnel, washed thoroughly with anhydrous methanol, and dried under reduced pressure (3 mm Hg) at 25 ºC for 1 h to give titanium superoxide 96% yield.

General experimental procedure for the preparation of benzamides:
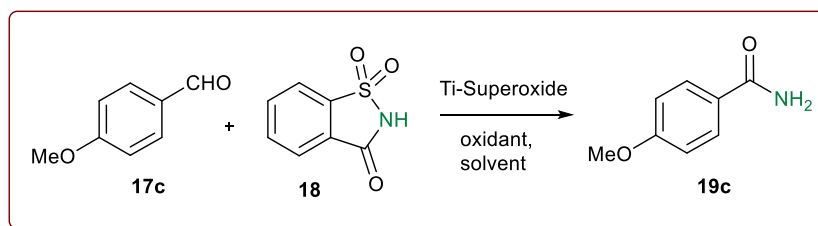
To a 25 mL, oven-dried round-bottom flask was added benzaldehydes (1 equiv.), Saccharin (1.2 equiv.) and titanium superoxide as catalyst (10 wt.%) in dry 1,4-Dioxane (4mL) was added TBHP in decane (3 equiv.) in a dropwise manner. The round-bottom flask was equipped with a condenser, and the resulting reaction mixture was refluxed to 90°C for 1h. The progress of the reaction was monitored by TLC. Upon completion of the reaction, the solvent was evaporated under reduced pressure then the reaction mixture was filtered through a sintered funnel using $NaHCO_3$ aqueous solution and EtOAc as eluent. Then the organic layer was extracted with EtOAc, dried over anhydrous Na_2SO_4, and evaporated under reduced pressure. The crude product was purified by column chromatography over silica (100-200 mesh) using petroleum ether/ethyl acetate (70:30 v/v) as an eluent to give the corresponding amides.

Experimental procedure for the gram scale synthesis of Moclobemide (24):
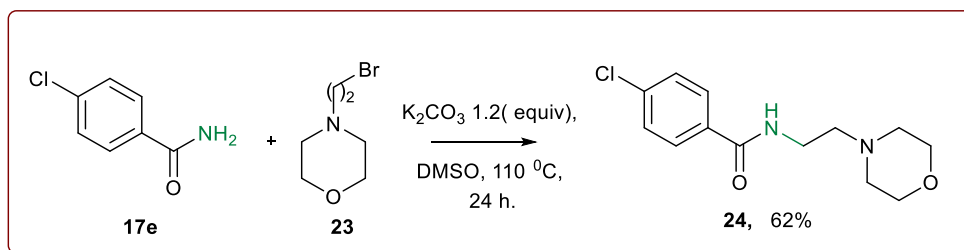
4-chlorobenzamide (5 g, 1equiv.), K_2CO_3 (6.67 g 1.5 equiv.), 4-(2-bromoethyl) morpholine (7.41 g 1.2 equiv.), and dry DMSO (25 mL) were placed in a two-neck round bottom flask. The mixture was heated at 110 $^\circ$C for 24 h under a nitrogen atmosphere, cooled, diluted with cold aq NH_4Cl solution, and extracted with EtOAc (3*30 mL). The organic layers were combined, washed with brine, and dried over anhyd. Na_2SO_4, and then concentrated. Further, the product was purified by column chromatography.

Benzamide (19a)

Yield: 104 mg (93%); White solid; mp:130-132 $^\circ$C; **^{1}H NMR** (400 MHz, DMSO-d_6): δ 7.38 - 7.55 (m, 4H), 7.88 - 7.98 (m, 2H), 8.07 (br.s.,1H); **^{13}C NMR** (101 MHz, DMSO-d_6): δ 128.0, 128.7, 131.7, 134.7, 168.6. **HRMS** (ESI) calculated [M+H]$^+$ for C_7H_8ON: 122.0527; found: 122.0528.

4-Methylbenzamide (19b)

Yield: 106 mg (95%); white solid; mp: 158-160°C; **^{1}H NMR** (400 MHz, DMSO-d_6) : δ 2.33 (s, 3H), 7.23 (d, J = 7.9 Hz, 2H), 7.31 (br. s., 1H), 7.79 (d, J = 7.9 Hz, 2H), 7.92 (br. s., 1H); **^{13}C NMR** (101 MHz, DMSO-d_6): δ 21.4 , 128.0, 129.2, 131.9, 141.5, 168.3; **HRMS** (ESI) calculated [M+H]$^+$ for $C_8H_{10}ON$: 136.0684; found: 136.0684.

4-Methoxybenzamide (19c)

Yield: 101 mg (91%); White solid; mp: 166-170°C; **^{1}H NMR** (400 MHz, DMSO-d_6): δ 3.80 (br. s., 3H), 6.96 (br. s., 2H), 7.21 (br. s., 1H), 7.85 (br. s., 3H); **^{13}C NMR** (101 MHz, DMSO-d_6): δ 55.5, 113.6, 126.7, 129.6, 161.8, 167.7, and 167.7; **HRMS** (ESI) calculated [M+H]$^+$ for $C_8H_{10}O_2N$: 152.0706; found: 152.0706.

4-(Tert-butyl)benzamide (19d)

Yield: 96 mg (88%); white solid; mp: 172-174°C; **^{1}H NMR** (400 MHz, *DMSO-d$_6$*): δ 1.26 (br. s., 9H), 7.32 (br. s., 1H), 7.44 (d, *J* = 8.2 Hz, 2H), 7.81 (t, *J* = 6.6 Hz, 2H), 7.95 (br. s., 1H); **^{13}C NMR** (101 MHz, *DMSO-d$_6$*): δ 31.0, 34.6, 125.0, 127.4, 131.6, 154.1, 168; **HRMS** (ESI) calculated [M+H]$^+$ for C$_1$H$_{16}$ON: 178.1226; found: 178.1227.

4-Chlorobenzamide (19e)

Yield: 87 mg (79%); White solid; mp: 178-180°C; **^{1}H NMR** (400 MHz, DMSO-d$_6$): δ 7.38 - 7.64 (m, 3H), 7.89 (d, *J* = 7.9 Hz, 2H), 8.06 (br. s., 1H); **^{13}C NMR** (101 MHz, DMSO-d$_6$): δ 128.6, 129.7, 133.3, 136.4, 167.2; **HRMS** (ESI) calculated [M+H]$^+$ for C$_7$H$_7$ONCl: 156.0137; found: 156.0139.

4-Iodobenzamide (19f)

Yield: 79 mg (75%); White solid; mp: 214-218°C; **^{1}H NMR** (400 MHz, DMSO-d$_6$): δ 7.48 (br. s., 1H), 7.66 (d, *J* = 6.9 Hz, 2H), 7.75 - 7.92 (m, 2H), 8.07 (br. s., 1H); **^{13}C NMR** (101 MHz, DMSO-d$_6$) : δ 99.5, 130.0, 134.2, 137.6, 167.9; **HRMS** (ESI) calculated [M+H]$^+$ for C$_7$H$_7$ONI: 247.9567; found: 247.9569.

4-Hydroxybenzamide(19g)

Yield: 42 mg (36%); off white solid; mp: 158-160°C; **^{1}H NMR** (400 MHz, DMSO-d$_6$): δ 6.81 (d, *J* = 8.5 Hz, 2H), 7.17 (br. s., 1H), 7.77 (d, *J* = 8.5 Hz, 3H), 10.00 (s, 1H); **^{13}C NMR** (101 MHz, DMSO-d$_6$) : δ 115.6, 125.7, 130.3, 161.0, 168.8; **HRMS** (ESI) calculated [M+H]$^+$ for C$_7$H$_8$O$_2$N: 138.0550; found: 138.0550.

4-Aminobenzamide(19h)

Yield: 41 mg (38%); white solid; mp: 182-184°C; **^{1}H NMR** (400 MHz, DMSO-d$_6$) : δ 5.66 (br. s., 2H), 6.63 (d, *J* = 7.9 Hz, 2H), 7.15 (br. s., 1H), 7.73 (d, *J* = 7.3 Hz, 3H); **^{13}C NMR** (101 MHz,

DMSO-d$_6$) : δ 113.0, 121.1, 129.6, 152.0, 169.1; **HRMS** (ESI) calculated [M+H]$^+$ for C$_7$H$_9$ON$_2$: 137.0709; found: 137.0711.

1-Naphthamide (19i)

Yield: 91 mg (78%); brown solid; mp: 208−210 $^°$C; **^{1}H NMR** (400 MHz, DMSO-d$_6$): δ 7.47 - 7.75 (m, 5H), 7.90 - 8.13 (m, 3H), 8.27 - 8.43 (m, 1H); **^{13}C NMR** (101 MHz, DMSO-d$_6$) : δ 125.3, 125.5, 126.0, 126.5, 127.0, 128.6, 130.1, 130.2, 133.6, 135.1, 171.0; **HRMS** (ESI) calculated [M+H]$^+$ for C$_{11}$H$_{10}$ON: 172.0757; found: 172.0757.

3-Nitrobenzamide (19j)

Yield: 78 mg (71%); white solid; mp: 140-142$^°$C; **^{1}H NMR** (400 MHz, DMSO-d$_6$): δ 7.68 - 7.83 (m, 2H), 8.35 (d, J = 7.3 Hz, 2H), 8.30 (d, J = 7.9 Hz, 2H), 8.68 (s, 1H). **^{13}C NMR** (101 MHz, DMSO-d$_6$): δ 122.3, 125.9, 130.1, 133.9, 135.8, 147.8, 165.9; **HRMS** (ESI) calculated [M+H]$^+$ for C$_7$H$_7$O$_3$N$_2$: 167.0451; found: 167.0452.

3-Fluorobenzamide (19k)

Yield: 83 mg (74%); white solid; mp: 128-130$^°$C; **^{1}H NMR** (400 MHz, DMSO-d$_6$): δ 7.31 (br. s., 1H), 7.45 (br. s., 1H), 7.52 (br. s., 1H), 7.60 - 7.74 (m, 2H), 8.06 (br. s., 1H); **^{13}C NMR** (101 MHz, DMSO-d$_6$): δ 114.6, 118.4, 124.0, 130.8, 137.1, 163.7, 167.1.

3-(Trifluoromethyl)benzamide (19l)

Yield: 77 mg (71%); white solid; mp: 182-186$^°$C; **^{1}H NMR** (400 MHz, DMSO-d$_6$): δ 7.55 - 7.79 (m, 2H), 7.87 (d, J = 7.3 Hz, 1H), 8.14 - 8.44 (m, 3H); **^{13}C NMR** (101 MHz, DMSO-d$_6$) : δ 123.1, 124.6, 125.8, 128.3, 129, 130.0, 132.0, 135.6, 166.9; **HRMS** (ESI) calculated [M+H]$^+$ for C$_8$H$_7$ONF$_3$: 190.0447; found: 190.0447.

3-Methoxybenzamide (19m)

Yield: 94 mg (84%); white solid; mp: 182-186°C; **^{1}H NMR** (400 MHz, DMSO-d$_6$): δ 3.79 (s, 3H), 6.92 - 7.20 (m, 1H), 7.29 - 7.58 (m, 4H), 7.99 (br. s., 1H); **^{13}C NMR** (101 MHz, DMSO-d$_6$): δ 55.5, 112.9, 117.3, 120.0, 129.6, 136.0, 159.4, 168.0; **HRMS** (ESI) calculated [M+H]$^+$ for C$_8$H$_{10}$O$_2$N: 152.0706; found: 152.0706.

2-Methylbenzamide (19n)

Yield: 102 mg (91%); white solid; mp:142-146°C; **^{1}H NMR** (400 MHz, DMSO-d$_6$): δ 2.36 (s, 3H), 7.16 - 7.25 (m, 2H), 7.28 - 7.40 (m, 3H), 7.70 (br. s., 1H); **^{13}C NMR** (101 MHz, DMSO-d$_6$): δ 20.0, 125.9, 127.4, 129.6, 130.9, 135.6, 137.5, 171.5; **HRMS** (ESI) calculated [M+H]$^+$ for C$_8$H$_{10}$ON: 136.0684; found: 136.0684.

2-Iodobenzamide (19o)

Yield: 84 mg (79%); white solid; mp: 180-182°C; **^{1}H NMR** (400 MHz, DMSO-d$_6$): δ 7.15 (td, *J* = 7.6, 1.6 Hz, 1H), 7.35 (dd, *J* = 7.6, 1.6 Hz, 1H), 7.43 (t, *J* = 7.4 Hz, 1H), 7.52 (br. s., 1H), 7.77 - 7.94 (m, 2H); **^{13}C NMR** (101 MHz, DMSO-d$_6$): δ 93.6, 128.3, 128.4, 131.1, 139.6, 143.6, 171.2; **HRMS** (ESI) calculated [M+H]$^+$ for C$_7$H$_7$ONI: 247.9567; found: 247.9566.

2-Bromobenzamide (19p)

Yield: 79 mg (73%); white solid; mp:156-158°C; **^{1}H NMR** (400 MHz, DMSO-d$_6$): δ 7.34 (br. s., 1 H), 7.41 (br. s., 2 H), 7.53 - 7.72 (m, 2H), 7.88 (br. s., 1H); **^{13}C NMR** (101 MHz, DMSO-d$_6$): δ 119.1, 128, 129, 131.1, 133.2, 139.8, 169.6.

2-Hydroxybenzamide (19q)

Yield: 53 mg (48%); off white solid; mp:137-139°C; **^{1}H NMR** (400 MHz, DMSO-d$_6$): δ 6.76 - 6.96 (m, 2H), 7.29 - 7.44 (m, 1H), 7.78 - 8.04 (m, 2H), 8.44 (br. s., 1H); **^{13}C NMR** (101 MHz, DMSO-d$_6$): δ 115.1, 118.1, 119.0, 128.8, 134.7, 161.8, 172.9; **HRMS** (ESI) calculated [M+H]$^+$ for C$_7$H$_8$O$_2$N: 138.0550; found: 138.0550.

2-Aminobenzamide (19r)

Yield: 30 mg (27%); white solid; mp:111-113°C; ^{1}**H NMR** (400 MHz, DMSO-d$_6$): δ 6.46 - 6.61 (m, 3H), 6.76 (d, J = 7.9 Hz, 1H), 7.09 - 7.33 (m, 2H), 7.62 (d, J = 7.9 Hz, 1H), 7.84 (br. s., 1H); ^{13}**C NMR** (101 MHz, DMSO-d$_6$): δ 114.4, 115.4, 117.2, 129.5, 132.8 , 150.8 , 172.3; **HRMS** (ESI) calculated [M+H]$^{+}$ for C$_7$H$_9$ON$_2$: 137.0709; found: 137.0709.

2-Ethoxybenzamide (19s)

Yield: 91 mg (79%); white solid; mp: 130-132 $^{\circ}$C; ^{1}**H NMR** (400 MHz, DMSO-d$_6$): δ 1.4 (t, J = 7.10 Hz, 3H), 4.1 (q, J = 6.87 Hz, 2H), 6.9 - 7.2 (m, 2H), 7.4 (td, J = 7.78, 1.83 Hz, 1H), 7.6 (br. s., 2H), 7.9 (dd, J = 7.79, 1.83 Hz, 1H); ^{13}**C NMR** (101 MHz, DMSO-d$_6$): δ 14.5 ,64.3, 112.9, 120.5, 122.6, 131.0, 132.6, 156.6, 166.5; **HRMS** (ESI) calculated [M+H]$^{+}$ for C$_9$H$_{12}$O$_2$N: 166.0863; found: 167.0862.

3,5-Dinitrobenzamide (19t)

Yield: 77 mg (72%); yellow solid; mp:180-182°C; ^{1}**H NMR** (400 MHz, DMSO-d$_6$):7.99 (br. s., 1H), 8.67 (br. s., 1H), 8.85 - 8.99 (m, 2H), 9.04 (d, J = 1.8 Hz, 2H); ^{13}**C NMR** (101 MHz, DMSO-d$_6$): δ 121.5, 128.4, 129.2, 137.7, 148.5, 148.8, 164.3; **HRMS** (ESI) calculated [M+H]$^{+}$ for C$_7$H$_6$O$_5$N$_3$: 212.0302; found: 212.1181.

3,5-Dimethylbenzamide (19u)

Yield: 105 mg (95%); white solid; mp:134-136°C; ^{1}**H NMR** (400 MHz, DMSO-d$_6$): δ 2.29 (s, 7H), 7.12 (s, 1H), 7.26 (br. s., 1H), 7.49 (s, 2H), 7.88 (br. s., 1H); ^{13}**C NMR** (101 MHz, DMSO-d$_6$): δ 21.3, 125.7, 132.9, 134.7, 137.7, 168.7; **HRMS** (ESI) calculated [M+H]$^{+}$ for C$_9$H$_{12}$ON: 150.0913; found: 150.0913.

2,3-Difluorobenzamide (19v)

Yield: 96 mg (85%); white solid; mp:118-120°C; **^{1}H NMR** (400 MHz, DMSO-d$_6$): δ 7.25 (br. s., 1H), 7.38 - 7.57 (m, 2H), 7.81 (br. s., 1H), 7.90 (br. s., 1H); **^{13}C NMR** (101 MHz, DMSO-d$_6$) : δ 119.4- 119.5 (1C J = 17 Hz), 125.0- 125.3 (1C J = 30 Hz), 126.6, 146.3 -146.4 (1C J = 12.5 Hz), 148.8 -148.9 (1C J = 13.5 Hz), 151.2-151.4 (1C J = 13.5 Hz), 164.7; **HRMS** (ESI) calculated [M+H]$^+$ for C$_7$H$_6$ONF$_2$: 158.0412; found: 158.0413.

2,6-Difluorobenzamide (19w)

Yield: 89 mg (81%); white solid; mp: 150-154°C; **^{1}H NMR** (400 MHz, DMSO-d$_6$): δ 7.14 (t, J = 8.0 Hz, 2H), 7.48 (quin, J = 7.6 Hz, 1H), 7.88 (br. s., 1H), 8.18 (br. s., 1H); **^{13}C NMR** (101 MHz, DMSO-d$_6$): δ 112.2-112.3 (1C J = 5 Hz), 112.4-112.4 (1C J = 5 Hz), 116.1, 116.3-116.5 (1C J = 23 Hz), 131.6, 131.7- 131.8 (1C J = 9.5 Hz), 157.9, 158.0 (1C J = 8.6 Hz), 160.4-160.5 (1C J = 8.6 Hz), 162.2; **HRMS** (ESI) calculated [M+H]$^+$ for C$_7$H$_6$ONF$_2$: 158.0412; found: 158.0413.

2-Phenylacetamide (19x)

Yield: 80 mg (71%); white solid; mp:154- 156°C; **^{1}H NMR** (400 MHz, DMSO-d$_6$): δ 3.48 (br. s., 2H), 6.94 (br. s., 1H), 7.21 - 7.26 (m, 1H), 7.28 (br. s., 5H), 7.52 (br. s., 1H); **^{13}C NMR** (101 MHz, DMSO-d$_6$) δ ppm 42.8, 126.8, 128.7, 129.6, 137.0, 172.9.

2-(4-Bromophenyl)acetamide (19y)

Yield: 79 mg; (74%); yellow solid; mp: 194 - 196°C; **^{1}H NMR** (400 MHz, DMSO-d$_6$): δ 3.40 (br. s., 3H), 6.96 (br. s., 1H), 7.25 (br. s., 3H), 7.41 (br. s., 1H), 7.48 (br. s., 1H), 7.55 (br. s., 1H); **^{13}C NMR** (101 MHz, DMSO-d$_6$): δ 42.1, 121.8, 128.7, 129.6, 130.7, 132.3, 139.6, 172.2; **HRMS** (ESI) calculated [M+H]$^+$ for C$_8$H$_9$ONBr: 213.9862; found: 213.9868.

2-(4-Hydroxyphenyl)acetamide (19z)

Yield: 61 mg (55%); white solid; mp: 175- 177°C; **^{1}H NMR** (400 MHz, DMSO-d$_6$): δ 3.28 (br. s., 2H), 6.63 - 6.81 (m, 2H), 6.82 - 7.00 (m, 1H), 7.04 - 7.16 (m, 2H), 7.43 (br. s., 1H), 9.19 - 9.35 (m, 1H); **^{13}C NMR** (101 MHz, DMSO-d$_6$): δ 41.8, 115.4, 126.9, 130.3, 156.2, 173.6.

2-(3,4-Dimethoxyphenyl)acetamide (19aa)

Yield: 93 mg (86%); brown solid; mp: 140-144°C; **^{1}H NMR** (400 MHz, DMSO-d$_6$): δ 3.28 (s, 2H), 3.72 (s, 3H), 3.71 (s, 3H), 6.74 - 6.79 (m, 1H), 6.80 - 6.89 (m, 3H), 7.37 (br. s., 1H); **^{13}C NMR** (101 MHz, DMSO-d$_6$): δ 42.5, 56.1, 56.2, 112.4 , 113.6, 121.7, 129.6, 148.1, 149.1, 173.2; **HRMS** (ESI) calculated [M+H]$^+$ for C$_{10}$H$_{14}$O$_3$N: 196.0968; found: 196.0969.

2-(3,4-Dichlorophenyl)acetamide (19ab)

Yield: 78 mg (74%); brown solid; **^{1}H NMR** (400 MHz, DMSO-d$_6$): δ 3.36 - 3.46 (m, 2H), 7.34 (br. s., 1H), 7.41 (br. s., 2H), 7.56 - 7.67 (m, 2H), 7.88 (br. s., 1H); **^{13}C NMR** (101 MHz, *DMSO-d$_6$*): δ 39, 118.7, 127.6, 128.6, 130.7, 132.8, 139.3, 169.2; **HRMS** (ESI) calculated [M+H]$^+$ for C$_8$H$_8$ONCl$_2$: 203.9977; found: 203.9980.

Octanamide (19ac)

Yield: 47 mg; (42%); white solid; mp: 107- 109°C; **^{1}H NMR** (400 MHz, CDCl$_3$): δ 0.82 - 0.95 (m, 3H), 1.30 (s, 4H), 1.27 (s, 5H), 1.56 - 1.70 (m, 2H), 2.21 (t, *J* = 7.6 Hz, 2 H), 5.54 (br. s., 1H), 5.86 (br. s., 1H); **^{13}C NMR** (101 MHz, CDCl$_3$): δ 14.0, 22.5, 25.5, 29.0, 29.1, 31.6, 35.9, 175.9.

Decanamide (19ad)

Yield: 42 mg (39%); white solid; mp: 101- 103°C; **^{1}H NMR** (400 MHz, DMSO-d$_6$): δ 0.85 (t, *J* = 6.4 Hz, 3H), 1.24 (s, 13H), 1.42 - 1.51 (m, 2H), 2.01 (t, *J* = 7.3 Hz, 2H), 6.66 (br. s., 1H), 7.21 (br. s., 1H); **^{13}C NMR** (101 MHz, DMSO-d$_6$): δ 14.0, 22.1, 25.1, 28.7, 28.7, 28.9, 29.0, 31.3, 35.1, 174.4; **HRMS** (ESI) calculated [M+H]$^+$ for C$_{10}$H$_{12}$ON: 172.1696; found: 172.1696.

Thiophene-2-carboxamide (19ae)

Yield: 68 mg (61%); white solid; mp:181- 183°C; **^{1}H NMR** (400 MHz, DMSO-d$_6$): δ 7.12 (br. s., 1H), 7.39 (br. s., 1H), 7.75 (s, 1H), 7.71 (s, 1H), 7.99 (br. s., 1H); **^{13}C NMR** (101 MHz, DMSO-d$_6$): δ 128.4, 129.2, 131.4, 140.7, 163.5; **HRMS** (ESI) calculated [M+H]$^+$ for C$_5$H$_6$ONS: 128.0165; found: 128.0165.

2-Picolinamide (19af)

Yield: 28 mg (25%); white solid; mp: 104- 108°C; **^{1}H NMR** (400 MHz, DMSO-d$_6$): δ 7.52 - 7.59 (m, 1H), 7.71 (br. s., 1H), 7.92 - 8.00 (m, 1H), 8.06 (d, J = 7.8 Hz, 1H), 8.17 (br. s., 1H), 8.61 (d, J = 2.7 Hz, 1H); **^{13}C NMR** (101 MHz, DMSO-d$_6$): δ 122.4, 126.9, 138.1, 148.9, 150.7 , 166.6; **HRMS** (ESI) calculated [M+H]$^+$ for C$_6$H$_7$ON$_2$: 123.0553; found: 123.0555.

2-Benzoylbenzo[d]isothiazol-3(2H)-one-1,1-dioxide (20)

White solid**; ^{1}H NMR** (400 MHz, DMSO-d$_6$) δ ppm 7.3 - 7.5 (m, 2H), 7.6 - 7.6 (m, 1H), 7.6 - 7.8 (m, 1H), 7.8 - 8.1 (m, 5H), 8.2 (d, J = 7.33 Hz, 1H). **^{13}C NMR** (101 MHz, DMSO-d$_6$): δ 121, 125, 127, 129, 131, 133, 135, 136, 139, 161, 167.

Moclobemide (24)

Yield: 5.35 gm (62%); white solid; mp: 135- 137°C; **^{1}H NMR** (500 MHz, CDCl$_3$): δ 2 (br. s., 4H), 3 (t, J = 5.91 Hz, 2H), 3 - 4 (m, 2H), 4 (t, J = 4.58 Hz, 4H), 7 (br. s., 1H), 7 (m, J = 8.77 Hz, 2H), 8 - 8 (m, 2H); **^{13}C NMR** (126 MHz, CDCl$_3$) : δ 36, 53, 57, 67, 128,128, 128, 133, 137, 166.

4.2.7 References

1   (a) Dawood, K. M.; Abbas, A. A. Inhibitory activities of indolizine derivatives: a patent review. *Expert Opin. Ther. Pat.* **2020**, *30*, 695-714. (b) Singh, G. S.; Mmatli, E. E. Recent progress in synthesis and bioactivity studies of indolizines. *Eur. J. Med. Chem*. **2011**, *46*, 5237-5257 (c) Movassaghi, M.; Ondrus, A. E.; Chen, B. Efficient and Stereoselective Dimerization of Pyrroloindolizine Derivatives Inspired by a Hypothesis for the Biosynthesis of Complex Myrmicarin Alkaloids. *J. Org. Chem.* **2007**, *72*, 10065-

10074. (d) Flitsch, W. In Comprehensive Heterocyclic Chemistry; Katritzky, A. R., Rees, C. W., Eds.; Pergamon Press: Oxford, U.K., 1984; Vol. 4, p 443. © Sharma, V.; Kumar, V. Indolizine: a Biologically Active Moiety. *Med. Chem. Res.* **2014,** *23*, 3593-3606. (f) de Souza, C. R.; Goncalves, A. C.; Amaral, M. F. Z. J.; Dos Santos, A. A.; Clososki, G. C. Recent Synthetic Developments and Reactivity of Aromatic Indolizines. *Targets Heterocycl. Syst.* **2016**, *20*, 265-392.

2   (a) Bloch, W. M.; Derwent-Smith, S. M.; Issa, F.; Morris, J. C.; Rendina, L. M.; Sumby, C. J. *Tetrahedron* **2011**, *67*, 9368-9375. (b) Hazra, A.; Mondal, S.; Maity, A.; Naskar, S.; Saha, P.; Paira, R.; Sahu, K. B.; Paira, P.; Ghosh, S.; Sinha, C.; Samanta, A.; Banerjee, S.; Mondal, N. B. *Eur. J. Med. Chem.* **2011**, *46*, 2132-2140. (c) Hagishita, S.; Yamada, M.; Shirahase, K.; Okada, T.; Murakami, Y.; Ito, Y.; Matsuura, T.; Wada, M.; Kato, T.; Ueno, M.; Chikazawa, Y.; Yamada, K.; Ono, T.; Teshirogi, I.; Ohtani, M. Potent Inhibitors of Secretory Phospholipase A2: Synthesis and Inhibitory Activities of Indolizine and Indene Derivatives. *J. Med. Chem*. **1996**, *39*, 3636-3658. (d) Lingala, S.; Nerella, R.; Cherukupally, R.; Das, A. K. *Int. J. Pharm. Sci. Rev. Res.* 2011, *6*, 128 © Abuhaie, C. M.; Bîcu, E.; Rigo, B.; Gautret, P.; Belei, D.; Farce, A.; Dubois, J.; Ghinet, A. Synthesis and anticancer activity of analogues of phenstatin, with a phenothiazine A-ring, as a new class of microtubule-targeting agents. *Bioorg. Med. Chem. Lett.* **2013**, 23, 147-152.

3   (a) Delcamp, J. H.; Yella, A.; Holcombe, T. W.; Nazeeruddin, M. K.; Grätzel, M. The molecular engineering of organic sensitizers for solar-cell applications. *Angew. Chem., Int. Ed.* **2013**, *52*, 376-380. (b) Yuan, Y. C.; Liu, T-Z.; Zhao, B-X. Metal-Free Catalyzed Synthesis of Fluorescent Indolizine Derivatives. *J. Org. Chem.* **2021**, *86*, 12737-12744 (c) Wan, J.; Zheng, C. J.; Fung, M. K.; Liu, X. K.; Lee, C. S.; Zhang, X. H. Multifunctional electron-transporting indolizine derivatives for highly efficient blue fluorescence, orange phosphorescence host and two-color based white OLEDs. *J. Mater. Chem.* **2012**, *22*, 4502-4510. (d) Zhang, Y.; Yu, Y.; Liang, B-b.; Pei, Y-y.; Liu, X.; Yao, H-g.; Cao, H. Synthesis of Pyrrolo[2,1,5-cd]indolizine Rings via Visible-LightInduced Intermolecular [3+2] Cycloaddition of Indolizines and Alkynes. *J. Org. Chem.* **2020**, *85*, 10719-10727. (e) Song, Y. R.; Lim, C. W.; Kim, T. W. Synthesis and photophysical properties of 1, 2-diphenylindolizine derivatives: fluorescent blue emitting materials for organic light-emitting device. *Luminescence,* **2016**, *31*, 364-371.

4   (a) Weide, T.; Arve, L.; Prinz, H.; Waldmann, H.; Kessler, H. 3-Substituted indolizine-1-carbonitrile derivatives as phosphatase inhibitors. *Bioorg. Med. Chem. Lett*. **2006**, 16, 59-63. (b) Krall, R. L.; Penry, J. K.; White, B. G.; Kupferberg, H. J.; Swinyard, E. A. Antiepileptic drug development: II. Anticonvulsant drug screening. *Epilepsia* **1978**, 19, 409-428. (c) Park, S.; Kwon, D. I.; Lee, J.; Kim, I. When Indolizine Meets Quinoline: Diversity-Oriented Synthesis of New Polyheterocycles and Their Optical Properties. *ACS Comb. Sci.* **2015**, *17*, 459-469. (d) Liu, X.; Song, D.; Zhang, Z.; Lin, J.; Zhuang, C.; Zhan, H.; Cao, H. Regioselective C–H dithiocarbamation of indolizines with tetraalkylthiuram disulfide under metal-free conditions. *Org. Biomol. Chem.*, **2021**,*19*, 5284-5288.

5   (a) Sadowski, B.; Klajn, J.; Gryko, D. T. Recent advances in the synthesis of indolizines and their π-expanded analogues. *Org. biomol. Chem.* **2016**, *14*, 7804-7828. (b) Lee, J. H.; Kim, I.

Cycloaromatization Approach to Polysubstituted Indolizines from 2-Acetylpyrroles: Decoration of the Pyridine Unit. *J. Org. Chem*. **2013**, *78*, 1283-1288.

6   Maiboroda, D. A.; Babaev, E, V.; Jug,K. On the Alternation Effect in Substituted Indolizines and Their Aza-analogs. *J. Org. Chem.* **1997,** *62*, 7100-7105.

7   Park, C-H.; Ryabova, V.; Seregin, I. V.; Sromek, A. W.; Gevorgyan, V. Palladium-Catalyzed Arylation and Heteroarylation of Indolizines. *Org. Lett*. **2004**, 6, 1159-1162.

8   Teng, L.; Liu, X.; Guo, P.; Yu, Y.; Cao, H. Visible-Light-Induced Regioselective Dicarbonylation of Indolizines with Oxoaldehydes via Direct C-H Functionalization. *Org. Lett.* **2020**, *22*, 10, 3841-3845.

9   (a) Penteado, F.; Gomes, C. S.; Monzon, L. I.; Perin, G.; Silveira, C. C.; Lenardão, E. J. Photocatalytic Synthesis of 3-Sulfanyl- and 1,3- Bis(223ulfonyl)indolizines Mediated by Visible Light. *Eur. J. Org. Chem.* **2020**, 2110-2115. (b) Li, B.; Chen, Z.; Cao, H.; Zhao, H. Transition-Metal-Free Regioselective Cross-Coupling: Controlled Synthesis of Mono- or Dithiolation Indolizines. *Org. Lett.* **2018**, *20*, 3291-3295.

10   (a) Guidotti, B. B.; Silva, T. S. d.; Correia, J. T. M.; Coelho, F. Brønsted-acid-catalyzed selective Friedel–Crafts monoalkylation of isatins with indolizines in water. *Org. Biomol. Chem.*, **2020**, *18*, 7330-7335 (b) Zhang, Y-Z.; Sheng, F-T.; Zhu, Z.; Li, Z-M.; Zhang, S.; Tan, W.; Shi, F. Organocatalytic C3-functionalization of indolizines: synthesis of biologically important indolizine derivatives. *Org. Biomol. Chem.*, 2020, 18, 5688-5696.

11   Xuan, J.; Cao, X.; Cheng, X. Advances in heterocycle synthesis via [3+m]-cycloaddition reactions involving an azaoxyallyl cation as the key intermediate. *Chem. Commun*., **2018**, *54*, 5154-5163.

12   (a) Sun, S.; Chen, R.; Wang, G.; Wang, J. Sodium carbonate promoted [3 + 2] annulation of α-halohydroxamates and isocyanates. *Org. Biomol. Chem.* **2018**, *16*, 8011-8014. (b) Acharya, A.; Montes, K.; Jeffrey, C. S. Access to 4-Oxazolidinones: A (3 + 2) Cycloaddition Approach. *Org. Lett*. **2016**, *18*, 6082−6085 (c) Zhang, Y.; Ma, H.; Liu, X.; Cui, X.; Wang, S.; Zhan, Z.; Pu, J.; Huang, G. The synthesis of multi-substituted pyrrolidinones *via* a direct [3 + 2] cycloaddition of azaoxyallyl cations with aromatic ethylenes. *Org. Biomol. Chem*. **2018**, *16*, 4439-4442. (d) Xu, X.; Zhang, K.; Li, P.; Yao, H.; Lin, A. [3 + 3] Cycloaddition of Azides with in Situ Formed Azaoxyallyl Cations To Synthesize 1,2,3,4-Tetrazines. *Org. Lett.* **2018**, 20, 1781-1784. © Jeffrey, C. S.; Barnes, K. L.; Eickhoff, J. A.; Carson, C. R. Generation and Reactivity of Aza-Oxyallyl Cationic Intermediates: Aza-[4 + 3] Cycloaddition Reactions for Heterocycle Synthesis. *J. Am. Chem. Soc.* **2011,** *133*, 7688-7691.

13   (a) Ansari, A. J.; Yadav, A.; Mukherjee, A.; Sathish, E.; Nagesh, K.; Singh, R. Metal free amination of congested and functionalized alkyl bromides at room temperature. *Chem. Commun*., **2020**, *56*, 4804-4807. (b) Kainz, Q. M.; Matier, C. D.; Bartoszewicz, A.; Zultanski, S. L.; Peters, J. C.; Fu, G. C. Asymmetric copper-catalyzed C-N cross-couplings induced by visible light. *Science*, **2016**, *351*, 681-684. (c) Jaiswal, V.; Mondal, B.; Singh, K.; Das, Dinabandhu,; Saha, J. [3 + 2]-Annulation of Azaoxyallyl Cations and Thiocarbonyls for the Assembly of Thiazolidin-4-ones**.** *Org. Lett.* 2019, 21, 15, 5848–5852.

14   Son, E. C.; Kim, S-G. Metal-free Nucleophilic Alkoxylation of in Situ-Generated Azaoxyallyl Cations: Synthesis of Hindered Dialkyl Ether Derivatives. *A. J. Org. Chem.* **2020**, 9, 914-917.

15   (a) Mane, K. D.; Kamble, R. B.; Suryavanshi, G. A visible light mediated, metal and oxidant free highly efficient cross dehydrogenative coupling (CDC) reaction between quinoxalin-2(1H)-ones and ethers. *New J. Chem.*, **2019**,*43*, 7403-7408.

16   (a) Fu, R.; Yang, Y.; Zhang, J.; Shao, J.; Xia, X.; Ma, Y.; Yuan, R. Direct oxidative amidation of aldehydes with amines catalyzed by heteropolyanion-based ionic liquids under solvent-free conditions via a dual-catalysis process. *Org. Biomol. Chem.* **2016**, *14,* 1784-1793. (b) Bode, J. W.; Emerging methods in amide-and peptide-bond formation. *Curr. Opin. Drug Discov. Devel.,* **2006**, *9,* 765 (c) Cupido, T.; Tulla-Puche, J.; Spengler, J.; Albericio, F.; The synthesis of naturally occurring peptides and their analogs. *Curr. Opin. Drug Discov. Devel.*, **2007**, *10,* 768 (d) Zhang, X.; Teo, W. T.; P. Chan, W. H. Efficient synthesis of di-and trisubstituted 2-aryloxazoles via ytterbium (III) triflate catalyzed cyclization of tertiary propargylic alcohols with aryl amides. *J. Organomet. Chem.,* **2011**, *696*, 331-337. (e) Allen, C. L.; Williams, J. M. J. Metal-catalysed approaches to amide bond formation. *Chem. Soc. Rev.,* **2011**, *40*, 3405-3415. (f) Humphrey, J. M.; Chamberlin, A. R. Chemical synthesis of natural product peptides: coupling methods for the incorporation of noncoded amino acids into peptides. *Chem. Rev.,* **1997**, *97,* 2243. (g) Zhao, H. P.; Liang, G. C.; Nie, S. M.; Lu, X.; Pan, C. X.; Zhong, X. X.; Su, G. F.; Mo, D.L. Metal-free graphene oxide-catalyzed aza-semipinacol rearrangement to prepare 2-(indol-2-yl)phenols and benzofuro[3,2-*b*]indolines containing quaternary carbon centers. *Green Chem*., **2019**,22, 404-410 (h) Liao, J. Y.; Wu, Q. Y.; Lu, X.; Zou, N.; Pan, C. X.; Liang, C.; Su, G. F.; Mo, D. L. A copper-catalyzed diastereoselective O-transfer reaction of N-vinyl-α, β-unsaturated nitrones with ketenes into γ-lactones through [5+ 2] cycloaddition and N–O bond cleavage. *Green Chem.*, **2019,** *21*, 6567-6573. (i) Zhang, T. S.; Zhang, H.; Fu, R.; Wang, J.; Hao, W. J.; Tu, S. J.; Jiang, B. tert-Butyl peroxide (TBHP)/KI-mediated dual C (sp2)–H bond amination of arylamines with α-diazo carbonyls toward 1, 2, 4-benzotriazines. *Chem. Commun*., **2019**, *55*, 13231-13234. (j) Wang, Z.; Hou, C.; Zhong, Y.F.; Lu, Y.X.; Mo, Z.Y.; Y. Pan, M.; Tang, H. T. Electrochemically Enabled Double C–H Activation of Amides: Chemoselective Synthesis of Polycyclic Isoquinolinones. *Org. Lett*. **2019**, *21*, 24, 9841–9845.

17   (a) Xu, F.; Song, Y-Y.; Li, Y-J.; Li, E-L.; Wang, X-R.; Li, W-Y.; Liu, C-S. Sulfur-Assisted Deprotection of Methylene Nitrile Group: One-Pot Synthesis of 4-Substituted-2*H*-1,2,3-triazoles. *Chemistry Select*, **2018**, *3*, 3474 (b) Carey, J. S.; Laffan, D.; Thomson, C.; Williams, M. T. Analysis of the reactions used for the preparation of drug candidate molecules. *Org. Biomol. Chem.,* **2006**, *4*, 2337-2347. (c) Bray, B. L. Large-scale manufacture of peptide therapeutics by chemical synthesis. *Nat. Rev. Drug Discov.*, **2003**, *2*, 587 (d) Allen, C. L.; Atkinson, B. N.; Williams, J. M. J. Transamidation of primary amides with amines using hydroxylamine hydrochloride as an inorganic catalyst. *Angew. Chem. Int. Ed.,* **2012**, *51*, 1383-1386. (e) Dragowich, P. S.; Prins, T. J.; Zhou, R.; Johnson, T. O.; Brown, F. L.; Maldonado, F. C.; Fuhrman, S. A.; Zalman, L. S.; Patick, A. K.; Mettews, D. A.; Hou,

X.; Meador, J. W.; Ferre, R. A.; Worland, S. T. Structure-based design, synthesis, and biological evaluation of irreversible human rhinovirus 3C protease inhibitors. Part 7: Structure–activity studies of bicyclic 2-pyridone-containing peptidomimetics. *Bioorg. Med. Chem. Lett*. **2002**, *12*, 733-738. (f) Reich, S. H.; Johnson, T.; Wallace, M. B.; Kephart, S. E.; Fuhrman, S. A.; Worland, S. T.; Matthews, D. A.; Hendrickson, T. F.; Chan, F.; Meador, J.; Ferre, R. A.; Brown, E. L.; Delisle, D. M.; Patick, A. K.; Binford, S. L.; Ford, C. E. Antitumor agents. 199. Three-dimensional quantitative structure-activity relationship study of the colchicine binding site ligands using comparative molecular field analysis. *J. Med. Chem*. **2000**, *43*, 167 (g) Narayana, B.; Vijay Raj, K. K.; Ashalatha, B. V.; Kumari, N. S.; Sarojini, B. K. E. Synthesis of some new 5-(2-substituted-1,3-thiazol-5-yl)-2-hydroxy benzamides and their 2-alkoxy derivatives as possible antifungal agents. *J. Med. Chem*. **2004,** *39*, 867.

18   (a) Lundberg, H.; Tinnis, F.; Selander, N.; Adolfsson, H. Catalytic amide formation from non-activated carboxylic acids and amines. *Chem. Soc. Rev*., **2014**, *43*, 2714 (b) Arzoumanidis, G.G.; Rauch; F. C.; Aromatic amines from carboxylic acids and ammonia. A homogeneous catalytic process. *J. Org. Chem*., **1981**, *46*, 3930 (c) Allen, C. L.; J. Williams, M. J. Metal-catalysed approaches to amide bond formation. *Chem. Soc. Rev.,* **2011**, *40,* 3405-3415.

19   (a) Wang, Z-P. A.; Tian, C-L.; Zheng; J-S. The recent developments and applications of the traceless-Staudinger reaction in chemical biology study. *RSC Adv*., **2015**, *5*, 107192-107199. (b) Rajput, P.; Sharma, A. Synthesis and biological importance of amide analogues. *J. Pharmacol. Med. Chem.*, **2018**; *2*, 22 (c) Lee, H-L.; Aubé, J. Intramolecular and intermolecular Schmidt reactions of alkyl azides with aldehydes. *Tetrahedron,* **2007**, *63*, 9007-9015. (d) Kuo, C-W.; Hsieh, M-T.; Gao, S.; Shao, Y-M.; Yao, C-F.; Shia, K-S. Beckmann rearrangement of ketoximes induced by phenyl dichlorophosphate at ambient temperature. *Molecules*, **2012**, *17,* 13662-13672. (e) Blatt, A. H. The Beckmann Rearrangement. *Chem. Rev.,* **1933**, *12* ,215 (f) Gao, B.; Zhang, G.; Zhou, X.; Huang, H. Palladium-catalyzed regiodivergent hydroaminocarbonylation of alkenes to primary amides with ammonium chloride. *Chem. Sci*., **2018**, *9*, 380 (f) Wang, G.; Yu, Q-Y.; Chen, S-Y.; Yu, X-Q. Et₄NI-catalyzed amidation of aldehydes and alcohols with ammonium salts. *Org. Biom. Chem.* **2014**, *12*, 414-417. (g) Tamura, M.; Tonomura, T.; Shimizu, K-i.; Satsuma, A. Transamidation of amides with amines under solvent-free conditions using a CeO₂ catalyst. *Green Chem.,* **2012**, *14*, 717-724.

20   (a) Fujiwara, H.; Ogasawara, Y.; Yamaguchi, K.; Mizuno, N. A One-Pot Synthesis of Primary Amides from Aldoximes or Aldehydes in Water in the Presence of a Supported Rhodium Catalyst. *Angew. Chem. Int. Ed.* **2007**, *46*, 5202-5297. (b) Thirukovela, N. S.; Balaboina, R.; Kankala, S.; Vadde, R.; Vasam, C. S. Activation of nitriles by silver (I) N-heterocyclic carbenes: An efficient on-water synthesis of primary amides. *Tetrahedron,* **2019**, *75*, 2637-2641. (c) Ghosh, S. C.; Ngiam, J. S. Y.; Seayad, A. M.; Tuan, D. T.; Chai, C. L. L. Chen, A. Copper-catalyzed oxidative amidation of aldehydes with amine salts: synthesis of primary, secondary, and tertiary amides. *J. Org. Chem.* **2012**, *77*, 18, 8007 (d) Fu, R.; Yang, Y.; Zhang, J.; Shao, J.; Xia, X.; Ma, Y.; Yuan, R. Direct oxidative amidation of aldehydes with amines catalyzed by heteropolyanion-based ionic liquids under solvent-free conditions

via a dual-catalysis process. *Org. Biomol. Chem.,* **2016**, *14,* 1784-1793. (e)   Yoo, W-J.; Li, C-J. Highly efficient oxidative amidation of aldehydes with amine hydrochloride salts. *J. Am. Chem. Soc*., **2006**, *128*, 40, 13064-13065. (f) Reddy, K. R.; Maheswari, C. U.; Venkateshwar, M.; Kantam, M. L. Oxidative Amidation of Aldehydes and Alcohols with Primary Amines Catalyzed by KI-TBHP. *Eur. J. Org. Chem.,* **2008**, 3619; (g) K. S. Goh, C-H. Tan; Metal-free pinnick-type oxidative amidation of aldehydes**.** *RSC Adv.,* **2012**, *2,* 5536; (h) D. Xu, L. Shi, D. Ge, X. Cao, H. Gu; *Sci. China Chem.,* **2016**, *59*, 478; (i) Liang, J.; Lv, J.; Shang, Z-C. Metal-free synthesis of amides by oxidative amidation of aldehydes with amines in PEG/oxidant system. *Tetrahedron*, **2011**, *67*, 8532; (j) Z. Wu, K. L. Hull; Rhodium-catalyzed oxidative amidation of allylic alcohols and aldehydes: effective conversion of amines and anilines into amides. *Chem. Sci.,* **2016**, *7*, 969; (k) Debbarma, S.; Maji, M. S. Cp*Rh[III]-Catalyzed Directed Amidation of Aldehydes with Anthranils. *Eur. J. Org. Chem.,* **2017**, 3699; (l) Wan, J-P.; Jing, Y. Recent advances in copper-catalyzed C–H bond amidation. *Beil. J. Org. Chem*., **2015**, 11, 2209-2222.

21   (a) Liu, X.; Jensen, K.F. Direct oxidative amidation of aromatic aldehydes using aqueous hydrogen peroxide in continuous flow microreactor systems. *Green Chem.,* **2012**, *14*, 1471-1474. (b) Yoo, W-J.; Li, C-J. Highly efficient oxidative amidation of aldehydes with amine hydrochloride salts. *J. Am. Chem. Soc.,* **2006**, *128*, 13064-13065.

22   (a) D. Leow; Org. Lett. 2014, 16, 5812; (b) Inagawa, H.; Uchida, S.; Yamaguchi, E.; Itoh, A. Metal-Free Oxidative Amidation of Aromatic Aldehydes using an Anthraquinone-Based Organophotocatalyst. *Asian J. Org. Chem*., **2019**, *8*, 1411 (c) Leung, F. K-C.; Cui, Dr. J-F.; Hui, T-W.; Kung, Dr. K. K-Y.; Wong, Dr. M-K. Photooxidative Amidation of Aldehydes with Amines Catalyzed by Rose Bengal. *Asian J. Org. Chem*., **2015,** *4*, 533.

23   (a) Wang, Y.; Yamaguchi, K.; Mizuno, N. Manganese Oxide Promoted Liquid-Phase Aerobic Oxidative Amidation of Methylarenes to Monoamides Using Ammonia Surrogates. *Angew. Chem. Int. Ed.,* **2012**, *51*, 7250-7253. (b) Zhao, Z.; Wang, T.; Yuan, L.; Hu, X.; Xiong, F.; Zhao, J. Oxidative coupling between methylarenes and ammonia: A direct approach to aromatic primary amides. *Adv. Synth. Catal.,* **2015**, *357*, 2566-2570.

24   (a) Ramezanpour, S.; Bigdelia, Z.; Alavijeha, N. S.; Rominger. F. Application of saccharin as an acidic partner in the Ugi reaction for the one-pot synthesis of 3-iminosaccharins. *Synlett*, **2017**, 28, 1214-1218. (b) Mohamadpour, F.; Maghsoodlou, M. T.; R. Heydari, Lashkari, M. Saccharin: a green, economical and efficient catalyst for the one-pot, multi-component synthesis of 3, 4-dihydropyrimidin-2-(1 H)-one derivatives and 1 H-pyrazolo [1, 2-b] phthalazine-5, 10-dione derivatives and substituted dihydro-2-oxypyrrole. *J. Iran. Chem. Soc*., **2016**, *13*, 1549-1560. (c) Naser, A. W.; Abdullah, A. F.; Synthesis of some new N-saccharin derivatives of possible biological activity. *J. Chem. Pharm. Res.,* **2014**, *6,* 872-879.

25   (a) Dey, S.; Gadakh, S. K.; Sudalai, A. Titanium superoxide–a stable recyclable heterogeneous catalyst for oxidative esterification of aldehydes with alkylarenes or alcohols using TBHP as an oxidant. *Org.*

Biomol. Chem., **2015**, *13*, 10631-10640. (b) Reddy, R. S.; Shaikh, T. M.; Rawat, V.; Karabal, P. U.; Dewkar, G.; Suryavanshi, G.; Sudalai, A. A novel synthesis and characterization of titanium superoxide and its application in organic oxidative processes. *Catal. Surv. Asia,* **2010**, *14*, 21-32. (c) Dewkar, G. K.; Nikalje, M. D.; Ali, I. S.; Paraskar, A. S.; Jagtap, H. S.; Sudalai, A. An Exceptionally Stable Ti Superoxide Radical Ion: A Novel Heterogeneous Catalyst for the Direct Conversion of Aromatic Primary Amines to Nitro Compounds. *Angew. Chem. Int. Ed.* **2001**, 40, 405-408. (d) Shaikh, T. M.; Karbhal, P. U.; Suryavanshi, G. M.; Sudalai, A. Titanium superoxide: a heterogeneous catalyst for anti-Markovnikov aminobromination of olefins. *Tetrahedron Lett.,* **2009,** *50*, 2815-2817.

26   (a) Wang, J.; Liu, C.; Yuana, J.; Lei, A.; Fe-Catalysed oxidative C–H/N–H coupling between aldehydes and simple amides. *Chem. Commun.,* **2014**, *50*, 4736-4739. (b) Adib, M.; Pashazadeh, R.; Daryasarei, S. R.; Mirzaei, P.; Gohari, S. J. A. Metal-free cross-dehydrogenative coupling of aryl aldehydes to give symmetrical carboxylic anhydrides promoted by the TBHP/nBu4PBr system. *Tetrahedron Lett.,* **2016** *57* 3071-3074.

ABSTRACT

Name of the Student: Kishor Dharmraj Mane   **Registration No.:** 10CC17J26029

Faculty of Study: Chemical Science   **Year of Submission:** 2022

AcSIR academic centre/CSIR Lab: **Name of the Supervisor:** Dr. Gurunath Suryavanshi

CSIR-National Chemical Laboratory, Pune   **Name of the Co-Supervisor:** Dr. S. A. R. Mulla

Title of the thesis: Enantioselective Synthesis of Bioactive Molecules and Development of Synthetic Methodologies Involving Formation of C-C, C-N Bonds**.**

Substituted piperidines are the most accessible structural motifs found among the biologically active *N*-heterocycles, which occurred naturally and synthetically. It has become the most reputed and impressive core structure as it is present in 72 small drug molecules having piperidine as an active site. Functional functionalized cyclic ethers are necessary scaffolds found in various natural products and pharmaceutical ingredients. Generally, tetrahydrofuran (THF), 1,4-dioxane, and tetrahydropyrans (THP) are examples of cyclic ethers. These compounds show a broad spectrum of biological activity, including antibacterial, anti-inflammatory, anti-cancer, and anti-diabetic. The natural and synthetic indolizine alkaloids are extensively used in SAR studies and this study reveals that the indolizine derivatives showed a broad spectrum biological activities. The amide bond constituting structural backbone of proteins and peptides, is abundantly found in natural products, pharmaceuticals, polymers and agrochemicals.

Chapter 1 includes the short enantioselective total synthesis of (+)-Tofacitinib and process for the production of key intermediate of (+)- Tofacitinib. Chapter 2 describes the development of metal-Free regioselective cross dehydrogenative coupling of cyclic ethers with aryl carbonyls and quinoxalin-2(1H)-ones. In chapter 3 includes development of new synthetic methodologies for the C-H functionalization of indolizines. In chapter 4 we have developed Ti-superoxide catalysed oxidative amidation of aldehydes and synthesis of congested indolizine amides.

List of Publications Emanating from the Thesis Work

1. **K. D. Mane,** A. Mukherjee, K. Vanka, G. Suryavanshi, Metal-Free Regioselective Cross Dehydrogenative Coupling of Cyclic Ethers and Aryl Carbonyls. *J. Org. Chem.* **2019**, *84,* 2039-2047

2. **K. D. Mane**, R. B. Kamble, G. Suryavanshi, A visible light mediated, metal and oxidant free highly efficient cross dehydrogenative coupling (CDC) reaction between quinoxalin-2(1H)-ones and ethers. *New J. Chem.*, **2019,** *43*, 7403-7408.

3. R. B. Kamble, **K. D. Mane,** B. D. Rupanawar, P. Korekar, A. Sudalai, G. Suryavanshi, Ti-superoxide catalyzed oxidative amidation of aldehydes with saccharin as nitrogen source: synthesis of primary amides. *RSC Adv.,* **2020**, *10*, 724-728.(***equal contribution***)

4. **K. D. Mane,** R. B. Kamble, G. Suryavanshi, Short enantioselective total synthesis of (+)-tofacitinib.*Tetrahedron Letters*, **2021**, *67*,152838.

5. **K. D. Mane**, A. Mukherjee, G. K. Das, G. Suryavanshi, Acetic Acid Catalyzed Regioselective $C(Sp^2)$-H Bond Functionalization of Indolizines: Concomitant Involvement of Synthetic and Theoretical Studies. *J. Org. Chem.* 2022, 87 (8), 5097-5112.

6. **K. D. Mane**, B. D. Rupanwar, G. Suryavanshi, Visible Light Promoted, Photocatalyst Free $C(Sp^2)$-H Bond Functionalization of Indolizines *via* EDA complexes. *E. J. Org. Chem.* **2022** (*Just Accepted*) https://doi.org/10.1002/ejoc.202200261

7. **K. D. Mane,** S. G. More, G. Suryavanshi, Metal-free Regioselective C-3 Alkylation of Indolizines *via* in situ Generated Azaoxyallyl Cations (*Manuscript under preparation*).

List of Publications Non-Emanating from the Thesis Work

8. S. G. More**, K. D. Mane,** G. Suryavanshi Metal-free and Mild Synthesis of Congested *N*-Alkyl Sulfoximines *via* In-situ Generated Aza-oxyallyl Cations from Functionalized Alkyl Bromides. (*Manuscript under communication*)

9. B. D. Rupanwar, **K. D. Mane,** G. Suryavanshi.; Hypervalent Iodine Mediated Oxidation Followed by Acetoxylation / Tosylation of *α*-Substituted Benzylamines Accesing to *α*-Acyloxy / Tosyloxy Ketones. (*Manuscript under communication*).

10. **K. D. Mane**, S. G. More, G. Suryavanshi. Lewis Acid Catalyzed Ring Opening Reactions of Donor-Acceptor Cyclopropanes with Indolizines (work under progress)

11. A. Mukherjee, R. Singh, **K. D. Mane,** G. K. Das; Regioselectivity in metalloradical catalyzed C-H bond activation: A theoretical study. *J. Organomet. Chem.* **2022**, *957*, 122179.

<div align="center">

<ins>List of Posters Presented with Details</ins>

</div>

1. National Science Day Poster Session at CSIR-National Chemical Laboratory, Pune (February 25-27, **2019**)

   Title: Metal-Free Regioselective Cross Dehydrogenative Coupling of Cyclic Ethers and Aryl carbonyls

   Abstract: A highly regioselective, efficient and metal free oxidative cross dehydrogenative coupling (CDC) of aryl carbonyls with cyclic ethers has been developed. This method offers easy access to substituted α-arylated cyclic ethers with high func-tional group tolerance in good to excellent yields. Regioselectivity of this CDC reaction was confirmed by DFT calculation studies.

2. National Science Day Poster Session at CSIR-National Chemical Laboratory, Pune (February 25-27, **2020**)

   Title: Visible Light Mediated, Metal and Oxidant Free Highly Efficient Cross Dehydrogenative Coupling (CDC) Reaction between Quinoxalin-2(1H)-ones and Ethers

   Abstract: An efficient and metal free, white light mediated 3C alkylation of quinoxalin-2(1H)-ones via cross dehydrogenative coupling (CDC) reaction with cyclic ethers using Eosin Y as photocatalyst has been described. This reaction has broad substrate scope and strong functional group tolerance with good to excellent yields.

Metal-Free Regioselective Cross Dehydrogenative Coupling of Cyclic Ethers and Aryl Carbonyls

Kishor D. Mane,[†,§] Anagh Mukherjee,[‡,§] Kumar Vanka,[‡,§] and Gurunath Suryavanshi*[,†,§]

†Chemical Engineering & Process Development Division, CSIR-National Chemical Laboratory, Dr. Homi Bhabha Road, Pune 411008, India

‡Physical and Material Chemistry Division, CSIR-National Chemical Laboratory, Dr. Homi Bhabha Road, Pune 411008, India

§Academy of Scientific and Innovative Research (AcSIR), New Delhi 110 025, India

Ⓢ *Supporting Information*

ABSTRACT: A highly regioselective, efficient, and metal-free oxidative cross dehydrogenative coupling (CDC) of aryl carbonyls with cyclic ethers has been developed. This method offers easy access to substituted α-arylated cyclic ethers with a high functional group tolerance in good to excellent yields. The regioselectivity of this CDC reaction was confirmed by density functional theory (DFT)-based calculations.

- Metal Free
- High Regioselective Reaction
- Broad Substrate Scope
- Yields up to 92%
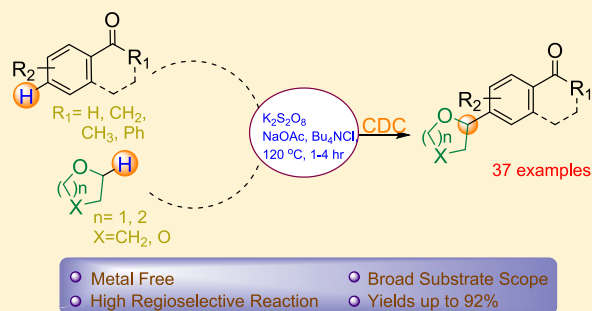
INTRODUCTION

Functionalized cyclic ethers are important scaffolds that are found in a variety of natural products and pharmaceutical ingredients.[1] Generally, tetrahydrofuran (THF), 1,4-dioxane, and tetrahydropyrans (THP) are the examples of cyclic ethers. These compounds show a broad spectrum of biological activity, including antibacterial,[2a] anti-inflammatory,[2b] anticancer,[2c−e] and antidiabetic.[2f,g] They have also been employed in the synthesis of agricultural pesticide **1** (Figure 1).[3]

Lignins are the class of natural compounds that exclusively contain substituted THF as a core unit.[5] Examples of lignins include sesamin **2** and galbacin **3** (Figure 1). These compounds are known to exhibit anticancer,[4a] antioxidant,[4b]

anti-inflammatory,[4c] and antiobesity[4d] properties. Strebluslignanol F **4**, a natural product, contains 1,4-dioxane as a core unit and shows potent antihepatitis B virus activity.[5a] On the other hand, omarigliptin **5** is an oral antidiabetic drug with substituted THP as the core moiety.[5b]

The formation of the C−C bond via C−H bond activation of sp3 and sp2 hybridized carbons as cross-coupling participants has generated renewed attention over the last few decades.[6a,b] However, sp3 C−H bond activation is a challenging task due to the inertness, gained from high bond energy and high pK_a values. Hence, CDC reactions have attracted the attention of organic chemists for the preparation of C−C bonds under metal and metal-free conditions in academic as well as industrial research.[6c−f]

After a careful survey of the literature, we realized that both metal and metal-free approaches have been employed for the oxidative cross dehydrogenative coupling of cyclic ethers with arenes and heteroarenes. Some of these important methods include the use of transition metals such as Cu(I)-catalyzed cross coupling between substituted 1,1′-diarylethenes and cyclic ethers,[7] Cu(II)-catalyzed addition of α-oxyalkyl radical to isoquinolinium salts,[8] and Fe(II)-catalyzed α-arylation of cyclic and acyclic ethers with azoles.[9] Also, Doyle and co-workers have achieved α-arylation of cyclic ethers through Ni(II)-catalyzed photoredox coupling between aryl halide and cyclic ethers, as shown in Scheme 1.[10]

Various electron-deficient heterocyclic arenes were subjected for α-arylation of cyclic and acyclic ethers under oxidative

Figure 1. Biologically active cyclic ethers.

Scheme 1. Strategies for the α-Arylation of Cyclic Ethers

Table 1. Optimisation Conditions for Cross Dehydrogenative Coupling

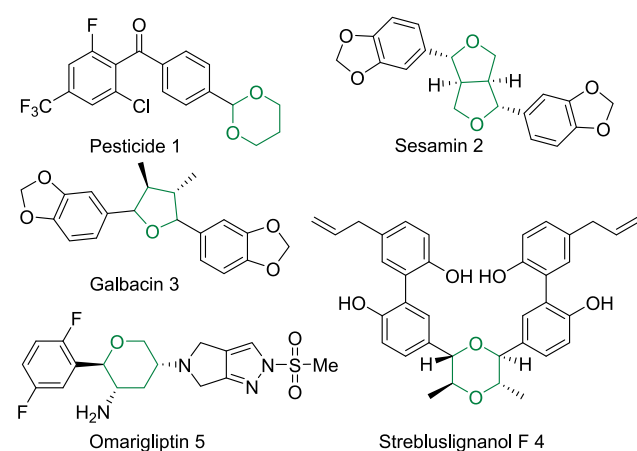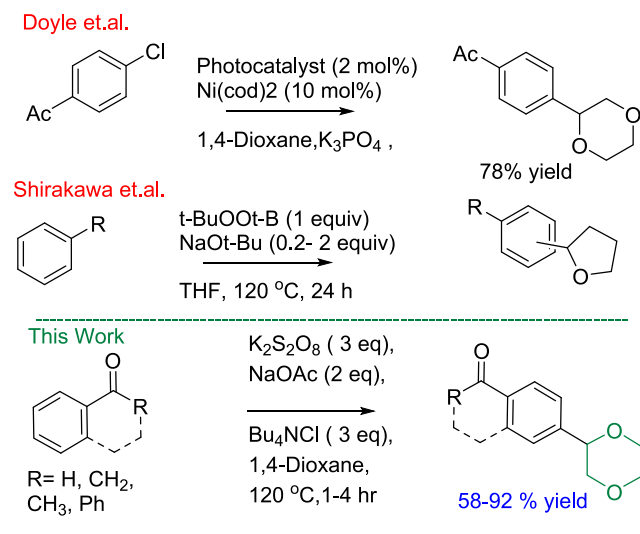| entry	oxidant (3 equiv)	additive (equiv)	base (equiv)	time (h)	yield (%)
1	K$_2$S$_2$O$_8$	A (2)	NaOAc (2)	4	51
2	K$_2$S$_2$O$_8$	A (2)	NaOAc (2)	12	45
3	K$_2$S$_2$O$_8$	A (3)	NaOAc (2)	4	57
4[a]	K$_2$S$_2$O$_8$	B (3)	NaOAc (2)	4	81
5	K$_2$S$_2$O$_8$	B (3)		4	NR
6	K$_2$S$_2$O$_8$		NaOAc (2)	12	NR
7	K$_2$S$_2$O$_8$	B (4)	NaOAc (2)	4	85
8	K$_2$S$_2$O$_8$	B (3)	NaOAc (4)	4	79
9	Na$_2$S$_2$O$_8$	B (3)	NaOAc (2)	12	31
10	(NH$_4$)$_2$S$_2$O$_8$	B (3)	NaOAc (2)	12	NR
11[b]	K$_2$S$_2$O$_8$	B (3)	NaOAc (2)	12	NR
12[c]	K$_2$S$_2$O$_8$	C (3)	NaOAc (2)	4	67
13	K$_2$S$_2$O$_8$	B (3)	K$_2$CO$_3$ (2)	4	NR
14	K$_2$S$_2$O$_8$	B (3)	NaOEt (2)	4	70
15	K$_2$S$_2$O$_8$	B (3)	Cs$_2$CO$_3$ (2)	4	NR
16	K$_2$S$_2$O$_8$	B (3)	NaO^{t}Bu(2)	4	NR
17	K$_2$S$_2$O$_8$		Bu$_4$NOH	4	NR
18	K$_2$S$_2$O$_8$	D (2)	NaOAc (2)	12	55
19	K$_2$S$_2$O$_8$	D (2)		12	NR
20	Oxone	B (3)	NaOAc (2)	4	17
21	TBHP	B (3)	NaOAc (2)	4	NR
22	DTBP	B (3)	NaOAc (2)	4	trace
23	BPO	B (3)	NaOAc (2)	4	NR

[a]TBACl in 50% aq solution. [b]Temp = 80 °C. [c]Bu$_4$NF·3H$_2$O. NR = no reaction.

metal-free conditions using a variety of oxidants such as DTBP, TBHP, BPO, and K$_2$S$_2$O$_8$. These heterocycles contain substituted pyridines,[11] thiophenes,[12] indoles,[13] quinines,[14] azoles,[15] and chromanes.[16] Although these methods are efficient toward yielding the CDC product, they are limited to activated heterocyclic systems. Recently, Shirakawa et al. reported base-promoted oxidative dehydrogenative coupling between a substituted benzene derivative and cyclic ethers, as well as amides, in the presence of DTBP oxidant and NaOt-Bu base.[17] Despite some advantages, the reaction suffers from certain limitations such as poor yields and poor regioselectivity when electron-withdrawing substituents were present on the aryl rings.

To overcome these shortcomings and inspired by metal-free approaches,[18] our motive has been to develop a synthetic method for the α-functionalization of cyclic ethers with better yields and regioselectivity (Scheme 1). Thus, we have described the metal-free CDC reaction via Csp^3−Csp^2 coupling between various cyclic ethers and aromatic carbonyls to generate a wide range of α-arylated cyclic ethers. The key features of this reaction are a short reaction time, good to excellent yields, and a high regioselectivity.

■ RESULTS AND DISCUSSION

We have started our investigation by taking acetophenone as a model substrate and 1,4-dioxane as a coupling partner as well as a solvent. The results are summarized in Table 1.

Initially, when acetophenone **6a** (1 equiv) and 1,4-dioxane (30 equiv, also acts as a solvent) are reacted at 120 °C in the presence of oxidant K$_2$S$_2$O$_8$ (3 equiv), tetrabutylammonium bromide (A) (2 equiv) as an additive, and NaOAc (2 equiv), to our delight we got the expected product **7a** in 51% yield within 4 h (Table 1, entry 1). When the reaction time was increased from 4 to 12 h, the yield of **7a** was reduced to 45%, as a result of decomposition of the obtained product (Table 1, entry 2). With an increased equivalence of tetrabutylammonium bromide (A) from 2 to 3 and refluxing at 120 °C, we obtained 57% yield of the desired product (Table 1, entry 3). When tetrabutylammonium chloride (B) was used instead of tetrabutylammonium bromide (A) as an additive and the mixture refluxed for 4 h, we got the expected product in 81% yield, which was a significant improvement (Table 1, entry 4)

in comparison to the first 3 entries (Table 1, entries 1−3). It was also observed that the reaction did not proceed in the absence of an additive as well as a base (Table 1, entries 5 and 6) and resulted in the recovery of the starting material. By increasing the additive tetrabutylammonium chloride (B) from 3 to 4 equiv, we observed an increase in yields only by 4% (Table 1, entry 7). Keeping the tetrabutylammonium chloride (B) (3 equiv) and K$_2$S$_2$O$_8$ (3 equiv) constant and increasing the stoichiometry of NaOAc (2 to 4 equiv) led to 79% yield for the CDC product (Table 1, entry 8). In continuation, the oxidant Na$_2$S$_2$O$_8$ offers only 31% yield of the desired product (Table 1, entry 9). No conversion was observed using (NH$_4$)$_2$S$_2$O$_8$ (Table 1, entry 10). However, no significant improvement was observed with the use of different combinations of additives and bases. Instead, most of the attempts were not fruitful (Table 1, entries 11−23). However, changing the bases did not lead to an enhancement in the yields. In order to examine the effect of atmospheric oxygen, the reaction was conducted under inert atmosphere, which did not affect the yield. In addition to this, the effect of the solvent was also studied (see the Supporting Information). Therefore,

the best regioselectivity and the highest yield of isolated product were achieved by using $K_2S_2O_8$ (3 equiv), tetrabutylammonium chloride (B) (3 equiv), and NaOAc (2 equiv) for the reaction at 120 °C for 4 h (Table1, entry 4).

With these optimized reaction conditions in hand (Table 1, entry 4), the substrate scope of this unique transformation and limitations of the CDC reaction were studied by evaluating a variety of aryl carbonyls in order to investigate the generality of this reaction.

As shown in Scheme 2, the CDC reaction proceeds without any difficulty for a wide range of substrates bearing various

gave the desired product **7e** in 66% yield. 1-Acetonaphthone also gave the expected α-arylated products of different cyclic ethers with excellent yields (**7d**, **7g**, **7o**). On the other hand, substituted cyclic ketones such as indanone and tetralone resulted in moderate yields of the products (**7l**–**7n**). It is noteworthy that thioxanthone successively yielded CDC product **7k** under oxidation conditions without any adverse effect of the sulfur. When acetophenone was subjected under the standardized reaction conditions using 1,3-benzodioxole as a solvent, the corresponding product **7r** was formed in 58% yield. Also, acyclic ethers as coupling partners led to undesired polymerization. Unfortunately this approach failed to yield the expected CDC products (**7s**–**7x**) when the reaction was carried out on N-substituted aryl carbonyls and heterocyclic aryl ketones.

Next, we examined the efficiency of substituted aldehydes as coupling partners under the optimized experimental conditions. Notably, it was observed that the rate of the CDC reaction between benzaldehydes and cyclic ethers was faster than for the aryl ketones.

Various substrates having electron-withdrawing substituents, such as Cl, Br, and F groups on the aromatic ring of the aldehydes were efficiently reacted to produce the substituted *para*-alkylated benzalehydes with excellent yields (Scheme 3, entries **9b**, **9e**, and **9g**). Surprisingly, hydroxy-substituted benaldehydes also offer good yields of alkylated aryl carbonyls under oxidative conditions (**9h** and **9i**). Benzaldehydes with different electron-donating substituents also led to the corresponding product with good to excellent yields. (**9c**, **9d**,

Scheme 2. CDC Reaction between Aromatic Ketones and Cyclic Ethers[a]

Scheme 3. CDC Reaction between Aromatic Aldehydes and Cyclic Ethers[a]

[a]Reaction conditions: **6a** (0.83 mmol), $K_2S_2O_8$ (2.5 mmol), TBACl (2.5 mmol 50% aq solution), NaOAc (1.66 mmol), 1,4-dioxane (3 mL), at 120 °C.
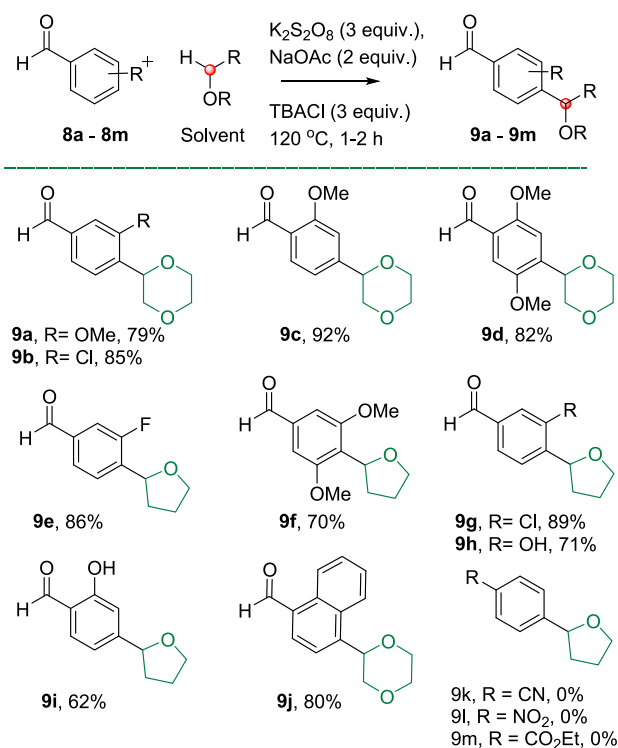
[a]Reaction conditions: **8a** (0.73 mmol), $K_2S_2O_8$ (2.20 mmol), TBACl (2.20 mmol 50% aq solution), NaOAc (1.47 mmol), 1,4-dioxane (3 mL) at 120 °C.

substituents at different positions on the aryl ketones, providing the coupling products in moderate to good yields. When the electron-withdrawing and electron-donating groups were present at the position meta to the acetyl group and the reaction was performed under optimized conditions, the desired products were obtained in excellent yields (**7b**, **7c**, **7f**). The unsubstituted acetophenone was subjected to the standard reaction conditions with THP as a coupling ether and

and **9f**). A reaction performed with 2,5-dimethoxy benzaldehyde on a 6 mmol scale provided **9d** in 79% yield. Cyano-, nitro-, and carboxylate-substituted aryl derivatives were unable to give the desired product with our optimized reaction conditions. (**9k–m**).

When benzil, α,α'-dimethyl acetal was subjected to the reaction under standard reaction conditions, it gave unexpected products. In THF, the acetal group remained unaffected, whereas, in 1,4-dioxane, it was deprotected to ketone (Scheme 4). An uncommon phenomenon that has

Scheme 4. Some Unexpected Result of the CDC Reaction
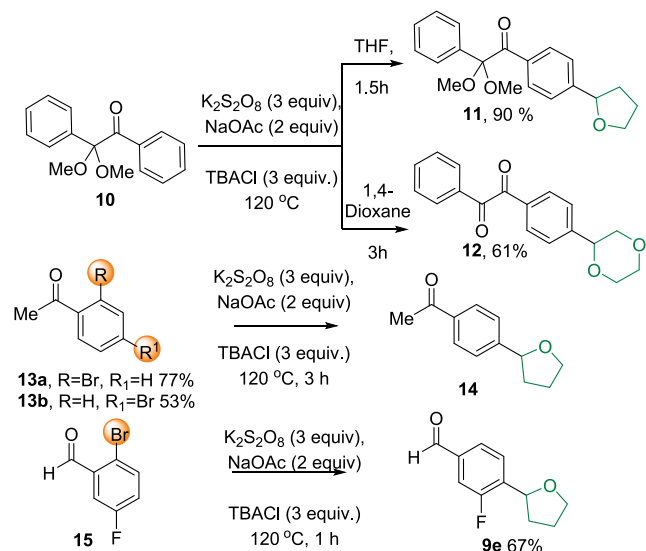
been observed is that the presence of bromine on the *ortho* or *para* position to the aryl carbonyls delivers unexpected debrominated products, i.e., **14** and **9e**, as shown in Scheme 4.

To show the utility of the reaction, the *para*-alkylated aryl carbonyl derivatives were further functionalized under various reaction conditions, as shown in Scheme 5. The compound **9d**

Scheme 5. Synthetic Transformations of the Products
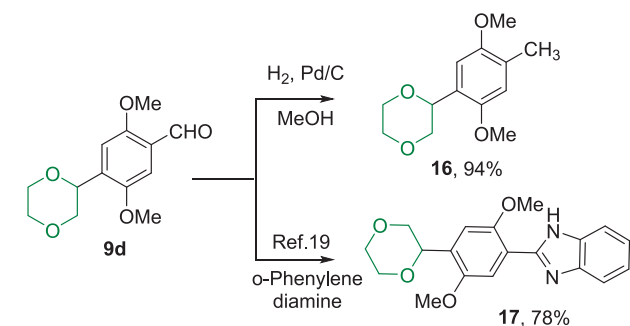
was subjected for the hydrogenation reaction using Pd/C; the aldehyde group of **9d** was reduced to methyl to give the toluene derivative **16** in a quantitative yield. Subsequently, the same compound **9d** was converted into its 1,2-benzimidazole derivative under the known protocol.[19]

In order to understand the mechanism of this CDC reaction, we carried out control experiments (Scheme 6), where 2 equiv of TEMPO (2,2,6,6-tetramethylpiperidine-*N*-oxide) were added into the reaction system under optimized reaction

Scheme 6. Control Experiments
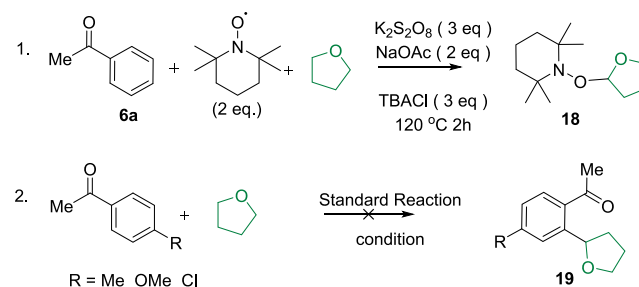
conditions. It was observed that the THF radical coupled with TEMPO to form a TEMPO–THF adduct **18**, instead of the expected product **7a**. This indicates that the reaction might be proceeding via the radical pathway. In the second control experiment, when the reaction was performed with *para*-substituted aryl ketone, we did not obtain the expected *ortho*-alkylated product **19**.

This indicates that the reaction regioselectively goes only to the *para* position. Based on the above control experiments and the reported literature,[20,21] the possible catalytic cycle was then initially proposed in Scheme 7, as the α-oxyalkyl radical **20** was

Scheme 7. Expected Reaction Mechanism of Dehydrogenative Coupling
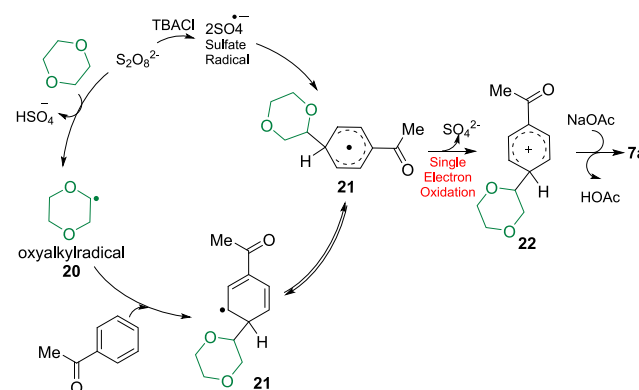
generated via hydrogen atom abstraction from 1,4-dioxane by persulfate.[20] Then, this α-oxyalkyl radical **20** reacted with acetophenone **6a** to generate the aryl radical species **21**. This was followed by single-electron oxidation to form the aryl cation species **22**.[21] The aryl cationic species further underwent aromatization to form the desired product **7a**.

In order to elucidate the reasons behind the *para* product being formed exclusively, quantum chemical calculations have been done using density functional theory (DFT). (See Figures S1 and S2 for more details.)

■ CONCLUSION

In conclusion, we have developed the first efficient and metal-free CDC reaction of aromatic carbonyls with inactive cyclic ethers to give the desired *p*-alkylated aryl aldehydes and ketones in good to excellent yields with a high regioselectivity. In addition, this reaction tolerates various functional groups under oxidative conditions and can be applied to obtain a wide range of substituted aromatic carbonyls. The utility of the products of CDC were shown by converting them to benzimidazole heterocycles and the toluene derivative.

■ EXPERIMENTAL SECTION

General Information. Solvents were purified and dried using standard procedures before use. All air- and moisture-sensitive reactions were carried out in flame-dried glassware under a positive pressure of dry argon using standard techniques. Commercially available chemicals were used without further purification unless otherwise mentioned. For moisture-sensitive reactions, tetrahydrofuran (THF) and dichloromethane (CH$_2$Cl$_2$) were dried using a standard solvent purification system. The following dry solvents are commercially available and were used without further purification: acetonitrile, Acros Organics, 99.9% extra dry, over molecular sieves; ethanol, Acros Organics, 99.5% extra dry; methanol, Acros Organics, 99.8% extra dry, over molecular sieves. Technical solvents for column chromatography were used after simple distillation. The reactions were monitored by TLC visualized by UV (254 nm) and/or with iodine. The purification was done using column chromatography on silica 60 (Merck, 230−400 mesh) with the indicated eluent mixtures (v/v)

Nuclear magnetic resonance spectra were recorded at room temperature on Bruker AVHD-200, AVHD-400, and AVHD-500 spectrometers in appropriate solvents using TMS as an internal standard or the solvent signals as secondary standards, and the chemical shifts are shown in δ scales. Coupling constants (J) are given in hertz (Hz), and the classical abbreviations are used to describe the signal multiplicities. ^{1}H NMR spectra were calibrated to the residual proton signal of chloroform-d_1 (δ = 7.27 ppm), and ^{13}C NMR spectra were referenced to the ^{13}C triplet of CDCl$_3$ (δ = 77.16 ppm). Apparent multiplets, which occur as a result of coupling constant equality between magnetically nonequivalent protons, are marked as virtual (virt). The following abbreviations for single multiplicities were used: br = broad, s = singlet, d = doublet, t = triplet, q = quartet, m = multiplet. High-resolution mass spectra (HRMS) for all new compounds were recorded on an ESI+ method and Orbitrap mass analyzer (Thermo Scientific Q-Exactive, Accela 1250 pump). All chemicals are purchased from Sigma-Aldrich and used without further purification.

Typical Experimental Procedure for the Synthesis of 1-(4-(1,4-Dioxan-2-yl)phenyl)ethan-1-one (7a). To a 25 mL round-bottom flask were added acetophenone **6a** (0.833 mmol, 100 mg), K$_2$S$_2$O$_8$ (2.5 mmol, 676 mg), tetrabutylammonium chloride (TBACl, 2.5 mmol, 1.4 mL), and NaOAc (1.66 mmol, 136 mg) in 1,4-dioxane (3 mL). The round-bottom flask was equipped with a condenser, and the resulting reaction mixture was refluxed to 120 °C for 4 h. The progress of the reaction was monitored by TLC. Upon completion of the reaction, the reaction mixture was dried under a vacuum. Then the crude reaction mixture was diluted with ethyl acetate (10 mL), washed with brine, and eluted with EtOAc (25 mL × 2). The organics were evaporated, and the crude residue was preadsorbed on silica gel and purified by column chromatography (100−200 mesh silica using 80:20 petroleum ether/ethyl acetate as the eluent to afford the corresponding compound **7a** in 81% yield.

1-(4-(1,4-Dioxan-2-yl)phenyl)ethan-1-one (7a): white solid, 81% yield (139 mg); mp 91−93 °C; ^{1}H NMR (500 MHz, CDCl$_3$) δ 7.99−7.87 (m, J = 8.4 Hz, 2H), 7.54−7.39 (m, J = 8.0 Hz, 2H), 4.68 (dd, J = 2.3, 9.9 Hz, 1H), 3.98−3.94 (m, 1H), 3.92 (dd, J = 2.3, 11.1 Hz, 1H), 3.89−3.86 (m, 1H), 3.83−3.79 (m, 1H), 3.74 (dd, J = 3.1, 11.4 Hz, 1H), 3.41 (t, J = 10.9 Hz, 1H), 2.59 (s, 3H); ^{13}C{^{1}H} NMR (126 MHz, CDCl$_3$) δ 197.6, 143.4, 136.7, 128.4, 126.2, 77.3, 72.1, 66.9, 66.2, 26.5; HRMS (ESI) m/z calcd for C$_{12}$H$_{15}$O$_3$ [M + H]$^+$ 207.1016, found 207.1019.

1-(3-Bromo-4-(1,4-dioxan-2-yl)phenyl)ethan-1-one (7b): white solid, 80% yield (114 mg); mp 87−89 °C; ^{1}H NMR (500 MHz, CDCl$_3$) δ 8.02 (d, J = 1.5 Hz, 1H), 7.83 (dd, J = 1.5, 8.0 Hz, 1H), 7.60 (d, J = 8.0 Hz, 1H), 4.92 (dd, J = 2.5, 9.7 Hz, 1H), 4.01 (dd, J = 2.5, 11.6 Hz, 1H), 3.91 (s, 1H), 3.90−3.88 (m, 1H), 3.77−3.74 (m, 1H), 3.69−3.63 (m, 1H), 3.15 (dd, J = 9.7, 11.6 Hz, 1H), 2.51 (s, 3H); ^{13}C{^{1}H} NMR (126 MHz, CDCl$_3$) δ 196.3, 142.6, 137.8, 132.4, 128.2, 127.4, 122.0, 77.0, 70.5, 67.1, 66.3, 26.6; HRMS (ESI) m/z calcd for C$_{12}$H$_{14}$O$_3$Br [M + H]$^+$ 285.0121, found 285.0127.

1-(4-(1,4-Dioxan-2-yl)-3-fluorophenyl)ethan-1-one (7c): white solid, 84% yield (136 mg); mp 116−118 °C; ^{1}H NMR (500 MHz, CDCl$_3$) δ 7.72−7.78 (m, 1H), 7.57−7.66 (m, 2H), 4.97 (dd, J = 9.9, 2.3 Hz, 1H), 3.91−4.00 (m, 3H), 3.80−3.84 (m, 1H), 3.70−3.77 (m, 1H), 3.36 (dd, J = 11.4, 9.9 Hz, 1H), 2.59 (s, 3H); ^{13}C{^{1}H} NMR (126 MHz, CDCl$_3$) δ 196.4, 160.4−158.4 (d, $J_{F−C}$ = 247.96 Hz), 138.4−138.3 (d, $J_{F−C}$ = 6.68 Hz), 130.8−130.7 (d, $J_{F−C}$ = 14.31 Hz), 128.04−128.01 (d, $J_{F−C}$ = 3.81 Hz), 124.4, 114.8−114.6 (d, $J_{F−C}$ = 22.89 Hz), 71.9, 70.9, 67.2, 66.3, 26.6; HRMS (ESI) m/z calcd for C$_{12}$H$_{14}$O$_3$F [M + H]$^+$ 225.0921, found 225.0928.

1-(4-(1,4-Dioxan-2-yl)naphthalen-1-yl)ethan-1-one (7d): gummy liquid, 75% yield (113 mg); ^{1}H NMR (200 MHz, CDCl$_3$) δ 8.87−8.64 (m, 1H), 8.15−8.05 (m, 1H), 7.93 (d, J = 7.6 Hz, 1H), 7.75 (d, J = 7.6 Hz, 1H), 7.66−7.51 (m, 2H), 5.43 (dd, J = 2.4, 9.7 Hz, 1H), 4.18−4.04 (m, 3H), 3.95−3.76 (m, 2H), 3.50 (dd, J = 10.0, 11.9 Hz, 1H), 2.75 (s, 3H); ^{13}C{^{1}H} NMR (126 MHz, CDCl$_3$) δ 201.7, 138.7, 135.5, 130.4, 129.9, 127.7, 127.3, 126.6, 126.5, 122.5, 122.1, 74.7, 71.9, 67.2, 66.4, 29.8; HRMS (ESI) m/z calcd for C$_{16}$H$_{17}$O$_3$ [M + H]$^+$ 257.1172, found 257.1171.

1-(4-(Tetrahydro-2H-pyran-2-yl)phenyl)ethan-1one (7e): whitish semisolid, 66% yield (112 mg); ^{1}H NMR (200 MHz, CDCl$_3$) δ 7.97−7.86 (m, J = 8.3 Hz, 2H), 7.49−7.38 (m, J = 8.2 Hz, 2H), 4.39 (d, J = 10.6 Hz, 1H), 4.17 (dd, J = 2.9, 10.9 Hz, 1H), 3.71−3.56 (m, 1H), 2.60 (s, 3H), 1.86 (d, J = 12.3 Hz, 1H), 1.75−1.47 (m, 5H); ^{13}C{^{1}H} NMR (101 MHz, CDCl$_3$) δ 197.9, 148.7, 136.1, 128.4, 125.8, 79.5, 68.9, 34.1, 26.6, 25.7, 23.9; HRMS (ESI) m/z calcd for C$_{13}$H$_{17}$O$_2$ [M + H]$^+$ 205.1223, found 205.1222.

1-(3-Bromo-4-(tetrahydro-2H-pyran-2-yl)phenyl)ethan-1-one (7f): clear oil, 79% yield (113 mg); ^{1}H NMR (500 MHz, CDCl$_3$) δ 8.08 (s, 1H), 7.88 (d, J = 8.0 Hz, 1H), 7.64 (d, J = 8.0 Hz, 1H), 4.65 (d, J = 10.7 Hz, 1H), 4.16 (d, J = 11.1 Hz, 1H), 3.65 (t, J = 10.7 Hz, 1H), 2.57 (s, 3H), 2.03 (d, J = 13.4 Hz, 1H), 1.93 (br s, 1H), 1.74−1.65 (m, 2H), 1.60 (d, J = 8.4 Hz, 1H), 1.31−1.24 (m, 1H); ^{13}C{^{1}H} NMR (126 MHz, CDCl$_3$) δ 196.4, 147.7, 137.1, 132.3, 127.5, 127.4, 121.5, 78.9, 69.0, 32.6, 26.5, 25.7, 23.7; HRMS (ESI) m/z calcd for C$_{13}$H$_{16}$O$_2$Br [M + H]$^+$ 283.0328, found 283.0333.

1-(4-(Tetrahydro-2H-pyran-2-yl)naphthalen-1-yl)ethan-1-one (7g): gummy oil, 82% yield (123 mg); ^{1}H NMR (400 MHz, CDCl$_3$) δ 8.78 (d, J = 7.9 Hz, 1H), 8.07 (d, J = 7.9 Hz, 1H), 7.93 (d, J = 7.9 Hz, 1H), 7.71 (d, J = 7.3 Hz, 1H), 7.62−7.51 (m, 2H), 5.09 (d, J = 11.0 Hz, 1H), 4.31−4.22 (m, 1H), 3.85−3.73 (m, 1H), 2.74 (s, 3H), 2.11−1.99 (m, 2H), 1.86−1.78 (m, 2H), 1.72−1.64 (m, 2H); ^{13}C{^{1}H} NMR (101 MHz, CDCl$_3$) δ 201.6, 143.8, 134.5, 130.2, 130.0, 128.0, 126.9, 126.3, 125.9, 122.9, 121.0, 76.6, 69.0, 33.2, 29.7, 25.6, 23.8; HRMS (ESI) m/z calcd for C$_{17}$H$_{19}$O$_2$ [M + H]$^+$ 255.1380, found 255.1378

(4-(1,4-Dioxan-2-yl)phenyl)(phenyl)methanone (7h): white solid, 72% yield (106 mg); mp 70−72 °C; ^{1}H NMR (200 MHz, CDCl$_3$) δ 7.84−7.77 (m, 4H), 7.65−7.55 (m, 1H), 7.54−7.44 (m, 4H), 4.73 (dd, J = 2.7, 10.2 Hz, 1H), 4.01−3.93 (m, 2H), 3.92−3.85 (m, 1H), 3.85−3.69 (m, 2H), 3.48 (dd, J = 10.2, 11.5 Hz, 1H); ^{13}C{^{1}H} NMR (101 MHz, CDCl$_3$) δ 195.6, 142.5, 137.3, 137.0, 132.0, 129.9, 129.7, 128.0, 126.3, 125.6, 125.1, 77.1, 72.0, 66.7, 66.0; HRMS (ESI) m/z calcd for C$_{17}$H$_{17}$O$_3$ [M + H]$^+$ 269.1172, found 269.1174.

(4-(1,4-Dioxan-2-yl)phenyl)(4-bromophenyl)methanone (7i): white solid, 67% yield (89 mg); mp 88−90 °C; ^{1}H NMR (200 MHz, CDCl$_3$) δ 7.81−7.74 (m, J = 8.3 Hz, 2H), 7.71−7.60 (m, 4H), 7.54−7.43 (m, J = 8.1 Hz, 2H), 4.73 (dd, J = 2.6, 10.0 Hz, 1H), 4.01−3.92 (m, 2H), 3.89 (d, J = 2.7 Hz, 1H), 3.84−3.69 (m, 2H), 3.46 (dd, J = 10.2, 11.6 Hz, 1H); ^{13}C{^{1}H} NMR (50 MHz, CDCl$_3$) δ 194.5, 142.4, 136.1, 135.6, 131.0, 130.8, 129.4, 127.6, 126.9, 126.6, 125.5, 76.7, 71.6, 66.3, 65.7; HRMS (ESI) m/z calcd for C$_{17}$H$_{16}$O$_3$Br [M + H]$^+$ 347.0277, found 347.0285.

(4-(1,4-Dioxan-2-yl)phenyl)(4-chlorophenyl)methanone (7j): white solid, 61% yield (85 mg); mp 90−92 °C; ^{1}H NMR (500 MHz, CDCl$_3$) δ 7.75 (d, J = 8.4 Hz, 2H), 7.77 (d, J = 8.0 Hz, 2H), 7.48 (dd, J = 9.9, 8.4 Hz, 4H), 4.73 (dd, J = 10.3, 2.7 Hz, 1H), 3.97−4.00 (m, 1H), 3.90−3.95 (m, 2H), 3.82−3.86 (m, 1H), 3.76 (td, J = 11.3, 3.2 Hz, 1H), 3.47 (dd, J = 11.4, 10.3 Hz, 1H); ^{13}C{^{1}H} NMR (101 MHz, CDCl$_3$) δ 194.7, 142.7, 138.6, 136.5, 135.5, 131.1, 129.8,

128.3, 125.8, 77.1, 71.9, 66.7, 66.0; HRMS (ESI) m/z calcd for $C_{17}H_{16}O_3Cl$ $[M + H]^+$ 303.0782, found 303.0789.

3-(1,4-Dioxan-2-yl)-9H-thioxanthen-9-one (7k): white solid, 74% yield (104 mg); mp 163−165 °C; ^{1}H NMR (400 MHz, CDCl$_3$) δ 8.54−8.66 (m, 2H), 7.56−7.66 (m, 3H), 7.46−7.53 (m, 1H), 7.42 (dd, J = 8.2, 1.8 Hz, 1H), 4.76 (dd, J = 10.1, 2.7 Hz, 1H), 3.91−4.05 (m, 3H), 3.85 (dd, J = 11.4, 2.7 Hz, 1H), 3.76 (td, J = 11.3, 3.4 Hz, 1H), 3.46 (dd, J = 11.9, 10.1 Hz, 1H); ^{13}C{^{1}H} NMR (101 MHz, CDCl$_3$) δ 179.7, 142.9, 137.6, 137.2, 132.3, 130.0, 129.8, 129.2, 128.8, 126.4, 126.0, 124.1, 123.2, 72.1, 67.0, 66.3; HRMS (ESI) m/z calcd for $C_{17}H_{15}O_3S$ $[M + H]^+$ 299.0736, found 299.0733.

5-(1,4-Dioxan-2-yl)-2,3-dihydro-1H-inden-1-one (7l): white solid, 67% yield (110 mg); mp 128−130 °C; ^{1}H NMR (400 MHz, CDCl$_3$) δ 7.50−7.70 (m, 2H), 7.39 (d, J = 6.7 Hz, 1H), 5.68 (d, J = 9.2 Hz, 1H), 3.92−4.08 (m, 3H), 3.82 (d, J = 11.0 Hz, 1H), 3.72 (td, J = 11.0, 3.7 Hz, 1H), 3.22 (t, J = 10.4 Hz, 1H), 3.05−3.17 (m, 2H), 2.58−2.83 (m, 2H); ^{13}C{^{1}H} NMR (101 MHz, CDCl$_3$) δ 207.0, 155.7, 138.5, 134.6, 132.6, 125.9, 124.6, 73.2, 71.7, 67.0, 66.3, 36.6, 25.6; HRMS (ESI) m/z calcd for $C_{13}H_{15}O_3$ $[M + H]^+$ 219.1016, found 219.1018.

4-Bromo-5-(tetrahydrofuran-2-yl)-2,3-dihydro-1H-inden-1-one (7m): off white solid, 70% yield (93 mg); mp 116−118 °C; ^{1}H NMR (200 MHz, CDCl$_3$) δ 7.62 (d, J = 8.2 Hz, 1H), 7.39 (d, J = 8.1 Hz, 1H), 5.64 (t, J = 6.9 Hz, 1H), 4.06 (q, J = 7.1 Hz, 1H), 3.79−3.97 (m, 1H), 2.92−3.06 (m, 2H), 2.43−2.69 (m, 3H), 1.72−2.06 (m, 2H), 1.34−1.55 (m, 1H); ^{13}C{^{1}H} NMR (126 MHz, CDCl$_3$) δ 206.5, 155.1, 144.2, 137.1, 134.5, 125.2, 120.1, 76.4, 69.1, 36.4, 34.0, 26.9, 25.8; HRMS (ESI) m/z calcd for $C_{13}H_{14}O_2Br$ $[M + H]^+$ 281.0172, found 281.0170.

6-(Tetrahydrofuran-2-yl)-3,4-dihydronaphthalen-1(2H)-one (7n). clear oil, 62% yield (91 mg); ^{1}H NMR (400 MHz, CDCl$_3$) δ 7.93 (d, J = 8.5 Hz, 1H), 7.13−7.24 (m, 2H), 4.85 (d, J = 6.7 Hz, 1H), 4.04 (d, J = 7.9 Hz, 1H), 3.89 (d, J = 7.3 Hz, 1H), 2.85−2.97 (m, 2H), 2.52−2.64 (m, 2H), 2.21−2.36 (m, 1H), 2.01−2.13 (m, 2H), 1.91−2.00 (m, 2H), 1.65−1.79 (m, 1H); ^{13}C{^{1}H} NMR (101 MHz, CDCl3) δ 197.9, 149.1, 144.4, 131.3, 127.0, 125.2, 123.6, 79.9, 68.6, 38.8, 34.3, 29.5, 29.4, 25.7, 23.0; HRMS (ESI) m/z calcd for $C_{14}H_{17}O_2$ $[M + H]^+$ 217.1223, found 217.1222.

1-(4-(Tetrahydrofuran-2-yl)naphthalen-1-yl)ethan-1-one (7o): white solid, 87% yield (123 mg); mp 65−67 °C; ^{1}H NMR (400 MHz, CDCl$_3$) δ 8.80 (d, J = 8.5 Hz, 1H), 7.94 (d, J = 7.3 Hz, 1H), 7.98 (d, J = 7.9 Hz, 1H), 7.70 (d, J = 7.3 Hz, 1H), 7.52−7.65 (m, 2H), 5.61−5.76 (m, 1H), 4.20−4.37 (m, 1H), 4.06 (q, J = 7.7 Hz, 1H), 2.75 (s, 3H), 2.54−2.70 (m, 1H), 1.96−2.13 (m, 2H), 1.87 (dt, J = 12.5, 6.6 Hz, 1H); ^{13}C{^{1}H} NMR (101 MHz, CDCl$_3$) δ 201.8, 144.9, 134.7, 130.6, 130.4, 128.5, 127.4, 126.8, 126.3, 123.4, 120.2, 77.7, 68.9, 34.0, 30.0, 25.9; HRMS (ESI) m/z calcd for $C_{16}H_{17}O_2$ $[M + H]^+$ 241.1223, found 241.1226.

1-(3-Methoxy-4-(tetrahydrofuran-2-yl)phenyl)ethan-1-one (7p): clear oil, 78% yield (114 mg); ^{1}H NMR (400 MHz, CDCl$_3$) δ 7.48−7.43 (m, 2H), 7.38 (s, 1H), 5.09 (t, J = 7.0 Hz, 1H), 4.10−4.00 (m, 1H), 3.90−3.85 (m, 1H), 3.84−3.80 (m, 3H), 2.52 (s, 3H), 2.36 (dd, J = 6.7, 12.8 Hz, 1H), 1.88 (qd, J = 6.9, 14.2 Hz, 2H), 1.62−1.55 (m, 1H); ^{13}C{^{1}H} NMR (101 MHz, CDCl$_3$) δ 197.8, 156.2, 138.4, 137.0, 125.3, 121.6, 108.6, 75.8, 68.6, 55.4, 33.0, 26.5, 25.8; HRMS (ESI) m/z calcd for $C_{13}H_{17}O_3$ $[M + H]^+$ 221.1172, found 221.1177.

1-(3-Bromo-4-(tetrahydrofuran-2-yl)phenyl)ethan-1-one (7q): clear oil, 84% yield (113 mg); ^{1}H NMR (400 MHz, CDCl$_3$) δ 8.08 (d, J = 1.5 Hz, 1H), 7.86 (dd, J = 8.0, 1.5 Hz, 1H), 7.59 (d, J = 8.0 Hz, 1H), 5.15 (t, J = 7.1 Hz, 1H), 4.17 (td, J = 7.6, 6.1 Hz, 1H), 3.97 (q, J = 7.2 Hz, 1H), 2.51−2.64 (m, 4H), 1.98 (td, J = 14.0, 7.1 Hz, 2H), 1.65 (dd, J = 12.6, 7.6 Hz, 1H); ^{13}C{^{1}H} NMR (126 MHz,CDCl$_3$) δ 196.4, 148.5, 137.2, 132.4, 127.3, 126.6, 121.5, 79.7, 69.2, 33.2, 26.5, 25.7; HRMS (ESI) m/z calcd for $C_{12}H_{14}O_2Br$ $[M + H]^+$ 269.0172, found 269.0178.

1-(4-(Benzo[d][1,3]dioxol-2-yl)phenyl)ethan-1-one (7r): white solid, 58% yield (116 mg); mp 70−72 °C; ^{1}H NMR (500 MHz, CDCl$_3$) δ 8.04 (s, 1H), 8.02 (s, 1H), 7.70 (s, 1H), 7.68 (s, 1H), 7.01 (s, 1H), 6.89 (s, 4H), 2.63 (s, 3H); ^{13}C{^{1}H} NMR (126 MHz, CDCl$_3$) δ 197.5, 147.2, 140.9, 138.4, 128.6, 126.6, 121.9, 108.8, 108.7,

26.7; HRMS (ESI) m/z calcd for $C_{15}H_{13}O_3$ $[M + H]^+$ 241.0859, found 241.0864.

Typical Experimental Procedure for the Synthesis of 4-(1,4-Dioxan-2-yl)-3-methoxybenzaldehyde (9a). To a 25 mL round-bottom flask were added 3-methoxybenzaldehyde **8a** (0.73 mmol), K$_2$S$_2$O$_8$ (2.20 mmol, 594 mg), tetrabutylammonium chloride (TBACl, 2.20 mmol, 1.2 mL), and NaOAc (1.47 mmol, 121 mg) in 1,4-dioxane (3 mL). The round-bottom flask was equipped with a condenser, and the resulting reaction mixture was refluxed to 120 °C for 1.5 h. The progress of the reaction was monitored by TLC. Upon completion of the reaction, the reaction mixture was dried under a vacuum. Then the crude reaction mixture was diluted with ethyl acetate (10 mL), washed with brine, and eluted with EtOAc (20 mL × 2). The organics were evaporated, and the crude residue was preadsorbed on silica gel and purified by column chromatography (100−200 mesh silica using 85:15 petroleum ether/ethyl acetate as the eluent to afford the corresponding compound **9a** in 79% yield.

4-(1,4-Dioxan-2-yl)-3-methoxybenzaldehyde (9a): clear oil, 79% yield (128 mg); ^{1}H NMR (500 MHz, CDCl$_3$) δ 9.97 (s, 1H), 7.67 (d, J = 7.6 Hz, 1H), 7.46−7.52 (m, 1H), 7.33−7.39 (m, 1H), 5.03 (dd, J = 9.7, 2.5 Hz, 1H), 4.02 (dd, J = 11.4, 2.7 Hz, 1H), 3.92−4.00 (m, 2H), 3.90 (s, 3H), 3.79−3.84 (m, 1H), 3.69−3.76 (m, 1H), 3.26 (dd, J = 11.3, 9.7 Hz, 1H); ^{13}C{^{1}H} NMR (126 MHz, CDCl$_3$) δ 191.6, 156.2, 136.7, 133.8, 127.0, 124.4, 107.9, 72.6, 70.7, 67.1, 66.2, 55.3; HRMS (ESI) m/z calcd for $C_{12}H_{15}O_4$ $[M + H]^+$ 223.0965, found 223.0964.

3-Chloro-4-(1,4-dioxan-2-yl)benzaldehyde (9b): pale yellow solid, 85% yield (137 mg); mp 72−74 °C; ^{1}H NMR (400 MHz, CDCl$_3$) δ 9.96 (s, 1H), 8.04−7.75 (m, 3H), 5.18−5.00 (m, 1H), 4.08 (d, J = 11.6 Hz, 1H), 4.04−3.93 (m, 2H), 3.84 (d, J = 12.2 Hz, 1H), 3.75 (dd, J = 4.0, 10.1 Hz, 1H), 3.36−3.17 (m, 1H); ^{13}C{^{1}H} NMR (101 MHz, CDCl$_3$) δ 190.1, 142.1, 136.5, 132.4, 129.6, 128.1, 127.9, 74.5, 70.1, 66.8, 66.0; HRMS (ESI) m/z calcd for $C_{11}H_{12}O_3Cl$ $[M + H]^+$ 227.0469, found 227.0467.

4-(1,4-Dioxan-2-yl)-2-methoxybenzaldehyde (9c): clear oil, 92% yield (150 mg); ^{1}H NMR (500 MHz, CDCl$_3$) δ 10.43 (s, 1H), 7.79 (d, J = 8.0 Hz, 1H), 7.04 (s, 1H), 6.95 (d, J = 8.0 Hz, 1H), 4.66 (dd, J = 2.7, 10.3 Hz, 1H), 3.98−3.93 (m, 4H), 3.91 (t, J = 3.4 Hz, 1H), 3.89−3.87 (m, 1H), 3.83−3.79 (m, 1H), 3.76−3.72 (m, 1H), 3.41 (dd, J = 10.3, 11.4 Hz, 1H); ^{13}C{^{1}H} NMR (126 MHz, CDCl$_3$) δ 189.1, 161.7, 146.5, 128.3, 124.0, 117.9, 108.8, 77.1, 71.8, 66.6, 66.0, 55.4; HRMS (ESI) m/z calcd for $C_{12}H_{15}O_4$ $[M + H]^+$ 223.0965, found 223.0963.

4-(1,4-Dioxan-2-yl)-2,5-dimethoxybenzaldehyde (9d): yellow solid, 82% yield (124 mg); mp 118−120 °C; ^{1}H NMR (500 MHz, CDCl$_3$) δ 10.43 (s, 1H), 7.27 (s, 1H), 7.19 (s, 1H), 4.98 (dd, J = 9.5, 2.3 Hz, 1H), 4.04 (dd, J = 11.3, 2.5 Hz, 1H), 3.96−3.99 (m, 1H), 3.92−3.96 (m, 4H), 3.82 (s, 3H), 3.79−3.81 (m, 1H), 3.69−3.76 (m, 1H), 3.22 (dd, J = 11.1, 9.9 Hz, 1H); ^{13}C{^{1}H} NMR (126 MHz, CDCl$_3$) δ 189.2, 156.9, 149.9, 135.5, 123.8, 110.8, 108.1, 73.1, 70.9, 67.3, 66.4, 56.2, 55.7; HRMS (ESI) m/z calcd for $C_{13}H_{17}O_5$ $[M + H]^+$ 253.1071, found 253.1069.

3-Fluoro-4-(tetrahydrofuran-2-yl) benzaldehyde (9e): clear oil, 86% yield (135 mg) and 67% yield (105 mg); ^{1}H NMR (200 MHz, CDCl$_3$) δ 9.96 (s, 1H), 7.72−7.61 (m, 2H), 7.52 (d, J = 9.9 Hz, 1H), 5.16 (t, J = 7.1 Hz, 1H), 4.12 (q, J = 6.8 Hz, 1H), 4.03−3.87 (m, 1H), 2.59−2.39 (m, 1H), 2.09−1.93 (m, 2H), 1.75 (dd, J = 7.6, 12.1 Hz, 1H); ^{13}C{^{1}H} NMR (50 MHz, CDCl$_3$) δ 190.7, 162.3−157.3 (d, J = 248.82 Hz), 138.4−138.1 (d, J = 14.27 Hz), 137.0−136.9 (d, J = 6.22 Hz), 127.4−127.3 (d, J = 4.39 Hz), 126.3−126.2 (d, J = 2.93 Hz), 115.0−114.6 (d, J = 22.32 Hz), 74.9−74.8 (d, J = 1.83 Hz), 68.8, 33.4, 25.9; HRMS (ESI) m/z calcd for $C_{11}H_{12}O_2F$ $[M + H]^+$ 195.0816, found 195.0815.

3,5-Dimethoxy-4-(tetrahydrofuran-2-yl)benzaldehydes (9f): clear oil, 70% yield (99 mg); ^{1}H NMR (500 MHz, CDCl$_3$) δ 10.43 (s, 1H), 7.27 (s, 1H), 7.19 (s, 1H), 4.98 (dd, J = 2.3, 9.5 Hz, 1H), 4.04 (dd, J = 2.5, 11.3 Hz, 1H), 3.99−3.97 (m, 1H), 3.96−3.91 (m, 4H), 3.82 (s, 3H), 3.81−3.79 (m, 1H), 3.75−3.70 (m, 1H), 3.22 (dd, J = 9.9, 11.1 Hz, 1H); ^{13}C{^{1}H} NMR (101 MHz, CDCl$_3$) δ 191.4, 158.8, 136.2,

124.5, 104.9, 71.8, 68.7, 55.6, 29.9, 27.4; HRMS (ESI) *m/z* calcd for $C_{13}H_{17}O_4$ [M + H]$^+$ 237.1121, found 237.1119.

3-Chloro-4-(tetrahydrofuran-2-yl)benzaldehydes (9g): clear oil, 89% yield (134 mg); ^{1}H NMR (400 MHz, CDCl$_3$) δ 9.86 (s, 1H), 7.75 (d, *J* = 1.5 Hz, 1H), 7.60−7.70 (m, 2H), 5.14 (t, *J* = 7.1 Hz, 1H), 4.03−4.17 (m, 1H), 3.90 (q, *J* = 7.3 Hz, 1H), 2.50 (dd, *J* = 12.5, 6.4 Hz, 1H), 1.83−2.02 (m, 2H), 1.51−1.65 (m, 1H); ^{13}C{^{1}H} NMR (101 MHz, CDCl$_3$) δ 190.3, 148.2, 135.9, 132.0, 129.6, 127.9, 126.6, 77.4, 68.8, 32.7, 25; HRMS (ESI) *m/z* calcd for $C_{11}H_{12}O_2Cl$ [M + H]$^+$ 211.0520, found 211.0519

3-Hydroxy-4-(tetrahydrofuran-2-yl)benzaldehydes (9h): yellow oil, 71% yield (111 mg); ^{1}H NMR (200 MHz, CDCl$_3$) δ 9.98 (s, 1H), 9.80 (s, 1H), 7.20−7.46 (m, 2H), 7.10 (dd, *J* = 7.5, 1.8 Hz, 1H), 5.89 (dd, *J* = 9.6, 6.2 Hz, 1H), 4.09−4.35 (m, 1H), 3.77−4.04 (m, 1H), 2.49−2.70 (m, 1H), 1.96−2.23 (m, 2H), 1.63−1.84 (m, 1H); ^{13}C{^{1}H} NMR (50 MHz, CDCl$_3$) δ 193.3, 157.2, 134.0, 128.5, 127.8, 124.7, 123.5, 80.2, 68.6, 32.9, 25.6; HRMS (ESI) *m/z* calcd for $C_{11}H_{11}O_3$ [M − H]$^+$ 191.0703, found 191.0702

2-Hydroxy-4-(tetrahydrofuran-2-yl)benzaldehydes (9i): clear oil, 62% yield (98 mg); ^{1}H NMR (200 MHz, CDCl$_3$) δ 11.07 (s, 1H), 9.86 (s, 1H), 7.52 (d, *J* = 8.5 Hz, 1H), 6.89−7.07 (m, 2H), 4.92 (t, *J* = 7.1 Hz, 1H), 3.90−4.16 (m, 2H), 2.37 (dd, *J* = 11.9, 6.3 Hz, 1H), 1.93−2.07 (m, 2H), 1.70−1.87 (m, 1H); ^{13}C{^{1}H} NMR (50 MHz, CDCl$_3$) δ 195.3, 161.1, 153.7, 133.1, 119.0, 116.4, 113.5, 79.3, 68.4, 33.9, 25.2; HRMS (ESI) *m/z* calcd for $C_{11}H_{12}O_3$ [M + H]$^+$ 193.0859, found 193.0858.

4-(1,4-Dioxan-2-yl)-1-naphthaldehyde (9j): clear oil, 80% yield (131 mg); ^{1}H NMR (200 MHz, CDCl$_3$) δ 10.29 (s, 1H), 9.17−9.35 (m, 1H), 8.01−8.10 (m, 1H), 7.93 (d, *J* = 7.5 Hz, 1H), 7.82 (d, *J* = 7.5 Hz, 1H), 7.50−7.68 (m, 2H), 5.37 (dd, *J* = 9.9, 2.3 Hz, 1H), 3.98−4.11 (m, 3H), 3.73−3.84 (m, 2H), 3.41 (dd, *J* = 11.9, 9.9 Hz, 1H); ^{13}C{^{1}H} NMR (50 MHz, CDCl$_3$) δ 192.7, 141.0, 135.7, 130.4, 130.0, 129.7, 128.0, 126.6, 125.1, 122.3, 122.2, 74.4, 71.5, 66.8, 66.0; HRMS (ESI) *m/z* calcd for $C_{15}H_{14}O_3Na$ [M + Na]$^+$ 265.0835, found 265.0832.

2,2-Dimethoxy-2-phenyl-1-(4-(tetrahydrofuran-2-yl)phenyl)-ethan-1-one (11): white semisolid, 90% yield (114 mg); ^{1}H NMR (400 MHz, CDCl$_3$) δ 8.04 (d, *J* = 7.9 Hz, 2H), 7.61 (d, *J* = 7.3 Hz, 2H), 7.20−7.46 (m, 5H), 4.74−4.98 (m, 1H), 4.00−4.12 (m, 1H), 3.81−3.98 (m, 1H), 3.21 (s, 6H), 2.21−2.40 (m, 1H), 1.90−2.07 (m, 2H), 1.72 (dt, *J* = 12.4, 7.9 Hz, 1H); ^{13}C{^{1}H} NMR (50 MHz, CDCl$_3$) δ 194.6, 148.8, 136.9, 133.0, 130.2, 128.8, 128.4, 126.9, 125.2, 103.5, 80.1, 68.8, 50.0, 34.4, 25.9; HRMS (ESI) *m/z* calcd for $C_{20}H_{22}O_4Na$ [M + Na]$^+$ 349.1410, found 349.1406.

1-(4-(1,4-Dioxan-2-yl)phenyl)-2-phenylethane-1,2-dione (12): yellow oil, 61% yield (70 mg); ^{1}H NMR (500 MHz, CDCl$_3$) δ 7.97 (d, *J* = 7.6 Hz, 4H), 7.61−7.73 (m, 1H), 7.43−7.58 (m, 4H), 4.61−4.81 (m, 1H), 3.86−4.00 (m, 3H), 3.82 (d, *J* = 10.7 Hz, 1H), 3.73 (td, *J* = 11.3, 2.9 Hz, 1H), 3.40 (t, *J* = 10.9 Hz, 1H); ^{13}C{^{1}H} NMR (50 MHz, CDCl$_3$) δ 194.4, 194.0, 145.5, 134.9, 132.9, 132.5, 130.0, 129.9, 129.0, 126.6, 77.2, 72.1, 66.9, 66.3; HRMS (ESI) *m/z* calcd for $C_{18}H_{16}O_4Na$ [M + Na]$^+$ 319.0941, found 319.0936.

1-(4-(Tetrahydrofuran-2-yl)phenyl)ethan-1-one (14): clear oil, 77% yield (121 mg) and 53% yield (83 mg); ^{1}H NMR (400 MHz, CDCl$_3$) δ 7.93 (d, *J* = 8.5 Hz, 2H), 7.42 (d, *J* = 8.5 Hz, 2H), 4.95 (t, *J* = 7.3 Hz, 1H), 4.14−4.07 (m, 1H), 3.97 (q, *J* = 7.3 Hz, 1H), 2.60 (s, 3H), 2.37 (dd, *J* = 6.4, 12.5 Hz, 1H), 2.02 (td, *J* = 7.0, 14.0 Hz, 2H), 1.81−1.74 (m, 1H); ^{13}C{^{1}H} NMR (101 MHz, CDCl$_3$) δ 197.8, 149.2, 136.1, 128.4, 125.6, 80.1, 68.9, 34.7, 26.6, 25.9; HRMS (ESI) *m/z* calcd for $C_{12}H_{14}O_2$ [M + H]$^+$ 191.1067, found 191.1062.

Experimental Procedure for the Synthesis of 2-(2,5-Dimethoxy-4-methylphenyl)-1,4-dioxane (16). Degassed methanol (4.0 mL) was added to the mixture of Pd/C (10 wt %) and **9d** (0.3 mmol, 76 mg). After stirring under 1 atm pressure of hydrogen for 12 h at room temperature, the reaction mixture was filtered and then evaporated under reduced pressure. The crude product was then purified by flash column chromatography (eluent 90:10 petroleum ether/ethyl acetate) to give hydrogenated product **16** (67 mg) as a clear oil.

2-(2,5-Dimethoxy-4-methylphenyl)-1,4-dioxane (16): clear oil, 94% yield (71 mg); ^{1}H NMR (400 MHz, CDCl$_3$) δ 6.89 (s, 1H),

6.59 (s, 1H), 4.95−4.82 (m, 1H), 3.92−3.83 (m, 3H), 3.75 (s, 3H), 3.72−3.62 (m, 5H), 3.22 (t, *J* = 10.4 Hz, 1H), 2.14 (s, 3H); ^{13}C{^{1}H} NMR (101 MHz, CDCl$_3$) δ 151.6, 149.2, 126.1, 124.1, 113.2, 108.8, 72.5, 71.2, 67.1, 66.1, 55.7, 55.6, 15.9; HRMS (ESI) *m/z* calcd for $C_{13}H_{18}O_4Na$ [M + Na]$^+$ 261.1097, found 261.1093.

Experimental Procedure for the Synthesis of 2-(4-(1,4-Dioxan-2-yl)-2,5-dimethoxyphenyl)-1H-benzo[d]imidazole (17). To a 25 mL round-bottom flask were added 4-(1,4-dioxan-2-yl)-2,5-dimethoxy-benzaldehyde (0.396 mmol, 100 mg), *o*-phenylenediamine (0.396 mmol, 42 mg), 30% H$_2$O$_2$ in water (94 mg, 0.82 mL), and 37% HCl in water (50.5 mg, 0.15 mL) in acetonitrile (3 mL). After stirring for 1 h at rt, the reaction mixture was evaporated under reduced pressure. Then the crude reaction mixture was diluted with ethyl acetate (10 mL), washed with brine, and eluted with EtOAc (15 mL × 2). The organics were evaporated, and the crude residue was preadsorbed on silica gel and purified by column chromatography (100−200 mesh silica using 70:30 petroleum ether/ethyl acetate as the eluent) to afford the corresponding compound **17** in 78% yield as a white solid.

2-(4-(1,4-Dioxan-2-yl)-2,5-dimethoxyphenyl)-1H-benzo[d]-imidazole (17): white solid, 78% yield (159 mg); ^{1}H NMR (500 MHz, CDCl$_3$) δ 10.80 (br s, 1H), 8.08 (s, 1H), 7.84 (br s, 1H), 7.52 (br s, 1H), 7.13−7.35 (m, 3H), 5.05 (dd, *J* = 9.7, 2.5 Hz, 1H), 4.07−4.13 (m, 4H), 3.96−4.05 (m, 2H), 3.95 (s, 3H), 3.82−3.87 (m, 1H), 3.74−3.81 (m, 1H), 3.31 (dd, *J* = 11.1, 10.3 Hz, 1H); ^{13}C{^{1}H} NMR (126 MHz, CDCl$_3$) δ 151.1, 150.2, 149.6, 129.7, 122.6, 122.1, 118.9, 116.9, 110.7, 110.5, 110.3, 72.7, 71.0, 67.1, 66.2, 56.3, 55.8; HRMS (ESI) *m/z* calcd for $C_{19}H_{21}O_4N_2$ [M + H]$^+$ 341.1496, found 341.1502.

■ ASSOCIATED CONTENT

Ⓢ Supporting Information

The Supporting Information is available free of charge on the ACS Publications website at DOI: 10.1021/acs.joc.8b03048.

Optimization and DFT studies, spectra, and X-ray crystal data for compound **7h** (PDF)

Crystallographic data for compound **7h** (CIF)

■ AUTHOR INFORMATION

Corresponding Author

*E-mail: gm.suryavanshi@ncl.res.in. Tel: 020-2590-2547. Fax: 020-2590-2676.

ORCID Ⓓ

Kumar Vanka: 0000-0001-7301-7573

Gurunath Suryavanshi: 0000-0002-6299-0914

Notes

The authors declare no competing financial interest.

■ ACKNOWLEDGMENTS

■ REFERENCES

(1) (a) Lorente, A.; Lamariano-Merketegi, J.; Albericio, F.; Álvarez, M. Tetrahydrofuran-Containing Macrolides: A Fascinating Gift from the Deep Sea. *Chem. Rev.* **2013**, *113*, 4567−4610. (b) Ward, R. S. Lignans, neolignans and related compounds. *Nat. Prod. Rep.* **1999**, *16*, 75−96. (c) Li, G.; Ju, H. K.; Chang, H. W.; Jahng, Y.; Lee, S.-H.; Son, J.-K. Melanin Biosynthesis Inhibitors from the Bark of Machilus thunbergii. *Biol. Pharm. Bull.* **2003**, *26*, 1039−1041. (d) Zhai, H.; Inoue, T.; Moriyama, M.; Esumi, T.; Mitsumoto, Y.; Fukuyama, Y.

Neuroprotective Effects of 2,5-Diaryl-3,4-dimethyltetrahydrofuran Neolignans. *Biol. Pharm. Bull.* **2005**, *28*, 289−293. (e) Teponno, R. B.; Kusari, S.; Spiteller, M. Recent advances in research on lignans and Neolignans. *Nat. Prod. Rep.* **2016**, *33*, 1044−1092. (f) Lee, W. S.; Baek, Y.; Kim, J.-R.; Cho, K.-H.; Sok, D.-E.; Jeong, T.-S. Antioxidant activities of a new lignan and a neolignan from Saururus chinensis. *Bioorg. Med. Chem. Lett.* **2004**, *14*, 5623−5628. (g) Saleem, M.; Kim, H. J.; Ali, M. S.; Lee, Y. S. An update on bioactive plant lignans. *Nat. Prod. Rep.* **2005**, *22*, 696−716. (h) Pan, J.-Y.; Chen, S.-L.; Yang, M.-H.; Wu, J.; Sinkkonen, J.; Zou, K. An update on lignans: natural products and synthesis. *Nat. Prod. Rep.* **2009**, *26*, 1251−1296. and references therein

(2) (a) Surivet, J.-P.; Zumbrunn, C.; Bruyere, T.; Bur, D.; Kohl, C.; Locher, H. H.; Seiler, P.; Ertel, E. A.; Hess, P.; Enderlin-Paput, M.; Enderlin-Paput, S.; Gauvin, J.-C.; Mirre, A.; Hubschwerlen, C.; Ritz, D.; Rueedi, G. Synthesis and Characterization of Tetrahydropyran-Based Bacterial Topoisomerase Inhibitors with Antibacterial Activity against Gram-Negative Bacteria. *J. Med. Chem.* **2017**, *60*, 3776−3794. (b) Saluja, B.; Thakkar, J. N.; Li, H.; Desai, U. R.; Sakagami, M. Novel low molecular weight lignins as potential anti-emphysema agents: In vitro triple inhibitory activity against elastase, oxidation and inflammation. *Pulm. Pharmacol. Ther.* **2013**, *26*, 296−304. (c) Lee, M.-A.; Kim, W. K.; Park, H. J.; Kang, S. S.; Lee, S. K. Anti-proliferative activity of hydnocarpin, a natural lignan, is associated with the suppression of Wnt/b-catenin signaling pathway in colon cancer cells. *Bioorg. Med. Chem. Lett.* **2013**, *23*, 5511−5514. (d) Katz, J. D.; Jewell, J. P.; Guerin, D. J.; Lim, J.; Dinsmore, C. J.; Deshmukh, S. V.; Pan, B.-S.; Marshall, C. G.; Lu, W.; Altman, M. D.; Dahlberg, W. K.; Davis, L.; Falcone, D.; Gabarda, A. E.; Hang, G.; Hatch, H.; Holmes, R.; Kunii, K.; Lumb, K. J.; Lutterbach, B.; Mathvink, R.; Nazef, N.; Patel, S. B.; Qu, X.; Reilly, J. F.; Rickert, K. W.; Rosenstein, C.; Soisson, S. M.; Spencer, K. B.; Szewczak, A. A.; Walker, D.; Wang, W.; Young, J.; Zeng, Q. Discovery of a 5H-Benzo[4,5]cyclohepta[1,2-b]pyridin-5-one (MK-2461) Inhibitor of c-Met Kinase for the Treatment of Cancer. *J. Med. Chem.* **2011**, *54*, 4092−4108. (e) González, A. G.; Silva, M. H.; Padrón, J. I.; León, F.; Reyes, E.; Álvarez-Mon, M. AÄ.; Pivel, J. P.; Quintana, J.; Estévez, F.; Bermejo, J. Synthesis and Antiproliferative Activity of a New Compound Containing an *α*-Methylene-*γ*-Lactone Group. *J. Med. Chem.* **2002**, *45*, 2358−2361. (f) Li, S.; Xu, H.; Cui, S.; Wu, F.; Zhang, Y.; Su, M.; Gong, Y.; Qiu, S.; Jiao, Q.; Qin, C.; Shan, J.; Zhang, M.; Wang, J.; Yin, Q.; Xu, M.; Liu, X.; Wang, R.; Zhu, L.; Li, J.; Xu, Y.; Jiang, H.; Zhao, Z.; Li, J.; Li, H. Discovery and Rational Design of Natural-Product-Derived 2-Phenyl-3,4-dihydro-2H-benzo[f]chromen-3-amine Analogs as Novel and Potent Dipeptidyl Peptidase 4 (DPP-4) Inhibitors for the Treatment of Type 2 Diabetes. *J. Med. Chem.* **2016**, *59*, 6772−6790. (g) Goodwin, N. C.; Ding, Z.-M.; Harrison, B. A.; Strobel, E. D.; Harris, A. L.; Smith, M.; Thompson, A. Y.; Xiong, W.; Mseeh, F.; Bruce, D. J.; Diaz, D.; Gopinathan, S.; Li, L.; O'Neill, E.; Thiel, M.; Wilson, A. G. E.; Carson, K. G.; Powell, D.; Rawlins, D. B. Discovery of LX2761, a Sodium-Dependent Glucose Cotransporter 1 (SGLT1) Inhibitor Restricted to the Intestinal Lumen, for the Treatment of Diabetes. *J. Med. Chem.* **2017**, *60*, 710−721.

(3) Miyazaki, H.; Uneme, H.; Katagiri, Y.; Yasser, S. A-K. S.; Salunke, G. B. Preparation of benzaldehyde oxime ether and phenyl alkyl ketone oxime ether compounds as pesticides. Patent JP 2014080385.

(4) (a) Liu, Z.; Saarinen, N. M.; Thompson, L. U. Sesamin Is One of the Major Precursors of Mammalian Lignans in Sesame Seed (Sesamum indicum) as Observed In Vitro and in Rats[1,2]. *J. Nutr.* **2006**, *136*, 906−912. (b) Kiso, Y. Antioxidative roles of sesamin, a functional lignan in sesame seed, and its effect on lipidand alcohol-metabolism in the liver: A DNA microarray study. *BioFactors* **2004**, *21*, 191−196. (c) Kong, P.; Chen, G.; Jiang, A.; Wang, Y.; Song, C.; Zhuang, J.; Xi, C.; Wang, G.; Ji, Y.; Yan, J. Sesamin inhibits IL-1*β*-stimulated inflammatory response in human osteoarthritis chondrocytes by activating Nrf2 signaling pathway. *Oncotarget.* **2016**, *7*, 83720−83726. (d) Nguyen, P. H.; Le, T. V. T.; Kang, H. W.; Chae, J.; Kim, S. K.; Kwon, K-i.; Seo, D. B.; Lee, S. J.; Oh, W. K. AMP-

activated protein kinase (AMPK) activators from Myristica fragrans (nutmeg) and their anti-obesity effect. *Bioorg. Med. Chem. Lett.* **2010**, *20*, 4128−4131.

(5) (a) Li, J.; Meng, A.-P.; Guan, X.-L.; Li, J.; Wu, Q.; Deng, S.-P.; Su, X.-J.; Yang, R.-Y. Anti-hepatitis B virus lignans from the root of Streblus asper. *Bioorg. Med. Chem. Lett.* **2013**, *23*, 2238−2244. (b) Burness, C. B. *Drugs* **2015**, *75*, 1947−1952.

(6) (a) Zhang, S.; Guo, L.; Wang, H.; Duan, X. Bu4NI-catalyzed decarboxylative acyloxylation of an sp3 C−H bond adjacent to a heteroatom with *α*-oxocarboxylic acids. *Org. Biomol. Chem.* **2013**, *11*, 4308−4311. (b) Doan, S. H.; Nguyen, V. H. H.; Nguyen, T. H.; Pham, P. H.; Nguyen, N. N.; Phan, A. N. Q.; Tu, T. N.; Phan, N. T. S. Cross-dehydrogenative coupling of coumarins with Csp3−H bonds using an iron−organic framework as a productive heterogeneous catalyst. *RSC Adv.* **2018**, *8*, 10736−10745. (c) Majji, G.; Rout, S. K.; Rajamanickam, S.; Guin, S.; Patel, B. K. Synthesis of esters via sp3 C−H functionalisation. *Org. Biomol. Chem.* **2016**, *14*, 8178−8211. (d) Evano, G.; Blanchard, N.; Toumi, M. Copper-Mediated Coupling Reactions and Their Applications in Natural Products and Designed Biomolecules Synthesis. *Chem. Rev.* **2008**, *108*, 3054. (e) Wang, H.; Guo, L.; Duan, X. Silver-catalyzed oxidative coupling/cyclization of acrylamides with 1,3-dicarbonyl compounds. *Chem. Commun.* **2013**, *49*, 10370−10372. (f) Lakshman, M. K.; Vuram, P. K. Cross-dehydrogenative coupling and oxidative-amination reactions of ethers and alcohols with aromatics and heteroaromatics. *Chem. Sci.* **2017**, *8*, 5845−5888.

(7) Liu, D.; Liu, C.; Li, H.; Lei, A. Copper-catalysed oxidative C−H/ C−H coupling between olefins and simple ethers. *Chem. Commun.* **2014**, *50*, 3623−3626.

(8) Sun, Q.; Zhang, Y.-Y.; Sun, J.; Han, Y.; Jia, X.; Yan, C.-G. Construction of C (sp2)−X (X = Br, Cl) Bonds through a Copper-Catalyzed Atom-Transfer Radical Process: Application for the 1,4-Difunctionalization of Isoquinolinium Salts. *Org. Lett.* **2018**, *20*, 987−990.

(9) Correa, A.; Fiser, B.; Gómez-Bengoa, E. Iron-catalyzed direct *α*-arylation of ethers with azoles. *Chem. Commun.* **2015**, *51*, 13365−13368.

(10) Shields, B. J.; Doyle, A. G. Direct C(sp3)−H Cross Coupling Enabled by Catalytic Generation of Chlorine Radicals. *J. Am. Chem. Soc.* **2016**, *138*, 12719−12722.

(11) Li, X.; Wang, H.-Y.; Shi, Z.-J. Transition-metal-free cross-dehydrogenative alkylation of pyridines under neutral conditions. *New J. Chem.* **2013**, *37*, 1704−1706.

(12) Kianmehr, E.; Fardpour, M.; Khan, K. M. Direct Regioselective Alkylation of Non-Basic Heterocycles with Alcohols and Cyclic Ethers through a Dehydrogenative Cross- Coupling Reaction under Metal-Free Conditions. *Eur. J. Org. Chem.* **2017**, *2017*, 2661−2668.

(13) Jin, L.; Feng, J.; Lu, G.; Cai, C. Di-tert-butyl Peroxide (DTBP)-Mediated Oxidative Cross- Coupling of Isochroman and Indole Derivatives. *Adv. Synth. Catal.* **2015**, *357*, 2105−2110.

(14) (a) Devari, S.; Shah, B. A. Visible light-promoted C−H functionalization of ethers and electron-deficient arenes. *Chem. Commun.* **2016**, *52*, 1490−1493. (b) Okugawa, N.; Moriyama, K.; Togo, H. Introduction of Ether Groups onto Electron-Deficient Nitrogen-Containing Heteroaromatics Using Radical Chemistry under Transition-Metal-Free Conditions. *Eur. J. Org. Chem.* **2015**, *2015*, 4973−4981. (c) Zhou, L.; Okugawa, N.; Togo, H. Hydroxymethylation of Quinolines with Na2S2O8 by a Radical Pathway. *Eur. J. Org. Chem.* **2017**, *2017*, 6239−6245.

(15) (a) Liu, S.; Liu, A.; Zhang, Y.; Wang, W. Direct Ca-heteroarylation of structurally diverse ethers via a mild N-hydroxysuccinimide mediated cross-dehydrogenative coupling reaction. *Chem. Sci.* **2017**, *8*, 4044−4050. (b) Xie, Z.; Cai, Y.; Hu, H.; Lin, C.; Chen, Z.; Wang, L.; Pan, Y.; Jiang, J. Cu-Catalyzed Cross-Dehydrogenative Coupling Reactions of (Benzo)thiazoles with Cyclic Ethers. *Org. Lett.* **2013**, *15*, 4600−4603.

(16) Jafarpour, F.; Darvishmolla, M. Peroxy mediated Csp2−Csp3 dehydrogenative coupling: regioselective functionalization of coumar-

ins and coumarin-3-carboxylic acids. *Org. Biomol. Chem.* **2018**, *16*, 3396−3401.

(17) Ueno, R.; Shirakawa, E. Base-promoted dehydrogenative coupling of benzene derivatives with amides or ethers. *Org. Biomol. Chem.* **2014**, *12*, 7469−7473.

(18) (a) Chavan, S. S.; Rupanawar, B. D.; Kamble, R. B.; Shelke, A. M.; Suryavanshi, G. Metal-free annulation of *β*-acylamino ketones: facile access to spirooxazolines and oxazolines via oxidative C−O bond formation. *Org. Chem. Front.* **2018**, *5*, 544−548. (b) Rupanwar, B. D.; Chavan, S. S.; Shelke, A. M.; Suryavanshi, G. Triflic acid-catalyzed metal-free synthesis of (E)-2-cyanoacrylamides and 3-substituted azetidine-2,4-diones. *New J. Chem.* **2018**, *42*, 6433−6440.

(19) Bahrami, K.; Khodaei, M. M.; Kavianinia, I. A Simple and Efficient One-Pot Synthesis of 2-Substituted Benzimidazoles. *Synthesis* **2007**, *4*, 547−550.

(20) (a) Ji, P.-Y.; Liu, Y.-F.; Xu, J.-W.; Luo, W.-P.; Liu, Q.; Guo, C.-C. Transition-Metal-Free Oxidative Decarboxylative Cross Coupling of *α,β*-Unsaturated Carboxylic Acids with Cyclic Ethers under Air Conditions: Mild Synthesis of *α*-Oxyalkyl Ketones. *J. Org. Chem.* **2017**, *82*, 2965−2971. (b) Handa, S.; Fennewald, J. C.; Lipshutz, B. H. Aerobic Oxidation in Nanomicelles of Aryl Alkynes, in Water at Room Temperature. *Angew. Chem., Int. Ed.* **2014**, *53*, 3432−3435. (c) Ledwith, A.; Russell, P. J.; Sutcliffe, L. H. *J. Chem. Soc. D* **1971**, 964.

(21) (a) Shi, Z.; Glorius, F. Synthesis of fluorenones via quaternary ammonium salt-promoted intramolecular dehydrogenative arylation of aldehydes. *Chem. Sci.* **2013**, *4*, 829−833. (b) Shirakawa, E.; Itoh, K.; Higashino, T.; Hayashi, T. tert-Butoxide-Mediated Arylation of Benzene with Aryl Halides in the Presence of a Catalytic 1,10-Phenanthroline Derivative. *J. Am. Chem. Soc.* **2010**, *132*, 15537−15539. (c) Devari, S.; Shah, B. A. Visible light-promoted C−H functionalization of ethers and electron-deficient arenes. *Chem. Commun.* **2016**, *52*, 1490−1493. (d) House, D. A. Kinetics and Mechanism of Oxidations by Peroxydisulfate. *Chem. Rev.* **1962**, *62*, 185. (e) Avetta, P.; Pensato, A.; Minella, M.; Malan-drino, M.; Maurino, V.; Minero, C.; Hanna, K.; Vione, D. Activation of Persulfate by Irradiated Magnetite: Implications for the Degradation of Phenol under Heterogeneous Photo-Fenton-Like Conditions. *Environ. Sci. Technol.* **2015**, *49*, 1043. (f) Dai, C.; Meschini, F.; Narayanam, J. M. R.; Stephenson, C. R. J. Friedel−Crafts Amidoalkylation via Thermolysis and Oxidative Photocatalysis. *J. Org. Chem.* **2012**, *77*, 4425. and references therein

NJC

Check for updates

A visible light mediated, metal and oxidant free highly efficient cross dehydrogenative coupling (CDC) reaction between quinoxalin-2(1H)-ones and ethers†

Kishor D. Mane,‡[ab] Rohit B. Kamble‡[ab] and Gurunath Suryavanshi ⓘ *[ab]

The efficient and metal free, white light mediated 3C alkylation of quinoxalin-2(1H)-ones *via* a cross dehydrogenative coupling reaction with cyclic ethers using eosin Y as a photocatalyst is described. This reaction has broad substrate scope and strong functional group tolerance with good to excellent yields.

Carbon–carbon (C–C) bond formation has always been one of the most useful and fundamental reactions in the development of organic chemistry, the C–C bond being considered a backbone of nearly every organic molecule. Hence C–C bond formation reactions have consistently contributed in the advancement of organic chemistry. The application of C–C bond formation is found in fine chemicals, agrochemicals, medicinal and pharmaceutical ingredients, therefore making this transformation one of the very crucial classes of reaction in organic chemistry.[1] Among the methods developed over the years,[2] metal-catalyzed and metal-free cross-dehydrogenative coupling (CDC) reactions have been reported as a straightforward and strong approach for the preparation of C–C bonds.[3] Recently, photocatalyzed CDC reactions are emerging as a powerful tool with transition metals as they have become an effective way for coupling of two C–H bonds with different chemical properties. Moreover photocatalytic C–H functionalization has attracted more attention due to its high atom economy and its following the green chemistry principle. The major advantage in performing CDC reactions as compared to traditional metal-catalyzed methods is the elimination of the most important step, *i.e.* prefunctionalization of starting materials.

Furthermore cyclic ethers follow the green chemistry principle and ethers are important synthons in organic chemistry which serve as a most versatile CDC reaction partner which we generally observe in various natural as well as synthetic molecules.[4]

In the metal and metal-free CDC reactions, various electron deficient heterocyclic, cyclic as well as acyclic ethers have been studied comprehensively. These heterocycles contain substituted pyridines, thiophenes, indoles, quinines, isoquinines, azoles and chromanes.[5] In addition to this some attempts have been made for C–N bond formation using photocatalytic CDC reaction.[6]

Recently, Adimurthy *et al.* studied C–H amination of imidazo-[1,2-*a*]pyridines under photocatalytic conditions using benzotri-azoles, benzoimidazoles, triazoles, pyrazoles, imidazoles and indazoles as amine source[7a] with $K_2S_2O_8$ as external oxidant, whereas Wei *et al.* efficiently carried out CDC amination reactions of quinoxalin-2(1H)-ones using blue LED and eosin Y as photocatalyst.[7b] Furthermore Wu and co-workers have developed photocatalyzed hydrogen atom transfer (HAT) reaction for C–H activation of ethers and subsequent 1,4-addition to various SOMO-philes as shown in Scheme 1.[8a]

Recently, Wei *et al.* have reported the photocatalytic CDC reaction between substituted quinoxalin-2(1H)-ones and ethers. However, this approach needs TBHP as oxidant and DABCO as base in stoichiometric amount.[8b]

The 3-alkyl-substituted quinoxalin-2(1H)-ones and their derivatives show a broad range of biological activities as pharmaceuticals and agrochemicals.[9] Some important activities include MDR antagonist (**1**),[10] antitumor (**2**),[11] antiviral, antimicrobial[12] and antidiabetic activity (**3**)[13] (Fig. 1). These molecules are widely used in organic synthesis as well as in synthesis of advanced materials. The high importance of these moieties attracts more attention of chemist towards new and easy routes for alkylation/arylation of quinoxalin-2(1H)-ones.[14] Numerous reports are accessible in the literature for 3C activation of quinoxalin-2(1H)-ones *via* C–H bond activation under metal-free condition.[15] Keeping in mind the importance of CDC reactions and our previous efforts towards developing metal-free approaches,[16] herein we report a metal-free photocatalytic CDC reaction for 3C alkylation of quinoxalin-2(1H)-ones with ethers.

To investigate our assumption concerning the CDC reaction, our initial attempts commenced with coupling between 1-methyl-quinoxalin-2(1H)-one (**5a**) and THF, using as photocatalyst rose

[a] *Chemical Engineering and Process Development Division, CSIR-National Chemical Laboratory, Pune, 411 008, India. E-mail: gm.suryavanshi@ncl.res.in*
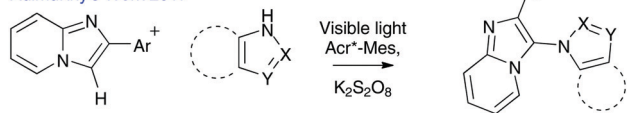[b] *Academy of Scientific and Innovative Research, Ghaziabad 201 002, India*
† Electronic supplementary information (ESI) available. See DOI: 10.1039/c9nj00075e
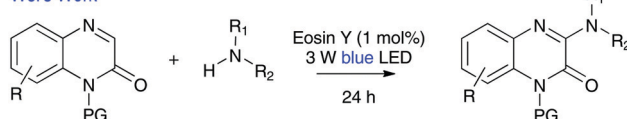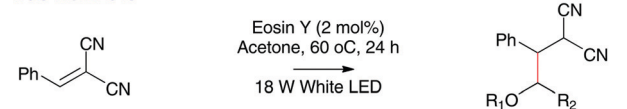‡ These authors contribute equally.

Previous Work

Adimurthy's Work 2017

Wei's Work

Wu's Work 2018

This Work

Scheme 1   The cross dehydrogenative coupling reaction.
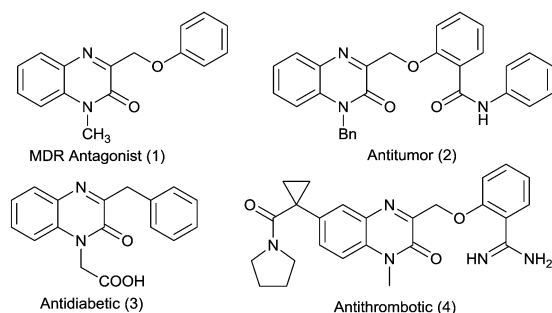

Fig. 1   Biologically active compounds.

Bengal (1 mol%) at 25 °C for 24 hrs. To our delight, the desired C-alkylated product was formed in 27% yield (Table 1, entry 1).

With this result in hand, to enhance the yield of product we varied the time and concentration of rose Bengal. Unfortunately yields were not promising and increased only up to 43% (entries 2–4). Hence, after careful analysis we speculated to use eosin Y as photocatalyst as an alternative to rose Bengal. When eosin Y (1 mol%) was used as catalyst, surprisingly, the yield of desired product increased to 68% in comparison with rose Bengal (entry 5). Further addition of TBHP as additive did not enhance the yield (entry 6) whereas on increasing the concentration of eosin Y to 2 mol% for 18 h the desired product was obtained in 88% yield (entry 7).

Moreover, on increasing the reaction time from 18 to 24 h keeping the concentration of eosin Y at 1 mol%, the yield of product was boosted dramatically to 95% (entry 8). With these results it can be concluded that the time of the reaction plays an important role in the formation of product (entries 9 and 10).

It is noteworthy that the reaction works well in the presence of water to afford 3C-alkylated product in 61% yield (entry 11).

Table 1   Optimization table for the CDC reaction

Entry	Photocatalyst	Time (h)	Yield^a (%)
1	Rose Bengal (1 mol%)	24	27
2	Rose Bengal (1 mol%)	36	35
3	Rose Bengal (2 mol%)	24	42
4	Rose Bengal (2 mol%)	48	43
5	Eosin Y (1 mol%)	18	68
6^b	Eosin Y (1 mol%)	18	69
7	Eosin Y (2 mol%)	18	88
8	Eosin Y (1 mol%)	24	95
9	Eosin Y (2 mol%)	24	94
10	Eosin Y (2 mol%)	36	96
11^c	Eosin Y (1 mol%)	24	61
12	—	36	nr
13	Eosin B (1 mol%)	24	30

^{a} Isolated yields. ^{b} Oxidant TBHP using 2 equivalents. ^{c} Water : THF used in a ratio of 1 : 0.3. nr = no reaction.

However, no reaction was observed in the absence of photocatalyst (entry 12). The reaction was attempted with eosin B as photocatalyst, affording only 30% yield of the desired product (entry 13). From the above observations it was concluded that entry 8 represents the suitable conditions for the CDC reaction between 1-methylquinoxalin-2(1H)-one (**5a**) and ethers.

With the optimized reaction conditions in hand, we next examined the substrate scope for this CDC reaction with various substituted quinoxalin-2(1H)-one derivatives. To our delight, the reaction serves as a really useful protocol for the syntheses of various 3C substituted quinoxalin-2(1H)-ones, affording moderate to excellent yields bearing both electron-donating and electron-withdrawing substituents.

When the amide group of quinoxalin-2(1H)-one was alkylated with groups such as methyl, benzyl and allyl groups subjected to photocatalytic CDC reaction conditions, high yields of desired products were observed without any adverse effect (**6a–6h**, Table 2).

We were glad to find that various cyclic ethers such as THF, THP and 1,4-dioxanes were compatible with the reaction conditions and yields of the corresponding 3C alkylated quinoxalin-2(1H)-one products were satisfactory. It is noteworthy that quinoxalin-2(1H)-ones bearing electron-donating groups such as methyl and dimethyl provided the highest yields (**6i–6m**, Table 2) whereas quinoxalin-2(1H)-ones with electron-withdrawing groups such as –Br and –Cl gave slightly lower yields of desired products (**6n–6o**).

Also, 6-benzoyl-substituted quinoxalin-2(1H)-one under the optimized reaction conditions forms the desired product in 81% yield (**6p**). The N-propylated quinoxalin-2(1H)-one derivative when subjected to optimized reaction conditions affords 3C alkylated product in 83% yield (**6q**, Table 2).

To show the synthetic utility of the developed protocol, 3C alkylated quinoxalin-2(1H)-one derivatives were further functionalized as shown in Scheme 2. 1-Allyl-3-(1,4-dioxan-2-yl)quinoxalin-2(1H)-one was subjected to hydrogenation using Pd/C as the catalyst

Table 2 Substrate scope for the CDC reaction

6a, R= Me, 95 %
6b, R= Bn, 90 %
6c, R= allyl, 92%

6d, R= Me, 49 %
6e, R= Bn, 42%
6f, R= allyl, 52%

6g, R= Me, 51%
6h, R= Bn, 39%

6i, 89 %

6j, X=CH₂, 55%
6k, X= O, 59%

6l, 41 %

6m, 84 %

6n, R= Br, 89 %
6o, R= Cl, 86 %

6p, 81%

6q, 83%
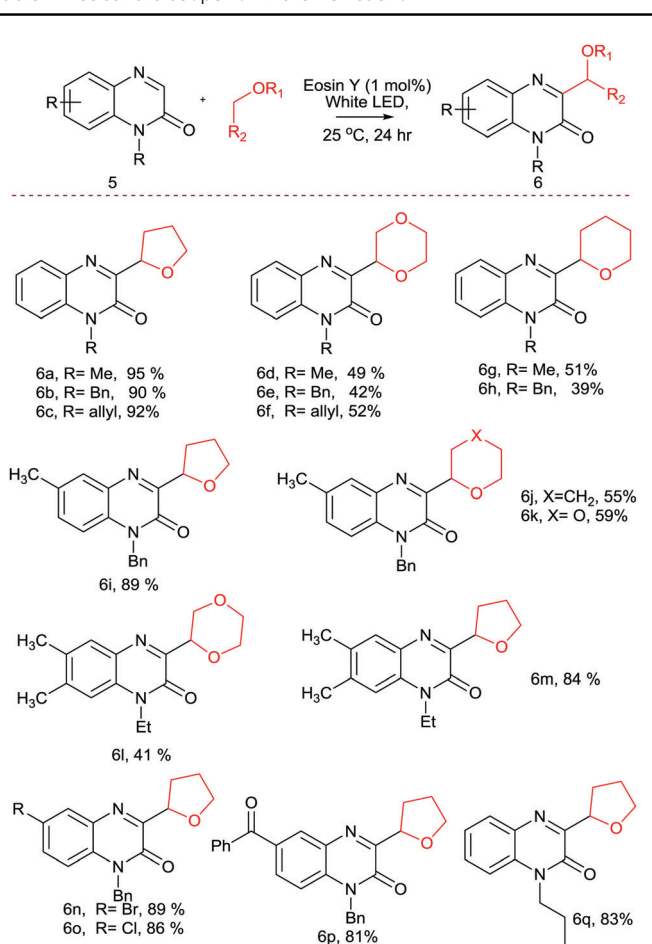
Reaction conditions: substituted quinoxalin-2(1*H*)-ones (5.1 mmol), eosin Y (0.01 mmol), in THF (15 mmol) at 25 °C under air for 24 h. The isolated yields were calculated based on quinoxalin-2(1*H*)-ones.

to give compound **7** in 94% yield. Next, 1-allyl-3-(1,4-dioxan-2-yl)quinoxalin-2(1*H*)-one was subjected to oxidative 1,3-dipolar addition[17] with 4-methoxybenzaldehyde oxime using PIDA as oxidant under nitrogen atmosphere to afford compound **8** in 75% yield (Scheme 2).

Besides, 1-allyl-3-(tetrahydrofuran-2-yl)quinoxalin-2(1*H*)-one (**6c**) could also be converted into the dihydroxylated product **9** in 89% yield which appears as a β-blocker type core structure (Scheme 2).

In order to gain insight into the reaction mechanism, a control experiment was performed between 1-methylquinoxalin-2(1*H*)-one (**5a**) and THF by the addition of 2 equivalents of TEMPO as a radical scavenger (Fig. 2). We observed the formation TEMPO-THF adduct **10** with trace amount of desired product. The formation of TEMPO-THF adduct **10** was confirmed by LCMS. From this experiment it can be concluded that the reaction works by formation of radicals. On the basis of control experiment and known literature, we propose a plausible reaction pathway for the eosin Y catalyzed CDC reaction.

The anionic eosin Y species A is activated in the presence of white light which promotes the HAT process[8] for the formation
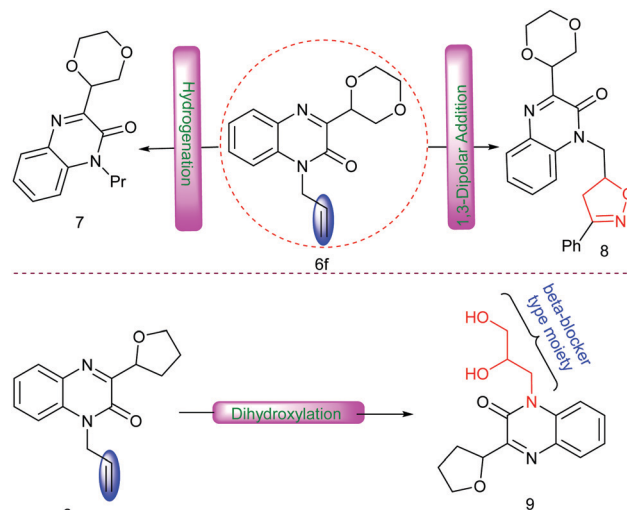
Scheme 2 Synthetic transformations of the products.
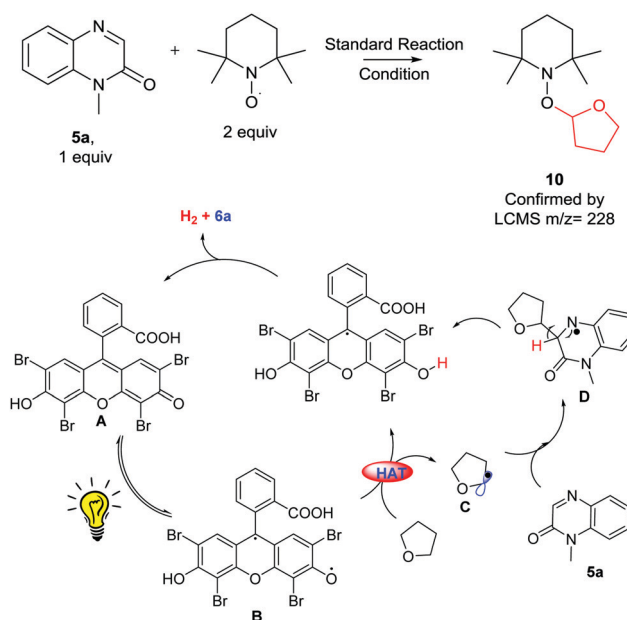
Fig. 2 Control experiment and a plausible reaction mechanism.

of carbon-centered radical C. The formed radical C adds to 1-methylquinoxalin-2(1*H*)-one (**5a**) to generate N-centered radical D. Then species D undergoes dehydrogenative aromatization reaction to give the desired product **6a** and eosin Y which will be further used for the next catalytic cycle.

In conclusion, we have developed an efficient white light mediated, eosin Y catalyzed C–C bond formation reaction between ethers and quinoxalin-2(1*H*)-ones to give 3C-alkylated quinoxalin-2(1*H*)-ones. This approach has a wide substrate scope with high functional group tolerance. Also it is a base- and oxidant-free approach under milder reaction conditions compared to previously reported methods. Further applications of the present methodology are underway in our laboratory.

Experimental section

General information

Solvents were purified and dried by standard procedures before use. ^{1}H NMR spectra and ^{13}C NMR spectra were recorded with Bruker AV 200/400/500 MHz spectrometers in appropriate solvents using TMS as internal standard or the solvent signals as secondary standards and the chemical shifts are shown as δ values. Purification was done using column chromatography (100–120 mesh) and/or with neutral alumina. The reactions were monitored by TLC visualized by UV (254 nm) and/or with iodine. Coupling constants are given in hertz (Hz) and the classical abbreviations are used to describe the signal multiplicities. HRMS data for all new compounds were recorded with a Thermo Scientific Q-Exactive, Accela 1250 pump. All chemicals are purchased from Sigma-Aldrich and used without further purification.

General procedure for the cross dehydrogenative coupling of quinoxalin-2(H)-ones with ethers

To a solution of quinoxalin-2(H)-one **5** (0.2 mmol), eosin Y (1 mol%) and ether (3 mL) were added and the reaction mixture was kept open to the air and stirred under irradiation of 3 W white LEDs at room temperature (27 °C) for 24 h. After completion of the reaction (monitored by TLC), the reaction mixture was dried under vacuum. Then the crude reaction mixture was diluted with ethyl acetate (10 mL) and washed with brine. It was eluted with EtOAc (10 mL × 2) and dried over anhydrous Na$_2$SO$_4$. The organics were evaporated and the crude residue was purified by flash column chromatography using a mixture of petroleum ether and ethyl acetate (70 : 30) as eluent to give the desired product **6**.

1-Methyl-3-(tetrahydrofuran-2-yl)quinoxalin-2(1H)-one (6a). Yield: 95% (95 mg); white solid; ^{1}H NMR (400 MHz, CDCl$_3$): δ 7.88–7.98 (m, 1H), 7.44–7.59 (m, 1H), 7.20–7.37 (m, 2H), 5.36 (dd, J = 7.32, 6.10 Hz, 1H), 4.21 (d, J = 6.71 Hz, 1H), 3.92–4.06 (m, 1H), 3.67 (s, 3H), 2.48 (d, J = 5.49 Hz, 1H), 1.95–2.08 (m, 3H). ^{13}C NMR (101 MHz, CDCl$_3$): δ 159.3, 153.9, 133.0, 132.3, 130.3, 130.0, 123.5, 113.4, 77.4, 69.0, 30.3, 28.7, 25.5.

1-Benzyl-3-(tetrahydrofuran-2-yl)quinoxalin-2(1H)-one (6b). Yield: 90% (70 mg); white solid; ^{1}H NMR (200 MHz, CDCl$_3$): δ 8.10 (dd, J = 8.02, 1.58 Hz, 1H), 7.85 (dd, J = 7.96, 1.64 Hz, 1H), 7.48–7.72 (m, 4H), 7.30–7.48 (m, 3H), 5.50–5.72 (m, 2H), 5.43 (dd, J = 7.45, 6.06 Hz, 1H), 4.13–4.33 (m, 1H), 3.92–4.11 (m, 1H), 2.34–2.57 (m, 1H), 1.94–2.23 (m, 3H). ^{13}C NMR (50 MHz, CDCl$_3$): δ 154.7, 149.7, 139.8, 138.2, 136.3, 129.3, 128.9, 128.3, 127.9, 126.5, 126.4, 76.8, 69.0, 67.9, 30.6, 25.6; HRMS (ESI) calculated [M + H]$^+$ for C$_{19}$H$_{19}$O$_2$N$_2$: 307.1441, found: 307.1442.

1-Allyl-3-(tetrahydrofuran-2-yl)quinoxalin-2(1H)-one (6c). Yield: 92% (88 mg); yellow gummy oil; ^{1}H NMR (500 MHz, CDCl$_3$): δ 7.85

(d, J = 8.01 Hz, 1H), 7.33–7.48 (m, 1H), 7.13–7.30 (m, 2H), 5.73–5.95 (m, 1H), 5.26–5.35 (m, 1H), 5.15 (d, J = 10.30 Hz, 1H), 5.06 (d, J = 17.55 Hz, 1H), 4.80 (br s, 2H), 4.13 (q, J = 6.61 Hz, 1H), 3.82–3.98 (m, 1H), 2.26–2.48 (m, 1H), 1.83–2.05 (m, 3H). ^{13}C NMR (126 MHz, CDCl$_3$): δ 159.2, 153.3, 132.3, 132.1, 130.3, 130.2, 129.8, 123.3, 117.8, 113.8, 77.2, 68.9, 44.0, 30.2, 25.4.

3-(1,4-Dioxan-2-yl)-1-methylquinoxalin-2(1H)-one (6d). Yield: 49% (52 mg); yellow solid; ^{1}H NMR (400 MHz, CDCl$_3$): δ 7.94 (d, J = 7.93 Hz, 1H), 7.50 (t, J = 7.93 Hz, 1H), 7.21–7.32 (m, 2H), 5.21 (dd, J = 9.46, 2.14 Hz, 1H), 4.19 (dd, J = 10.99, 1.83 Hz, 1H), 4.03 (d, J = 11.60 Hz, 1H), 3.86–3.95 (m, 1H), 3.75 (d, J = 6.10 Hz, 2H), 3.62 (s, 3H), 3.53–3.60 (m, 1H). ^{13}C NMR (101 MHz, CDCl$_3$): δ 155.0, 153.5, 133.0, 132.4, 130.7, 130.5, 123.7, 113.5, 74.5, 69.3, 67.4, 66.2, 28.9; HRMS (ESI) calculated [M + Na]$^+$ for C$_{13}$H$_{14}$O$_3$N$_2$Na: 269.0897, found: 269.0898.

1-Benzyl-3-(1,4-dioxan-2-yl)quinoxalin-2(1H)-one (6e). Yield: 42% (35 mg); white solid; ^{1}H NMR (500 MHz, CDCl$_3$): δ 8.07 (d, J = 8.01 Hz, 1H), 7.76 (d, J = 8.01 Hz, 1H), 7.57 (t, J = 7.63 Hz, 1H), 7.46–7.51 (m, 1H), 7.43 (d, J = 7.25 Hz, 2H), 7.29–7.35 (m, 2H), 7.23–7.28 (m, 1H), 5.38–5.61 (m, 2H), 5.19 (dd, J = 9.54, 2.29 Hz, 1H), 4.00–4.10 (m, 2H), 3.91 (td, J = 11.44, 3.05 Hz, 1H), 3.71–3.82 (m, 2H), 3.64 (t, J = 10.68 Hz, 1H). ^{13}C NMR (126 MHz, CDCl$_3$): δ 154.1, 144.8, 139.7, 138.3, 135.8, 129.8, 128.9, 128.3, 127.9, 127.9, 126.5, 126.5, 73.8, 69.2, 68.0, 67.2, 66.0; HRMS (ESI) calculated [M + H]$^+$ for C$_{19}$H$_{19}$O$_3$N$_2$: 323.1390, found: 323.1391.

1-Allyl-3-(1,4-dioxan-2-yl)quinoxalin-2(1H)-one (6f). Yield: 52% (53 mg); yellow solid; ^{1}H NMR (500 MHz, CDCl$_3$): δ 7.95 (dd, J = 8.20, 1.34 Hz, 1H), 7.39–7.55 (m, 1H), 7.10–7.33 (m, 2H), 5.74–5.95 (m, 1H), 5.15–5.27 (m, 2H), 5.08 (d, J = 17.17 Hz, 1H), 4.74–4.88 (m, 2H), 4.19 (dd, J = 11.44, 2.67 Hz, 1H), 4.03 (d, J = 11.44 Hz, 1H), 3.86–3.94 (m, 1H), 3.70–3.80 (m, 2H), 3.60 (dd, J = 11.06, 9.54 Hz, 1H). ^{13}C NMR (126 MHz, CDCl$_3$): δ 155.1, 153.2, 132.7, 132.2, 130.7, 130.7, 130.3, 123.7, 118.2, 114.1, 74.4, 69.3, 67.4, 66.2, 44.4.

1-Methyl-3-(tetrahydro-2H-pyran-2-yl)quinoxalin-2(1H)-one (6g). Yield: 51% (54 mg); yellow solid; ^{1}H NMR (500 MHz, CDCl$_3$): δ 8.05 (d, J = 8.0 Hz, 1H), 7.55 (t, J = 7.6 Hz, 1H), 7.25–7.41 (m, 2H), 5.00 (d, J = 10.7 Hz, 1H), 4.29 (d, J = 10.7 Hz, 1H), 3.62–3.80 (m, 4H), 2.15 (d, J = 12.6 Hz, 1H), 1.98 (d, J = 10.3 Hz, 1H), 1.72–1.90 (m, 2H), 1.52–1.68 (m, 2H). ^{13}C NMR (126 MHz, CDCl$_3$): δ 158.5, 153.3, 132.7, 132.4, 130.3, 129.9, 123.4, 113.2, 76.1, 69.1, 29.9, 28.6, 25.3, 23.3; HRMS (ESI) calculated [M + H]$^+$ for C$_{14}$H$_{17}$O$_2$N$_2$: 245.1285 found: 245.1279.

1-Benzyl-3-(tetrahydro-2H-pyran-2-yl)quinoxalin-2(1H)-one (6h). Yield: 39% (32 mg); white solid; ^{1}H NMR (200 MHz, CDCl$_3$): δ 8.06 (dd, J = 7.89, 1.58 Hz, 1H), 7.37–7.47 (m, 1H), 7.22–7.36 (m, 7H), 5.32–5.68 (m, 2H), 4.87–5.20 (m, 1H), 4.32 (dd, J = 10.55, 3.09 Hz, 1H), 3.60–3.89 (m, 1H), 2.20 (d, J = 10.74 Hz, 1H), 1.53–2.08 (m, 6H). ^{13}C NMR (50 MHz, CDCl$_3$): δ 158.3, 153.1, 134.5, 132.3, 131.7, 130.0, 129.6, 128.2, 127.0, 126.1, 123.1, 113.6, 68.8, 45.1, 29.6, 24.9, 23.0.

1-Methyl-3-(tetrahydrofuran-2-yl)quinoxalin-2(1H)-one (6i). Yield: 89% (79 mg); colorless oil; ^{1}H NMR (200 MHz, CDCl$_3$): δ 7.54–7.91 (m, 1H), 7.06–7.33 (m, 7H), 5.30–5.52 (m, 2H), 3.86–4.07 (m, 1H), 2.39–2.56 (m, 1H), 2.26–2.38 (m, 3H), 2.12–2.25 (m, 1H), 1.89–2.11 (m, 3H).

1-Benzyl-7-methyl-3-(tetrahydro-2H-pyran-2-yl)quinoxalin-2(1H)-one (6j). Yield: 55% (51 mg); colorless oil; ^{1}H NMR (200 MHz, CDCl$_3$): δ 7.73–7.91 (m, 1H), 6.93–7.28 (m, 7H), 5.17–5.57 (m, 2H), 4.89–5.07 (m, 1H), 4.14–4.31 (m, 1H), 3.54–3.76 (m, 1H), 2.30 (s, 3H), 2.01–2.16 (m, 1H), 1.39–1.99 (m, 5H). ^{13}C NMR (50 MHz, CDCl$_3$): δ 157.5, 153.6, 141.0, 135.2, 133.5, 131.4, 131.1, 130.4, 130.3, 128.8, 127.6, 126.9, 126.7, 125.0, 114.2, 114.0, 69.4, 45.7, 30.2, 25.6, 23.6, 22.0, 20.5; HRMS (ESI) calculated [M + H]$^+$ for C$_{21}$H$_{23}$O$_2$N$_2$: 335.1754, found: 335.1741.

1-Benzyl-3-(1,4-dioxan-2-yl)-7-methylquinoxalin-2(1H)-one (6k). Yield: 59% (55 mg); colorless oil; ^{1}H NMR (400 MHz, CDCl$_3$): δ 7.77 (s, 1H), 7.17–7.26 (m, 4H), 7.13 (t, J = 6.49 Hz, 2H), 7.04–7.10 (m, 1H), 5.41–5.51 (m, 1H), 5.23–5.40 (m, 2H), 4.23 (dd, J = 11.44, 2.29 Hz, 1H), 4.01–4.10 (m, 1H), 3.86–3.98 (m, 1H), 3.72–3.84 (m, 2H), 3.63 (dd, J = 11.06, 9.54 Hz, 1H), 2.32 (s, 3H). ^{13}C NMR (101 MHz, CDCl$_3$): δ 154.7, 153.4, 141.4, 134.6, 133.5, 132.4, 131.7, 130.2, 130.1, 129.8, 128.6, 127.4, 126.4, 125.0, 114.0, 113.8, 74.2, 69.1, 67.2, 67.1, 66.0, 45.4, 45.4, 29.3, 20.2; HRMS (ESI) calculated [M + H]$^+$ for C$_{20}$H$_{21}$O$_3$N$_2$: 337.1547, found: 337.1534.

3-(1,4-Dioxan-2-yl)-1-ethyl-6,7-dimethylquinoxalin-2(1H)-one (6l). Yield: 41% (40 mg); white solid; ^{1}H NMR (400 MHz, CDCl$_3$): δ 7.89 (s, 1H), 7.55 (s, 1H), 5.21 (dd, J = 9.77, 2.44 Hz, 1H), 4.42–4.68 (m, 2H), 4.07–4.19 (m, 2H), 3.99 (td, J = 11.29, 3.05 Hz, 1H), 3.79–3.92 (m, 2H), 3.69 (t, J = 10.68 Hz, 1H), 2.41 (d, J = 6.10 Hz, 6H), 1.46 (t, J = 7.02 Hz, 3H). ^{13}C NMR (101 MHz, CDCl$_3$): δ 154.1, 143.4, 139.9, 138.4, 136.8, 136.0, 128.2, 125.8, 73.8, 69.3, 67.2, 65.9, 62.0, 29.3, 19.9, 19.6, 14.1; HRMS (ESI) calculated [M + H]$^+$ for C$_{16}$H$_{21}$O$_3$N$_2$: 289.1547, found: 289.1543.

1-Ethyl-6,7-dimethyl-3-(tetrahydrofuran-2-yl)quinoxalin-2(1H)-one (6m). Yield: 84% (79 mg); semi solid; ^{1}H NMR (200 MHz, CDCl$_3$): δ 7.73 (s, 1H), 7.48 (s, 1H), 5.19–5.42 (m, 1H), 4.34–4.60 (m, 2H), 4.08–4.25 (m, 1H), 3.86–4.02 (m, 1H), 2.34 (d, J = 2.40 Hz, 7H), 1.95–2.11 (m, 3H), 1.39 (t, J = 7.07 Hz, 3H). ^{13}C NMR (101 MHz, CDCl$_3$): δ 155.0, 148.5, 139.5, 138.7, 136.9, 136.0, 128.4, 126.1, 77.2, 69.1, 62.1, 30.7, 25.9, 20.2, 19.9, 14.5; HRMS (ESI) calculated [M + H]$^+$ for C$_{16}$H$_{21}$O$_2$N$_2$: 273.1598, found: 273.1598.

1-Benzyl-6-bromo-3-(tetrahydrofuran-2-yl)quinoxalin-2(1H)-one (6n). Yield: 89% (76 mg); white solid; ^{1}H NMR (200 MHz, CDCl$_3$): δ 7.88 (q, J = 2.06 Hz, 2H), 7.21–7.50 (m, 6H), 5.38–5.53 (m, 3H), 4.14 (q, J = 7.33 Hz, 1H), 3.96 (td, J = 7.67, 5.75 Hz, 1H), 2.20–2.31 (m, 2H), 1.89–2.16 (m, 2H). ^{13}C NMR (101 MHz, CDCl$_3$): δ 155.6, 150.8, 141.1, 135.6, 134.7, 132.6, 128.6, 128.3, 128.0, 127.9, 124.5, 122.6, 76.2, 68.9, 68.4, 29.6, 25.3; HRMS (ESI) calculated [M + H]$^+$ for C$_{19}$H$_{18}$O$_2$N$_2$Br: 385.0546, found: 385.0543.

1-Benzyl-7-chloro-3-(tetrahydrofuran-2-yl)quinoxalin-2(1H)-one (6o). Yield: 86% (76 mg); reddish viscous oil; ^{1}H NMR (200 MHz, CDCl$_3$): δ 7.75–8.12 (m, 1H), 7.17–7.40 (m, 7H), 5.32–5.65 (m, 3H), 4.17–4.34 (m, 1H), 3.97–4.16 (m, 1H), 2.40–2.67 (m, 1H), 1.95–2.26 (m, 3H). ^{13}C NMR (50 MHz, CDCl$_3$): δ 160.5, 153.2, 134.1, 132.6, 130.9, 130.5, 129.5, 129.2, 128.4, 127.2, 126.1, 123.5, 114.9, 113.6, 76.8, 68.6, 62.7, 45.2, 29.9, 25.0; HRMS (ESI) calculated [M + H]$^+$ for C$_{19}$H$_{18}$O$_2$N$_2$Cl: 341.1051, found: 341.1040.

6-Benzoyl-1-benzyl-3-(tetrahydrofuran-2-yl)quinoxalin-2(1H)-one (6p). Yield: 81% (68 mg); gummy oil; ^{1}H NMR (200 MHz, CDCl$_3$): δ 7.95–8.19 (m, 1H), 7.70–7.83 (m, 2H), 7.59–7.68 (m, 2H), 7.36–7.57 (m, 3H), 7.26–7.34 (m, 3H), 7.14–7.26 (m, 2H), 5.31–5.69 (m, 3H), 4.19–4.42 (m, 1H), 3.93–4.16 (m, 1H), 2.41–2.80 (m, 1H), 1.97–2.21 (m, 3H). ^{13}C NMR (101 MHz, CDCl$_3$): δ 194.8, 161.9, 153.7, 137.8, 136.4, 134.6, 134.5, 132.9, 132.4, 132.2, 131.7, 130.9, 130.2, 129.6, 129.5, 128.8, 128.1, 127.7, 127.6, 126.7, 126.5, 124.7, 116.3, 77.3, 69.0, 45.3, 30.4, 25.4; HRMS (ESI) calculated [M + H]$^+$ for C$_{26}$H$_{23}$O$_3$N$_2$: 411.1703, found: 411.1715.

1-Propyl-3-(tetrahydrofuran-2-yl)quinoxalin-2(1H)-one (6q). Yield: 83% (79 mg); gummy oil; ^{1}H NMR (400 MHz, CDCl$_3$): δ 7.97 (d, J = 7.9 Hz, 1H), 7.54 (t, J = 7.6 Hz, 1H), 7.23–7.39 (m, 2H), 5.29–5.53 (m, 1H), 4.15–4.38 (m, 3H), 3.94–4.10 (m, 1H), 2.42–2.64 (m, 1H), 2.05 (br s, 3H), 1.74–1.88 (m, 2H), 1.05 (t, J = 7.6 Hz, 3H). ^{13}C NMR (101 MHz, CDCl$_3$): δ 159.5, 153.8, 132.8, 132.3, 130.7, 130.0, 123.4, 113.6, 77.6, 69.2, 43.6, 30.5, 25.6, 20.6, 11.4; HRMS (ESI) calculated [M + H]$^+$ for C$_{15}$H$_{19}$O$_2$N$_2$: 259.1441, found: 259.1435.

3-(1,4-Dioxan-2-yl)-1-propylquinoxalin-2(1H)-one (7). Yield: 94% (57 mg); off-white solid; ^{1}H NMR (500 MHz, CDCl$_3$): δ 8.04 (d, J = 7.6 Hz, 1H), 7.57 (t, J = 7.4 Hz, 1H), 7.26–7.41 (m, 2H), 5.23–5.44 (m, 1H), 4.17–4.31 (m, 3H), 4.12 (d, J = 11.4 Hz, 1H), 3.95–4.04 (m, 1H), 3.84 (d, J = 5.0 Hz, 2H), 3.67 (t, J = 10.3 Hz, 1H), 1.73–1.88 (m, 2H), 1.05 (t, J = 7.2 Hz, 3H). ^{13}C NMR (126 MHz, CDCl$_3$): δ 154.8, 153.1, 132.5, 132.0, 130.6, 130.4, 123.3, 113.3, 74.2, 69.1, 67.2, 66.0, 43.4, 20.3, 11.0; HRMS (ESI) calculated [M + H]$^+$ for C$_{15}$H$_{18}$N$_2$O$_3$: 274.1308, found: 274.1309.

3-(1,4-Dioxan-2-yl)-1-((3-(4-methoxyphenyl)-4,5-dihydroisoxazol-5-yl)methyl)quinoxalin-2(1H)-one (8). Yield: 75% (65 mg); white solid; ^{1}H NMR (200 MHz, CDCl$_3$): δ 7.80–8.32 (m, 1H), 7.39–7.77 (m, 4H), 7.25–7.39 (m, 1H), 6.50–7.04 (m, 2H), 5.00–5.42 (m, 2H), 4.55 (td, J = 13.8, 4.3 Hz, 1H), 3.86–4.45 (m, 4H), 3.70–3.86 (m, 5H), 3.12–3.70 (m, 3H); ^{13}C NMR (50 MHz, CDCl$_3$): δ 161.4, 156.8, 154.6, 154.1, 132.8, 131.1, 130.8, 128.5, 124.2, 121.4, 114.7, 114.3, 78.2, 74.5, 67.6, 66.4, 55.4, 46.1, 39.2, 29.7; HRMS (ESI) calculated [M + H]$^+$ for C$_{23}$H$_{24}$O$_5$N$_3$: 422.1710, found: 422.1698.

1-(2,3-Dihydroxypropyl)-3-(tetrahydrofuran-2-yl)quinoxalin-2(1H)-one (9). Yield: 89% (60 mg); colorless gummy oil; ^{1}H NMR (200 MHz, CDCl$_3$): δ 7.87 (d, J = 7.83 Hz, 1H), 7.47 (d, J = 3.79 Hz, 2H), 7.23–7.36 (m, 1H), 5.21–5.37 (m, 1H), 4.35–4.50 (m, 1H), 3.86–4.32 (m, 4H), 3.63 (d, J = 9.35 Hz, 2H), 3.51 (br s, 1H), 3.00 (s, 1H), 2.22–2.49 (m, 1H), 1.81–2.11 (m, 3H), 1.18 (s, 1H). ^{13}C NMR (50 MHz, CDCl$_3$): δ 158.1, 154.3, 132.2, 131.8, 129.9, 129.9, 123.6, 113.5, 76.6, 68.9, 68.5, 62.7, 62.7, 44.0, 42.6, 29.6, 29.5, 29.0, 25.0; HRMS (ESI) calculated [M + H]$^+$ for C$_{15}$H$_{19}$O$_4$N$_2$: 291.1339, found: 291.1345.

Conflicts of interest

There are no conflicts to declare.

Notes and references

1 (a) G. Brahmachari, *RSC Adv.*, 2016, **6**, 64676–64725; (b) V. Resch, J. H. Schrittwieser, E. Siirola and W. Kroutil, *Curr. Opin. Biotechnol.*, 2011, **22**, 793–799; (c) D. J. Hart, *Science*, 1984, **223**, 883–887; (d) J. Yamaguchi, A. D. Yamaguchi and K. Itami, *Angew. Chem., Int. Ed.*, 2012, **51**, 8960–9009.

2 C.-H. Jun, *Chem. Soc. Rev.*, 2004, **33**, 610–618.

3 (*a*) M. K. Lakshman and P. K. Vurama, *Chem. Sci.*, 2017, **8**, 5845–5888; (*b*) B. V. Varun, J. Dhineshkumar, K. R. Bettadapur, Y. Siddaraju, K. Alagiri and K. R. Prabhu, *Tetrahedron Lett.*, 2017, **58**, 803–824; (*c*) Z. Li, D. S. Bohle and C.-J. Li, *PNAS*, 2006, **24**, 8928–8933; (*d*) C.-J. Li, *Acc. Chem. Res.*, 2009, **42**, 335–344; (*e*) C. S. Yeung and V. M. Dong, *Chem. Rev.*, 2011, **111**, 1215–1292; (*f*) S. A. Girard, T. Knauber and C.-J. Li, *Angew. Chem., Int. Ed.*, 2014, **53**, 74–100; (*g*) C. Zhang, C. Tanga and N. Jiao, *Chem. Soc. Rev.*, 2012, **41**, 3464–3484; (*h*) D. Ravelli, S. Protti and M. Fagnoni, *Chem. Rev.*, 2016, **116**, 9850–9913; (*i*) D. P. Hari and B. KÖnig, *Org. Lett.*, 2011, **13**, 3852–3855; (*j*) G. Wei, C. Basheer, C.-H. Tan and Z. Jiang, *Tetrahedron Lett.*, 2016, **57**, 3801–3809.

4 (*a*) T. Martín, J. I. Padrón and V. S. Martín, *Synlett*, 2014, 12–32; (*b*) J. Rutkowski and B. Brzezinski, *BioMed Res. Int.*, 2013, 162513; (*c*) I. Kadota and Y. Yamamoto, *Acc. Chem. Res.*, 2005, **38**, 423–432; (*d*) N. Li, Z. Shi, Y. Tang, J. Chen and X. Li, *Beilstein J. Org. Chem.*, 2008, **4**, 1–62; (*e*) T. Nakata, *Chem. Rev.*, 2005, **105**, 4314–4347.

5 (*a*) X. Li, H.-Y. Wanga and Z.-J. Shi, *New J. Chem.*, 2013, **37**, 1704–1706; (*b*) E. Kianmehr, M. Fardpour and K. M. Khan, *Eur. J. Org. Chem.*, 2017, 2661–2668; (*c*) L. Jin, J. Feng, G. Lu and C. Cai, *Adv. Synth. Catal.*, 2015, **357**, 2105–2110; (*d*) S. Devariab and B. A. Shah, *Chem. Commun.*, 2016, **52**, 1490–1493; (*e*) N. Okugawa, K. Moriyama and H. Togo, *Eur. J. Org. Chem.*, 2015, 4973–4981; (*f*) L. Zhou, N. Okugawa and H. Togo, *Eur. J. Org. Chem.*, 2017, 6239–6243; (*g*) S. Liu, A. Liu, Y. Zhang and W. Wang, *Chem. Sci.*, 2017, **8**, 4044–4050; (*h*) Z. Xie, Y. Cai, H. Hu, C. Lin, Z. Chen, L. Wang and Y. Pan, *Org. Lett.*, 2013, **15**, 4600–4603; (*i*) F. Jafarpour and M. Darvishmolla, *Org. Biomol. Chem.*, 2018, **16**, 3396–3401.

6 (*a*) Y. Zhao, B. Huang, C. Yang, B. Li, B. Gou and W. Xia, *ACS Catal.*, 2017, **7**, 2446–2451; (*b*) Y. Zhaoa and W. Xia, *Chem. Soc. Rev.*, 2018, **47**, 2591–2608; (*c*) Y. Zhao, B. Huang, C. Yang and W. Xia, *Org. Lett.*, 2016, **18**, 3326–3329.

7 (*a*) S. Samanta, C. Ravi, S. N. Rao, A. Joshi and S. Adimurthy, *Org. Biomol. Chem.*, 2017, **15**, 9590–9594; (*b*) W. Wei, L. Wang, P. Bao, Y. Shao, H. Yue, D. Yang, X. Yang, X. Zhao and H. Wang, *Org. Lett.*, 2018, **20**, 7125–7130.

8 (*a*) X.-Z. Fan, J.-W. Rong, H.-L. Wu, Q. Zhou, H.-P. Deng, J. D. Tan, C.-W. Xue, L.-Z. Wu, H.-R. Tao and J. Wu, *Angew. Chem., Int. Ed.*, 2018, **57**, 8514–8518; (*b*) W. Wei, L. Wang, H. Yue, P. Bao, W. Liu, C. Hu, D. Yang and H. Wang, *ACS Sustainable Chem. Eng.*, 2018, **6**, 17252–17257.

9 (*a*) O. O. Ajani, *Eur. J. Med. Chem.*, 2014, **85**, 688–715; (*b*) D. Wang and F. Gao, *Chem. Cent. J.*, 2013, **7**, 95; references therein.

10 D. S. Lawrence, J. E. Copper and C. D. Smith, *J. Med. Chem.*, 2001, **44**, 594–601.

11 Z. Liu, S. Yu, D. Chen, G. Shen, Y. Wang, L. Hou, D. Lin, J. Zhang and F. Ye, *Drug Des., Dev. Ther.*, 2016, **10**, 1489–1500.

12 (*a*) J. Harmenberg, A. Akesson-Johansson, A. Graslund, T. Malmfors, J. Bergman, B. Wahren, S. Akerfeldt, L. Lundblad and S. Cox, *Antiviral Res.*, 1991, **15**, 193–204; (*b*) N. C. Desai, A. Dodiya and N. Shihory, *J. Saudi Chem. Soc.*, 2013, **17**, 259–267.

13 X. Qin, X. Hao, H. Han, S. Zhu, Y. Yang, B. Wu, S. Hussain, S. Parveen, C. Jing, B. Ma and C. Zhu, *J. Med. Chem.*, 2015, **58**, 1254–1267.

14 (*a*) B. Ramesh, R. Reddy, G. R. Kumar and B. V. S. Reddy, *Tetrahedron Lett.*, 2018, **59**, 628–631; (*b*) K. Yin and R. Zhang, *Org. Lett.*, 2017, **19**, 1530–1533; (*c*) L. Yang, P. Gao, X.-H. Duan, Y.-R. Gu and L.-N. Guo, *Org. Lett.*, 2018, **20**, 1034–1037.

15 (*a*) H. I. Jung, J. H. Lee and D. Y. Kim, *Bull. Korean Chem. Soc.*, 2018, **39**, 1003–1006; (*b*) P. S. Akula, B.-C. Hong and G.-H. Lee, *RSC Adv.*, 2018, **8**, 19580–19584; (*c*) J. Yuan, S. Liu and L. Qu, *Adv. Synth. Catal.*, 2017, **359**, 4197–4207; (*d*) S. Paul, J. H. Ha, G. E. Park and Y. R. Lee, *Adv. Synth. Catal.*, 2017, **359**, 1515–1521.

16 (*a*) S. S. Chavan, B. D. Rupanawar, R. B. Kamble, A. M. Shelke and G. Suryavanshi, *Org. Chem. Front.*, 2018, **5**, 544–548; (*b*) B. D. Rupanawar, S. S. Chavan, A. M. Shelke and G. Suryavanshi, *New J. Chem.*, 2018, **42**, 6433–6440; (*c*) A. H. Bansode and G. Suryavanshi, *RSC Adv.*, 2018, **8**, 32055–32062; (*d*) K. D. Mane, A. Mukherjee, K. Vanka and G. Suryavanshi, *J. Org. Chem.*, 2019, **84**, 2039–2047; (*e*) S. G. More and G. Suryavanshi, *Org. Biomol. Chem.*, 2019, **17**, 3239–3248.

17 B. A. Mendelsohn, S. Lee, S. Kim, F. Teyssier, V. S. Aulakh and M. A. Ciufolini, *Org. Lett.*, 2009, **11**, 1539–1542.

RSC Advances

PAPER

Check for updates

Ti-superoxide catalyzed oxidative amidation of aldehydes with saccharin as nitrogen source: synthesis of primary amides†

Rohit B. Kamble, ‡[ab] Kishor D. Mane, ‡[ab] Bapurao D. Rupanawar, [ab] Pranjal Korekar,[c] A. Sudalai[ab] and Gurunath Suryavanshi *[ab]

A new heterogeneous catalytic system (Ti-superoxide/saccharin/TBHP) has been developed that efficiently catalyzes oxidative amidation of aldehydes to produce various primary amides. The protocol employs saccharin as amine source and was found to tolerate a wide range of substrates with different functional groups. Moderate to excellent yields, catalyst reusability and operational simplicity are the main highlights. A possible mechanism and the role of the catalyst in oxidative amidation have also been discussed.

Introduction

The amide bond constituting the structural backbone of proteins and peptides is abundantly found in natural products, pharmaceuticals, polymers and agrochemicals.[1] In particular, primary amides ($RCONH_2$) play an important role in organic synthesis as building blocks exhibiting a wide range of industrial applications and pharmacological interests[2] (Fig. 1).

Traditionally, amide synthesis has been achieved by the reaction of an amine with an activated carboxylic acid derivative, that often employs coupling reagents.[3] Subsequently, several alternate strategies[4] emerged for amide formation that include: (i) the Staudinger reaction; (ii) the Schmidt reaction; (iii) the Beckmann rearrangement; (iv) hydroamination of alkynes; (v) dehydrogenative amidation of alcohols; (vi) hydro-amino carbonylation of alkenes; (vii) iodonium promoted nitroalkene amine coupling reaction; (viii) transamidation of primary amides; *etc.* In this context, oxidative amidation of aldehydes with amine salts is synthetically preferred and has been achieved with a variety of reagent systems[5] (*e.g.* I_2, NBS, MnO_2, 3,3′,5,5′-tetra-*tert*-butyldiphenoquinone and TBHP as oxidant, *N*-heterocyclic carbene, transition metals such as Pd, Rh, Ru, Ni, Cu/Ag, Fe. Au, Pt and lanthanides). It may also be noted that several researchers have developed catalyst-free methods using TBHP and H_2O_2 as oxidants.[6] Quite recently, visible light was utilized to trigger a photoredox catalytic

oxidative amidation of aldehydes.[7] This reaction, however, relied on phenazinium salt, rose bengal or anthraquinone-based organophotocatalyst and air as the oxidant. Also, oxidative amidation of methylarenes catalyzed by Mn or Fe in combination with NH_3 or urea as amine source and oxidants has been reported[8] for amide synthesis (Scheme 1). The existing methods utilize homogeneous, rare and costly transition metals as catalyst. Also, these homogeneous reaction mixtures did not allow recyclability of used metals. To the best of our knowledge, metal catalyzed direct oxidative amidation of aldehydes under heterogeneous conditions has not explored. In this strategy, we wish to report Ti-superoxide catalyzed oxidative amidation of aldehydes and catalyst reused for more than three catalytic cycles (Scheme 1).
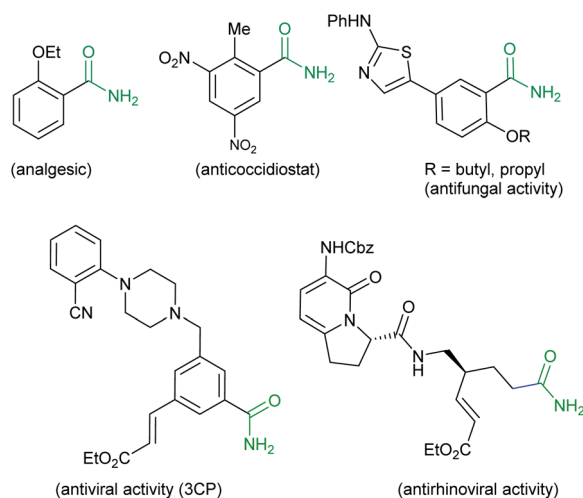
[a]Chemical Engineering and Process Development Division, CSIR-National Chemical Laboratory, Pune, Maharashtra, India-411 008. E-mail: gm.suryavanshi@ncl.res.in
[b]Academy of Scientific and Innovative Research, Ghaziabad, UP, India-201002
[c]Department of Chemistry, MES Abasaheb Garware College, Pune, India-411004

† Electronic supplementary information (ESI) available. See DOI: 10.1039/c9ra10413e

‡ These authors contribute equally.

Fig. 1 Some biologically important primary amides.

Previous work

a. Transition-metal catalyzed oxidative amidation
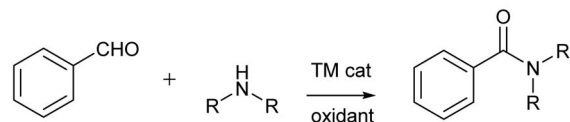
b. Visible light photocatalytic amide synthesis
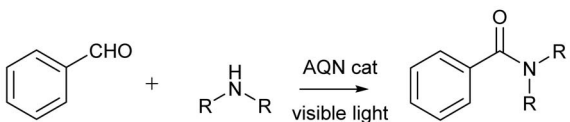
c. Oxidative amidation using urea or NH₃ as nitrogen source
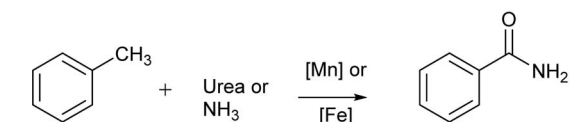
d. This work
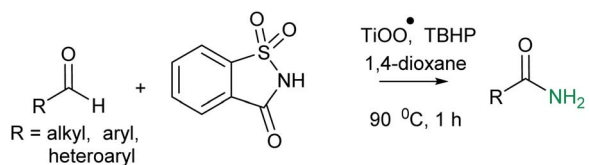
Scheme 1 Primary amide synthesis *via* direct oxidative amidation of aldehydes or methyl arenes.

Saccharin (2) is an artificial sweetener used in the production of various foods and pharmaceutical products. It is also used in the preparation of disubstituted amines from halides *via* nucleophilic substitution followed by Gabriel synthesis.[9]

Sometime ago, we have reported an elegant synthesis and catalytic applications of exceptionally stable titanium

superoxide for C–O, C–N and C–Br bond forming reactions.[10] Keeping this in mind, it was of interest to explore the cross dehydrogenative coupling between benzaldehyde and saccharin under Ti-superoxide catalysis in the presence of TBHP as oxidant to produce *N*-benzoylsaccharin (8). Surprisingly, the reaction underwent oxidative amidation to produce benzamide (56%). Thus, in seeking to develop a general condition for amide synthesis, we proposed that saccharin (2) could serve as nitrogen source. In this paper, we wish to report, for the first time, that titanium superoxide efficiently catalyzes oxidative amidation of aldehydes, under truly heterogeneous conditions, to produce primary amides (3) in excellent yields employing saccharin (2) as amine source and TBHP as oxidant (Scheme 1).

Table 1 shows the results of optimization studies of oxidative amidation of anisaldehyde with saccharin as amine source over Ti-superoxide using TBHP as oxidant.

When they were combined in equimolar amounts in 1,2-dichloroethane with Ti-superoxide (10 wt%) as catalyst at RT, no reaction took place. However, with increase in TBHP concentration (2–3 equiv.) and temperature at 90 °C, amide 3c was indeed obtained in low yields (19–22%). With change of solvent to 1,4-dioxane, considerable improvement in yield of 3c was achieved (41%). Further, increase of temperature to 110 °C, however, had a deleterious effect on yield (22%) (entry 3). When the catalyst concentration was increased to 20 wt%, yield of 3c was increased to 65%. Interestingly, a substantial improvement in yield was observed from 65 to 83% as the reaction time was decreased from 12 h to 4 h. Finally, a dramatic improvement in yield (95%) was realized with the reduction in time to 1 h. Further, reduction in TBHP concentration to 2 equiv. resulted in lowered yield of amide 3c (51%) (entry 5). Unfortunately, other solvents such as CH₃CN, DMSO, DMF and THF were found to be unsuitable for the reaction. Also, several oxidants such as DTBP, K₂S₂O₈ and H₂O₂ and other Ti catalysts (titanium silicalite-1 and TiO₂) were found to be less favoured for oxidative amidation. It may be noted that the reaction failed to proceed with

Table 1 Optimization of oxidative amidation of anisaldehyde with saccharin as amine source over Ti-superoxide[a]

No.	Cat[b] (wt%)	Oxidant (equiv.)	Solvent	T (°C)	T (h)	Yield[c] (%)
1	10	TBHP (1)[d]	DCE[e]	25	12	N R
2	10	TBHP (2)	DCE	90	12	19 (22)[f]
3	10	TBHP (3)	1,4-Dioxane	90	12	41 (22)[g]
4	20	TBHP (3)	1,4-Dioxane	90	12	65 (71)[h], (83)[i]
5	20	TBHP (3)	1,4-Dioxane	90	1	95 (51)[j]
6	20	DTBP (3)[k] or K₂S₂O₈ (3)	1,4-Dioxane	90	1	N R
7	20	30% H₂O₂ (3)	1,4-Dioxane	90	1	11

[a] Reaction conditions: anisaldehyde (1 mmol), saccharin (1.2 mmol), solvent (4 mL). [b] Titanium superoxide. [c] Isolated yield. [d] 5–6 M TBHP in hexane was used. [e] 1,2-Dichloroethane. [f] 3 equiv. of TBHP was used. [g] Temperature was 110 °C. [h] Time was 8 h. [i] Time was 4 h. [j] 2 equiv. of TBHP was used. [k] Di-*tert*-butylperoxide.

Table 2 Substrate scope for the oxidative amidation of aldehydes[a]

3a, R = H, 93%
3b, R = Me, 95%
3c, R = OMe, 91%
3d, R = t-Bu, 88%
3e, R = Cl, 79%
3f, R = I, 75%
3g, R = OH, 36%
3h, R = NH$_2$, 38%

3i, 78%

3j, R = NO$_2$, 71%
3k, R = F, 74%
3l, R = CF$_3$, 71%
3m, R = OMe, 84%

3n, R = Me, 91%
3o, R = I, 79%
3p, R = Br, 73%
**3q**, R = OH, 48%
3r, R = NH$_2$, 27%
3s, R = OEt, 79%

3t, R = NO$_2$, 72%
3u, R = Me, 95%

3v, R = F, R$_1$ = H; 85%
3w, R = H, R$_1$ = F; 81%

3x, R = H, 71%
3y, R = Br, 74%
3z, R = OH, 55%

3aa, R, R$_1$= OMe, 86%
3ab, R, R$_1$= Cl, 74%

3ac, n = 4, 42%
**3ad**, n = 6, 39%

3ae, 61%

3af, 25%
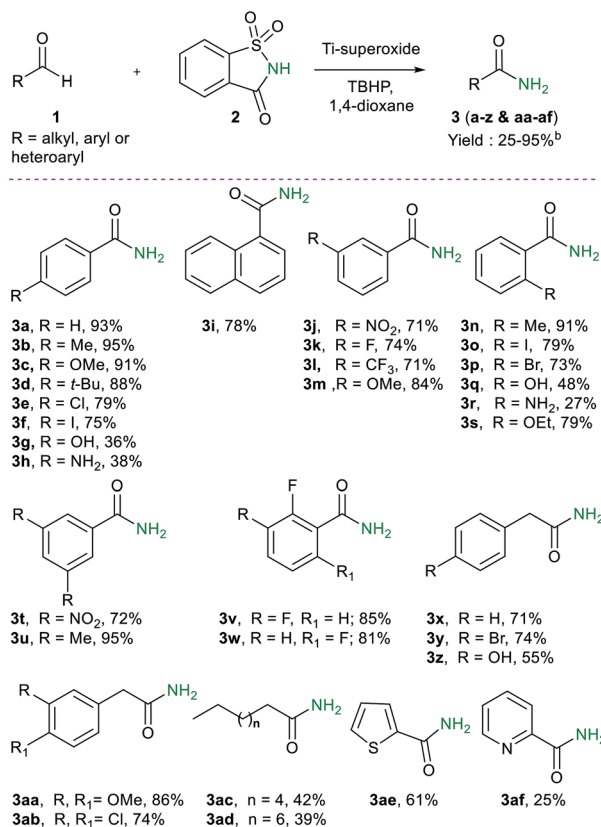
[a] Reaction conditions: aldehyde (1 mmol), saccharin (1.2 mmol), 5–6 M TBHP in hexane (3 mmol), Ti-superoxide (20 wt%), 1,4-dioxane (4 mL), 90 °C, 1 h. [b] Isolated yield.

other amine sources such as ammonia or its salts (Cl$^-$, OAc$^-$ or NO$_3^-$) as well.

To determine the scope and limitations of this reaction, a wide range of aldehydes were reacted under the optimized reaction conditions (Table 2). In general, good to excellent yields of primary amides were obtained in most cases. For instance, aromatic aldehydes, bearing electron–donating and electron withdrawing groups in different ring positions, gave the desired products (**3a–w**) in good to excellent yields (27–95%), indicating that the reaction is not sensitive to electronic effects. Thus, various functional groups with potential synthetic applications are well-suited for this reaction, although substrates having sensitive NH$_2$ and OH groups gave a diminished yield (27–36%). Interestingly, phenyl acetaldehydes possessing a variety of substituents with different electronic effect (Br, OH, OMe and Cl) gave the desired primary amides (**3x–z** & **3aa-3ab**) in high yields (36–86%). Aliphatic (C$_8$- and C$_{10}$-), heteroaryl (2-thienyl and 2-pyridyl), and naphthyl aldehydes were tolerated as well, thus providing the desired amides (**3ae, 3af** & **3i**) in good yields (25–78%). Nevertheless, it should be noted that unsaturated aldehydes such as cinnamaldehyde and acrolein are less favoured substrates under the oxidative amidation condition.
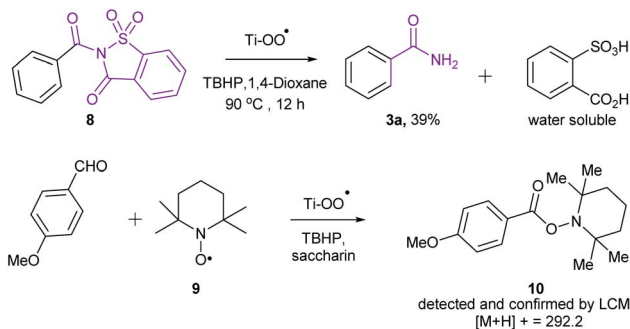
Scheme 2 Mechanistic studies to establish the involvement of radical pathway.
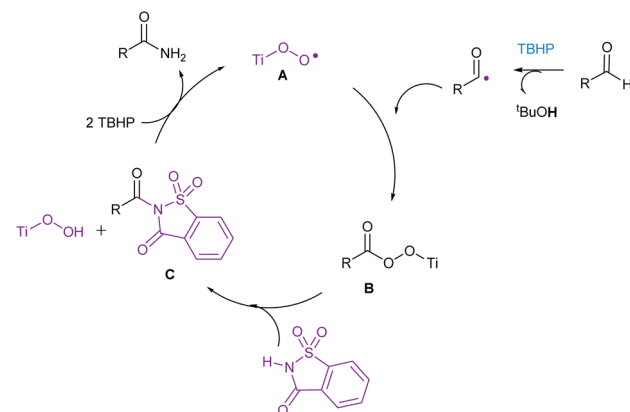
Scheme 3 Catalytic cycle for the oxidative amination of aldehydes.

In order to get an insight into the mechanism of this reaction, we have conducted the following two experiments (Scheme 2). When N-benzoyl saccharin **8** was subjected to the optimized reaction conditions, benzamide (**3a**) was indeed isolated in 39% yield, confirming the involvement of **8** as the key intermediate. Also, when oxidative amidation of anisaldehyde was carried out in the presence of radical scavenger TEMPO (1.1 equiv.), the corresponding TEMPO adduct **10** was detected and confirmed by LCMS, thus establishing the formation of benzoyl radical that underwent radical coupling in the reaction. On the basis of the above experiments and literature precedence,[11] a plausible catalytic cycle is proposed in Scheme 3. Initially, combination of acyl radical, generated from aldehyde on oxidation with TBHP, in the presence of Ti catalyst **A** produces Ti peroxo species **B**. Subsequently, **B** undergoes displacement with saccharin to produce N-acylsaccharin **C** along with TiOOH. Finally, 2 equiv. of TBHP are utilized: (i) to regenerate Ti catalyst **A**; (ii) to form amides from intermediate **C** via oxidative hydrolysis.
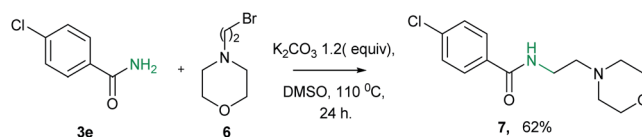
Scheme 4 Synthesis of moclobemide on 5 g scale.
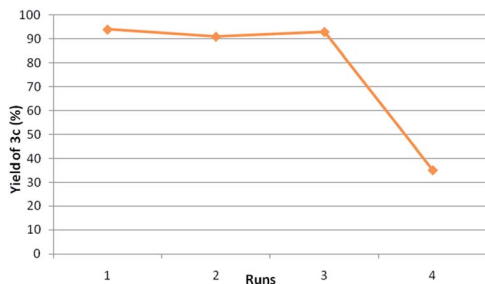
Fig. 2 Reusability studies of Ti catalyst. [a]Reaction conditions: ani-saldehyde (2 mmol), saccharin (2.4 mmol), TBHP (6 mmol), 1,4-dioxane, 90 °C, 1 h; [b]isolated yiled.

This methodology is amply demonstrated in the synthesis of drugs namely ethenzamide **3s** and moclobemide **7**. Scheme 4 shows the single step synthesis of moclobemide, a reversible inhibitor of monoamine oxidase **A** via N-alkylation of **3e** with **6**.

Fig. 2 shows the results on reusability studies. Ti-superoxide catalyst was readily recovered quantitatively by simple filtration and reused again at least for 3 cycles without the loss of catalytic activity (runs 1–3). The catalyst performed under truly hetero-geneous manner as no leaching of Ti was observed in the aqueous part.

Conclusions

In conclusion, we have described here a simple, convenient and environment-friendly protocol for primary amide synthesis directly from aldehydes using Ti-superoxide as a mild and cheap catalyst and saccharin as amine source using TBHP as oxidant. The presented strategy has several advantages that include: (i) Ti catalyst is recyclable; (ii) good functional group compatibility; (iii) wide range of substrate scope; (iv) mild reaction conditions; (v) no additives and can be easily scaled up; (vi) saccharin as cheaply available amine source. We envisage that this new catalytic method would be used as an alternative to other existing methods for the primary amide synthesis.

Conflicts of interest

There are no conflicts to declare.

Acknowledgements

Notes and references

1 (a) R. Fu, Y. Yang, J. Zhang, J. Shao, X. Xia, Y. Ma and R. Yuan, *Org. Biomol. Chem.*, 2016, **14**, 1784; (b) J. W. Bode, *Curr. Opin. Drug Discovery Dev.*, 2006, **9**, 765; (c) T. Cupido, J. Tulla-Puche, J. Spengler and F. Albericio, *Curr. Opin. Drug Discovery Dev.*, 2007, **10**, 768; (d) X. Zhang, W. T. Teo and P. W. H. Chan, *J. Organomet. Chem.*, 2011, **696**, 331; (e) C. L. Allen and J. M. J. Williams, *Chem. Soc. Rev.*, 2011, **40**, 3405; (f) J. M. Humphrey and A. R. Chamberlin, *Chem. Rev.*, 1997, **97**, 2243; (g) H. P. Zhao, G. C. Liang, S. M. Nie, X. Lu, C. X. Pan, X. X. Zhong, G. F. Su and D. L. Mo, *Green Chem.*, 2020, DOI: 10.1039/C9GC03345A; (h) J. Y. Liao, Q. Y. Wu, X. Lu, N. Zou, C. X. Pan, C. Liang, G. F. Su and D. L. Mo, *Green Chem.*, 2019, **21**, 6567–6573; (i) T. S. Zhang, H. Zhang, R. Fu, J. Wang, W. J. Hao, S. J. Tu and B. Jiang, *Chem. Commun.*, 2019, **55**, 13231–13234; (j) Z. Wang, C. Hou, Y. F. Zhong, Y. X. Lu, Z. Y. Mo, Y. M. Pan and H. T. Tang, *Org. Lett.*, 2019, **21**, 9841–9845.

2 (a) F. Xu, Y.-Y. Song, Y.-J. Li, E.-L. Li, X.-R. Wang, W.-Y. Li and C.-S. Liu, *ChemistrySelect*, 2018, **3**, 3474; (b) J. S. Carey, D. Laffan, C. Thomson and M. T. Williams, *Org. Biomol. Chem.*, 2006, **4**, 2337; (c) B. L. Bray, *Nat. Rev. Drug Discovery*, 2003, **2**, 587; (d) C. L. Allen, B. N. Atkinson and J. M. J. Williams, *Angew. Chem., Int. Ed.*, 2012, **51**, 1383; (e) P. S. Dragowich, T. J. Prins, R. Zhou, T. O. Johnson, F. L. Brown, F. C. Maldonado, S. A. Fuhrman, L. S. Zalman, A. K. Patick, D. A. Mettews, X. Hou, J. W. Meador, R. A. Ferre and S. T. Worland, *Bioorg. Med. Chem. Lett.*, 2002, **12**, 733; (f) S. H. Reich, T. Johnson, M. B. Wallace, S. E. Kephart, S. A. Fuhrman, S. T. Worland, D. A. Matthews, T. F. Hendrickson, F. Chan, J. Meador, R. A. Ferre, E. L. Brown, D. M. Delisle, A. K. Patick, S. L. Binford and C. E. Ford, *J. Med. Chem.*, 2000, **43**, 1670; (g) B. Narayana, K. K. Vijay Raj, B. V. Ashalatha, N. S. Kumari and B. K. Sarojini, *Eur. J. Med. Chem.*, 2004, **39**, 867.

3 (a) H. Lundberg, F. Tinnis, N. Selander and H. Adolfsson, *Chem. Soc. Rev.*, 2014, **43**, 2714; (b) G. G. Arzoumanidis and F. C. Rauch, *J. Org. Chem.*, 1981, **46**, 3930; (c) C. L. Allen and J. M. J. Williams, *Chem. Soc. Rev.*, 2011, **40**, 3405.

4 (a) Z.-P. A. Wang, C.-L. Tian and J.-S. Zheng, *RSC Adv.*, 2015, **5**, 107192; (b) P. Rajput and A. Sharma, *J. Pharm. Med. Chem.*, 2018, **2**, 22; (c) H.-L. Lee and J. Aubé, *Tetrahedron*, 2007, **63**, 9007; (d) C.-W. Kuo, M.-T. Hsieh, S. Gao, Y.-M. Shao, C.-F. Yao and K.-S. Shia, *Molecules*, 2012, **17**, 13662; (e) A. H. Blatt, *Chem. Rev.*, 1933, **12**, 215; (f) B. Gao, G. Zhang, X. Zhou and H. Huang, *Chem. Sci.*, 2018, **9**, 380; (g) G. Wang, Q.-Y. Yu, S.-Y. Chen and X.-Q. Yu, *Org. Biomol. Chem.*, 2014, **12**, 414; (h) M. Tamura, T. Tonomura, K.-i. Shimizu and A. Satsuma, *Green Chem.*, 2012, **14**, 717–724.

5 (a) H. Fujiwara, Y. Ogasawara, K. Yamaguchi and N. Mizuno, *Angew. Chem., Int. Ed.*, 2007, **46**, 5202; (b) N. S. Thirukovela, R. Balaboina, S. Kankala, R. Vadde and C. S. Vasam, *Tetrahedron*, 2019, **75**, 2637; (c) S. C. Ghosh, J. S. Y. Ngiam, A. M. Seayad, D. T. Tuan, C. L. L. Chai and A. Chen, *J. Org. Chem.*, 2012, **77**, 18; (d) R. Fu, Y. Yang, J. Zhang, J. Shao, X. Xia, Y. Ma and R. Yuan, *Org. Biomol. Chem.*, 2016, **14**, 1784; (e) W.-J. Yoo and C.-J. Li, *J. Am. Chem. Soc.*, 2006, **128**(40), 13064; (f) K. R. Reddy, C. U. Maheswari, M. Venkateshwar and M. L. Kantam, *Eur. J. Org. Chem.*, 2008, 3619; (g) K. S. Goh and C.-H. Tan, *RSC Adv.*, 2012, **2**, 5536; (h) D. Xu, L. Shi, D. Ge, X. Cao and H. Gu, *Sci. China: Chem.*, 2016, **59**, 478; (i) J. Liang, J. Lv and Z.-C. Shang,

Tetrahedron, 2011, **67**, 8532; (*j*) Z. Wu and K. L. Hull, *Chem. Sci.*, 2016, **7**, 969; (*k*) S. Debbarma and M. S. Maji, *Eur. J. Org. Chem.*, 2017, 3699; (*l*) J.-P. Wan and Y. Jing, *Beilstein J. Org. Chem.*, 2015, **11**, 2209.

6 (*a*) X. Liu and K. F. Jensen, *Green Chem.*, 2012, **14**, 1471; (*b*) W.-J. Yoo and C.-J. Li, *J. Am. Chem. Soc.*, 2006, **128**, 13064.

7 (*a*) D. Leow, *Org. Lett.*, 2014, **16**, 5812; (*b*) H. Inagawa, S. Uchida, E. Yamaguchi and A. Itoh, *Asian J. Org. Chem.*, 2019, **8**, 1411; (*c*) F. K. -C. Leung, J. -F. Cui, T. -W. Hui, K. K. -Y. Kung and M. -K. Wong, *Asian J. Org. Chem.*, 2015, **4**, 533.

8 (*a*) Y. Wang, K. Yamaguchi and N. Mizuno, *Angew. Chem., Int. Ed.*, 2012, **51**, 7250; (*b*) Z. Zhao, T. Wang, L. Yuan, X. Hu, F. Xiong and J. Zhao, *Adv. Synth. Catal.*, 2015, **357**, 2566; (*c*) D. D. Subhedar, S. S. R. Gupta and B. M. Bhanage, *Catal. Lett.*, 2018, **148**, 3102; (*d*) J. W. Comerford, J. H. Clark, D. J. Macquarrie and S. W. Breeden, *Chem. Commun.*, 2009, 2562.

9 (*a*) S. Ramezanpour, Z. Bigdelia, N. S. Alavijeha and F. Rominger, *Synlett*, 2017, **28**, 1214; (*b*) F. Mohamadpour, M. T. Maghsoodlou and R. H. M. Lashkari, *J. Iran. Chem. Soc.*, 2016, **13**(8), 1549; (*c*) A. W. Naser and A. F. Abdullah, *J. Chem. Pharm. Res.*, 2014, **6**, 872.

10 (*a*) S. Dey, S. K. Gadakh and A. Sudalai, *Org. Biomol. Chem.*, 2015, **13**, 10631; (*b*) R. S. Reddy, T. M. Shaikh, V. Rawat, P. U. Karabal, G. Dewkar, G. Suryavanshi and A. Sudalai, *Catal. Surv. Asia*, 2010, **14**, 21; (*c*) G. K. Dewkar, M. D. Nikalje, I. S. Ali, A. S. Paraskar, H. S. Jagtap and A. Sudalai, *Angew. Chem., Int. Ed.*, 2001, **40**(2), 405; (*d*) T. M. Shaikh, P. U. Karbhal, G. M. Suryavanshi and A. Sudalai, *Tetrahedron Lett.*, 2009, **50**, 2815.

11 (*a*) J. Wang, C. Liu, J. Yuana and A. Lei, *Chem. Commun.*, 2014, **50**, 4736; (*b*) M. Adib, R. Pashazadeh, S. R. Daryasarei, P. Mirzaei and S. J. A. Gohari, *Tetrahedron Lett.*, 2016, **57**, 3071.

Short enantioselective total synthesis of (+)-tofacitinib

Kishor D. Mane [a,b], Rohit B. Kamble [a,b], Gurunath Suryavanshi [a,b,*]

[a] Chemical Engineering & Process Development Division, CSIR-National Chemical Laboratory, Dr. Homi Bhabha Road, Pune, Maharashtra 411008, India
[b] Academy of Scientific and Innovative Research, Ghaziabad 201 002, India

ARTICLE INFO

ABSTRACT

An enantioselective total synthesis of Tofacitinib (CP-690,550), a Janus tyrosine kinase (JAK3) specific inhibitor has been achieved from the readily available 4-piperidone. Proline catalysed hydroxylation is the key step for the synthesis of enantiopure 1-benzyl-4-methylpiperidin-3-ol.

© 2021 Elsevier Ltd. All rights reserved.

Introduction

Substituted piperidines are the most accessible structural motifs found among the biologically active *N*-heterocycles which occurred naturally as well as synthetically [1]. It has become the most reputed and impressive core structure as it is present in 72 small drug molecules having piperidine as active site [2]. Due to the impact of piperidines in pharmaceutical industry it has attracted the attention of chemists towards its synthesis [3]. The Janus protein tyrosine kinase also known as jakinibs, are a type of medication that act for inhibiting the movement of one or more of the Janus kinase family of enzymes (JAK1, JAK2 and JAK3) thereby interrupting with the JAK-STAT signalling pathway [4]. Hence it has become an important task to develop JAK inhibitors which will prevent such uncontrolled inflammation [5].

In recent studies, 3, 4-disubstituted piperidines has shown a promising candidate as JAK inhibitors [6a]. Whereas in 2012, tofacitinib (1) became the first JAK inhibitor drug approved by the Food and Drug Administration (FDA) for the treatment of rheumatoid arthritis, also in 2017 it was further approved for the treatment of active rheumatoid arthritis (RA) [6b], psoriatic arthritis [6c], and ulcerative colitis [6d].

It is a promising immunosuppressant, developed by Pfizer and approved for treatment during the organ transplant rejection [7]. Tofacitinib (CP-690,550) (1) with two chiral centers having the

substituted piperidines and amino deazapurine core as shown in Fig. 1. Also, it shows promising clinical activities against autoimmune related diseases such as psoriasis, inflammatory bowel disease and Crohn's disease [8].

Due to the increasing importance of tofacitinib in medicinal and pharmaceutical fields, several synthetic approaches have been well reported in the literature [9a]. Among the reported methods, asymmetric synthesis of tofacitinib is rarely explored [9b-d].

In 2013, Maricán et al. reported the preparation of key synthetic intermediate *tert*-butyl-(3*S*,4*R*)-3-hydroxy-4-methyl piperidine-1-carboxylate from (*S*)-5-hydroxypiperidin-2-one in 6 steps [10]. Preliminary the key steps of this route are selenoxide elimination, Grignard methyl cuprate addition, with an overall yield of 18%.

Initially, Ripin and co-workers from Pfizer has developed a synthetic route for the preparation of key intermediate **2** from 4-picoline, followed by late stage resolution to achieve the enantiomeric purity [11a]. In 2017, Uang et al. accomplished the formal asymmetric synthesis of tofacitinib via a stereoselective Michael addition of the corresponding enolate of chiral 1,3-dioxolanone to methyl crotonate. The enantioselectivity was introduced by using chiral auxiliary *i.e.* homochiral 1,3-dioxolanon synthesized from derivative of camphor sulfonic acid and glycolic acid [9d].

For the synthesis of enantiopure piperidine moiety above method requires late stage resolution techniques which results in the loss of yield. Furthermore, use of chiral auxiliary and harsh reaction conditions make the above approaches impractical. Hence, to overcome this limitation, we have developed an enantioselective synthesis of key intermediate **2a** with 18% overall yield and high enantiopurity of the **2a** was achieved by hydrolytic
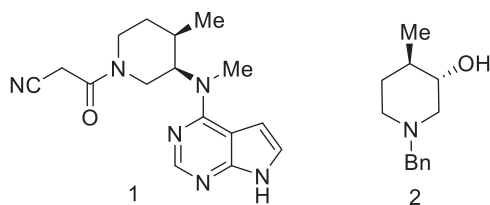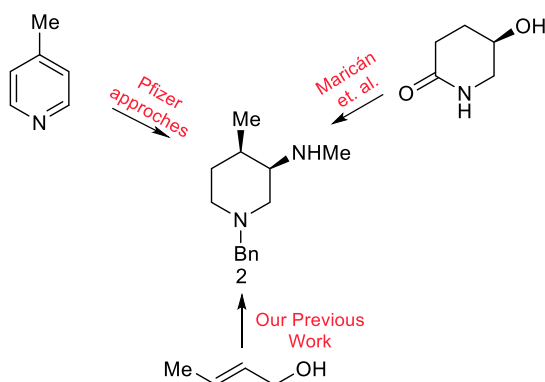
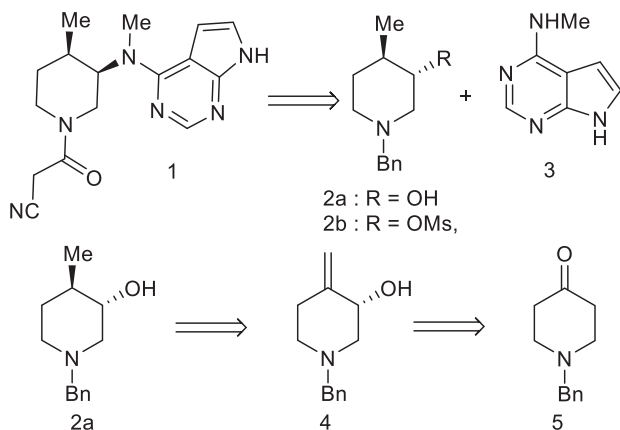**Fig. 1.** Structure of Tofacitinib and Key Intermediate.

Scheme 1. Various Routes for synthesis of intermediate 2 from pyridines.

kinetic resolution starting from crotyl alcohol as shown in Scheme 1 [12b].

The presence of enantiopure piperidine moiety as a core structure in tofacitinib and our continuous efforts towards the synthesis of these moieties [12], we have outlined a retro synthetic approach for the tofacitinib (**1**). As shown in Scheme 2, the synthesis of tofacitinib (**1**) could be accomplished from stereoselective inversion of 1-benzyl-4-methylpiperidin-3-yl methanesulfonate **2b** via nucleophilic substitution reaction with *N*-methyl dezapurine amine **3**. Further, the key intermediate **2a** can be synthesized from the *N*-protected piperidone **5** by using proline catalysed one pot α-aminoxylation and Wittig reaction, followed by reduction of allylic alcohol **4**.

Our approach towards the synthesis of key intermediate **2a** commences from *N*-benzyl protection of 4-piperidone **6** under basic condition using K$_2$CO$_3$, BnBr in H$_2$O and chloroform, gives *N*-benzyl protected 4-piperidone **5** in 87% yield [13]. The compound **5** was then subjected for direct proline-catalyzed asymmet-

ric α-aminoxylation reaction using ʟ-proline as organocatalyst and nitrosobenzene as aminoxylating source in DMF under N$_2$ atmosphere for 62 hrs, followed by one carbon Wittig reaction using methyl triphenylphosphonium iodide (CH$_3$PPh$_3$I) and *t*-BuOK as base in THF for 12 hrs which gives intermediate **7** as shown in Scheme 3.

After consumption of starting material, the *O*—*N* bond cleavage of intermediate **7** was achieved in situ by addition of CuSO$_4$·5H$_2$O in the reaction mixture and kept for another 12 h to give the corresponding chiral allylic alcohol **4** in 47% yield over three steps with 97% *ee* [14].

Furthermore, the formed allylic alcohol **4** was subjected for diastereoselective hydrogenation reaction using 1 atm pressure of hydrogen and 10% Pd on carbon to form the compound **2a** in
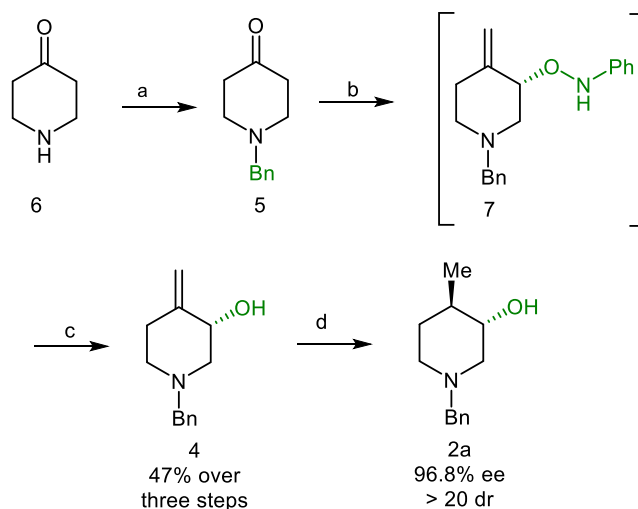
Scheme 3. Synthesis of Enantiopure Hydroxypiperidine via Proline Catalysed α-aminoxylation; Reaction Conditions: (a) BnBr, K$_2$CO$_3$, H$_2$O:CHCl$_3$ (1:1), 12 h, rt 87%; (b) (i) ʟ-proline, PhNO, DMF, 0 °C, 62 h; (ii) CH$_3$PPh$_3$I, *t*-BuOK, LiCl (1.1 eq.), THF, 50 °C; (c) CuSO$_4$·5H$_2$O (30 mol %), MeOH, 25 °C, 12 h; (d) 10% Pd/C, H$_2$ (1 atm), AcOEt, 5 h, rt, 93%.

Scheme 2. Retrosynthetic Analysis of Tofacitinib (CP-690,550).
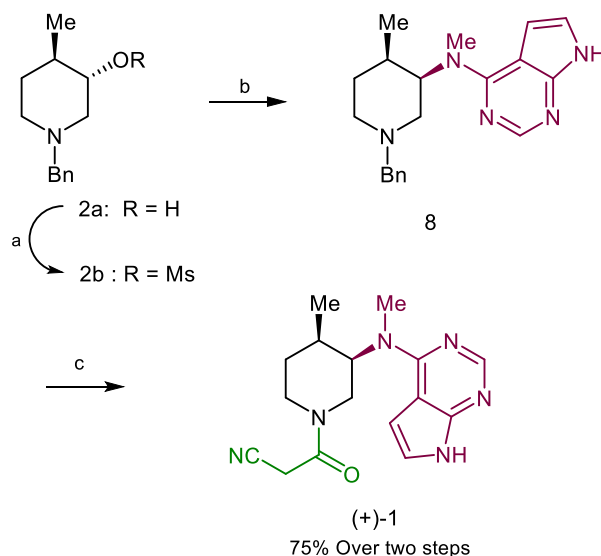
Scheme 4. Synthesis of (+)-Tofacitinib: (a) MsCl, TEA, DCM, 0 °C, 1 h, 97%; (b) **3**, K$_2$CO$_3$, DMF, 60 °C, 12 h, 81%; (c) 20 wt% Pd(OH)$_2$, H$_2$ (1 atm), TFA, MeOH, 45 °C 12 h then, ClCOCH$_2$CN, DCM, TEA, 0 °C to rt, 2 h.

93% yield with 96.8% *ee*. The formation of compound **2a** was confirmed by previous literature report and its optical rotation is in well agreement with the reported value. Then the enantiopure piperidine alcohol **2a** was utilized for the synthesis of tofacitinib as shown in the Scheme 4.

Further, the compound **2a** was utilized for mesylation reaction using MsCl and Et$_3$N, followed by base mediated S$_N$2 reaction with *N*-Methyl dezapurine **3** under basic condition to give compound **8** in 81% yield. Then *N*-benzyl deprotection of compound **8** was carried out under hydrogenation condition using 20 wt% Pd(OH)$_2$ and 1 atm H$_2$ pressure followed by in situ *N*-acylation using 2-cyanoacetyl chloride to give (+)-tofacitinib **(1)** in 75% yield over two steps. The formation of tofacitinib **(1)** was confirmed by ^{1}H, ^{13}C NMR and its values are in well agreement with previous reports [15].

In conclusion, the (+)-tofacitinib **(1)** was synthesized in 8 steps commenced from 4-piperidinone in 22.4% overall yield with 96.8% *ee*. The key steps involved are ʟ-proline catalyzed α-aminohydroxylation followed by Wittig olefination and hydrogenation reactions.

Declaration of interests

There are no conflicts to declare.

Declaration of Competing Interest

The authors declare that they have no known competing financial interests or personal relationships that could have appeared to influence the work reported in this paper.

Acknowledgments

Appendix A. Supplementary data

Supplementary data (experimental procedures, HRMS Data, ^{1}H and ^{13}C-NMR spectra of all synthesized compounds, HPLC Data.) to this article can be found online at https://doi.org/10.1016/j.tetlet.2021.152838.

References

[1] (a) P. Goel, O. Alam, M.J. Naim, F. Nawaz, M. Iqbal, M.I. Alam, Eur. J. Med. Chem. 157 (2018) 480–502;
(b) C. Oefner, A. Binggeli, V. Breu, D. Bur, J.-P. Clozel, A. D'Arcy, A. Dorn, W. Fischli, F. Grfininger, R. Gtillert, G. Hirth, H.P. Marki, S. Mathews, M. Miiller, R. G. Ridley, H. Stadler, E. Vieira, M. Wilhelm, F.K. Winkler, W. Wostl, Chem. Biol. 6 (1999) 127–131;
(c) R.D. Fabio, R. Giovannini, B. Bertani, M. Borriello, A. Bozzoli, D. Donati, A. Falchi, D. Ghirlanda, C.P. Leslie, A. Pecunioso, G. Rumboldt, S. Spada, Bioorg. Med. Chem. Lett. 16 (2006) 1749–1752.
[2] (a) E. Vitaku, D.T. Smith, J.T. Njardarson, J. Med. Chem. 57 (2014) 10257–10274;
(b) R.D. Taylor, M. MacCoss, A.D.G. Lawson, J. Med. Chem. 57 (2014) 5845–5859.
[3] (a) P.D. Bailey, P.A. Millwood, P.D. Smith, Chem. Commun. (1998) 633–640;
(b) J. Jiang, R.J. DeVita, G.A. Doss, M.T. Goulet, M.J. Wyvratt, J. Am. Chem. Soc. 121 (1999) 593–594.
[4] M.H. Kaplan, STAT signaling in inflammation, JAKSTAT 2 (2013) 24198.
[5] (a) H.L. Lightfoot, F.W. Goldberg, J. Sedelmeier, ACS Med. Chem. Lett. 10 (2019) 153–160;
(b) J.D. Clark, M.E. Flanagan, J.-B. Telliez, J. Med. Chem. 57 (2014) 5023–5038;
(c) D.M. Schwartz, Y. Kanno, A. Villarino, M. Ward, M. Gadina, J.J. O'Shea, Nat. Rev. Drug. Discov. 16 (2017) 843–862.
[6] (a) A. Thorarensen, M.E. Dowty, M.E. Banker, B. Juba, J. Jussif, T. Lin, F. Vincent, R.M. Czerwinski, A. Casimiro-Garcia, R. Unwalla, J.I. Trujillo, S. Liang, P. Balbo, Y. Che, A.M. Gilbert, M.F. Brown, M. Hayward, J. Montgomery, L. Leung, X. Yang, S. Soucy, M. Hegen, J. Coe, J. Langille, F. Vajdos, J. Chrencik, J.B. Telliez, J. Med. Chem. 60 (2017) 1971–1993;
(b) L. Vijayakrishnan, R. Venkataramana, P. Gulati, Trends Pharmacol. Sci. 32 (2011) 25–34;
(c) M.M. Seavey, P.B. Dobrzanski, Biochem. Pharmacol. 83 (2012) 1136–1145;
(d) J.D. Clark, M.E. Flanagan, J.-B. Telliez, J. Med. Chem. 57 (2014) 5023–5038.
[7] P.S. Changelian, M.E. Flanagan, D.J. Ball, C.R. Kent, K.S. Magnuson, W.H. Martin, B.J. Rizzuti, P.S. Sawyer, B.D. Perry, W.H. Brissette, S.P. McCurdy, E.M. Kudlacz, M.J. Conklyn, E.A. Elliott, E.R. Koslov, M.B. Fisher, T.J. Strelevitz, K. Yoon, D.A. Whipple, J. Sun, M.J. Munchhof, J.L. Doty, J.M. Casavant, T.A. Blumenkopf, M. Hines, M.F. Brown, et al., Science 302 (2003) 875–878.
[8] (a) S. Dhillon, Drugs. 77 (2017) 1987–2001;
(b) A. Berekmeri, F. Mahmood, M. Wittmann, P. Helliwell, Expert Rev. Clin. Immunol. 14 (2018) 719–730;
(c) A. Fernandez-Clotet, J. Castro-Poceiro, J. Panes, Expert Rev. Clin. Immunol. 14 (2018) 881;
(d) M.S. Zand, Transplant. Rev. (Copenhagen, Den.) 27 (2013) 85–89;
(e) L.C.S. De Vries, M.E. Wildenberg, W.J. De Jonge, G.R. D'Haens, J. Crohn's Colitis. 11 (2017) 885–893.
[9] (a) L.C.R. Carvalho, A. Lourenço, L.M. Ferreira, P.S. Branco, J. Eur. Org. Chem. (2019) 615–624;
(b) A. Maricán, M.J. Simirgiotis, L.S. Santos, Tetrahedron Lett. 54 (2013) 5096–5098;
(c) B.-Y. Hao, J.-Q. Liu, W.-H. Zhang, X.-Z. Chen, Synthesis 8 (2011) 1208–1212;
(d) H.C. Liao, B.J. Uang, Tetrahedron: Asymmetry 28 (2017) 105–109.
[10] A. Maricán, M.J. Simirgiotis, L.S. Santos, Tetrahedron Lett. 54 (2013) 5096–5098.
[11] D.H.B. Ripin, S. Abele, W. Cai, T. Blumenkopf, J.M. Casavant, J.L. Doty, M. Flanagan, C. Koecher, K.W. Laue, K. Mccarthy, C. Meltz, M. Munchhoff, K. Pouwer, B. Shah, J. Sun, J. Teixeira, T. Vries, D.A. Whipple, G. Wilcox, Org. Process Res. Dev. 7 (2003) 2169.
[12] (a) R.B. Kamble, S.H. Gadre, G.M. Suryavanshi, Tetrahedron Lett. 56 (2015) 1263–1265;
(b) R.B. Kamble, G.M. Suryavanshi, Synth. Commun. 48 (2018) 1045–1051.
[13] M.M.A.R. Moustafa, B.L. Pagenkopf, Org. Lett. 12 (2010) 3168–3171.
[14] (a) D.A. Devalankar, P.V. Chouthaiwale, A. Sudalai, Tetrahedron: Asymmetry 23 (2012) 240–244;
(b) Y. Hayashi, J. Yamaguchi, T. Sumiya, K. Hibino, M. Shoji, J. Org. Chem. 69 (2004) 5966–5973.
[15] J-k Jiang, K. Ghoreschi, F. Deflorian, Z. Chen, M. Perreira, M. Pesu, J. Smith, E. Liu, W. Leister, S. Costanzic, J.J. O'Shea, C.J. Thomas, J. Med. Chem. 51 (2008) 8012–8018.

Article

Acetic Acid-Catalyzed Regioselective C(sp²)−H Bond Functionalization of Indolizines: Concomitant Involvement of Synthetic and Theoretical Studies

Kishor D. Mane, Anirban Mukherjee, Gourab Kanti Das, and Gurunath Suryavanshi*
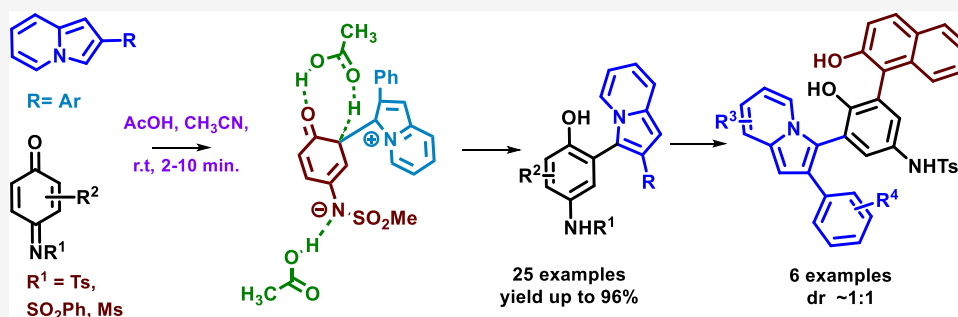
Read Online

ACCESS | 📊 Metrics & More | 📰 Article Recommendations | 🆘 Supporting Information

ABSTRACT: An atom economical and environmentally benign protocol has been developed for the regioselective C(sp²)−H bond functionalization of indolizines. The acetic acid-catalyzed cross-coupling reaction proceeds under metal-free conditions, producing a wide range of synthetically useful indolizine derivatives. The present protocol showed good functional group tolerance and broad substrate scope in good to excellent yields. Quantum mechanical investigation using density functional theory (DFT) has played a crucial role in understanding that acetic acid is the key player in determining the actual pathway as the catalyst and its ultrafast nature. Different pathways involving inter- and intramolecular proton transfer, with or without acetic acid, were investigated. Calculated results revealed that a proton shuttle mechanism is involved for the least energetic, most favorable acetic acid-catalyzed pathway. Furthermore, regioselectivity has also been explained theoretically.

■ INTRODUCTION

N-heterocyclic compounds are found ubiquitously in many natural products and the core structure of active pharmaceutical ingredients. The indolizines are one of the most important fused *N*-heterocyclic compounds isolated from different plants and fungal sources[1] and, furthermore, these compounds have been drawn into the spotlight due to their unique physical and pharmacological properties. Natural and synthetic indolizine alkaloids are extensively used in structure−activity relationship (SAR) studies. In this study, various biological activities of indolizine derivatives are reported, including anticancer, antibiotic, antitubercular, antioxidant, antimicrobial, anti-inflammatory, and antimycobacterial properties (Figure 1).[2,3] The fluorescent indolizine derivatives are effectively used in Alzheimer's disease (a neurodegenerative disorder) to detect accumulated amyloid-β (Aβ) peptide monomers, dimers, and plaques in the brain of the 5XFAD Alzheimer transgenic mouse model.[4] To determine the mode of action of the antiangiogenic drug, a fluorescent indolizine core derivative was used to prepare a drug−biotin conjugate.[5] Additionally, substituted indolizine derivatives exhibit fluorescence properties that make them ideal candidates in dye-sensitized solar cells as organic sensitizers,[6] FRET fluorescence sensors for

detecting Hg²⁺ and Cu²⁺ in the living cell,[7] pH fluorescent probe for imaging living cells,[8] and fluorescent blue-emitting indolizines for organic light-emitting devices.[9] Indolizine β-cyclodextrin compounds are used as molecular chemosensors for detecting volatile organic compounds and biological markers.[10]

The unique physical and pharmacological properties of indolizine derivatives were able to draw attention among research groups. A variety of strategies have been reported for the synthesis[11] and functionalization of indolizines,[12] and among these reactions, metal-free and visible light-mediated reactions are particularly effective in providing a new set of indolizines.[13] Quinone monoimines show excellent electrophilic properties and are effectively used with various
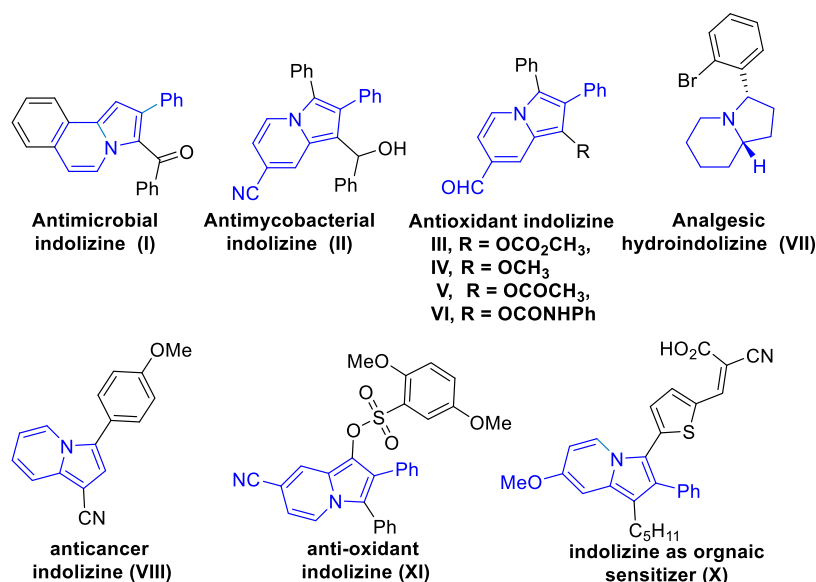
Figure 1. Fluorescent and biologically active indolizines.

Scheme 1. Different Approaches on C−H Functionalization of Indolizines
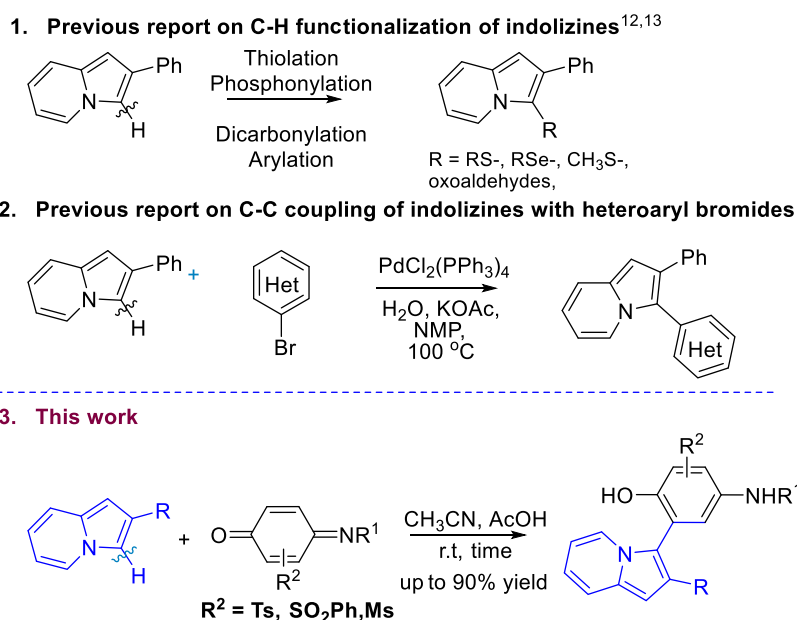
nucleophiles such as indoles,[17] naphthols,[17b,c] and napthyla-mines.[17d]

In 2004, Gevorgyan and co-workers developed C−H functionalization of heteroaryl such as indolizines with heteroaryl bromides using a palladium catalyst, and it provided a wide range of biheteroaryl structural motifs in excellent yields (Scheme 1).[13e] To the best of our knowledge, there are very few reports present so far for the metal-free C−H functionalization of indolizines.[14] Continuing our research efforts on developing efficient and straightforward methods,[15] we have developed a metal-free, regioselective C−H functionalization of indolizines using a catalytic amount of acetic acid.

As the reaction involves only two starting materials and solvent while investigating the reaction pathway theoretically, our initial assumption was that a simple nucleophilic attack of indolizine to the electrophilic monoimine might take place, followed by the intramolecular four or five-membered proton abstractions. Based on prior research,[16] upon calculating the energetics against our initial hypothesis using DFT, it was observed that the activation barriers for different transition states did not fit with the reaction conditions. Hence, this hypothesis will not stand. At this point, the complexity arises and we started connecting the missing dots; it came out of the discussion that the monoimine we were using is the crude mixture for which we did not do the column. For the synthesis of the quinone monoimine, (diacetoxyiodo)benzene (PIDA) was used and we obtained acetic acid as a byproduct in the system, which can also be easily recognized by its smell. Since we were using the crude monoimine with acetic acid for the reported reaction, the presence of acetic acid might cause the reaction to occur very fast, our next assumption. Based on this hypothesis, we again performed DFT quantum mechanical studies that showed the energetics to fit finely with the reaction

Table 1. Reaction Optimization[a]
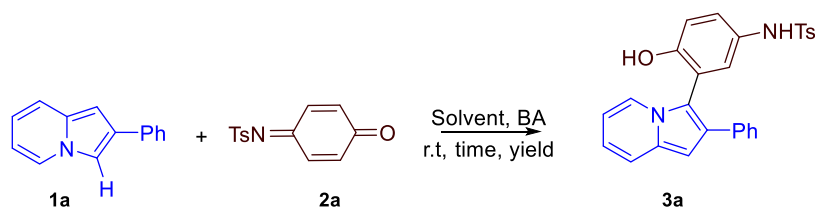
entry	additive	solvent	time	yield (%)
1		CH$_3$CN	12 h	trace
2	HCl	CH$_3$CN	12 h	trace
3	AcOH (10 mol %)	CH$_3$CN	12 h	88
4	AcOH (20 mol %)	CH$_3$CN	12 h	87
5	AcOH (50 mol %)	CH$_3$CN	12 h	74
6	AcOH (100 mol %)	CH$_3$CN	12 h	69
7	AcOH (20 mol %)	CH$_3$CN	1 h	88
8	AcOH (20 mol %)	CH$_3$CN	20 min	89
9	AcOH (20 mol %)	CH$_3$CN	10 min	92
10	**AcOH (20 mol %)**	**CH$_3$CN**	**2 min**	**92**
11	AcOH (20 mol %)	DCE	10 min	71
12	AcOH (20 mol %)	THF	10 min	78
13	AcOH (20 mol %)	DCM	10 min	81
14	AcOH (20 mol %)	CH$_3$CN	10 min	55[b]

[a]Reaction conditions: **1a** (1 equiv), **2a** (1 equiv), AcOH (20 mol %), CH$_3$CN, rt, 2 min. [b]Reaction carried out at 0 °C.

conditions, which have a global activation barrier of only 17.67 kcal mol^{-1}. With these computational results in our hands, we now started looking into the synthetic evidence and support. We removed acetic acid impurity present in the starting material. The purified quinone monoimine was subjected to optimized reaction conditions, but the yield of the product reduced drastically. This is the first and direct support of our hypothesis and theory. The yield was significantly increased by the addition of one drop of acetic acid externally into the reaction mixture. Hence, we have shown a delicate control over synthesis and computation: a computation-driven synthesis and a synthesis-driven computation. We were now interested in finding the origin of regioselectivity, which upon investigation showed that the transition state for the nucleophilic attack from the C-3 position is 5.68 kcal mol^{-1} more stabilized than from the C-1 position of indolizine. Three different gauche conformations have been studied to identify the most stable transition state for the nucleophilic attack.
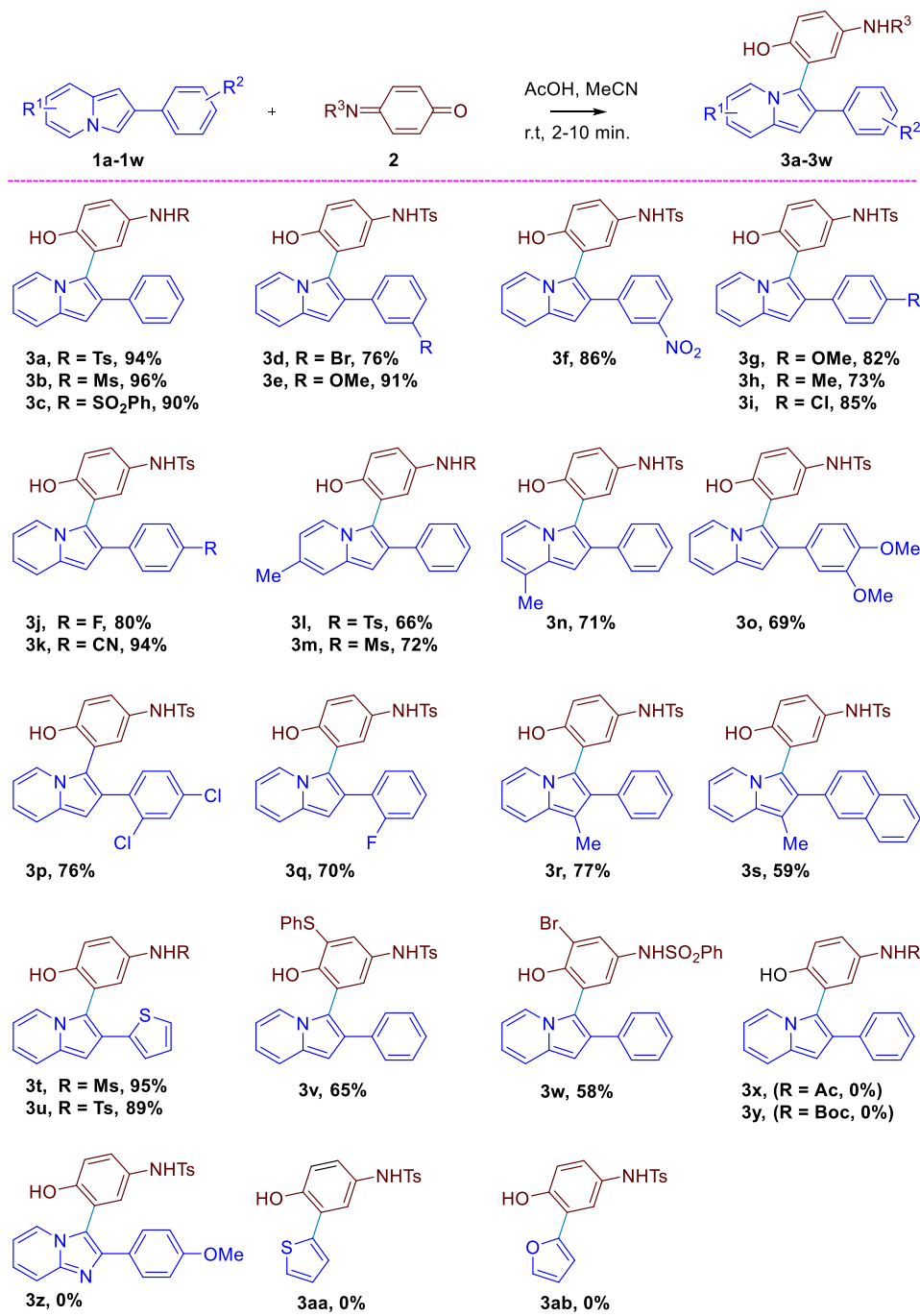
RESULTS AND DISCUSSION

As an initial investigation, indolizine (**1a**) and quinone monoimine (**2a**) were used as a model substrate for the optimization of reaction conditions (Table 1). First, the desired product C-3-functionalized indolizine **3a** was observed in a trace amount of isolated yield in the presence of HCl or without any additive at rt in 12 h (Table 1, entries 1 and 2). Furthermore, we found that the reaction works well in acetonitrile with a catalytic amount of acetic acid as an additive (Table 1, entry 3). With CH$_3$CN as a solvent, we investigated different concentrations of acetic acid and reaction times at room temperature, which resulted in comparative yields of the expected product (see Table 1, entries 3−6). Excellent yields were obtained even when reactions were conducted for a short period of time, beginning with 1 h, 20, 10, and 2 min (Table 1, entries 7−10). Furthermore, different solvents were screened to promote the reaction yields (Table 1, entries 11−13). Entries 11−13 demonstrate that the

reaction works well in all of the solvents but not better than acetonitrile. With lowering reaction temperature, the rate of the reaction slows down (Table 1, entry 14). Thus, we choose entry 10 as the most optimal reaction condition to form **3a**.

With optimized reaction conditions in hand (Table 1, entry 10), we investigated the scope of the reported reaction by screening a wide range of indolizine and quinone monoimine derivatives (Scheme 2). In the reaction of *N*-sulfonyl quinone monoimines with substituted indolizines containing electron-withdrawing, electron-donating, halo, and hetero substituents, coupled products (**3a−3w**) were obtained in good to excellent yields, as shown in Scheme 2. Using standard reaction conditions, *N*-tosyl-, mesyl-, and sulfonyl-protected quinone monoimines gave 90−96% yields for the expected products (**3a−3c**) upon reaction with indolizine. With ortho-, meta-, and para-substituted electron-donating groups on the phenyl rings of indolizines, we obtained the desired products (**3e, 3g, 3h, 3o**) in good yields (up to 91%). Halogen substitutions at ortho-, meta-, and para-positions on indolizines were also examined under optimized reaction conditions that gave the corresponding products (**3d, 3i, 3j, 3p, 3q**) with good to excellent yields.

In addition, electron-withdrawing substitution on indolizine offered the desired products (**3f, 3k**) in 86 and 94% yields, respectively. With substituents present at the C-1, C-6, and C-7 positions of indolizines, the reaction gave the coupled products (**3l-3n, 3r-3s**) with 59−77% yields. Furthermore, indolizines with heterocyclic rings are also capable of forming coupled products (**3t and 3u**) with comparable yields. The substituted quinone monoimines also gave moderate yields of the coupled products **3v** and **3w**. Unfortunately, *N*-acyl-protected quinone monoimine and various electron-rich heterocycles failed to give the expected products (**3x−3ab**).

Additionally, we investigated the effect of other quinone monoimine reactions with different indolizines, and the results are summarized in Schemes 3 and 4. For the quinone monoimine derivative (**5**), the standard reaction conditions

Scheme 2. Substrate Scope for C-3-Functionalized Indolizines with Quinone Monoimine Derivatives[a]

3a, R = Ts, 94%
3b, R = Ms, 96%
3c, R = SO$_2$Ph, 90%

3d, R = Br, 76%
3e, R = OMe, 91%

3f, 86%

3g, R = OMe, 82%
3h, R = Me, 73%
3i, R = Cl, 85%

3j, R = F, 80%
3k, R = CN, 94%

3l, R = Ts, 66%
3m, R = Ms, 72%

3n, 71%

3o, 69%

3p, 76%

3q, 70%

3r, 77%

3s, 59%

3t, R = Ms, 95%
3u, R = Ts, 89%

3v, 65%

3w, 58%

3x, (R = Ac, 0%)
3y, (R = Boc, 0%)

3z, 0%

3aa, 0%

3ab, 0%

[a]Reaction conditions: **1a** (1 equiv, 0.191 mmol), **2a** (1 equiv, 0.191 mmol), AcOH (20 mol %), CH$_3$CN, rt, 2−10 min.

were applied to produce a wide range of synthetically important molecules of axially chiral BINOLs with substituted indolizine cores.

As shown in Scheme 3, several indolizines with electron-donating, electron-withdrawing, and halo groups reacted well with quinone monoimine **5** under standard reaction conditions and provided corresponding products (**6a**−**6f**) in 57−74% yields. For the axially chiral BINOL products, four possible stereoisomers are possible. Since we have used a racemic starting material, a pair of diastereomers have formed, each of which exists as a racemic mixture.

We also synthesized symmetric indolizine **8** and one-pot synthesis **3a** from *N*-tosyl-*p*-aminophenol **9**, as shown in Scheme 4. Compound **3u** is oxidized to give quinonone monoimine derivative **7**, followed by the addition of heterocyclic indolizine **1u**, which yields symmetric indolizine **8** in 67% yield. Additionally, we successfully synthesized product **3a** directly from *N*-tosyl-*p*-aminophenol **9** in a one-pot reaction using PIDA with 61% yield. In a scale-up reaction of **1u** with quinone monoimine **2a**, 1.27 grams of compound **3u** was obtained with 90% yield.

Density Functional Theory (DFT) Studies. *Design of Reaction Pathways.* The selected model structures of quinone

Scheme 3. Synthesis of Indolizine-Functionalized BINOLs[a]
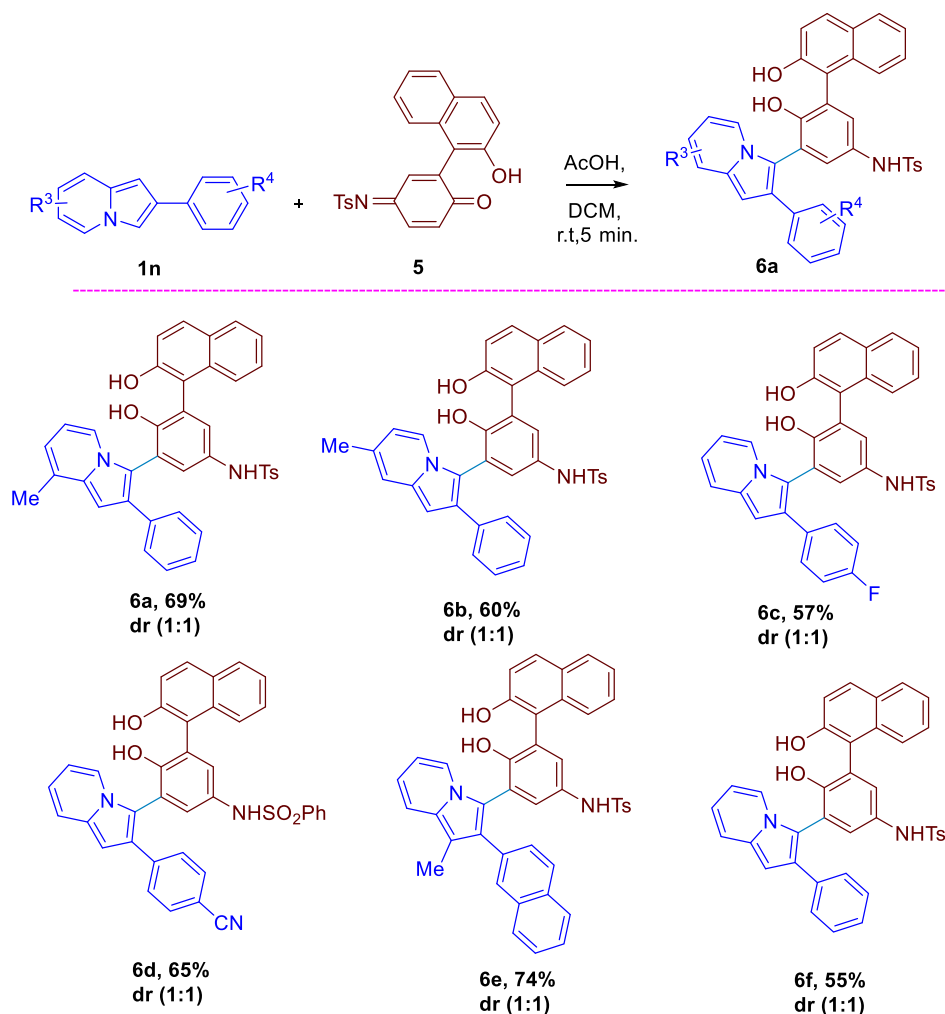
monoimine S_1 and indolizine S_2 in Figure 2 have been used to investigate the probable mechanistic pathways for the reaction. The investigated pathways are shown in Schemes 5, 6, and 7, respectively.

In pathway 1, the reaction proceeds *via* a [1, 4] proton transfer, whereas a [1, 3] proton abstraction mechanism is seen in pathway 2 (Scheme 5). Pathways 3, 4, 5, and 6 show an acetic acid-catalyzed proton shuttle mechanism (Scheme 6) as well as substrate activation (Scheme 7). The potential energy surface (PES) of the studied pathways are shown in Figure S1 (refer Supporting Information), 5, and 6, respectively. Stationary points for the minima have been designated using the letters "S", "I", and "P". "TS" is used for the saddle point. Subscript on the right- and left-hand sides, respectively, indicates the species number and the pathway it belongs. "F" in subscript represents "final," "Ac" represents "acetic acid-catalyzed pathway", and "PT" represents proton transfer.

Analysis of the Pathways. *Conformational Analysis for the Nucleophilic Attack.* Initially, the indolizine S_2 from its C-3 position makes the nucleophilic attack to the electrophilic monoimine S_1 through TS_1 to produce the intermediate I_1. We found that three different gauche conformations can be possible for TS_1, which are indicated as TS_{1a}, TS_{1b}, and TS_{1c}

in Figure 3. DFT quantum mechanical calculations revealed that the activation barriers for TS_{1a}, TS_{1b}, and TS_{1c} are 24.09, 20.54, and 17.67 kcal mol^{-1}, respectively. Hence, TS_{1c} is the most stable conformer for the nucleophilic attack.

Pathways 1 and 2. We suspect that two different ways of proton transfer could be possible after the nucleophilic attack (Scheme 5). In pathway 1, an intramolecular [1, 4] proton transfer is observed, which has an activation barrier of 27.5 kcal mol^{-1}, whereas a [1, 3] intramolecular proton transfer is associated with pathway 2. The TS for [1, 3] proton abstraction has an energy barrier of 71.48 kcal mol^{-1}. (Energy profile for pathways 1 and 2 are given in the Supporting Information; refer to Figure S1 in the Supporting Information.) Therefore, the observed energetics did not fit with the current reaction conditions. Hence, our initial hypothesis for the intramolecular proton abstraction pathways did not stand anymore.

Pathway 3. At this point, we again started understanding the system and found that acetic acid has an important role in making the reaction catalytic and very fast, which led us to pathway 3 (Scheme 6 and Figure 4). After the initial nucleophilic attack, intermediate I_1 is formed through TS_{1c} associated with an activation barrier of 17.67 kcal mol^{-1}. Here,

Scheme 4. Synthetic Utility and Scale-Up Experiment
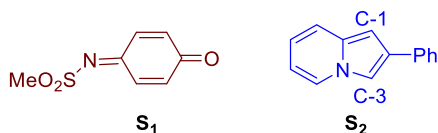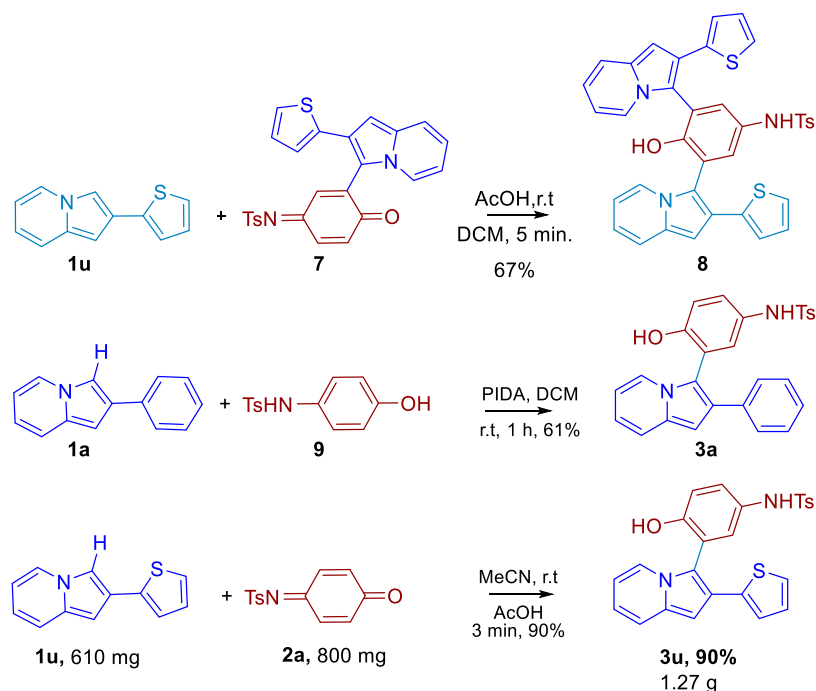
Figure 2. Structures of the model starting materials.

in this pathway 3, I_1 is getting far more stabilized than pathways 1 and 2 due to the acetic acid support in the system through hydrogen bonding ($_{Ac}I_2$). An eight-membered proton

shuttle mechanism was observed in the very next step by which an intermolecular proton abstraction from acetic acid to I_1 and from I_1 to acetic acid is occurring simultaneously through $_{Ac}TS_2$ to form $_{Ac}I_3$ and, therefore, we are getting acetic acid back (Scheme 6 and Figure 4). This step has an activation barrier of 10.48 kcal mol^{-1}. The intermediate $_{Ac}I_3$ forms $_{Ac}I_4$, followed by $_{Ac}I_5$ and acetate anion through $_{Ac}I_{PT}$. Finally, the aromatization occurs through a proton transfer from $_{Ac}I_3$ to acetate anion *via* $_{Ac}TS_3$, which has an activation barrier of 0.18 kcal mol^{-1} and, hence, we obtain the final product $_{Ac}P_F$ with

Scheme 5. Initial Hypothesis for the Probable Pathways
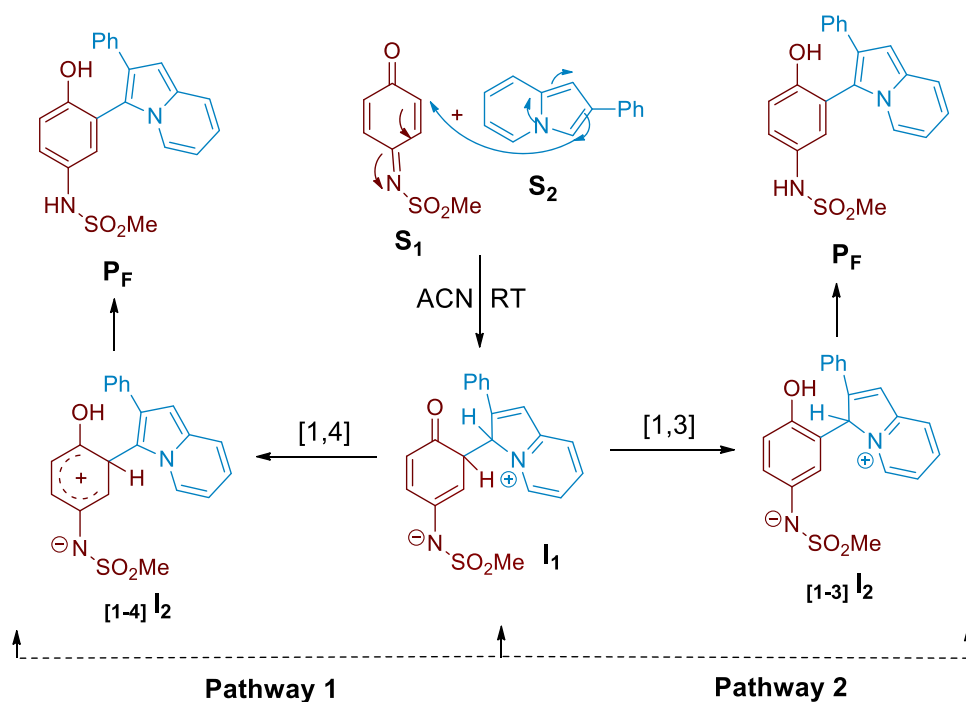
Scheme 6. Proposed Catalytic Cycle for the Acetic Acid-Catalyzed Pathway
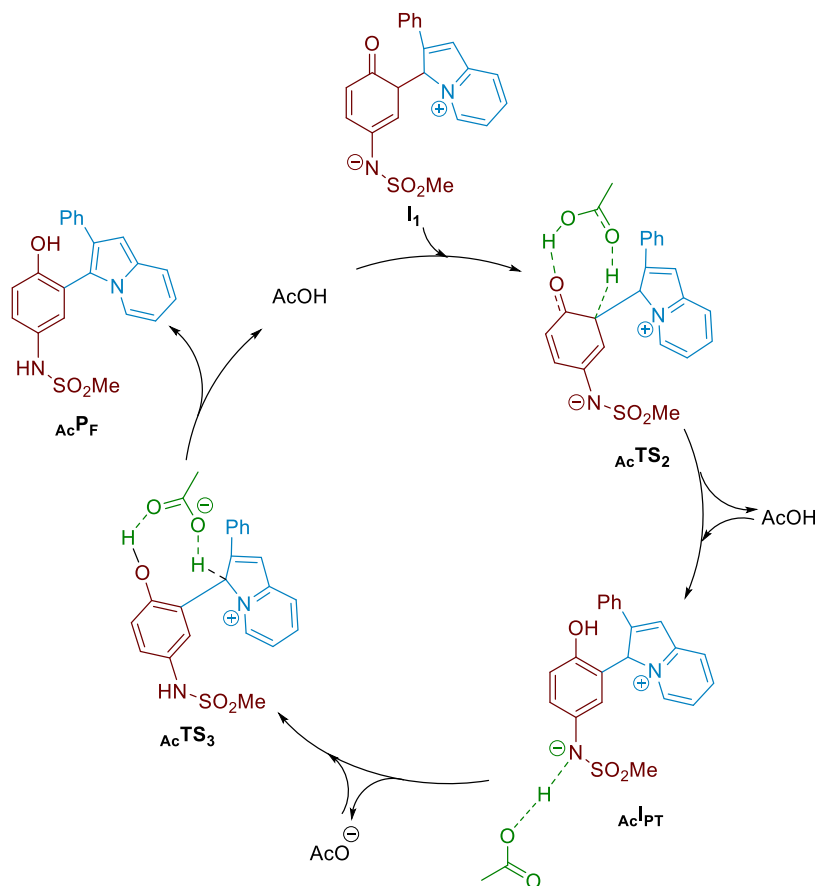
the recovery of the acetic acid, which is further used to perform the next catalytic cycle.

Hence, this pathway 3 is a direct support for the crucial role of acetic acid to make the reaction very fast and the energetics for pathway 3 now exactly fits with our current reaction conditions. However, as shown in Scheme 6 and in pathway 3, the acetic acid participates after the initial nucleophilic attack, and also, there are various negatively charged intermediates and TS in the mechanistic route. At this point, a few questions may arise, viz. why acetic acid is not taking part in the initial nucleophilic attack step by activating the reactant and also why the negatively charged intermediates and TS are not getting stabilized by the acetic acid in the catalytic cycle. Considering these facts, our further investigation led us to three different pathways (pathways 4, 5, and 6), as shown in Scheme 7 and Figure 5. Based on our conformational analysis, as shown in Figure 3, we chose the most stable conformer TS_{1c} to probe the effect of activation by acetic acid.

Pathway 4. In pathway 4, the quinone monoimine gets protonated ($_{Ac}S_{1b}$) for activation at the very first step. This protonation leads to a barrierless TS for the nucleophilic attack by indolizine S_2 to form the intermediate $_{Ac}I_{1b}$. The proton abstraction takes place by a proton shuttle mechanism through $_{Ac}TS_{2b}$ with an activation barrier of 13.57 kcal mol^{-1}. The intermediate $_{Ac}I_{2b}$ is further stabilized when one acetate molecule got inserted by replacing one molecule of acetic acid, forming the intermediate $_{Ac}I_{3b}$. Next, protonation occurs to give rise to the hydrogen-bonded aromatized intermediate $_{Ac}I_{4b}$ through $_{Ac}TS_{3b}$ having a −0.18 kcal mol^{-1} activation energy barrier. Finally, $_{Ac}P_F$ is formed.

Pathway 5. In pathway 5, the quinone monoimine S_1 initially gets activated by the acetic acid through hydrogen bonding ($_{Ac}S_{1a}$), which facilitates the nucleophilic attack by the indolizine S_2 through $_{Ac}TS_{1a}$ with an energy barrier of 8.48 kcal mol^{-1} forming the intermediate $_{Ac}I_{1a}$ that undergoes a proton shuttle mechanism through $_{Ac}TS_{2a}$, which has an activation barrier of 17.85 kcal mol^{-1}, to end up with intermediate $_{Ac}I_{2a}$. At this point, the nitrogen on the quinone monoimine moiety gets protonated by the acetic acid and forms the intermediate $_{Ac}I_{3b}$. Further proton abstraction to give the aromatized hydrogen-bonded intermediate $_{Ac}I_{4b}$ occurs through $_{Ac}TS_{3b}$ with an activation barrier of −0.18 kcal mol^{-1}. Finally, $_{Ac}P_F$ is formed.

Pathway 6. Pathway 6 also follows the common step up to intermediate $_{Ac}I_{2a}$. Then, instead of protonating the nitrogen (pathway 5), one acetic acid molecule goes out and one acetate molecule gets inserted to provide intermediate $_{Ac}I_{3a}$ that undergoes proton abstraction through $_{Ac}TS_{3a}$ by crossing an activation barrier of only 0.18 kcal mol^{-1}. Furthermore, the hydrogen-bonded negatively charged aromatized intermediate $_{Ac}I_{4a}$ gets protonated to provide the final product $_{Ac}P_F$ with initializing another catalytic cycle. Comparing all of the possible mechanistic pathways, it can be concluded from the energy profile that pathway 6 has the least energetic or most favorable geometries of intermediates and transition states. Therefore, pathway 6 is the most plausible investigated path for the reported reaction, which has a global free energy barrier of 19.73 kcal mol^{-1}.

Regioselectivity. The indolizine S_2 has two reactive sites for the nucleophilic attack. In our current reaction conditions, we

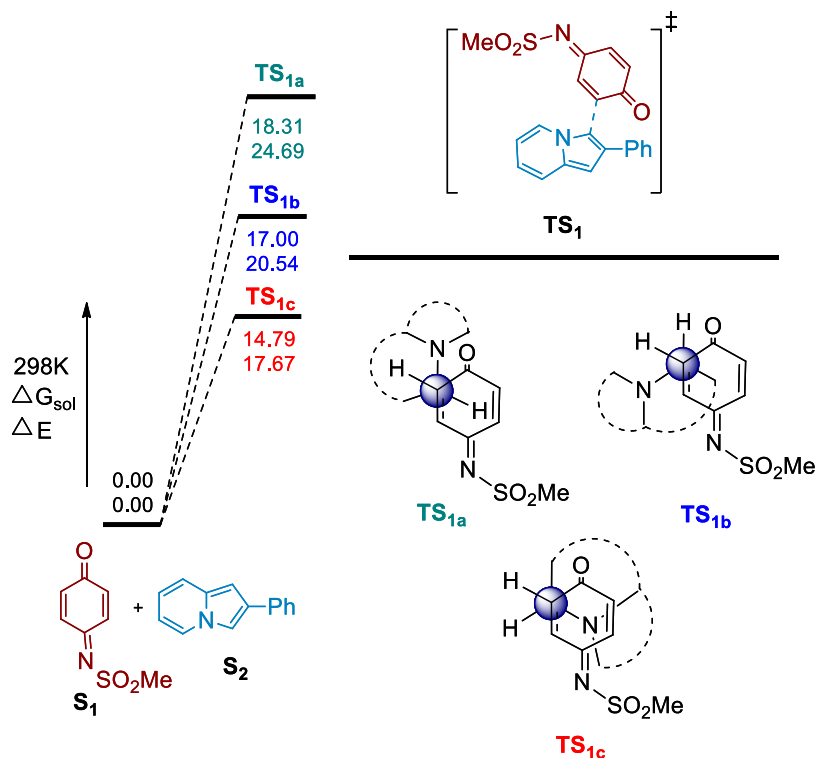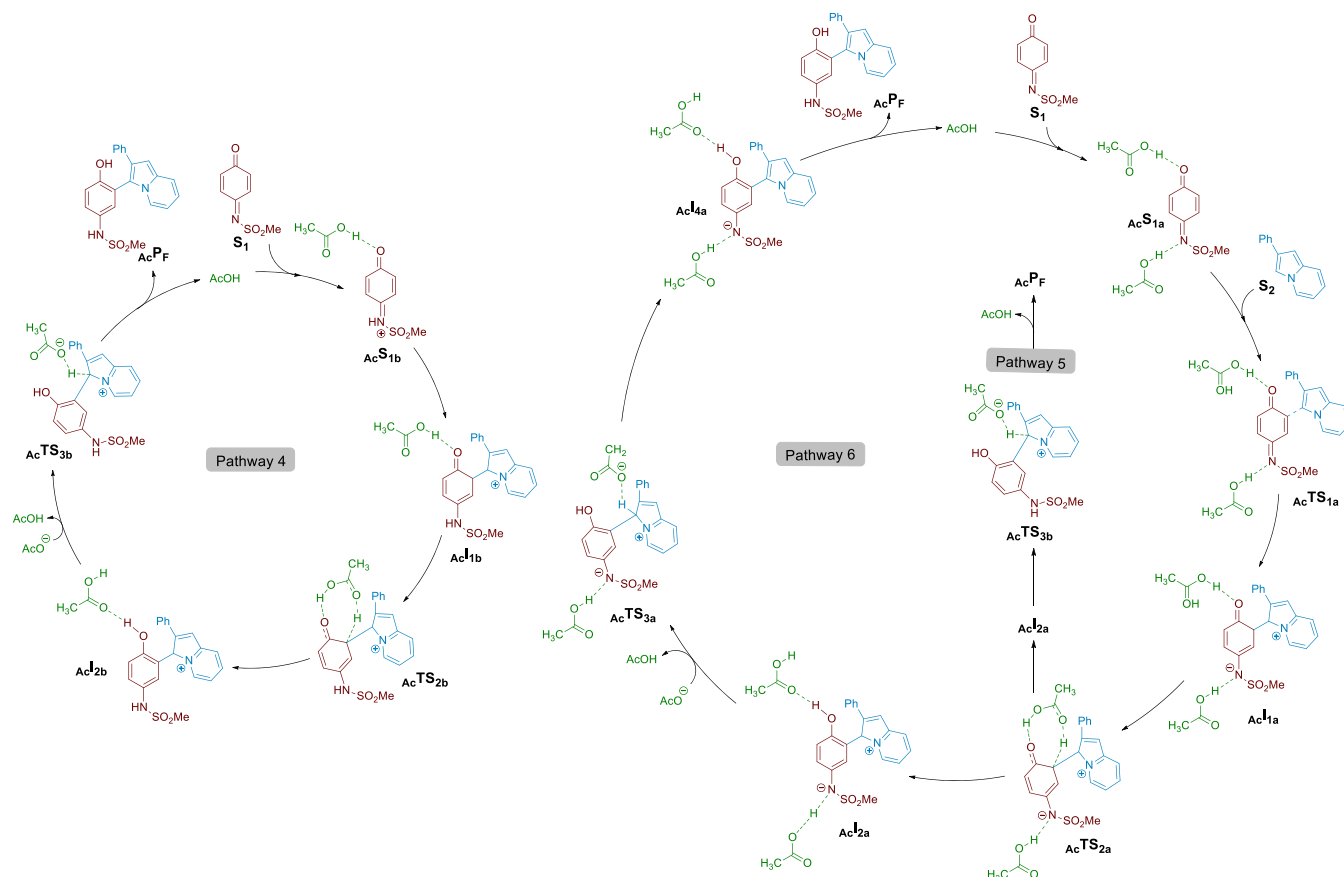## Scheme 7. Outline of Pathways 4, 5, and 6

Figure 3. Conformation analysis for the nucleophilic attack.

have shown a selective control for the functionalization of C-3 hydrogen over C-1 (Figure 2). To understand such

regioselectivity, we again performed DFT quantum mechanical calculations for determining the transition state involving the
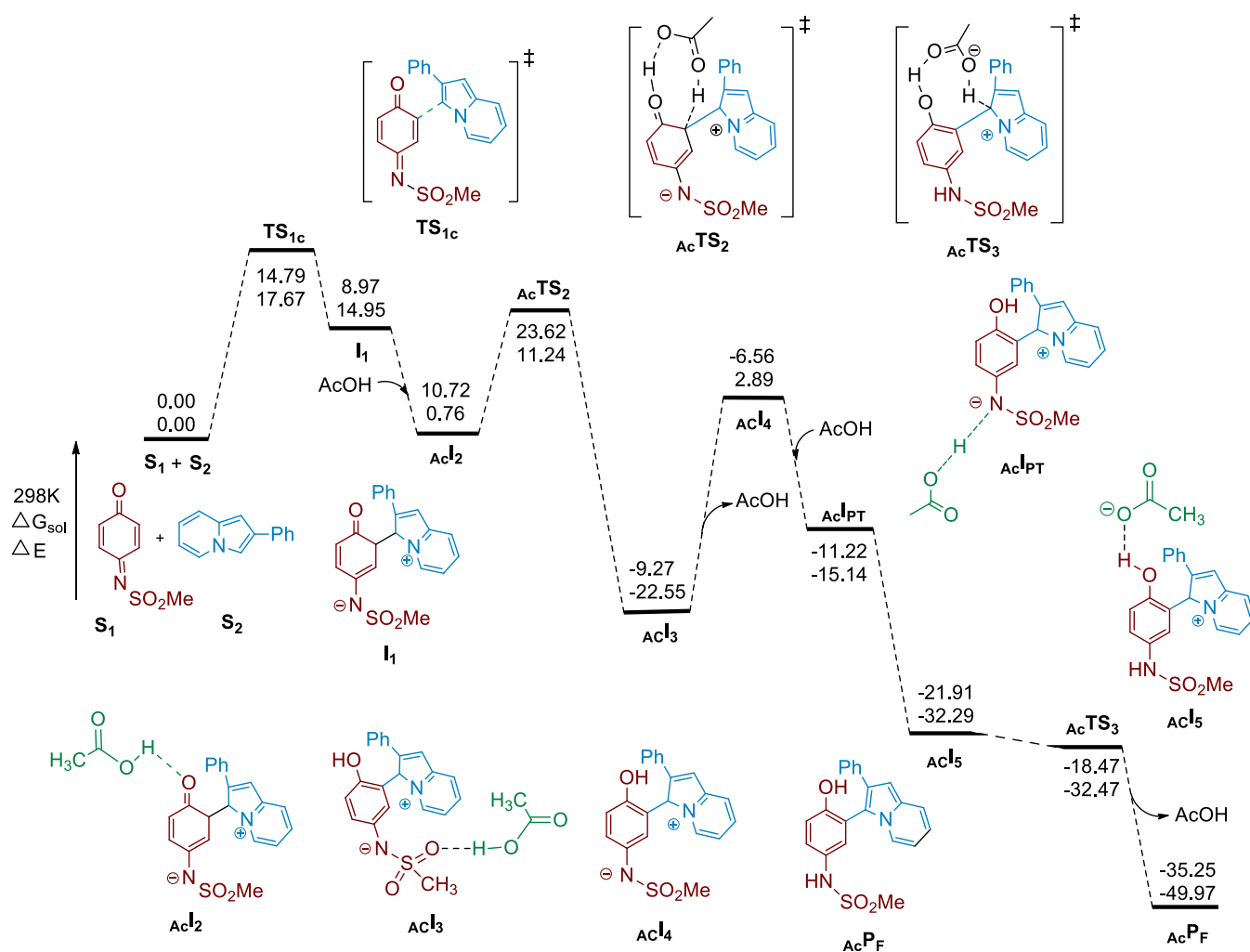
Figure 4. PES along with structures and thermodynamic parameters for pathway 3.

C-1 site of indolizine and compared the energetics between C-1 and C-3. It can be clearly seen from the energy profile in Figure 6 that after activating by acetic acid the quinone monoimine ($_{Ac}S_{1a}$) when comes into contact with the indolizine S_2, the drop of energy leading to the respective transition states is much more in the case of C-3 than C-1, which is due to the additional pi-stacking interaction between the molecules. Furthermore, the transition state involving the C-3 site is more stabilized by an amount of 3.91 kcal mol^{-1}. Finally, the thermodynamic stability of the intermediate ($_{C-3Ac}I_{1a}$) via C-3 TS is much higher than the intermediate ($_{C-1Ac}I_{1a}$) via C-1 TS. Hence, the C-3 site is the chosen one for the reported reaction.

CONCLUSIONS

We have developed an operationally simple and environmentally friendly protocol for the regioselective C−H functionalization of indolizines using a catalytic amount of acetic acid. We have demonstrated the application of the present methodology by synthesizing functionally important BINOL-substituted derivatives of indolizines. The energetics from DFT quantum mechanical investigations showed that our preliminary hypothesis of intramolecular proton abstractions did not fit with the current reaction conditions; instead, it gave rise to some complex path that revealed the role of acetic acid

toward unfolding the inherent mechanism for this ultrafast catalytic reaction. This theoretical result was also confirmed by synthetic experiments. Additionally, the choice of regioselectivity was also addressed.

EXPERIMENTAL SECTION

General Information. All solvents were purified and dried by standard procedures before use. ^{1}H and ^{13}C NMR spectra were recorded with Jeol 400 (^{1}H 400 MHz,^{13}C 101 MHz) and Bruker AV 200/400/500 MHz spectrometers in suitable solvents using TMS as the internal standard or the solvent signals as secondary standards, and the chemical shifts are shown as δ scales. Purification was performed using column chromatography (100−120 and 230−400 mesh). The reactions were monitored by TLC visualized by UV (254 nm) and/or with iodine. Coupling constants are given in hertz (Hz), and the classical abbreviations are used to describe the signal multiplicities (m, multiplet; q, quartet; t, triplet; d, doublet, and s, singlet). HRMS data for all purified compounds were recorded by the ESI$^+$ method and an Orbitrap mass analyzer with a Thermo Scientific Q-Exactive, Accela 1250 pump.

Typical Procedure for the Synthesis of Quinone Monoimines. *N*-tosyl-*p*-aminophenol (2.64 g) was added in 50 mL of DCM, followed by the addition of PhI(OAc)$_2$ (1 equiv, 3.23 g) and stirred for 1 h at room temperature. Then, 25 mL of water was added to the mixture and extracted with EtOAc (25 mL × 3). The combined organic layers were washed with brine and dried over sodium sulfate. The solvent evaporated under reduced pressure. The crude residue is purified using flash column chromatography (100−200 mesh silica) using 85/
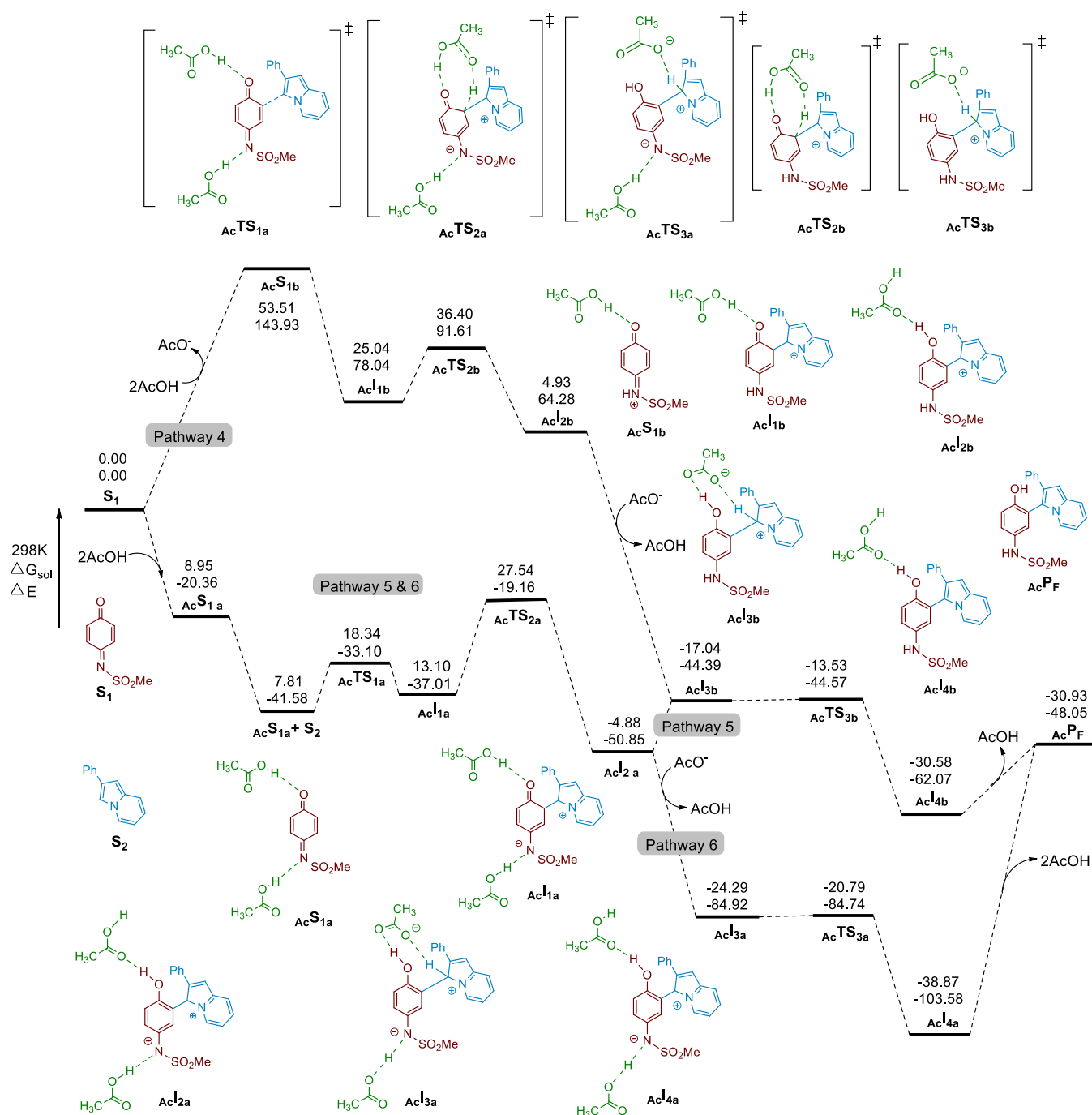
Figure 5. PES along with structures and thermodynamic parameters for pathways 4, 5, and 6.

15 petroleum ether/ethyl acetate as the eluent to afford the corresponding compound as an orange solid. All quinone monoimines (2a–2c, 5, and 7) are synthesized using the above method.

General Procedure for the Synthesis of 3a. To a 25 mL oven-dried round-bottom flask containing CH_3CN (1 mL) were added indolizine 1a (0.191 mmol, 37 mg), quinone monoimine 2a (0.191 mmol, 50 mg), and AcOH (0.038 mmol, 0.2 mL). Then, the resulting reaction mixture was stirred at 25 °C for 2 min. Upon completion of the reaction, the reaction mixture was dried under vacuum. Then, the crude reaction mixture was diluted with ethyl acetate (5 mL), washed with brine, and eluted with EtOAc (5 mL × 2). The organic layer was evaporated, and the crude residue was preadsorbed on silica gel and purified by column chromatography (100−200 mesh silica) using 80/20 to 80/30 petroleum ether/ethyl acetate as the eluent to afford the

corresponding compound 3a in 94% yield as a faint yellow semisolid (81 mg).

N-(4-Hydroxy-3-(2-phenylindolizin-3-yl)phenyl)-4-methylbenzenesulfonamide (3a). White semisolid, 94% yield (81 mg). ^{1}H NMR (400 MHz, CDCl₃) δ 7.57 (d, J = 8.4 Hz, 2H), 7.35−7.44 (m, 2H), 7.20−7.29 (m, 5H), 7.11−7.19 (m, 3H), 6.95 (d, J = 2.6 Hz, 1H), 6.89 (d, J = 8.8 Hz, 1H), 6.65−6.81 (m, 3H), 6.34−6.45 (m, 1H), 5.21 (br. s., 1H), 2.36 (s, 3H). ^{13}C{^{1}H} NMR (101 MHz, CDCl₃) δ 152.7, 143.4, 135.3, 134.3, 133.8, 129.2, 128.9, 128.8, 128.2, 127.4, 127.0, 127.0, 126.6, 126.6, 122.2, 118.6, 118.2, 117.9, 116.7, 112.7, 110.6, 98.7, 21.2. HRMS (ESI) m/z calcd for $C_{27}H_{23}O_3N_2S$ [(M + H)[+]] 455.1424 found 455.1417.

N-(4-Hydroxy-3-(2-phenylindolizin-3-yl)phenyl)-methanesulfonamide (3b). White solid, 96% yield (94 mg). MP. 92−94 °C. ^{1}H NMR (500 MHz, CDCl₃) δ 7.65 (d, J = 7.2 Hz, 1H),
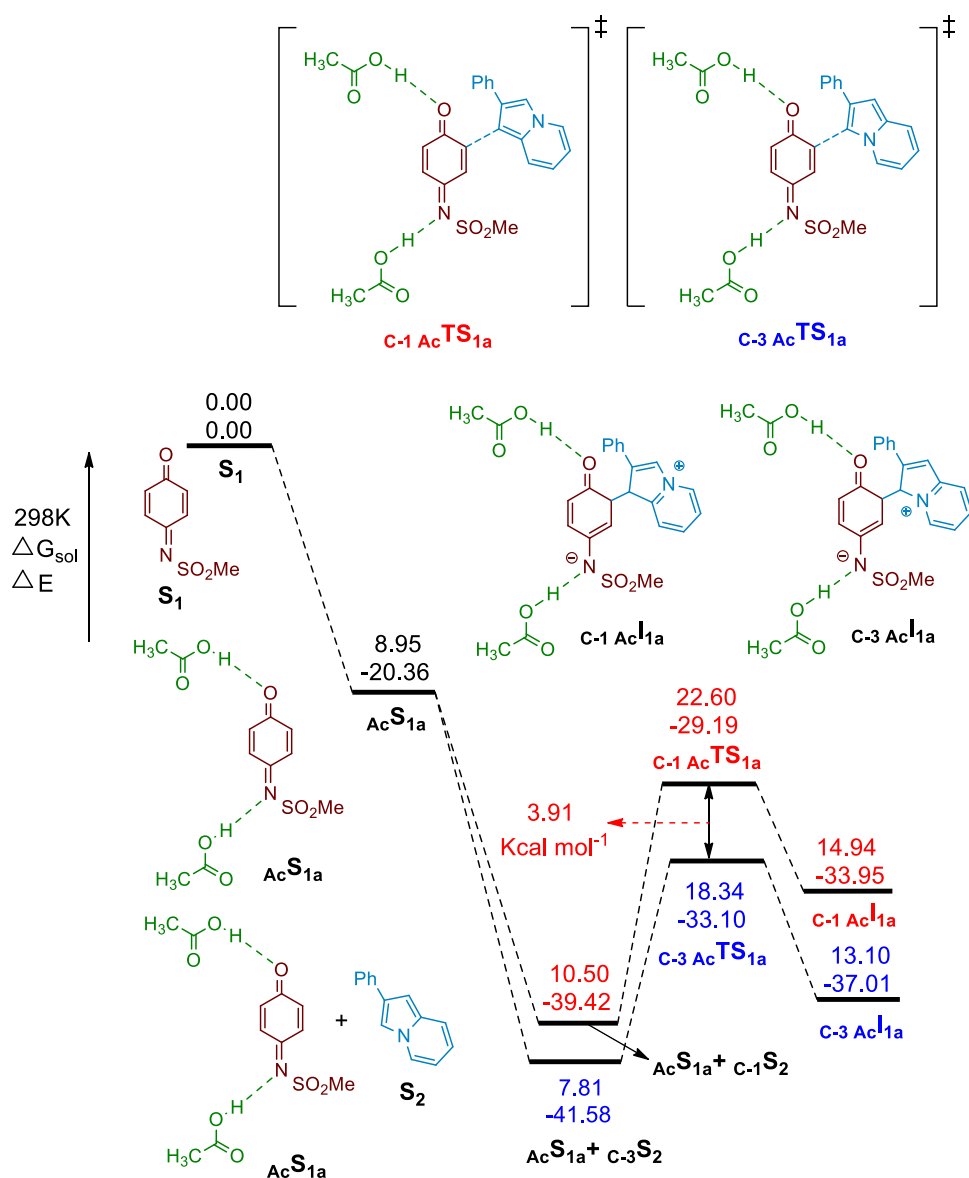
Figure 6. PES for regioselectivity.

7.45 (d, J = 9.2 Hz, 1H), 7.34 (d, J = 7.6 Hz, 2H), 7.24−7.29 (m, 4H), 7.17−7.23 (m, 1H), 7.11 (d, J = 2.3 Hz, 1H), 7.04 (d, J = 8.8 Hz, 1H), 6.70−6.87 (m, 2H), 6.52 (t, J = 6.7 Hz, 1H), 6.38 (br. s., 1H), 2.84 (s, 3H). ^{13}C{^{1}H} NMR (126 MHz, CDCl$_3$) δ 153.0, 134.6, 133.9, 129.3, 129.0, 128.3, 127.9, 127.1, 126.6, 125.9, 122.6, 118.8, 118.6, 118.3, 117.1, 113.3, 111.0, 99.2, 38.7. HRMS (ESI) m/z calcd for C$_{21}$H$_{18}$O$_3$N$_2$NaS [(M + Na)$^+$] 401.0930 found 401.0911.

N-(4-Hydroxy-3-(2-phenylindolizin-3-yl)phenyl)-benzenesulfonamide (3c). White amorphous solid, 90% yield (101 mg). ^{1}H NMR (500 MHz, CDCl$_3$) δ 7.70 (d, J = 8.0 Hz, 2H), 7.47−7.58 (m, 1H), 7.33−7.45 (m, 4H), 7.18−7.31 (m, 5H), 7.14 (dd, J = 8.8, 2.7 Hz, 1H), 6.95 (d, J = 2.3 Hz, 1H), 6.89 (d, J = 8.8 Hz, 1H), 6.67−6.78 (m, 2H), 6.40 (t, J = 6.7 Hz, 1H). ^{13}C{^{1}H} NMR (126 MHz, CDCl$_3$) δ 152.8, 138.3, 134.3, 133.9, 132.6, 128.8, 128.8, 128.7, 128.3, 127.5, 127.1, 127.1, 126.8, 126.7, 122.3, 118.7, 118.3, 118.0, 116.9, 112.6, 110.8, 98.8. HRMS (ESI) m/z calcd for C$_{26}$H$_{21}$O$_3$N$_2$S [(M + H)$^+$] 441.1267 found 441.1260.

N-(3-(2-(3-Bromophenyl)indolizin-3-yl)-4-hydroxyphenyl)-4-methylbenzenesulfonamide (3d). White amorphous solid, 76% yield (74 mg). ^{1}H NMR (500 MHz, CDCl$_3$) δ 7.58 (m, J = 8.4 Hz, 2H), 7.51 (t, J = 1.5 Hz, 1H), 7.40−7.47 (m, 2H), 7.36 (d, J = 8.0 Hz, 1H), 7.20 (m, J = 8.0 Hz, 2H), 7.13−7.17 (m, 2H), 7.06−7.11 (m, 1H), 6.93−6.99 (m, 2H), 6.79 (dd, J = 8.6, 7.1 Hz, 1H), 6.72 (s, 1H),

6.44−6.50 (m, 1H), 6.41 (s, 1H), 5.11 (s, 1H), 2.38 (s, 3H). ^{13}C{^{1}H} NMR (126 MHz, CDCl$_3$) δ 153.1, 147.3, 143.8, 136.9, 135.8, 134.2, 130.7, 130.0, 129.8, 129.6, 129.3, 127.6, 127.5, 127.3, 126.1, 122.7, 122.6, 119.1, 118.8, 117.8, 117.2, 113.2, 111.3, 99.1, 21.6. HRMS (ESI) m/z calcd for C$_{27}$H$_{22}$O$_3$N$_2$BrS [(M + H)$^+$] 533.0529 found 533.0527.

N-(4-Hydroxy-3-(2-(3-methoxyphenyl)indolizin-3yl)-phenyl)-4-methylbenzenesulfonamide (3e). White solid, 91% yield (98 mg). ^{1}H NMR (500 MHz, CDCl$_3$) δ 7.52−7.62 (m, 2H), 7.38−7.45 (m, 2H), 7.10−7.19 (m, 4H), 6.96 (d, J = 2.7 Hz, 1H), 6.87−6.92 (m, 2H), 6.81−6.85 (m, 1H), 6.71−6.78 (m, 3H), 6.65−6.68 (m, 1H), 6.36−6.45 (m, 1H), 5.22 (br. s., 1H), 3.62 (s, 3H), 2.36 (s, 3H). ^{13}C{^{1}H} NMR (126 MHz, CDCl$_3$) δ 159.6, 153.1, 143.8, 135.9, 135.7, 134.1, 129.6, 129.5, 129.3, 128.9, 127.4, 127.3, 127.1, 125.7, 122.5, 120.2, 119.0, 118.6, 118.3, 117.0, 115.9, 113.0, 112.7, 111.0, 99.1, 55.0, 21.5. HRMS (ESI) m/z calcd for C$_{28}$H$_{25}$O$_4$N$_2$S [(M + H)$^+$] 485.1530 found 485.1524.

N-(4-Hydroxy-3-(2-(3-nitrophenyl)indolizin-3-yl)phenyl)-4-methylbenzenesulfonamide (3f). Yellow solid, 86% yield (89 mg). MP.: 98−100 °C. ^{1}H NMR (400 MHz, CDCl$_3$) δ 8.20 (t, J = 2.0 Hz, 1H), 8.05 (ddd, J = 8.3, 2.3, 1.0 Hz, 1H), 7.54−7.61 (m, 3H), 7.43−7.50 (m, 2H), 7.37 (t, J = 8.0 Hz, 1H), 7.20 (d, J = 8.0 Hz, 2H), 7.10 (dd, J = 8.8, 2.8 Hz, 1H), 7.03 (d, J = 2.5 Hz, 1H), 6.94 (d, J = 8.8 Hz, 1H),

6.78–6.85 (m, 2H), 6.59 (s, 1H), 6.50 (td, J = 6.9, 1.0 Hz, 1H), 2.38 (s, 3H). ^{13}C{^{1}H} NMR (101 MHz, CDCl$_3$) δ 152.6, 148.2, 143.6, 136.4, 135.4, 134.0, 133.0, 129.3, 129.0, 127.2, 127.0, 126.9, 126.2, 122.4, 122.0, 121.1, 118.9, 118.8, 117.2, 116.9, 113.5, 111.3, 98.7, 21.2. HRMS (ESI) m/z calcd for C$_{27}$H$_{22}$O$_5$N$_3$S [(M + H)$^+$] 500.1275 found 500.1268.

N-(4-Hydroxy-3-(2-(4-methoxyphenyl)indolizin-3yl)-phenyl)-4-methylbenzenesulfonamide (3g). White solid, 82% yield (88 mg). MP.: 100–102 °C. ^{1}H NMR (500 MHz, CDCl$_3$) δ 7.5–7.6 (m, 2H), 7.3–7.5 (m, 2H), 7.2–7.2 (m, 4H), 7.1 (dd, J = 8.4, 2.7 Hz, 1H), 7.0 (d, J = 2.7 Hz, 1H), 6.9 (d, J = 8.8 Hz, 1H), 6.8–6.8 (m, 2H), 6.7–6.8 (m, 1H), 6.7 (s, 1H), 6.3–6.5 (m, 2 H), 5.1 (s, 1 H), 3.8 (s, 3 H), 2.4 (s, 3 H). ^{13}C{^{1}H} NMR (101 MHz, CDCl$_3$) δ 158.7, 153.0, 143.7, 135.7, 134.1, 129.6, 129.2, 128.8, 127.4, 127.3, 126.9, 125.7, 122.5, 118.8, 118.4, 118.4, 117.1, 115.9, 114.1, 112.5, 110.7, 98.7, 55.2, 21.5. HRMS (ESI) m/z calcd for C$_{28}$H$_{25}$O$_4$N$_2$S [(M + H)$^+$] 485.1530 found 485.1509.

N-(4-Hydroxy-3-(2-(p-tolyl)indolizin-3-yl)phenyl)-4-methylbenzenesulfonamide (3h). White semisolid, 73% yield (82 mg). ^{1}H NMR (500 MHz, CDCl$_3$) δ 7.60 (m, J = 7.6 Hz, 2H), 7.35–7.48 (m, 2H), 7.15–7.24 (m, 5H), 7.04–7.10 (m, 2H), 6.98 (br. s, 1H), 6.92 (d, J = 8.4 Hz, 1H), 6.68–6.80 (m, 2H), 6.50 (s, 1H), 6.42 (t, J = 6.7 Hz, 1H), 5.17 (br. s, 1H), 2.39 (s, 3H), 2.34 (s, 3H). ^{13}C{^{1}H} NMR (126 MHz, CDCl$_3$) δ 153.0, 143.7, 136.7, 135.8, 134.2, 131.6, 129.6, 129.4, 129.2, 129.1, 127.6, 127.4, 127.1, 126.4, 122.5, 118.9, 118.5, 118.4, 117.1, 112.6, 110.9, 99.0, 21.6, 21.2. HRMS (ESI) m/z calcd for C$_{28}$H$_{25}$O$_3$N$_2$S [(M + H)$^+$] 469.1580 found 469.1577.

N-(3-(2-(4-Chlorophenyl)indolizin-3-yl)-4-hydroxyphenyl)-4-methylbenzenesulfonamide (3i). White solid, 85% yield (90 mg). MP.: 188–190 °C. ^{1}H NMR (500 MHz, CDCl$_3$) δ 7.57 (d, J = 8.0 Hz, 2H), 7.38–7.46 (m, 2H), 7.26 (s, 1H), 7.21 (s, 1H), 7.18 (s, 4H), 7.14 (dd, J = 8.8, 2.7 Hz, 1H), 6.89–7.01 (m, 2H), 6.73–6.81 (m, 1H), 6.69 (s, 1H), 6.54 (s, 1H), 6.37–6.49 (m, 1H), 5.15 (s, 1H), 2.39 (s, 3H). ^{13}C{^{1}H} NMR (126 MHz, CDCl$_3$) δ 153.0, 143.9, 135.7, 134.2, 133.2, 132.7, 129.6, 129.4, 128.9, 128.7, 127.9, 127.4, 127.2, 126.9, 122.6, 119.0, 118.8, 118.0, 117.1, 113.0, 111.2, 98.9, 21.6. HRMS (ESI) m/z calcd for C$_{27}$H$_{22}$O$_3$N$_2$SCl [(M + H)$^+$] 489.1034 found 489.1025.

N-(3-(2-(4-Fluorophenyl)indolizin-3-yl)-4-hydroxyphenyl)-4-methylbenzenesulfonamide (3j). White solid, 80% yield (87 mg). ^{1}H NMR (500 MHz, CDCl$_3$) δ 7.58 (d, J = 8.0 Hz, 2H), 7.38–7.46 (m, 2H), 7.18–7.25 (m, 4H), 7.14 (dd, J = 8.8, 2.7 Hz, 1H), 6.98 (d, J = 2.7 Hz, 1H), 6.89–6.96 (m, 3H), 6.77 (dd, J = 9.0, 6.7 Hz, 1H), 6.68 (s, 1H), 6.39–6.52 (m, 2H), 2.39 (s, 3H). ^{13}C{^{1}H} NMR (101 MHz, CDCl$_3$) δ 163.1, 160.7, 152.9, 148.2, 147.3, 145.5, 143.8, 143.6, 135.7, 134.1, 131.3, 130.7, 129.7, 129.6, 129.5, 129.3, 129.3, 129.2, 128.8, 128.2, 127.4, 127.3, 127.2, 126.9, 126.4, 125.7, 122.6, 118.9, 118.7, 118.0, 117.1, 115.9, 115.6, 115.4, 112.9, 111.1, 98.9, 21.5. ^{19}F NMR (376 MHz, CDCl$_3$) δ −115.41 (s, 1F). HRMS (ESI) m/z calcd for C$_{27}$H$_{22}$O$_3$N$_2$FS [(M + H)$^+$] 473.1330 found 473.1321.

N-(3-(2-(4-Cyanophenyl)indolizin-3-yl)-4-hydroxyphenyl)-4-methylbenzenesulfonamide (3k). White solid, 94% yield (103 mg). MP.: 185–187 °C. ^{1}H NMR (500 MHz, DMSO-d_6) δ 9.75 (d, J = 9.5 Hz, 2H), 7.66 (d, J = 8.4 Hz, 2H), 7.49–7.56 (m, 1H), 7.46 (m, J = 8.0 Hz, 2H), 7.36–7.43 (m, 2H), 7.25–7.34 (m, 3H), 7.13 (dd, J = 8.8, 2.7 Hz, 1H), 6.96 (d, J = 8.8 Hz, 1H), 6.83–6.87 (m, 1H), 6.79 (dd, J = 8.8, 6.9 Hz, 1H), 6.64 (d, J = 2.7 Hz, 1H), 6.51–6.59 (m, 1H), 2.34 (s, 3H). ^{13}C{^{1}H} NMR (126 MHz, DMSO-d_6) δ 153.9, 142.9, 140.6, 136.4, 132.2, 129.4, 127.9, 126.6, 126.4, 125.6, 125.0, 123.9, 123.1, 119.1, 118.9, 118.4, 118.0, 117.5, 116.8, 115.5, 110.9, 108.2, 98.6, 21.0. HRMS (ESI) m/z calcd for C$_{28}$H$_{22}$O$_3$N$_3$S [(M + H)$^+$] 480.1376 found 480.1371.

N-(4-Hydroxy-3-(7-methyl-2-phenylindolizin-3-yl)phenyl)-4-methylbenzenesulfonamide (3l). White solid, 66% yield (74 mg). ^{1}H NMR (500 MHz, CDCl$_3$) δ 7.60 (d, J = 8.0 Hz, 2H), 7.36 (d, J = 6.9 Hz, 1H), 7.24–7.31 (m, 5H), 7.18–7.23 (m, 3H), 7.16 (dd, J = 8.8, 2.7 Hz, 1H), 6.98 (d, J = 2.7 Hz, 1H), 6.93 (d, J = 8.8 Hz, 1H), 6.61 (s, 1H), 6.54 (s, 1H), 6.28 (dd, J = 7.2, 1.5 Hz, 1H), 5.20 (br. s, 1H), 2.40 (s, 3H), 2.32 (s, 3H). ^{13}C{^{1}H} NMR (126 MHz, CDCl$_3$) δ 152.8, 143.5, 135.5, 134.5, 134.3, 129.3, 128.9, 128.8, 128.6, 128.3,

127.4, 127.2, 127.1, 126.7, 126.6, 121.8, 118.2, 116.7, 113.5, 111.7, 97.3, 21.3, 20.7. HRMS (ESI) m/z calcd for C$_{28}$H$_{25}$O$_3$N$_2$S [(M + H)$^+$] 469.1580 found 469.1566.

N-(4-Hydroxy-3-(7-methyl-2-phenylindolizin-3-yl)phenyl)-methanesulfonamide (3m). White semisolid, 72% yield (67 mg). ^{1}H NMR (500 MHz, CD$_3$CN) δ 7.55 (d, J = 7.1 Hz, 1H), 7.47 (s, 1H), 7.39 (d, J = 2.7 Hz, 1H), 7.31–7.34 (m, 2H), 7.26 (d, J = 7.6 Hz, 2H), 7.21–7.23 (m, 2H), 7.15–7.18 (m, 1H), 7.03 (d, J = 8.7 Hz, 1H), 6.92 (d, J = 2.7 Hz, 1H), 6.60 (s, 1H), 6.38 (d, J = 5.5 Hz, 1H), 2.67 (s, 3H), 2.28 (s, 4H). ^{13}C{^{1}H} NMR (101 MHz, CD$_3$CN) δ 155.1, 137.1, 134.4, 131.0, 130.1, 129.4, 129.3, 129.2, 129.1, 128.7, 127.6, 127.2, 126.4, 124.2, 120.1, 118.0, 117.6, 114.0, 98.4, 38.8, 21.0. HRMS (ESI) m/z calcd for C$_{22}$H$_{21}$O$_3$N$_2$S [(M + H)$^+$] 393.1267 found 393.1259.

N-(4-Hydroxy-3-(8-methyl-2-phenylindolizin-3-yl)phenyl)-4-methylbenzenesulfonamide (3n). White semisolid, 71% yield (80 mg). MP.: 108–110 °C. ^{1}H NMR (400 MHz, CD$_3$CN) δ 7.54–7.59 (m, 1H), 7.45–7.50 (m, 2H), 7.28–7.32 (m, 2H), 7.19–7.26 (m, 6H), 7.11 (dd, J = 8.7, 2.7 Hz, 1H), 6.91 (d, J = 8.6 Hz, 1H), 6.75 (s, 1H), 6.71 (d, J = 2.6 Hz, 1H), 6.58 (d, J = 6.6 Hz, 1H), 6.43 (t, J = 6.8 Hz, 1H), 2.44 (s, 3H), 2.32 (s, 3H). ^{13}C{^{1}H} NMR (101 MHz, CD$_3$CN) δ 155.2, 144.9, 137.1, 136.9, 134.9, 130.8, 130.6, 129.4, 129.0, 128.9, 128.9, 128.2, 127.3, 127.0, 122.0, 120.1, 117.9, 117.8, 117.5, 116.9, 111.7, 98.5, 21.6, 18.2. HRMS (ESI) m/z calcd for C$_{28}$H$_{25}$O$_3$N$_2$S [(M + H)$^+$] 469.1580 found 469.1566.

N-(3-(2-(3,4-Dimethoxyphenyl)indolizin-3-yl)-4-hydroxyphenyl)-4-methylbenzenesulfonamide (3o). White solid, 69% yield (69 mg). ^{1}H NMR (500 MHz, CDCl$_3$) δ 7.61 (m, J = 8.4 Hz, 2H), 7.39–7.46 (m, 2H), 7.22 (m, J = 8.0 Hz, 2H), 7.16 (dd, J = 8.8, 2.7 Hz, 1H), 7.01–7.08 (m, 1H), 6.92–6.98 (m, 2H), 6.76–6.84 (m, 3H), 6.73 (s, 1H), 6.53 (s, 1H), 6.36–6.47 (m, 1H), 5.23 (br. s, 1H), 3.89 (s, 3H), 3.59 (s, 3H), 2.40 (s, 3H). ^{13}C{^{1}H} NMR (126 MHz, CDCl$_3$) δ 153.0, 148.7, 148.0, 143.8, 135.7, 134.1, 129.6, 129.3, 129.2, 128.8, 127.3, 127.2, 127.0, 126.6, 122.4, 119.9, 118.7, 118.5, 116.9, 115.9, 112.5, 111.3, 110.8, 98.5, 55.7, 55.4, 21.5. HRMS (ESI) m/z calcd for C$_{29}$H$_{27}$O$_5$N$_2$S [(M + H)$^+$] 515.1635 found 515.1619.

N-(3-(2-(2,4-Dichlorophenyl)indolizin-3-yl)-4hydroxyphenyl)-4-methylbenzenesulfonamide (3p). White solid, 76% yield (75 mg). ^{1}H NMR (500 MHz, CDCl$_3$) δ 7.49–7.58 (m, 3H), 7.46 (d, J = 8.8 Hz, 1H), 7.42 (d, J = 1.9 Hz, 1H), 7.24 (d, J = 8.0 Hz, 2H), 7.09 (dd, J = 8.4, 2.3 Hz, 1H), 7.04 (d, J = 8.4 Hz, 1H), 6.97–7.01 (m, 2H), 6.79–6.85 (m, 2H), 6.75 (s, 1H), 6.45–6.56 (m, 1H), 5.23 (br. s, 1H), 2.43 (s, 3H). ^{13}C{^{1}H} NMR (126 MHz, CDCl$_3$) δ 152.4, 143.5, 135.5, 133.8, 133.3, 133.2, 132.6, 132.4, 129.3, 128.8, 127.0, 126.8, 126.6, 126.0, 125.7, 122.5, 118.9, 118.3, 117.3, 116.7, 115.0, 111.0, 101.2, 21.3. HRMS (ESI) m/z calcd for C$_{27}$H$_{21}$O$_3$N$_2$Cl$_2$S [(M + H)$^+$] 523.0644 found 523.0630.

N-(3-(2-(2-Fluorophenyl)indolizin-3-yl)-4-hydroxyphenyl)-4-methylbenzenesulfonamide (3q). White solid, 70% yield (77 mg). MP.: 86–88 °C. ^{1}H NMR (500 MHz, CDCl$_3$) δ 7.54 (d, J = 8.4 Hz, 2H), 7.38–7.49 (m, 2H), 7.15–7.24 (m, 3H), 7.11 (td, J = 7.6, 1.5 Hz, 1H), 7.02–7.08 (m, 2H), 6.96–7.00 (m, 1H), 6.93 (d, J = 2.7 Hz, 1H), 6.87 (d, J = 8.8 Hz, 1H), 6.73–6.81 (m, 2H), 6.54 (br. s, 1H), 6.39–6.49 (m, 1H), 5.19 (br. s, 1H), 2.38 (s, 3H). ^{13}C{^{1}H} NMR (126 MHz, CDCl$_3$) δ 160.8, 158.8, 153.0, 143.7, 135.8, 133.8, 131.0, 131.03, 131.0, 129.7, 129.5, 129.1, 128.8, 128.7, 127.4, 127.3, 126.9, 125.8, 124.0, 123.2, 122.6, 122.5, 119.1, 118.4, 118.1, 116.9, 116.0, 115.9, 115.8, 114.5, 111.1, 101.1, 21.6. ^{19}F NMR (376 MHz, CDCl$_3$) δ −115.13 (s, 1F). HRMS (ESI) m/z calcd for C$_{27}$H$_{22}$O$_3$N$_2$FS [(M + H)$^+$] 473.1330 found 473.1314.

N-(4-Hydroxy-3-(1-methyl-2-phenylindolizin-3-yl)phenyl)-4-methylbenzenesulfonamide (3r). White semisolid, 77% yield (87 mg). ^{1}H NMR (400 MHz, CDCl$_3$) δ 7.54 (d, J = 8.3 Hz, 2H), 7.42 (d, J =7.1 Hz, 1H), 7.36–7.39 (m, 1H), 7.23–7.28 (m, 3H), 7.13–7.21 (m, 4H), 6.94–7.02 (m, 2H), 6.78 (d, J = 8.5 Hz, 1H), 6.70 (dd, J = 8.8, 7.3 Hz, 1H), 6.33–6.41 (m, 1H), 2.38 (s, 3H), 2.37 (s, 3H). ^{13}C{^{1}H} NMR (101 MHz, CDCl$_3$) δ 152.8, 148.1, 147.2, 145.5, 143.6, 135.7, 134.2, 131.6, 129.7, 129.5, 128.9, 128.3, 127.3, 126.7, 126.4, 122.3, 118.1, 117.4, 116.9, 116.8, 113.5, 110.7, 106.9, 21.6, 9.4.

HRMS (ESI) m/z calcd for $C_{28}H_{25}O_3N_2S$ [(M + H)$^+$] 469.1580 found 469.1576.

N-(4-Hydroxy-3-(1-methyl-2-(naphthalen-2-yl)indolizin-3-yl)-phenyl)-4-methylbenzenesulfonamide (3s). White solid, 59% yield (58 mg). MP.: 129−131 °C. ^{1}H NMR (500 MHz, CDCl$_3$) δ 7.79−7.86 (m, 1H), 7.68−7.77 (m, 3H), 7.42−7.55 (m, 6H), 7.18−7.30 (m, 2H), 7.03−7.11 (m, 3H), 6.97 (dd, J = 8.8, 2.7 Hz, 1H), 6.70−6.81 (m, 2H), 6.42 (t, J = 6.7 Hz, 2H), 2.43 (s, 3H), 2.34 (s, 3H). ^{13}C{^{1}H} NMR (126 MHz, CDCl$_3$) δ 152.6, 143.4, 135.6, 133.1, 131.9, 131.6, 129.2, 128.7, 128.6, 128.3, 127.7, 127.6, 127.6, 127.4, 127.3, 127.0, 126.3, 125.8, 125.6, 122.1, 118.0, 117.3, 116.8, 116.6, 113.3, 110.6, 107.0, 21.3, 9.2. HRMS (ESI) m/z calcd for $C_{32}H_{26}O_3N_2NaS$ [(M + Na)$^+$] 541.1556 found 541.1538.

N-(4-Hydroxy-3-(2-(thiophen-2-yl)indolizin-3-yl)phenyl)-methanesulfonamide (3t). White solid, 95% yield (91 mg). MP.: 95−97 °C. ^{1}H NMR (500 MHz, CDCl$_3$) δ 7.55 (d, J = 6.9 Hz, 1H), 7.38 (d, J = 8.8 Hz, 1H), 7.33 (dd, J = 8.8, 2.7 Hz, 1H), 7.19 (d, J = 2.7 Hz, 1H), 7.11−7.15 (m, 1H), 7.07 (d, J = 8.4 Hz, 1H), 6.96−7.00 (m, 1H), 6.92 (dd, J = 5.0, 3.8 Hz, 1H), 6.67−6.84 (m, 2H), 6.55 (br. s., 1H), 6.43−6.51 (m, 1H), 5.33 (br. s., 1H), 2.93 (s, 3H). ^{13}C{^{1}H} NMR (126 MHz, CDCl$_3$) δ 153.7, 137.0, 134.1, 129.5, 127.4, 126.7, 124.6, 124.2, 123.2, 122.8, 118.9, 118.8, 118.1, 117.5, 112.7, 111.3, 98.5, 39.0. HRMS (ESI) m/z calcd for $C_{19}H_{16}O_3N_2NaS_2$ [(M + H)$^+$] 407.0495 found 407.0479.

N-(4-Hydroxy-3-(2-(thiophen-2-yl)indolizin-3-yl)phenyl)-4-methylbenzenesulfonamide (3u). White solid, 89% yield (102 mg). MP.: 90−92 °C. ^{1}H NMR (500 MHz, CDCl$_3$) δ 7.59 (m, J = 8.0 Hz, 2H), 7.31−7.38 (m, 2H), 7.22 (dd, J = 8.8, 2.7 Hz, 1H), 7.17 (m, J = 8.4 Hz, 2H), 7.13 (dd, J = 5.0, 1.1 Hz, 1H), 6.97 (d, J = 8.8 Hz, 1H), 6.89−6.94 (m, 2H), 6.87 (dd, J = 3.6, 1.0 Hz, 1H), 6.70−6.77 (m, 2H), 6.62 (s, 1H), 6.35−6.48 (m, 1H), 5.21 (s, 1H), 2.35 (s, 3H). ^{13}C{^{1}H} NMR (126 MHz, CDCl$_3$) δ 153.4, 143.5, 136.7, 135.4, 133.8, 129.3, 129.2, 127.5, 127.4, 127.2, 124.2, 123.7, 122.8, 122.3, 118.6, 118.5, 117.3, 116.9, 112.0, 110.8, 98.1, 21.3. HRMS (ESI) m/z calcd for $C_{25}H_{21}O_3N_2S_2$ [(M + H)$^+$] 461.0988 found 461.0971.

N-(4-Hydroxy-3-(2-phenylindolizin-3-yl)-5-(phenylthio)- phenyl)-4-methylbenzenesulfonamide (3v). White semisolid, 65% yield (92 mg). ^{1}H NMR (500 MHz, CDCl$_3$) δ 7.54 (d, J = 7.6 Hz, 2H), 7.39−7.46 (m, 2H), 7.23−7.35 (m, 10H), 7.12−7.20 (m, 3H), 7.06−7.12 (m, 2H), 6.98−7.04 (m, 1H), 6.81−6.88 (m, 1H), 6.70−6.80 (m, 1H), 6.44 (t, J = 6.5 Hz, 1H), 2.39 (s, 3H). ^{13}C{^{1}H} NMR (126 MHz, CDCl$_3$) δ 153.4, 143.7, 135.7, 135.5, 134.5, 133.6, 130.7, 129.3, 129.2, 129.0, 128.3, 128.2, 128.1, 127.9, 127.4, 127.3, 127.2, 126.8, 126.4, 125.5, 122.8, 121.9, 120.3, 119.4, 118.9, 117.9, 114.9, 110.6, 99.1, 21.5. HRMS (ESI) m/z calcd for $C_{33}H_{27}O_3N_2S_2$ [(M + H)$^+$] 563.1458 found 563.1446.

N-(3-Bromo-4-hydroxy-5-(2-phenylindolizin-3-yl)phenyl)-benzenesulfonamide (3w). White semisolid, 58% yield (76 mg). ^{1}H NMR (500 MHz, CDCl$_3$) δ 7.69−7.77 (m, 2H), 7.48−7.55 (m, 2H), 7.36−7.44 (m, 4H), 7.33 (d, J = 7.6 Hz, 1H), 7.10−7.17 (m, 2H), 7.03−7.08 (m, 1H), 6.89−6.99 (m, 2H), 6.71−6.79 (m, 2H), 6.68 (s, 1H), 6.43 (t, J = 6.7 Hz, 1H). ^{13}C{^{1}H} NMR (126 MHz, CDCl$_3$) δ 153.1, 138.6, 136.9, 134.1, 132.9, 130.6, 130.0, 129.8, 129.1, 129.0, 128.4, 127.5, 127.3, 126.1, 123.3, 122.6, 119.1, 118.8, 117.9, 117.2, 113.2, 111.3, 99.1. HRMS (ESI) m/z calcd for $C_{26}H_{20}O_3N_2BrS$ [(M + H)$^+$] 519.0373 found 519.0358.

Experimental Procedure for the Synthesis of 6. To a 25 mL oven-dried round-bottom flask containing DCM (3 mL) were added quinone monoimine **5** (0.197 mmol, 80 mg), indolizine **1n** (0.197 mmol, 45 mg), and AcOH (0.039 mmol). Then, the resulting reaction mixture was stirred at room temperature for 5 min. Upon completion of the reaction (monitored by TLC), the reaction mixture was dried under vacuum. Then, the crude reaction mixture was diluted with ethyl acetate (5 mL), washed with brine, and eluted with EtOAc (5 mL × 3). The organic layer was evaporated, and the crude residue was preadsorbed on silica gel and purified by column chromatography (100−200 mesh silica) using 80/20 to 80/50 petroleum ether/ethyl acetate as the eluent to afford the corresponding product **6a** in 69% yield (91 mg).

N-(4-Hydroxy-3-(2-hydroxynaphthalen-1-yl)-5-(8-methyl-2-phenylindolizin-3-yl)phenyl)-4-methylbenzenesulfonamide (6a). White gummy semisolid, 69% yield (91 mg). ^{1}H NMR (500 MHz, CDCl$_3$) δ 8.13 (d, J = 6.9 Hz, 1H), 8.10 (d, J = 6.9 Hz, 1H), 7.89−7.84 (m, 2H), 7.84−7.79 (m, 2H), 7.50 (d, J = 8.0 Hz, 2H), 7.47−7.43 (m, J = 8.4 Hz, 2H), 7.41−7.36 (m, 4H), 7.36−7.30 (m, 5H), 7.26−7.21 (m, 5H), 7.20−7.14 (m, 5H), 7.13−7.06 (m, 5H), 7.05−7.00 (m, J = 8.0 Hz, 2H), 6.97 (d, J = 9.2 Hz, 4H), 6.67−6.61 (m, 2H), 6.61−6.50 (m, 4H), 2.45 (s, 3H), 2.43 (s, 3H), 2.33 (s, 3H), 2.30 (s, 3H). ^{13}C{^{1}H} NMR (101 MHz, CDCl$_3$) δ 152.5, 152.4, 151.8, 151.8, 144.1, 144.0, 137.5, 136.3, 135.7, 135.4, 134.6, 134.5, 132.8, 132.6, 132.3, 132.2, 131.0, 130.4, 130.2, 129.3, 129.3, 129.1, 129.1, 129.1, 128.4, 128.4, 128.3, 128.3, 128.1, 128.1, 128.0, 127.8, 127.5, 127.4, 127.4, 127.4, 127.3, 127.2, 127.1, 126.8, 126.7, 126.3, 126.2, 126.0, 123.9, 123.9, 120.4, 120.3, 119.9, 119.9, 118.4, 118.4, 118.0, 117.9, 117.3, 117.3, 115.9, 115.8, 113.3, 113.2, 111.5, 111.5, 97.3, 97.3, 21.5, 21.5, 17.6, 17.6. HRMS (ESI) m/z calcd for $C_{38}H_{31}O_4N_2S$ [(M + H)$^+$] 611.1999 found 611.1984.

N-(4-Hydroxy-3-(2-hydroxynaphthalen-1-yl)-5-(7-methyl-2-phenylindolizin-1-yl)phenyl)-4-methylbenzenesulfonamide (6b). White solid, 60% yield (45 mg). MP.: 142−144 °C. ^{1}H NMR (500 MHz, CDCl$_3$) δ 8.22 (s, 1H), 8.14 (dd, J = 14.8, 7.2 Hz, 1H), 7.82−7.87 (m, 2H), 7.77−7.81 (m, 2H), 7.74 (dd, J = 9.0, 5.3 Hz, 1H), 7.60−7.67 (m, 1H), 7.55 (dd, J = 8.1, 4.1 Hz, 1H), 7.47 (d, J = 8.5 Hz, 1H), 7.43 (d, J = 8.2 Hz, 1H), 7.33−7.39 (m, 7H), 7.27−7.32 (m, 7H), 7.19−7.26 (m, 4H), 7.13−7.18 (m, 5H), 7.08−7.12 (m, 1H), 7.03−7.07 (m, 1H), 6.99 (d, J = 7.9 Hz, 3H), 6.86−6.96 (m, 3H), 6.62−6.66 (m, 1H), 6.58 (d, J = 11.9 Hz, 1H), 6.43−6.50 (m, 2H), 6.38−6.42 (m, 1H), 6.26 (d, J = 2.7 Hz, 1H), 2.43 (s, 3H), 2.31 (s, 3H), 2.27−2.30 (m, 6H). ^{13}C{^{1}H} NMR (126 MHz, CDCl$_3$) δ 151.8, 151.5, 147.8, 142.4, 141.6, 139.7, 136.2, 134.5, 132.8, 132.2, 131.5, 131.0, 130.8, 130.7, 129.7, 129.4, 129.2, 129.1, 129.0, 128.7, 128.6, 128.3, 128.1, 128.0, 127.9, 127.8, 127.6, 127.4, 127.3, 127.3, 127.1, 127.0, 126.7, 126.6, 126.3, 126.1, 125.8, 125.0, 124.2, 124.1, 123.9, 123.9, 123.8, 123.5, 122.0, 121.9, 121.5, 120.1, 118.0, 117.9, 117.7, 117.4, 117.3, 117.1, 116.6, 116.5, 115.7, 114.1, 106.3, 97.2, 29.7, 29.3, 21.4, 21.0. HRMS (ESI) m/z calcd for $C_{38}H_{31}O_4N_2S$ [(M + H)$^+$] 611.1999 found 611.1990.

HPLC: (Chiralpak IC Column, i PrOH/hexane = 05/95, flow rate = 1 mL/min, λ = 254 nm, 23 °C): tR$_1$ = 35.78 min, tR$_2$ = 39.16 min, dr = 1:1.

N-(3-(2-(4-Fluorophenyl)indolizin-1-yl)-4-hydroxy-5-(2-hydroxynaphthalen-1-yl)phenyl)-4-methylbenzenesulfonamide (6c). Off-white solid, 57% yield (52 mg). MP.: 132−134 °C. ^{1}H NMR (500 MHz, CDCl$_3$) δ 8.21 (d, J = 6.9 Hz, 1H), 8.17 (d, J = 6.9 Hz, 1H), 7.85−7.88 (m, 2H), 7.78−7.84 (m, 2H), 7.64 (d, J = 8.0 Hz, 1H), 7.50 (d, J = 8.4 Hz, 2H), 7.46 (m, J = 8.0 Hz, 2H), 7.33−7.42 (m, 7H), 7.30−7.33 (m, 2H), 7.18−7.25 (m, 4H), 7.13−7.16 (m, 2H), 7.08−7.11 (m, 1H), 7.05 (m, J = 8.0 Hz, 2H), 6.96−7.03 (m, 6H), 6.85−6.92 (m, 2H), 6.80−6.85 (m, 2H), 6.75−6.79 (m, 2H), 6.57−6.67 (m, 2H), 6.52 (d, J = 4.2 Hz, 2H), 6.40−6.49 (m, 1H), 2.35 (s, 3H), 2.32 (s, 3H). ^{13}C{^{1}H} NMR (126 MHz, CDCl$_3$) δ 162.9, 162.7, 160.9, 160.7, 152.4, 152.4, 151.5, 151.2, 147.7, 147.6, 144.0, 143.8, 142.5, 141.0, 139.1, 138.6, 138.2, 136.0, 135.2, 134.9, 132.5, 132.3, 132.2, 130.8, 130.5, 130.3, 129.8, 129.7, 129.4, 129.1, 128.8, 128.1, 128.0, 127.7, 127.5, 127.3, 127.1, 126.9, 126.1, 125.9, 125.6, 125.3, 123.7, 123.6, 123.5, 123.3, 122.1, 122.0, 121.6, 120.7, 120.5, 120.3, 120.0, 119.0, 118.7, 117.8, 117.7, 117.4, 117.2, 117.1, 116.4, 116.2, 116.2, 115.6, 115.4, 114.8, 114.8, 114.6, 114.4, 113.1, 112.9, 111.2, 110.8, 106.7, 102.8, 98.4, 21.3, 21.2. ^{19}F NMR (376 MHz, CDCl$_3$) δ −113.77 (s, 1F), −114.58 (s, 1F), −115.56 (s, 1F). HRMS (ESI) m/z calcd for $C_{37}H_{28}O_4N_2FS$ [(M + H)$^+$] 615.1748 found 615.1734.

HPLC: (Chiralpak IC Column, i PrOH/hexane = 20/80, flow rate = 1 mL/min, λ = 254 nm, 23 °C): tR$_1$ = 17.94 min, tR$_2$ = 21.62 min, dr = 1:1.

N-(3-(2-(4-Cyanophenyl)indolizin-1-yl)-4-hydroxy-5-(2-hydroxynaphthalen-1-yl)phenyl)benzenesulfonamide (6d). Off-white gummy semisolid, 65% yield (40 mg). ^{1}H NMR (500 MHz, CDCl$_3$) δ 8.13 (dd, J = 6.5, 4.6 Hz, 1H), 7.81−7.85 (m, 2H),

7.77−7.80 (m, 2H), 7.65−7.75 (m, 3H), 7.56−7.63 (m, 4H), 7.44−7.50 (m, 6H), 7.36−7.41 (m, 6H), 7.29−7.34 (m, 4H), 7.22−7.26 (m, 6H), 7.12−7.20 (m, 4H), 7.08−7.11 (m, 1H), 7.02−7.07 (m, 1H), 6.97 (d, J = 9.5 Hz, 2H), 6.87−6.92 (m, 1H), 6.81−6.87 (m, 2H), 6.74−6.81 (m, 1H), 6.66−6.73 (m, 1H), 6.54−6.65 (m, 3H), 6.34−6.47 (m, 1H). ^{13}C{^{1}H} NMR (101 MHz, CDCl$_3$) δ 152.5, 152.4, 151.2, 151.0, 147.7, 138.9, 138.9, 138.8, 138.8, 134.5, 134.3, 133.1, 132.5, 132.3, 131.9, 131.8, 131.6, 131.6, 131.2, 131.0, 130.7, 130.7, 128.7, 128.7, 128.6, 128.6, 128.4, 128.3, 128.1, 128.0, 127.7, 127.4, 127.4, 126.9, 126.9, 126.9, 126.8, 125.7, 125.3, 125.3, 125.2, 123.6, 123.6, 123.5, 123.5, 123.3, 121.9, 121.9, 120.6, 120.5, 119.4, 118.9, 118.4, 118.3, 117.6, 117.6, 117.4, 117.2, 117.2, 115.4, 115.4, 113.2, 113.2, 111.8, 109.7, 109.7, 98.4. HRMS (ESI) m/z calcd for C$_{37}$H$_{26}$O$_4$N$_3$S [(M + H)$^+$] 608.1639 found 608.1629.

N-(4-Hydroxy-3-(2-hydroxynaphthalen-1-yl)-5-(1-methyl-2-(naphthalen-2-yl)indolizin-3-yl)phenyl)-4-methylbenzenesulfonamide (6e). Gummy semisolid, 74% yield (57 mg). ^{1}H NMR (400 MHz, CDCl$_3$) δ 8.12 (d, J = 6.9 Hz, 2H), 7.78−7.88 (m, 4H), 7.44 (d, J = 8.3 Hz, 3H), 7.49 (d, J = 8.1 Hz, 2H), 7.30−7.40 (m, 11H), 7.20−7.25 (m, 5H), 7.14−7.20 (m, 5H), 7.04−7.14 (m, 7H), 6.93−7.04 (m, 7H), 6.57−6.66 (m, 3H), 6.50−6.57 (m, 3H), 2.44 (s, 3H), 2.42 (s, 3H), 2.31 (s, 3H), 2.29 (s, 3H). ^{13}C{^{1}H} NMR (126 MHz, CDCl$_3$) δ 152.8, 151.5, 151.4, 151.2, 147.5, 143.5, 139.0, 138.6, 137.2, 136.0, 136.0, 135.2, 135.0, 133.1, 132.8, 132.6, 132.5, 132.4, 132.1, 131.9, 131.3, 131.2, 130.7, 130.4, 130.0, 129.6, 128.9, 128.9, 128.7, 128.5, 128.1, 128.0, 127.9, 127.8, 127.7, 127.5, 127.4, 127.2, 127.2, 127.1, 127.0, 126.9, 126.0, 125.9, 125.6, 125.5, 125.4, 123.8, 123.7, 123.6, 123.5, 121.9, 121.8, 121.7, 121.2, 119.9, 119.8, 119.3, 117.7, 117.6, 117.6, 117.4, 117.4, 117.1, 116.9, 116.8, 116.5, 116.4, 115.5, 113.9, 113.1, 113.0, 112.6, 110.9, 106.4, 106.3, 94.1, 21.3, 21.0, 9.6, 9.1. HRMS (ESI) m/z calcd for C$_{42}$H$_{33}$O$_4$N$_2$S [(M + H)$^+$] 661.2156 found 661.2154.

N-(4-Hydroxy-3-(2-hydroxynaphthalen-1-yl)-5-(2-phenylindolizin-3-yl)phenyl)-4-methylbenzene sulfonamide (6f). Off-white semisolid, 55% yield (49 mg). ^{1}H NMR (500 MHz, CDCl$_3$) δ 8.26 (d, J = 7.1 Hz, 1H), 8.23 (d, J = 6.9 Hz, 1H), 8.05 (t, J = 1.8 Hz, 1H), 8.02 (t, J = 1.8 Hz, 1H), 7.93 (dd, J = 8.1, 1.5 Hz, 1H), 7.90 (dd, J = 8.2, 1.6 Hz, 1H), 7.80−7.85 (m, 4H), 7.74−7.79 (m, 2H), 7.72 (d, J = 8.0 Hz, 2H), 7.45 (dd, J = 8.2, 5.7 Hz, 5H), 7.40−7.42 (m, 2H), 7.36−7.39 (m, 2H), 7.33−7.36 (m, 4H), 7.28−7.32 (m, 2H), 7.24−7.26 (m, 4H), 7.18−7.23 (m, 2H), 7.07−7.15 (m, 1H), 7.03−7.05 (m, 1H), 7.02 (s, 1H), 6.90−6.97 (m, 4H), 6.88 (s, 1H), 6.82−6.86 (m, 1H), 6.64−6.69 (m, 2H), 6.63 (s, 2H), 5.22 (br. s, 1H), 2.25 (s, 6H). ^{13}C{^{1}H} NMR (126 MHz, CDCl$_3$) δ 152.5, 151.7, 151.6, 148.0, 147.4, 144.4, 137.4, 136.0, 135.9, 135.2, 135.1, 133.9, 133.9, 132.8, 132.7, 131.9, 131.0, 130.2, 129.3, 129.1, 128.9, 128.9, 128.6, 128.3, 128.3, 127.7, 127.4, 127.3, 126.3, 126.1, 125.2, 124.9, 124.8, 124.7, 124.6, 124.2, 123.9, 123.8, 122.7, 122.6, 122.4, 122.1, 121.2, 120.8, 120.7, 119.9, 119.1, 118.7, 118.0, 118.0, 117.8, 117.7, 117.6, 117.5, 116.4, 116.1, 115.6, 115.5, 114.0, 113.5, 113.5, 112.0, 98.4, 98.3, 21.3, 21.3.

Experimental Procedure for the Synthesis of 8. To a 25 mL oven-dried round-bottom flask containing DCM (3 mL) were added quinone monoimine 7 (0.108 mmol, 50 mg), indolizine 1u (0.108 mmol, 22 mg), and AcOH (0.021 mmol). Then, the resulting reaction mixture was stirred at room temperature for 5 min. Upon completion of the reaction (monitored by TLC), the reaction mixture was dried under vacuum and purified by column chromatography (100−200 mesh silica) using 80/10 to 80/20 petroleum ether/ethyl acetate as the eluent to afford the corresponding product 8 in 67% yield (48 mg).

N-(4-Hydroxy-3,5-bis(2-(thiophen-2-yl)indolizin-3-yl) phenyl)-4-methylbenzenesulfonamide (8). White semisolid, 67% yield (48 mg). ^{1}H NMR (500 MHz, CDCl$_3$) δ 7.62 (d, J = 8.4 Hz, 2H), 7.48−7.52 (m, 1H), 7.37−7.40 (m, 2H), 7.32−7.36 (m, 1H), 7.23 (s, 2H), 7.20 (dt, J = 4.4, 2.4 Hz, 3H), 7.10−7.13 (m, 1H), 6.99−7.03 (m, 3H), 6.92−6.94 (m, 1H), 6.88−6.91 (m, 1H), 6.74−6.81 (m, 2H), 6.70−6.73 (m, 2H), 6.43−6.49 (m, 2H), 6.39−6.42 (m, 1H), 5.37 (s, 1H), 2.38 (s, 3H). ^{13}C{^{1}H} NMR (101 MHz, CDCl$_3$) δ 152.6, 152.4, 143.8, 137.5, 137.2, 135.8, 135.7, 133.8, 129.9, 129.7, 129.7, 129.6,

129.3, 129.2, 127.8, 127.6, 127.5, 127.3, 125.0, 124.4, 124.3, 124.2, 123.0, 122.9, 122.8, 122.7, 122.6, 119.4, 119.3, 119.2, 118.9, 118.8, 118.5, 118.4, 113.9, 113.7, 111.4, 110.9, 110.8, 98.7, 98.7, 21.6. HRMS (ESI) m/z calcd for C$_{37}$H$_{28}$O$_3$N$_3$S$_3$ [(M + H)$^+$] 658.1287 found 658.1271.

Experimental Procedure for the Synthesis of 3a from N-Tosyl-p-aminophenol. To a 50 mL round-bottom flask containing DCM (10 mL) were added *N*-tosyl-p-aminophenol **9** (0.380 mmol, 100 mg), indolizine **1a** (0.380 mmol, 74 mg), and PIDA (0.418 mmol, 135 mg). Then, the resulting reaction mixture was stirred at room temperature for 1 h. Upon completion of the reaction (monitored by TLC), the reaction mixture was dried under vacuum. Then, the crude reaction mixture was diluted with ethyl acetate (10 mL), washed with brine, and eluted with EtOAc (10 mL × 3). The organic layer was evaporated, and the crude residue was preadsorbed on silica gel and purified by column chromatography (100−200 mesh silica) using 80/30 petroleum ether/ethyl acetate as the eluent to afford the corresponding product **3a** in 61% yield (105 mg).

Large-Scale Synthesis of 3u. The reaction mixture of **1u** (3.065 mmol, 610 mg), **2a** (3.065 mmol, 800 mg), and AcOH (0.6 mL) in MeCN was stirred at rt for 10 min and dried under vacuum. Then, the crude reaction mixture was diluted with ethyl acetate (30 mL), washed with brine, and eluted with EtOAc (25 mL × 3). Then, the crude residue was purified by column chromatography (100−200 mesh silica) using 80/30 petroleum ether/ethyl acetate as the eluent to produce **3u** in 90% yield (1.27 g).

Large-Scale Synthesis of 3i. To an oven-dried 100 mL round-bottom flask containing MeCN were added indolizine **1i** (2.87 mmol, 652 mg), quinone monoimine **2a** (2.87 mmol, 750 mg), and AcOH (0.5 mL), stirred at rt for 20 min, and then the reaction mixture was dried under vacuum. Then, the crude reaction mixture was diluted with ethyl acetate (30 mL), washed with brine, and eluted with EtOAc (30 mL × 3). Then, the crude residue was purified by column chromatography (100−200 mesh silica) using 80/20 petroleum ether/ethyl acetate as the eluent to produce **3i** in 79% yield (1.21 g).

■ ASSOCIATED CONTENT

Ⓢ Supporting Information

The Supporting Information is available free of charge at https://pubs.acs.org/doi/10.1021/acs.joc.1c03019.

> Analytical data (^{1}H, ^{13}C, mass copies of all new compounds and DFT calculation studies) (PDF)
>
> Full reference of Gaussian software; computational methods; PES for Pathway 1 and Pathway 2; cartesian co-ordinate, frequencies, absolute energies, and ball and stick models for each computed stationary point (PDF)

■ AUTHOR INFORMATION

Corresponding Author

Gurunath Suryavanshi − *Chemical Engineering & Process Development Division, CSIR-National Chemical Laboratory, Pune 411008, India; Academy of Scientific and Innovative Research (AcSIR), Ghaziabad 201 002, India;* ⦿ orcid.org/0000-0002-6299-0914; Phone: 020-2590-2547; Email: gm.suryavanshi@ncl.res.in; Fax: 020-2590-2676

Authors

Kishor D. Mane − *Chemical Engineering & Process Development Division, CSIR-National Chemical Laboratory, Pune 411008, India; Academy of Scientific and Innovative Research (AcSIR), Ghaziabad 201 002, India*

Anirban Mukherjee − *Organic Chemistry Division, CSIR-National Chemical Laboratory, Pune 411008, India; The Institute of Scientific and Industrial Research (ISIR), Osaka University, Ibaraki-shi, Osaka 567- 0047, Japan;* ⦿ orcid.org/0000-0001-7083-7322

Gourab Kanti Das − *Department of Chemistry, Institute of Science (Siksha Bhavana), Santiniketan 731235 West Bengal, India;* ● orcid.org/0000-0002-1235-3298

■ REFERENCES
(1) (a) Tewari, D.; Kumar, P.; Sharma, P. Pharmacognostical Evaluation of Elaeocarpus sphaericus (Rudraksha) Leaves. *Int. J. Pharmacogn. Phytochem. Res.* **2013**, *5*, 147−150. (b) Colegate, S. M.; Dorling, P. R. *Handbook of Plant and Fungal Toxicants*; D'Mello, J. P. F., Ed.; CRC Press: Boca Raton, 1997; Chapter 1, pp 1−18.
(2) (a) Mehta, L. K.; Parrick, J. The Synthesis of Three Indolizine Derivatives of Interest as Non-Isomerizable Analogues of Tamoxifen. *J. Heterocycl. Chem.* **1995**, *32*, 391−394. (b) Sharma, V.; Kumar, V. Indolizine: A Biologically Active Moiety. *Med. Chem. Res.* **2014**, *23*, 3593−3606. (c) Hazra, A.; Mondal, S.; Maity, A.; Naskar, S.; Saha, P.; Paira, R.; Sahu, K. B.; Paira, P.; Ghosh, S.; Sinha, C.; Samanta, A.; Banerjee, S.; Mondal, N. B. Amberlite-IRA-402(OH): Ion Exchange Resin Mediated Synthesis of Indolizines, Pyrrolo [1,2-a] Quinolines and Isoquinolines: Antibacterial and Antifungal Evaluation of the Products. *Eur. J. Med. Chem.* **2011**, *46*, 2132−2140. (d) Gundersen, L. L.; Negussie, A. H.; Rise, F.; Ostby, O. B. Antimycobacterial Activity of 1-Substituted Indolizines. *Arch. Pharm. Med. Chem.* **2003**, *336*, 191−195. (e) Nasir, A. I.; Gundersen, L.-L.; Rise, F.; Antonsen, O.; Kristensen, T.; Langhelle, B.; Bast, A.; Custers, I.; Haenen, G. R.; Wikstrom, H. Inhibition of Lipid Peroxidation Mediated by Indolizines. *Bioorg. Med. Chem. Lett.* **1998**, *8*, 1829−1832.
(3) (a) Gundersen, L.-L.; Charnock, C.; Negussie, A.-H.; Rise, F.; Teklu, S. Synthesis of indolizine derivatives with selective antibacterial activity against Mycobacterium tuberculosis. *Eur. J. Pharm. Sci.* **2007**, *30*, 26−35. (b) Narajji, C.; Karvekar, M. D.; Das, A. K. Synthesis and antioxidant activity of 3,3′-diselanediylbis (N, N-disubstituted indolizine-1-carboxamide) and derivatives. *S. Afr. J. Chem.* **2008**, *61*, 53−55. (c) Sandeep, C.; Venugopala, K. N.; Gleiser, R. M.; Chetram, A.; Padmashali, B.; Kulkarni, R. S.; Venugopala, R.; Odhav, B. Greener synthesis of indolizine analogue using water as a base and solvent: Study for larvicidal activity against Anopheles arabiensis. *Chem. Biol. Drug. Des.* **2016**, *88*, 899−904. (d) Huang, W.; Zuo, T.; Luo, X.; Jin, H.; Liu, Z.; Yang, Z.; Yu, X.; Zhang, L.; Zhang, L. Indolizine derivatives as HIV-1 VIF-Elongin C interaction inhibitors. *Chem. Biol. Drug. Des.* **2013**, *81*, 730−741.
(4) Kim, D.; Lee, J. H.; Kim, H. Y.; Shin, J.; Kim, K.; Lee, S.; Park, J.; Kim, J.; Kim, Y. Fluorescent indolizine derivative YI-13 detects amyloid-β monomers, dimers, and plaques in the brain of 5XFAD Alzheimer transgenic mouse model. *PLoS One* **2020**, *15*, No. e0243041.
(5) Arvin-Berod, M.; Desroches-Castan, A.; Bonte, S.; Brugière, S.; Coute, Y.; Guyon, L.; Feige, J.-J.; Baussanne, I.; Demeunynck, M. Indolizine-based scaffolds as efficient and versatile tools: Application to the synthesis of biotin-tagged antiangiogenic drugs. *ACS Omega* **2017**, *2*, 9221−9230.

(6) (a) Huckaba, A. J.; Giordano, F.; McNamara, L. E.; Dreux, K. M.; Hammer, N. I.; Tschumper, G. S.; Zakeeruddin, S. M.; Grätzel, M.; Nazeeruddin, M. K.; Delcamp, J. H. Indolizine-Based Donors as Organic Sensitizer Components for Dye-Sensitized Solar Cells. *Adv. Energy Mater.* **2014**, *5*, No. 1401629. (b) Huckaba, A. J.; Yella, A.; Brogdon, P.; Murphy, J. S.; Nazeeruddin, M. K.; Grätzel, M.; Delcamp, J. H. A Low Recombination Rate Indolizine Sensitizer for Dye-Sensitized Solar Cells. *Chem. Commun.* **2016**, *52*, 8424−8427.
(7) (a) Ji, R.; Liu, A.; Shen, S.; Cao, X.; Li, F.; Ge, Y. An indolizine-rhodamine-based FRET fluorescence sensor for highly sensitive and selective detection of Hg²⁺ in living cells. *RSC Adv.* **2017**, *7*, 40829−40833. (b) Zheng, X.; Ji, R.; Cao, X.; Ge, Y. FRET-based radiometric fluorescent probe for Cu²⁺ with a new indolizine fluorophore. *Anal. Chimi. Acta* **2017**, *978*, 48−54.
(8) Ge, Y.; Liu, A.; Dong, J.; Duan, G.; Cao, X.; Li, F. A simple pH fluorescent probe based on new fluorophore indolizine for imaging of living cells. *Sens. Actuators, B* **2017**, *247*, 46−52.
(9) Song, Y. R.; Lim, C. W.; Kim, T. W. Synthesis and photophysical properties of 1,2-diphenylindolizine derivatives: fluorescent blue-emitting materials for organic light-emitting device. *Luminescence* **2016**, *31*, 364−371.
(10) (a) Becuwe, M.; Landy, D.; Delattre, F.; Cazier, F.; Fourmentin, S. Fluorescent Indolizine-β-Cyclodextrin Derivatives for the Detection of Volatile Organic Compounds. *Sensors* **2008**, *8*, 3689−3705. (b) Surpateanu, G. G.; Becuwe, M.; Lungu, N. C.; Dron, P. I.; Fourmentin, S.; Landy, D.; Surpateanu, G. Photochemical behaviour upon the inclusion for some volatile organic compounds in new fluorescent indolizine β-cyclodextrin sensors. *J. Photochem. Photobiol., A* **2007**, *185*, 312−320.
(11) (a) Sadowski, B.; Klajn, J.; Gryko, D. T. Recent advances in the synthesis of indolizines and their π-expanded analogues. *Org. Biomol. Chem.* **2016**, *14*, 7804−7828. (b) Lee, J. H.; Kim, I. Cyclo-aromatization Approach to Polysubstituted Indolizines from 2-Acetylpyrroles: Decoration of the Pyridine Unit. *J. Org. Chem.* **2013**, *78*, 1283−1288. (c) Joshi, D. R.; Kim, I. Correction to "Michael-Aldol Double Elimination Cascade to Make Pyridines: Use of Chromone for the Synthesis of Indolizines. *J. Org. Chem.* **2021**, *86*, 10235−10248.
(12) (a) Lins, C. L.; Block, J. H.; Doerge, R. F. Nitro-para-and meta-substituted 2-phenylindolizines as potential antimicrobial agents. *J. Pharm. Sci.* **1982**, *71*, 556−561. (b) Wu, Y.; Ding, H.; Zhao, M.; Ni, Z.-H.; Cao, J.-P. Electrochemical and direct C-H methylthiolation of electron-rich aromatics. *Green Chem.* **2020**, *22*, 4906−4911. (c) Yu, Y.; Yue, Z.; Ding, L. G.; Zhou, Y.; Cao, H. Mn (OAc)₃ -Mediated Regioselective C-H Phosphonylation of Indolizines with H-Phosphonates. *Chem. Select* **2019**, *4*, 1117−1120. (d) Penteado, F.; Gomes, C. S.; Monzon, L. I.; Perin, G.; Silveira, C. C.; Lenardão, E. J. Photocatalytic Synthesis of 3-Sulfanyl- and 1,3-Bis(sulfanyl)-indolizines Mediated by Visible Light. *Eur. J. Org. Chem.* **2020**, *2020*, 2110−2115. (e) Xia, J.-B.; Wang, X.-Q.; You, S.-L. Synthesis of Biindolizines through Highly Regioselective Palladium-Catalyzed C-H Functionalization. *J. Org. Chem.* **2009**, *74*, 456−458. (f) Xia, J.-B.; You, S.-L. Synthesis of 3-Haloindolizines by Copper(II) Halide Mediated Direct Functionalization of Indolizines. *Org. Lett.* **2009**, *11*, 1187−1190. (g) Seregin, I. V.; Ryabova, V.; Gevorgyan, V. Direct Palladium-Catalyzed Alkynylation of N-Fused Heterocycles. *J. Am. Chem. Soc.* **2007**, *129*, 7742−7743. (h) Yang, Y.; Cheng, K.; Zhang, Y. Highly Regioselective Palladium-Catalyzed Oxidative Coupling of Indolizines and Vinylarenes via C-H Bond Cleavage. *Org. Lett.* **2009**, *11*, 5606−5609. (i) Jung, Y.; Kim, I. C3 functionalization of indolizines via In(III)-catalyzed three-component reaction. *Org. Biomol. Chem.* **2015**, *13*, 10986−10994.
(13) (a) Teng, L.; Liu, X.; Guo, P.; Yu, Y.; Cao, H. Visible-Light-Induced Regioselective Dicarbonylation of Indolizines with Oxoaldehydes via Direct C−H Functionalization. *Org. Lett.* **2020**, *22*, 3841−3845. (b) Masumura, M.; Yamashita, Y. Addition reactions of indolizine derivatives with diethyl azodicarboxylate. *Heterocycles* **1979**, *12*, 787−790. (c) Joshi, D. R.; Seo, Y.; Heo, Y.; Park, S-h.; Lee, Y.; Namkung, W.; Kim, I. Domino [4 + 2] Annulation Access to

Quinone-Indolizine Hybrids: Anticancer *N*-Fused Polycycles. *J. Org. Chem.* **2020**, *85*, 10994−11005. (d) Lee, S.; Kim, S.; Yoon, S. H.; Dagar, A.; Kim, I. Diastereoselective Synthesis of Densely Functionalized 3a,8a-Dihydro-8*H*-furo[3,2-*a*]pyrrolizines through One-Pot Three-Component Assembly. *J. Org. Chem.* **2021**, *86*, 12367−12377. (e) Park, C.-H.; Ryabova, V.; Seregin, I. V.; Sromek, A. W.; Gevorgyan, V. Palladium-Catalyzed Arylation and Heteroarylation of Indolizines. *Org. Lett.* **2004**, *6*, 1159−1162.

(14) (a) Chen, F.-M.; Huang, F.-D.; Yao, X.-Y.; Li, T.; Liu, F. S. Direct C-H heteroarylation by an acenaphthyl based *α*-diimine palladium complex: improvement of the reaction efficiency for bi(hetero)aryls under aerobic conditions. *Org. Chem. Front.* **2017**, *4*, 2336−2342. (b) Correia, J. T. M.; List, B.; Coelho, f. Catalytic Asymmetric Conjugate Addition of Indolizines to *α*,*β*-Unsaturated Ketones. *Angew. Chem., Int. Ed.* **2017**, *56*, 7967−7970. (c) Zhang, Y.-Z.; Sheng, F.-T.; Zhu, Z.; Li, Z.-M.; Zhang, S.; Tan, W.; Shi, F. Organocatalytic C3-functionalization of indolizines: synthesis of biologically important indolizine derivatives. *Org. Biomol. Chem.* **2020**, *18*, 5688−5696.

(15) (a) Bansode, A. H.; Suryavanshi, G. Visible-Light-Induced Controlled Oxidation of N-Substituted 1,2,3,4-Tetrahydroisoquinolines for the Synthesis of 3,4-Dihydroisoquinolin-1(2*H*)-ones and Isoquinolin-1(2*H*)-ones. *Adv. Synth. Catal.* **2021**, *363*, 1390−1400. (b) Bhoite, S. P.; Bansode, A. H.; Suryavanshi, G. Radical Rearrangement of Aryl/Alkylidene Malononitriles via Aza Michael Addition/Decynoformylation/Addition Sequence: An Access to *α*-Aminonitriles and *α*-Aminoamides. *J. Org. Chem.* **2020**, *85*, 14858−14865. (c) More, S. G.; Kamble, R. B.; Suryavanshi, G. Oxidative Radical-Mediated Addition of Ethers to Quinone Imine Ketals: An Access to Hemiaminals. *J. Org. Chem.* **2021**, *86*, 2107−2116.

(16) (a) Mane, K. D.; Mukherjee, A.; Vanka, K.; Suryavanshi, G. Metal-Free Regioselective Cross Dehydrogenative Coupling of Cyclic Ethers and Aryl Carbonyls. *J. Org. Chem.* **2019**, *84*, 2039−2047. (b) Mukherjee, A.; Ansari, A. J.; Reddy, S. R.; Das, G. K.; Singh, R. Mechanistic Investigations for the Formation of Active Hexafluoroisopropyl Benzoates Involving Aza-Oxyallyl Cation and Anthranils. *Asian J. Org. Chem.* **2020**, *9*, 2136−2143. (c) Mukherjee, A.; Singh, R.; Mane, K. D.; Das, G. K. Regioselectivity in metalloradical catalyzed C-H bond activation: A theoretical study. *J. Organomet. Chem.* **2022**, *957*, No. 122179.

(17) (a) Liu, J.-Y.; Yang, X.-C.; Liu, Z.; Luo, Y.-C.; Lu, H.; Gu, Y.-C.; Fang, R.; Xu, P.-F. An Atropo-enantioselective Synthesis of Benzo-Linked Axially Chiral Indoles via Hydrogen-Bond Catalysis. *Org. Lett.* **2019**, *21*, 5219−5224. (b) Li, X.-Q.; Yang, H.; Wang, J.-J.; Gou, B.-B.; Chen, J.; Zhou, L. Asymmetric Arylative Dearomatization of *β*-Naphthols Catalyzed by a Chiral Phosphoric Acid. *Chem. - Eur. J.* **2017**, *23*, 5381−5385. (c) Wang, J.-Z.; Jhou, J.; Xu, C.; Sun, H.; Kürti, L.; Xu, Q.-L. Symmetry in Cascade Chirality-Transfer Processes: A Catalytic Atroposelective Direct Arylation Approach to BINOL Derivatives. *J. Am. Chem. Soc.* **2016**, *138*, 5202−5205. (d) Chen, Y. H.; Qi, L. W.; Fang, F.; Tan, B. Organocatalytic Atroposelective Arylation of 2-Naphthylamines as a Practical Approach to Axially Chiral Biaryl Amino Alcohols. *Angew. Chem., Int. Ed.* **2017**, *56*, 16308−16312.

☐ Recommended by ACS

Visible Light-Promoted, Photocatalyst-Free C(sp²)—H Bond Functionalization of Indolizines *via* EDA Complexes

Kishor D. Mane,[a, b] Bapurao D. Rupanawar,[a, b] and Gurunath Suryavanshi*[a, b]

The catalyst and additive-free, photo-driven cross dehydrogenative coupling (CDC) reaction initiated by electron donor-acceptor (EDA) complexes between electron rich indolizines and electron poor quinones has been demonstrated. This green transformation reveals the advantages of operational simplicity, mild reaction conditions and good functional group tolerances.

Introduction

In the past decade, visible-light photocatalysis has become a hot area in synthetic organic chemistry for initiating various organic transformations under environmentally friendly and very mild reaction conditions. However, photoredox catalysis suffered from costly exogenous photosensitizers and complex organic dyes used in electron transfer (ET) processes.[1] At present, with the increasing demand for greener chemical processes, photo-driven organic transformations without external photocatalysts have gained significant attention due to their excellent synthetic value and high atom economy. The development of new organic transformations triggered by the photo-excitation of electron donor-acceptor (EDA) complexes is a field in its golden age.[2]

In recent years, the construction of important organic products by exciting the electron donor-acceptor (EDA) complexes has turned up as an efficient and straightforward pathway.[3] Generally, typical EDA complexes are a novel class of molecular clusters having the combination of electron rich donor molecules and electron poor acceptor substrates, which are called the charge-transfer (CT) complexes.[4]

While the electron acceptor molecule (A) and donor (D) may be colorless on their own whereas, after charge transfer, interlinkage between D and A results in a bathochromic shift to produce a visible light absorbing colored aggregate which upon excitation under visible light, gives reactive intermediates (charged radical ions) without the assistance of external photocatalyst (Figure 1).[5]

Indolizine and quinones are two privileged structures widely common in numerous bioactive natural products, pharmaceuticals, agrochemicals, approved commercial drugs, and functional organic materials.[6] The reduced form of indolizine
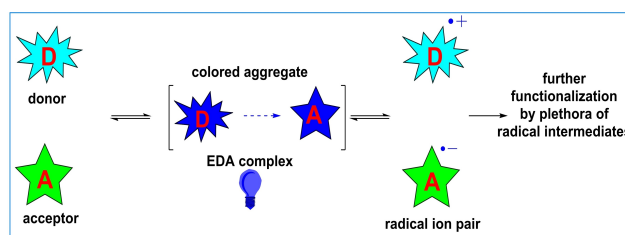
Figure 1. EDA complex driven photoionization

derivative is a well-known core nucleus in many alkaloids in natural product chemistry.[7] Indolizines are a bioisostere for indole, widely present in many biologically active molecules. They can apply in important fluorescent sensors and fluorescent materials in materials chemistry (Figure 2),[8] thus justifying current efforts towards C—H functionalization of indolizines. In the past few years, chemists have spent a great deal of time for synthesis and C—H functionalization of indolizines.[9] Direct C—H functionalization of indolizines at C-3 position has provided an ideal and dynamic method to grant the useful indolizine derivatives. To do that, transition metals are commonly employed in catalyzing borylation,[10] arylation,[11] acyloxylation[12] and propargylation[13] reactions. Despite this, few metal-free approaches are available in the literature for C—H functionalization of indolizines such as electrochemical sulfonylation,[14] alkylation,[15] and C—H dithiocarbamation[16]

[a] K. D. Mane, Dr. B. D. Rupanawar, Dr. G. Suryavanshi
    Chemical Engineering & Process Development Division,
    CSIR-National Chemical Laboratory,
    Dr. Homi Bhabha Road, Pune-411008, India
    E-mail: gm.suryavanshi@ncl.res.in
    www.ncl-india.org
[b] K. D. Mane, Dr. B. D. Rupanawar, Dr. G. Suryavanshi
    Academy of Scientific and Innovative Research (AcSIR),
    Ghaziabad 201002, India
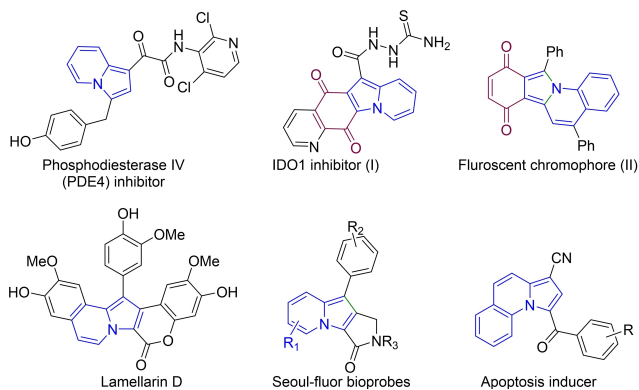
Figure 2. Some bioactive indolizine and quinones

EurJOC
European Journal of Organic Chemistry

Research Article
doi.org/10.1002/ejoc.202200261

**Chemistry
Europe**
European Chemical
Societies Publishing

reactions. More recently, visible light-induced operations on indolizines have arisen as a new functionalization strategy.[17] Nevertheless, examples of visible light-mediated C(sp^2)−H bond activation reactions by using indolizine as a donor are still unknown in the literature.

Recently in 2020, Lenardao and a co-worker reported the visible light-mediated mono and dithiolation of indolizines by using eosin Y as a photocatalyst[18] (Scheme 1a). Also, Cao et al. developed the cross dehydrogenative coupling (CDC) between oxoaldehyde and indolizine (Scheme 1b) by using visible light under very mild reaction conditions.[19] Inspired by the previous literature reports and our continuous efforts towards visible-light-induced C−H functionalization of heteroarenes,[20] herein we have described the photo-driven cross dehydrogenative coupling reaction between indolizines with quinones via EDA complexes as shown in Scheme 1c.

Results and Discussion

To measure the formation of electron donor-acceptor complexes from **1** and **2**, we investigated the UV-vis absorption spectroscopic properties of 0.05 M solutions **1** and **2** and the mixture of **1** and **2** in acetonitrile, respectively (Figure 3A). A blue color appeared when yellow colored **1** was mixed with

colorless **2**, a new band appeared, which could be attributed to the generation of charge-transfer (CT) band (Figure 3B).

Sunden and co-workers reported that the visible light promoted annulation reaction between N,N-substituted dialkyl anilines, and alkenes to synthesize substituted tetrahydroquinolines via EDA complexes.[21] Accordingly, we began our investigation by taking naphthoquinone **1a**, and indolizine **2a** as a model substrate in DCM under irradiation with blue LED (homemade setup), the desired product **3a** was formed in 35% yield (Table 1, entry 1). To our delight, the expected product **3a** was isolated in 61% yield along with difunctionalized by-product **3a'** in 6% yield, when MeCN is used as a solvent instead of DCM (Table 1, entry 2). An examination of other routine solvents, such as dichloroethane (DCE), 1,4-dioxane, tetrahydrofuran (THF), and dimethyl formamide (DMF), and the experimental results showed that DMF displayed a higher efficiency compared with other solvents (Table 1, entries 3–6). When the reaction was carried out with 2 equiv. of naphthoquinone, the desired product **3a** was isolated in 64% yield and slightly increment of **3a'** (13% yield) in 8 hours of reaction time (Table 1, entry 7).

The yield of **3a** and **3a'** was dramatically reduced to 21% and 0%, respectively, when the reaction time was increased to 16 hours (Table 1, entry 8). Surprisingly when reaction time was reduced from 8 to 4 hours, then the desired product was observed in 67% yield (Table 1, entry 9). From entries 8 and 9, it can be concluded that reaction time plays a crucial role in the formation of desired product; as the reaction is stirred for a longer time, the decomposition of products may occur.

The absence of light suppressed the formation of product **3a**, confirming the requirement for an excitation source (Table 1, entry 10). A trace amount of product formation was observed when the reaction was carried out in the dark (Table 1, entry 11). White LED is used instead of blue LED; no
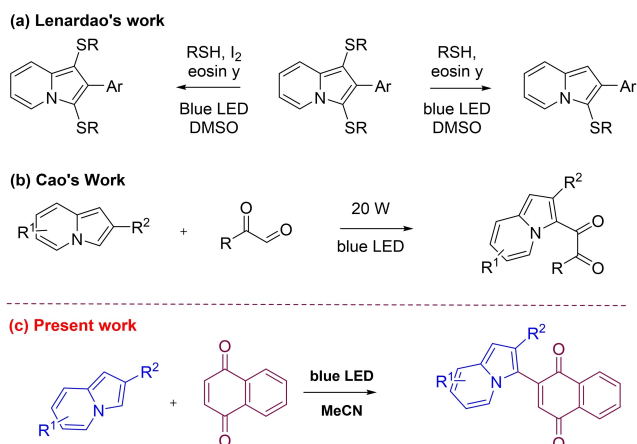
Scheme 1. Strategies for the C(sp^2)−H bond Functionalization of indolizines.
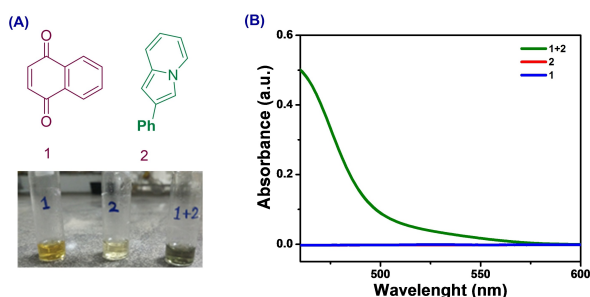
Figure 3. (A) Photos of 1, 2, and 1+2 in CH$_3$CN (0.05 M) (B) the charge transfer band of (1+2) EDA complex.

Table 1. Reaction Optimization.[a]

Entry	Solvent	Light source	Time [h]	Yield of **3a** [%]	Yield of **3a'** [%]
1	DCM	blue LED	8	35	0
2	MeCN	blue LED	8	61	6
3	DCE	blue LED	8	27	0
4	1,4-Dioxane	blue LED	8	trace	0
5	THF	blue LED	8	0	0
6	DMF	blue LED	8	47	0
7[b]	MeCN	blue LED	8	64	13
8[c]	MeCN	Blue LED	16	21	0
9	**MeCN**	**blue LED**	**4**	**67(44)[e]**	**8**
10[d]	MeCN	–	6	trace	0
11	MeCN	dark	6	trace	0
12	MeCN	White LED	4	51	0

[a] Reaction condition: **1a** (0.14 mmol), **2a** (0.14 mmol) in 2 mL of solvent irradiated with homemade setup of light in room temperature (blue LED 12 W); [b,c] Reaction was carried out by using 0.28 mmol of **1a**; [d] in the absence of light; [e] time of reaction is 2 h.

EurJOC
European Journal of Organic Chemistry

Research Article
doi.org/10.1002/ejoc.202200261

Chemistry Europe
European Chemical
Societies Publishing

such improvement in the yield of expected product is observed (Table 1, entry 12). We have also checked the solvent effect and the difference in UV-Vis absorption due to the solvent (see SI, Figure S1).

Under the optimal photocatalytic conditions (Table 1, entry 9), we proceeded to evaluate the scope for substituted indolizines. As shown in Scheme 2, several indolizines (**2a–2p**) with different substitution patterns such as electron withdrawing, electron releasing, and halo groups (Cl, Br, and F) were comparable with our cross dehydrogenative coupling (CDC) protocol. The para-position of phenyl ring on indolizine

substituted with -H, Cl, and OMe groups produce the expected CDC products (**3a,3b** & **3l**) in good yields with the minimal amount of side product (**3a′, 3b′**, & **3l′**) (Scheme 2). Methyl group present on C1, C6, and C7 position of indolizine gave the desired products in compatible yields (**3d, 3e, 3h** & **3i**). Halogen substituted indolizines including F, Cl, and Br are suitable donors and gave the expected products with 60–66% yields (**3c, 3f, 3k** & **3m**). Electron releasing group such as OMe, Me produces the coupled products (**3g** & **3j**) with 59% and 70%, respectively. Electron withdrawing groups present on indolizine rings gave excellent yields of CDC products (**3n** &
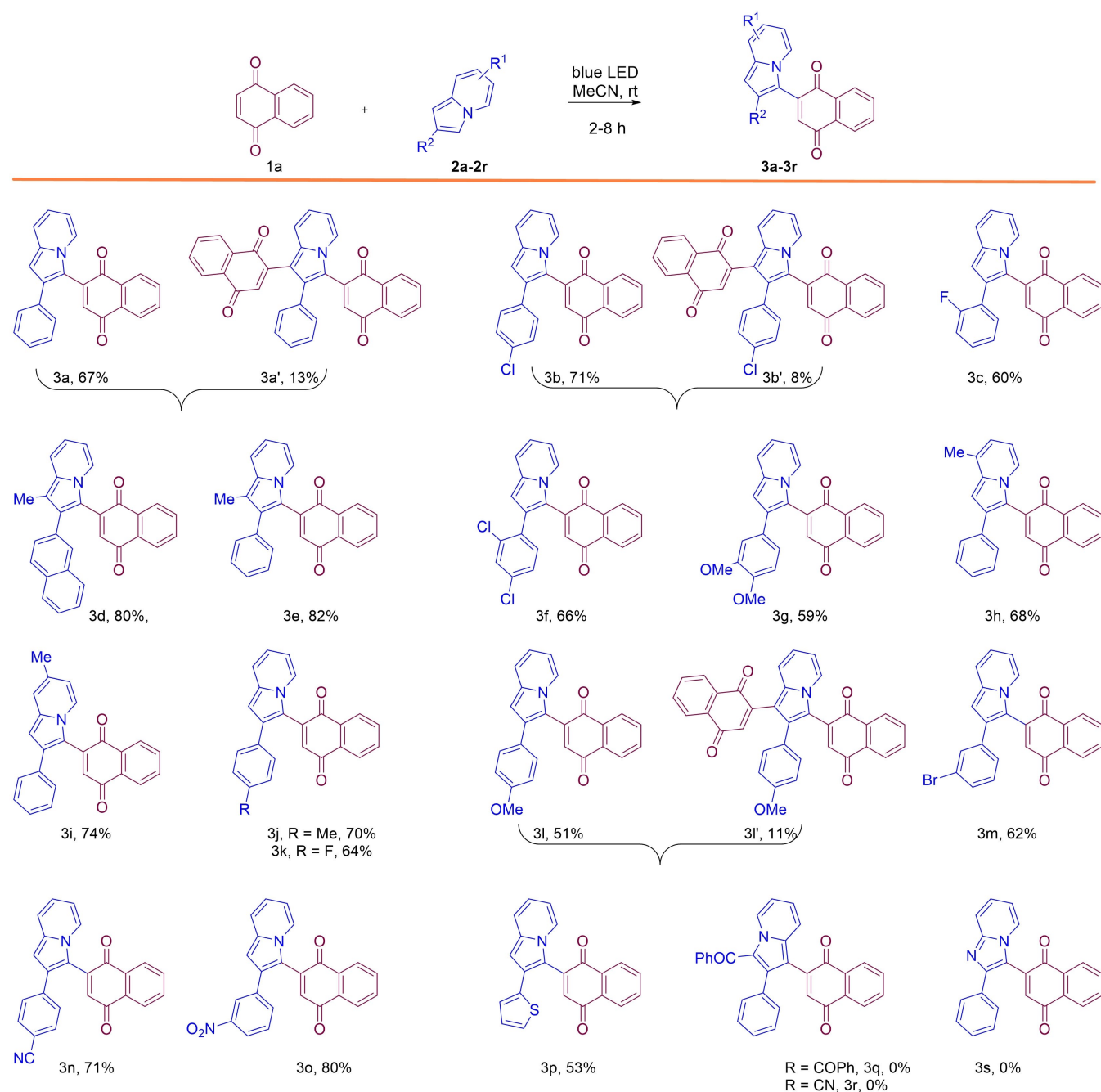
Scheme 2. Reaction conditions: **1a** (0.31 mmol), **2a** (0.31 mmol) and MeCN 3 mLwere irradiated with blue LEDs (12 W), r.t, for 2–8 h.

EurJOC
European Journal of Organic Chemistry

Research Article
doi.org/10.1002/ejoc.202200261

Chemistry
Europe
European Chemical
Societies Publishing

3o). Additionally, the heterocyclic indolizine also forms EDA complex and produces the desired product (**3p**) in 53% yield. Imidazopyridine and indolizines substituted at C-3 with electron-withdrawing groups is not suitable donors for the present transformation (**3r** & **3q**). After examining the substrate scope for indolizines, we next focused on investigating the scope of substituted quinones (Scheme 3). Naphthoquinone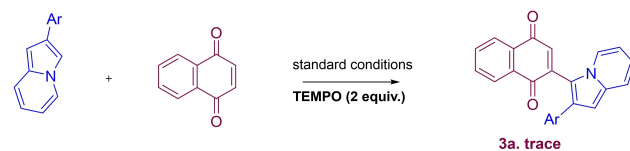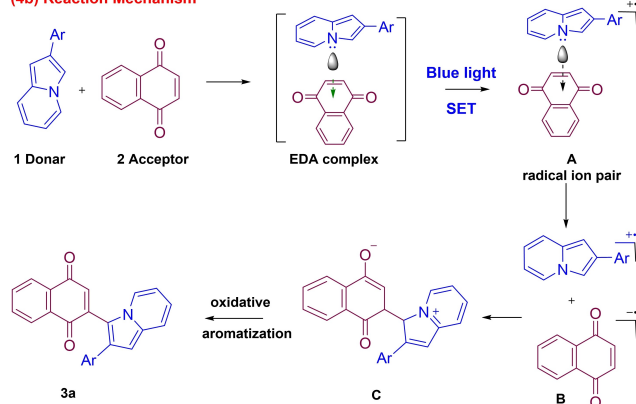s substituted with groups like Cl, NO2, and Br can form the stable EDA complex and give the CDC products (**5a–5c**) with acceptable yields as shown in Scheme 3.
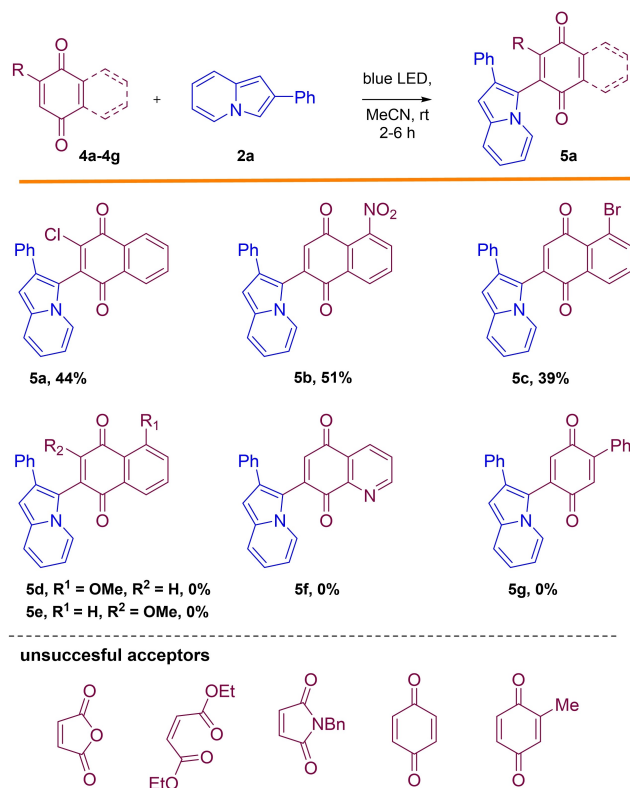
Electron donating groups present on the quinone moiety are not suitable for forming EDA complex (**5d–5e**). Also, the heterocyclic naphthoquinone and substituted benzoquinone could not produce the desired products (**5f** & **5g**). It was reasoned that the electron deficient conjugated π-system might be essential for forming the EDA complex and the following electron transfer process. Other acceptor moieties such as maleic anhydride, maleic ester, maleimides, and benzoquinones are remains unreacted in the reaction mixture.

Concerning the mechanistic aspects, when the 2,2,6,6-tetramethylpiperidine-1-oxyl (TEMPO) was added in the standard reaction condition, only a trace amount of the product was obtained (Scheme 4a). Next, we applied Job's method of continuous variations to determine the ratio of molar **1a/2a**, which was found to be 1:1 in CH_3CN (Figure 4). Based on previous reports[22] and experimental observations, a possible reaction mechanism is depicted in Scheme 4b. The interaction between indolizine **1** and naphthoquinone **2** can produce an EDA complex, followed by visible light (blue LED) initiated single electron transfer (SET) to give a radical ion pair **A**. Upon irradiation with visible light, generating the aryl radical ion pairs (**B**) simultaneously, followed by the oxidative addition of radical ion pairs, furnishes the expected coupled product **3a**.

Scheme 3. Reaction condition: **4a** (1 equiv.), **2a** (1 equiv.), MeCN (3 mL) were irradiated with blue LEDs (12 W), rt, for 2–8 h.

Scheme 4. Possible reaction mechanism.

Conclusion

In conclusion, we have developed a visible light promoted operationally simple and mild reaction conditions to construct functionally important derivatives of indolizine. Interestingly, this photo-driven CDC transformation can go ahead without adding any photocatalyst or additive. In place of catalyst, the formation of EDA complex between indolizine and quinone drives this photochemical reaction. Further attempts are ongoing in our laboratory to employ the freshly developed
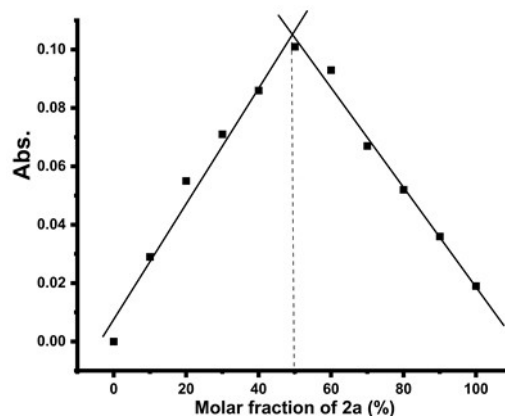

Figure 4. Job plot for a mixture of **1a** and **2a** in CH_3CN.

EurJOC
European Journal of Organic Chemistry

Research Article
doi.org/10.1002/ejoc.202200261

Chemistry Europe
European Chemical
Societies Publishing

predecessors in other transformations, which will be reported in due course.

Experimental Section

General Information

Commercially available solvents and reagents were used without further purification. Acetonitrile: Acros Organics, 99.9% extra dry, over molecular sieves. Technical solvents for column chromatography were used after simple distillation. The reactions were monitored by TLC visualized by UV (254 nm). The purification was done using column chromatography on silica gel (230–400 mesh). Nuclear Magnetic Resonance Spectra were recorded at room AV-400, AV-500, and Jeol-400 spectrometers in appropriate solvents using solvent signals as secondary standards, and the chemical shifts are shown in δ scales. High-Resolution Mass Spectra (HRMS) for all new compounds were recorded on an ESI$^+$ method and ORBITRAP mass analyzer (Thermo Scientific Q-Exactive, Accela 1250 pump). The ^{1}H and ^{13}C NMR spectra were recorded on Jeol-400 MHz NMR, 400 MHz NMR, and 500 MHz NMR spectrometers using residue solvent signals as an internal standard. ^{1}H NMR spectra were calibrated to the residual proton signal of chloroform-d$_1$ (δ = 7.27 ppm), Acetonitrile-d$_3$ (δ = 1.94 ppm) and ^{13}C NMR spectra were referenced to the ^{13}C triplet of CDCl$_3$ (δ = 77.16 ppm).

General Experimental Procedure for synthesis of 3a

A solution of indolizine 1a (0.31 mmol, 50 mg), quinone 2a (0.31 mmol, 61 mg), and CH$_3$CN (3 mL) were added into a 25 mL oven-dried quartz tube. Then the mixture was stirred under blue LED (12 W) at room temperature for 4 h monitored by TLC. The crude reaction mixture was diluted with ethyl acetate (5 mL) and water 5 mL, washed with brine and eluted with EtOAc (5 mL×2). The collected organic layer was evaporated, and the crude residue was purified by using silica gel column chromatography (100–200 mesh silica) and isolated by using 95/05 to 90/10 petroleum ether/ethyl acetate to give the product 3a.

2-(2-phenylindolizin-3-yl)naphthalene-1,4-dione(3a). Blue colored solid; mp: 158–160 °C; yield: 67% (74 mg).^{1}H NMR (400 MHz, CDCl$_3$) δ 8.14–8.08 (m, 1H), 8.07–8.02 (m, 1H), 7.94 (qd, J = 0.9, 7.2 Hz, 1H), 7.76 (m, J = 1.6, 7.4 Hz, 2H), 7.44 (td, J = 1.1, 9.0 Hz, 1H), 7.39–7.35 (m, 2H), 7.33–7.27 (m, 2H), 7.27–7.24 (m, 1H), 6.96 (s, 1H), 6.84 (ddd, J = 0.9, 6.6, 8.9 Hz, 1H), 6.72–6.68 (m, 1H), 6.61–6.54 (m, 1H).^{13}C{^{1}H} NMR (101 MHz, CDCl$_3$) δ 184.5 (CO), 183.8 (CO), 140.4 (Cq), 136.3 (CH), 136.0 (Cq), 135.7 (Cq), 134.0 (CH), 133.7 (Cq), 133.7 (CH), 132.7 (Cq), 132.2 (Cq), 128.9 (2CH), 128.6 (2CH), 127.1 (CH), 126.9 (CH), 126.1 (CH), 124.7 (CH), 119.9 (CH), 119.2 (CH), 114.9 (Cq), 111.6 (CH), 102.6 (CH). **HRMS** (ESI) m/z calculated for C$_{24}$H$_{16}$O$_2$N [(M+H)$^+$] 350.1176, found 350.1173

2,2′-(2-phenylindolizine-1,3-diyl)bis(naphthalene-1,4-dione) (3a′). Blue colored solid; mp: 254–256 °C; yield: 13% (20 mg).^{1}H NMR (400 MHz, CDCl$_3$) δ 8.06–8.13 (m, 3H), 7.98–8.04 (m, 1H), 7.90 (dt, J = 7.0, 1.0 Hz, 1H), 7.76–7.81 (m, 2H), 7.68–7.75 (m, 2H), 7.50 (dt, J = 9.1, 1.1 Hz, 1H), 7.16–7.26 (m, 5H), 7.04 (ddd, J = 9.1, 6.7, 1.0 Hz, 1H), 6.84 (s, 1H), 6.81 (s, 1H), 6.73 (td, J = 6.9, 1.3 Hz, 1H).^{13}C{^{1}H} NMR (101 MHz, CDCl$_3$) δ 184.7(CO), 184.4 (CO), 184.4 (CO), 183.5 (CO), 143.7(Cq), 139.8 (Cq), 138.6 (CH), 136.1 (CH), 135.2 (Cq), 134.2 (CH), 133.9 (CH), 133.9 (CH), 133.6 (CH), 133.5 (CH), 133.0 (Cq), 132.7 (Cq), 132.5 (Cq), 132.2 (Cq), 132.0 (Cq), 130.0 (2CH), 128.7 (2CH), 127.4 (CH), 127.2 (CH), 126.9 (CH), 126.3 (CH), 125.9 (CH), 125.2 (Cq), 122.2 (CH), 118.8 (CH), 117.8 (Cq), 112.6 (CH), 108.0 (Cq). **HRMS** (ESI) m/z calculated for C$_{34}$H$_{20}$O$_4$N [(M+H)$^+$] 506.1387, found 506.1387.

2-(2-(4-chlorophenyl)indolizin-3-yl)naphthalene-1,4-dione (3b). Blue colored solid; mp: 188–190 °C; yield: 71% (86 mg).^{1}H NMR (500 MHz, CDCl$_3$) δ 8.13 (dd, J = 1.4, 7.5 Hz, 1H), 8.07 (dd, J = 1.4, 7.5 Hz, 1H), 7.95 (d, J = 7.0 Hz, 1H), 7.83–7.75 (m, 2H), 7.45 (d, J = 8.9 Hz, 1H), 7.33–7.27 (m, 4H), 6.99 (s, 1H), 6.94–6.79 (m, 1H), 6.68 (br. s., 1H), 6.63–6.58 (m, 1H).^{13}C{^{1}H} NMR (101 MHz, CDCl$_3$) δ 184.5 (CO), 183.7 (CO), 140.2 (CH), 136.4 (CH), 136.1 (Cq), 134.3 (Cq), 134.1 (CH), 133.8 (CH), 133.0 (Cq), 132.6 (Cq), 132.4 (Cq), 132.1 (Cq), 130.1 (2CH), 128.9 (2CH), 127.2 (CH), 126.1 (CH), 124.6 (CH), 120.1 (CH), 119.3 (CH), 114.7 (Cq), 111.8 (CH), 102.5 (CH). **HRMS** (ESI) m/z calculated for C$_{24}$H$_{15}$O$_2$NCl [(M+H)$^+$] 384.0786, found 384.0771.

2,2′-(2-(4-chlorophenyl)indolizine-1,3-diyl)bis(naphthalene-1,4-dione) (3b′). Off white solid, mp: 280–282 °C; yield: 8% (13 mg).^{1}H NMR (400 MHz, CDCl$_3$) δ 8.14–8.07 (m, 3H), 8.04–7.98 (m, 1H), 7.91 (td, J = 1.0, 7.0 Hz, 1H), 7.84–7.78 (m, 2H), 7.77–7.70 (m, 2H), 7.51 (td, J = 1.1, 9.0 Hz, 1H), 7.24–7.20 (m, 2H), 7.19–7.12 (m, 2H), 7.05 (ddd, J = 1.0, 6.7, 9.1 Hz, 1H), 6.88 (s, 1H), 6.86 (s, 1H), 6.74 (dt, J = 1.3, 6.8 Hz, 1H). ^{13}C{^{1}H} NMR (101 MHz, CDCl$_3$) δ 184.7 (CO), 184.3 (CO), 183.3 (CO), 143.4 (Cq), 139.6 (Cq), 138.7 (CH), 136.2 (CH), 135.1 (Cq), 134.3 (CH), 134.0 (CH), 133.8 (CH), 133.6 (CH), 133.5 (Cq), 132.6 (Cq), 132.6 (Cq), 132.3 (Cq), 132.2 (Cq), 132.0 (Cq), 131.6 (Cq), 131.1 (2CH), 129.0 (2CH), 127.2 (CH), 127.0 (CH), 126.3 (CH), 126.0 (CH), 125.1 (CH), 122.3 (CH), 118.7 (CH), 117.6 (Cq), 112.8 (CH), 107.9 (Cq). **HRMS** (ESI) m/z calculated for C$_{34}$H$_{19}$O$_4$NCl [(M+H)$^+$] 540.0997, found 540.0996.

2-(2-(2-fluorophenyl)indolizin-3-yl)naphthalene-1,4-dione (3c). Blue colored solid; mp: 125–127 °C; yield: 60% (69 mg). ^{1}H NMR (500 MHz, CDCl$_3$) δ 8.10 (d, J = 7.2 Hz, 2H), 7.93 (d, J = 6.9 Hz, 1H), 7.71-7.81 (m, 2H), 7.46 (d, J = 8.8 Hz, 1H), 7.40 (td, J = 7.4, 1.5 Hz, 1H), 7.23–7.27 (m, 1H), 7.11–7.17 (m, 1H), 6.96–7.07 (m, 1H), 6.81–6.90 (m, 2H), 6.71 (s, 1H), 6.60 (t, J = 6.3 Hz, 1 H). ^{13}C{^{1}H} NMR (126 MHz, CDCl$_3$) δ 184.8 (CO), 183.5 (CO), 158.2-160.2 (d, J = 247 Hz,) 140.5 (Cq), 138.7 (Cq), 135.8 (Cq), 135.4 (CH), 134.0 (CH), 133.7 (CH), 132.6 (Cq), 132.1 (Cq), 131.6, 129.0 (d, J = 7.63 Hz), 127.1 (CH), 126.7 (Cq), 126.1 (CH), 124.8 (CH), 124.4 (CH), 123.3-123.4 (d, J = 14.31 Hz), 119.8 (CH), 119.3, 115.9-116.0 (d, J = 22.89 Hz), 111.7 (CH), 103.3 (CH). ^{19}F NMR (376 MHz, CDCl$_3$) δ −114.9 (s, 1F). **HRMS** (ESI) m/z calculated for C$_{24}$H$_{15}$O$_2$NF [(M+H)$^+$] 368.1081, found 368.1068.

2-(1-methyl-2-(naphthalen-2-yl)indolizin-3-yl)naphthalene −1,4-dione (3d). Blue colored solid; mp: 115–117 °C; yield: 80% (100 mg).^{1}H NMR (400 MHz, CDCl$_3$) δ 8.08–8.02 (m, 1H), 7.99–7.96 (m, 1H), 7.94 (dd, J = 1.2, 7.6 Hz, 1H), 7.85–7.79 (m, 2H), 7.79–7.74 (m, 2H), 7.73–7.64 (m, 2H), 7.49–7.44 (m, 3H), 7.40 (dd, J = 1.6, 8.4 Hz, 1H), 6.87 (ddd, J = 0.9, 6.5, 9.0 Hz, 1H), 6.83 (s, 1H), 6.59 (dt, J = 1.3, 6.8 Hz, 1H), 2.36 (s, 3H).

^{13}C{^{1}H} NMR (101 MHz, CDCl$_3$) δ 184.4 (CO), 184.0 (CO), 140.2 (Cq), 135.0 (CH), 134.6 (Cq), 133.9 (CH), 133.5 (CH), 133.4 (Cq), 132.9 (Cq), 132.8 (Cq), 132.6 (Cq), 132.2 (Cq), 132.2 (Cq), 129.0 (CH), 128.3 (CH), 128.1 (CH), 127.9 (CH), 127.7 (CH), 127.0 (CH), 126.1 (CH), 126.0 (CH), 125.9 (CH), 125.0 (CH), 119.1 (CH), 117.8 (CH), 115.7 (Cq), 111.6 (CH), 110.5 (Cq), 9.3 (CH$_3$). **HRMS** (ESI) m/z calculated for C$_{29}$H$_{20}$O$_2$N [(M+H)$^+$] 414.1489, found 414.1489.

2-(1-methyl-2-phenylindolizin-3-yl)naphthalene-1,4-dione (3e). Blue colored solid; mp: 123–125 °C; yield: 82% (94 mg).^{1}H NMR (400 MHz, CDCl$_3$) δ 8.04–8.09 (m, 1H), 7.96–8.01 (m, 1H), 7.93 (dt, J = 7.1, 1.0 Hz, 1H), 7.66–7.76 (m, 2H), 7.41 (dt, J = 8.9, 1.2 Hz, 1H), 7.30–7.36 (m, 2H), 7.23–7.29 (m, 3H), 6.81–6.85 (m, 1H), 6.79 (s, 1H), 6.47–6.65 (m, 1H), 2.30 (s, 3H).^{13}C{^{1}H} NMR (101 MHz, CDCl$_3$) δ 184.4 (CO), 184.0 (CO), 140.1 (Cq), 135.0 (Cq), 134.9 (CH), 134.4 (Cq), 133.8 (CH), 133.4 (CH), 133.0 (Cq), 132.8 (Cq), 132.2 (Cq), 130.1 (2CH), 128.4 (2CH), 126.9 (CH), 126.9 (CH), 125.9 (CH), 124.9 (CH), 119.0 (CH), 117.7 (CH), 115.5 (Cq), 111.4 (CH), 110.2 (Cq), 9.2 (CH$_3$). **HRMS**

EurJOC
European Journal of Organic Chemistry

Research Article
doi.org/10.1002/ejoc.202200261

Chemistry
Europe
European Chemical
Societies Publishing

(ESI) m/z calculated for $C_{25}H_{18}O_2N$ [(M+H)$^+$] 364.1332, found 364.1332.

2-(2-(2,4-dichlorophenyl)indolizin-3-yl)naphthalene-1,4-dione (3f).
Blue colored solid; mp: 129–131°C; yield: 66% (86 mg).[1]**H NMR** (500 MHz, CDCl$_3$) δ 8.08–8.14 (m, 2H), 7.95 (d, J=6.9 Hz, 1H), 7.76–7.81 (m, 2H), 7.47 (d, J=9.2 Hz, 1H), 7.43 (d, J=1.9 Hz, 1H), 7.29 (d, J=1.5 Hz, 1H), 7.23–7.27 (m, 1H), 6.86–6.95 (m, 1H), 6.76 (s, 1H), 6.60–6.67 (m, 2H). **^{13}C{^{1}H} NMR** (126 MHz, CDCl$_3$) δ 184.3 (CO), 183.2 (CO), 139.7 (Cq), 135.3 (Cq), 135.1 (CH), 133.8 (Cq), 133.6 (Cq), 133.5 (Cq), 132.6 (CH), 132.2 (Cq), 131.7 (Cq), 129.5 (CH), 129.0 (Cq), 126.9 (CH), 126.8 (CH), 125.9 (CH), 124.8 (CH), 121.4 (CH), 119.9 (CH), 119.0 (CH), 116.1 (Cq), 111.5 (CH), 109.7 (CH), 103.4 (CH). **HRMS** (ESI) m/z calculated for $C_{24}H_{14}O_2NCl_2$ [(M+H)$^+$] 418.0396, found 418.0392.

2-(2-(3,4-dimethoxyphenyl)indolizin-3-yl)naphthalene-1,4-dione (3g). Blue colored solid; mp: 170–172°C; yield: 59% (76 mg).[1]**H NMR** (500 MHz, CDCl$_3$) δ 8.14 (dd, J=7.2, 1.1 Hz, 1H), 8.06 (dd, J=7.6, 1.1 Hz, 1H), 8.00 (d, J=7.2 Hz, 1H), 7.74–7.83 (m, 2H), 7.46 (d, J=9.2 Hz, 1H), 7.07 (s, 1H), 6.93 (dq, J=4.2, 2.0 Hz, 2H), 6.87 (dd, J=8.6, 6.7 Hz, 1H), 6.81–6.85 (m, 1H), 6.58–6.64 (m, 1H), 6.71 (s, 1H), 3.89 (s, 3H), 3.74 (s, 3H). **^{13}C{^{1}H} NMR** (101 MHz, CDCl$_3$) δ 184.5 (CO), 183.9 (CO), 148.9 (Cq), 148.2 (Cq), 140.7 (Cq), 136.1 (CH), 135.6 (CH), 134.0 (CH), 133.7 (CH), 133.6 (Cq), 132.7 (Cq), 132.1 (Cq), 128.5 (Cq), 127.1 (CH), 126.0 (CH), 124.5 (CH), 121.3 (CH), 120.0 (CH), 119.1 (CH), 114.8 (Cq), 112.1 (CH), 111.5 (CH), 111.4 (CH), 102.4 (CH), 55.8 (CH$_3$), 55.7 (CH$_3$). **HRMS** (ESI) m/z calculated for $C_{26}H_{20}O_4N$ [(M+H)$^+$] 410.1387, found 410.1381.

2-(8-methyl-2-phenylindolizin-3-yl)naphthalene-1,4-dione (3h).
Blue colored solid; mp: 148–150°C; yield: 68% (77 mg).[1]**H NMR** (400 MHz, CD$_3$CN) δ 8.04–8.09 (m, 1H), 7.97–8.01 (m, 1H), 7.91 (d, J=0.8 Hz, 1H), 7.83 (ddd, J=7.6, 5.3, 1.7 Hz, 2H), 7.41–7.50 (m, 2H), 7.28–7.33 (m, 2H), 7.26 (d, J=7.3 Hz, 1H), 6.94 (s, 1H), 6.77 (d, J=0.8 Hz, 1H), 6.70 (s, 1H), 6.50–6.61 (m, 1H), 2.46 (s, 3H). **^{13}C{^{1}H} NMR** (101 MHz, CD$_3$CN) δ 185.8 (CO), 185.1 (CO), 141.9 (Cq), 138.9 (CH), 137.3 (Cq), 137.1 (Cq), 135.4 (CH), 135.2 (CH), 134.1 (Cq), 133.5 (Cq), 133.3 (Cq), 130.1 (2CH), 129.9 (2CH), 129.4 (Cq), 128.0 (CH), 127.9 (CH), 126.9 (CH), 124.1 (CH), 120.1 (CH), 116.3 (Cq), 112.7 (CH), 101.5 (CH), 18.4 (CH$_3$). **HRMS** (ESI) m/z calculated for $C_{25}H_{18}O_2N$ [(M+H)$^+$] 364.1332, found 364.1321.

2-(7-methyl-2-phenylindolizin-3-yl)naphthalene-1,4-dione (3i). Blue colored solid; mp: 143–145°C; yield: 74% (68 mg).[1]**H NMR** (500 MHz, CDCl$_3$) δ 8.13 (d, J=7.2 Hz, 1H), 8.02–8.08 (m, 1H), 7.92 (d, J=7.2 Hz, 1H), 7.71–7.85 (m, 2H), 7.36–7.43 (m, 2H), 7.33 (t, J=7.4 Hz, 2H), 7.23–7.28 (m, 1H), 6.96 (s, 1H), 6.60 (s, 1H), 6.46 (dd, J=7.2, 1.5 Hz, 1H), 2.35 (s, 3H). **^{13}C{^{1}H} NMR** (101 MHz, CDCl$_3$) δ 184.6 (CO), 184.1 (CO), 140.4 (Cq), 136.7 (Cq), 136.0 (Cq), 135.1 (CH), 134.2 (Cq), 133.9 (CH), 133.6 (CH), 132.9 (Cq), 132.3 (Cq), 130.8 (Cq), 128.9 (2CH), 128.6 (2CH), 127.1 (CH), 126.9 (CH), 126.0 (CH), 124.4 (Cq), 117.5 (CH), 114.4 (CH), 114.4 (CH), 101.7 (CH), 21.0 (CH$_3$). **HRMS** (ESI) m/z calculated for $C_{25}H_{18}O_2N$ [(M+H)$^+$] 364.1332, found 364.1320.

2-(2-(p–tolyl)indolizin-3-yl)naphthalene-1,4-dione (3j). Blue colored solid; mp: 74–76°C; yield: 70% (63 mg). [1]**H NMR** (500 MHz, CD$_3$CN) δ 8.06 (dd, J=7.2, 1.5 Hz, 1H), 7.97–8.03 (m, 2H), 7.75–7.91 (m, 2H), 7.46 (d, J=8.8 Hz, 1H), 7.31 (m, J=8.0 Hz, 2H), 7.12 (m, J=8.0 Hz, 2H), 6.91 (s, 1H), 6.86 (dd, J=9.0, 6.7 Hz, 1H), 6.70 (s, 1H), 6.51–6.64 (m, 1H), 2.30 (s, 3H). **^{13}C{^{1}H} NMR** (126 MHz, CD$_3$CN) δ 185.6 (CO), 184.9 (CO), 141.6 (Cq), 138.6 (CH), 137.7 (Cq), 136.4 (Cq), 135.2 (CH), 135.0 (CH), 133.9 (Cq), 133.8 (Cq), 133.6 (Cq), 133.3 (Cq), 130.3 (2CH), 129.8 (2CH), 127.7 (CH), 126.7 (CH), 126.0 (CH), 120.8 (CH), 119.8 (CH), 115.6 (Cq), 112.3 (CH), 102.6 (CH), 21.2 (CH$_3$). **HRMS** (ESI) m/z calculated for $C_{25}H_{18}O_2N$ [(M+H)$^+$] 364.1332, found 364.1333.

2-(2-(4-fluorophenyl)indolizin-3-yl)naphthalene-1,4-dione (3k). Blue colored solid; mp: 298–300°C; yield: 64% (59 mg).[1]**H NMR** (400 MHz, CDCl$_3$) δ 8.07–8.01 (m, 1H), 7.98 (dd, J=1.4, 7.4 Hz, 1H), 7.86 (d, J=7.1 Hz, 1H), 7.69 (dquin, J=1.5, 7.3 Hz, 2H), 7.36 (d, J=8.9 Hz, 1H), 7.28–7.22 (m, 2H), 6.93 (t, J=8.7 Hz, 2H), 6.88 (s, 1H), 6.78 (dd, J=6.8, 8.4 Hz, 1H), 6.58 (br. s., 1H), 6.54–6.47 (m, 1H).**^{13}C {^{1}H} NMR** (101 MHz, CDCl$_3$) δ 184.5 (CO), 183.8 (CO), 160.8-163.2 (J$_{F-Cq}$, 247 Hz), 140.3 (Cq), 136.3 (CH), 136.0 (CH), 134.1 (CH), 133.7 (CH), 132.7 (Cq), 132.1 (Cq), 131.8 (J$_{F-Cq}$, 3.6 Hz) 130.4 (2CH, J$_{F-C}$, 7.9 Hz), 127.1 (CH), 126.1 (CH), 124.6 (CH), 120.1 (Cq), 119.2 (2CH), 115.5-115.7 (2 CH, J$_{F-C}$, 21 Hz), 114.8 (Cq), 111.7 (CH), 102.6 (CH).

HRMS (ESI) m/z calculated for $C_{24}H_{15}O_2NF$ [(M+H)$^+$] 368.1081, found 368.1080.

2-(2-(4-methoxyphenyl)indolizin-3-yl)naphthalene-1,4-dione (3l). Blue colored solid; mp: 151–153°C; yield: 51% (49 mg).[1]**H NMR** (400 MHz, CDCl$_3$) δ 8.09–8.16 (m, 1H), 8.03–8.08 (m, 1H), 7.96 (dd, J=7.1, 0.8 Hz, 1H), 7.77 (dquin, J=7.3, 1.6 Hz, 2H), 7.45 (d, J=8.9 Hz, 1H), 7.21 (t, J=7.9 Hz, 1H), 7.00 (s, 1H), 6.91–6.97 (m, 2H), 6.86 (ddd, J=8.9, 6.6, 0.8 Hz, 1H), 6.77–6.83 (m, 1H), 6.71 (s, 1H), 6.53–6.64 (m, 1H), 3.73 (s, 3H). **^{13}C{^{1}H} NMR** (101 MHz, CDCl$_3$) δ 184.6 (CO), 183.9 (CO), 159.7 (Cq), 140.5 (Cq), 137.2 (Cq), 136.1 (CH), 136.0 (CH), 134.0 (CH), 133.7 (2CH), 133.6 (Cq), 132.8 (Cq), 132.2 (Cq), 129.6 (2CH), 127.1 (CH), 126.1 (CH), 124.6 (CH), 121.5 (CH), 120.0 (CH), 119.3 (CH), 115.0 (Cq), 114.5 (CH), 112.5 (CH), 111.7 (CH), 102.6 (CH), 55.2 (CH$_3$). **HRMS** (ESI) m/z calculated for $C_{25}H_{18}O_3N$ [(M+H)$^+$] 380.1281, found 380.1264.

2,2′-(2-(4-methoxyphenyl)indolizine-1,3-diyl)bis(naphthalene −1,4-dione) (3l′). Blue colored solid; mp: 255–257°C; yield: 11% (14 mg). [1]**H NMR** (500 MHz, CDCl$_3$) δ 8.06–8.17 (m, 3H), 8.04 (dd, J=7.4, 1.3 Hz, 1H), 7.88 (d, J=6.9 Hz, 1H), 7.68–7.82 (m, 4H), 7.48 (d, J=9.2 Hz, 1H), 7.09–7.15 (m, 2H), 6.97–7.05 (m, 1H), 6.85 (s, 1H), 6.75–6.82 (m, 3H), 6.64–6.74 (m, 1H), 3.75 (s, 3H). **^{13}C{^{1}H} NMR** (101 MHz, CDCl$_3$) δ 184.7 (CO), 184.5 (CO), 184.4 (CO), 183.5 (CO), 158.8 (Cq), 143.8 (Cq), 139.9 (Cq), 138.6 (CH), 136.1 (CH), 135.1 (Cq), 134.2 (CH), 133.9 (CH), 133.6 (CH), 133.4 (CH), 132.7 (Cq), 132.7 (Cq), 132.4 (Cq), 132.2 (Cq), 132.0 (2CH), 131.1 (CH), 127.2 (CH), 126.9 (CH), 126.2 (CH), 125.9 (2CH), 125.2 (CH), 122.1 (CH), 118.7 (Cq), 117.7 (Cq), 114.2 (2CH), 112.5 (CH), 108.0 (Cq), 55.1 (CH$_3$). **HRMS** (ESI) m/z calculated for $C_{35}H_{22}O_5N$ [(M+H)$^+$] 536.1492, found 536.1490.

2-(2-(3-bromophenyl)indolizin-3-yl)naphthalene-1,4-dione (3m). Blue colored solid; mp: 114–116°C; yield: 62% (67 mg).[1]**H NMR** (500 MHz, CDCl$_3$) δ 8.15 (dd, J=7.4, 1.3 Hz, 1H), 8.09 (dd, J=7.4, 1.3 Hz, 1H), 7.97 (d, J=7.2 Hz, 1H), 7.75–7.86 (m, 2H), 7.60 (t, J=1.7 Hz, 1H), 7.47 (d, J=8.8 Hz, 1H), 7.40 (d, J=8.0 Hz, 1H), 7.27–7.31 (m, 1H), 7.12–7.21 (m, 1H), 7.00 (s, 1H), 6.89 (dd, J=8.6, 6.7 Hz, 1H), 6.72 (s, 1H), 6.59–6.67 (m, 1H). **^{13}C{^{1}H} NMR** (126 MHz, CDCl$_3$) δ 184.2 (CO), 183.5 (CO), 139.9 (Cq), 137.7 (Cq), 136.1 (CH), 135.8 (Cq), 133.8 (CH), 133.5 (CH), 132.4 (Cq), 131.9 (Cq), 131.7 (Cq), 131.5 (CH), 129.8 (CH), 127.3 (CH), 126.9 (CH), 125.9 (CH), 124.3 (CH), 122.5 (Cq), 119.9 (CH), 119.1 (CH), 114.6 (Cq), 111.7 (CH), 102.3 (CH). **HRMS** (ESI) m/z calculated for $C_{24}H_{15}O_2NBr$ [(M+H)$^+$] 428.0281, found 428.0277.

4-(3-(1,4-dioxo-1,4-dihydronaphthalen-2-yl)indolizin-2-yl)benzonitrile (3n). Blue colored solid; mp: 207–209°C; yield: 71% (66 mg).[1]**H NMR** (500 MHz, CD$_3$CN) δ 8.05–8.13 (m, 2H), 7.98–8.03 (m, 2H), 7.80–7.89 (m, 2H), 7.64 (m, J=8.4 Hz, 2H), 7.60 (m, J=8.4 Hz, 2H), 7.52 (d, J=8.8 Hz, 1H), 7.03 (s, 1H), 6.91 (dd, J=8.6, 6.7 Hz, 1H), 6.82 (s, 1H), 6.60–6.71 (m, 1H). **^{13}C{^{1}H} NMR** (126 MHz, CD$_3$CN) δ 185.6 (CO), 184.7 (CO), 141.8 (Cq), 140.9 (Cq), 139.2 (CH), 136.5 (Cq), 135.4 (CH), 135.1 (CH), 133.8 (Cq), 133.5 (2CH), 131.4 (Cq), 130.5 (2CH), 127.8 (CH), 126.8 (CH), 125.9 (CH), 121.2 (CH), 120.2 (CH), 119.9 (Cq), 118 (Cq), 117.7 (CH), 115.9 (CH), 113.0 (CH), 111.0 (Cq), 102.6 (CH). **HRMS** (ESI) m/z calculated for $C_{25}H_{15}O_2N_2$ [(M+H)$^+$] 375.1128, found 375.1125.

2-(2-(3-nitrophenyl)indolizin-3-yl)naphthalene-1,4-dione (3o). Blue colored solid; mp: 198–200°C; yield: 80% (79 mg).[1]**H NMR**

EurJOC
European Journal of Organic Chemistry

Research Article
doi.org/10.1002/ejoc.202200261

Chemistry
Europe
European Chemical
Societies Publishing

(500 MHz, CDCl$_3$) δ 8.30 (t, J=1.8 Hz, 1H), 8.16–8.09 (m, 2H), 8.05 (dd, J=1.2, 7.6 Hz, 1H), 7.99 (d, J=7.0 Hz, 1H), 7.86–7.71 (m, 2H), 7.67 (d, J=7.9 Hz, 1H), 7.53–7.41 (m, 2H), 7.02 (s, 1H), 6.97–6.86 (m, 1H), 6.78 (s, 1H), 6.72–6.60 (m, 1H). ^{13}C{^{1}H} NMR (126 MHz, CDCl$_3$) δ 184.4 (CO), 183.7 (CO), 148.5 (Cq), 139.8 (Cq), 137.8 (CH), 136.7 (Cq), 136.2 (CH), 134.7 (CH), 134.3 (CH), 133.9 (Cq), 132.5 (Cq), 132.1 (Cq), 130.9 (CH), 129.5 (CH), 127.2 (CH), 126.3 (CH), 124.5 (CH), 123.6 (CH), 121.7 (CH), 120.5 (CH), 119.5 (CH), 114.8 (Cq), 112.3 (CH), 102.6 (CH). **HRMS** (ESI) m/z calculated for C$_{24}$H$_{15}$O$_4$N$_2$ [(M+H)$^+$] 395.1026, found 395.1023.

2-(2-(thiophen-2-yl)indolizin-3-yl)naphthalene-1,4-dione (3p). Blue colored solid; mp: 158–160 °C; yield: 53% (47 mg).^{1}H NMR (500 MHz, CDCl$_3$) δ 8.13–8.18 (m, 1H), 8.07–8.13 (m, 1H), 7.67–7.91 (m, 4H), 7.42 (d, J=8.8 Hz, 1H), 7.22 (d, J=4.6 Hz, 1H), 7.18 (s, 1H), 7.06 (d, J=3.1 Hz, 1H), 6.99 (dd, J=5.0, 3.4 Hz, 1H), 6.84 (dd, J=8.4, 6.9 Hz, 1H), 6.57 (t, J=6.5 Hz, 1H). ^{13}C{^{1}H} NMR (101 MHz, CDCl$_3$) δ 184.6 (CO), 183.7 (CO), 140.2 (Cq), 137.6 (CH), 137.3 (Cq), 135.6 (Cq), 134.0 (CH), 133.8 (CH), 132.8 (Cq), 132.2 (Cq), 127.6 (CH), 127.2 (CH), 126.2 (CH), 125.8 (Cq), 125.6 (CH), 125.4 (CH), 124.4 (CH), 120.0 (CH), 119.2 (CH), 114.6 (Cq), 111.7 (CH), 102.1 (CH). **HRMS** (ESI) m/z calculated for C$_{22}$H$_{14}$O$_2$NS [(M+H)$^+$] 356.0740, found 356.0737.

General Experimental Procedure for synthesis of 5a

A solution of indolizine **4a** (1 equiv.), quinone **2a** (1 equiv.), and CH$_3$CN (3 mL) was added into a 25 mL oven-dried quartz tube. Then the mixture was stirred under blue LED (12 W) at room temperature for 2–8 h monitored by TLC. The crude reaction mixture was diluted with ethyl acetate (5 mL) and water 5 mL, washed with brine and eluted with EtOAc (5 mL×3). The collected organic layer was evaporated and the crude residue was purified using silica gel column chromatography (100-200 mesh silica) and isolated using 95/05 to 90/10 petroleum ether/ethyl acetate to give the product **5a**.

2-chloro-3-(2-phenylindolizin-3-yl)naphthalene-1,4-dione (5a). Blue colored solid; mp: 212–214 °C; yield: 44% (46 mg).^{1}H NMR (500 MHz, CDCl$_3$) δ 8.12 (d, J=7.2 Hz, 1H), 8.06 (d, J=7.2 Hz, 1H), 8.01 (d, J=7.6 Hz, 1H), 7.95 (d, J=6.9 Hz, 1H), 7.73–7.82 (m, 2H), 7.44–7.59 (m, 2H), 7.37–7.42 (m, 2H), 7.28–7.32 (m, 3H), 7.23 (d, J=5.3 Hz, 1H), 6.88–6.94 (m, 1H), 6.82 (s, 1H), 6.71 (s, 1H), 6.66 (t, J=6.5 Hz, 1H). ^{13}C{^{1}H} NMR (101 MHz, CDCl$_3$) δ 184.2 (CO), 183.5 (CO), 140.1 (Cq), 135.9 (CH), 135.4 (Cq), 134.0 (Cq), 133.6 (CH), 133.3 (CH), 132.4 (Cq), 131.8 (Cq), 128.6 (2CH), 128.3 (2CH), 127.8 (CH), 127.2 (CH), 126.8 (CH), 126.6 (CH), 125.7 (CH), 124.3 (CH), 119.6 (Cq), 118.9 (CH), 114.6 (Cq), 111.3 (CH), 111.0 (Cq), 102.3 (CH), 101.3 (Cq). **HRMS** (ESI) m/z calculated for C$_{24}$H$_{15}$O$_2$NCl [(M+H)$^+$] 384.0786, found 384.0775.

5-nitro-2-(2-phenylindolizin-3-yl)naphthalene-1,4-dione (5b). faint blue colored solid; mp: 181–183 °C; yield: 51% (36 mg).^{1}H NMR (400 MHz, CDCl$_3$) δ 8.19–8.11 (m, 1H), 8.08–8.02 (m, 1H), 7.99 (dd, J=0.7, 7.2 Hz, 1H), 7.85–7.74 (m, 2H), 7.63–7.56 (m, 2H), 7.52–7.44 (m, 3H), 7.02 (s, 1H), 6.90 (ddd, J=6.6, 8.9 Hz, 1H), 6.73 (s, 1H), 6.68–6.61 (m, 1H).

^{13}C{^{1}H} NMR (101 MHz, CDCl$_3$) δ 184.0 (CO), 183.2 (CO), 140.5 (Cq), 139.4 (Cq), 136.2 (CH), 135.9 (Cq), 134.0 (CH), 133.6 (CH), 132.1 (2CH), 131.7 (Cq), 131.2 (Cq), 129.0 (2CH), 126.9 (CH), 125.9 (CH), 124.1 (CH), 120.1 (Cq), 119.2 (CH), 118.6 (Cq), 114.4 (Cq), 112.0 (CH), 110.1 (CH), 102.2 (CH).

5-bromo-2-(2-phenylindolizin-3-yl)naphthalene-1,4-dione (5c). Blue colored solid; mp: 133–135 °C; yield: 39% (17 mg). ^{1}H NMR (500 MHz, CD$_3$CN) δ 8.10–8.03 (m, 2H), 8.02–7.99 (m, 1H), 7.86–7.83 (m, 1H), 7.50 (d, J=9.2 Hz, 1H), 7.43 (d, J=7.2 Hz, 2H), 7.36–7.29 (m, 2H), 7.28–7.23 (m, 1H), 6.94 (s, 1H), 6.89 (dd, J=6.9, 8.4 Hz, 1H), 6.75

(s, 1H), 6.62 (t, J=6.7 Hz, 1H). ^{13}C{^{1}H} NMR (126 MHz, CD$_3$CN) δ 185.6 (CO), 184.9 (CO), 141.5 (Cq), 138.7 (CH), 136.8 (Cq), 136.4 (Cq), 135.3 (CH), 135.0 (CH), 133.9 (Cq), 133.4 (Cq), 129.9 (2CH), 129.7 (2CH), 127.9 (CH), 127.7 (CH), 126.7 (CH), 126.1 (CH), 120.9 (Cq), 119.9 (Cq), 112.4 (CH), 102.6 (CH).

Acknowledgements

Conflict of Interest

The authors declare no conflict of interest.

Data Availability Statement

The data that support the findings of this study are available in the supplementary material of this article.

[1] a) N. A. Romero, D. A. Nicewicz, *Chem. Rev.* **2016**, *116*, 10075–10166; b) C. K. Prier, D. A. Rankic, D. W. C. MacMillan, *Chem. Rev.* **2013**, *113*, 5322–5363; c) Y. Xi, H. Yi, A. Lei, *Org. Biomol. Chem.* **2013**, *11*, 2387–2403; d) J. M. R. Narayanam, C. R. J. Stephenson, *Chem. Soc. Rev.* **2011**, *40*, 102–113; e) M. Reckenthaler, A. G. Griesbeck, *Adv. Synth. Catal.* **2013**, *355*, 2727–2744.

[2] a) G. E. M. Crisenza, D. Mazzarella, P. Melchiorre, *J. Am. Chem. Soc.* **2020**, *142*, 5461–5476; b) Y.-Q. Yuan, S. Majumder, M.-H. Yang, S.-R. Guo, *Tetrahedron Lett.* **2020**, *61*, (8),151506.

[3] C. G. S. Lima, T. de M. Lima, M. Duarte, I. D. Jurberg, M. W. Paixao, *ACS Catal.* **2016**, *6*, 1389–1407.

[4] S. V. Rosokha, J. K. Kochi, *Acc. Chem. Res.* **2008**, *41*, 641–653.

[5] a) R. S. Mulliken, *J. Am. Chem. Soc.* **1952**, *74*, 811–824; b) Z.-Y. Cao, T. Ghosh, P. Melchiorre, *Nat. Commun.* **2018**, *9*, 3274–3283; c) J. Liu, Z. Zhua, F. Liu, *Org. Chem. Front.* **2019**, *6*, 241–244.

[6] a) G. S. Singh, E. E. Mmatli, *Eur. J. Med. Chem.* **2011**, *46*, 5237–5257; b) W. Chai, J. G. Breitenbucher, A. Kwok, X. Li, V. Wong, N. I. Carruthers, T. W. Lovenberg, C. Mazur, S. J. Wilson, F. U. Axe, T. K. Jones, *Bioorg. Med. Chem. Lett.* **2003**, *13*, 1767–1770; c) K. M. Dawood, A. A. Abbas, *Expert Opin. Ther. Pat.* **2020**, 30, 695–714.

[7] a) J. P. Michael, *Nat. Prod. Rep.* **2008**, *25*, 139–165; b) M. Movassaghi, A. E. Ondrus, B. Chen, *J. Org. Chem.* **2007**, *72*, 10065–10074.

[8] a) S. Chen, Z. Xia, M. Nagai, R. Lu, E. Kostik, T. Przewloka, M. Song, D. Chimmanamada, D. James, S. Zhang, *MedChemComm* **2011**, *2*, 176–180; b) H. Yang, H.-W. Wang, T.-W. Zhu, L.-M. Yu, J.-W. Chen, L.-X. Wang, L. Shi, D. Li, L.-Q. Gu, Z.-S. Huang, L.-K. An, *Eur. J. Med. Chem.* **2017**, *127*, 166–173; c) R. Yang, Y. Chen, L. Pan, Y. Yang, Q. Zheng, Y. Hu, Y. Wang, L. Zhang, Y. Sun, Z. Li, X. Meng, *Bioorg. Med. Chem.* **2018**, *26*, 4886–4897; d) L. Zheng, T. Gao, Z. Ge, Z. Maa, J. Xu, W. Ding, L. Shena, *Eur. J. Med. Chem.* **2021**, *214*, 1132262; e) V. Sharma, V. Kumar, *Med. Chem. Res.* **2014**, *23*, 3593–3606; f) E. Kim, Y. Lee, S. Lee, S. B. Park, *Acc. Chem. Res.* **2015**, *48*, 538–547; g) S. Park, D. I. Kwon, J. Lee, I. Kim, *ACS Comb. Sci.* **2015**, *17*, 459–469.

[9] a) B. Sadowski, J. Klajn, D. T. Gryko, *Org. Biomol. Chem.* **2016**, *14*, 7804–7828; b) Y. M. Shen, G. Grampp, N. Leesakul, H. W. Hu, J.-H. Xu, *Eur. J. Org. Chem.* **2007**, *22*, 3718–3726; c) J. Sung, Y. Lee, J. H. Cha, S. B. Park, E. Kim, *Dyes Pigm.* **2017**, *145*, 461–468; d) D–T. Yang, J. Radtke, S. K. Mellerup, K. Yuan, X. Wang, M. Wagner, S. Wang, *Org. Lett.* **2015**, *17*,

2486–2489; e) J. Hui, Y. Ma, J. Zhao, H. Cao, *Org. Biomol. Chem.* **2021**, *19*, 10245–10258.

[10] C. R. d. S. Bertallo, T. R. Arroio, M. F. Z. J. Toledo, S. A. Sadler, R. Vessecchi, P. G. Steel, G. C. Clososki, *Eur. J. Org. Chem.* **2019**, *2019*, 5205–5213.

[11] a) C. Wang, H. Jia, Z. Li, H. Zhang, B. Zhao, *RSC Adv.* **2016**, *6*, 21814–21821; b) C.-H. Park, V. Ryabova, I. V. Seregin, A. W. Sromek, V. Gevorgyan, *Org. Lett.* **2004**, *6*, 1159–1162.

[12] J. Sun, F. Wang, Y. Shen, H. Zhi, H. Wu, Y. Liu, *Org. Biomol. Chem.* **2015**, *13*, 10236–10243.

[13] L. Yang, X. Pu, D. Niu, Z. Fu, X. Zhang, *Org. Lett.* **2019**, *21*, 8553–8557.

[14] W. Kim, H. Y. Kim, K. Oh, *J. Org. Chem.* **2021**, *86*, 22, 15973–15991.

[15] a) Y–Z. Zhanga, F–T. Sheng, Z. Zhu, Z–M. Li, S. Zhang, W. Tan, F. Shi, *Org. Biomol. Chem.* **2020**,*18*, 5688–5696.

[16] X. Liu, D. Song, Z. Zhang, J. Lin, C. Zhuang, H. Zhan, H. Cao, *Org. Biomol. Chem.* **2021**, *19*, 5284–5288.

[17] a) Y. Zhang, Y. Yu, B. Liang, Y-y. Pei, X. Liu, H. Yao, H. Cao, *J. Org. Chem.* **2020**, *85*, 10719–10727; b) Y. Liang, L. Teng, Y. Wang, Q. He, H. Cao, *Green Chem.* **2019**, *21*, 4025–4029.

[18] F. Penteado, C. S. Gomes, L. I. Monzon, G. Perin, C. C. Silveira, E. J. Lenardão, *Eur. J. Org. Chem.* **2020**, 2110–2115.

[19] L. Teng, X. Liu, P. Guo, Y. Yu, H. Cao, *Org. Lett.* **2020**, *22*, 10, 3841–3845.

[20] K. D. Mane, R. B. Kamble, G. Suryavanshi, *New J. Chem.* **2019**,*43*, 7403–7408.

[21] A. Runemark, S. C. Zacharias, H. Sunden, *J. Org. Chem.* **2021**, *86*, 1901–1910.

[22] a) C. Hu, F. Q. Shen, G. Feng, J. Jin, *Org. Lett.* **2021**, *23*, 10, 3913–3918; b) V. Quint, N. Chouchène, M. Askri, J. Lalevée, A. C. Gaumonta, S. Lakhdar, *Org. Chem. Front.* **2019**, *6*, 41–44; c) J. Kaur, A. Shahin, J. P. Barham, *Org. Lett.* **2021**, *23*, 6, 2002–2006; d) L. Zheng, Y. E. Qian, Y. Z. Hu, J.-A. Xiao, Z. P. Ye, K. Chen, H. Y. Xiang, X. Q. Chen, H. Yang, *Org. Lett.* **2021**, *23*, 5, 1643–1647.